

Georgia State University

ScholarWorks @ Georgia State University

Chemistry Dissertations

Department of Chemistry

12-10-2018

**Design and Development of Prodrugs of Sulfur Dioxide and
Design and Synthesis of Prodrugs of Thiamine Monophosphate
Mimics as Pyruvate Dehydrogenase Kinase Inhibitors**

Wenyi Wang

Follow this and additional works at: https://scholarworks.gsu.edu/chemistry_diss

Recommended Citation

Wang, Wenyi, "Design and Development of Prodrugs of Sulfur Dioxide and Design and Synthesis of Prodrugs of Thiamine Monophosphate Mimics as Pyruvate Dehydrogenase Kinase Inhibitors." Dissertation, Georgia State University, 2018.
https://scholarworks.gsu.edu/chemistry_diss/151

This Dissertation is brought to you for free and open access by the Department of Chemistry at ScholarWorks @ Georgia State University. It has been accepted for inclusion in Chemistry Dissertations by an authorized administrator of ScholarWorks @ Georgia State University. For more information, please contact scholarworks@gsu.edu.

DESIGN AND DEVELOPMENT OF PRODRUGS OF SULFUR DIOXIDE
AND
DESIGN AND SYNTHESIS OF PRODRUGS OF THIAMINE MONOPHOSPHATE MIMICS
AS PYRUVATE DEHYDROGENASE KINASE INHIBITORS

by

WENYI WANG

Under the Direction of Binghe Wang, PhD

ABSTRACT

SO₂ is widely recognized as an air pollutant and is a known cause of acid rain. At a sufficiently high level, it also causes respiratory diseases. There is mounting evidence that SO₂ is produced during normal cellular metabolism and may possibly function as a signaling molecule in normal physiology. One difficulty in studying the biological and pharmacological roles of SO₂ is the lack of adequate tools for its controllable and precise delivery. Traditional methods of using SO₂ gas or mixed sulfite salts do not meet research need for several reasons. Therefore, there has been increasing attention on the need of developing SO₂ donors or prodrugs that can be used as tools for the elucidation of SO₂'s physiological roles, pharmacological effects, and

possible mechanism(s) of action. In the first chapter, we provided two strategies to deliver SO₂ in its molecule form to allow SO₂ release with tunable release rate. Such SO₂ donors and prodrugs would serve as useful tools for researchers to probe the mystery of SO₂ as a gasotransmitter.

A decreased level of thiamine-dependent enzyme pyruvate dehydrogenase (PDH) is an important characteristic of cancer cells. Pyruvate dehydrogenase kinase (PDK) inhibits the activity of PDH which helps cancer cells to gain more energy by converting glucose into lactate. Therefore, inhibiting the activity of PDK can be a promising approach for cancer therapy. Thiamine at a high concentration was found to have inhibitory effect on cancer cell proliferation as a PDK inhibitor. From previous studies, a series of thiamine analogues were designed, synthesized, and tested *in vitro* for anti-proliferative effect. However, all the analogues demonstrate low inhibitory effect on cancer cell proliferation. We hypothesize that the low inhibitory activity may be due to a lack of phosphorylation inside the cell. A phosphate prodrug strategy that can release thiamine monophosphate mimetics inside the cell may overcome this problem. In the second chapter, we describe the design, synthesis, and preliminary biological evaluation of several prodrugs of thiamine monophosphate mimics. Cancer cell proliferation tests suggest significantly increased inhibitory effect of the phosphate prodrugs compared with respective thiamine analogues without the phosphate prodrug moiety.

INDEX WORDS: Gasotransmitter, Sulfur dioxide, Prodrugs, PDK inhibitors, Thiamine analogues, Phosphate prodrugs.

DESIGN AND DEVELOPMENT OF PRODRUGS OF SULFUR DIOXIDE
AND
DESIGN AND SYNTHESIS OF PRODRUGS OF THIAMINE MONOPHOSPHATE MIMICS
AS PYRUVATE DEHYDROGENASE KINASE INHIBITORS

by

WENYI WANG

A Dissertation Submitted in Partial Fulfillment of the Requirements for the Degree of

Doctor of Philosophy

in the College of Arts and Sciences

Georgia State University

2018

Copyright by
Wenyi Wang
2018

DESIGN AND DEVELOPMENT OF PRODRUGS OF SULFUR DIOXIDE
AND
DESIGN AND SYNTHESIS OF PRODRUGS OF THIAMINE MONOPHOSPHATE MIMICS
AS PYRUVATE DEHYDROGENASE KINASE INHIBITORS

by

WENYI WANG

Committee Chair: Binghe Wang

Committee: Peng Wang

Ivaylo Ivanov

Electronic Version Approved:

Office of Graduate Studies

College of Arts and Sciences

Georgia State University

December 2018

DEDICATION

This dissertation is dedicated to my dearest parents: Mr. Leping Wang and Mrs. Yan Lin, and my beloved husband Mr. Guangming Jing.

I want to thank my parents for raising me to a person who I am. Without their unconditional love, I won't be able to go through the hard times in my life. They care about my well-being as if I were a little kid, and respect all the decisions I made, no matter good or bad. I want to thank them for always backing me up. Their encouragement and advices have made all the bitterness into memorable experiences. I am very proud to be their daughter.

I also want to thank my husband for his companion. Studying abroad is never easy. Meeting him in this journey is one the best things that happened to me. He's not only a husband, but also a mentor, a healer, and a best friend. His understanding and support have carried me through my darkest time. He makes me believe that the best has yet to come.

ACKNOWLEDGEMENTS

I would like to thank my advisor Dr. Binghe Wang for his guidance throughout my graduate study. He accepted me when I was almost ignorant about chemistry and coached me into a chemist that I am today. He is a great educator that truly cares about every of his students. His advice will benefit me through my whole life. I would also like to thank Dr. Peng Wang and Dr. Ivaylo Ivanov for their support and advices. I would like to express my special thanks to Dr. Chaofeng Dai, and Dr. Xingyue Ji, who trained me almost everything I know about organic synthesis. I would like to thank Dr. Siming Wang, Dr. Zhenming Du, Dr. Kaili Ji, Dr. Xiaoxiao Yang, and Dr. Yueqin Zheng, for instrumental trainings and many inspiring discussions. Also, I would like to thank Dr. Danzhu Wang, Dr. Ke Wang, Dr. Alexander Draganov, Zhixiang Pan, and Manjusha Choudhury for making my days in the lab loaded with happy memories. Last but not least, I would like to thank all the group members of Dr. Binghe Wang's lab I've been working with and wish all of them my very best.

TABLE OF CONTENTS

ACKNOWLEDGEMENTS	V
LIST OF TABLES	VIII
LIST OF FIGURES	IX
LIST OF ABBREVIATIONS	XI
1 DESIGN AND DEVELOPMENT OF SO₂ PRODRUGS	1
1.1 Introduction	1
<i>1.1.1 SO₂ chemistry</i>	<i>2</i>
<i>1.1.2 SO₂ donors and prodrugs</i>	<i>9</i>
<i>1.1.3 Expected Results</i>	<i>17</i>
1.2 Click reaction-based SO₂ prodrugs	18
<i>1.2.1 Results and discussion</i>	<i>18</i>
<i>1.2.2 Experimental procedures</i>	<i>24</i>
1.3 Esterase-sensitive SO₂ prodrugs	39
<i>1.3.1 Results and discussion</i>	<i>40</i>
<i>1.3.2 Experimental procedures</i>	<i>49</i>
 2 DESIGN AND SYNTHESIS OF PRODRUGS OF THIAMINE	
MONOPHOSPHATE MIMICS AS PYRUVATE DEHYDROGENASE KINASE	
INHIBITORS	77
2.1 Introduction	77

2.1.1	<i>PDC structure and funtion</i>	78
2.1.2	<i>PDC regulation by PDK and PDP</i>	79
2.1.3	<i>PDK inhibition for cancer therapy</i>	80
2.2	Results and discussion	84
2.3	Experimental procedures	84
2.3.1	<i>Materials and Methods</i>	90
2.3.2	<i>Synthesis</i>	91
	REFERENCES	120
	APPENDICES	139
	Appendix A NMR spectra of compounds in Chapter 1	139
	<i>Appendix A.1 NMR spectra of compound in Chapter 1.2</i>	139
	<i>Appendix A.2 NMR spectra of compound in Chapter 1.3</i>	163
	Appendix B NMR spectra of compound in Chapter 2	192

LIST OF TABLES

Table 1-1 Kinetics study of SO ₂ donor pairs	23
Table 1-2 SO ₂ release rate monitored by HPLC	44
Table 2-1 IC ₅₀ of first-batch thiamine analogues	86
Table 2-2 IC ₅₀ of phosphate prodrugs of thiamine analogues	90

LIST OF FIGURES

Figure 1-1 Interconversion of SO ₂ derivatives	3
Figure 1-2 Endogenous production of SO ₂	7
Figure 1-3 DTNB test mechanism	20
Figure 1-4 UV absorption at 412 nm of DTNB test	20
Figure 1-5 SO ₂ donor pairs	22
Figure 1-6 Fluorescent SO ₂ donor and product after SO ₂ release (100 μM in MeOH)	22
Figure 1-7 Coalescence of cheletropic product (6 + 1) observed in ¹³ C NMR (DEPT-135) with increasing temperature	22
Figure 1-8 Kinetics studies of cycloaddition reactions by UV-vis absorbance change.....	35
Figure 1-9 Kinetics studies of cycloaddition reaction between 7 and 1 by monitoring fluorescence changes	36
Figure 1-10 Quantum yield determination of 7 using QS as the reference	38
Figure 1-11 Quantum yield determination of 21 using QS as the reference	39
Figure 1-12 Structures of compounds 10-13	46
Figure 1-13 Kinetics of esterase triggered release monitored by HPLC	46
Figure 1-14 Stability of compound 13 in 1% DMSO/PBS.....	46
Figure 1-15 Esterase triggered release of compound 13 under different conditions	47
Figure 1-16 Cell imaging study of SO ₂ release from 13 in HeLa cells	48
Figure 1-17 DTNB test results.....	64
Figure 1-18 Kinetics studies of compounds 7a-e by measuring 2-OHBT peak areas using HPLC	65

Figure 1-19 An example of reaction of 7e monitored by HPLC. Peaks at 8.87~8.88 min: compound 7e	67
Figure 1-20 An example of stability tests of compound 9 monitored by HPLC	68
Figure 1-21 An example of stability tests of compound 10 monitored by HPLC	70
Figure 1-22 An example of stability studies of compound 13 monitored by HPLC	72
Figure 1-23 Kinetics study of esterase-triggered SO ₂ release from compound 10-13 by fluorescent probe 14	75
Figure 2-1 Reactions catalyzed by PDC	79
Figure 2-2 Representative PDK inhibitors.....	82
Figure 2-3 Prodrug strategy to deliver phosphorylated thiamine analogue into the cell	87
Figure 2-4 Prodrug structures	88

LIST OF ABBREVIATIONS

AAT	Aspartate aminotransferase
ATP	Adenosine triphosphate
BT	Benzothiazole
CDO	Cysteine dioxygenase
CHD	Congenital heart disease
DCA	Dichloroacetate
DNS	2,4-Dinitrophenylsulfone
<i>E. coli</i>	<i>Escherichia coli</i>
GSSH	Glutathione persulfide
HIF1 α	Hypoxia inducible factor 1 α
IC	Ion chromatography
I/R	Ischemia-reperfusion
LPS	Lipopolysaccharid
MCT	Monocrotaline
MIC	Minimum inhibitory concentrations
MRSA	Methicillin-resistant <i>Staphylococcus aureus</i>
MSBT	Methyl sulfonyl benzothiazole
MSSA	Methicillin sensitive <i>Staphylococcus aureus</i>
<i>Mtb</i>	<i>Mycobacterium tuberculosis</i>
NADPH	Nicotinamide adenine dinucleotide phosphate
NEM	<i>N</i> -ethylmaleimide

HEK29	Human embryonic kidney 293 cells
2-OHBT	2-Hydroxybenzothiazole
PDC	Pyruvate dehydrogenase complex
PDH	Pyruvate dehydrogenase
PDK	Pyruvate dehydrogenase kinase
PDP	Pyruvate dehydrogenase phosphatase
QS	Quinine sulfate
SHR	Spontaneous hypertensive rat
TCA	Tricarboxylic acid
TIL	Tumor-infiltrating lymphocytes
TPP	Thiamine pyrophosphate
VSMC	Vascular smooth muscle cells

1 DESIGN AND DEVELOPMENT OF SO₂ PRODRUGS

1.1 Introduction

SO₂ has long been recognized as an air pollutant produced by fossil fuel consumption and volcano eruptions. Upon oxidation and/or hydration, SO₂ can serve as a precursor of acid species such as H₂SO₃ and H₂SO₄, which cause acidification of rain water, and thus acid pollution. In terms of toxicology, overexposure to SO₂ may induce respiratory tract irritation and damage to many organs.¹⁻⁴ Besides forming acid which causes mucous irritation, the mechanism of SO₂'s toxicity is generally thought to involve the oxidation process of its derivatives.⁵ For example, it has been demonstrated that the DNA damage effect of SO₂ can be induced by SO₃^{•-} and SO₄^{•-} radicals produced by autoxidation of sulfite (SO₃²⁻).⁶⁻⁷ However, as a matter of fact, SO₂ and its derivatives have a long history of being applied in food industry as preservatives. Moreover, endogenous SO₂ can be produced enzymatically through the metabolism of sulfur-containing amino acids or non-enzymatically through oxidation of H₂S in neutrophils under oxidative stress.^{5, 8} A recent review by Huang et al. considered SO₂ as the fourth gasotransmitter after nitric oxide (NO), carbon monoxide (CO), and hydrogen sulfide (H₂S).⁹ By the same token, it is hard to imagine that O₂ and CO₂ do not have regulatory roles and should not be considered as gasotransmitters as well. Indeed, sensing for O₂ and CO₂ are essential for their regulatory roles and have been extensively studied.¹⁰⁻¹² Therefore, one may consider the gasotransmitter family having at least 6 members.

In recent years, accumulating evidence demonstrates that SO₂ possesses many bioactivities, especially in the cardiovascular system.¹³⁻¹⁴ Besides the biological effect SO₂ demonstrated under physiological concentration, it has been shown that abnormal levels of SO₂ are related to many pathological conditions such as hypertension and pulmonary hypertension.⁹

Its regulatory effects in the cardiovascular system may have therapeutic potential and thus require more detailed studies for its mechanism of activity.¹⁵

1.1.1 *SO₂ chemistry*

Much of the recent rise in interest for SO₂ originates from its possible roles as an endogenous signaling molecule. As a gaseous molecule, SO₂ has a Henry's constant of 1.23 mol kg⁻¹ bar⁻¹.¹⁶ It can readily dissolve in water and form hydrated SO₂ complex (SO₂·H₂O), which in turn undergoes first and second dissociation to give bisulfite (HOSO₂⁻ or HSO₃⁻) and sulfite (SO₃²⁻) ions.¹⁷⁻¹⁹ The first and second pK_as of SO₂·H₂O are 1.81 and 6.97. Accordingly, it can be calculated that under physiological pH, the bisulfite and sulfite are formed in a molar ratio of about 1: 3. Dimerization of bisulfite would form disulfite (S₂O₅⁻). The interconversion of these species is summarized in Figure 1-1. Due to the abundance of water in biological system, all the species exist in an equilibrium. Therefore, it will be hard to isolate one species out and study its sole effect; and it is important to study SO₂ and its derivatives as a whole. Besides hydration, another important aspect of SO₂ chemistry is its redox chemistry, which is much more complex in a biological setting. SO₂ and its derivatives are interconnected with many other sulfur species through enzymatic or non-enzymatic processes. Generally speaking, SO₂ is produced as an intermediate of metabolism of sulfur-containing compounds and can be oxidized further to generate other sulfur species. For example, SO₂ can be produced from L-cysteine through sequential catalysis of cysteine dioxygenase and aspartate aminotransferase (AAT); oxidation of sulfite through sulfite oxidase can produce sulfate; H₂S can be generated from L-cysteine by cystathionine β-synthase, and further oxidation by NADPH oxidase would generate SO₂; under ambient conditions, more reactive species such as SO₃⁻ and SO₄⁻ can be produced through autoxidation of sulfite.^{7, 9, 20}

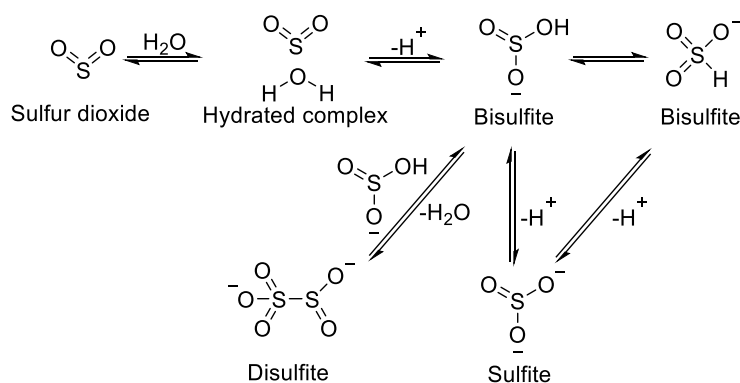


Figure 1-1 Interconversion of SO₂ derivatives

Taken together the chemistry of SO₂ and current reports about SO₂'s biological activity, one may see some contradictory results. On one hand, SO₂ and its derivatives seems to be toxic intermediates produced in sulfur metabolism. The high oxidation state of endogenous SO₂ produced by oxidation of sulfur species at lower oxidation states (e.g. cysteine, H₂S) can pose oxidative stress on cells and tissue, causing oxidative damage.⁴ Moreover, deficiency of sulfite oxidase, which catalyzes the oxidation of sulfite to sulfate as the last oxidative step of sulfur metabolism, is known to result in fatal neurological symptoms.²¹⁻²² On the other hand, the potential for further oxidation allows SO₂ and its derivatives to function as an antioxidant. Indeed, SO₂ plays a protective role against oxidative stress under certain circumstances.²³⁻²⁶ For example, Chen *et al.* have demonstrated that endogenous SO₂ offers protection against oleic acid-induced acute lung injury by suppressing oxidative stress.²⁶ Also, SO₂ preconditioning was shown to be effective in preventing ischemia-reperfusion injury in cardiovascular system.²³ It is nonetheless clear that the chemical reaction to go from SO₂ to SO₃ is only a 2-electron process. Thus, the scavenging capacity of SO₂ is far lower than that of H₂S, which can give 6 electrons to go to the oxidation state of SO₂ and 8 electrons to that of SO₃. The dual role of SO₂ and its “inefficiency” as antioxidant makes us wonder what would be the reason for SO₂ to be used as

an antioxidant by nature. Does SO_2 perform its “antioxidant” role through direct reduction/scavenging of an oxidizing species or through regulatory functions that make cells more resilient under an oxidizing environment? The interconversion rates among sulfur species are also very important in considering the meaning of using SO_2 as signaling molecule. Enzymatic processes not only provide more precise control of substrate concentration compared with non-enzymatic process, but also offer potential targets for regulation. In addition, bisulfite and sulfite are strong nucleophiles and such properties may contribute to their biological activities. For all these reasons and more, it is very important to understand the chemistry issues when studying its biology and developing its donors and prodrugs. However, such relationships are very convoluted that makes deciphering the precise role of SO_2 very hard, given that the enzymes and reaction kinetics involved are not so clear.

For a signal molecule to function, the existence of relevant biological target(s) is a critical question. For small organic molecules, proteins, peptides, lipids and others, binding to a macromolecular target is often the mechanism of action. The issue is nevertheless more challenging for gasotransmitters. There are well-established mechanism(s) of action at the molecular level for NO , H_2S ²⁷ and CO .²⁸ Specifically, NO can bind to a heme moiety at the distal site of soluble form of guanylyl cyclase, and thus activates guanylyl cyclase, leading to elevated levels of cGMP.²⁹ Hydrogen sulfide in its persulfide form is known to be responsible for protein persulfidation, which is a well-established regulatory process.³⁰ For CO , there is also strong evidence that binding to heme and other metal-containing biomolecules is a critical first step.^{28, 31} For example, CO can bind a soluble form of guanylyl cyclase much the same way as NO , except with decreased ability to activate the cyclase. CO is also reported to inhibit cytochrome C oxidase leading to increased production of ROS, which in turn leads to the production of the

persulfide form of glutathione (GSSG).³²⁻³⁴ GSSG is known to facilitate protein glutathionylation, a known form of protein post-translational modification, and plays a regulatory role. With SO₂, molecular level studies have been scarce, though various regulation effects of SO₂ and its derivatives on other biological molecules have been observed, especially in the cardiovascular system.⁹ However, the binding targets of SO₂ or its derivatives are not yet clear. It is not hard to envision that the equilibrium between SO₂ and other sulfur species would play an important role in maintaining the intracellular redox balance. Therefore, enzymes involved in generating related species may serve as potential binding targets. Moreover, the varied concentration of SO₂ in different tissue hints that SO₂ may have tissue-specific target.³⁵ Furthermore, as a strong nucleophile and Lewis base, bisulfite's interaction with certain metal-containing proteins (e.g. sulfite oxidase) and reaction with electrophiles could play a role in regulating the biological functions of these molecules.³⁶ With such knowledge, SO₂ donors and prodrugs with desirable properties will help us understand the molecular mechanism of SO₂'s action.

1.1.2 Endogenous production and physiological effects of SO₂.

SO₂ can be produced endogenously through several pathways (Figure 1-2). In the aspartate aminotransferase (AAT) pathway, L-cysteine is first oxidized to L-cysteine sulfinic acid by cysteine dioxygenase (CDO). AAT then catalyzes the transamination between L-cysteine sulfinic acid and α -ketoglutarate to form β -sulfinylpyruvate. The spontaneous decomposition of the latter would yield SO₂ and pyruvate.³⁷ SO₂ can also be produced from the oxidation of H₂S, another metabolite of sulfur-containing amino acids. The oxidation could be directly through NADPH oxidase in activated neutrophils, or through oxidation by sulfide oxidase followed by thiosulfate sulfurtransferase or glutathione-dependent thiosulfate reductase.³⁸⁻⁴⁰ Zhang et al.

have shown that the endogenous production of SO_2 is closely related to endogenous H_2S . Endogenous H_2S can inhibit endothelial SO_2 production through suppressing AAT activity, while impaired H_2S production pathway would lead to upregulation of SO_2 production.⁴¹ The excretion of SO_2 is through hydration and oxidation by sulfite oxidase to sulfate followed by renal clearance to urine.⁴²

The most profound effect of SO_2 under physiological conditions was found in the cardiovascular system. Du et al. tested various vascular tissues and found the highest SO_2 content in the aorta.³⁵ Using a mixture of bisulfite/sulfite salt as an SO_2 source, a slight relaxation effect was observed on isolated rat aortic rings while a concentration-dependent relaxation was observed with higher dosages. The same effect was also observed using SO_2 gas and SO_2 gas solution as later demonstrated by Meng et al.⁴³⁻⁴⁴ Such result indicates the role SO_2 plays in maintaining normal vascular tone and blood pressure. SO_2 was also found to have a negative inotropic effect as observed on isolated perfused rat heart, which in turn affects the heart rate and left ventricular developed pressure.⁴⁵ Besides in the cardiovascular system, SO_2 was also found to be involved in lipid metabolism, possibly due to its oxidant effect.⁴⁶⁻⁴⁷ More interestingly, aligned with the well-known antimicrobial activity of SO_2 and its derivatives, Nojima and colleagues have demonstrated that sulfite is a neutrophil mediator of host defense that *in vivo* administration of lipopolysaccharide (LPS) would trigger sulfite release from neutrophil and increase serum sulfite concentration in rats.⁴⁸

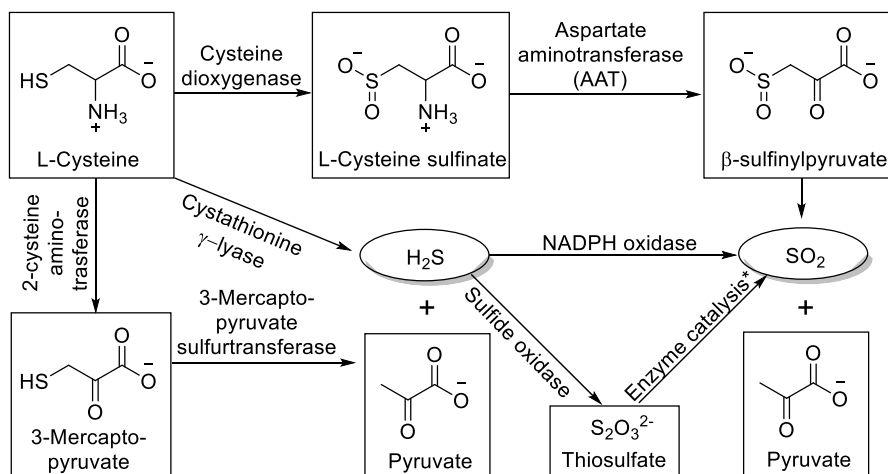


Figure 1-2 Endogenous production of SO_2 .

* Process catalyzed by thiosulfate sulfurtransferase or glutathione-dependent thiosulfate reductase.

1.1.3 Pathophysiological effect of SO_2

Many research papers and excellent reviews have been published in recent years addressing the pathophysiological effect of SO_2 .^{9, 14} Here we give a brief summary to provide a background for readers to understand the therapeutic potential and future application of SO_2 .

Compared with the SO_2 's therapeutic potential, the toxicity of SO_2 is more widely accepted by the public; and is likely to be attributed to SO_2 's oxidative property. Meng has suggested that SO_2 as an oxidative agent can cause lipid peroxidation and changes anti-oxidation status in multiple organs.⁴ Chronic exposure to SO_2 was also found to promote atherosclerosis.⁴⁹ Controversially, in atherosclerosis rats, a decreased level of plasma and aortic SO_2 content, as well as AAT activity, was reported by Li et al.⁵⁰ Further, treatment of SO_2 derivatives could diminish the size of atherosclerotic plaques in rat coronary artery. Under certain physiological or pathological conditions, the regulation of endogenous SO_2 level may vary, resulting from or contributing to the formation of the pathological condition.

The fluctuation of endogenous SO_2 level has been observed in several animal disease models and human. An elevated level of serum sulfite content was found in patients with chronic renal failure and pneumonia.⁵¹⁻⁵² Corresponding with afore mentioned LPS stimulated sulfite release stimulated by LPS, the serum level of SO_2 was found to increase significantly in pediatric patients with acute lymphoblastic leukemia with bacteria-induced inflammation, which is likely a defensive mechanism indicating SO_2 's anti-inflammatory role.⁵³

SO_2 's pathophysiological roles have been widely studied in cardiovascular disease models. In spontaneous hypertensive rats (SHRs), a significantly lower level of SO_2 and AAT activity was observed in serum and aorta.⁵⁴ In a study conducted on children with congenital heart disease (CHD), serum SO_2 level showed a negative relationship with pulmonary hypertension. For example, in the CHD group with severe pulmonary hypertension, the SO_2 concentration was only half of that of the group without pulmonary hypertension.⁵⁵ Similarly, in rats under hypoxic conditions, a decreased SO_2 level in plasma and lung tissue was observed simultaneously with pulmonary hypertension, pulmonary vascular structural remodeling, and increased vascular inflammatory response.⁵⁶ In rat model with monocrotaline-induced pulmonary vascular collagen remodeling, SO_2 content and AAT activity were significantly increased.⁵⁷ Meanwhile, in rats with monocrotaline (MCT) induced pulmonary hypertension, higher SO_2 level, AAT expression and activity were observed compared to the control group, indicating a protective role of endogenous SO_2 .⁵⁸ Additionally, in rat myocardial ischemia-reperfusion (I/R) models, AAT1 protein expression showed a significant decrease.⁵⁹ In isoproterenol induced myocardial injury rat model, the SO_2 /AAT pathway also showed a down regulation.²⁴ Subjecting such animal models to treatment or pretreatment with SO_2 derivatives or SO_2 gas led to alleviation of the pathology, indicating a strong therapeutic potential of SO_2 .

1.1.4 SO₂ donors and prodrugs

For biological assessment, SO₂ gas and mixed sulfite salts (NaHSO₃ and Na₂SO₃ in 1: 3 molar ratio) have been most widely used as sources of SO₂. SO₂ gas was used for preparation of stock solution or administration to small animals by inhalation. The dosage can be controlled through partial pressure. In such applications, using gaseous SO₂ requires special laboratory equipment and settings as well as prolonged exposure time at low concentration to avoid acute toxicity or irritation. Neither does it offer precise dosage control nor future prospect of human use. The second method of using mixed sulfite salts to generate SO₂ depends on the complex kinetics of the dynamic equilibrium between gaseous SO₂ and its hydrated derivatives (Figure 1-1). Using such donors lacking controllable release rate cannot mimic endogenous production of SO₂ and may lead to transient effect and overdosing. The quick renal clearance rate may also limit the efficiency of using mixed salt as SO₂, especially when prolonged exposure at low dosage is required. Moreover, efficiency of SO₂ delivery to cell or tissue can hardly be guaranteed and may result in irreproducible experiment results. According to Meng and co-workers, gaseous SO₂ may have much stronger vasorelaxant effect compared with mixed sulfite salts.⁴³ Another way of donating SO₂ is through overexpression of two isoenzymes of AAT.⁶⁰ AAT is an upstream enzyme in the SO₂ generation pathway, which can catalyze the transamination of L-cysteine sulfinic acid to form β-sulfinylpyruvate and generate SO₂. Therefore, the activity of AAT may directly influence SO₂ production. Vascular smooth muscle cells (VSMCs) transfected with AAT1 or AAT2 plasmids showed suppressed serum-induced proliferation, while AAT1 or AAT2 knocked-down VSMCs showed exacerbated serum-induced proliferation. Such approaches could serve as a powerful research tools in cell-based assays. Nevertheless, the same kind of studies at the tissue, organ, or animal level would require much

more complicated work.⁶¹ The lack of reliable donors that can generate SO₂ in a controllable manner has hampered the delineation of SO₂'s precise biological and regulatory roles. To overcome these obstacles, SO₂ donors and prodrugs with different triggering mechanisms have been developed in recent years.

1.1.4.1 Thiol-activated SO₂ prodrugs

Chakrapani's group pioneered in the work of developing SO₂ prodrugs. They first developed a series of 2,4-dinitrophenylsulfonamide compounds as prodrugs that release SO₂ upon thiol triggering for antimycobacterial purpose (Scheme 1-1).⁶² 2,4-Dinitrophenylsulfonamide was previously employed in thiol-detection systems, which produces SO₂ as a byproduct upon decomposition. In their design, mycothiol (MSH), which exists in *Mycobacterium tuberculosis* (*Mtb*) in millimolar concentrations, would serve as the thiol source to trigger the release. Depleting thiols and generating SO₂ at the same time would disrupt cellular redox equilibrium and damage biomacromolecules, causing *Mtb* growth inhibition. A first batch of 17 compounds were synthesized with varied substitutions on both the amino group and the sulfonyl group through simple substitution reactions using the corresponding amines and sulfonyl chlorides. The compounds were incubated in pH 7.4 buffer with cysteine and tested of SO₂ release by a *p*-rosaniline-based assay. Release rates were measured by ion chromatography (IC) with a conductivity detector. Antimycobacterial activity of the compounds against *Mtb* was quantified as minimum inhibitory concentrations (MICs, the minimum concentration required to inhibit 99% of bacterial growth). Eleven compounds containing the 2,4-dinitrophenylsulfone (DNS) moiety showed SO₂ release within 30 min and demonstrated greater antimycobacterial activity than the non-releasing compounds, indicating a correlation between SO₂ release and *Mtb* inhibition. The release mechanism was proposed to go through Jackson-Meisenheimer complex

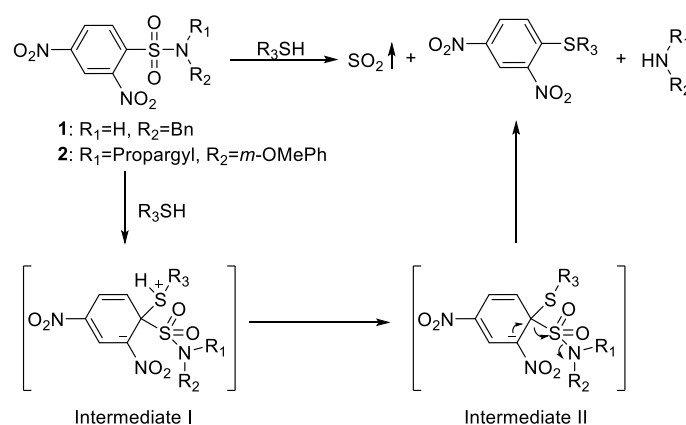
intermediates to produce SO₂, benzylamine, and 2,4-dinitrophenylthioether (Scheme 1-1). *N*-Benzyl-2,4-dinitrophenylsulfonamide (**1**, Scheme 1-1) showed 100% SO₂ release within 30 min (estimated half-life ~ 2 min) and was found to have the best *Mtb* inhibitory potency with a MIC of 0.15 μM, which is lower than the clinically used agent isoniazid (0.37 μM) tested under the same conditions. Moreover, compound **1** showed no cytotoxicity at such concentration towards human embryonic kidney 293 cells (HEK293) (IC₅₀ = 7 μM). Further studies of the relationship between SO₂ release rates and MICs on 6 compounds (*t*_{1/2} = 2~63 min) with similar clogP values found a good correlation between fast SO₂ release rates and inhibitory potency.

To better understand this relationship as well as the structure-activity relationship (SAR), the same group synthesized a total of 19 structural analogues of compound **1** with varied amino substitutions and comparable clogP values.⁶³ The results showed only decreased SO₂ release rates and MICs compared with compound **1**, regardless of modifications made. Seven compounds with potent MICs (highest MIC = 2.13 μM) were found better than clinically used drugs ethambutol and pyrazinamide tested under the same conditions. According to Spearman rank correlation analysis, a correlation between MIC and SO₂ yield after 5 min was established that higher SO₂ yield is related to lower MIC.

This strategy was further tested on methicillin sensitive *Staphylococcus aureus* (MSSA, Gram+), methicillin-resistant *Staphylococcus aureus* (MRSA, Gram+), *Enterococcus faecalis* (*E. faecalis*, Gram+), and *Escherichia coli* (*E. coli*, Gram-).⁶⁴ A library of 38 2,4-dinitrophenylsulfonamides (including compound **1**) were synthesized, among which 12 compounds were in “dimerized” forms. All compounds were shown to be able to release SO₂ under physiological conditions with different rates. Compound **2** (Scheme 1-1) showed good MICs of 4 μg/mL (~10 μM) against both strains of *S. aureus* and 8 μg/mL MIC against *E.*

faecalis. However, no compound was found to be effective against *E. coli*, possibly due to the permeation barrier presented by the outer membrane of Gram-negative bacteria in general. The inhibitory mechanism remains to be determined since evidence suggests that the SO₂ generating ability of these compounds is not the sole reason responsible for the inhibitory effect. The capability of the compounds to permeate cells and deplete thiols may as well affect the inhibitory effect, since thiols in presence of oxidative stress can be primarily oxidized to disulfide species. Indeed, compound **2** showed much better capacity depleting intracellular thiols compared with compounds with poor inhibitory activity. Furthermore, compound **2** was also capable of inhibiting several patient-derived MRSA strains with MIC values of 2~4 µg/mL. Cytotoxicity was also assessed against A549 lung carcinoma cells. A GI₅₀ of 27 µM and a selectivity index (GI₅₀/MIC) of 5.2 were determined.

Besides antibacterial applications, compound **1** has been extensively used as an intracellular SO₂ source in validation of utility of many SO₂ probes in biological settings.⁶⁵⁻⁶⁹ Depletion of thiol with thiol scavenger (*N*-ethylmaleimide, NEM) would easily disable SO₂ release from the prodrug, offering a good method for conducting control experiments.



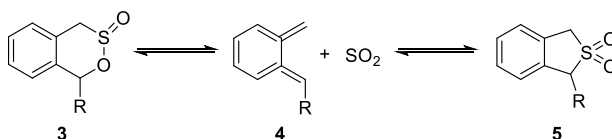
Scheme 1-1 Thiol-activated SO₂ prodrugs.

1.1.4.2 Thermally activated SO₂ prodrugs

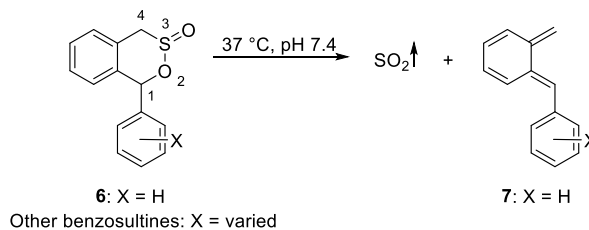
Another class of SO₂ prodrugs developed by Chakrapani's groups uses the benzosultine scaffold (Scheme 1-2).⁷⁰ By design, such prodrugs would release SO₂ through a thermal retro-Diels-Alder reaction. The substitutions on the 1-position would allow reactivity tuning and thus cycloreversion at physiological temperature. As such, benzosultine and 1-substituted (Me, Ph) benzosultines were subjected to *ab initio* calculations. Reaction energies (ΔE_{rxn}), Gibbs free energies (ΔG_{rxn}), and Gibbs free-energy barriers (ΔG^{\ddagger}) of different conformations of the benzosultines and sulfones to produce dienes and SO₂ were calculated to predict the stable conformations and favorable reaction paths (Scheme 1-2). Results showed that, compared with benzosultine, 1-substituted benzosultines have lower Gibbs energy barriers (ΔG^{\ddagger}) and would be expected to have enhanced cycloreversion rates. Besides, phenyl substitution (**6**) would further reduce cycloreversion barrier than methyl substitution, leading to faster reactions at the same temperature. All three compounds were synthesized and tested under varied thermal conditions. Compound **6** was shown to be an active SO₂ donor at physiological pH and 37 °C with a release rate constant k of 0.0140 min⁻¹, while the other two compounds were found to be unreactive under similar conditions. Moreover, calculations predicted conversion of 1-phenyl-benzosultine (**3**) to form 1-phenyl-benzosulfone (**5**) as a more stable form (Scheme 2). This prediction was confirmed by experiments. When compound **6** was incubated in MeCN solution at 37 °C, it was fully converted to 1-phenyl-benzosulfone (**7**), presumably through a retro-Diels-Alder reaction followed by *in situ* cheletropic addition of SO₂. Based on this result, the authors further developed UV-light sensitive SO₂ donors based on the sulfone structure, which is discussed in the next section. The utility of compound **6** as a SO₂ prodrug was demonstrated using a DNA cleavage assay. Compound **6** showed the same potency as mixed sulfite salts in cleaving plasmid

DNA. 1-Aryl-benzosultines with varied substitution groups were prepared to further explore the tunability of the reaction rate. These compounds showed release half-lives ranging from 10 to 68 min at pH 7.4 in 30–40% MeCN/PBS mixture at 37 °C. According to Hammett plot of rate constants, the substitution groups were found to have a weak electronic effect on the reaction rate that electron-donating group would accelerate the reaction. However, none of these compounds showed complete release of SO₂, with maximal SO₂ yield ranging from 59% to 89%. This incomplete conversion was thought to be caused by decomposition of sultine through uncharacterized process(es).

Ab initio calculation:



Thermally activated prodrugs:



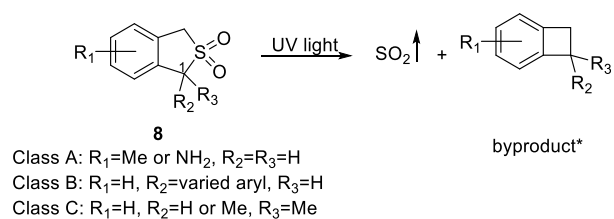
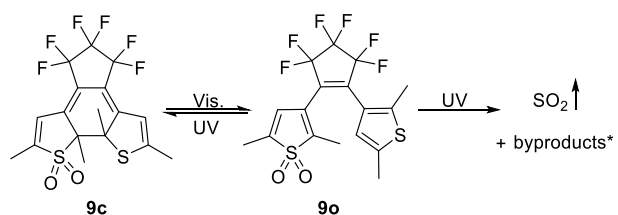
Scheme 1-2 Thermally activated retro-Diels-Alder reaction-based SO₂ prodrugs.

1.1.4.3 Photochemically activated SO₂ prodrugs

1-Phenyl-benzosulfone (**7**) was found to be a more stable form of 1-phenyl-benzosultine (**6**).⁷⁰ To develop UV light-triggered SO₂ prodrugs, Chakrapani's group further exploited the stability of benzosulfones.⁷¹ Three classes of benzosulfone were designed with varied substitution groups on the 1-position and the aryl ring (**8**, Scheme 1-3). A total of 17 compounds were synthesized and subjected to UV irradiation in pH 7.4 buffered solution (30–40% MeCN or

EtOH in PBS). All tested compounds successfully released SO₂ within 10 min with yields ranging from 12% to 90%. Fifteen compounds gave yields of more than 93% after 60 min. Structure-activity analysis showed that electron-donating groups on the aryl ring and substitutions on 1-position both have promoting effect on SO₂ release, possibly through stabilizing the radical intermediates. No biological applications of these prodrugs have been reported so far.

Sumaru and Uchida's group later reported another UV light triggered SO₂ donor based on an dithienylethene structure and demonstrated its application in inducing cell death "on demand" (Scheme 1-3).⁷² Close-ring compound **9c** was found to be stable upon heating up to 70 °C. While upon visible light ($\lambda > 480$ nm) or UV light ($300 \text{ nm} < \lambda < 365$ nm) irradiation, **9c** undergoes cycloreversion reaction to form open-ring isomer **9o**. Further irradiation by UV light ($300 \text{ nm} < \lambda < 365$ nm) of **9o** would lead to both SO₂ gas formation and cyclization reaction to form **9c**. Therefore, SO₂ gas can be stored in the form of **9c** as a thermally stable reagent and be released upon UV irradiation. Compounds **9c** and **9o** were then coated on substrates as thin layers and tested for cell death-inducing effect. NIH/3T3 and MDCK cells were disseminated on the thin layers and light at 365 or 436 nm was used in a striped pattern. It was found that 365 nm light would induce cell damage and detachment from the thin layers of both **9c** and **9o** in the patterned area, demonstrating an on-demand feature of killing cells.

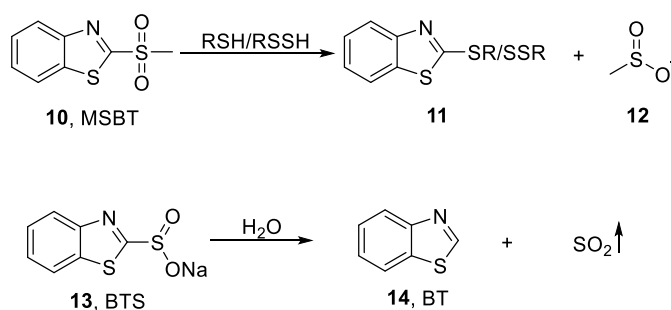
Benzosulfone-based prodrugs:*Diarylethene-based prodrugs:**Scheme 1-3 UV-triggered SO₂ prodrugs.*

* *Byproducts not fully characterized in original literature*

1.1.4.4 Hydrolysis-based SO₂ prodrugs

Xian's group later reported sodium benzothiazole sulfinate (**13**, BTS, Scheme 1-4) as a water-soluble prodrug features slow-release of SO₂.⁷³ The inspiration came from their previous finding that methyl sulfonyl benzothiazole (**10**, MSBT) selectively blocks protein thiols through electrophilic substitution on the C2 position of benzothiazole (**14**, BT), and produce methyl sulfinic acid (**12**) as a byproduct (Scheme 1-4).⁷⁴ Therefore, replacing the methyl sulfone group with a sulfonate group would allow BTS to undergo self-elimination and to release SO₂ and benzothiazole upon hydrolysis. This idea was well supported by experimental results. BTS was obtained as crystalline solid through basic hydrolysis of benzothiazole methyl sulfinic ester. As a salt, it has solubility as high as 100 mM in water. Production of SO₂ through decomposition of BTS and formation of BT was monitored by HPLC. The release of SO₂ was shown to be second-order that the rate depends on both pH (proton concentration) and concentration of BTS itself. At pH 7.4 and 37 °C, 0.4 mM BTS would slowly release SO₂ with a half-life of about 13 days. Lower pH would promote SO₂ release that at pH 4, the same concentration of BTS has a half-life

of only 7.5 min. SO₂ release was further confirmed using a reported ratiometric fluorescent probe (Mito-Ratio-SO₂).⁷⁵ This prodrug was then applied in a vasorelaxation experiment using rat aorta rings. 250 μM to 4 mM of BTS was applied to aorta rings and demonstrated dose-dependent relaxation effect. When compared with SO₂ gas, the same concentration of BTS (2 mM) showed weaker but longer-lasting vasorelaxant effect, while SO₂ gas has a stronger but shorter effect. Such results are consistent with the slow releasing property of BTS compared with SO₂ gas.



Scheme 1-4 Hydrolysis-based SO₂ prodrug.

1.1.5 Expected Results

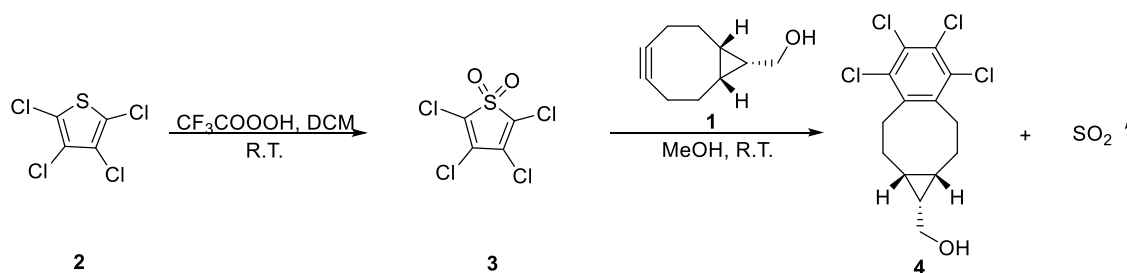
Despite the remarkable progress in making SO₂ donors and the associated beautiful chemistry, there are still unresolved issues including the reliance on other sulfur species for SO₂ release, the need for two components in the bimolecular reaction-based prodrugs, and the delicate and sometimes difficult balance between stability and rapid release of SO₂ from unimolecular systems without the use of a trigger. Our group has a long-standing interest in studying gasotransmitters.⁷⁶⁻⁸¹ Herein we aim to provide strategies that allows the release of SO₂ in a controllable fashion.

1.2 Click reaction-based SO₂ prodrugs

Previously, we have demonstrated the feasibility of using an extrusion reaction as a way to deliver carbon monoxide.⁷⁷ Herein we describe a strategy to cage SO₂ in thiophene dioxide and use a strained alkyne to trigger the release of SO₂ in a controllable fashion (Scheme 1-5). By varying the substituents on the thiophene dioxide scaffold, the release rates can also be tuned.

1.2.1 Results and discussion

As early as 1976, Stille already examined the reaction of thiophene dioxide and a terminal alkyne under reflux condition in toluene. Though conditions were “harsh”, the cheletropic reaction yielded a cyclized product with the release of SO₂.⁸² We planned to take advantage of this reaction to construct caged SO₂ for release under near physiological conditions (room temperature to 37 °C, pH 7.4, and aqueous solution). A key issue in this project was how to lower the reaction temperature to ambient temperature for applications under near physiological conditions. 2,3,4,5-Tetrachlorothiophene dioxide has been shown to possess high reactivity in cycloaddition reactions with a variety of olefines. Specifically, it was shown to react steadily with ethylene and to give a cyclohexyldiene product and SO₂ at 28 °C.⁸³ We reasoned that a strained alkyne with increased HOMO energy would promote this cycloaddition reaction. The formation of a stable phenyl ring should also help to drive the subsequent cheletropic reaction with the concomitant release of SO₂. Therefore, we synthesized 2,3,4,5-tetrachlorothiophene dioxide **3** from commercially available perchlorothiophene **2**. Then we first examined the reaction of **3** (20 mM in MeOH) with *endo*-BCN (**1**, 4 equiv.) at room temperature as a proof-of-concept test. Indeed, after 5 min, we saw complete conversion of **3** into a new product, which was spectroscopically characterized as **4** (Scheme 1-5).



Scheme 1-5 Proof-of-concept test of SO₂ donor system

We then examined the reaction kinetics. The UV absorption of the product is significantly lower than that of the reactants at 328 nm. Therefore, we used UV absorbance decrease to monitor the reaction progress. The second order rate constant was determined by first using a large excess of **1** to examine the pseudo-first order reaction followed by plotting the pseudo-first order reaction rate constants against different **1** concentration. The second order rate constant was determined to be $1.50 \text{ M}^{-1} \text{ s}^{-1}$ in MeOH at room temperature, allowing the reaction to be finished in about 3 hours at mid- μM levels (Figure 1-8).

To further confirm the formation of SO₂, we performed the DTNB test, which has been applied in SO₂ measurement in atmosphere and food samples.⁸⁴⁻⁸⁶ DTNB would react with SO₃²⁻ ion to give an reduced product, which can be quantitatively measured by UV absorbance at 412 nm (Figure 1-3).⁸⁴ To allow hydration of SO₂, we performed this test in 5% DMSO/PBS. A reaction mixture was incubated at room temperature or 37 °C for 45 min (about 1 $t_{1/2}$) and then the DTNB probe was added. Afterwards, the test solution was incubated at room temperature for another 15 min and subjected to UV absorbance reading at 412 nm. The experimental group showed higher absorbance at both room temperature and 37 °C than the negative control groups, confirming the formation of SO₃²⁻. Both experimental groups and positive control groups showed lower SO₃²⁻ formation at 37 °C than at room temperature, presumably due to increased SO₂ escape at higher temperature (Figure 1-4).

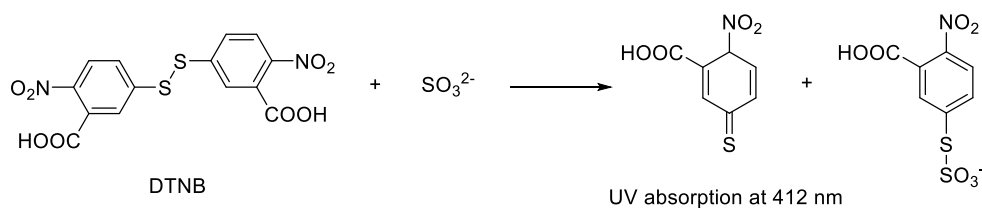


Figure 1-3 DTNB test mechanism

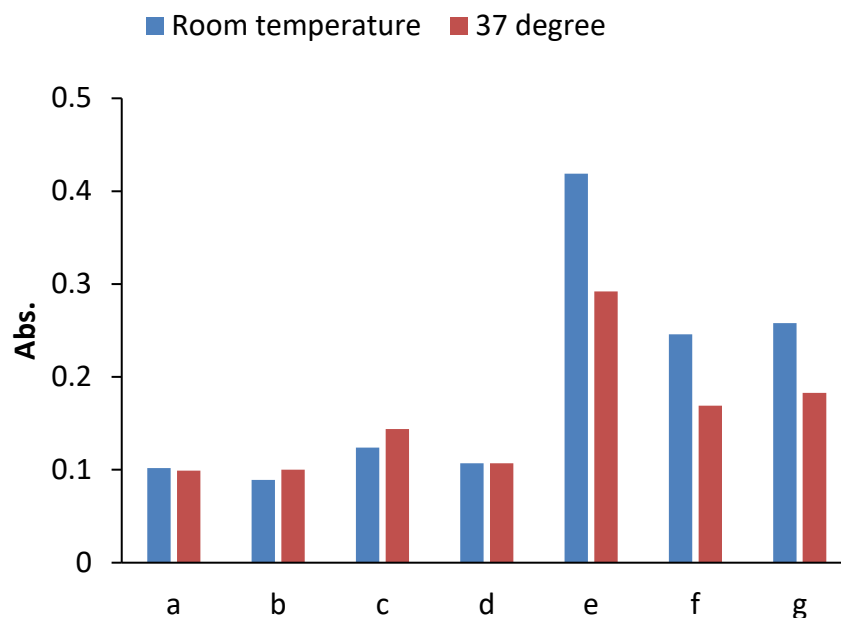


Figure 1-4 UV absorption at 412 nm of DTNB test

After 45 min incubation at room temperature or 37 °C (a) blank (5% DMSO/PBS), (b) 250 μM of **3** only, (c) 2.5 mM of **1** only, (d) 250 μM of **4** only, (e) 250 μM of **3** + 2.5 mM of **1**, (f) 50 μM of Na_2SO_3 , (g) 50 μM of NaHSO_3 .

Encouraged by the initial success, we went on to synthesize additional analogues to see whether we can tune the reaction rates for various applications. Thus, we synthesized compounds **5** and **6** with electron withdrawing groups at different positions (Figure 1-5). We reasoned that by varying the electron density on the thiophene ring, different LUMO energy will result in varied reaction rate with BCN. We also tested reaction with a trans-cyclooctene compound (**8**, equatorial isomer), which is known to have high strain energy and high HOMO, to see if the

reaction rate can be further enhanced. In all these reactions at room temperature, we successfully isolated the cheletropic reaction products. Interestingly, we had initial difficulties in analysing the room temperature NMR spectra of the products containing the bicyclo(6.1.0)non-4-ene structure. This was due to line broadening caused peak overlap in ^1H NMR. Structure elucidation by ^{13}C NMR is equally difficult because of missing peak(s) at high field. Given HRMS confirmation, we reasoned that this phenomenon is caused by the slow flipping of eight-member ring between the “chair” and “boat” conformations. We successfully observed two conformations by tracking the $-\text{CH}_2$ group next to the $-\text{OH}$ group at low temperature (270 K). As temperature increases, the exchange rate of the two populations increases, and the two peaks observed for the $-\text{CH}_2$ group coalesced and then averaged to give a sharp peak. Unfortunately, within the temperature range tested, the exchange rate is not fast enough to average the $-\text{CH}_2$ and $-\text{CH}$ groups from the bicyclo(6.1.0)non-4-ene structure, which become broad above 278 K and hard to track (Figure 1-7). However, this phenomenon has been observed exclusively with *endo*-product. As for product obtained from reaction between **6** and *exo*-BCN, sharp peaks at high field were observed at room temperature. By contrast, with chlorine substitutions, we are able to track the carbons at room temperature because of their fast flipping rate. Edited HSQC experiment gave clear evidence of geminal protons splitting from the eight-membered ring, confirming the structures of cheletropic products. We studied the reaction kinetics for these reactions and obtained k_2 values ranging from 0.02 to $0.33 \text{ M}^{-1}\text{s}^{-1}$ (Table 1; Figure 1-8).

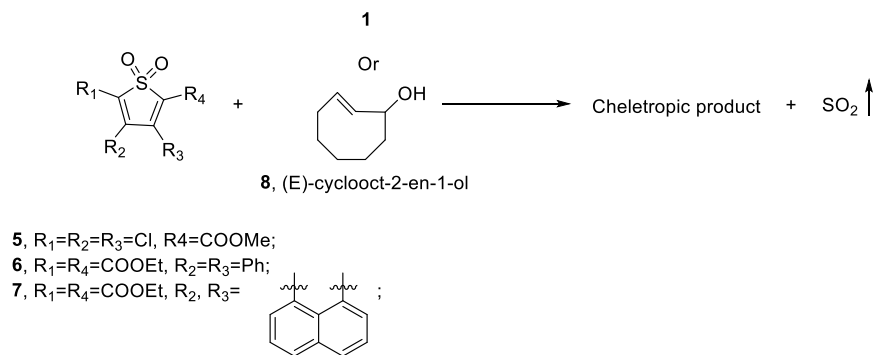


Figure 1-5 SO₂ donor pairs

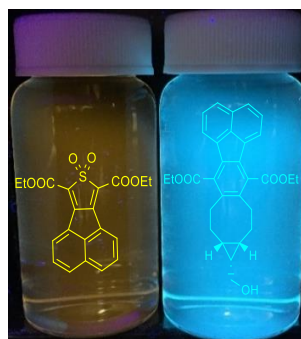
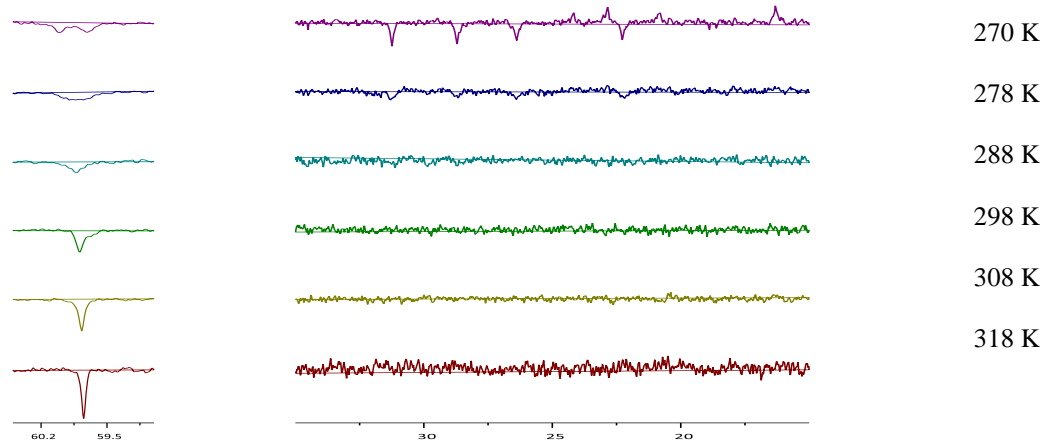


Figure 1-6 Fluorescent SO₂ donor and product after SO₂ release (100 μM in MeOH)

–CH₂OH

–CH₂ and –CH groups

from the bicyclo(6.1.0)non-4-ene structure



*Figure 1-7 Coalescence of cheletropic product (**6** + **1**) observed in ¹³C NMR (DEPT-135) with increasing temperature*

Currently, several elegant fluorescent probes for SO₂ have been developed based on the nucleophilicity of SO₃²⁻/HSO₃⁻. However, few of them are suitable for real-time monitoring of SO₂ generation due to delayed response.⁸⁷ One alternative strategy for real time monitoring of SO₂ release is to devise such SO₂ prodrugs that would become fluorescent after SO₂ release. Therefore, we were interested in designing SO₂ prodrugs that would lead to the formation of a fluorescent reporter, which allows for real-time monitoring of SO₂ release. We reasoned that attaching an aromatic substituent to the thiophene ring would allow formation of an expanded conjugation system after the cheletropic reaction and thus result in pronounced changes in the spectroscopic behavior of the aromatic system after the reaction. Therefore, we synthesized thiophene dioxide with naphthalene conjugated at the 3,4 positions (**7**, Figure 1-5). The compound itself has weak yellow fluorescence with an excitation wavelength of 299 nm, emission wavelength of 556 nm, and a quantum yield of 0.006. After reaction with BCN and SO₂ release, the resulting product shows strong cyan fluorescence with an emission wavelength of 470 nm, excitation wavelength of 296 nm, and quantum yield of 0.138 (Figure 1-6). We also established the kinetics profile of this reaction by monitoring the fluorescence increase at 470 nm. A k₂ of 0.01 M⁻¹s⁻¹ was obtained (Table 1-1; Figure 1-6; Figure 1-9).

Table 1-1 Kinetics study of SO₂ donor pairs

SO ₂ donor pairs	3 + 1	3 + 8	5 + 1	6 + 1	7 + 1	6 +<i>exo</i>-BCN
k ₂ (M ⁻¹ s ⁻¹)	1.50 ^a	0.02 ^a	0.33 ^b	0.05 ^a	0.01 ^c	0.04 ^a

Note: a. Measured in MeOH under room temperature. b. Measured in ACN under room temperature. c. Measured in DMSO/PBS 4:1 at 37 °C.

In summary, we have developed a SO₂ donor system, which releases SO₂ through a Diels-Alder reaction with a strained alkyne/alkene as a trigger. We explored the initial tunability of the releasing rate by varying the electron density of thiophene dioxide ring. With a small set of

compounds, we were able to tune the reaction rate in the range of $0.01\text{--}1.50\text{ M}^{-1}\text{s}^{-1}$, giving a 150-fold variation in reactivity. This work has been published in *Chem. Commun.*, **2017**, 53, 1370–1373.

1.2.2 Experimental procedures

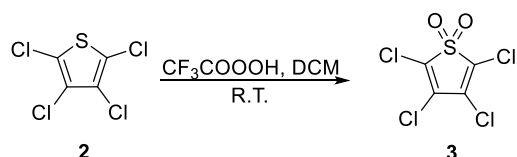
1.2.2.1 Materials and Methods

All reagents and chemicals were purchased from commercial suppliers as reagent grade or higher, and were used without further purification unless otherwise noted. NMR spectra were recorded on a Bruker Avance NMR spectrometer at 400 MHz for ^1H and 101 MHz for ^{13}C at room temperature unless otherwise specified. Solvent peaks were served as internal standard. Mass spectral analyses were performed by the GSU Mass Spectrometry Facilities. UV-Vis absorption spectra were recorded on a Shimadzu PharmaSpec UV-1700 UV-Visible spectrophotometer. Fluorescence spectra were recorded on a Shimadzu RF- 5301PC fluorimeter.

1.2.2.2 Synthesis of thiophene dioxides

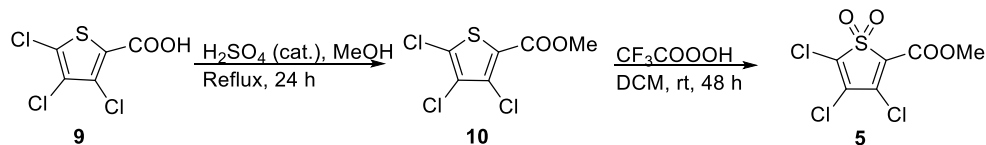
General method for the oxidation of thiophenes:

Thiophene S-dioxides were synthesized following a literature procedure using peroxytrifluoroacetic acid as the oxidant.⁸⁸



Tetrachlorothiophene-1,1-dioxide (3)

Tetrachlorothiophene-1,1-dioxide was synthesized following the general procedure of thiophene oxidation. Off-white solid was obtained. Yield: 85% ^{13}C NMR (CDCl_3): δ 131.2, 127.4 ppm. IR: 1598 cm^{-1} , 1337 cm^{-1} , 1166 cm^{-1} .

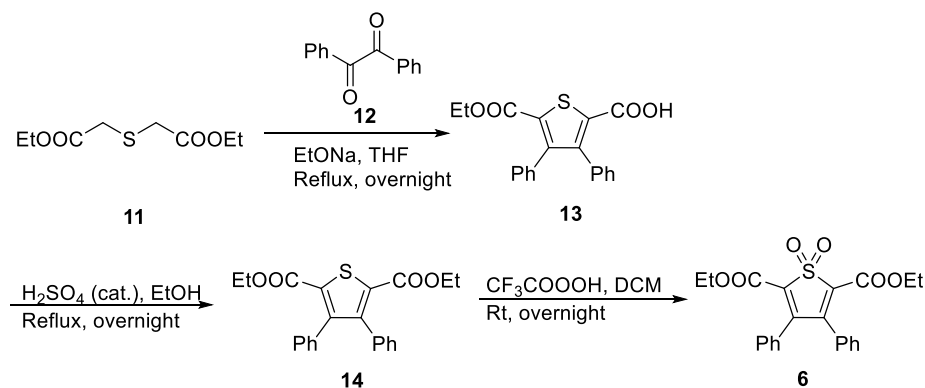


Methyl 3,4,5-trichlorothiophene-2-carboxylate (10)

500 mg 3,4,5-trichlorothiophene-2-carboxylic acid (**9**, 2.16 mmol) was dissolved in 10 mL MeOH. 1 mL concentrated H₂SO₄ was added dropwise with stirring. The reaction mixture was stirred under reflux for 1 day. Then the reaction mixture was cooled down to room temperature and stirred for another 2 days. White precipitate was filtered off. Filter cake was kept. The filtrate was dried over vacuum, washed with sat. NaHCO₃ solution, and extracted with EtOAc. The organic phase was dried over Na₂SO₄ followed by solvent evaporation with rotavap. Solid was combined with filter cake and recrystallized in MeOH. 400 mg beige needle crystals were obtained. Yield: 75%. ¹H NMR (CDCl₃): δ 3.91 (s, 3H) ppm. HRMS (ESI): calcd for C₆H₄Cl₃O₂S [M+H]⁺ 244.8992, found 244.9002.

Methyl 3,4,5-trichlorothiophene-2-carboxylate 1,1-dioxide (5)

Methyl 3,4,5-trichlorothiophene-2-carboxylate 1,1-dioxide was synthesized following the general procedure of thiophene oxidation from methyl 3,4,5-trichlorothiophene-2-carboxylate (**10**). Pale yellow cylinder crystals were obtained. Yield: 60%. ¹H NMR (CDCl₃): δ 3.99 (s, 3H) ppm. ¹³C NMR (CDCl₃): δ 156.3, 145.0, 133.0, 130.7, 127.8, 53.7 ppm. IR : 1727, 1564, 1437, 1335, 1244, 1196, 1172 cm⁻¹. HRMS (ESI): calcd for C₆H₃Cl₂O₄S [M-Cl]⁺ 240.9124, found 240.9134.



5-(Ethoxycarbonyl)-3,4-diphenylthiophene-2-carboxylic acid (13)

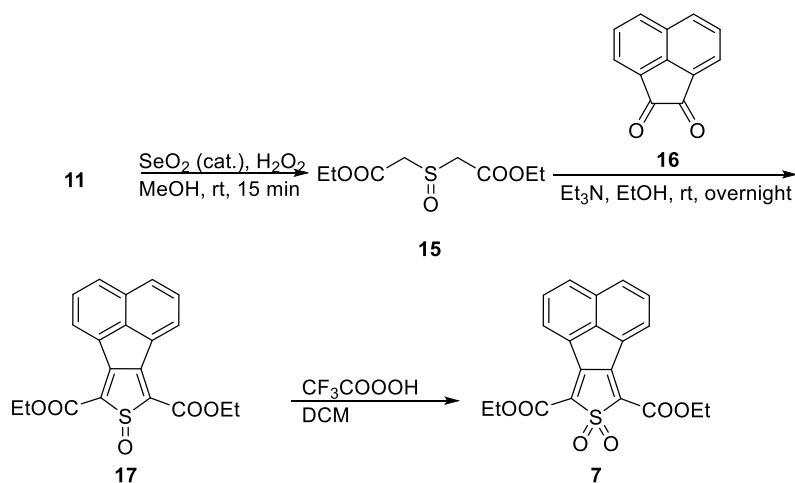
1500 mg diethyl 2,2'-thiodiacetate (**11**, 7.26 mmol) and 1270 mg benzil (**12**, 6.05 mmol) were dissolved in 30 mL dry THF. 850 mg EtONa (12.50 mmol) was then added. The reaction mixture was refluxed overnight under argon protection. Then the reaction was quenched by pouring onto ice followed by washing with EtOAc. The aqueous phase was acidified using 1N HCl. The solid was filtered off and kept. The filtrate was extracted with EtOAc. The organic phase was dried over Na₂SO₄. Solvent was removed by vacuum. The remaining solid was combined with filter cake and directly used for the next step as crude (1.42 g). Crude yield: 67%.

Diethyl 3,4-diphenylthiophene-2,5-dicarboxylate (14)

1.42 g crude 5-(ethoxycarbonyl)-3,4-diphenylthiophene-2-carboxylic acid (**13**) was dissolved in 50 mL EtOH. 2 mL concentrated H₂SO₄ was added. The reaction mixture was refluxed with stirring for 2 days and then cooled to room temperature. Solid was filtered out and kept. The solution was then dried under vacuum. To the residue was added with sat. NaHCO₃ solution. The resulting solution was extracted with EtOAc. Organic phase was dried over Na₂SO₄ followed by solvent evaporation under vacuum. Solid was combined with the filter cake and recrystallized in EtOH to give 576 mg product. Combined yield of two steps: 25%. ¹H NMR (CDCl₃): δ 7.23 – 7.11 (m, 6H), 7.02 (dd, *J* = 6.5, 3.1 Hz, 4H), 4.20 (q, *J* = 7.1 Hz, 4H), 1.18 (t, *J* = 7.1 Hz, 6H) ppm.

Diethyl 3,4-diphenylthiophene-2,5-dicarboxylate 1,1-dioxide (6)

Diethyl 3,4-diphenylthiophene-2,5-dicarboxylate 1,1-dioxide was synthesized following the general procedure of thiophene oxidation from diethyl 3,4-diphenylthiophene-2,5-dicarboxylate (**14**). Product was obtained as yellow solid. Yield: 65%. $^1\text{H NMR}$ (CDCl_3): δ 7.32 (t, $J = 7.5$ Hz, 2H), 7.22 (t, $J = 7.6$ Hz, 4H), 6.93 (d, $J = 7.3$ Hz, 4H), 4.30 (q, $J = 7.1$ Hz, 4H), 1.26 (t, $J = 7.1$ Hz, 6H) ppm. $^{13}\text{C NMR}$ (CDCl_3): δ 157.7, 150.1, 130.0, 129.9, 129.5, 128.9, 127.8, 62.5, 13.8 ppm. IR: 3061, 1725, 1583, 1311, 1241, 1194 cm^{-1} . HRMS (ESI): calcd for $\text{C}_{22}\text{H}_{21}\text{O}_6\text{S}$ $[\text{M}+\text{H}]^+$ 413.1053, found 413.1045.



Diethyl 2,2'-sulfinyldiacetate (15)

1 g diethyl 2,2'-thiodiacetate (**11**, 4.84 mmol) and 30 mg SeO_2 (0.27 mmol) were dissolved in 10 mL MeOH and added with 1.22 mL H_2O_2 (~27% w/w in water, ~10 mmol) slowly. The reaction mixture was stirred under room temperature for 15 min. Then the reaction mixture was concentrated over a rotavap. The residue was dissolved in water (10 mL) and extracted with DCM (20 mL \times 3). The organic phase was combined. Removal of solvent yielded 1.05 g crude oil, which was used directly in the next step. Crude yield: 98%. $^1\text{H NMR}$ (CDCl_3): δ

4.25 (q, $J = 7.2$ Hz, 4H), 4.05 (d, $J = 14.3$ Hz, 2H), 3.83 (d, $J = 14.3$ Hz, 2H), 1.30 (t, $J = 7.1$ Hz, 6H) ppm.

Diethyl acenaphtho(1,2-c)thiophene-7,9-dicarboxylate 8-oxide (17)

373 mg acenaphthylene-1,2-dione (**16**, 2.05 mmol) and 500 mg diethyl 2,2'-sulfinyldiacetate (**15**, 2.25 mmol) were dissolved in 2.5 mL ethanol. 456 mg trimethylamine (4.51 mmol) was added slowly to the reaction mixture. Then the reaction mixture was stirred at room temperature overnight. Then the precipitates were filtered out and recrystallized using DCM/hexane. 400 mg yellow crystals were obtained. Yield: 53%. ^1H NMR (CDCl_3): δ 8.75 (d, $J = 7.2$ Hz, 2H), 8.05 (d, $J = 8.2$ Hz, 2H), 7.76 (t, $J = 7.7$ Hz, 2H), 4.54 (m, 4H), 1.50 (t, $J = 7.1$ Hz, 6H) ppm. ^{13}C NMR (CDCl_3): δ 161.3, 151.2, 147.1, 133.2, 131.1, 130.4, 129.0, 128.6, 128.4, 62.6, 14.5 ppm.

Diethyl acenaphtho(1,2-c)thiophene-7,9-dicarboxylate 8,8-dioxide (7)

Diethyl acenaphtho(1,2-c)thiophene-7,9-dicarboxylate 8,8-dioxide was synthesized following the general procedure of thiophene oxidation. 100 mg diethyl acenaphtho(1,2-c)thiophene-7,9-dicarboxylate 8-oxide (**17**, 0.27 mmol) was dissolved in 2 mL DCM and added with 1 mL freshly prepared peroxytrifluoroacetic acid. The reaction mixture was stirred at room temperature for 1 day. Then the reaction mixture was dried under vacuum and redissolved in DCM. The drying process was repeated several times till the residue is free of acid. Recrystallization from EtOAc/DCM yielded orange solid 46 mg. Yield: 45%. ^1H NMR (CDCl_3): δ 8.90 (d, $J = 7.3$ Hz, 2H), 8.11 (d, $J = 8.2$ Hz, 2H), 7.86-7.77 (m, 2H), 4.55 (q, $J = 7.1$ Hz, 4H), 1.51 (t, $J = 7.1$ Hz, 6H) ppm. ^{13}C NMR (CDCl_3): δ 158.9, 147.8, 145.2, 131.0, 130.9, 129.1, 129.1, 128.0, 124.3, 62.7, 14.2 ppm. IR: 1707, 1654, 1581, 1318, 1259, 1231, 1196 cm^{-1} . HRMS (ESI): calcd for $\text{C}_{20}\text{H}_{17}\text{O}_6\text{S}$ $[\text{M}+\text{H}]^+$ 385.0740, found 385.0729.

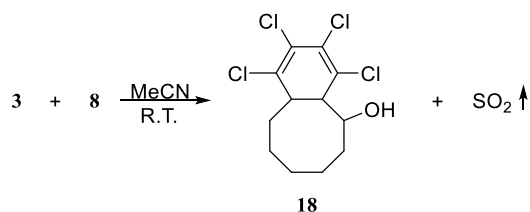
General procedure of the reaction between thiophene dioxides and strained alkyne/alkene

Thiophene dioxide was dissolved in a small amount of MeCN or MeOH to give a final concentration of around 50~100 mM. 1~1.5 equiv. of strained alkyne (or *trans*-alkene) was then added to the solution. TLC was used to monitor the procession of the reaction. After completion, the reaction mixture was directly dried on a rotavap and purified by column chromatography to yield the product after SO₂ release.

((1*s*,1*aR*,9*aS*)-4,5,6,7-tetrachloro-1*a*,2,3,8,9,9*a*-hexahydro-1*H*-benzo(*a*)cyclopropano(*e*)(8)annulen-1-yl)methanol (**4**)

Product obtained as white solid. Yield: 53%. ¹H NMR (600 MHz, DMSO-*d*₆): δ 4.35 (br, 1H), 3.52 (br, 2H), 3.26 (br, 2H), 3.00 (br, 2H), 2.18 (br, 2H), 1.78 (br, 2H), 0.82 (br, 1H), 0.32 (br, 2H) ppm. ¹³C NMR (CDCl₃): δ 140.6, 132.4, 130.5, 59.7, 29.9, 21.1, 16.3 ppm.

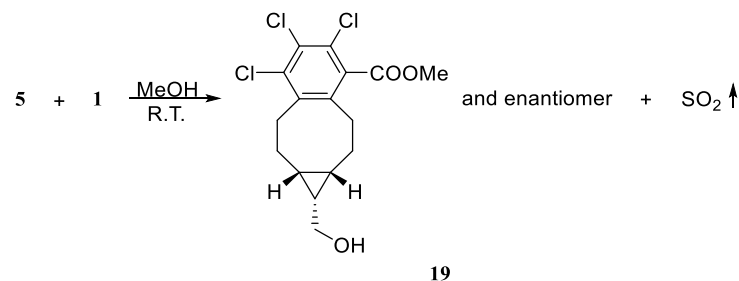
To allow HRMS characterization, compound **4** was acetylated by reacting with acetic anhydride (3 equiv.) and triethylamine (3 equiv.) in DCM in the presence of DMAP (0.1 equiv.) at room temperature overnight. Reaction mixture was dried over vacuum and purified by column chromatography (eluent: EtOAc/Hex 1:2). HRMS of acetyl derivative (ESI): calcd for C₁₆H₁₆O₂Cl₄Na [M+Na]⁺ 402.9797, found 402.9814.



1,2,3,4-Tetrachloro-4*a*,5,6,7,8,9,10,10*a*-octahydrobenzo(8)annulen-5-ol (**18**)

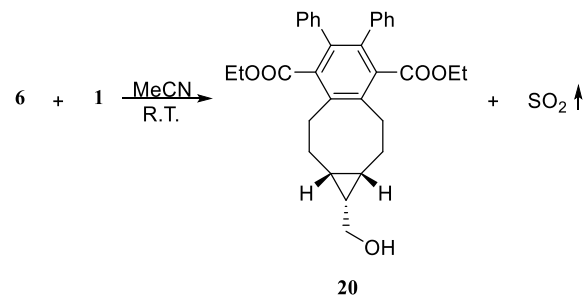
Product obtained as white solid. Yield: 77%. ¹H NMR (CDCl₃): δ 4.29 – 4.15 (m, 1H), 2.94 – 2.78 (m, 1H), 2.73 – 2.63 (m, 1H), 2.15 (d, *J* = 2.9 Hz, 1H), 2.09 – 1.73 (m, 6H), 1.73 – 1.58 (m, 2H), 1.53 – 1.42 (m, 1H), 1.16 – 1.00 (m, 1H) ppm. ¹³C NMR (CDCl₃): δ 133.6, 129.3,

125.2, 122.7, 74.3, 47.2, 43.0, 36.6, 30.6, 27.9, 26.2, 23.3 ppm. HRMS (ESI): calcd for $C_{12}H_{14}Cl_4NaO$ $[M+Na]^+$ 336.9691, found 336.9681.



Methyl (1*S*,1*aS*,9*aR*)-5,6,7-trichloro-1-(hydroxymethyl)-1*a*,2,3,8,9,9*a*-hexahydro-1*H*-benzo(*a*) cyclopropa(*e*)(8)annulene-4-carboxylate and enantiomer (19)

Product obtained as white solid. Yield: 61%. 1H NMR ($CDCl_3$): δ 3.98 (s, 3H), 3.75 (br, 2H), 3.28 (br, 1H), 2.96 (br, 2H), 2.80-2.65 (m, 1H), 2.50-2.35 (m, 1H), 2.24 (br, 1H), 1.75 (br, 1H), 1.38-1.00 (br, 3H), 0.95-0.44 (br, 2H). ^{13}C NMR ($CDCl_3$): δ 167.5, 140.8, 138.8, 134.7, 129.9, 127.5, 59.7, 53.0 30.5, 28.8, 22.3, 21.0, 20.4, 16.9, 15.7. HRMS (ESI): calcd for $C_{16}H_{17}O_3NaCl_3$ $[M+Na]^+$ 385.0141, found 385.0128.

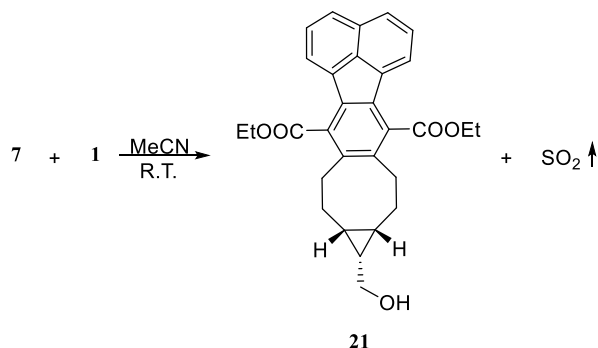


Diethyl (1*s*,1*aR*,9*aS*)-1-(hydroxymethyl)-5,6-diphenyl-1*a*,2,3,8,9,9*a*-hexahydro-1*H*-benzo(*a*) cyclopropa(*e*)(8)annulene-4,7-dicarboxylate (20)

Product obtained as yellowish solid. Yield: 46%. 1H NMR ($CDCl_3$): δ 7.16 – 7.05 (m, 6H), 7.02 (br, 4H), 3.94 (q, $J = 7.1$ Hz, 4H), 3.75 (br, 2H), 2.98 (br, 2H), 2.90 – 2.74 (m, 2H), 2.31 (br, 2H), 1.87 – 1.64 (br, 1H), 1.55 – 1.29 (br, 2H), 1.21 – 0.98 (br, 3H), 0.89 (t, $J = 7.1$ Hz,

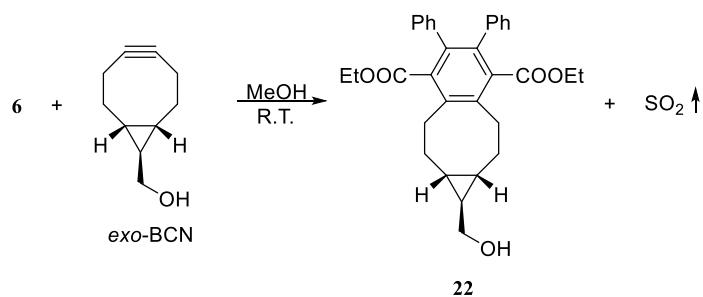
6H) ppm. ^{13}C NMR (CDCl_3): δ 169.6, 138.3, 136.5, 130.4, 127.2, 126.8, 61.0, 59.8, 13.7 ppm.

HRMS (ESI): calcd for $\text{C}_{32}\text{H}_{35}\text{O}_5$ $[\text{M}+\text{H}]^+$ 499.2479, found: 499.2479.



Diethyl (9aR,10s,10aS)-10-(hydroxymethyl)-9,9a,10,10a,11,12-hexahydro-8H-cyclopropa(5,6) cycloocta(1,2-k)fluoranthene-7,13-dicarboxylate (21)

Product obtained as yellow solid. Yield: 60%. ^1H NMR (CDCl_3): δ 7.85 (d, $J = 8.2$ Hz, 2H), 7.77 (d, $J = 7.1$ Hz, 2H), 7.65 – 7.55 (m, 2H), 4.60 (q, $J = 7.1$ Hz, 4H), 3.81 – 3.57 (m, 2H), 3.17 – 2.95 (m, 2H), 2.95 – 2.78 (m, 2H), 2.33 (br, 2H), 1.83 – 1.52 (m, 2H), 1.51 – 1.37 (m, 6H), 1.17 – 0.62 (m, 4H) ppm. ^{13}C NMR (CDCl_3): δ 169.8, 134.2, 133.7, 132.7, 129.9, 127.9, 127.4, 121.9, 61.7, 59.8, 14.3 ppm. HRMS (ESI): calcd for $\text{C}_{30}\text{H}_{30}\text{O}_5\text{Na}$ $[\text{M}+\text{Na}]^+$ 493.1991, found: 493.1987.



Diethyl (1r,1aR,9aS)-1-(hydroxymethyl)-5,6-diphenyl-1a,2,3,8,9,9a-hexahydro-1H-benzo(a) cyclopropa(e)(8)annulene-4,7-dicarboxylate (22)

Product obtained as yellowish solid. Yield: 58%. ^1H NMR (CDCl_3) δ 7.08 (s, 6H), 7.01 (s, 4H), 4.07 – 3.78 (m, 4H), 3.44 (d, $J = 6.7$ Hz, 2H), 3.03 – 2.88 (m, 2H), 2.88 – 2.68 (m, 2H),

2.62 – 2.38 (br, 2H), 1.49 – 1.31 (br, 3H), 0.89 (t, $J = 7.1$ Hz, 6H), 0.85 – 0.72 (br, 2H) ppm. ^{13}C NMR (CDCl_3) δ 169.6, 138.5, 138.3, 136.4, 136.3, 130.4, 130.2, 127.2, 126.8, 66.5, 61.0, 30.4, 29.7, 29.5, 21.6, 13.7 ppm. HRMS (ESI): calcd for $\text{C}_{32}\text{H}_{35}\text{O}_5$ $[\text{M}+\text{H}]^+$ 499.2479, found: 499.2462.

1.2.2.3 Confirmation of SO_2 release by the DTNB test

3 was prepared as 500 μM stock solution in 5% DMSO/PBS. **1** was prepared as 5 mM stock solution in 5% DMSO/PBS. DTNB was prepared as 1.5 mM stock solution in 10% EtOH/PBS stock solution. NaHSO_3 and Na_2SO_3 as positive controls were prepared as 500 μM stock solution in 5% DMSO/PBS, respectively.

Room temperature incubation: Each group (2 mL) was prepared in 4 mL glass vial, sealed with Parafilm[®] M, and incubated at room temperature (21 °C) for 45 min. 2 mL DTNB stock solution was then added to each group. The solutions were allowed to stand at room temperature for another 15 min. Then the solution was filtered through 0.45 μm micron filters and its UV-vis absorption measured at 412 nm in a quartz cuvette.

37 °C incubation: Each group (2 mL) was prepared in 4 mL glass vial, added with 0.3 mL silicon fluid (to minimize SO_2 escape), and sealed with Parafilm[®] M. Then all the groups were incubated in a 37 °C water bath for 45 min. Then the solutions were taken out and allowed 15 min to cool to room temperature. 2 mL DTNB was then added to each group. The solution was allowed to stand at room temperature for another 15 min. Then the water phase of each solution was taken out by syringe and filtered through 0.45 μm micron filters. The UV-vis absorption of the filtrate was measured at 412 nm in a quartz cuvette.

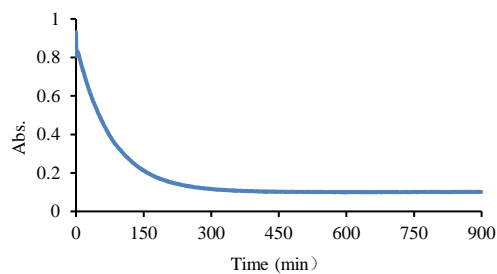
All DTNB tests were in triplicates.

1.2.2.4 Kinetics studies of cycloaddition reactions

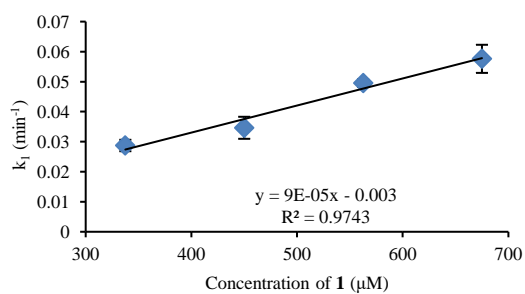
Second order reaction rate constants (k_2) were obtained as slopes of pseudo-first reaction rate constants (k_1) plotted linearly against concentrations of strained alkyne/alkene.

UV-vis kinetic measurements: Separate stock solutions of thiophene dioxide (**3**, **5**, or **6**) and BCN (**1**) or *trans*-cyclooctene (**8**) (concentration 10 ~18 times of respective thiophene dioxide) were prepared in HPLC-grade solvent (MeOH, MeCN) at room temperature. The “click-release” reaction led to significant changes in the UV-vis spectrum of thiophene dioxide. Thiophene dioxide stock solution (200 μL), BCN (or *trans*-alkene) (300, 400, 500, 600 μL), and solvent (300, 200, 100, 0 μL) were added into 10 mm quartz cuvettes, thoroughly mixed and sealed with a PTFE cap and monitored for time-dependent UV-vis absorption changes. All kinetic runs were in triplicates. Curve fitting was operated using the SigmaPlot[®] 10 software (Figure 1-8).

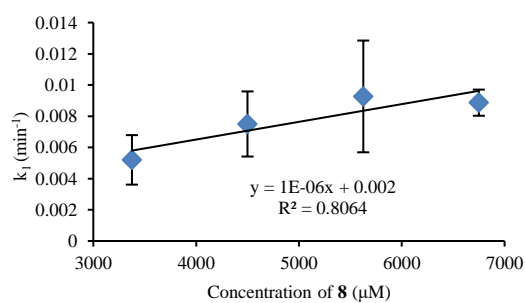
(A)



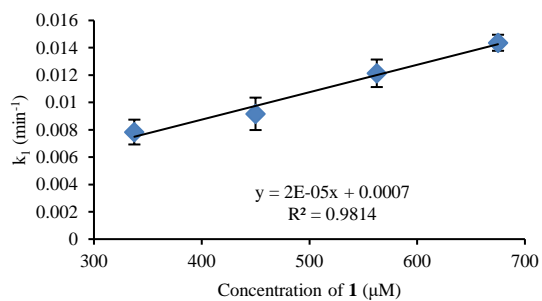
(B) a)



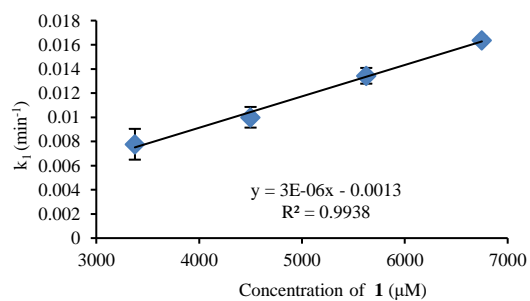
b)



c)



d)



e)

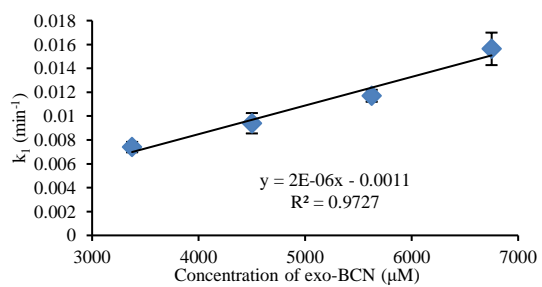


Figure 1-8 Kinetics studies of cycloaddition reactions by UV-vis absorbance change
(A) *Example of pseudo-first reaction monitored by UV absorbance decrease. A typical curve shows reaction between 125 μM **6** and 5.625 mM **1** in MeOH at room temperature. $\lambda = 324 \text{ nm}$.*
(B) *Linear plot of k_1 at different concentrations of **1** or **8**. SO₂ donor pairs and solvents: a) **3** + **1**, MeOH; b) **3** + **8**, MeOH; c) **5** + **1**, MeCN; d) **6** + **1**, MeOH; e) **6** + *exo*-BCN.*

Fluorescence kinetics measurements: Separate solutions of thiophene dioxide (**7**, 500 μM) and **1** (5 mM) were prepared in HPLC-grade solvent (DMSO/PBS 4:1) at room temperature. The “click-release” reaction gives a fluorescent product that can be monitored by fluorimeter. The solutions containing thiophene dioxide (200 μL), BCN (300, 400, 500, 600 μL), and solvent (300, 200, 100, 0 μL) were added into quartz cuvettes, thoroughly mixed and sealed with a PTFE cap, kept at 37 °C in water bath, and tested for fluorescence emission change ($\lambda_{\text{ex}}=350 \text{ nm}$, $\lambda_{\text{em}}=470 \text{ nm}$). All kinetics runs were in triplicates. Curve fitting was done using the SigmaPlot[®] 10 software (Figure 1-9).

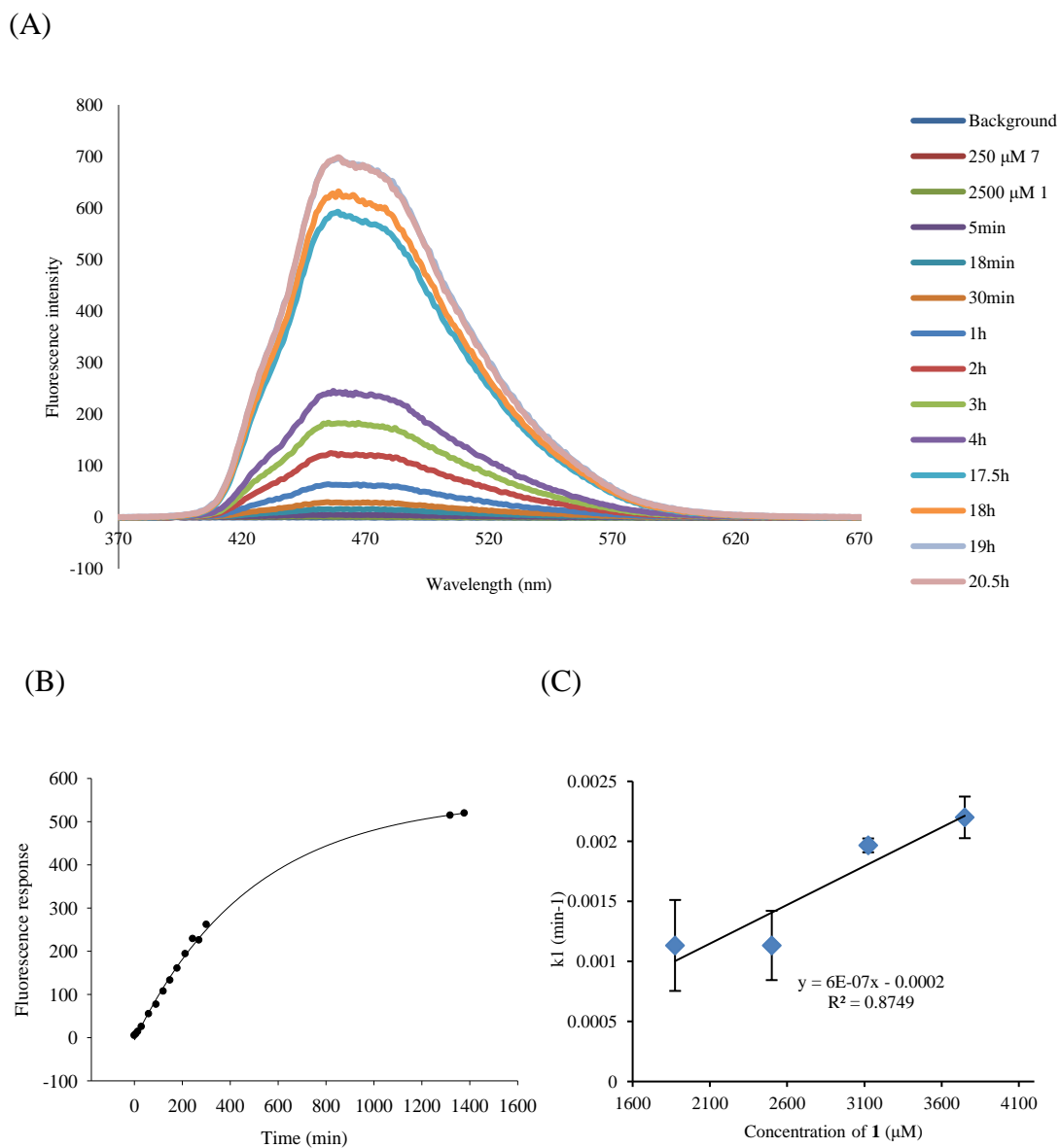


Figure 1-9 Kinetics studies of cycloaddition reaction between **7** and **1** by monitoring fluorescence changes

(A) Time-dependent fluorescence increases. Conditions: $250 \mu\text{M}$ **7** + $2500 \mu\text{M}$ **1** in 4:1 DMSO/PBS at 37°C . (B) Example of pseudo-first reaction monitored by fluorescence increase. Conditions: $125 \mu\text{M}$ **7** + 3.125mM **1** in 4:1 DMSO/PBS at 37°C . $\lambda_{ex}=350 \text{ nm}$, $\lambda_{em}=470 \text{ nm}$; slit width: ex 3 nm, em 1.5 nm. (C) Linear plot of k_1 at different concentrations of **1**.

1.2.2.5 Determination of fluorescence quantum yields

Quinine sulfate (QS) in 0.1M H₂SO₄ water solution was chosen as the standard (ex: 350 nm, em: 400-600 nm). Literature⁸⁹ quantum yield: 0.54. The quantum yields of compound **7** and compound **21** were determined according to the equation:

$$\Phi_X = \Phi_{ST} \left(\frac{Grad_X}{Grad_{ST}} \right) \left(\frac{\eta_X^2}{\eta_{ST}^2} \right)$$

Where Φ is the fluorescence quantum yield, the subscripts ST and X denote standard and test compounds respectively, *Grad* is the gradient from the plot of integrated fluorescence intensity versus UV-vis absorbance, and η is the refractive index of the solvent (1.3330 for water, 1.3284 for methanol). Excitation wavelength were chosen as UV-vis absorbance < 0.1 to avoid reabsorption effect.

Quantum yield determination of **7**:

Solutions of compound **7** at 0, 2, 4, 6, 8, 10 μ M in methanol were prepared at room temperature. Each solution was tested for absorbance at 345 nm and fluorescence emission at 380-680 nm under 345 nm excitation (slit width: ex: 5, em: 3; fluorescence cuvette: 10 mm). Fluorescence responses were integrated in the same range to obtain AUC readings. Then AUC readings were plotted against absorbance readings to obtain *Grad_X* as the slope of linear regression equation. *Grad_{ST}* of QS were determined in the same manner using 0, 0, 1, 1, 2, 2 μ M solutions instead (Figure 1-10). Calculated quantum yield for **7** was 0.006.

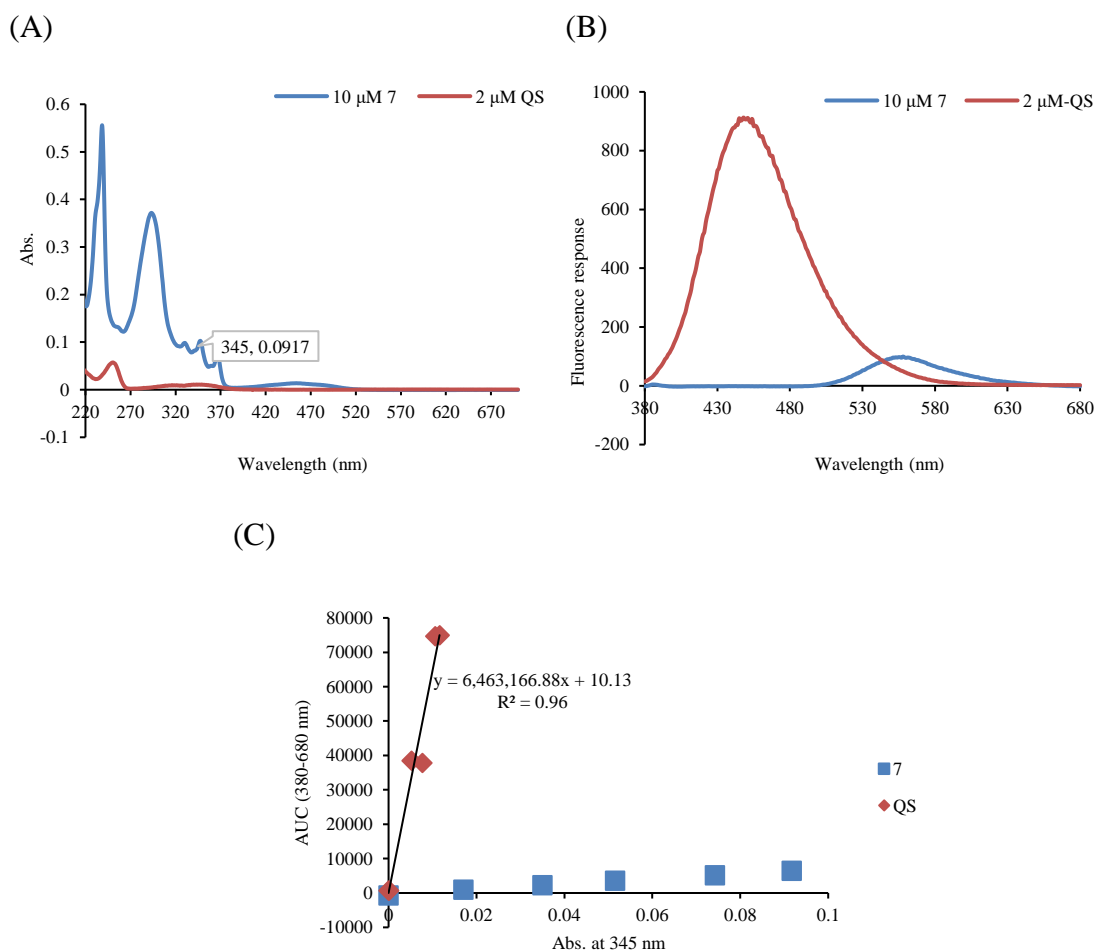


Figure 1-10 Quantum yield determination of **7** using QS as the reference (A) UV-vis absorbance spectrum. (B) Fluorescence response spectrum (λ_{ex} : 345 nm; slit width: ex: 5 nm, em: 3 nm; fluorescence cuvette: 10 mm). (C) Plot of AUC versus UV-vis absorbance (integration range: 380 nm to 680 nm).

Quantum yield determination of **21**:

Solutions of compound **21** at 0, 2, 4, 6, 8, 10, 12 μ M in methanol were prepared at room temperature. Each solution was tested for absorbance at 364 nm and fluorescence emission at 380-620 nm under 364 nm excitation (slit width: ex: 3 nm, em: 1.5 nm; fluorescence cuvette: 10 mm). Fluorescence responses were integrated at the same range to obtain AUC readings. Then AUC readings were plotted against absorbance readings to get $Grad_X$ as the slope of linear

regression equation. $Grad_{ST}$ of QS were determined in the same manner using 0, 5, 10, 15, 20, 25 μM solution instead (Figure 1-11). Calculated quantum yield for **21** is 0.138.

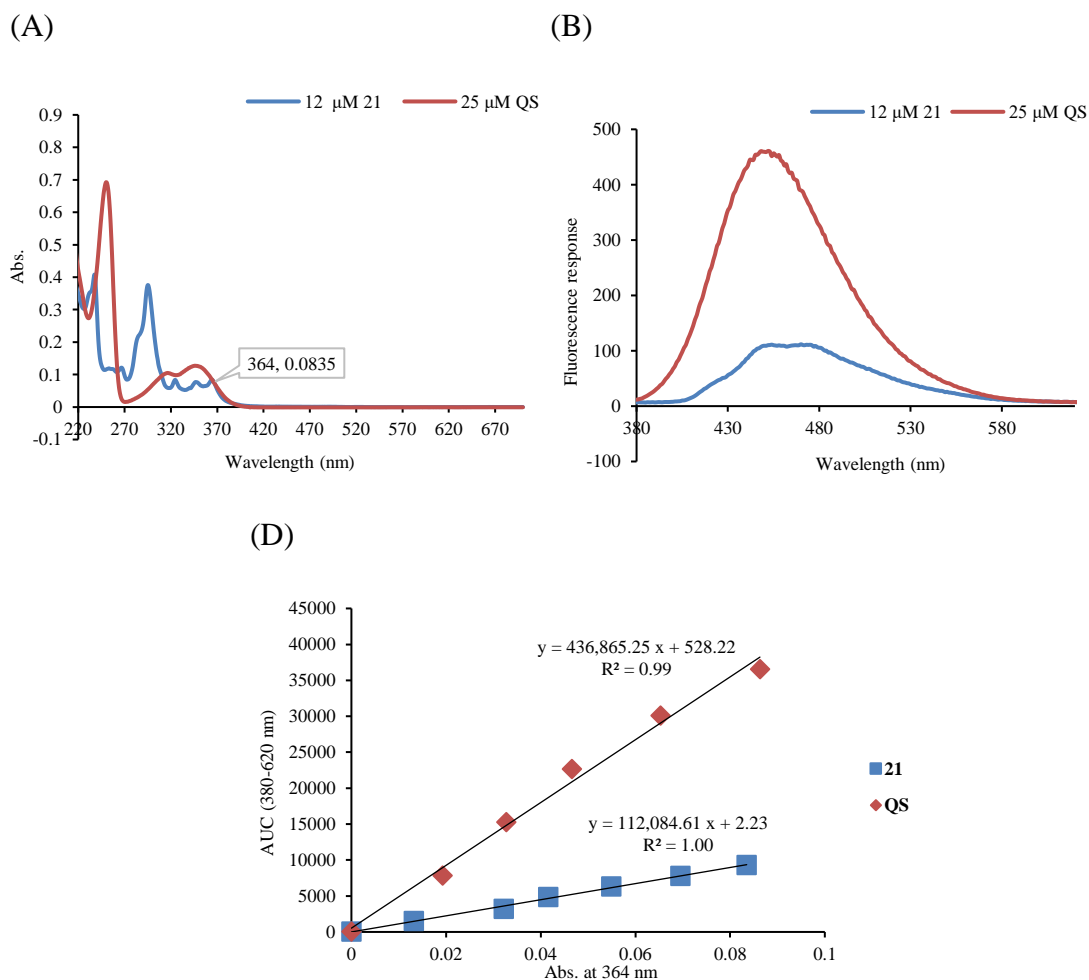


Figure 1-11 Quantum yield determination of **21** using QS as the reference (A) UV-vis absorbance spectrum. (B) Fluorescence response spectrum (λ_{ex} : 364 nm; slit width: ex: 3 nm, em: 1.5 nm; fluorescence cuvette: 10 mm). (C) Plot of AUC versus UV-vis absorbance (integration range: 380 nm to 620 nm).

1.3 Esterase-sensitive SO_2 prodrugs

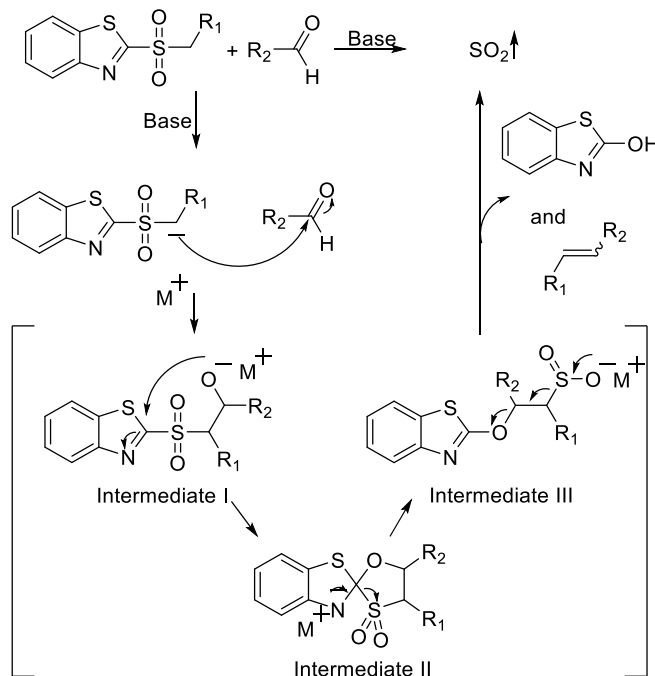
Despite the remarkable progress in making SO_2 donors and the associated beautiful chemistry, there are still unresolved issues including the reliance on other sulfur species for SO_2 release, the need for two components in the bimolecular reaction-based prodrugs, and the

delicate and sometimes difficult balance between stability and rapid release of SO₂ from unimolecular systems without the use of a trigger. Herein, we describe a series of esterase-sensitive SO₂ prodrugs. Such SO₂ prodrugs would release SO₂ under physiological conditions with a bio-compatible triggering mechanism. We envision that prodrugs with an enzyme-sensitive release mechanism would simulate the endogenous SO₂ generating process and offer unique advantages as research tools. We understand that it is unlikely that a single triggering mechanism, such as the esterase-sensitive triggering mechanism, would meet the demand of all research needs. We further envision that the general method used can be a platform approach that allows for the incorporation of other triggering mechanisms to provide research tools applicable in different situations.

1.3.1 Results and discussion

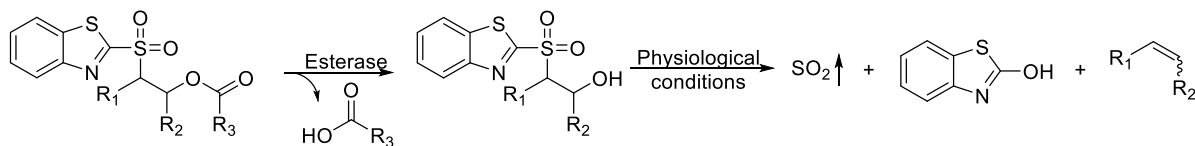
In our search for the chemistry needed for developing esterase-sensitive SO₂ prodrugs, we found SO₂ is formed as a byproduct in modified Julia olefination (also known as one-pot Julia olefination). Modified Julia olefination as well as Julia reaction have been widely applied in organic synthesis for fragment connection (Scheme 1-6).⁹⁰⁻⁹⁵ Briefly, benzothiazole sulfone is first deprotonated by a base. The carbanion formed then can undergo an aldol condensation-type of reaction leading to an alkoxide intermediate (**I**). Intramolecular addition-elimination followed by extrusion of SO₂ and 2-hydroxybenzothiazole (2-OHBT) gives the final product with a double bond. As to the reaction itself, strongly basic condition is required in the first step to generate the carbanion as nucleophile. This need for strongly basic conditions present an obstacle in the development of prodrugs that can release SO₂ under physiological conditions. However, if we could “trap” the β-alkoxysulfone intermediate (**I**) as the donor molecule, the subsequent

intramolecular reaction should readily occur under physiological conditions. As a result, we designed the esterase-sensitive prodrug system described in Scheme 1-7.



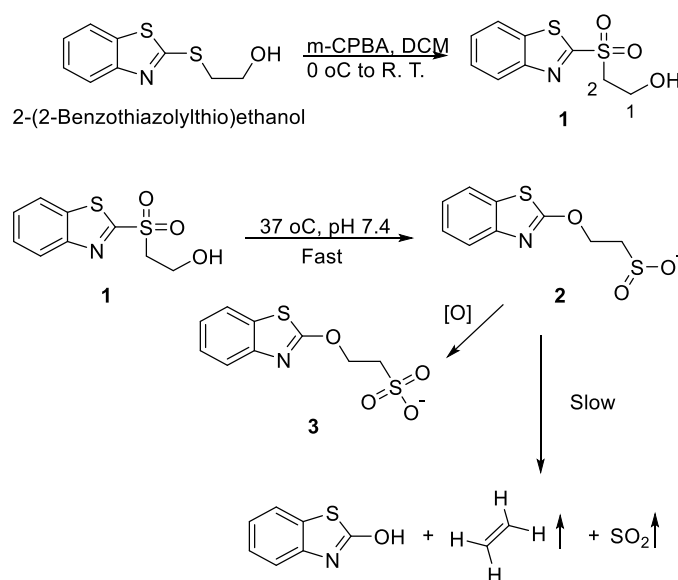
Scheme 1-6 Modified Julia olefination

As a first step, we were interested in studying the SO_2 release chemistry from compound **1** and its analogues. Thus compound **1** was synthesized from commercially available 2-(2-benzothiazolylthio)ethanol in one step (Scheme 1-8). It should be noted that besides benzothiazole (BT), various heterocycles have been applied in modified Julia olefination.⁹¹ We reasoned that BT holds certain advantage for the easy accessibility of 2-substituted BT derivatives and its strong UV absorption for easy detection.



Scheme 1-7 Design of SO_2 prodrug

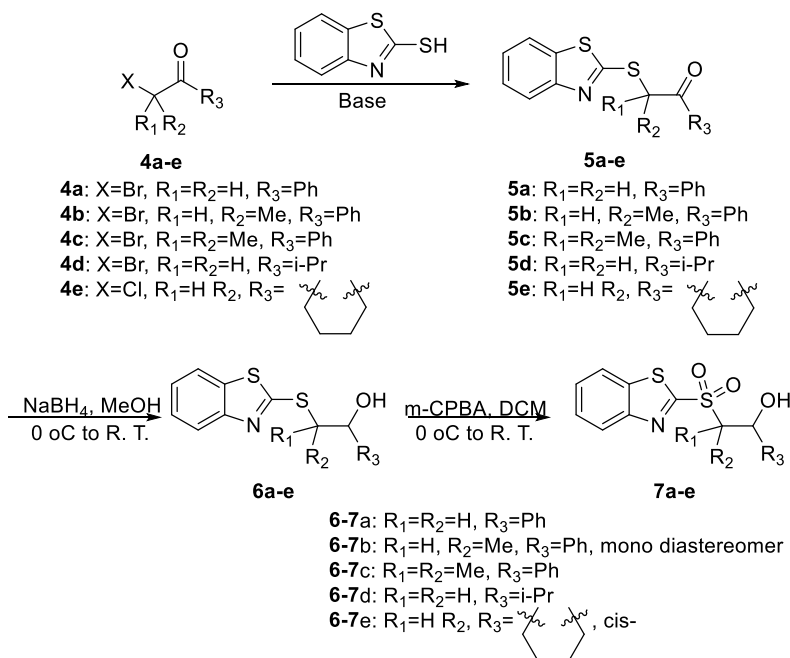
To gain an initial understanding of the SO₂ release tendency, we incubated compound **1** (200 μM) in 10% DMSO/PBS (pH 7.4) at 37 °C and monitored the reaction with HPLC. Over a period of 4 days, only a small amount of 2-OHBT was formed, and yet compound **1** was fully consumed (Scheme 1-8, data not shown). Mass spectral analysis of the reaction mixture suggest the formation of 2-(benzo(d)thiazol-2-yloxy)ethane-1-sulfonic acid (**3**). This was likely formed through oxidation of corresponding sulfinic acid (**2**), and indicates successful “cyclization” to the 2-position of BT. Possible issues that hinder the elimination step might include the lack of stabilization of the transition state.⁹⁶



*Scheme 1-8 Synthesis and proposed reaction route of compound **1** under physiological conditions*

According to computational studies by Robiette and Pospíšil, introduction of substituents on the linker portion (1,2-positions) can offer electronic stabilization to the transition state of the elimination step.⁹⁶ It is also well known that introduction of substituents can significantly affect the outcome of cyclization reactions.⁹⁷⁻⁹⁸ Thus, there is a need to study analogues with various substitution patterns on the linker portion to facilitate the steps leading to SO₂ production. We

synthesized a set of compounds (compound **7a-e**) with different substituents at the 1- and 2-positions (Scheme 1-9). These β -alkoxysulfones were readily prepared through a 3-step synthesis route by first condensing 2-thiolbenzothiazole with α -bromoketone (or α -chloroketone) under basic conditions. The resulting β -ketosulfides were then reduced with NaBH_4 to give the respective β -alkoxysulfides. The final product was obtained by S-oxidation using 2.5~3 equivalents of m-CPBA. The final compounds were incubated in PBS (with 1~10% DMSO to solubilize) at 37 °C. Formation of 2-OHBT was monitored with HPLC as an indication of reaction progress. Compounds **7a-d** successfully yielded 2-OHBT peaks, whereas compound **7e** with the sulfone group locked in a *cis*- configuration with the hydroxyl group failed to release 2-OHBT, suggesting the need for an antiperiplanary relationship for the final elimination step, as expected (Figure 1-19).²⁴



Scheme 1-9 Synthesis of sulfone compounds with different substitution groups

Studies of reaction kinetics of **7a-d** were conducted at 50 μM in 10% DMSO/PBS at 37 °C. The overall reaction was treated as single first-order reaction. k_{obs} was calculated

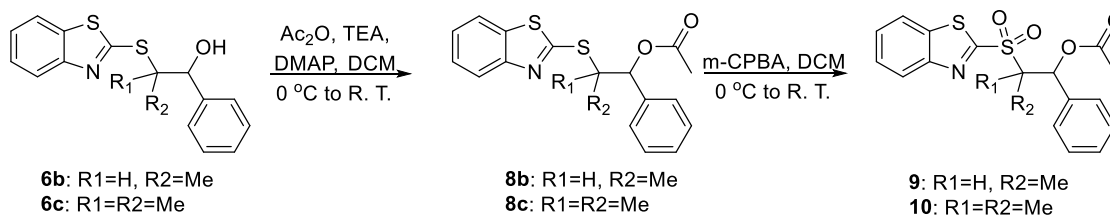
accordingly. The resulting half-life ($t_{1/2}$) of 7a-d ranges from 1.7 to 86.6 min (Table 1-2; Figure 1-18).

Table 1-2 SO₂ release rate monitored by HPLC

Compound	7a	7b	7c	7d
k_{obs}^a (min ⁻¹)	0.014±0.001	0.397±0.081	0.168±0.028	0.008±0.000
$t_{1/2}$ (min)	49.5	1.7	4.1	86.6

Note: a. Measured at 37 °C with 50 μM compound in 10% DMSO/PBS in triplicates; Curve fitted as first-order reaction.

To further confirm the release of SO₂, the DTNB test was performed using a modified method that has been previously reported (Figure 1-17).⁸⁶ The positive responses from such tests confirmed SO₂ formation.



Scheme 1-10 Synthesis of compound 9 and 10

In designing an esterase-sensitive prodrug approach, we masked the hydroxy group as an ester. The ester group should be labile to hydrolysis by esterases in the blood and in cell. A hydrophobic ester group can also increase the membrane permeability of the prodrug. Therefore, compound **9** (**BW-SO₂-201**) was prepared from **6b** (Scheme 1-10). We first tested the stability of compound **9** in PBS (with 1% DMSO at 37 °C) by HPLC. It was surprising to find that **9** was not stable, leading to slow decomposition with elimination of the ester group and neighboring hydrogen without 2-OHBT formation (Figure 1-20). Such results can be explained by the good leaving ability of the newly attached ester group. We reasoned that we should be able to avoid this self-elimination problem by replacing the susceptible hydrogen with a methyl group. We

therefore synthesized compound **10** (**BW-SO₂-202**) following the same synthetic route from **6c** (Scheme 1-10). Compound **10** did not show degradation within the time range (3~4 h) examined (Figure 1-21). When incubated with porcine liver esterase (PLE, 5 unit/mL) in 10% DMSO/PBS at 37 °C, 2-OHBT formation was readily observed, affirming the validity of our design. The observed half-life ($t_{1/2\text{obs}}$, ~1 h) is much slower than **7c**, indicating the esterase cleavage step is the rate-limiting step in the releasing process (Figure 1-13).

From previous work in our group, it has been shown that esterase-catalyzed hydrolysis is tunable by varying the acyl moiety.⁸¹ Therefore, we designed and synthesized compounds **11-13** (**BW-SO₂-203-205**) with different acyl groups in order to tune the SO₂ release rate. Indeed, significant differences in release rates were observed (Figure 1-13). Compounds **11** and **13** exhibited the fastest release rates, with $t_{1/2\text{obs}}$ being ~10 min and ~9 min respectively. Compound **12** with a bulky *t*-butyl group exhibited the slowest release rate with only ~10% release after 2 hours. Compound **10** falls somewhere in between that showed ~70% release within 2 hours. The kinetics were also monitored using a literature reported bisulfite probe **14** (Figure 1-16; Figure 1-23).⁹⁹ Results are consistent with that of HPLC studies that compound **10-13** demonstrated significantly different release rates. Compound **13** with an α -dimethyl amino group is expected to possess much higher water solubility compared with compounds **10-12**. Thus, we hope this compound will be especially useful as a prodrug for future work. We have further tested the stability and esterase-triggered release kinetics of **13** in 1% DMSO/PBS solution at 37 °C using HPLC. The results show that the ester group slowly hydrolyzed with $t_{1/2}$ of about 24 h in the absence of PLE. With 1 unit/mL PLE, the release was complete within 90 min (Figures 1-13, 1-14). Therefore, the esterase-triggered release is the dominant pathway for SO₂ release.

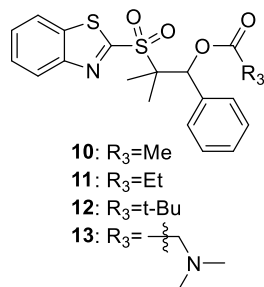


Figure 1-12 Structures of compounds 10-13

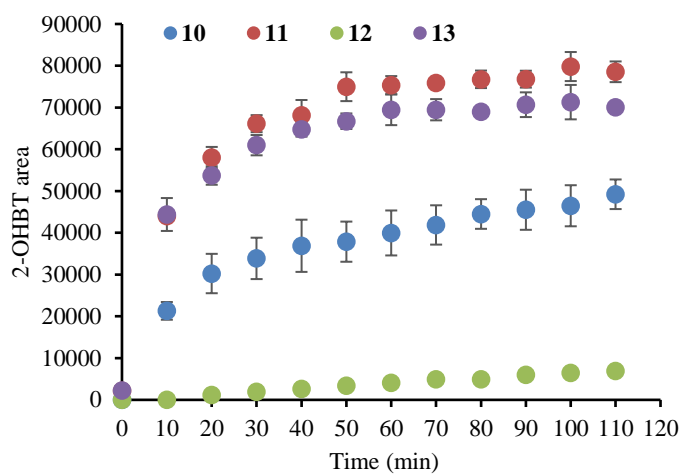


Figure 1-13 Kinetics of esterase triggered release monitored by HPLC
 Condition: 50 μM compound in 10% DMSO/PBS at 37 $^{\circ}\text{C}$ with 5 unit/mL PLE, n=3.

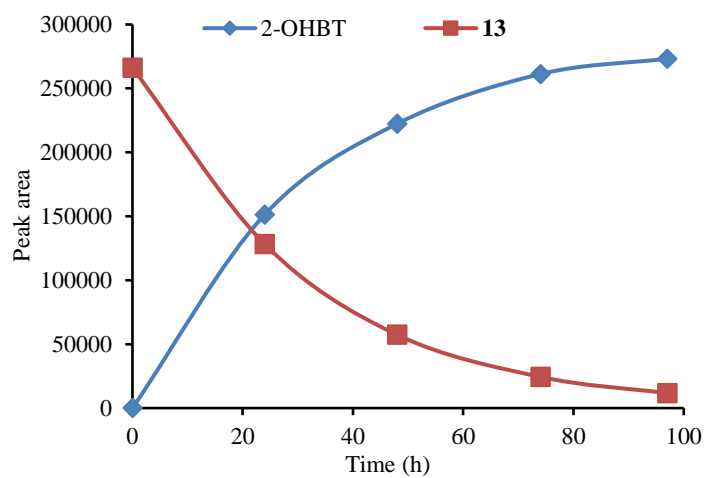
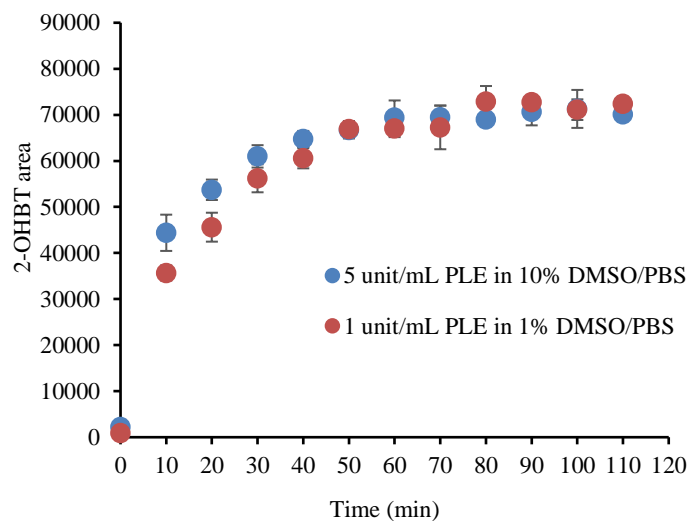


Figure 1-14 Stability of compound 13 in 1% DMSO/PBS



*Figure 1-15 Esterase triggered release of compound **13** under different conditions*

With these esterase-sensitive SO₂ prodrugs in hand, we further tested whether they can be applied in biological systems. Using the fast-releasing prodrug **13** as a representative, we used probe **14** for cell imaging studies. Briefly, HeLa cells were incubated with 100 μM prodrug at 37 °C for 2 h. Then the cells were washed with PBS and incubated with 10 μM of probe **14** for another 0.5 h (Figure 1-16). The experimental group showed strong fluorescence inside the cells while the negative control groups showed no fluorescence or very weak fluorescence. It is worth noting that NaHSO₃ gives much weaker fluorescence than **13** even at 400 μM. Such results

indicate that prodrug **13** has much better capacity to deliver SO₂ into the cell than the widely used NaHSO₃ as a SO₂ donor.

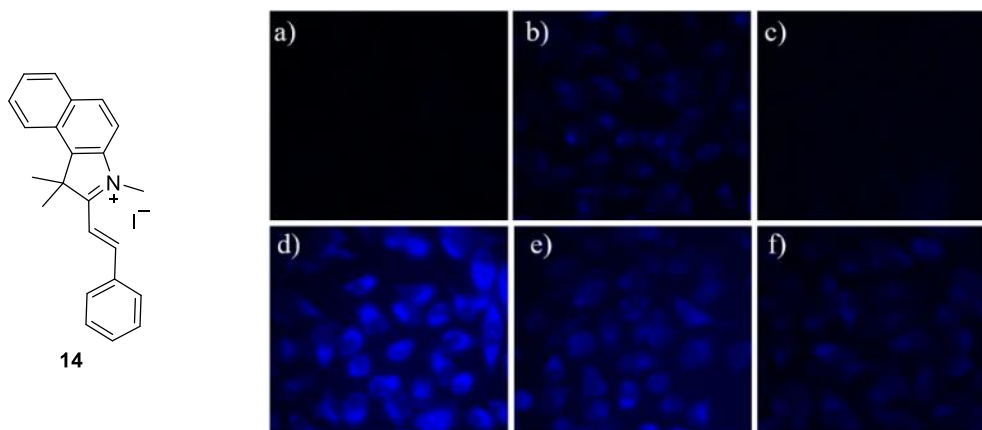


*Figure 1-16 Cell imaging study of SO₂ release from **13** in HeLa cells*

*a) cell only; b) **14** only (10 μM); c) **13** only (100 μM); d) **13** (100 μM) + **14** (10 μM); e) NaHSO₃ (400 μM) + **14** (10 μM); f) product (2-OHBT and 2-methyl-1-phenyl-propene, 100 μM each) + **14** (10 μM)*

In summary, a series of SO₂ prodrugs inspired by modified Julia olefination was designed and synthesized. The release kinetics were determined by HPLC through monitoring the formation of 2-OHBT, a byproduct generated simultaneously with SO₂. Through manipulating the substitution patterns, the release rate has been tuned with $t_{1/2}$ ranging from ~ 2 min to ~1.5 h. More importantly, by attaching an acyl group at the free hydroxyl group of compound **7c**, esterase-sensitive SO₂ prodrugs were prepared. Tunable release rate was also achieved using different esterase-sensitive acyl groups. Prodrug **13** exhibited the fastest release and was selected for cell imaging studies. It exhibited high efficiency in releasing SO₂ in biological environment. Other triggering mechanisms are equally possible with proper modification to serve different research purposes. Most SO₂ donors and prodrugs in this paper were obtained in the solid form, and they remain stable under normal storage condition for several months (-20 °C, data not

shown). We feel that these SO₂ prodrugs will be very useful tools in elucidating SO₂ biology.

This work has been published in *Chem. Commun.*, **2017**, 53, 10124-10127.

1.3.2 Experimental procedures

1.3.2.1 Materials and Methods

All chemicals, reagents, and solvents were purchased from commercial suppliers as reagent grade and were used without further purification. NMR spectra were recorded on a Bruker Avance NMR spectrometer at 400 MHz for ¹H spectra and 101 MHz for ¹³C spectra at room temperature. Solvent peaks were used as internal standards. Mass spectral analyses were performed by the GSU Mass Spectrometry Facilities. HPLC analyses were performed on a Shimadzu HPLC equipped with UV detector. Column: Shimadzu C18 3μm 4.6×50 mm column.

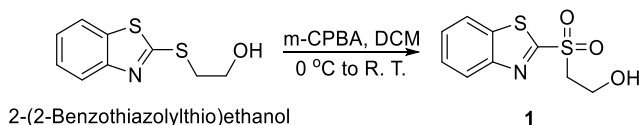
1.3.2.2 Synthesis

General procedure of the oxidation of sulfide to sulfone:

Sulfone compounds were synthesized following similar procedure with necessary adjustments using 3-chloroperoxybenzoic acid (m-CPBA) as the oxidant.

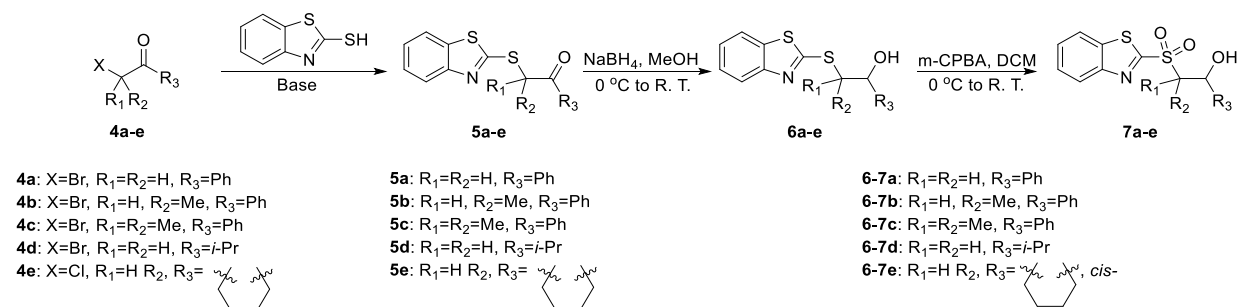
Generally, 1 equiv. of sulfide was dissolved in dichloromethane (DCM) at a concentration of ~0.5 mmol/10 mL. The resulting solution was treated with 2.5~3 equiv. of m-CPBA in small portions under stirring at room temperature (ice bath can be applied for large scale reaction). Reaction process was monitored by thin layer chromatography (TLC). Usual reaction time is between 1~4 hours. When reaction finished, the reaction was quenched with an equal volume of sat. NaHCO₃ aqueous solution. For small scale reactions, dilution with DCM was used to facilitate separation and washing. The aqueous phase was separated with separatory funnel and back-extracted with fresh DCM twice. Combined organic phase was washed with brine and dried over Na₂SO₄. Solvent was then removed under reduced pressure. Column chromatography was

used for purification. Further washing with sat. NaHCO₃ solution was used to remove residual m-CPBA/m-CBA.



2-(Benzo(d)thiazol-2-ylsulfonyl)ethan-1-ol (1)

Synthesis followed the general procedure of oxidation of sulfide to sulfone. Product was obtained as white solid. Yield: 77%. ¹H NMR (CDCl₃) δ 8.21 (d, *J* = 7.9 Hz, 1H), 8.04 (d, *J* = 7.9 Hz, 1H), 7.72 – 7.56 (m, 2H), 4.21 (s, 2H), 3.81 – 3.73 (m, 2H), 2.97 (s, 1H) ppm. ¹³C NMR (CDCl₃) δ 166.2, 152.4, 136.6, 128.3, 127.9, 125.42, 122.4, 57.7, 56.5 ppm. IR: ν_{max}/cm⁻¹ 3388 (O-H), 2929 (C-H), 1322 (S=O), 1301 (C-O), 1128 (S=O). HRMS (ESI): calcd. for C₉H₁₀NO₃S₂⁺ [M+H]⁺ 244.0097, found 244.0089.



2-(Benzo(d)thiazol-2-ylthio)-1-phenylethan-1-one (5a)

2-Mercaptobenzothiazole (1.0 g, 6.0 mmol) and 2-bromoacetophenone (1.2 g, 6.0 mmol) were dissolved in 50 mL acetone and treated with K₂CO₃ (0.83 g, 6.0 mmol). The reaction mixture was heated at reflux temperature for 0.5 h and then cooled down to room temperature. Solvent was evaporated under reduced pressure. The residue was re-dissolved in ethyl acetate (EA, ~50 mL) and washed with brine (~50 mL). Organic phase was then dried over Na₂SO₄, and concentrated *in vacuo*. Residue was recrystallized in ethanol to yield 1.4 g of product as yellow

needle crystals. Yield: 82%. ^1H NMR (CDCl_3) δ 8.13 – 8.05 (m, 2H), 7.81 (dd, $J = 8.1, 0.4$ Hz, 1H), 7.75 (dd, $J = 8.0, 0.6$ Hz, 1H), 7.68 – 7.58 (m, 1H), 7.56 – 7.47 (m, 2H), 7.43 – 7.37 (m, 1H), 7.33 – 7.27 (m, 1H), 4.98 (s, 2H) ppm. ^{13}C NMR (CDCl_3) δ 193.0, 165.2, 152.9, 135.6, 133.9, 128.8, 128.6, 126.1, 124.4, 121.5, 121.1, 41.0 ppm. HRMS (ESI): calcd. for $\text{C}_{15}\text{H}_{11}\text{NOS}_2\text{Na}^+$ $[\text{M}+\text{Na}]^+$ 308.0174, found 308.0189.

2-(Benzo(d)thiazol-2-ylthio)-1-phenylpropan-1-one (5b)

To a solution of 2-mercaptobenzothiazole (334 mg, 2 mmol) in 4 mL DCM was added triethylamine (TEA, 0.39 mL, 2.8 mmol). The 2-bromopropiophenone (0.30 mL, 2 mmol) was added dropwise. The reaction mixture was stirred at room temperature for 1 h and then dried under vacuum. The residue was re-dissolved in 10 mL EA and washed with water (10 mL \times 2). Water phase was back extracted with 15 mL EA. Combined organic phase was dried over Na_2SO_4 , concentrated in vacuo, and purified by column chromatography (EA/Hex 1:20 to 1:10). Product (470 mg) was obtained as yellow oil. Yield: 78%. ^1H NMR (CDCl_3) δ 8.11 (dt, $J = 8.5, 1.7$ Hz, 2H), 7.83 (dd, $J = 8.1, 0.4$ Hz, 1H), 7.75 (dd, $J = 8.0, 0.6$ Hz, 1H), 7.64 – 7.54 (m, 1H), 7.53 – 7.45 (m, 2H), 7.42 (ddd, $J = 8.3, 7.4, 1.2$ Hz, 1H), 7.35 – 7.27 (m, 1H), 5.88 (q, $J = 7.1$ Hz, 1H), 1.77 (d, $J = 7.1$ Hz, 3H) ppm. ^{13}C NMR (CDCl_3) δ 197.3, 164.7, 152.9, 135.7, 135.0, 133.6, 128.9, 128.8, 126.1, 124.5, 121.6, 121.1, 47.1, 18.3 ppm. HRMS (ESI): calcd. for $\text{C}_{16}\text{H}_{13}\text{NOS}_2\text{Na}^+$ $[\text{M}+\text{Na}]^+$ 322.0331, found 322.0352.

2-(Benzo(d)thiazol-2-ylthio)-2-methyl-1-phenylpropan-1-one (5c)

A solution of 2-mercaptobenzothiazole (167 mg, 1 mmol) in 2 mL DCM was added with 0.20 mL TEA (1.4 mmol). To the solution was then added 2-bromo-2-methylpropiophenone (0.17 mL, 1 mmol) dropwise. The reaction mixture was stirred at room temperature for 0.5 h and then heated to 60 $^\circ\text{C}$ for 4 h. After cooling to room temperature, solvent was removed by reduced

pressure. Residue was re-dissolved in 10 mL EA and washed with water (10 mL \times 2). Aqueous phase was back extracted with 15 mL EA. Combined organic phase was dried over Na₂SO₄, concentrated *in vacuo*, and purified by column chromatography (EA/Hex 1:20 to 1:10). 175 mg product was obtained as yellow oil. Yield: 56%. ¹H NMR (CDCl₃) δ 8.13 – 8.05 (m, 2H), 7.89 (d, *J* = 8.1 Hz, 1H), 7.71 (d, *J* = 8.0 Hz, 1H), 7.50 – 7.43 (m, 1H), 7.43 – 7.35 (m, 3H), 7.33 – 7.27 (m, 1H), 1.86 (s, 6H) ppm. ¹³C NMR (CDCl₃) δ 200.6, 161.4, 153.1, 136.7, 136.3, 131.8, 129.1, 127.9, 126.1, 125.0, 122.5, 121.0, 58.1, 27.4 ppm. HRMS (ESI): calcd. for C₁₇H₁₆NOS₂⁺ [M+H]⁺ 314.0668, found 314.0655.

1-(Benzo(d)thiazol-2-ylthio)-3-methylbutan-2-one (5d)

1-Bromo-3-methyl-2-butanone (0.12 mL, 1 mmol) and 2-mercaptobenzothiazole (167 mg, 1 mmol) were dissolved in 5 mL acetone. To the solution was added K₂CO₃ (138 mg, 1 mmol). The reaction mixture was stirred at room temperature for 1 h then dried under reduced pressure. The residue was re-dissolved in 10 mL EA and washed with water (10 mL \times 2). The aqueous phase was back extracted with EA (15 mL \times 2). Combined organic phase was dried over Na₂SO₄ and concentrated over vacuum. The crude product was purified by column chromatography (EA/Hex 1:20 to 1:10). 204 mg product was obtained as white solid. Yield: 81%. ¹H NMR (CDCl₃) δ 7.81 (d, *J* = 8.1 Hz, 1H), 7.74 (d, *J* = 8.0 Hz, 1H), 7.44 – 7.36 (m, 1H), 7.32 – 7.27 (m, 1H), 4.35 (s, 2H), 2.97 (dt, *J* = 13.9, 6.9 Hz, 1H), 1.22 (d, *J* = 6.9 Hz, 6H) ppm. ¹³C NMR (CDCl₃) δ 207.3, 165.3, 152.9, 135.6, 126.1, 124.4, 121.4, 121.1, 41.4, 40.1, 18.4 ppm. HRMS (ESI): calcd. for C₁₂H₁₄NOS₂⁺ [M+H]⁺ 252.0511, found 252.0505.

2-(Benzo(d)thiazol-2-ylthio)cyclohexan-1-one (5e)

To a solution of 2-mercaptobenzothiazole (500 mg, 3.0 mmol) and trimethylamine (0.58 mL, 4.2 mmol) in 6 mL DCM was added 2-chlorocyclohexan-1-one (0.36 mL, 3.1 mmol)

slowly. The solution was heated at reflux for 4.5 h, then cooled to room temperature, and stirred overnight. The reaction mixture was diluted with DCM to 15 mL and washed with water (10 mL \times 2). The combined aqueous phase was back extracted with DCM (15 mL \times 2). Combined organic phase was dried over Na₂SO₄, concentrated in vacuo, and purified by column chromatography (EA/Hex 1:10 to 1:5) to yield the product (454 mg) as yellow solid. Yield: 57%. ¹H NMR (CDCl₃) δ 7.89 (d, J = 8.2 Hz, 1H), 7.77 (dd, J = 8.0, 0.6 Hz, 1H), 7.50 – 7.39 (m, 1H), 7.38 – 7.30 (m, 1H), 4.93 (dd, J = 10.2, 5.7 Hz, 1H), 2.82 – 2.65 (m, 2H), 2.65 – 2.48 (m, 1H), 2.25 – 2.09 (m, 1H), 2.05 – 1.74 (m, 4H) ppm. ¹³C NMR (CDCl₃) δ 205.5, 164.8, 153.1, 135.5, 126.0, 124.4, 121.6, 121.0, 57.4, 41.6, 35.5, 27.6, 25.1 ppm. HRMS (ESI): calcd. for C₁₃H₁₃NOS₂Na⁺ [M+Na]⁺ 286.0331, found 286.0339.

General procedure of reducing β -ketosulfides to β -alkoxysulfides:

Compounds **6a-e** were prepared by reducing compounds **5a-e** with NaBH₄. In general, 1 equiv. of compounds **5a-e** was dissolved in MeOH (10~15 mL/mmol) and cooled to 0 °C in an ice bath. NaBH₄ (4 equiv.) was added to the solution in small portions. The reaction was then allowed to warm up to room temperature. The reaction process was monitored by TLC. After completion, the reaction was quenched with sat. NH₄Cl aqueous solution. The mixture was then extracted with EA and washed with water and brine. The organic phase was dried over Na₂SO₄ and concentrated under reduced pressure. Crude product was purified by column chromatography.

2-(Benzo(d)thiazol-2-ylthio)-1-phenylethan-1-ol (**6a**)

Synthesis followed the general procedure of reducing β -ketosulfides to β -alkoxysulfides from **5a**. Product was obtained as yellow solid. Yield: 99%. ¹H NMR (CDCl₃) δ 7.92 (d, J = 8.1 Hz, 1H), 7.76 (d, J = 7.9 Hz, 1H), 7.57 – 7.25 (m, 7H), 5.31 – 5.05 (m, 2H), 3.74 (dd, J = 14.3,

2.5 Hz, 1H), 3.58 (dd, $J = 14.3, 7.9$ Hz, 1H) ppm. ^{13}C NMR (CDCl_3) δ 167.9, 152.5, 142.9, 135.5, 128.6, 127.9, 126.3, 125.9, 124.7, 121.4, 121.1, 73.6, 42.8 ppm. HRMS (ESI): calcd. for $\text{C}_{15}\text{H}_{13}\text{NOS}_2\text{Na}^+$ $[\text{M}+\text{Na}]^+$ 310.0331, found 310.0340.

2-(Benzo(d)thiazol-2-ylthio)-1-phenylpropan-1-ol (6b)

Synthesis followed the general procedure of reducing β -ketosulfides to β -alkoxysulfides from **5b**. Two isomers were obtained in (Ratio of 35:65 between the compounds with a high and low R_f) with a total yield of 100 %. Both isomers were obtained as clear oil. Isomer with the lower R_f on TLC was characterized as below and used for the next step. ^1H NMR (CDCl_3) δ 7.95 (d, $J = 8.1$ Hz, 1H), 7.79 (d, $J = 7.7$ Hz, 1H), 7.51 – 7.29 (m, 7H), 4.88 (d, $J = 7.2$ Hz, 1H), 4.12 – 4.02 (m, 1H), 1.45 (d, $J = 7.2$ Hz, 3H) ppm. ^{13}C NMR (CDCl_3) δ 166.9, 152.5, 142.5, 135.6, 128.4, 127.9, 126.7, 126.3, 124.8, 121.5, 121.1, 78.5, 52.3, 18.3 ppm. HRMS (ESI): calcd. for $\text{C}_{16}\text{H}_{16}\text{NOS}_2^+$ $[\text{M}+\text{H}]^+$ 302.0668, found 302.0661.

2-(Benzo(d)thiazol-2-ylthio)-2-methyl-1-phenylpropan-1-ol (6c)

Synthesis followed the general procedure of reducing β -ketosulfides to β -alkoxysulfides from **5c**. Product obtained as white solid. Yield: 87%. ^1H NMR (CDCl_3) δ 7.99 (d, $J = 8.1$ Hz, 1H), 7.81 (d, $J = 7.6$ Hz, 1H), 7.56 – 7.44 (m, 1H), 7.44 – 7.35 (m, 3H), 7.35 – 7.27 (m, 3H), 4.95 (s, 1H), 1.58 (s, 3H), 1.41 (s, 3H) ppm. ^{13}C NMR (CDCl_3) δ 165.3, 152.6, 141.0, 136.1, 128.1, 127.7, 127.7, 126.5, 125.2, 121.9, 121.1, 81.7, 60.1, 27.1, 24.1 ppm. HRMS (ESI): calcd. for $\text{C}_{17}\text{H}_{17}\text{NOS}_2\text{Na}^+$ $[\text{M}+\text{Na}]^+$ 338.0644, found 338.0663.

1-(Benzo(d)thiazol-2-ylthio)-3-methylbutan-2-ol (6d)

Synthesis followed the general procedure of reducing β -ketosulfides to β -alkoxysulfides from **5d**. Product was obtained as clear oil. Yield: 90%. ^1H NMR (CDCl_3) δ 7.84 (d, $J = 8.1$ Hz, 1H), 7.74 (d, $J = 8.0$ Hz, 1H), 7.48 – 7.37 (m, 1H), 7.37 – 7.27 (m, 1H), 4.37 (s, br, 1H), 3.76

(ddd, $J = 8.2, 6.0, 2.5$ Hz, 1H), 3.52 (dd, $J = 14.4, 2.5$ Hz, 1H), 3.38 (dd, $J = 14.4, 7.9$ Hz, 1H), 1.88 (dq, $J = 13.4, 6.7$ Hz, 1H), 1.05 (d, $J = 6.8$ Hz, 3H), 1.00 (d, $J = 6.8$ Hz, 3H) ppm. ^{13}C NMR (CDCl_3) δ 168.0, 152.5, 135.4, 126.2, 124.6, 121.3, 121.0, 76.6, 38.8, 33.6, 18.7, 17.8 ppm.

HRMS (ESI): calcd. for $\text{C}_{12}\text{H}_{16}\text{NOS}_2^+$ $[\text{M}+\text{H}]^+$ 254.0668, found 254.0660.

***cis*-2-(benzo(d)thiazol-2-ylthio)cyclohexan-1-ol (6e)**

Synthesis followed the general procedure of reducing β -ketosulfides to β -alkoxysulfides from **5e**. Both *cis*- and *trans*-products were obtained in about 5:4 ratio (according to crude NMR). Total yield: 91%. *cis*-product was characterized as below and used for further synthesis.

^1H NMR (CDCl_3) δ 7.84 (d, $J = 8.1$ Hz, 1H), 7.73 (d, $J = 7.9$ Hz, 1H), 7.47 – 7.35 (m, 1H), 7.35 – 7.27 (m, 1H), 4.38 – 4.23 (m, 1H), 4.23 – 4.08 (m, 1H), 2.15 – 2.01 (m, 1H), 1.92 (dtd, $J = 10.3, 6.4, 4.1$ Hz, 1H), 1.85 – 1.67 (m, 3H), 1.64 – 1.49 (m, 2H), 1.49 – 1.33 (m, 1H). ^{13}C NMR (CDCl_3) δ 167.4, 152.7, 135.4, 126.2, 124.5, 121.4, 121.0, 70.2, 53.9, 31.5, 29.2, 23.9, 21.8 ppm.

HRMS (ESI): calcd. for $\text{C}_{13}\text{H}_{15}\text{NOS}_2\text{Na}^+$ $[\text{M}+\text{Na}]^+$ 288.0487, found 288.0497.

Trans-product characterization: ^1H NMR (CDCl_3) δ 7.86 (d, $J = 8.1$ Hz, 1H), 7.74 (d, $J = 7.9$ Hz, 1H), 7.48 – 7.35 (m, 1H), 7.35 – 7.27 (m, 1H), 4.67 (s, 1H), 3.73 – 3.56 (m, 2H), 2.33 – 2.14 (m, 2H), 1.84 – 1.72 (m, 2H), 1.66 – 1.29 (m, 4H) ppm. ^{13}C NMR (CDCl_3) δ 167.4, 152.5, 135.6, 126.3, 124.7, 121.6, 121.0, 75.0, 55.6, 35.6, 32.2, 26.1, 24.1 ppm. HRMS (ESI): calcd. for $\text{C}_{13}\text{H}_{16}\text{NOS}_2^+$ $[\text{M}+\text{H}]^+$ 266.0668, found 266.0672.

2-(Benzo(d)thiazol-2-ylsulfonyl)-1-phenylethan-1-ol (7a)

Synthesis followed the general procedure of the oxidation of sulfide to sulfone from **6a**. Product was obtained as white solid. Yield: 78%. ^1H NMR (CDCl_3) δ 8.28 – 8.17 (m, 1H), 8.09 – 7.97 (m, 1H), 7.75 – 7.54 (m, 2H), 7.42 – 7.27 (m, 5H), 5.51 (dd, $J = 9.7, 1.8$ Hz, 1H), 3.94 (dd, $J = 14.9, 9.7$ Hz, 1H), 3.82 (dd, $J = 14.9, 2.1$ Hz, 1H), 3.59 (s, 1H) ppm. ^{13}C NMR (CDCl_3) δ

166.3, 152.4, 140.3, 136.7, 128.9, 128.6, 128.3, 127.9, 125.7, 125.5, 122.4, 68.7, 63.0 ppm. IR: $\nu_{\max}/\text{cm}^{-1}$ 3347 (O-H), 2930 (C-H), 1334 (S=O) and 1141 (S=O). HRMS (ESI): calcd. for $\text{C}_{15}\text{H}_{13}\text{NO}_3\text{S}_2^+$ $[\text{M}+\text{H}]^+$ 320.0410, found 320.0400.

2-(Benzo(d)thiazol-2-ylsulfonyl)-1-phenylpropan-1-ol (7b)

Synthesis followed the general procedure of the oxidation of sulfide to sulfone from **6b**.

Product was obtained as white solid. Yield: 23% ^1H NMR (CDCl_3) δ 8.33 – 8.18 (m, 1H), 8.09 – 7.95 (m, 1H), 7.73 – 7.63 (m, 1H), 7.63 – 7.57 (m, 1H), 7.40 – 7.28 (m, 5H), 5.18 (d, $J = 9.1$ Hz, 1H), 4.08 – 3.94 (m, 1H), 3.59 (d, $J = 1.9$ Hz, 1H), 1.13 (d, $J = 7.2$ Hz, 3H) ppm. ^{13}C NMR (CDCl_3) δ 166.0, 152.7, 139.5, 136.9, 128.9, 128.8, 128.1, 127.7, 127.1, 125.6, 122.3, 74.0, 66.2, 11.9 ppm. IR: $\nu_{\max}/\text{cm}^{-1}$ 3484 (O-H), 2851 (C-H), 1313 (S=O), and 1137(S=O). HRMS (ESI): calcd. for $\text{C}_{16}\text{H}_{15}\text{NO}_3\text{S}_2\text{Na}^+$ $[\text{M}+\text{Na}]^+$ 356.0386, found 356.0381.

2-(Benzo(d)thiazol-2-ylsulfonyl)-2-methyl-1-phenylpropan-1-ol (7c)

Synthesis followed the general procedure of the oxidation of sulfide to sulfone from **6c**.

Product was obtained as white solid. Yield: 35%. ^1H NMR (CDCl_3) δ 8.33 – 8.22 (m, 1H), 8.09 – 7.99 (m, 1H), 7.72 – 7.56 (m, 2H), 7.39 – 7.27 (m, 5H), 5.54 (s, 1H), 1.54 (s, 3H), 1.22 (s, 3H) ppm. ^{13}C NMR (CDCl_3) δ 164.9, 152.8, 138.0, 137.3, 128.5, 128.2, 128.1, 128.0, 127.8, 125.7, 122.2, 74.8, 70.4, 20.8, 14.4 ppm. IR: $\nu_{\max}/\text{cm}^{-1}$ 3335 (O-H), 1314 (S=O), and 1158 (S=O). HRMS (ESI): calcd. for $\text{C}_{17}\text{H}_{18}\text{NO}_3\text{S}_2^+$ $[\text{M}+\text{H}]^+$ 348.0723, found 348.0718.

1-(Benzo(d)thiazol-2-ylsulfonyl)-3-methylbutan-2-ol (7d)

Synthesis followed the general procedure of the oxidation of sulfide to sulfone from **6d**.

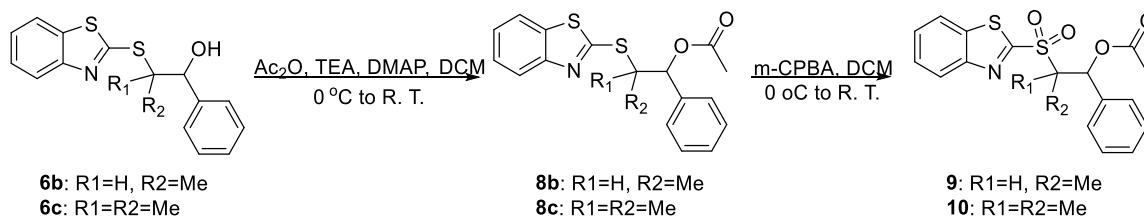
Product was obtained as white solid. Yield: 70%. ^1H NMR (CDCl_3) δ 8.21 (dd, $J = 7.5, 1.3$ Hz, 1H), 8.02 (dd, $J = 7.1, 1.1$ Hz, 1H), 7.71 – 7.51 (m, 2H), 4.19 (ddd, $J = 9.0, 5.1, 2.1$ Hz, 1H), 3.68 (dd, $J = 14.7, 2.1$ Hz, 1H), 3.61 (dd, $J = 14.7, 9.0$ Hz, 1H), 1.91 – 1.73 (m, 1H), 0.96 (t, $J =$

6.7 Hz, 6H) ppm. ^{13}C NMR (CDCl_3) δ 166.4, 152.4, 136.6, 128.2, 127.8, 125.4, 122.4, 70.5, 59.5, 33.5, 18.1, 17.1 ppm. IR: $\nu_{\text{max}}/\text{cm}^{-1}$ 3540 (O-H), 2969 (C-H), 1304 (S=O), and 1126(S=O). HRMS (ESI): calcd. for $\text{C}_{12}\text{H}_{16}\text{NO}_3\text{S}_2^+$ $[\text{M}+\text{H}]^+$ 286.0566, found 286.0561.

cis-2-(benzo(d)thiazol-2-ylsulfonyl)cyclohexan-1-ol (**7e**)

Synthesis followed the general procedure of the oxidation of sulfide to sulfone from **6e**.

Product was obtained as white solid. Yield: 79%. ^1H NMR (CDCl_3) δ 8.29 – 8.13 (m, 1H), 8.09 – 7.93 (m, 1H), 7.72 – 7.51 (m, 2H), 4.59 (s, 1H), 3.59 – 3.43 (m, 1H), 3.29 (s, 1H), 2.20 – 1.85 (m, 4H), 1.85 – 1.63 (m, 1H), 1.55 – 1.20 (m, 3H). ^{13}C NMR (CDCl_3) δ 165.5, 152.7, 136.9, 128.2, 127.8, 125.5, 122.4, 67.2, 63.8, 32.5, 25.1, 19.5, 18.6 ppm. IR: $\nu_{\text{max}}/\text{cm}^{-1}$ 3548 (OH) 2925 (C-H), 1318 (S=O) and 1141 (S=O). HRMS (ESI): calcd. for $\text{C}_{13}\text{H}_{16}\text{NO}_3\text{S}_2^+$ $[\text{M}+\text{H}]^+$ 298.0566, found 298.0565.



2-(Benzo(d)thiazol-2-ylthio)-1-phenylpropyl acetate (**8b**)

A solution of **6b** (100 mg, 0.33 mmol) in 2 mL DCM was treated with Ac_2O (0.09 mL, 1 mmol), TEA (0.14 mL, 1 mmol), and *N,N*-dimethylaminopyridine (DMAP, 4 mg, 0.03 mmol) under stirring at room temperature. After 1 hour, the reaction mixture was directly dried under reduced pressure and purified by column chromatography (EA/Hex 1:20). Product was obtained as clear oil. Yield: 98%. ^1H NMR (CDCl_3) δ 7.89 (d, $J = 8.1$ Hz, 1H), 7.75 (dd, $J = 7.9, 0.5$ Hz, 1H), 7.42 (dd, $J = 11.2, 4.1$ Hz, 3H), 7.38 – 7.27 (m, 4H), 5.98 (d, $J = 7.1$ Hz, 1H), 4.50 (p, $J = 7.1$ Hz, 1H), 2.03 (s, 3H), 1.42 (d, $J = 7.0$ Hz, 3H) ppm. ^{13}C NMR (CDCl_3) δ 169.8, 165.6,

153.2, 137.5, 135.4, 128.6, 128.4, 127.3, 126.1, 124.4, 121.7, 121.0, 77.8, 48.3, 21.0, 18.1 ppm.

HRMS (ESI): calcd. for $C_{18}H_{18}NO_2S_2^+$ $[M+H]^+$ 344.0773, found 344.0768.

2-(Benzo(d)thiazol-2-ylthio)-2-methyl-1-phenylpropyl acetate (8c)

A solution of **6c** (63 mg, 0.20 mmol) in 2 mL DCM was treated with Ac_2O (0.06 mL, 0.60 mmol), TEA (0.08 mL, 0.6 mmol), and DMAP (2 mg, 0.02 mmol) under stirring at room temperature. After 1 hour, the reaction mixture was directly dried under reduced pressure and purified by column chromatography (EA/Hex 1:20). Product was obtained as clear oil. Yield: 90%. 1H NMR ($CDCl_3$) δ 8.03 (d, $J = 7.9$ Hz, 1H), 7.80 (dd, $J = 8.0, 0.5$ Hz, 1H), 7.50 – 7.44 (m, 1H), 7.44 – 7.27 (m, 6H), 6.36 (s, 1H), 2.08 (s, 3H), 1.60 (s, 3H), 1.51 (s, 3H) ppm. ^{13}C NMR ($CDCl_3$) δ 169.6, 162.6, 153.7, 136.9, 136.4, 128.3, 128.2, 127.9, 126.2, 125.1, 122.8, 120.9, 79.7, 56.4, 25.7, 24.3, 21.1 ppm. HRMS (ESI): calcd. for $C_{19}H_{19}NO_2S_2Na^+$ $[M+Na]^+$ 380.0794, found 380.0761.

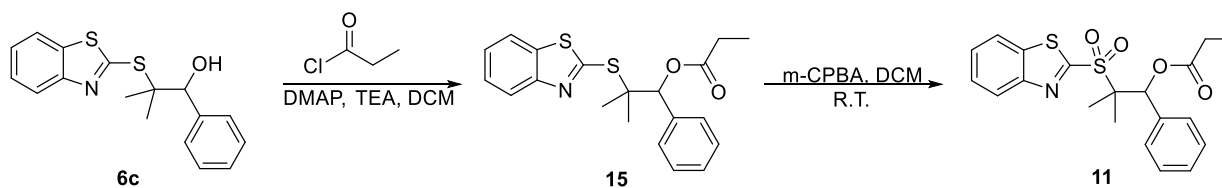
2-(Benzo(d)thiazol-2-ylsulfonyl)-1-phenylpropyl acetate (9)

Synthesis procedure followed the general procedure of the oxidation of sulfide to sulfone from **8b**. Product obtained as pale white oil. Yield: 83%. 1H NMR ($CDCl_3$) δ 8.27 (dd, $J = 8.1, 0.5$ Hz, 1H), 8.03 (dd, $J = 8.0, 0.6$ Hz, 1H), 7.72 – 7.63 (m, 1H), 7.63 – 7.55 (m, 1H), 7.39 – 7.28 (m, 5H), 6.05 (d, $J = 9.7$ Hz, 1H), 4.35 (dq, $J = 9.7, 7.3$ Hz, 1H), 1.53 (s, 3H), 1.26 (d, $J = 7.3$ Hz, 3H) ppm. ^{13}C NMR ($CDCl_3$) δ 168.7, 166.9, 152.8, 136.7, 136.6, 129.2, 128.9, 128.1, 127.8, 127.6, 125.5, 122.27, 74.9, 62.8, 20.6, 10.6 ppm. IR: ν_{max}/cm^{-1} 2941 (C-H), 1745 (C=O), 1317 (S=O), 1221 (C-O), and 1145 (S=O). HRMS (ESI): calcd. for $C_{18}H_{18}NO_4S_2^+$ $[M+H]^+$ 376.0672, found 376.0666.

2-(Benzo(d)thiazol-2-ylsulfonyl)-2-methyl-1-phenylpropyl acetate (10)

Synthesis followed the general procedure of the oxidation of sulfide to sulfone from **8c**.

Product was obtained as white solids. Yield: 85%. $^1\text{H NMR}$ (CDCl_3) δ 8.27 (d, $J = 7.7$ Hz, 1H), 8.02 (d, $J = 7.6$ Hz, 1H), 7.69 – 7.62 (m, 1H), 7.60 (td, $J = 7.7, 1.3$ Hz, 1H), 7.36 – 7.24 (m, 5H), 6.29 (s, 1H), 1.76 (s, 3H), 1.66 (s, 3H), 1.31 (s, 3H) ppm. $^{13}\text{C NMR}$ (CDCl_3) δ 168.7, 165.3, 153.1, 137.3, 135.8, 128.8, 128.4, 128.1, 127.8, 127.7, 125.7, 122.2, 75.7, 69.1, 20.7, 20.3, 16.5 ppm. IR: $\nu_{\text{max}}/\text{cm}^{-1}$ 2992 (C-H), 1748 (C=O), 1312 (S=O) 1225 (C-O), 1153 (S=O). HRMS (ESI): calcd. for $\text{C}_{19}\text{H}_{19}\text{NO}_4\text{S}_2\text{Na}^+$ $[\text{M}+\text{Na}]^+$ 412.0648, found 412.0651.



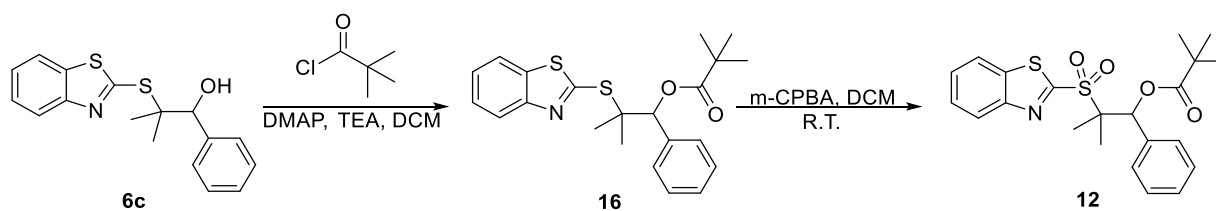
2-(Benzo(d)thiazol-2-ylthio)-2-methyl-1-phenylpropyl propionate (15)

A solution of **6c** (150 mg, 0.48 mmol) was dissolved in 1 mL DCM. To the solution was added DMAP (6 mg, 0.05 mmol), TEA (0.13 mL, 0.96 mmol), and propionyl chloride (0.05 mL, 0.58 mmol) sequentially under stirring. The reaction mixture was heated to 60 °C for 8 hours and then stirred at room temperature overnight. The reaction mixture was directly dried over reduced pressure and purified by column chromatography (EA/Hex 1:20). Product was obtained as clear oil. Yield: 52%. $^1\text{H NMR}$ (CDCl_3) δ 8.04 (d, $J = 7.8$ Hz, 1H), 7.80 (dd, $J = 8.0, 0.5$ Hz, 1H), 7.53 – 7.27 (m, 7H), 6.38 (s, 1H), 2.48 – 2.27 (m, 2H), 1.61 (s, 3H), 1.52 (s, 3H), 1.15 (t, $J = 7.6$ Hz, 3H) ppm. $^{13}\text{C NMR}$ (CDCl_3) δ 172.9, 162.6, 153.7, 137.1, 136.4, 128.2, 128.2, 127.9, 126.2, 125.1, 122.8, 120.9, 79.4, 56.5, 27.8, 25.6, 24.4, 9.1 ppm. HRMS (ESI): calcd. for $\text{C}_{20}\text{H}_{21}\text{NO}_2\text{S}_2\text{Na}^+$ $[\text{M}+\text{Na}]^+$ 394.0906, found 394.0905.

2-(Benzo(d)thiazol-2-ylsulfonyl)-2-methyl-1-phenylpropyl propionate (11)

Synthesis followed the general procedure of the oxidation of sulfide to sulfone from **11**.

Product was obtained as clear oil. Yield: 81%. ^1H NMR (CDCl_3) δ 8.26 (d, $J = 7.7$ Hz, 1H), 8.01 (d, $J = 7.6$ Hz, 1H), 7.70 – 7.61 (m, 1H), 7.61 – 7.54 (m, 1H), 7.36 – 7.23 (m, 5H), 6.31 (s, 1H), 2.02 – 1.79 (m, 2H), 1.76 (s, 3H), 1.30 (s, 3H), 0.89 (t, $J = 7.5$ Hz, 3H) ppm. ^{13}C NMR (CDCl_3) δ 172.0, 165.3, 153.1, 137.2, 135.9, 128.8, 128.4, 128.1, 127.8, 127.7, 125.7, 122.1, 75.4, 69.1, 27.3, 20.4, 16.5, 8.5 ppm. IR: $\nu_{\text{max}}/\text{cm}^{-1}$ 2985 (C-H), 1746 (C=O), 1319 (S=O), 1151 (S=O). HRMS (ESI): calcd. for $\text{C}_{20}\text{H}_{21}\text{NO}_4\text{S}_2\text{Na}^+$ $[\text{M}+\text{Na}]^+$ 426.0804, found 426.0821.



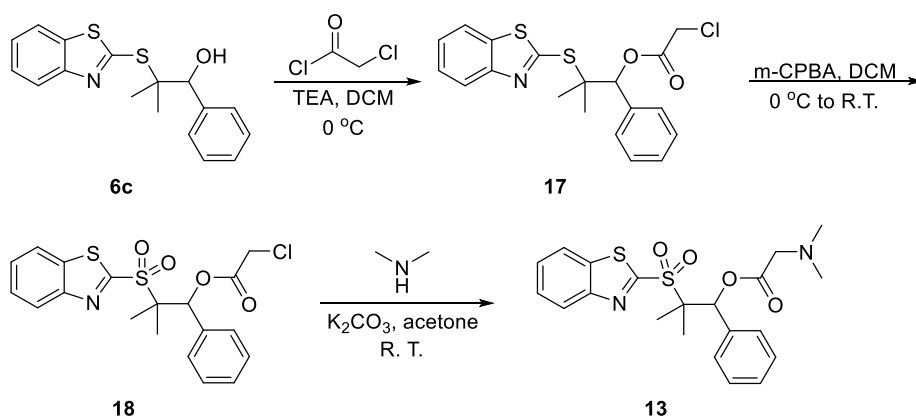
2-(Benzo(d)thiazol-2-ylthio)-2-methyl-1-phenylpropyl pivalate (**16**)

Compound **6c** (200 mg, 0.63 mmol) and DMAP (7 mg, 0.06 mmol) were dissolved in 2 mL DCM. To this solution was added TEA (0.18 mL, 1.26 mmol) and pivaloyl chloride (0.09 mL, 0.73 mmol) slowly under stirring. The reaction mixture was heated at 60 °C for 8 hours, then cooled to room temperature, and stirred overnight. The reaction mixture was diluted with 10 mL DCM, and washed with 8 mL water. The aqueous phase was back extracted with DCM (10 mL \times 2). Combined organic phase was dried over Na_2SO_4 , concentrated in vacuo, and purified by column chromatography (DCM/Hex 1:2 to 1:1 to pure DCM). Product was obtained as clear oil. Yield: 63%. ^1H NMR (CDCl_3) δ 8.03 (d, $J = 7.8$ Hz, 1H), 7.80 (dd, $J = 8.0, 0.5$ Hz, 1H), 7.52 – 7.28 (m, 7H), 6.35 (s, 1H), 1.61 (s, 3H), 1.52 (s, 3H), 1.26 (s, 9H) ppm. ^{13}C NMR (CDCl_3) δ 176.6, 162.6, 153.8, 137.1, 136.3, 128.2, 128.1, 127.8, 126.1, 125.0, 122.8, 120.9, 79.09, 56.7, 39.0, 27.2, 25.5, 24.4 ppm. HRMS (ESI): calcd. for $\text{C}_{22}\text{H}_{26}\text{NO}_2\text{S}_2^+$ $[\text{M}+\text{H}]^+$ 400.1399, found 400.1384.

2-(Benzo(d)thiazol-2-ylsulfonyl)-2-methyl-1-phenylpropyl pivalate (12)

Synthesis followed the general procedure of the oxidation of sulfide to sulfone from **15**.

Product yielded as white solid. Yield: 86%. ^1H NMR (CDCl_3) δ 8.32 – 8.20 (m, 1H), 8.09 – 7.93 (m, 1H), 7.72 – 7.53 (m, 2H), 7.37 – 7.27 (m, 5H), 6.33 (s, 1H), 1.77 (s, 3H), 1.23 (s, 3H), 1.15 (s, 9H) ppm. ^{13}C NMR (CDCl_3) δ 176.1, 164.6, 153.2, 137.3, 136.0, 128.8, 128.4, 128.1, 127.9, 127.6, 125.8, 122.2, 74.9, 68.6, 38.8, 26.9, 21.6, 16.4 ppm. IR: $\nu_{\text{max}}/\text{cm}^{-1}$ 2975 (C-H), 1734 (C=O), 1321 (S=O), 1139 (S=O). HRMS (ESI): calcd. for $\text{C}_{22}\text{H}_{26}\text{NO}_4\text{S}_2^+$ $[\text{M}+\text{H}]^+$ 432.1298, found 432.1284.



2-(Benzo(d)thiazol-2-ylthio)-2-methyl-1-phenylpropyl 2-chloroacetate (17)

Compound **6c** (140 mg, 0.44 mmol) was dissolved in 5 mL DCM. To this solution was added TEA (0.11 mL, 0.80 mmol). The solution was cooled to 0 °C in ice bath. 2-Chloroacetyl chloride (0.04 mL, 0.50 mmol) was then added slowly to the solution. The reaction mixture was stirred at 0 °C for 90 min. Then 5 mL water was added into the reaction mixture. The aqueous layer was extracted with DCM (10 mL \times 3). Combined organic phase was washed with brine, dried over Na_2SO_4 , concentrated, and purified by column chromatography (EA/Hex 1:40 to 1:20). Product was obtained as clear oil. Yield: 50%. ^1H NMR (CDCl_3) δ 8.03 (dd, $J = 8.1, 0.4$ Hz, 1H), 7.81 (dd, $J = 8.0, 0.6$ Hz, 1H), 7.53 – 7.45 (m, 1H), 7.45 – 7.28 (m, 6H), 6.54 (s, 1H),

4.10 (s, 2H), 1.61 (s, 3H), 1.51 (s, 3H) ppm. ^{13}C NMR (CDCl_3) δ 165.8, 162.3, 153.7, 136.2, 136.1, 128.6, 128.1, 128.0, 126.2, 125.2, 122.8, 121.0, 81.2, 56.1, 41.0, 25.4, 24.1 ppm. HRMS (ESI): calcd. for $\text{C}_{19}\text{H}_{18}\text{ClNO}_2\text{S}_2\text{Na}^+$ $[\text{M}+\text{Na}]^+$ 414.0360, found 414.0383.

2-(Benzo(d)thiazol-2-ylsulfonyl)-2-methyl-1-phenylpropyl 2-chloroacetate (18)

Synthesis followed the general procedure of the oxidation of sulfide to sulfone from **16**. Product was obtained as white solid. Yield: 88%. ^1H NMR (CDCl_3) δ 8.35 – 8.17 (m, 1H), 8.10 – 7.91 (m, 1H), 7.76 – 7.56 (m, 2H), 7.42 – 7.27 (m, 5H), 6.41 (s, 1H), 3.88 – 3.68 (m, 2H), 1.73 (s, 3H), 1.31 (s, 3H) ppm. ^{13}C NMR (CDCl_3) δ 165.2, 164.7, 153.0, 137.3, 134.8, 129.2, 128.6, 128.3, 127.9, 127.8, 125.7, 122.3, 77.1, 69.0, 40.8, 20.4, 16.3 ppm. IR: $\nu_{\text{max}}/\text{cm}^{-1}$ 2989 (C-H), 1743 (C=O), 1313 (S=O), 1152 (S=O). HRMS (ESI): calcd. for $\text{C}_{19}\text{H}_{18}\text{ClNO}_4\text{S}_2\text{Na}^+$ $[\text{M}+\text{Na}]^+$ 446.0258, found 446.0271.

2-(Benzo(d)thiazol-2-ylsulfonyl)-2-methyl-1-phenylpropyl dimethylglycinate (13)

Compound **17** (100 mg, 0.24 mmol) was dissolved in 5 mL acetone and added with K_2CO_3 (66 mg, 0.48 mmol). Dimethylamine (2.0 M in methanol, 0.24 mL, 0.48 mmol) was added into this solution and then the reaction mixture was stirred overnight. Subsequently, the reaction mixture was filtered. The filtrate was concentrated under reduced pressure. Residue was purified by column chromatography (EA/Hex 1:4 to 1:1). Product was obtained as yellowish solid. Yield: 62%. ^1H NMR (CDCl_3) δ 8.27 (d, $J = 7.8$ Hz, 1H), 8.01 (d, $J = 7.5$ Hz, 1H), 7.72 – 7.62 (m, 1H), 7.62 – 7.50 (m, 1H), 7.36 – 7.26 (m, 5H), 6.33 (s, 1H), 2.86 (d, $J = 16.9$ Hz, 1H), 2.71 (d, $J = 16.9$ Hz, 1H), 2.14 (s, 6H), 1.76 (s, 3H), 1.30 (s, 3H) ppm. ^{13}C NMR (CDCl_3) δ 168.5, 165.2, 153.1, 137.2, 135.6, 128.9, 128.4, 128.1, 127.85, 127.7, 125.8, 122.2, 75.5, 69.0, 59.6, 44.9, 20.5, 16.4 ppm. IR: $\nu_{\text{max}}/\text{cm}^{-1}$ 2934 (C-H), 1742 (C=O), 1320 (S=O), 1110 (S=O). HRMS (ESI): calcd. for $\text{C}_{21}\text{H}_{25}\text{N}_2\text{O}_4\text{S}_2^+$ $[\text{M}+\text{H}]^+$ 433.1250, found 433.1244.

1.3.2.3 Confirmation of SO₂ release by DTNB test

DTNB test was adopted from a published method.⁸⁶ **7b** and **7c** were prepared as 500- μ M DMSO stock solutions. DTNB was prepared as 15-mM EtOH stock solution. NaHSO₃ as positive control was prepared as a 1-mM PBS (pH 7.4) stock solution and stored on ice before use. 2-OHBT and 2-methyl-1-phenyl-propene as negative controls were prepared as 500- μ M DMSO stock solutions respectively.

Each group (200 μ L total volume) was prepared by adding 20 μ L stock solution into the wells of a 96-well plate followed by addition of 180 μ L PBS. Each final solution contained 10% DMSO. The plate was incubated at 37 °C for 0.5 h with gentle shaking on a Barnstead shaker. Then 20 μ L DTNB was added into each well. After incubating at room temperature for another 15 min, the UV absorption was read by a PerkinElmer multiplate reader at 405 nm (n=3).

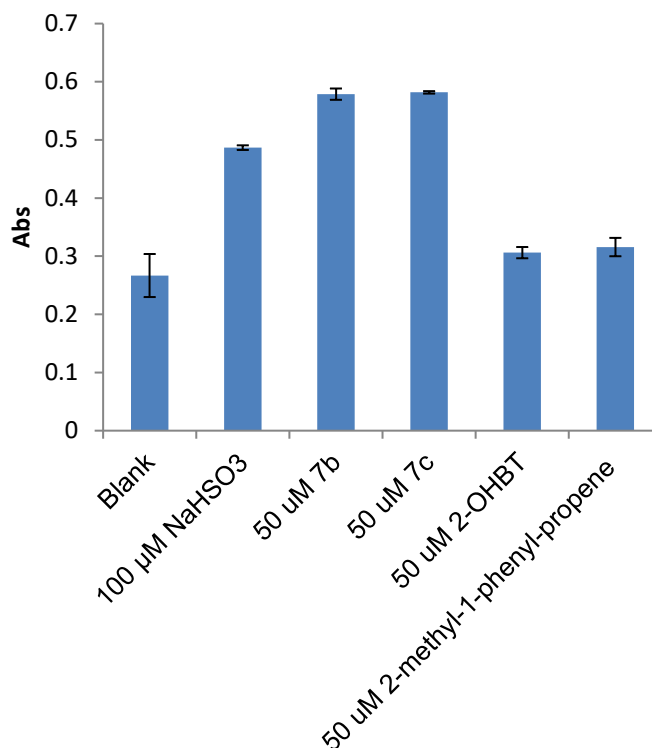


Figure 1-17 DTNB test results.

1.3.2.4 Kinetics study of compound 7a-e by HPLC

Compounds **7a-d** were prepared as 500- μM DMSO stock solution at room temperature. Test solution (50 μM) was prepared in 8 mL glass vial by adding 200 μL of a DMSO stock solution into 1800 μL PBS and the resulting solution was incubated immediately in a water bath at 37 $^{\circ}\text{C}$. 100 μL of samples for analysis were taken at random time points ($n = 10$) and were mixed with 300 μL ACN in a 1.5-mL eppendorf tube and stored at -80 $^{\circ}\text{C}$. Frozen samples were thawed and centrifuged with benchtop microcentrifuge shortly to allow salt precipitation. Supernatant was subjected to HPLC analysis. Standards of 2-OHBT, styrene, and substituted styrenes were purchased from commercial vendors. k_{obs} was calculated using 2-OHBT peak areas. All kinetic runs were in triplicates. Curve fitting was conducted using the SigmaPlot 10 software (Figure 1-18).

HPLC conditions:Binary solvent system: Solvent A: H₂O with 0.05% TFA; Solvent B: ACN

Gradient elution: Solvent B 15% to 60%

UV detector wavelength: 254 nm

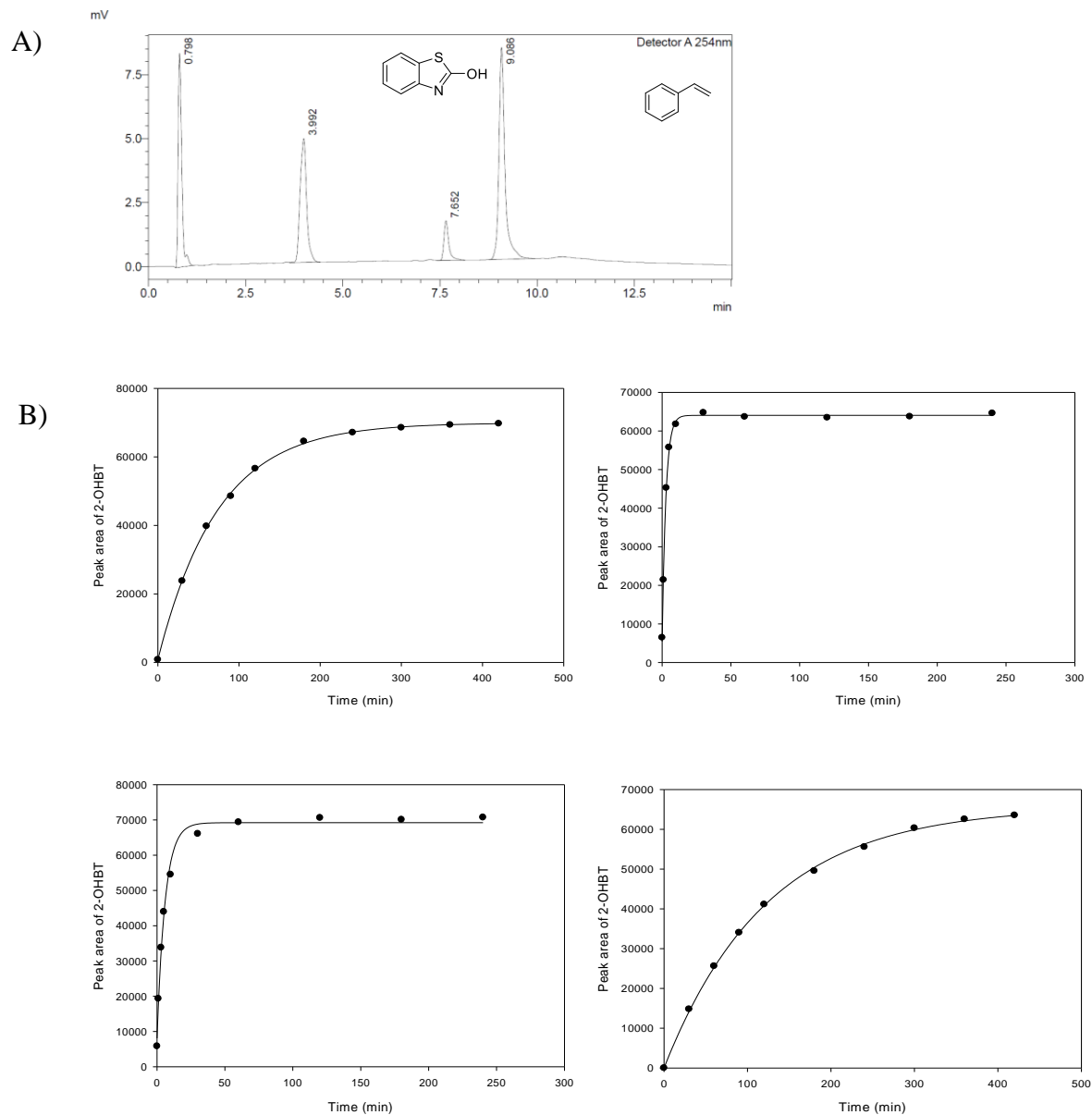
Injection volume: 20 μ L

Figure 1-18 Kinetics studies of compounds **7a-e** by measuring 2-OHBT peak areas using HPLC

(A) An example of HPLC chromatogram obtained by HPLC. Chromatogram showing 50 μM **7a** in 10% DMSO/PBS (pH 7.4) at 37 °C at the 120-min time point. Peak at 3.992 min: 2-OHBT; peak at 7.652 min: compound **7a**; peak at 9.086 min: styrene. (B) Examples of first-order reaction monitored by measuring 2-OHBT peak areas. Upper left: **7a**; upper right: **7b**; lower left: **7c**; lower right: **7d**.

Compound **7e** was prepared as a 20-mM DMSO stock solution at room temperature. Test solution (200 μM) was prepared in 1.5 mL eppendorf tube by adding 10 μL of the DMSO stock solution into 990 μL PBS followed by incubation in a water bath at 37 °C. Samples for HPLC analyses were taken at random time points and subjected to HPLC analysis directly. 2-OHBT standard was pretested for retention time (\sim 3.8 min). Kinetic runs were in triplicates (Figure 1-19).

HPLC conditions:

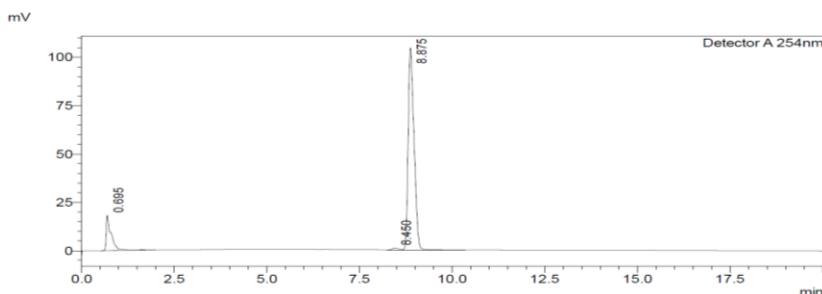
Binary solvent system: Solvent A: H₂O with 0.05% TFA; Solvent B: ACN

Gradient elution: Solvent B 15% to 40%

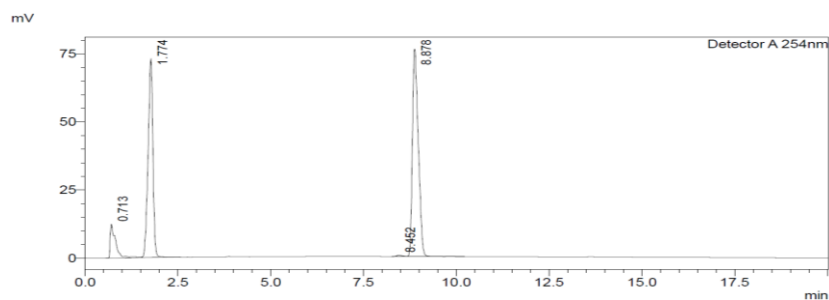
UV detector wavelength: 254 nm

Injection volume: 20 μL

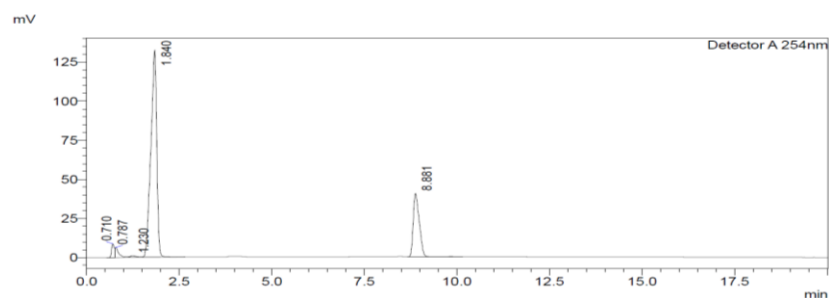
0 min:



65 min:



196 min:



Overlay (0~196 min):

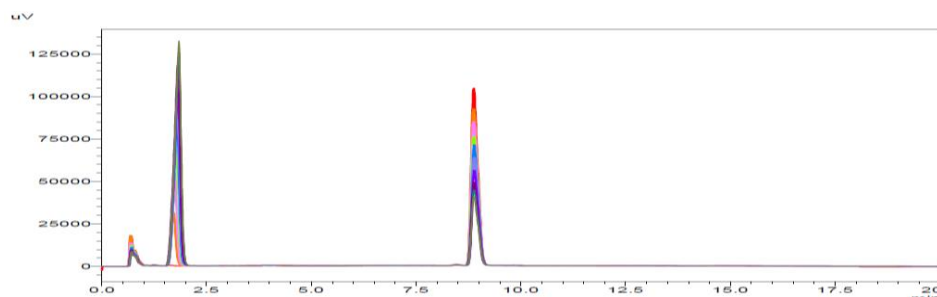


Figure 1-19 An example of reaction of **7e** monitored by HPLC. Peaks at 8.87~8.88 min: compound **7e**

1.3.2.5 Stability study of compound **9**, **10**, and **13** by HPLC

Compound **9** was prepared as a 5-mM DMSO stock solution at room temperature. Test solution (50 μ M) was prepared in a 1.5 mL eppendorf tube by adding 10 μ L of the DMSO stock solution into 990 μ L PBS followed by incubation at 37 $^{\circ}$ C in a water bath. Samples for HPLC analysis were taken at random time points (n = 10) and subjected to HPLC analysis directly. Stability tests were in duplicates (Figure 1-20).

HPLC conditions:

Binary solvent system: Solvent A: H₂O with 0.05% TFA; Solvent B: ACN

Gradient elution: Solvent B 15% to 60%

UV detector wavelength: 254 nm

Injection volume: 20 μ L

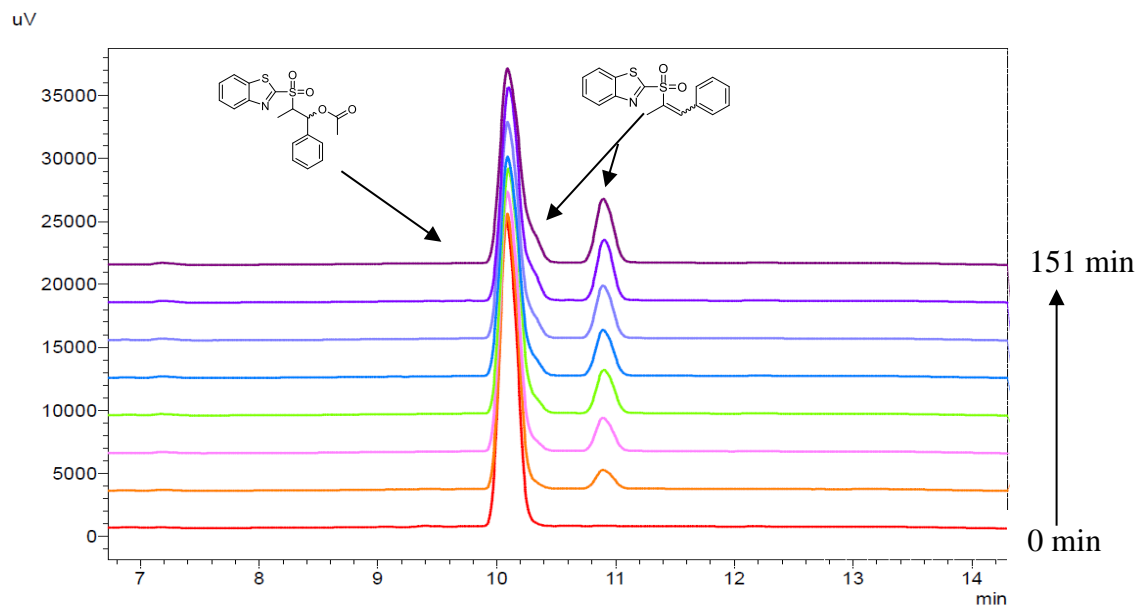


*Figure 1-20 An example of stability tests of compound 9 monitored by HPLC
Peaks at 10.07~10.08 min: compound 9; shoulder peaks and peaks at 10.87~10.89 min:
elimination product.*

Compound **10** was prepared as 100- μ M DMSO stock solution at room temperature. Test solution (10 μ M) was prepared in an 8-mL glass vial by adding 500 μ L of the DMSO stock solution into 4.5 mL PBS followed by incubation at 37 $^{\circ}$ C in a water bath with stirring. Samples for HPLC analysis were taken at random time points ($n = 5$) and subjected to HPLC analysis directly. Stability tests were in duplicates (Figure 1-21).

HPLC conditions:

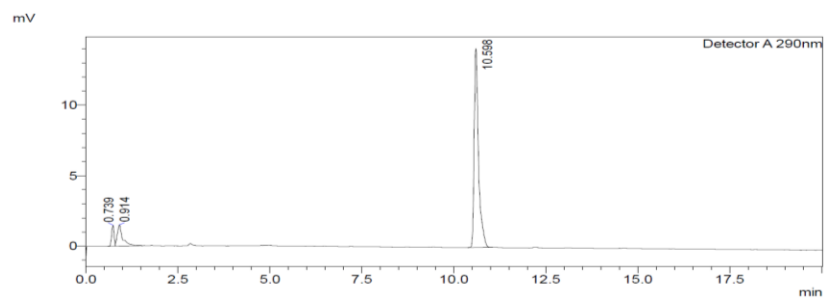
Binary solvent system: Solvent A: H₂O with 0.05% TFA; Solvent B: ACN

Gradient elution: Solvent B 15% to 60%

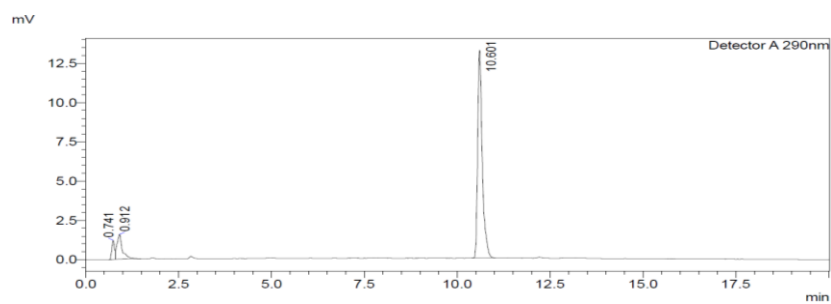
UV detector wavelength: 254 nm

Injection volume: 20 μ L

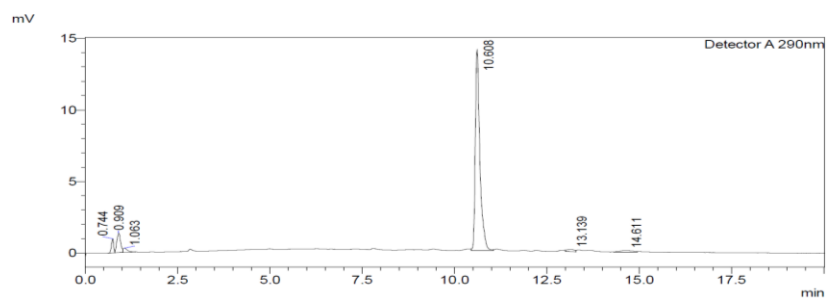
0 min:



86 min:



240 min:



Overlay (0~240 min):

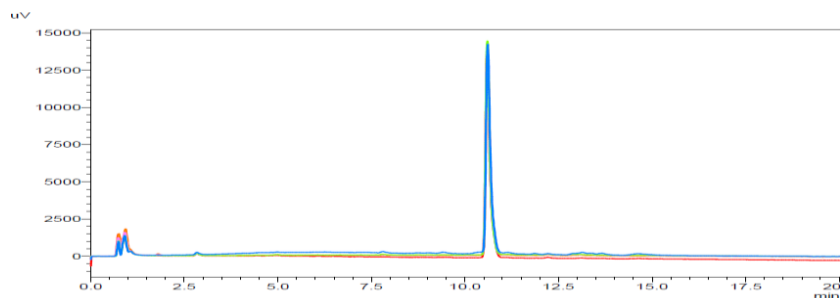


Figure I-21 An example of stability tests of compound **10** monitored by HPLC
Peaks at 10.60~10.61 min: compound **10**

A 5-mM stock solution of Compound **13** was prepared at room temperature in DMSO. Test solution (50 μ M) was prepared in an 8-mL glass vial by adding 20 μ L of the DMSO stock solution into 1980 μ L of PBS followed by incubation at 37 °C in a water bath. Samples for HPLC analysis were taken at random time points (n = 5) and subjected to HPLC analysis directly. Stability tests were in duplicates (Figure 1-22).

HPLC conditions:

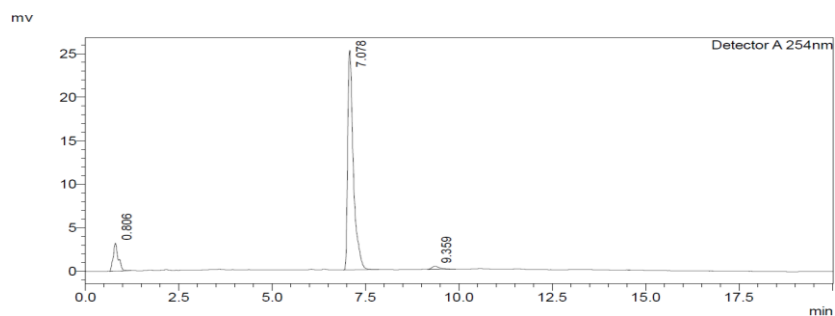
Binary solvent system: Solvent A: H₂O with 0.05% TFA; Solvent B: ACN

Gradient elution: Solvent B 15% to 60%

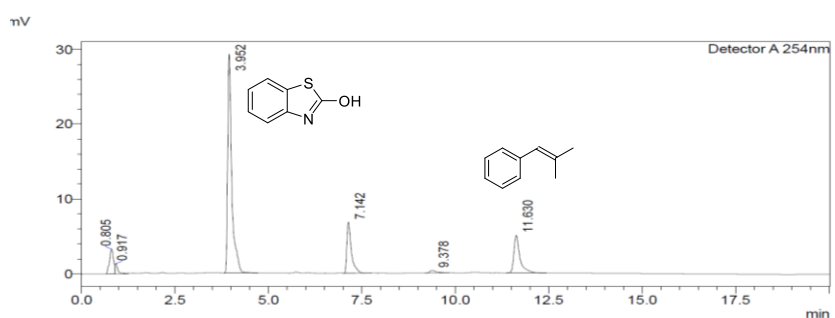
UV detector wavelength: 254 nm

Injection volume: 20 μ L

0 h:



48 h:



97 h:

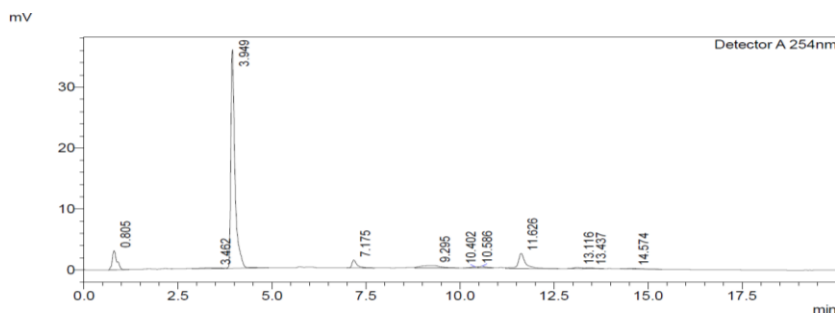


Figure 1-22 An example of stability studies of compound **13** monitored by HPLC
Peaks at 3.94~3.95min: 2-OHBT; peaks at 7.07~7.17 min: compound **13**; peaks at 11.62~11.63 min: 2-methyl-1-phenyl-propene.

1.3.2.6 Kinetics study of esterase-triggered SO_2 release of compound 10-13 by HPLC

Stock solutions (500 μM) of compounds **10-13** were prepared in DMSO at room temperature. Porcine liver esterase (PLE, 18 unit/mg) was prepared as 0.1 unit/ μL PBS stock solution. Test solution (50 μM with 5 unit/mL PLE) was prepared in an 8-mL glass vial by first

adding 200 μL of the DMSO stock solution into 1700 μL of PBS and thoroughly mixed. Then to the solution was added 100 μL of the PLE stock solution followed by incubation at 37 $^{\circ}\text{C}$ in a water bath. 100 μL samples for analysis were taken every 10 minutes ($n=12$) and mixed with 300 μL ACN in a 1.5-mL eppendorf tube and stored at -80 $^{\circ}\text{C}$. Frozen samples were thawed and centrifuged with benchtop micro-centrifuge at 14.5×10^3 rpm for 4 min to allow esterase and salt to precipitate. Supernatant was subjected to HPLC analysis. 2-OHBT, styrene, and substituted styrenes were used as standard and pre-tested for retention time. All kinetic runs were in triplicates. Microsoft Excel was used for plotting. Kinetics studies of the esterase-triggered SO_2 release from compound **13** in 1% DMSO/PBS with 1 unit/mL PLE used the same method. Stock solutions were prepared accordingly.

HPLC conditions:

Binary solvent system: Solvent A: H_2O with 0.05% TFA; Solvent B: ACN

Gradient elution: Solvent B 15% to 60%

UV detector wavelength: 254 nm

Injection volume: 20 μL

1.3.2.7 Kinetics studies of esterase-triggered SO_2 release from compound 10-13 as examined with fluorescent probe 14

Standard curve:

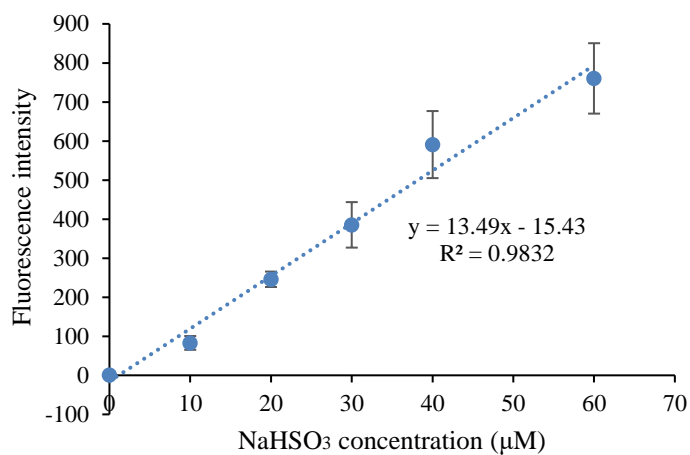
500 μM probe **14** DMSO stock solution was prepared at room temperature. NaHSO_3 solutions of different concentrations were prepared in PBS. The test solution was prepared in a 4 mL (10 mm \times 10 mm) quartz cuvette by adding 300 μL probe DMSO stock solution into 2700 μL NaHSO_3 solution. Final solution contains 50 μM probe **14** and 10% DMSO. The test solution was sealed with a cap, thoroughly mixed, and incubated at room temperature for 2 min.

Fluorescent emission at 465 nm was then recorded on a Shimadzu RF- 5301PC fluorimeter. ($\lambda_{\text{ex}}=400$ nm; slit width: ex: 5nm, em: 3 nm) Experiments were conducted in triplicates. Standard curves were fitted with Microsoft Excel 2016 (Figure 1-23 (A)).

Studies of reaction kinetics:

Stock solutions (1 mM) of compounds **10-13** were prepared in DMSO at room temperature. PLE (18 unit/mg) was prepared as 0.1 unit/ μL PBS stock solution. Probe **14** was prepared as 1 mM DMSO stock solution. Test solution (50 μM prodrug with 50 μM probe and 5 unit/mL PLE) was prepared by adding 150 μL of the prodrug DMSO stock solution, 150 μL of the probe **14** DMSO stock solution, 2550 μL of PBS, and 150 μL PLE stock solution sequentially into a 4 mL (10 mm \times 10 mm) quartz cuvette. The test solution was sealed with a cap, and thoroughly mixed; and fluorescent emission at 465 nm was recorded every 10 minutes ($n=13$) ($\lambda_{\text{ex}}=400$ nm; slit width: ex: 5nm, em: 3 nm). Fluorescence intensities obtained were converted to NaHSO_3 concentrations using the standard curve described above. All runs were in triplicates (Figure 1-23(B)).

(A)



(B)

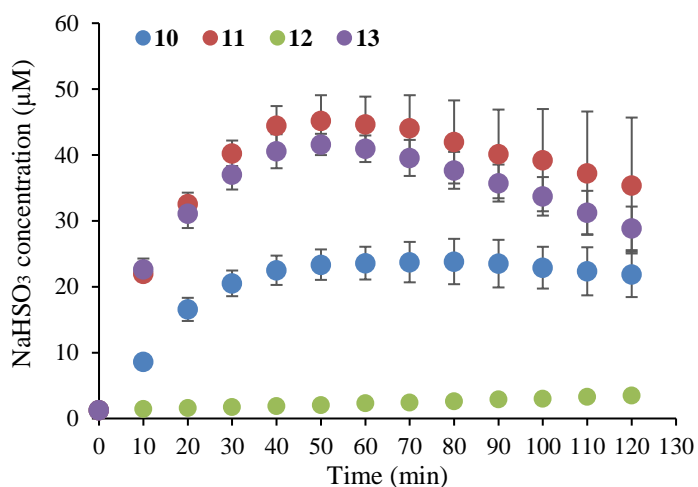


Figure 1-23 Kinetics study of esterase-triggered SO₂ release from compound **10-13** by fluorescent probe **14**.

(A) Standard curve. (B) Kinetics of esterase-triggered SO₂ release from compounds **10-13** monitored with fluorescent probe **14**.

1.3.2.8 Cell imaging study

Cell culture:

HeLa cells were maintained in Dulbecco's Modified Eagle's Medium (DMEM) supplemented with 10 % fetal bovine serum and 1% penicillin-streptomycin at 37 °C with 5 %

CO₂. The media was changed every other day. Experiment was done within 10 passages of HeLa cells.

Cell imaging:

HeLa cells were pre-seeded onto coverslips in 6-well plate a day before experiment. A 2-mM DMSO stock solution of probe **14** was prepared. Compound **13** was prepared as 20-mM DMSO stock solution. Cells were first treated with compound **13** to make a final concentration of 100 μ M (0.5% DMSO). 400 μ M NaHSO₃ was used as a positive control. A mixture containing 100 μ M 2-OHBT and 100 μ M 2-methyl-1-phenyl-propene was used as the negative control. Cell only group was also used as negative controls. All final media contained 0.5% DMSO. The cells were incubated at 37 °C for 2 hours and washed with PBS once. 2 mL of fresh DMEM media was added into each well. The cells were then treated with probe **14** to give a final concentration of 10 μ M. Cells were incubated for another 0.5 h at 37 °C. After washing twice with PBS, the cells were fixed with 4% paraformaldehyde for 30 min at room temperature. The cells were then washed once with PBS. Then 25 mM glycine in PBS was added to quench the extra formaldehyde. After storing at 4 °C overnight. The glycine solution was discarded. All coverslips were immersed in DI water and mounted onto glass slides using DAPI-free mounting media (ProLong Live Antifade Reagent; P36974). Fluorescent imaging was performed on a Zeiss fluorescent microscope using the DAPI channel (λ_{ex} : 358 nm, λ_{em} : 461 nm).

2 DESIGN AND SYNTHESIS OF PRODRUGS OF THIAMINE MONOPHOSPHATE MIMICS AS PYRUVATE DEHYDROGENASE KINASE INHIBITORS

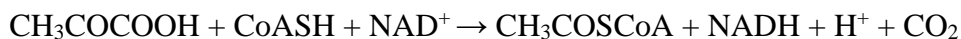
2.1 Introduction

An increased glucose uptake followed by fermentation to lactate is the most common feature of metabolism change of cancer cells. This effect was named as “Warburg effect” after its discoverer Otto Warburg.¹⁰⁰ Unlike the upregulation of fermentation in normal cells as a response to hypoxia environment, excessive fermentation was observed in many cancer cells even in the presence of oxygen and was thus termed as “aerobic glycolysis” by Warburg and his colleagues.¹⁰¹ Though early thought to result from damaged mitochondrial function, Racker and colleagues later revealed that the aerobic glycolysis also exists in presence of fully functional mitochondria.¹⁰⁰ Despite the recent advances of genetic and pharmacological study, well accepted explanation of its origin remains unavailable. Nevertheless, several hypotheses have been put forward to give some rationale of this effect.¹⁰² Although “uneconomic” in terms of glucose consumption, the ATP production rate of glycolysis is 10 to 100 times faster than mitochondrial oxidative phosphorylation, affording a comparable rate to compensate the energy demand of cancer cell growth.¹⁰³ This fast consumption of glucose can also provide cancer cells advantage to compete for more glucose, providing carbon source for biosynthesis of nucleotides, lipids, proteins, and most importantly NADPH, which is in greater need than ATP in cell proliferation.¹⁰⁴⁻¹⁰⁵ Moreover, the acidification of the microenvironment caused by increase production of lactate can facilitate cancer cell metastasis by altering the tumor-stroma interface while competition for glucose would suppress the function of tumor-infiltrating lymphocytes (TIL), whose function is to kill tumor cells.¹⁰⁶⁻¹⁰⁷

The alteration of cancer cell energy metabolism has provided potential targets for cancer therapy. The decreased activity of thiamine-dependent enzyme - pyruvate dehydrogenase complex (PDC, PDH complex) is one of the most critical steps that regulate the enhanced glycolytic activity in cancer cells. PDC converses pyruvate into carbon dioxide and acetyl-CoA through pyruvate decarboxylation while producing NADH. A reduced activity of PDC will limit the carbon flux into the tricarboxylic acid (TCA) cycle and force glucose carbons into lactic acid fermentation.¹⁰⁸

2.1.1 PDC structure and function

Human PDC is a large enzyme consisting of multiple copies of six major components: pyruvate dehydrogenase (PDH, E1), dihydrolipoyl transacetylase (E2), dihydrolipoyl dehydrogenase (E3), E3 binding protein (E3BP), and two regulatory enzymes: pyruvate dehydrogenase kinase (PDK) and pyruvate dehydrogenase phosphatase (PDP).¹⁰⁹⁻¹¹⁰ The complex structure is organized around a scaffold of E2 that allows pyruvate to go through sequential reactions in the complex to produce CO₂ and acetyl-CoA (Figure 2-1). PDH is an $\alpha_2\beta_2$ heterotetramer with two active sites that catalyze the decarboxylation of pyruvate under the assistance of thiamine pyrophosphate (TPP, or vitamin B₁) to produce CO₂. It also catalyzes the reductive acetylation of the lipoyl groups of E2. Sequentially, E2 transfers the acetyl group to coenzyme A to form acetyl-CoA. E3 catalyzes the electron transfer from the dihydrolipoyl moieties of E2 to FAD⁺. FADH₂ will be oxidized back to FAD⁺ while reducing NAD⁺ to NADH. The overall reaction catalyzed by PDC is as follows:¹¹¹



In this process, the decarboxylation step catalyzed by PDH is the rate-limiting step.¹¹¹⁻¹¹²

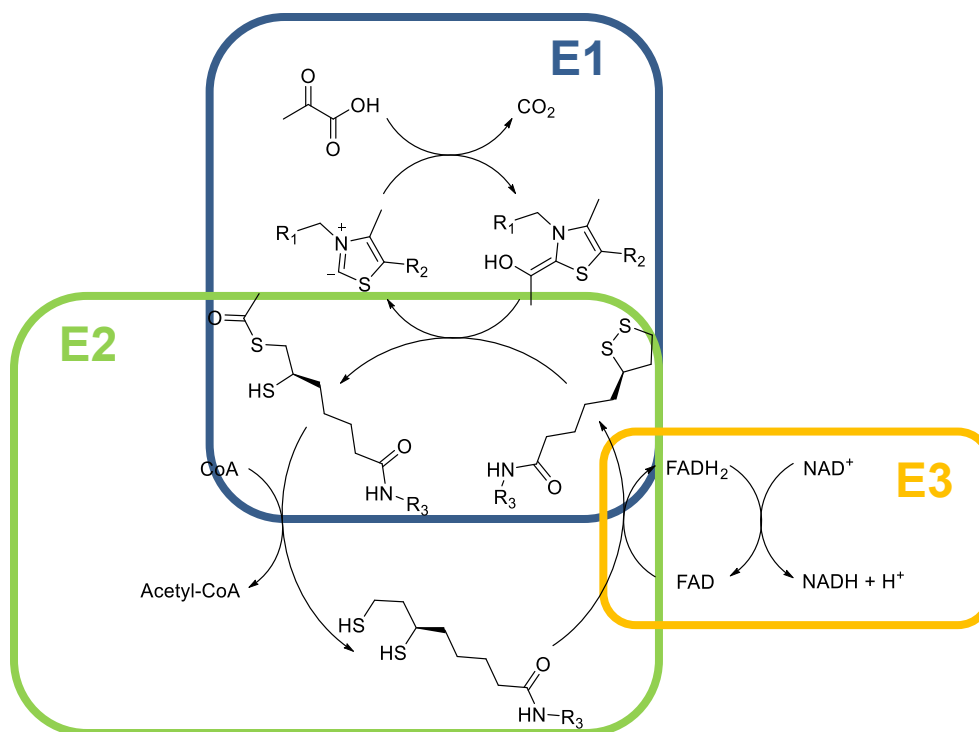


Figure 2-1 Reactions catalyzed by PDC

2.1.2 PDC regulation by PDK and PDP

The activity of mammalian PDC is primarily regulated by reversible phosphorylation of PDH by PDK and PDP.¹¹¹⁻¹¹² PDK attaches to one of the two lipoyl domains (L2) of E2 to reach PDH core and inactivates PDH by phosphorylating one or more of its three serine residues (site 1: Ser-293, site 2: Ser-300, and site 3: Ser-232) on the α subunit of PDH.¹¹³ Phosphorylation of site 1 is the fastest and most well-known mechanism of deactivating PDC, while reactivation of PDC by PDP dephosphorylation are of similar rates at all three sites.¹¹⁴

Mammalian PDK family consists of four isozymes (PDK1, PDK2, PDK3, and PDK4) with varied tissue distribution. PDK1 is mainly expressed in heart; PDK3 is primarily expressed in testis; PDK2 is universally expressed in all tissues only with lower level in spleen and lung; PDK4 was found in skeletal muscle and heart.¹¹⁵ An elevated level of PDK1 expression has been

observed in various cancer cells such as breast, head and neck, and lung cancers.¹¹⁶⁻¹¹⁷ The tissue-specific distribution of PDK isoenzymes would provide potential targets for treating diabetes, heart ischemia, and cancer.^{110, 118} Knock-down of PDK1 will result in restored PDH activity and glucose oxidation, as well as reduced lactate production and suppressed tumor growth.¹¹⁹ Despite the tissue distribution specificity, PDK isozymes also showed site selective phosphorylation on the PDH serine residues. Site 1 and site 2 can be phosphorylated by all four isozymes, while site 3 can only be phosphorylated by PDK1.¹²⁰

Inhibition of PDC activity by PDK are associated with many physiological and pathophysiological processes such as lactic acidosis, diabetes, cerebrovascular and cardiovascular diseases, late-onset neurodegenerative diseases, pulmonary arterial hypertension, aging, and cancer.¹²¹ The activity of PDK isozymes can be stimulated by ATP, NADH, and acetyl-CoA with different sensitivity, while pyruvate and ADP can inhibit PDK activity.¹¹⁴ PDK family also serves as direct transcriptional target of hypoxia inducible factor 1 α (HIF1 α), which is upregulated in hypoxic tumor cells.¹²²⁻¹²⁴ Therefore, the overexpression of PDK is adopted by cancer cells to inactivate PDH as an important way to guarantee cancer cells' survival.

2.1.3 PDK inhibition for cancer therapy

The fact that PDK expression and activity can be upregulated by HIF1 α and downregulated by tumor suppressor protein p53 further supported the important role PDK plays in cancer development.¹²⁵ Inhibition of PDK-mediated phosphorylation of PDH has been considered a promising way for reducing cancer cell proliferation.^{121, 126-127} Restoring PDH activity by blocking PDK-regulated deactivation can lead to normalized glycolysis and redirect glucose carbons into TCA cycle, forcing the production of ROS by mitochondria, which in turn leads to HIF1 α downregulation and apoptosis.¹²⁶ On the other hand, decreased production of

lactate through glycolysis may limit the biosynthesis of nucleotides, which may also lead to growth inhibition of cancer cells. Moreover, PDK overexpression in cancer cells provides an opportunity to target PDK activity selectively to avoid cytotoxicity towards normal tissue.¹²⁸

Compounds that can inhibit PDK activity would help to re-establish PDH activity in cancer cells and inhibit cell proliferation. It has been demonstrated both *in vitro* and *in vivo* that inhibiting PDK activity will lead to decreased viability in multiple types of cancer cells.¹²⁹⁻¹³⁰ Despite substrate-level regulation by pyruvate, NAD⁺, and CoA, many PDK inhibitors have been reported so far targeting four binding sites: pyruvate binding site, lipoamide binding site, and allosteric site located in the regulatory N-terminal R domain, and an nucleotide binding site (Figure 2-2).^{114, 121}

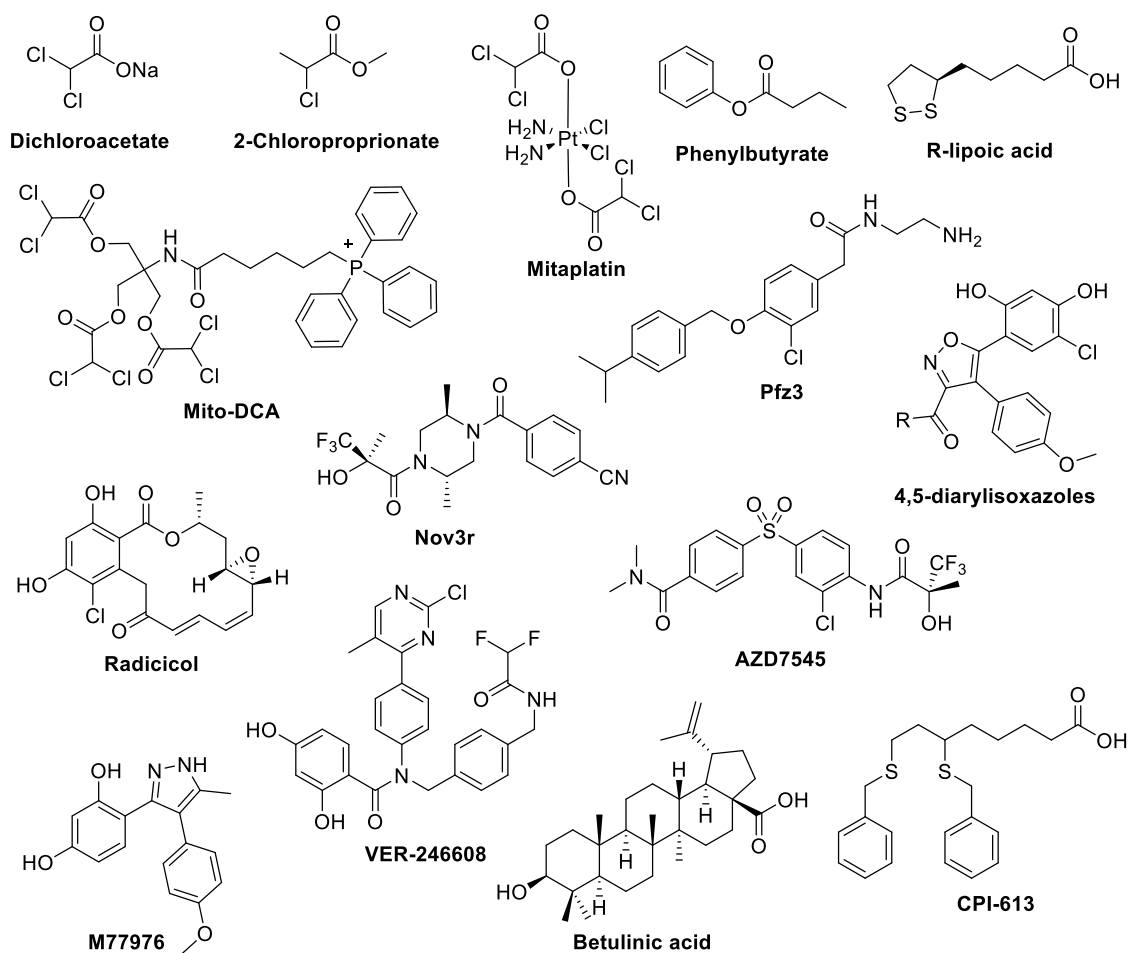


Figure 2-2 Representative PDK inhibitors

2.1.3.1 Dichloroacetate (DCA)

Dichloroacetate (DCA) is the first PDK inhibitor developed into clinical use for treatment of multiple PDC deficiency diseases including type 2 diabetes, hyperlipoproteinemias, myocardial ischemia and failure, and lactic acidosis.^{121, 131} In recent years, DCA has also shown profound effect in inhibiting tumor cell growth in a number of cancer cell lines including breast, endometrial, lung, and colorectal by acting as a pyruvate mimic.^{126-128, 132-133} DCA was shown to be able to bind to two sites on PDK: the pyruvate binding pocket, which would adversely affect the binding of PDK to PDC;¹³⁴ and the allosteric site, which would cause conformational changes to the nucleotide and lipoamide binding sites.¹³⁵⁻¹³⁶ DCA can be well tolerated by

human only with minor reversible effects on the nervous system and liver upon chronic administration.¹³⁷ Upon oral or parenteral administration, DCA can be rapidly absorbed and can penetrate the blood-brain barrier. As a result, DCA was therefore widely investigated on human glioblastoma (GBM) cells, which is the most prevalent and malignant form of brain tumor.¹²¹ Besides its stimulating effect on tumor oxygen consumption, it was reported that DCA can also inhibit mitochondrial fatty acid β -oxidation, which would lead to inhibition of endothelial cell growth.¹³⁸

Despite the great academic interest in its potential as an anti-cancer agent, DCA in its original form received little investment from the pharmaceutical industry, since it is no longer patentable after its debut in the public more than 30 years ago. Therefore, many DCA prodrugs with multi-molar DCA loading and DCA mimics have been reported over the years (Figure 2-2). For example, 2-chloropropionate replaced one chlorine in DCA with a methyl group; Mitaplatin contains two molecules of DCA bound to cisplatin; Mito-DCA contains 3 molecules of DCA and a mitochondria-targeting triphenylphosphonium moiety. (Figure 2-2) Besides patentability interest, such modifications would also provide improved drug properties such as higher potency and increased stability.¹²¹

2.1.3.2 Thiamine and analogues as PDK inhibitors

Thiamine, also known as vitamin B₁, is an important dietary supplement that can be found in many food sources such as whole grains, meat, and fish. Cellular uptake of thiamine is through active transportation by thiamine transporters (THTRs). In mammalian cells, thiamine can be di-phosphorylated by thiamine diphosphokinase to produce thiamine pyrophosphate (TPP), which is an important coenzyme for several enzymes. Therefore, thiamine is regarded as the transport form of TPP to allow transmembrane delivery.¹³⁹ TPP is also a coenzyme of PDH,

whose function is essential for PDH catalyzed trans-acetylation. (Figure 2-1) It has been reported that binding of TPP to PDH alters the rate and stoichiometry of phosphorylation of the individual sites.¹²⁰ TPP decreased both the rate and extent of PDH phosphorylation by PDK isoforms.

Therefore, increased TPP concentration may help restore PDH activity. Previous research from Cascante's group showed that thiamine demonstrated a dichotomous effect that stimulates cancer cell growth at low concentration (12.5 to 75 times of recommended daily allowance, 20 µg/kg) and inhibits cell growth at high concentration (above 75 times of recommended daily allowance).¹⁴⁰ Also reported by our collaborator, Dr. Jason Zastre's group, high-dose thiamine decreased proliferation in a mechanism similar to that of DCA by reducing phosphorylation of PDH.¹⁴¹ Thiamine showed lower IC₅₀ in both SK-N-BE (4.9 mM) and Panc-1 (5.4 mM) cell lines, when compared with DCA (23.8 for SK-N-BE and 10.3 mM for Panc-1). Moreover, as a dietary supplement, thiamine can be very well tolerated by human that an oral dosage as high as 1.5g/day showed no adverse effects in healthy patients.¹⁴² Therefore, thiamine analogues with PDK inhibitory potency would provide a new strategy to target cancer cell metabolism.

2.2 Results and discussion

PDK has four isoenzymes: PDK1, PDK2, PDK3, and PDK4. Evaluation of the amino acid sequences of the isozymes proved that the ATP binding pockets of the isozymes are identical despite minor differences of tertiary structures. PDK1 and PDK4 possess complete ATP binding site structure and are therefore suitable for binding modeling assays. Moreover, increased expression of PDK1 is observed in multiple types of cancer cells. Therefore, PDK1 would be the most suitable isozyme for anticancer study. Previously in our group, four novel thiamine analogues (**BW-VB-1** to **BW-VB-4**, Table 2-1) were designed and tested *in silico* against PDK1. Two of the analogues – **BW-VB-3** and **BW-VB-4** showed good potency in

docking studies with docking score of 5.9 and 5.45, respectively, indicating the best binding affinity towards PDK1. We further expanded the data base to 19 analogues in collaboration with Dr. Bowen Ke's group (**BW-VB-1** to **BW-VB-19**, Table 2-1). Modifications have been made on the pyrimidine ring and ethanolic chain, while the thiazolium ring was replaced by triazole ring. The principle of making such modifications is to introduce enough structural difference to allow binding optimization. The synthesized analogues were tested against HCT116 cells for inhibitory effect. To our disappointment, these thiamine analogues demonstrate only limited inhibitory effect on cancer cell proliferation with the lowest IC_{50} being 0.612 mM (**BW-VB-13**).

Table 2-1 IC_{50} of first-batch thiamine analogues

Compound	Structure	IC_{50} (mM)	Compound	Structure	IC_{50} (mM)
Thiamine		>1	BW-VB-10		>1
BW-VB-1		5.923	BW-VB-11		>1
BW-VB-2		>10	BW-VB-12		0.725
BW-VB-3		7.82	BW-VB-13		0.612
BW-VB-4		6.23	BW-VB-14		0.828
BW-VB-5		1.09	BW-VB-15		0.875
BW-VB-6		3.32	BW-VB-16		>1.0
BW-VB-7		1.026	BW-VB-17		>1.0
BW-VB-8*		>1	BW-VB-18		0.814
BW-VB-9*		>1	BW-VB-19		>1.0

Note: * Compounds were tested against Panc-1 cell line.

We hypothesize that the low inhibitory effect may be caused by a lack of phosphorylation of the analogues. *In silico* binding assay indicates phosphorylated thiamine analogue would have much higher binding affinity to PDK compared with respective non-phosphorylated analogue.

Since kinases that can phosphorylate thiamine could be selective towards thiamine structure, the analogues may not be able to be phosphorylated inside the cell. In this case, we could either screen thiamine analogues that serve as substrate for specific kinases, or we would directly deliver phosphorylated thiamine analogues. The first method can be very time and effort consuming considering the possibility that the substrates of thiamine diphosphokinase and PDK inhibitor may not share the same structure(s). While the second method is also problematic since phosphorylated thiamine analogue may not be permeable enough to cross cell membrane due to the high polarity introduced by a phosphate group. To address this problem, we turned to phosphate prodrug strategy that have been widely applied in delivery of antiviral nucleoside phosphates and phosphonates.¹⁴³ (Figure 2-3)

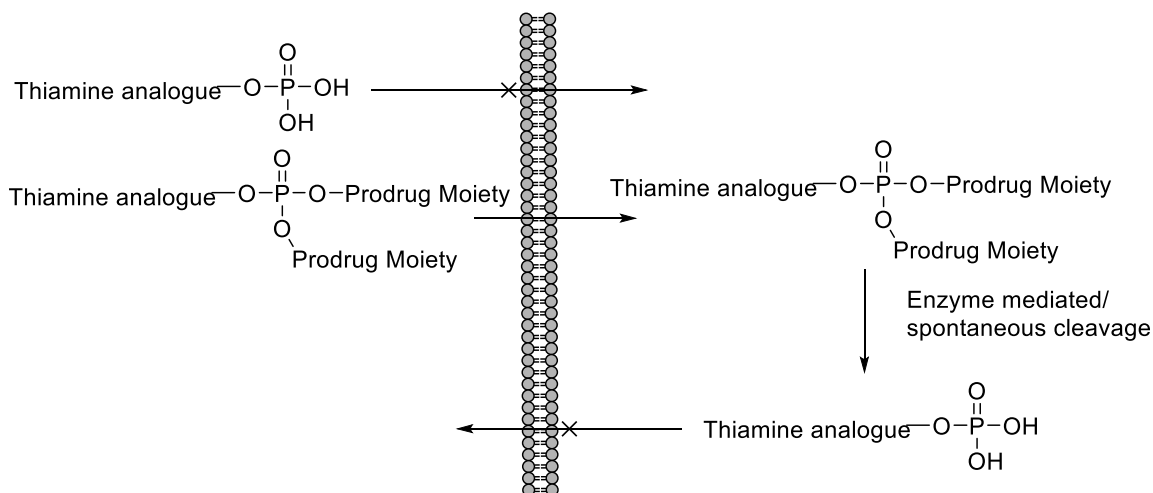


Figure 2-3 Prodrug strategy to deliver phosphorylated thiamine analogue into the cell

To test this idea, we planned to attach a phosphate moiety on the hydroxyl group of each of the thiamine analogues to better mimic the binding mode of thiamine metabolites. To mask the charges on phosphate group, the free phosphate groups were attached with prodrug moieties. (Figure 2-4) Once the molecule is delivered into the cell, prodrug moiety can be cleaved either by enzyme mediated hydrolysis or by spontaneous hydrolysis. Then phosphorylated thiamine

analogue would be released. The high polarity of free phosphate would prevent the drug molecule from permeating out of the cell, which would allow better interaction with intracellular target(s).

We used several thiamine analogues as the “drug” part and attached different phosphate prodrug moieties on the hydroxy group. We picked three phosphate prodrug approaches with synthetic ease and proved release efficiency: 1. bis(*S*-acyl-2-thioethyl), bis(SATE); 2. aryloxyphosphoramidate, ProTide; 3. (bis(pivaloyloxymethyl), bis(POM). Besides, we made a small modification on the SATE moiety and obtained a carbonothionate structure (2-(*t*-butoxycarbonylthio)ethoxyl, BOCTE). We expected this structure to be less stable under physiological condition and be more susceptible to hydrolysis compared with SATE prodrugs. (Figure 2-4) The phosphate prodrug moieties were attached to the hydroxyl group of the respective alkyne following literature reported procedure with necessary modification.¹⁴⁴⁻¹⁴⁵ (Figure 2-4) The prodrugs were then assembled through copper(I)-catalyzed “click” reaction with 5-(azidomethyl)-2,4-dimethoxypyrimidine. The resulted prodrugs were subjected to cell proliferation assay using HCT116 cells. (Table 2-2)

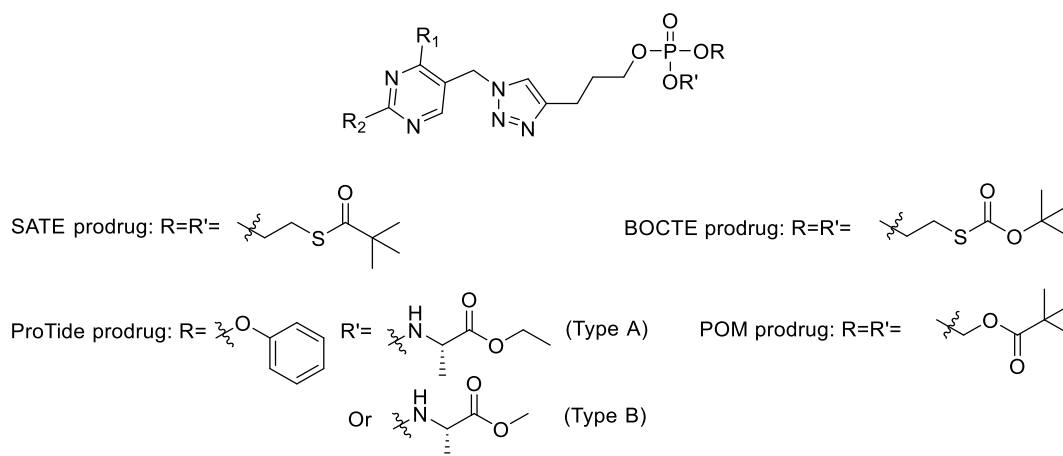
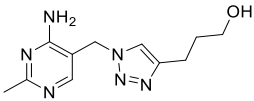
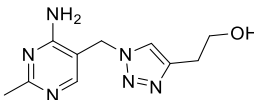
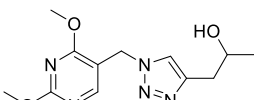
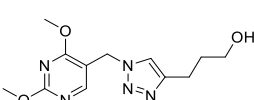
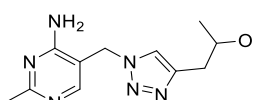
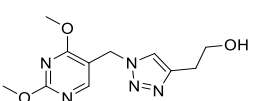
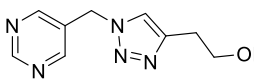


Figure 2-4 Prodrug structures

From cell proliferation assay results, we can see that compared with the thiamine analogues without phosphate groups, the phosphate prodrugs demonstrated significantly higher inhibitory effects against cancer cell lines than the drug itself. Several compounds have shown IC_{50} lower than 100 μ M, indicating a >10 times higher potency than the corresponding thiamine analogues. The inhibitory potency demonstrated by the prodrugs seems to have little connection with their parental drug. Comparing different prodrug strategies, SATE prodrugs and POM prodrugs showed the best inhibitory effects in general. This advantage could be the result from the chemical stability of the prodrug moieties that SATE and POM prodrugs are more prone to release phosphate drugs under tested conditions. It is also possible that the side products associated with these two prodrug moieties have certain cytotoxicity. Different prodrug moieties may also cause varied uptake efficiency of the prodrugs by the cells. The results confirmed our hypothesis that the phosphate prodrug strategy could increase the potency of thiamine analogues.

To better understand the inhibitory mechanism, more specific research is going on in Dr. Zastre's lab. Candidate optimization is an iterative process. It is important to build structure-activity relationship (SAR) to allow better understanding of the binding between phosphorylated thiamine analogues and PDK. These problems will be further investigated in the future.

Table 2-2 IC_{50} of phosphate prodrugs of thiamine analogues

Thiamine analogue/ IC_{50}	Structure	Compound # (BW-VB-#) / IC_{50} (mM)				
		SATE prodrug	BOCTE prodrug	ProTide prodrug (Type A)	ProTide prodrug (Type B)	POM prodrug
BW-VB-2/ >10		29/0.04	--	30/0.107	41/0.336	31/0.081
BW-VB-3/ 7.82		27/0.085	--	34/>>0.25	40/0.656	28/0.075
BW-VB-8/ >1		21/0.049	23/0.111	26/0.1	--	--
BW-VB-11/ >1		20/0.060	22/0.105	24/0.248	--	25/0.044
BW-VB-14/ 0.828		35/0.088	--	42/0.624	--	--
BW-VB-39/ >1		32/0.043	--	--	--	33/0.045
BW-VB-43/ 0.339		44/0.126	45/0.256	46/0.557	47/0.501	--

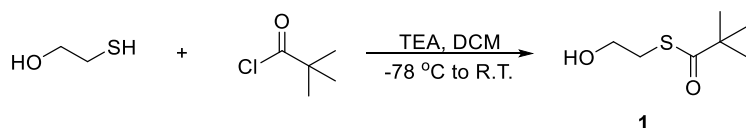
2.3 Experimental procedures

2.3.1 Materials and Methods

All reagents and chemicals were purchased from commercial suppliers as reagent grade or higher and were used without further purification unless otherwise noted. NMR spectra were recorded on a Bruker Avance NMR spectrometer at 400 MHz for ^1H , 101 MHz for ^{13}C , and 162

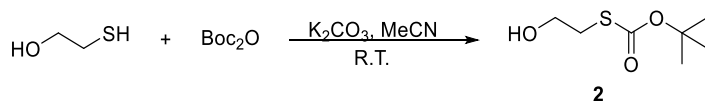
MHz for 31P at room temperature unless otherwise specified. Solvent peaks were used as internal standards. Mass spectral analyses were performed by the GSU Mass Spectrometry Facilities. The synthesis of compounds **BW-VB-1** to **BW-VB-7** were previous reported by Dr. Hieu Dinh in his Master thesis.¹⁴⁶ Compound **BW-VB-12** to **BW-VB-19** were provided by Dr. Bowen Ke's lab. Cell proliferation assays were conducted by Dr. Jason Zastre's lab.

2.3.2 Synthesis



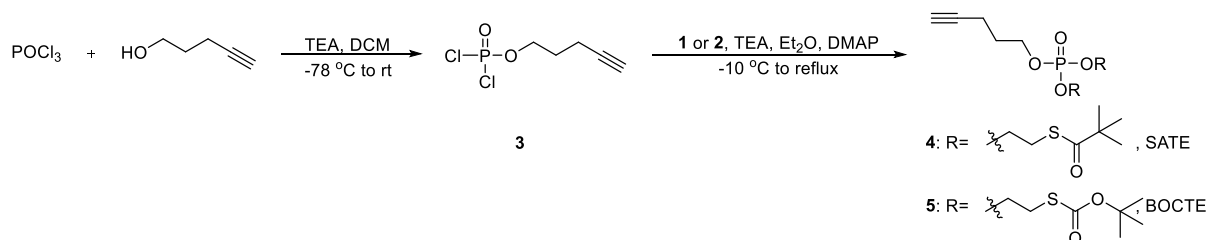
S-(2-hydroxyethyl) 2,2-dimethylpropanethioate (1)

Synthesis of *S*-(2-hydroxyethyl) 2,2-dimethylpropanethioate followed literature procedures.¹⁴⁵ Briefly, 0.32 mL pivaloyl chloride (2.6 mmol) was added to a stirred solution of 2-mercaptoethanol (0.18 mL, 2.6 mmol) and trimethylamine (TEA, 0.36 mL, 2.6 mmol) in 5 mL dichloromethane (DCM) at -78 °C under argon protection. The reaction mixture was stirred at -78 °C for 1 h, and then allowed to warm up to room temperature. The reaction was stirred for an additional 1 h and quenched by water (3mL). The organic layer was separated. The aqueous phase was extracted with DCM (3×10 mL). The combined organic phase was dried over Na₂SO₄ and concentrated *in vacuo*. Column chromatography was used to purify the residue (silica gel, hexane/EtOAc 10:1 to 4:1). 410 mg of the title product was obtained as clear oil. Yield: 97%. NMR data matched that of the literature report.



O-(*tert*-butyl) S-(2-hydroxyethyl) carbonothioate (2)

718 mg K_2CO_3 (5.2 mmol) and 568 mg Boc_2O (2.6 mmol) were added to a 50-mL round bottom flask with 20 mL MeCN. 2-Mercaptoethanol was then added into the solution. The solution was stirred at room temperature for 2 days. K_2CO_3 was filtered off. MeCN was used to wash the filter cake. The filtrate was then dried over Na_2SO_4 and concentrated in vacuo. The oil-like residue was purified by column chromatography (silica gel, hexane/EtOAc 10:1 to 2:1) to give 381 mg product as clear oil. Yield: 82%. NMR data match well with literature report.¹⁴⁷



Pent-4-yn-1-yl phosphorodichloridate (3)

1 mL phosphorus oxychloride (10.7 mmol) was added to a solution of 4-pentyn-1-ol (10.7 mmol) in 25 mL DCM at -78°C under argon protection. TEA (1.64 mL, 11.77 mmol, 1.1 equiv.) was added dropwise to the solution. The reaction mixture was slowly warmed up to room temperature and stirred for another 10 min. Then the solution was quenched by pouring onto ice and extracted with DCM (2×30 mL). The combined organic phase was dried over Na_2SO_4 and concentrated in vacuo. The residue was purified by column chromatography (silica gel, hexane/EtOAc 10:1). 1.2 g product was obtained as clear oil. Yield: 56%. ^1H NMR (CDCl_3) δ 4.59 – 4.40 (m, 2H), 2.41 (t, $J = 6.8$ Hz, 2H), 2.14 – 1.91 (m, 3H). ^{13}C NMR (CDCl_3) δ 81.7, 70.4 (d, $J = 9.2$ Hz), 70.0, 28.3 (d, $J = 9.3$ Hz), 14.6. ^{31}P NMR (162 MHz, CDCl_3) δ 7.06.

Pent-4-yn-1-yl bis(SATE) phosphate (4)

Pent-4-yn-1-yl phosphorodichloridate (3, 200 mg, 1 mmol) and DMAP (13 mg, 0.1 mmol, 0.1 equiv.) were dissolved in 15 mL Et_2O and cooled to -10°C under argon protection. Then *S*-(2-hydroxyethyl) 2,2-dimethylpropanethioate (1, 648 mg, 4 mmol, 4 equiv.) was added

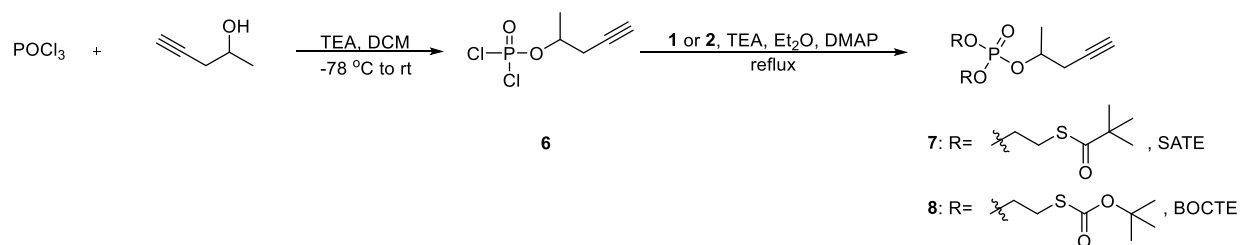
to the solution in one portion. TEA (0.29 mL, 2.1 mmol, 2.1 equiv.) was added dropwise to the solution with stirring. The reaction mixture was allowed to warm up to room temperature and heated up to reflux overnight. Then the reaction mixture was mixed with 10 mL of water and extracted with EtOAc (3×30 mL). The combined organic phase was dried over Na₂SO₄, concentrated in vacuo and purified by column chromatography (silica gel, hexane/EtOAc 20:1 to 5:1). 164 mg product was obtained as clear oil. Yield: 36%. ¹H NMR (CDCl₃) δ 4.18 (dd, *J* = 13.1, 6.2 Hz, 2H), 4.14 – 4.03 (m, 4H), 3.14 (q, *J* = 6.4 Hz, 4H), 2.33 (td, *J* = 7.0, 2.7 Hz, 2H), 1.97 (t, *J* = 2.7 Hz, 1H), 1.90 (dd, *J* = 7.0, 6.1 Hz, 2H), 1.24 (s, 18H). ¹³C NMR (CDCl₃) δ 205.7, 82.7, 69., 66.4 (d, *J* = 6.0 Hz), 66.1 (d, *J* = 5.7 Hz), 50.7, 46.5, 29.0 (d, *J* = 7.2 Hz), 28.6 (d, *J* = 7.5 Hz), 27.3, 14.7. ³¹P NMR (CDCl₃) δ -1.82 (dt, *J* = 14.9, 7.4 Hz). HRMS (ESI): calcd for C₁₉H₃₃NaO₆PS₂ [M+Na]⁺ 475.1348, found 475.1335.

Pent-4-yn-1-yl bis(2-((*tert*-butoxycarbonyl)thio)ethanyl) phosphate (5)

The synthesis of **5** follows similar procedure with the synthesis of **4**. Pent-4-yn-1-yl phosphorodichloridate (**3**, 200 mg, 1 mmol) and DMAP (13 mg, 0.1 mmol, 0.1 equiv.) were dissolved in 15 mL Et₂O and cooled to -10 °C under argon protection. Then O-(*tert*-butyl) S-(2-hydroxyethyl) carbonothioate (**2**, 380 mg, 2.13 mmol, 2.13 equiv.) was added to the solution in one portion. TEA (0.29 mL, 2.1 mmol, 2.1 equiv.) was added dropwise to the stirring solution. The reaction mixture was allowed to warm up to room temperature and heated up to reflux overnight. Then to the reaction mixture was added 10 mL of water and resulting solution was extracted with EtOAc (3×30 mL). The combined organic phase was dried over Na₂SO₄, concentrated in vacuo and purified by column chromatography (silica gel, hexane/EtOAc 20:1 to 5:1). 173 mg product was obtained as clear oil. Yield: 36%. ¹H NMR (CDCl₃) δ 4.25 – 4.08 (m, 6H), 3.07 (t, *J* = 6.6 Hz, 4H), 2.32 (td, *J* = 7.0, 2.6 Hz, 2H), 1.96 (t, *J* = 2.7 Hz, 1H), 1.92 – 1.81

(m, 2H), 1.48 (s, 18H). ^{13}C NMR (CDCl_3) δ 168.2, 85.4, 82.7, 69.3, 66.3 (dd, $J = 21.2, 5.8$ Hz), 30.9 (d, $J = 7.4$ Hz), 29.0 (d, $J = 7.3$ Hz), 28.2, 14.7. ^{31}P NMR (CDCl_3) δ -1.42 – -2.16 (m).

HRMS (ESI): calcd for $\text{C}_{19}\text{H}_{33}\text{NaO}_8\text{PS}_2$ [$\text{M}+\text{Na}$] $^+$ 507.1247, found 507.1258.



Pent-4-yn-2-yl phosphorodichloridate (6)

1 mL phosphorus oxychloride (10.7 mmol) was added to a solution of 4-pentyn-2-ol (10.7 mmol) in 25 mL DCM at -78°C under argon protection. TEA (1.64 mL, 11.77 mmol, 1.1 equiv.) was added dropwise to the solution. The reaction mixture was slowly warmed up to room temperature and stirred for another 10 min. Then the solution was quenched by pouring onto ice and extracted with DCM (2×30 mL). The combined organic phase was dried over Na_2SO_4 and concentrated in vacuo. The residue was purified by column chromatography (silica gel, hexane/ EtOAc 10:1). 1.0 g product was obtained as clear oil. Yield: 47%. ^1H NMR (CDCl_3) δ 5.11 – 4.83 (m, 1H), 2.82 – 2.55 (m, 2H), 2.12 (t, $J = 2.4$ Hz, 1H), 1.59 (d, $J = 6.2$ Hz, 3H). ^{13}C NMR (CDCl_3) δ 79.2 (d, $J = 9.1$ Hz), 77.7, 72.0, 27.0 (d, $J = 7.1$ Hz), 20.5 (d, $J = 4.4$ Hz). ^{31}P NMR (162 MHz, CDCl_3) δ 6.61 (d, $J = 11.1$ Hz).

Pent-4-yn-2-yl bis(SATE) phosphate (7)

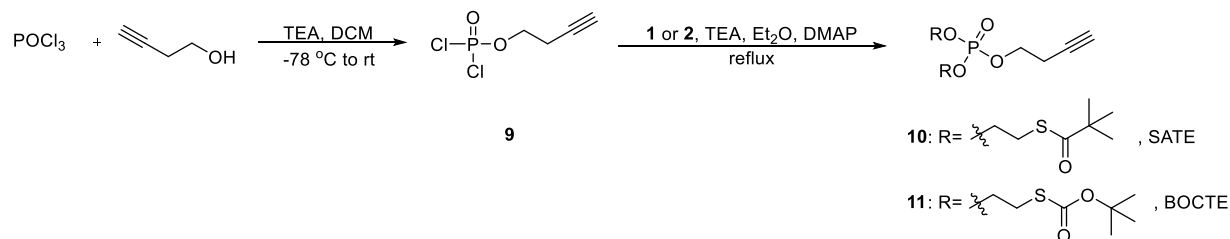
Pent-4-yn-2-yl phosphorodichloridate (6, 200 mg, 1 mmol) and DMAP (13 mg, 0.1 mmol, 0.1 equiv.) were dissolved in 15 mL Et_2O and cooled to -10°C under argon protection. Then S-(2-hydroxyethyl) 2,2-dimethylpropanethioate (1, 366 mg, 2.2 mmol, 2.2 equiv.) was added to the solution in one portion. TEA (0.29 mL, 2.1 mmol, 2.1 equiv.) was added dropwise

to the solution with stirring. The reaction mixture was allowed to warm up to room temperature and then heated at reflux overnight. Then to the reaction mixture was added 10 mL of water and the resulting mixture was extracted with EtOAc (3×30 mL). The combined organic phase was dried over Na₂SO₄, concentrated in vacuo and purified by column chromatography (silica gel, hexane/EtOAc 20:1 to 5:1). 163 mg racemic product was obtained as clear oil. Yield: 36%. ¹H NMR (CDCl₃) δ 4.62 (dp, *J* = 12.8, 6.3 Hz, 1H), 4.22 – 3.99 (m, 4H), 3.15 (td, *J* = 6.6, 1.6 Hz, 4H), 2.66 – 2.42 (m, 2H), 2.04 (t, *J* = 2.7 Hz, 1H), 1.45 (d, *J* = 6.2 Hz, 3H), 1.24 (s, 18H). ¹³C NMR (CDCl₃) δ 177.9, 78.8, 74.4 (d, *J* = 8.4 Hz), 71.4, 62.7 (dd, *J* = 4.8, 2.7 Hz), 38.8, 30.8 – 30.5 (m), 27.5 (d, *J* = 5.6 Hz), 27.1, 21.1 (d, *J* = 3.9 Hz). ³¹P NMR (CDCl₃) δ 54.30 (pd, *J* = 16.5, 10.5 Hz). HRMS (ESI): calcd for C₁₉H₃₃NaO₆PS₂ [M+Na]⁺ 475.1348, found 475.1348.

Pent-4-yn-2-yl bis(2-((*tert*-butoxycarbonyl)thio)ethanyl) phosphate (8)

Pent-4-yn-2-yl phosphorodichloridate (**6**, 200 mg, 1 mmol) and DMAP (13 mg, 0.1 mmol, 0.1 equiv.) were dissolved in 15 mL Et₂O and cooled to -5 °C under argon protection. Then O-(*tert*-butyl) S-(2-hydroxyethyl) carbonothioate (**2**, 375 mg, 2.1 mmol, 2.1 equiv.) was added to the solution in one portion. TEA (0.29 mL, 2.1 mmol, 2.1 equiv.) was added dropwise to the solution stirring. The reaction mixture was allowed to warm up to room temperature and heated up at reflux overnight. Then to the reaction mixture was added 10 mL of water and the resulting mixture was extracted with EtOAc (3×30 mL). The combined organic phase was dried over Na₂SO₄, concentrated in vacuo and purified by column chromatography (silica gel, hexane/EtOAc 20:1 to 5:1). 288 mg racemic product was obtained as clear oil. Yield: 60%. ¹H NMR (CDCl₃) δ 4.62 (dp, *J* = 12.5, 6.2 Hz, 1H), 4.25 – 4.09 (m, 4H), 3.08 (td, *J* = 6.7, 2.0 Hz, 3H), 2.64 – 2.45 (m, 2H), 2.04 (t, *J* = 2.7 Hz, 1H), 1.49 (s, 18H), 1.45 (d, *J* = 6.2 Hz, 3H). ¹³C

NMR (CDCl₃) δ 168.2, 85.4, 79.3, 73.7 (d, $J = 5.9$ Hz), 71.1, 66.2 (dd, $J = 5.8, 2.4$ Hz), 30.9 (d, $J = 7.6$ Hz), 28.2, 27.2 (d, $J = 6.2$ Hz), 20.8 (d, $J = 4.1$ Hz). ³¹P NMR (CDCl₃) δ -2.93 (h, $J = 7.6$ Hz). HRMS (ESI): calcd for C₁₉H₃₄O₈PS₂ [M+H]⁺ 485.1427, found 485.1140.



Using the same method described above, compound **9**, **10**, and **11** were prepared accordingly.

But-3-yn-1-yl phosphorodichloridate (**9**)

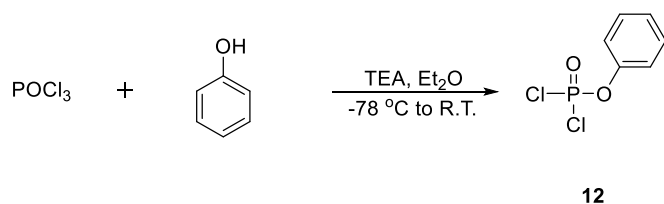
Yield 40%. ¹H NMR (CDCl₃) δ 4.43 (dt, $J = 10.4, 6.8$ Hz, 2H), 2.74 (tdd, $J = 6.8, 2.6, 0.4$ Hz, 2H), 2.12 (t, $J = 2.7$ Hz, 1H). ¹³C NMR (CDCl₃) δ 77.8, 71.5, 68.9 (d, $J = 9.0$ Hz), 20.2 (d, $J = 10.0$ Hz). ³¹P NMR (CDCl₃) δ 7.29 (t, $J = 9.6$ Hz).

But-3-yn-1-yl bis(SATE) phosphate (**10**)

Yield: 59%. ¹H NMR (CDCl₃) δ 4.31 (dd, $J = 14.0, 7.6$ Hz, 4H), 4.28 – 4.19 (m, 2H), 3.17 (dt, $J = 16.5, 6.4$ Hz, 4H), 2.64 (t, $J = 6.6$ Hz, 2H), 2.03 (s, 1H), 1.21 (s, 18H). ³¹P NMR (CDCl₃) δ 55.99 (ddd, $J = 26.0, 16.8, 9.4$ Hz). HRMS (ESI): calcd for C₁₈H₃₁NaO₆PS₂ [M+Na]⁺ 461.1192, found 461.1179.

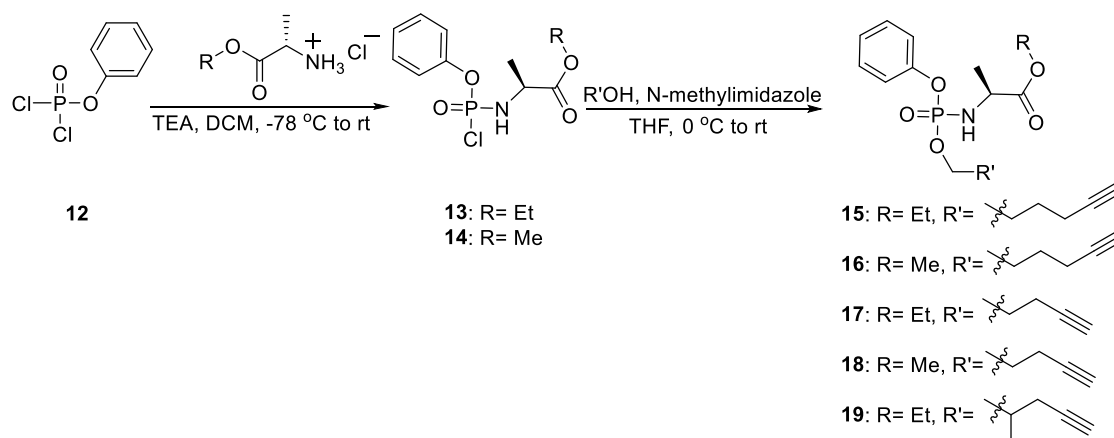
But-3-yn-1-yl bis(2-((tert-butoxycarbonyl)thio)ethyl) phosphate (**11**)

Yield: 46%. ¹H NMR (CDCl₃) δ 4.28 – 3.96 (m, 6H), 3.06 (t, $J = 6.7$ Hz, 4H), 2.58 (td, $J = 6.8, 2.6$ Hz, 2H), 2.01 (t, $J = 2.6$ Hz, 1H), 1.47 (s, 18H). ¹³C NMR (CDCl₃) δ 168.2, 85.4, 79.3, 70.5, 66.3 (d, $J = 5.7$ Hz), 65.5 (d, $J = 5.8$ Hz), 30.9 (d, $J = 7.4$ Hz), 28.2, 20.6 (d, $J = 7.3$ Hz). ³¹P NMR (CDCl₃) δ -2.15 (hept, $J = 7.9$ Hz). HRMS (ESI): calcd for C₁₈H₃₂O₈PS₂ [M+H]⁺ 471.1271, found 471.1260.



Phenyl phosphorodichloridate (12)

To a solution of phosphorus oxychloride (1 mL, 10.7 mmol) in 25 mL of anhydrous diethyl ether was added dropwise a solution of phenol (1.01 g, 10.7 mmol) and TEA (1.5 mL, 10.7 mmol) in 25 mL of anhydrous diethyl ether at $-78\text{ }^{\circ}\text{C}$ under argon atmosphere over 1 h. The solution was allowed to slowly warm up to room temperature and stirred overnight. Then the solution was filtered using Celite[®]. The filtrate was immediately dried over vacuum and kept under high vacuum for 3 h. The crude product was directly used for the next step without further purification.



General procedure of preparing compound 13 and 14

The crude product of phenyl phosphorodichloridate (12) described above was dissolved in 10 mL DCM together with L-alanine alkyl ester hydrogen chloride (10.7 mmol) and cooled to $-78\text{ }^{\circ}\text{C}$ under argon protection. 3 mL TEA (21.4 mmol) dissolved in 10 mL DCM was slowly added to the reaction solution. The reaction solution was allowed to slowly warm up to room temperature and reacted overnight under stirring. Then the reaction was filtered over Celite[®]

(wash with DCM). The filtrate was concentrated and purified by column (silica gel, hexane/EtOAc 20:1 to 2:1).

Ethyl (chloro(phenoxy)phosphoryl)-L-alaninate (13)

Total yield of two steps: 17%. Spectra data correspond well with literature report.¹⁴⁸

Methyl (chloro(phenoxy)phosphoryl)-L-alaninate (14)

Total yield of two steps: 13%. Spectra data correspond well with literature report.¹⁴⁹

General procedure of preparing compound 15, 16, 17, 18, and 19

Alkyl (chloro(phenoxy)phosphoryl)-L-alaninate (**13** or **14**) was prepared as 1 M stock solution in THF. To a solution of alkynyl alcohol (1.19 mmol) and *N*-methylimidazole in 1 mL THF at 0 °C was added dropwise 1.19 mL stock solution of compound **13** or **14**. The resulting mixture was stirred at room temperature for 3 days. Then the reaction mixture was dried over rotavap, premixed with silica gel, and purified by column (silica gel, hexane/EtOAc 20:1 to 2:1) to yield the product.

Ethyl ((pent-4-yn-1-yloxy)(phenoxy)phosphoryl)-L-alaninate (15)

Product (mixture of two diastereomers) was obtained as clear oil. Yield: 46%. ¹H NMR (CDCl₃) δ 7.37 – 7.23 (m, 2H), 7.19 (t, *J* = 7.6 Hz, 2H), 7.11 (t, *J* = 7.3 Hz, 1H), 4.26 – 4.07 (m, 4H), 4.04 – 3.89 (m, 1H), 3.78 (m, *J* = 16.0, 10.5 Hz, 1H), 2.25 (m, 2H), 1.95 (m, 1H), 1.90 – 1.77 (m, 2H), 1.34 (m, 3H), 1.22 (m, 3H). ¹³C NMR (CDCl₃) δ 173.5 (m), 150.8 (m), 129.6 (d, *J* = 2.8 Hz), 124.7, 120.2 (m), 82.9, 69.2 (d, *J* = 4.3 Hz), 65.5 (m), 61.4, 50.4 – 50.1 (m), 29.0 (d, *J* = 7.3 Hz), 21.0 (m), 14.7 (d, *J* = 3.1 Hz), 14.1 (d, *J* = 3.7 Hz). ³¹P NMR (CDCl₃) δ 2.98 – 1.68 (m). HRMS (ESI): calcd for C₁₆H₂₃NO₅P [M+H]⁺ 340.1308, found 340.1299.

Methyl ((pent-4-yn-1-yloxy)(phenoxy)phosphoryl)-L-alaninate (16)

Product (mixture of two diastereomers) was obtained as clear oil. Yield: 24 %. ^1H NMR (CDCl_3) δ 7.41 – 7.24 (m, 2H), 7.23 – 7.15 (m, 2H), 7.15 – 7.05 (m, 1H), 4.27 – 4.13 (m, 2H), 4.00 (dt, $J = 9.2, 1.7$ Hz, 1H), 3.73 – 3.57 (m, 4H), 2.26 (qd, $J = 7.1, 2.6$ Hz, 2H), 1.94 (q, $J = 2.7$ Hz, 1H), 1.86 (dd, $J = 14.2, 6.9$ Hz, 2H), 1.35 (dd, $J = 7.0, 5.0$ Hz, 3H). ^{13}C NMR (CDCl_3) δ 174.1 – 173.8 (m), 150.8 (dd, $J = 6.7, 3.7$ Hz), 129.6 (d, $J = 2.1$ Hz), 124.8, 120.2 (dd, $J = 4.9, 3.3$ Hz), 82.9, 69.2 (d, $J = 3.7$ Hz), 65.5 (t, $J = 5.9$ Hz), 52.4 (d, $J = 2.4$ Hz), 50.3 – 50.1 (m), 29.0 (d, $J = 7.1$ Hz), 21.1 – 20.8 (m), 14.7 (d, $J = 3.7$ Hz). ^{31}P NMR (162 MHz, CDCl_3) δ 2.55 – 1.82 (m). HRMS (ESI): calcd for $\text{C}_{15}\text{H}_{21}\text{NO}_5\text{P}$ $[\text{M}+\text{H}]^+$ 326.1152, found 326.1145.

Ethyl ((but-3-yn-1-yloxy)(phenoxy)phosphoryl)-L-alaninate (17)

Yield: 21%. ^1H NMR (CDCl_3) δ 7.36 – 7.24 (m, 2H), 7.24 – 7.15 (m, 2H), 7.15 – 7.05 (m, 1H), 4.17 (ddq, $J = 21.5, 12.6, 7.0$ Hz, 4H), 4.02 (ddd, $J = 23.0, 8.3, 7.4$ Hz, 1H), 3.79 (dt, $J = 17.4, 10.5$ Hz, 1H), 2.57 (dtd, $J = 9.4, 6.9, 2.6$ Hz, 2H), 2.01 (dt, $J = 5.4, 2.7$ Hz, 1H), 1.37 (dd, $J = 7.0, 3.2$ Hz, 3H), 1.24 (dt, $J = 10.8, 7.1$ Hz, 3H). ^{13}C NMR (CDCl_3) δ 173.4 (d, $J = 7.9$ Hz), 150.9 – 150.6 (m), 129.6 (d, $J = 2.1$ Hz), 124.8, 120.2 (t, $J = 4.7$ Hz), 79.6 (d, $J = 2.5$ Hz), 70.3 (d, $J = 3.1$ Hz), 64.8 – 64.4 (m), 61.5 (d, $J = 2.2$ Hz), 50.2 (d, $J = 6.8$ Hz), 21.0 (t, $J = 4.8$ Hz), 20.6 (dd, $J = 7.5, 4.7$ Hz), 14.1 (d, $J = 3.4$ Hz). ^{31}P NMR (CDCl_3) δ 2.63 – 1.85 (m). HRMS (ESI): calcd for $\text{C}_{15}\text{H}_{21}\text{NO}_5\text{P}$ $[\text{M}+\text{H}]^+$ 326.1152, found 326.1151.

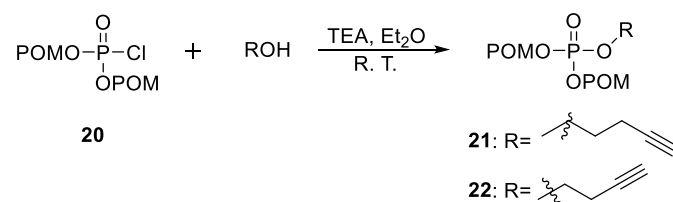
Methyl ((but-3-yn-1-yloxy)(phenoxy)phosphoryl)-L-alaninate (18)

Yield: 39%. ^1H NMR (CDCl_3) δ 7.41 – 7.23 (m, 2H), 7.19 (ddd, $J = 7.7, 6.9, 1.0$ Hz, 2H), 7.15 – 7.01 (m, 1H), 4.27 – 4.08 (m, 2H), 4.02 (d, $J = 6.8$ Hz, 1H), 3.83 (s, 1H), 3.72 – 3.53 (m, 3H), 2.67 – 2.41 (m, 2H), 1.99 (dt, $J = 5.4, 2.6$ Hz, 1H), 1.36 (dd, $J = 7.1, 3.4$ Hz, 3H). ^{13}C NMR (CDCl_3) δ 173.9 (d, $J = 7.7$ Hz), 150.7 (dd, $J = 6.8, 3.5$ Hz), 129.6 (d, $J = 2.1$ Hz), 124.9, 120.2 (dd, $J = 4.8, 3.2$ Hz), 79.6 (d, $J = 1.6$ Hz), 70.4 (d, $J = 4.2$ Hz), 64.9 – 64.5 (m), 52.5 (d, $J = 3.6$

Hz), 50.2 (d, $J = 6.5$ Hz), 20.9 (t, $J = 5.5$ Hz), 20.6 (dd, $J = 7.6, 5.1$ Hz). ^{31}P NMR (CDCl_3) δ 2.10. HRMS (ESI): calcd for $\text{C}_{14}\text{H}_{19}\text{NO}_5\text{P}$ $[\text{M}+\text{H}]^+$ 312.0995, found 312.0984.

Ethyl ((pent-4-yn-2-yloxy)(phenoxy)phosphoryl)-L-alaninate (**19**)

Yield: 21%. ^1H NMR (CDCl_3) δ 7.38 – 7.24 (m, 2H), 7.24 – 7.16 (m, 2H), 7.12 (t, $J = 7.3$ Hz, 1H), 4.78 – 4.54 (m, 1H), 4.24 – 4.08 (m, 2H), 4.09 – 3.92 (m, 1H), 3.70 – 3.46 (m, 1H), 2.62 – 2.38 (m, 2H), 2.07 – 1.96 (m, 1H), 1.44 (dd, $J = 14.5, 6.2$ Hz, 1H), 1.40 – 1.30 (m, 5H), 1.30 – 1.14 (m, 3H). ^{13}C NMR (CDCl_3) δ 173.5 (d, $J = 8.2$ Hz), 150.9, 129.6, 124.8, 120.3 (dd, $J = 9.1, 4.7$ Hz), 79.6, 79.4, 72.9 (dd, $J = 10.7, 5.4$ Hz), 70.9 (d, $J = 3.0$ Hz), 61.5, 50.3 (d, $J = 6.4$ Hz), 27.5 – 27.1 (m), 21.0 (t, $J = 15.6$ Hz), 20.8 – 20.3 (m), 14.1 (d, $J = 2.2$ Hz). ^{31}P NMR (CDCl_3) δ 1.67 – 0.74 (m). calcd for $\text{C}_{16}\text{H}_{22}\text{NaNO}_5\text{P}$ $[\text{M}+\text{Na}]^+$ 362.1128, found 362.1137.



Chlorophosphoryl-bisPOM (**20**)

Synthesis of chlorophosphoryl-bisPOM (**20**) starting from trimethyl phosphate followed literature reported procedure.¹⁵ However, we found the products in the sequential four steps are hard to visualize on TLC using commonly used staining reagents. None of previous literature recorded method for this problem. So, we tried a series of staining reagents and found acidic α -naphthol stain can efficiently visualize compounds contains POM moiety in these four reactions.

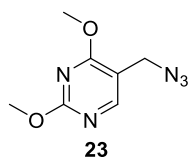
Pent-4-yn-2-yl bisPOM phosphate (**21**)

To a stirred solution of 4-pentyn-1-ol (21 μL , 0.22 mmol) and chlorophosphoryl-bisPOM (**20**, 380 mg, 1.10 mmol, 5 equiv.) in 2 mL Et_2O was added TEA (0.3 mL, 2.20 mmol, 10 equiv.) dropwise at room temperature. The solution was stirred under room temperature overnight. Then

the reaction was quenched with saturated ammonium chloride solution and extracted with EtOAc (3×10 mL). The organic phase was dried over Na₂SO₄ and purified by column (silica gel, hexane/EtOAc 10:1). 47 mg product was obtained. Yield: 55%. ¹H NMR (CDCl₃) δ 5.63 (d, *J* = 13.6 Hz, 4H), 4.19 (dd, *J* = 13.4, 6.2 Hz, 2H), 2.30 (td, *J* = 7.0, 2.7 Hz, 2H), 1.95 (t, *J* = 2.7 Hz, 1H), 1.92 – 1.81 (m, 2H), 1.26 – 1.14 (m, 18H). ¹³C NMR (CDCl₃) δ 176.7, 82.8 (d, *J* = 5.1 Hz), 82.5, 69.4, 67.0 (d, *J* = 6.1 Hz), 38.8, 28.9 (d, *J* = 7.4 Hz), 26.9, 14.7. ³¹P NMR (CDCl₃) δ -3.82 (ddd, *J* = 20.6, 13.8, 7.1 Hz). HRMS (ESI): calcd for C₁₇H₂₉NaO₈P [M+Na]⁺ 415.1492, found 415.1495.

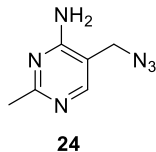
But-3-yn-1-yl bisPOM phosphate (22)

The synthesis of compound **22** followed the same procedure with compound **21** using but-3-yn-1-ol. Yield: 58%. ¹H NMR (CDCl₃) δ 5.75 – 5.51 (m, 4H), 4.13 (q, *J* = 7.3 Hz, 2H), 2.55 (t, *J* = 6.9 Hz, 2H), 1.98 (s, 1H), 1.19 (s, 18H). ¹³C NMR (CDCl₃) δ 176.7, 82.8 (d, *J* = 5.1 Hz), 78.8, 70.7, 65.8 (d, *J* = 5.7 Hz), 38.8, 26.8, 20.5 (d, *J* = 7.7 Hz). ³¹P NMR (CDCl₃) δ -3.94 – -4.62 (m). HRMS (ESI): calcd for C₁₆H₂₇NaO₈P [M+Na]⁺ 401.1336, found 401.1322.



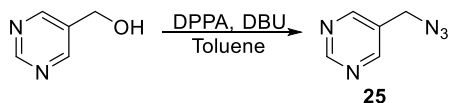
5-(Azidomethyl)-2,4-dimethoxypyrimidine (23)

Compound **23** was prepared using literature reported procedure from 2,4-dimethoxypyrimidine-5-carbaldehyde.¹⁵⁰⁻¹⁵¹ ¹H NMR (CDCl₃) δ 8.16 (s, 1H), 4.27 (s, 2H), 4.06 (s, 3H), 4.03 (s, 3H). ¹³C NMR (CDCl₃) δ 169.6, 165.6, 158.1, 109.7, 55.0, 54.3, 47.1. HRMS (ESI): calcd for C₇H₉N₅NaO₂ [M+Na]⁺ 218.0648, found 218.0661.



5-(Azidomethyl)-2-methylpyrimidin-4-amine (24)

Compound **24** was prepared using reported procedure.¹⁴⁶ Spectra data correspond well with literature report.



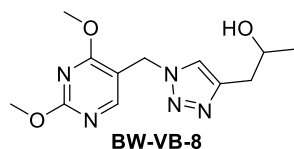
5-(Azidomethyl)pyrimidine (25)

Pyrimidin-5-ylmethanol (266 mg, 2.42 mmol) and DPPA (0.73 mL, 3.39 mmol) were dissolved in 15 mL dry toluene and cooled to 0 °C in an ice bath under N₂ protection. Then DBU (0.51 mL, 3.39 mmol) was slowly added to the solution with a syringe. The reaction mixture was allowed to slowly warm up to room temperature and stirred overnight. The reaction mixture was then diluted with EtOAc and washed with 1N HCl solution. The organic phase was dried over Na₂SO₄, concentrated, and purified with Al₂O₃ column. Product was obtained as yellowish oil with a 75% yield. ¹H NMR (CDCl₃) δ 9.21 (s, 1H), 8.72 (s, 2H), 4.44 (s, 2H). ¹³C NMR (CDCl₃) δ 158.7, 156.4, 129.3, 49.8. HRMS (ESI): calcd for C₅H₆N₅ [M+Na]⁺ 136.0618, found 136.0623.

General procedure for “click” reaction

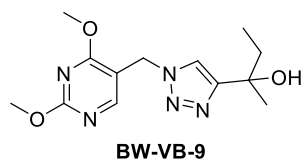
Azide was prepared as 50 mg/mL stock solution in MeOH beforehand. 1 mL of this solution was added into a 20-mL glass vial. 1 equiv. of the respective alkyne was added into the solution. 0.63 mL (0.05 equiv.) freshly made 20 mM CuSO₄/sodium ascorbate stock solution (50 mg CuSO₄·5H₂O, 40 mg sodium ascorbate dissolved in 10 mL water) was slowly added to the reaction solution. The reaction mixture was stirred at room temperature overnight. Then solvent

was removed with vacuum. The residue was premixed with silica gel and purified by column chromatography (silica, pure EtOAc to EtOAc/MeOH 20:1).



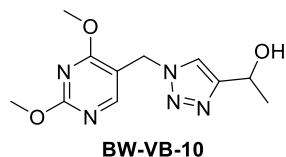
1-(1-((2,4-Dimethoxypyrimidin-5-yl)methyl)-1H-1,2,3-triazol-4-yl)propan-2-ol (BW-VB-8)

Yield: 73%. ¹H NMR (CDCl₃) δ 8.14 (s, 1H), 7.38 (s, 1H), 5.34 (s, 2H), 4.07 (s, 1H), 3.96 (dd, *J* = 16.1, 5.1 Hz, 6H), 3.21 (s, 1H), 2.80 (dd, *J* = 14.9, 3.8 Hz, 1H), 2.70 (dd, *J* = 14.9, 8.0 Hz, 1H), 1.19 (d, *J* = 6.2 Hz, 3H). ¹³C NMR (CDCl₃) δ 169.3, 165.9, 159.2, 145.7, 122.1, 109.3, 67.2, 55.3, 54.6, 46.2, 35.1, 23.1. HRMS (ESI): calcd for C₁₂H₁₇N₅NaO₃⁺ [M+Na]⁺ 302.1224, found 302.1243.



2-(1-((2,4-Dimethoxypyrimidin-5-yl)methyl)-1H-1,2,3-triazol-4-yl)butan-2-ol (BW-VB-9)

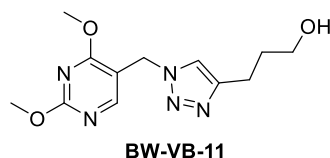
Yield: 98%. ¹H NMR (CDCl₃) δ 8.13 (s, 1H), 7.41 (s, 1H), 5.33 (s, 2H), 3.93 (d, *J* = 12.5 Hz, 6H), 3.00 (s, 1H), 1.80 (d, *J* = 6.4 Hz, 2H), 1.49 (s, 3H), 0.75 (t, *J* = 7.0 Hz, 3H). ¹³C NMR (CDCl₃) δ 169.2, 165.8, 159.0, 155.1, 120.3, 109.3, 71.4, 55.6, 54.5, 46.2, 36.0, 28.2, 8.4. HRMS (ESI): calcd for C₁₃H₁₉N₅NaO₃⁺ [M+Na]⁺ 316.1380, found 316.1389.



1-(1-((2,4-Dimethoxypyrimidin-5-yl)methyl)-1H-1,2,3-triazol-4-yl)ethan-1-ol (BW-VB-10)

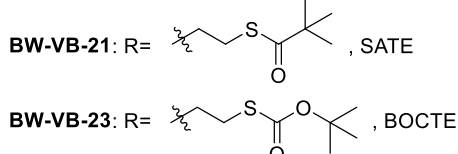
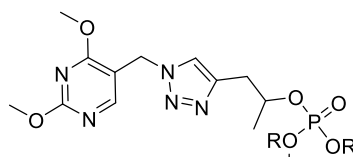
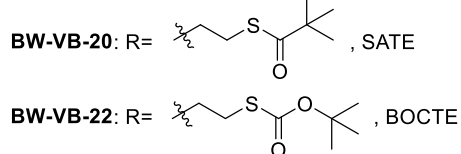
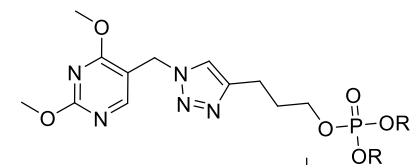
Yield: 67%. ¹H NMR (CDCl₃) δ 8.18 (s, 1H), 7.48 (s, 1H), 5.37 (s, 2H), 5.04 (d, *J* = 4.0 Hz, 1H), 3.98 (d, *J* = 15.6 Hz, 6H), 3.18 (s, 1H), 1.53 (d, *J* = 6.2 Hz, 3H). ¹³C NMR (CDCl₃) δ

169.4 166.0, 159.3, 153.1, 120.4, 109.2, 63.3, 55.4, 54.7, 46.4, 23.495. HRMS (ESI): calcd for $C_{11}H_{15}N_5NaO_3^+ [M+Na]^+$ 288.1067, found 288.1078.



3-(1-((2,4-Dimethoxypyrimidin-5-yl)methyl)-1H-1,2,3-triazol-4-yl)propan-1-ol (BW-VB-11)

Yield: 52%. 1H NMR ($CDCl_3$) δ 8.17 (s, 1H), 7.31 (s, 1H), 5.36 (s, 2H), 3.99 (d, $J = 16.1$ Hz, 6H), 3.67 (s, 2H), 2.78 (t, $J = 7.3$ Hz, 2H), 2.64 (s, 1H), 2.01 – 1.79 (m, 2H). ^{13}C NMR ($CDCl_3$) δ 169.4, 166.0, 159.2, 148.1, 121.2, 109.4, 62.1, 55.4, 54.7, 46.3, 32.3, 22.4. HRMS (ESI): calcd for $C_{12}H_{17}N_5NaO_3^+ [M+Na]^+$ 302.1224, found 302.1237.



3-(1-((2,4-dimethoxypyrimidin-5-yl)methyl)-1H-1,2,3-triazol-4-yl)propyl bis-SATE phosphate (BW-VB-20)

Yield: 64%. 1H NMR ($CDCl_3$) δ 8.18 (s, 1H), 7.39 (s, 1H), 5.37 (s, 2H), 4.15 – 4.04 (m, 6H), 4.00 (d, $J = 19.2$ Hz, 6H), 3.12 (t, $J = 6.7$ Hz, 4H), 2.81 (t, $J = 7.5$ Hz, 2H), 2.13 – 1.97 (m, 2H), 1.76 (s, 2H), 1.22 (s, 18H). ^{13}C NMR ($CDCl_3$) δ 205.7, 165.71, 158.9, 146.8, 121.6, 109.2, 67.1, 66.1 (d, $J = 5.7$ Hz), 55.1, 54.4, 46.5, 46.0, 29.8, 28.6 (d, $J = 7.5$ Hz), 27.3, 21.6. ^{31}P NMR ($CDCl_3$) δ -1.67 (dq, $J = 15.1, 7.5$ Hz). HRMS (ESI): calcd for $C_{26}H_{42}N_5O_8NaPS_2 [M+Na]^+$ 670.2105, found 670.2133.

1-(1-((2,4-dimethoxypyrimidin-5-yl)methyl)-1H-1,2,3-triazol-4-yl)propan-2-yl bisSATE phosphate (BW-VB-21)

Product was obtained as racemic mixture. Yield: 53%. ^1H NMR (CDCl_3) δ 8.20 (s, 1H), 7.55 (s, 1H), 5.42 (s, 2H), 4.87 – 4.68 (m, 2H), 4.15 – 3.91 (m, 10H), 3.18 – 2.97 (m, 6H), 1.39 (d, $J = 6.2$ Hz, 3H), 1.24 (d, $J = 1.8$ Hz, 18H). ^{13}C NMR (CDCl_3) δ 205.7, 169.0, 165.7, 158.8, 143.3, 122.5, 109.2, 75.3, 65.9, 55.1, 54.4, 46.5, 46.1, 33.7, 28.5, 27.3, 21.1. ^{31}P NMR (CDCl_3) δ -2.8 (h, $J = 7.4$ Hz). HRMS (ESI): calcd for $\text{C}_{26}\text{H}_{42}\text{N}_5\text{O}_8\text{NaPS}_2$ $[\text{M}+\text{Na}]^+$ 670.2105, found 670.2123.

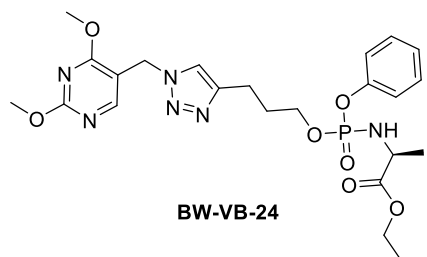
3-(1-((2,4-dimethoxypyrimidin-5-yl)methyl)-1H-1,2,3-triazol-4-yl)propyl bis(2-((tert-butoxycarbonyl)thio)ethyl) phosphate (BW-VB-22)

Yield: 37%. ^1H NMR (CDCl_3) δ 8.19 (s, 1H), 7.39 (s, 1H), 5.37 (s, 2H), 4.17 (q, $J = 7.0$ Hz, 4H), 4.09 (q, $J = 6.4$ Hz, 2H), 4.03 (s, 3H), 3.98 (s, 3H), 3.06 (t, $J = 6.6$ Hz, 4H), 2.81 (t, $J = 7.4$ Hz, 2H), 2.06 (p, $J = 6.6$ Hz, 2H), 1.47 (s, 18H). ^{13}C NMR (CDCl_3) δ 169.1, 168.2, 165.7, 158.9, 146.8, 121.3, 109.2, 85.4, 67.1 (d, $J = 6.1$ Hz), 66.2 (d, $J = 5.7$ Hz), 55.1, 54.4, 46.0, 30.9 (d, $J = 7.4$ Hz), 29.8 (d, $J = 7.1$ Hz), 28.2, 21.6. ^{31}P NMR (CDCl_3) δ -1.64 (dt, $J = 15.2, 7.5$ Hz). HRMS (ESI): calcd for $\text{C}_{26}\text{H}_{42}\text{N}_5\text{O}_{10}\text{NaPS}_2$ $[\text{M}+\text{Na}]^+$ 702.2003, found 702.2041.

1-(1-((2,4-dimethoxypyrimidin-5-yl)methyl)-1H-1,2,3-triazol-4-yl)propan-2-yl bis(2-((tert-butoxycarbonyl)thio)ethyl) phosphate (BW-VB-23)

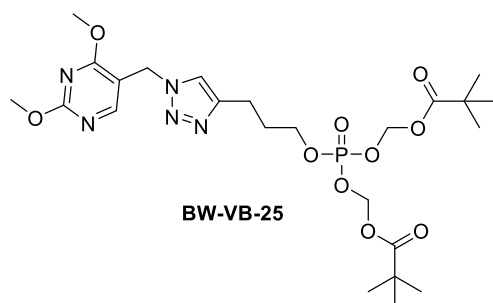
Product was obtained as racemic mixture. Yield: 92%. ^1H NMR (CDCl_3) δ 8.19 (s, 1H), 7.53 (s, 1H), 5.39 (s, 2H), 4.82 – 4.62 (m, 1H), 4.10 (ddd, $J = 7.7, 5.2, 3.9$ Hz, 4H), 4.04 (dd, $J = 21.9, 10.7$ Hz, 7H), 3.08 – 2.95 (m, 6H), 1.65 (s, 4H), 1.48 (d, $J = 1.9$ Hz, 18H), 1.37 (d, $J = 6.2$ Hz, 3H). ^{13}C NMR (CDCl_3) δ 169.0, 168.1, 165.7, 158.8, 143.2, 122.5, 109.2, 85.4, 75.4 (d, $J = 6.2$ Hz), 66.0 (dd, $J = 5.6, 4.2$ Hz), 55.1, 54.4, 46.0, 33.7 (d, $J = 6.2$ Hz), 30.8 (d, $J = 7.5$ Hz),

28.1, 21.1 (d, $J = 3.4$ Hz). ^{31}P NMR (CDCl_3) δ -2.78 (dd, $J = 15.1, 7.5$ Hz). HRMS (ESI): calcd for $\text{C}_{26}\text{H}_{42}\text{N}_5\text{O}_{10}\text{NaPS}_2$ $[\text{M}+\text{Na}]^+$ 702.2003, found 702.2032.



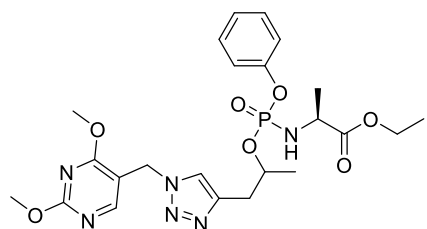
Ethyl ((3-(1-((2,4-dimethoxypyrimidin-5-yl)methyl)-1H-1,2,3-triazol-4-yl)propoxy)(phenoxy)phosphoryl)-L-alaninate (BW-VB-24)

Product was obtained as mixture of two diastereomers. Yield: 94%. ^1H NMR (CDCl_3) δ 8.18 (s, 1H), 7.34 (s, 1H), 7.30 (m, 2H), 7.19 (t, $J = 7.8$ Hz, 2H), 7.13 (t, $J = 7.3$ Hz, 1H), 5.36 (s, 2H), 4.22 – 4.05 (m, 4H), 4.02 (s, 3H), 3.98 (s, 3H), 3.75 – 3.61 (m, 1H), 2.86 – 2.69 (m, 2H), 2.04 (m, 2H), 1.36 (m, 3H), 1.23 (q, $J = 7.2$ Hz, 3H). ^{13}C NMR (CDCl_3) δ 173.5 (d, $J = 7.8$ Hz), 169.0, 165.7, 158.8, 150.8 (d, $J = 6.8$ Hz), 129.6 (d, $J = 2.1$ Hz), 124.8, 121.3, 120.4 – 120.1 (m), 109.2, 66.3 – 65.8 (m), 61.5 (d, $J = 2.3$ Hz), 55.1, 54.4, 50.3 (d, $J = 3.8$ Hz), 46.0, 29.9 – 29.7 (m), 21.5 (d, $J = 4.8$ Hz), 21.0 (t, $J = 4.6$ Hz), 14.1 (d, $J = 3.0$ Hz). ^{31}P NMR (CDCl_3) δ 2.44 (dd, $J = 17.1, 8.8$ Hz). HRMS (ESI): calcd for $\text{C}_{23}\text{H}_{31}\text{N}_6\text{O}_7\text{NaP}$ $[\text{M}+\text{Na}]^+$ 557.1884, found 557.1871.



3-(1-((2,4-dimethoxypyrimidin-5-yl)methyl)-1H-1,2,3-triazol-4-yl)propyl bisPOM phosphate (BW-VB-25)

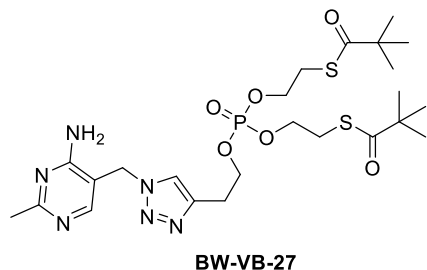
Yield: 63%. ^1H NMR (CDCl_3) δ 8.18 (s, 1H), 7.37 (s, 1H), 5.62 (d, $J = 13.4$ Hz, 4H), 5.37 (s, 2H), 4.14 – 4.05 (m, 2H), 4.02 (s, 3H), 3.97 (s, 3H), 2.78 (t, $J = 7.4$ Hz, 2H), 2.15 – 1.98 (m, 2H), 1.21 (d, $J = 5.9$ Hz, 18H). ^{13}C NMR (CDCl_3) δ 176.7, 165.7, 158.9, 146.6, 121.3, 109.2, 82.7 (d, $J = 5.1$ Hz), 67.5 (d, $J = 6.0$ Hz), 55.1, 54.4, 46.0, 38.7, 29.6 (d, $J = 7.2$ Hz), 26.8, 21.4 (s). ^{31}P NMR (CDCl_3) δ -3.87 (dtt, $J = 20.5, 13.4, 6.7$ Hz). HRMS (ESI): calcd for $\text{C}_{24}\text{H}_{39}\text{N}_5\text{O}_{10}\text{P}$ $[\text{M}+\text{H}]^+$ 588.2429, found 588.2414.



BW-VB-26

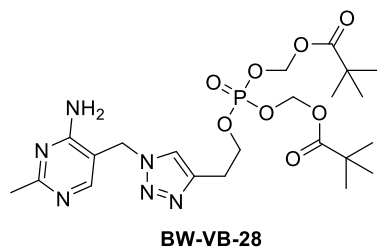
Ethyl (((1-(1-((2,4-dimethoxypyrimidin-5-yl)methyl)-1H-1,2,3-triazol-4-yl)propan-2-yl)oxy)(phenoxy)phosphoryl)-L-alaninate (BW-VB-26)

Product was obtained as mixture of two diastereomers. Yield: 34%. ^1H NMR (CDCl_3) δ 8.15 (d, $J = 26.2$ Hz, 1H), 7.48 (d, $J = 13.0$ Hz, 1H), 7.37 – 7.17 (m, 5H), 7.17 – 7.06 (m, 4H), 5.37 (d, $J = 2.0$ Hz, 2H), 5.28 (s, 1H), 4.87 (ddd, $J = 18.5, 12.1, 5.9$ Hz, 2H), 4.20 – 4.06 (m, 3H), 3.96 (dt, $J = 15.8, 10.3$ Hz, 11H), 3.74 – 3.40 (m, 2H), 3.04 (dd, $J = 14.4, 5.3$ Hz, 3H), 1.42 – 1.10 (m, 15H). ^{13}C NMR (CDCl_3) δ 173.6, 169.0 (d, $J = 8.3$ Hz), 165.7, 150.9, 129.5 (d, $J = 3.0$ Hz), 124.7, 122.4, 120.3 (dd, $J = 8.9, 4.2$ Hz), 109.2, 74.3, 61.6 – 61.3 (m), 55.1, 54.4 (d, $J = 4.7$ Hz), 50.3, 46.0 (d, $J = 9.5$ Hz), 21.2, 21.0, 14.1. ^{31}P NMR (CDCl_3) δ 1.52, 1.19. HRMS (ESI): calcd for $\text{C}_{23}\text{H}_{31}\text{N}_6\text{O}_7\text{P}$ $[\text{M}+\text{H}]^+$ 535.2065, found 535.2065.



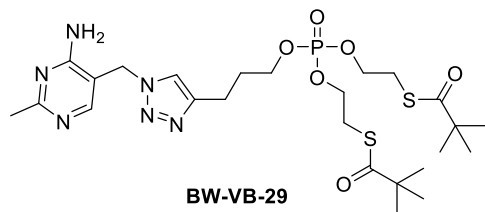
2-(1-((4-amino-2-methylpyrimidin-5-yl)methyl)-1H-1,2,3-triazol-4-yl)ethyl bisSATE phosphate (BW-VB-27)

Yield: 64%. ^1H NMR (CDCl_3) δ 8.20 (s, 1H), 7.52 (s, 1H), 5.73 (s, 2H), 5.35 (s, 2H), 4.40 (dd, $J = 15.2, 6.4$ Hz, 2H), 4.24 (t, $J = 6.4$ Hz, 4H), 3.10 (dt, $J = 14.8, 6.2$ Hz, 6H), 2.47 (s, 3H), 1.19 (s, 18H). ^{13}C NMR (CDCl_3) δ 178.1, 156.0, 144.2, 122.3, 108.1, 66.5 (d, $J = 8.2$ Hz), 62.8 (d, $J = 4.4$ Hz), 48.6, 38.8, 30.4 (d, $J = 3.4$ Hz), 27.1, 25.6. ^{31}P NMR (CDCl_3) δ 56.32 – 55.58 (m). HRMS (ESI): calcd for $\text{C}_{24}\text{H}_{39}\text{N}_6\text{O}_6\text{PS}_2$ $[\text{M}+\text{H}]^+$ 603.2183, found 603.2184.



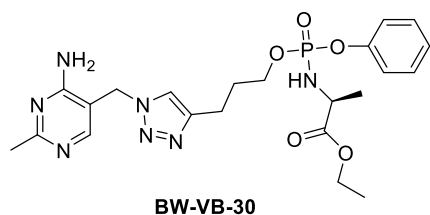
2-(1-((4-amino-2-methylpyrimidin-5-yl)methyl)-1H-1,2,3-triazol-4-yl)ethyl bisPOM phosphate (BW-VB-28)

Yield: 44%. ^1H NMR (CDCl_3) δ 8.19 (s, 1H), 7.53 (s, 1H), 5.70 (s, 2H), 5.58 (d, $J = 13.2$ Hz, 4H), 5.33 (s, 2H), 4.31 (q, $J = 6.6$ Hz, 2H), 3.08 (t, $J = 6.1$ Hz, 2H), 2.46 (s, 3H), 1.19 (s, 18H). ^{13}C NMR (CDCl_3) δ 176.8, 168.9, 162.0, 156.2, 144.3, 122.3, 108.1, 82.7 (d, $J = 5.0$ Hz), 67.0 (d, $J = 5.8$ Hz), 48.7, 38.7, 27.4 – 26.9(m), 27.1 – 26.7 (m), 25.6. ^{31}P NMR (CDCl_3) δ -4.44 (qd, $J = 13.3, 6.5$ Hz). HRMS (ESI): calcd for $\text{C}_{22}\text{H}_{35}\text{N}_6\text{O}_8\text{P}$ $[\text{M}+\text{H}]^+$ 543.2327, found 543.2326.



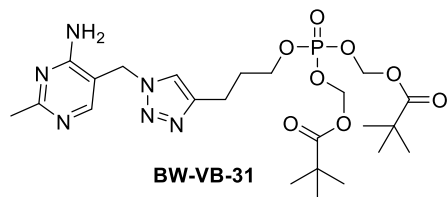
3-(1-((4-amino-2-methylpyrimidin-5-yl)methyl)-1H-1,2,3-triazol-4-yl)propyl bisSATE phosphate (BW-VB-29)

Yield: 42%. ¹H NMR (CDCl₃) δ 8.14 (s, 1H), 7.41 (s, 1H), 5.83 (s, 2H), 5.29 (s, 2H), 4.24 (t, *J* = 6.4 Hz, 4H), 4.14 (dd, *J* = 14.7, 6.2 Hz, 2H), 3.08 (dt, *J* = 16.6, 6.5 Hz, 4H), 2.76 (t, *J* = 7.3 Hz, 2H), 2.42 (s, 3H), 2.10 – 2.00 (m, 2H), 1.14 (s, 18H). ¹³C NMR (CDCl₃) δ 178.0, 168.8, 162.0, 156.0, 147.3, 121.5, 108.2, 66.9 (d, *J* = 8.3 Hz), 62.7 (d, *J* = 4.6 Hz), 48.6, 38.8, 30.4 (d, *J* = 3.3 Hz), 29.5 (d, *J* = 7.0 Hz), 27.1, 25.5, 21.5. ³¹P NMR (CDCl₃) δ 56.10 – 55.33 (m). HRMS (ESI): calcd for C₂₅H₄₁N₆O₆PS₂ [M+H]⁺ 617.2339, found 617.2341.



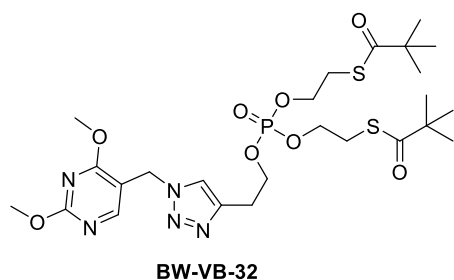
Ethyl ((3-(1-((4-amino-2-methylpyrimidin-5-yl)methyl)-1H-1,2,3-triazol-4-yl)propoxy)(phenoxy)phosphoryl)-L-alaninate (BW-VB-30)

Yield: 34%. ¹H NMR (CDCl₃) δ 8.16 (s, 1H), 7.29 (dd, *J* = 16.3, 8.7 Hz, 3H), 7.15 (dt, *J* = 14.8, 7.1 Hz, 3H), 5.75 (s, 2H), 5.29 (s, 2H), 4.21 – 3.89 (m, 5H), 3.75 (dd, *J* = 24.1, 10.6 Hz, 1H), 2.75 (q, *J* = 7.5 Hz, 2H), 2.47 (s, 3H), 2.01 (dd, *J* = 13.8, 6.3 Hz, 3H), 1.35 (dd, *J* = 6.9, 2.8 Hz, 3H), 1.22 (q, *J* = 6.7 Hz, 4H). ¹³C NMR (CDCl₃) δ 173.6, 162.0, 156.0, 150.8, 147.7, 129.7 (d, *J* = 2.2 Hz), 124.9, 121.5, 120.2 (t, *J* = 5.3 Hz), 100.0, 65.8, 61.5, 50.3 (d, *J* = 8.1 Hz), 48.7, 29.5, 25.6, 21.5 (d, *J* = 3.3 Hz), 21.0, 14.1 (d, *J* = 3.1 Hz). ³¹P NMR (CDCl₃) δ 3.14 – 1.78 (m). HRMS (ESI): calcd for C₂₂H₃₀N₇O₅P [M+H]⁺ 504.2119, found 504.2113.



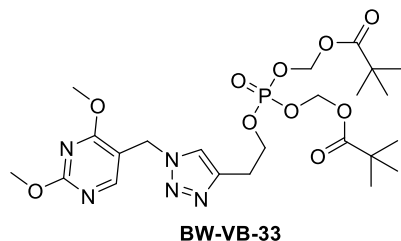
3-(1-((4-amino-2-methylpyrimidin-5-yl)methyl)-1H-1,2,3-triazol-4-yl)propyl bisPOM phosphate (BW-VB-31)

Yield: 48%. ^1H NMR (CDCl_3) δ 8.20 (s, 1H), 7.41 (s, 1H), 5.66 (s, 2H), 5.61 (d, $J = 13.4$ Hz, 4H), 5.33 (s, 2H), 4.07 (q, $J = 6.2$ Hz, 2H), 2.79 (t, $J = 7.2$ Hz, 2H), 2.47 (s, 3H), 2.03 (dt, $J = 13.1, 6.6$ Hz, 3H), 1.20 (s, 18H). ^{13}C NMR (CDCl_3) δ 176.8, 168.8, 162.1, 156.0, 147.3, 121.6, 108.2, 82.7 (d, $J = 5.1$ Hz), 67.3 (d, $J = 6.1$ Hz), 48.6, 38.7, 30.9, 29.3 (d, $J = 7.3$ Hz), 26.8, 25.6, 21.3. ^{31}P NMR (CDCl_3) δ -3.59 – -4.40 (m). HRMS (ESI): calcd for $\text{C}_{23}\text{H}_{38}\text{N}_6\text{O}_8\text{P}$ $[\text{M}+\text{H}]^+$ 557.2483, found 557.2482.



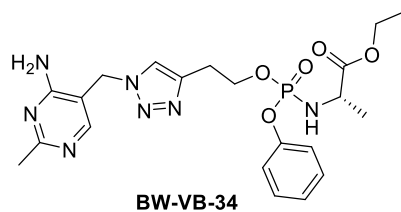
2-(1-((2,4-dimethoxypyrimidin-5-yl)methyl)-1H-1,2,3-triazol-4-yl)ethyl bisSATE phosphate (BW-VB-32)

Yield: 56%. ^1H NMR (CDCl_3) δ 8.20 (s, 1H), 7.49 (s, 1H), 5.39 (s, 2H), 4.41 (dd, $J = 14.5, 6.2$ Hz, 2H), 4.26 (t, $J = 6.4$ Hz, 4H), 4.00 (d, $J = 18.9$ Hz, 6H), 3.32 – 3.01 (m, 6H), 1.18 (s, 18H). ^{13}C NMR (CDCl_3) δ 178.0, 169.0, 66.6 (d, $J = 8.2$ Hz), 62.7 (d, $J = 4.6$ Hz), 55.1, 54.4, 46.1, 38.7, 30.4 (d, $J = 3.3$ Hz), 27.0 (d, $J = 5.6$ Hz). ^{31}P NMR (CDCl_3) δ 56.23 – 55.35 (m). HRMS (ESI): calcd for $\text{C}_{25}\text{H}_{40}\text{N}_5\text{O}_8\text{PS}_2$ $[\text{M}+\text{H}]^+$ 634.2129, found 634.2130.



**2-(1-((2,4-dimethoxypyrimidin-5-yl)methyl)-1H-1,2,3-triazol-4-yl)ethyl bisPOM phosphate
(BW-VB-33)**

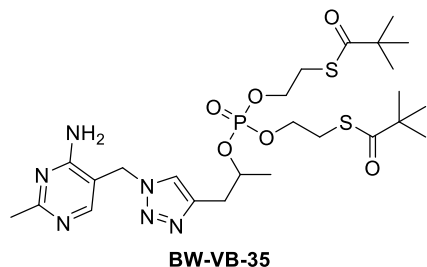
Yield: 33%. ^1H NMR (CDCl_3) δ 8.20 (s, 1H), 7.49 (s, 1H), 5.60 (d, $J = 13.4$ Hz, 4H), 5.38 (s, 2H), 4.32 (q, $J = 6.8$ Hz, 2H), 4.00 (d, $J = 18.9$ Hz, 6H), 3.09 (t, $J = 6.4$ Hz, 2H), 1.21 (d, $J = 12.1$ Hz, 18H). ^{13}C NMR (CDCl_3) δ 176.7, 169.1, 165.7, 158.9, 143.3, 122.2, 109.1, 100.0, 82.7 (d, $J = 5.0$ Hz), 67.1 (d, $J = 6.1$ Hz), 55.1, 54.4, 46.1, 38.7, 27.1 – 26.7 (m). ^{31}P NMR (CDCl_3) δ -3.91 – -4.49 (m). HRMS (ESI): calcd for $\text{C}_{23}\text{H}_{36}\text{N}_5\text{O}_{10}\text{NaP}$ $[\text{M}+\text{Na}]^+$ 596.2092, found 596.2073.



Ethyl ((2-(1-((4-amino-2-methylpyrimidin-5-yl)methyl)-1H-1,2,3-triazol-4-yl)ethoxy)(phenoxy)phosphoryl)-L-alaninate (BW-VB-34)

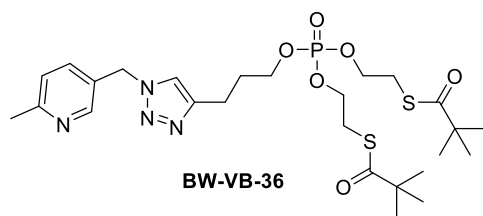
Yield: 72%. ^1H NMR (CDCl_3) δ 8.14 (s, 1H), 7.34 (d, $J = 8.4$ Hz, 1H), 7.27 (t, $J = 7.0$ Hz, 2H), 7.14 (t, $J = 7.3$ Hz, 3H), 5.92 (s, 2H), 5.26 (s, 2H), 4.41 – 4.23 (m, 2H), 4.17 – 4.05 (m, 2H), 4.08 – 3.82 (m, 2H), 3.06 (q, $J = 6.4$ Hz, 2H), 2.45 (s, 3H), 1.32 (t, $J = 7.7$ Hz, 3H), 1.21 (t, $J = 6.9$ Hz, 3H). ^{13}C NMR (CDCl_3) δ 173.6 (t, $J = 7.5$ Hz), 168.7, 162.0, 156.1, 150.7 (d, $J = 6.8$ Hz), 144.7 (d, $J = 4.7$ Hz), 129.6 (d, $J = 3.0$ Hz), 124.9, 122.2, 120.3 – 120.0 (m), 108.1, 65.5, 61.5, 50.3 (d, $J = 4.7$ Hz), 48.5, 27.1 (d, $J = 7.3$ Hz), 25.5, 21.0 – 20.6 (m), 14.1 (d, $J = 2.3$ Hz).

^{31}P NMR (CDCl_3) δ 2.79 – 1.97 (m). HRMS (ESI): calcd for $\text{C}_{21}\text{H}_{29}\text{N}_7\text{O}_5\text{P}$ $[\text{M}+\text{H}]^+$ 490.1962, found 490.1946.



2-(1-((4-amino-2-methylpyrimidin-5-yl)methyl)-1H-1,2,3-triazol-4-yl)-1-methyl-ethyl bisSATE phosphate (BW-VB-35)

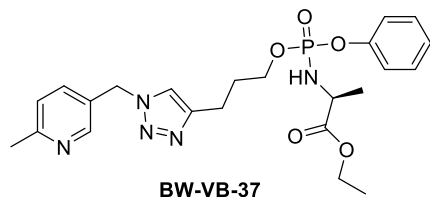
Yield: 42%. ^1H NMR (CDCl_3) δ 8.21 (s, 1H), 7.53 (s, 1H), 5.67 (s, 2H), 5.36 (s, 2H), 5.11 – 4.74 (m, 1H), 4.25 (dt, $J = 12.6, 6.5$ Hz, 4H), 3.19 – 2.85 (m, 6H), 2.48 (s, 3H), 1.42 (d, $J = 6.2$ Hz, 3H), 1.20 (s, 18H). ^{13}C NMR (CDCl_3) δ 178.1, 162.0, 143.8, 122.8, 76.36 (d, $J = 8.7$ Hz), 62.9 – 62.6 (m), 48.7, 38.8, 33.9 (d, $J = 5.7$ Hz), 30.7 (d, $J = 3.4$ Hz), 30.4 (d, $J = 3.2$ Hz), 27.2, 25.6, 21.7 (d, $J = 3.2$ Hz). ^{31}P NMR (CDCl_3) δ 54.15 (td, $J = 16.9, 10.6$ Hz). HRMS (ESI): calcd for $\text{C}_{25}\text{H}_{41}\text{N}_6\text{O}_6\text{PS}_2$ $[\text{M}+\text{H}]^+$ 617.2339, found 617.2340.



3-(1-((6-methylpyridin-3-yl)methyl)-1H-1,2,3-triazol-4-yl)propyl bisSATE phosphate (BW-VB-36)

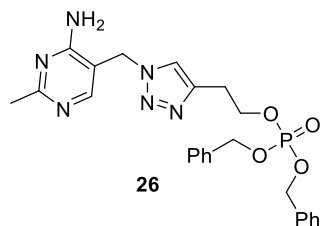
Yield: 62%. ^1H NMR (CDCl_3) δ 8.43 (s, 1H), 7.45 (d, $J = 7.9$ Hz, 1H), 7.33 (s, 1H), 7.11 (d, $J = 8.0$ Hz, 1H), 5.44 (s, 2H), 4.25 (t, $J = 6.4$ Hz, 4H), 4.15 (dd, $J = 14.7, 6.3$ Hz, 2H), 3.09 (dt, $J = 16.5, 6.4$ Hz, 4H), 2.77 (t, $J = 7.4$ Hz, 2H), 2.50 (s, 3H), 2.06 (p, $J = 6.6$ Hz, 2H), 1.15 (s, 19H). ^{13}C NMR (CDCl_3) δ 178.0, 159.2, 148.5, 147.0, 136.1, 127.6, 123.6, 121.2, 67.0 (d, $J =$

8.2 Hz), 62.7 (d, $J = 4.6$ Hz), 51.2, 38.8, 30.4 (d, $J = 3.3$ Hz), 29.7 (d, $J = 7.0$ Hz), 27.1, 24.2, 21.6. ^{31}P NMR (CDCl_3) δ 56.13 – 55.36 (m). HRMS (ESI): calcd for $\text{C}_{26}\text{H}_{42}\text{N}_4\text{O}_6\text{PS}_2$ $[\text{M}+\text{H}]^+$ 601.2278, found 601.2259.



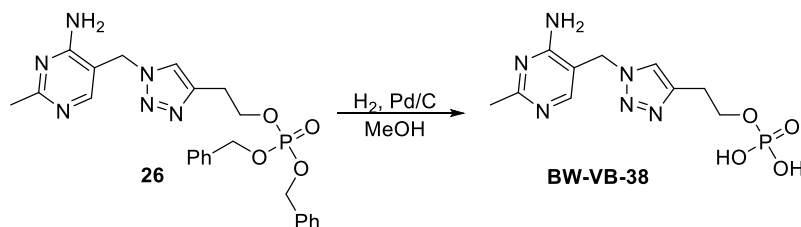
Ethyl ((3-(1-((6-methylpyridin-3-yl)methyl)-1H-1,2,3-triazol-4-yl)propoxy)(phenoxy)phosphoryl)-L-alaninate (BW-VB-37)

Yield: 44%. ^1H NMR (CDCl_3) δ 8.49 (s, 1H), 7.49 (d, $J = 7.9$ Hz, 1H), 7.34 – 7.24 (m, 3H), 7.17 (dt, $J = 23.9, 7.3$ Hz, 4H), 5.47 (s, 2H), 4.25 – 4.05 (m, 4H), 4.01 (dt, $J = 15.9, 7.9$ Hz, 1H), 3.69 (td, $J = 10.3, 4.5$ Hz, 1H), 2.78 (dd, $J = 15.3, 7.6$ Hz, 2H), 2.56 (s, 3H), 2.06 (dt, $J = 14.0, 6.8$ Hz, 2H), 1.37 (t, $J = 5.9$ Hz, 3H), 1.25 (q, $J = 6.9$ Hz, 3H). ^{13}C NMR (CDCl_3) δ 173.5 (d, $J = 7.7$ Hz), 159.1, 151.0 – 150.7 (m), 148.4, 147.3, 136.1, 129.6 (d, $J = 2.2$ Hz), 127.7, 124.8, 123.6, 121.1, 120.2 (t, $J = 5.1$ Hz), 66.1 – 65.8 (m), 61.5 (d, $J = 2.2$ Hz), 51.2, 50.3 (d, $J = 6.0$ Hz), 29.7 (dd, $J = 7.2, 3.0$ Hz), 24.2, 21.5 (d, $J = 4.9$ Hz), 21.0 (t, $J = 4.8$ Hz), 14.1 (d, $J = 2.9$ Hz). ^{31}P NMR (CDCl_3) δ 2.45 (dd, $J = 16.9, 7.8$ Hz). HRMS (ESI): calcd for $\text{C}_{23}\text{H}_{31}\text{N}_5\text{O}_5\text{P}$ $[\text{M}+\text{H}]^+$ 488.2057, found 488.2038.



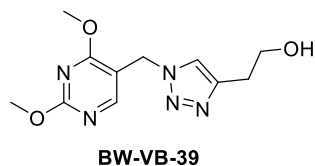
2-(1-((4-amino-2-methylpyrimidin-5-yl)methyl)-1H-1,2,3-triazol-4-yl)ethyl dibenzyl phosphate (26)

Yield: 40%. ^1H NMR (CDCl_3) δ 8.11 (s, 1H), 7.36 – 7.28 (m, 10H), 5.78 (s, 2H), 5.22 (s, 2H), 5.04 – 4.90 (m, 4H), 4.22 (dd, $J = 13.7, 6.5$ Hz, 2H), 3.00 (t, $J = 6.3$ Hz, 2H), 2.46 (s, 3H). ^{13}C NMR (CDCl_3) δ 168.9, 162.0, 156.0, 144.6, 135.7 (d, $J = 6.6$ Hz), 128.6 (d, $J = 1.8$ Hz), 128.0, 122.1, 108.0, 69.4 (d, $J = 5.6$ Hz), 66.2 (d, $J = 5.9$ Hz), 48.6, 27.0 (d, $J = 7.1$ Hz), 25.6. ^{31}P NMR (CDCl_3) δ -0.82 – -1.44 (m). HRMS (ESI): calcd for $\text{C}_{24}\text{H}_{28}\text{N}_6\text{O}_4\text{P}$ $[\text{M}+\text{H}]^+$ 495.1904, found 495.1933.



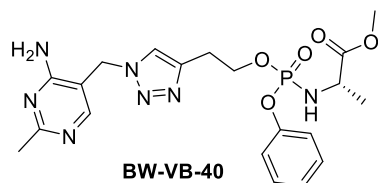
2-(1-((4-amino-2-methylpyrimidin-5-yl)methyl)-1H-1,2,3-triazol-4-yl)ethyl dihydrogen phosphate (BW-VB-38)

70 mg compound **26** was dissolved in 5 mL MeOH in a round-bottom flask equipped with a 3-way switch. 8.8 mg Pd/C was added to the solution carefully. The round bottom flask was flushed with N_2 and then equipped with a H_2 balloon. The solution was stirred under room temperature overnight. Then the reaction mixture was filtered through a Celite[®] pad. The filtrate was concentrated and dried over high vacuum. Yield: 56%. ^1H NMR (D_2O) δ 7.86 (d, $J = 9.9$ Hz, 2H), 5.48 (s, 2H), 3.99 (q, $J = 6.2$ Hz, 2H), 2.94 (t, $J = 6.0$ Hz, 2H), 2.47 (s, 3H). ^{13}C NMR (D_2O) δ 163.2, 162.6, 145.6, 143.2, 124.5, 109.7, 64.0 (d, $J = 5.2$ Hz), 46.6, 26.4 (d, $J = 7.4$ Hz), 20.8. ^{31}P NMR (D_2O) δ 0.26. HRMS (ESI): calcd for $\text{C}_{10}\text{H}_{16}\text{N}_6\text{O}_4\text{P}$ $[\text{M}+\text{H}]^+$ 315.0965, found 315.0968.



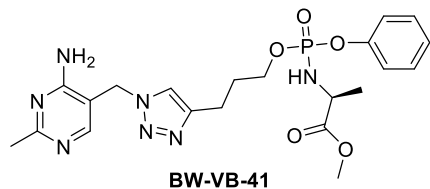
2-(1-((2,4-Dimethoxypyrimidin-5-yl)methyl)-1H-1,2,3-triazol-4-yl)ethan-1-ol (BW-VB-39)

Yield: 32%. ^1H NMR (MeOD) δ 8.29 (s, 1H), 7.84 (s, 1H), 5.45 (s, 2H), 4.00 (d, $J = 15.5$ Hz, 6H), 3.31 (s, 1H), 2.86 (s, 2H). ^{13}C NMR (CDCl_3) δ 169.1, 165.7, 158.9, 109.1, 61.5, 55.1, 54.4, 46.1, 28.7. HRMS (ESI): calcd for $\text{C}_{11}\text{H}_{16}\text{N}_5\text{O}_3$ $[\text{M}+\text{H}]^+$ 266.1248, found 266.1239.



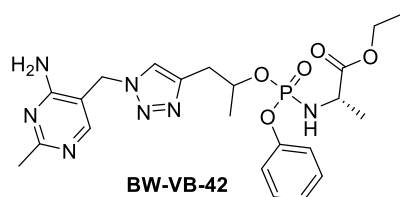
Methyl ((2-(1-((4-amino-2-methylpyrimidin-5-yl)methyl)-1H-1,2,3-triazol-4-yl)ethoxy)(phenoxy)phosphoryl)-L-alaninate (BW-VB-40)

Yield: 84%. ^1H NMR (CDCl_3) δ 8.13 (s, 1H), 7.32 (d, $J = 11.8$ Hz, 1H), 7.29 – 7.20 (m, 2H), 7.12 (t, $J = 7.3$ Hz, 3H), 5.82 (s, 2H), 5.25 (s, 2H), 4.29 (tt, $J = 6.4, 4.5$ Hz, 2H), 4.05 – 3.78 (m, 2H), 3.65 (d, $J = 1.3$ Hz, 3H), 3.42 (s, 1H), 3.04 (dd, $J = 14.4, 6.4$ Hz, 2H), 2.44 (s, 3H), 1.30 (dd, $J = 9.5, 6.6$ Hz, 3H). ^{13}C NMR (CDCl_3) δ 174.2 – 173.8 (m), 168.8, 162.0, 156.1 (d, $J = 1.9$ Hz), 150.7 (d, $J = 6.9$ Hz), 144.7 (d, $J = 4.9$ Hz), 129.6 (d, $J = 2.5$ Hz), 124.9, 122.2, 120.2 (dd, $J = 4.8, 3.1$ Hz), 108.1, 65.6 (d, $J = 5.1$ Hz), 52.5 (d, $J = 1.8$ Hz), 50.2 (d, $J = 5.5$ Hz), 48.6, 27.1 (d, $J = 7.1$ Hz), 25.6, 21.0 – 20.7 (m). ^{31}P NMR (CDCl_3) δ 2.63 – 1.87 (m). HRMS (ESI): calcd for $\text{C}_{20}\text{H}_{27}\text{N}_7\text{O}_5\text{P}$ $[\text{M}+\text{H}]^+$ 476.1806, found 476.1786.



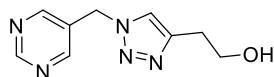
Methyl ((3-(1-((4-amino-2-methylpyrimidin-5-yl)methyl)-1H-1,2,3-triazol-4-yl)propoxy)(phenoxy)phosphoryl)-L-alaninate (BW-VB-41)

Yield: 75%. ^1H NMR (CDCl_3) δ 8.12 (s, 1H), 7.31 (d, $J = 3.4$ Hz, 1H), 7.26 (dd, $J = 7.9$, 6.8 Hz, 2H), 7.20 – 7.11 (m, 2H), 7.09 (t, $J = 7.3$ Hz, 1H), 5.84 (s, 2H), 5.26 (s, 2H), 4.13 – 3.88 (m, 4H), 3.65 (d, $J = 8.4$ Hz, 3H), 2.72 (dd, $J = 14.7$, 7.5 Hz, 2H), 2.43 (s, 3H), 1.99 (dt, $J = 17.7$, 6.7 Hz, 2H), 1.32 (dd, $J = 6.4$, 3.4 Hz, 3H). ^{13}C NMR (CDCl_3) δ 174.3 – 173.9 (m), 168.7, 162.0, 156.0, 150.8 (d, $J = 9.2$ Hz), 147.5, 129.6 (d, $J = 1.8$ Hz), 124.8, 121.4, 120.2 (t, $J = 4.5$ Hz), 108.1, 66.0 – 65.5 (m), 52.4 (d, $J = 3.3$ Hz), 50.2 (d, $J = 8.6$ Hz), 48.5, 29.5 (d, $J = 7.3$ Hz), 25.5, 21.4 (d, $J = 2.8$ Hz), 21.3 – 20.7 (m). ^{31}P NMR (CDCl_3) δ 2.42 (ddd, $J = 32.8$, 17.0, 8.3 Hz). HRMS (ESI): calcd for $\text{C}_{21}\text{H}_{29}\text{N}_7\text{O}_5\text{P}$ $[\text{M}+\text{H}]^+$ 490.1962, found 490.1943.



Ethyl (((1-(1-((4-amino-2-methylpyrimidin-5-yl)methyl)-1H-1,2,3-triazol-4-yl)propan-2-yl)oxy)(phenoxy)phosphoryl)-L-alaninate (BW-VB-42)

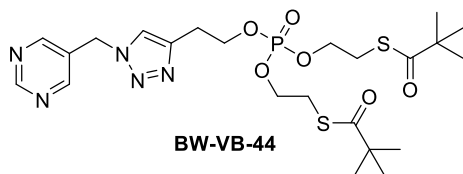
Product is a mixture of two diastereomers. Yield: 37%. ^1H NMR (CDCl_3) δ 8.14 (d, $J = 29.2$ Hz, 1H), 7.53 (d, $J = 20.7$ Hz, 1H), 7.28 (t, $J = 7.6$ Hz, 2H), 7.13 (dd, $J = 15.5$, 7.7 Hz, 3H), 5.86 (d, $J = 10.8$ Hz, 2H), 5.31 (d, $J = 3.3$ Hz, 1H), 5.18 (t, $J = 10.1$ Hz, 1H), 4.83 (dt, $J = 18.4$, 6.1 Hz, 1H), 4.27 – 4.02 (m, 2H), 4.01 – 3.72 (m, 2H), 3.16 – 2.83 (m, 2H), 2.46 (s, 3H), 1.39 – 1.17 (m, 9H). ^{13}C NMR (CDCl_3) δ 173.7, 168.7, 162.0, 156.1 (d, $J = 17.4$ Hz), 150.8 (d, $J = 7.0$ Hz), 144.6 – 144.0 (m), 129.6 (d, $J = 3.9$ Hz), 124.8 (d, $J = 3.9$ Hz), 122.8 – 122.4 (m), 120.2 (dd, $J = 11.2$, 6.0 Hz), 108.1, 74.3, 74.0, 61.5, 50.5 – 50.0 (m), 48.5, 34.0 – 33.5 (m), 25.5, 21.1 (dd, $J = 42.2$, 9.0 Hz), 14.1. ^{31}P NMR (CDCl_3) δ 1.79 – 0.89 (m). HRMS (ESI): calcd for $\text{C}_{22}\text{H}_{31}\text{N}_7\text{O}_5\text{P}$ $[\text{M}+\text{H}]^+$ 504.2119, found 504.2111.



BW-VB-43

2-(1-((Pyrimidin-5-ylmethyl)-1H-1,2,3-triazol-4-yl)ethan-1-ol (BW-VB-43)

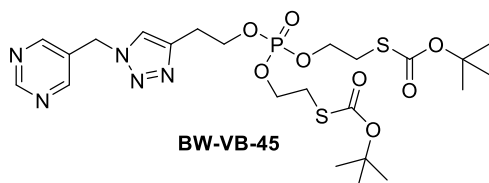
Yield: 35%. ^1H NMR (CDCl_3) δ 9.16 (s, 1H), 8.68 (s, 2H), 7.48 (s, 1H), 5.53 (s, 2H), 3.88 (t, $J = 6.0$ Hz, 2H), 2.91 (t, $J = 6.0$ Hz, 3H). ^{13}C NMR (CDCl_3) δ 158.9, 156.5, 146.6, 128.8, 121.9, 61.2, 49.1, 28.8. HRMS (ESI): calcd for $\text{C}_9\text{H}_{12}\text{N}_5\text{O}$ $[\text{M}+\text{H}]^+$ 206.1039, found 206.1029.



BW-VB-44

2-(1-((Pyrimidin-5-ylmethyl)-1H-1,2,3-triazol-4-yl)ethyl bisSATE phosphate (BW-VB-44)

Yield: 26%. ^1H NMR (CDCl_3) δ 9.18 (s, 1H), 8.70 (s, 2H), 7.58 (s, 1H), 5.56 (s, 2H), 4.30 (dd, $J = 13.9, 6.3$ Hz, 2H), 4.02 (dd, $J = 14.5, 6.8$ Hz, 4H), 3.15 – 3.02 (m, 6H), 1.19 (s, 18H). ^{13}C NMR (CDCl_3) δ 205.8, 158.9, 156.4, 144.6, 128.8, 122.3, 66.5 (d, $J = 5.9$ Hz), 66.1 (d, $J = 5.7$ Hz), 49.1, 46.5, 28.5 (d, $J = 7.4$ Hz), 27.4 – 26.9 (m). ^{31}P NMR (CDCl_3) δ -1.98 (dt, $J = 15.5, 7.7$ Hz). HRMS (ESI): calcd for $\text{C}_{23}\text{H}_{37}\text{N}_5\text{O}_6\text{PS}_2$ $[\text{M}+\text{H}]^+$ 574.1917, found 574.1906.



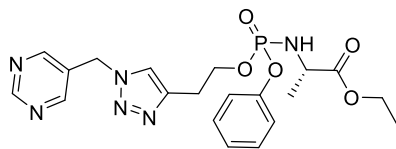
BW-VB-45

2-(1-((Pyrimidin-5-ylmethyl)-1H-1,2,3-triazol-4-yl)ethyl bis(2-((tert-butoxycarbonyl)thio)ethyl) phosphate (BW-VB-45)

Yield: 23%. ^1H NMR (CDCl_3) δ 9.19 (s, 1H), 8.70 (s, 2H), 7.56 (s, 1H), 5.55 (s, 2H), 4.30 (dd, $J = 13.8, 6.3$ Hz, 2H), 4.12 (dt, $J = 7.8, 6.6$ Hz, 4H), 3.11 (t, $J = 6.2$ Hz, 2H), 3.01 (t, $J = 6.6$ Hz, 4H), 1.45 (s, 18H). ^{13}C NMR (CDCl_3) δ 168.1, 159.0, 156.4, 144.6, 128.8, 122.3, 85.5,

66.6 (d, $J = 5.9$ Hz), 66.3 (d, $J = 5.7$ Hz), 49.1, 30.9 (d, $J = 7.4$ Hz), 28.2, 27.1 (d, $J = 7.0$ Hz).

^{31}P NMR (CDCl_3) δ -1.96 (dt, $J = 15.5, 7.7$ Hz). HRMS (ESI): calcd for $\text{C}_{23}\text{H}_{37}\text{N}_5\text{O}_8\text{PS}_2$ $[\text{M}+\text{H}]^+$ 606.1816, found 606.1815.

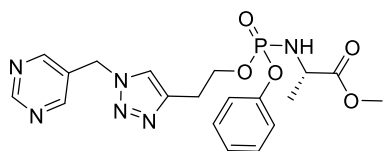


BW-VB-46

Ethyl (phenoxy(2-(1-(pyrimidin-5-ylmethyl)-1H-1,2,3-triazol-4-yl)ethoxy)phosphoryl)-L-alaninate (BW-VB-46)

Yield: 36%. ^1H NMR (CDCl_3) δ 9.17 (s, 1H), 8.66 (d, $J = 1.7$ Hz, 2H), 7.37 (d, $J = 10.0$ Hz, 1H), 7.25 (ddd, $J = 9.1, 6.9, 2.3$ Hz, 2H), 7.12 (dd, $J = 16.2, 8.3$ Hz, 3H), 5.46 (s, 2H), 4.43 – 4.21 (m, 2H), 4.18 – 4.02 (m, 2H), 3.97 – 3.71 (m, 2H), 3.08 (dd, $J = 14.8, 6.3$ Hz, 2H), 1.30 (dd, $J = 8.8, 7.1$ Hz, 3H), 1.20 (td, $J = 7.1, 2.8$ Hz, 3H). ^{13}C NMR (CDCl_3) δ 173.5 (t, $J = 7.1$ Hz), 158.9, 156.4 (d, $J = 1.8$ Hz), 150.7 (d, $J = 4.3$ Hz), 144.7 (d, $J = 4.6$ Hz), 129.6 (d, $J = 2.8$ Hz), 128.8, 124.9, 122.2, 120.2 (t, $J = 4.7$ Hz), 65.7 – 65.3 (m), 61.5, 50.3 (d, $J = 3.8$ Hz), 49.0, 27.1 (d, $J = 6.9$ Hz), 21.0 – 20.6 (m), 14.1 (d, $J = 2.0$ Hz). ^{31}P NMR (CDCl_3) δ 2.68 – 1.85 (m).

HRMS (ESI): calcd for $\text{C}_{20}\text{H}_{26}\text{N}_6\text{O}_5\text{P}$ $[\text{M}+\text{H}]^+$ 461.1697, found 461.0942.



BW-VB-47

Methyl (phenoxy(2-(1-(pyrimidin-5-ylmethyl)-1H-1,2,3-triazol-4-yl)ethoxy)phosphoryl)-L-alaninate (BW-VB-47)

Yield: 37%. ^1H NMR (CDCl_3) δ 9.15 (s, 1H), 8.65 (s, 2H), 7.37 (d, $J = 13.2$ Hz, 1H), 7.24 (dt, $J = 7.5, 1.7$ Hz, 2H), 7.11 (dt, $J = 15.3, 4.2$ Hz, 3H), 5.45 (s, 2H), 4.36 – 4.19 (m, 2H),

4.01 – 3.79 (m, 2H), 3.63 (d, $J = 0.8$ Hz, 3H), 3.06 (dt, $J = 9.1, 6.2$ Hz, 2H), 1.29 (dd, $J = 9.1, 6.7$ Hz, 3H). ^{13}C NMR (CDCl_3) δ 174.0 (dd, $J = 8.9, 6.9$ Hz), 158.8, 156.4 (d, $J = 1.0$ Hz), 150.8 – 150.6 (m), 144.7 (d, $J = 4.4$ Hz), 129.6 (d, $J = 2.7$ Hz), 128.8, 124.9, 122.3, 120.4 – 120.1 (m), 65.5 (t, $J = 5.3$ Hz), 52.5 (d, $J = 2.3$ Hz), 50.2 (d, $J = 5.1$ Hz), 49.0, 27.1 (d, $J = 7.1$ Hz), 20.8 (t, $J = 4.9$ Hz). ^{31}P NMR (CDCl_3) δ 3.03 – 1.49 (m). HRMS (ESI): calcd for $\text{C}_{19}\text{H}_{24}\text{N}_6\text{O}_5\text{P}$ $[\text{M}+\text{H}]^+$ 461.1697, found 461.0942.

REFERENCES

1. Iwasawa, S.; Kikuchi, Y.; Nishiwaki, Y.; Nakano, M.; Michikawa, T.; Tsuboi, T.; Tanaka, S.; Uemura, T.; Ishigami, A.; Nakashima, H.; Takebayashi, T.; Adachi, M.; Morikawa, A.; Maruyama, K.; Kudo, S.; Uchiyama, I.; Omae, K., Effects of SO₂ on Respiratory System of Adult Miyakejima Resident 2 Years after Returning to the Island. *J. Occup. Health* **2009**, *51* (1), 38-47.
2. Sang, N.; Yun, Y.; Li, H.; Hou, L.; Han, M.; Li, G., SO₂ inhalation contributes to the development and progression of ischemic stroke in the brain. *Toxicol. Sci.* **2010**, *114* (2), 226-36.
3. Meng, Z.; Qin, G.; Zhang, B.; Bai, J., DNA damaging effects of sulfur dioxide derivatives in cells from various organs of mice. *Mutagenesis* **2004**, *19* (6), 465-8.
4. Meng, Z., Oxidative damage of sulfur dioxide on various organs of mice: sulfur dioxide is a systemic oxidative damage agent. *Inhal. Toxicol.* **2003**, *15* (2), 181-95.
5. Mathew, N. D.; Schlipalius, D. I.; Ebert, P. R., Sulfurous gases as biological messengers and toxins: comparative genetics of their metabolism in model organisms. *J. Toxicol.* **2011**, *2011*, 394970.
6. Shi, X. L.; Mao, Y., 8-Hydroxy-2'-deoxyguanosine Formation and DNA Damage Induced by Sulfur Trioxide Anion Radicals. *Biochem. Biophys. Res. Commun.* **1994**, *205* (1), 141-147.
7. Muller, J. G.; Hickerson, R. P.; Perez, R. J.; Burrows, C. J., DNA damage from sulfite autoxidation catalyzed by a nickel(II) peptide. *J Am Chem Soc* **1997**, *119* (7), 1501-1506.
8. Mitsuhashi, H.; Yamashita, S.; Ikeuchi, H.; Kuroiwa, T.; Kaneko, Y.; Hiromura, K.; Ueki, K.; Nojima, Y., Oxidative stress-dependent conversion of hydrogen sulfide to sulfite by activated neutrophils. *Shock* **2005**, *24* (6), 529-34.

9. Huang, Y.; Tang, C.; Du, J.; Jin, H., Endogenous Sulfur Dioxide: A New Member of Gasotransmitter Family in the Cardiovascular System. *Oxid. Med. Cell. Longevity* **2016**, *2016*, 8961951.
10. Kaelin, W. G., Jr.; Ratcliffe, P. J., Oxygen sensing by metazoans: the central role of the HIF hydroxylase pathway. *Mol. Cell* **2008**, *30* (4), 393-402.
11. Lopez-Barneo, J.; Ortega-Saenz, P.; Pardal, R.; Pascual, A.; Piruat, J. I., Carotid body oxygen sensing. *Eur. Respir. J.* **2008**, *32* (5), 1386-98.
12. Cummins, E. P.; Selfridge, A. C.; Sporn, P. H.; Sznajder, J. I.; Taylor, C. T., Carbon dioxide-sensing in organisms and its implications for human disease. *Cell. Mol. Life Sci.* **2014**, *71* (5), 831-45.
13. Liu, D.; Jin, H.; Tang, C.; Du, J., Sulfur dioxide: a novel gaseous signal in the regulation of cardiovascular functions. *Mini-Rev. Med. Chem.* **2010**, *10* (11), 1039-45.
14. Wang, X. B.; Du, J. B.; Cui, H., Sulfur dioxide, a double-faced molecule in mammals. *Life Sci.* **2014**, *98* (2), 63-7.
15. Wang, X. B.; Du, J. B.; Cui, H., Signal pathways involved in the biological effects of sulfur dioxide. *Eur. J. Pharmacol.* **2015**, *764*, 94-9.
16. Goldberg, R. N.; Parker, V. B., Thermodynamics of solution of SO₂(g) in water and of aqueous sulfur dioxide solutions. *J. Res. Natl. Bur. Stand. (U. S.)* **1985**, *90* (5), 341.
17. Townsend, T. M.; Allanic, A.; Noonan, C.; Sodeau, J. R., Characterization of sulfurous acid, sulfite, and bisulfite aerosol systems. *J. Phys. Chem. A* **2012**, *116* (16), 4035-46.
18. Voegele, A. F.; Tautermann, C. S.; Rauch, C.; Loerting, T.; Liedl, K. R., On the Formation of the Sulfonate Ion from Hydrated Sulfur Dioxide. *J. Phys. Chem. A* **2004**, *108* (17), 3859-3864.

19. Tolmachev, Y. V.; Scherson, D. A., Electrochemical reduction of bisulfite in mildly acidic buffers: Kinetics of sulfur dioxide bisulfite interconversion. *J. Phys. Chem. A* **1999**, *103* (11), 1572-1578.
20. Bora, P.; Chauhan, P.; Pardeshi, K. A.; Chakrapani, H., Small molecule generators of biologically reactive sulfur species. *RSC Adv.* **2018**, *8* (48), 27359-27374.
21. Wang, S. S.; Zhang, Y. X.; Yang, F.; Huang, Z. Q.; Tang, J.; Hu, K. D.; Zhang, H., Sulfur dioxide alleviates programmed cell death in barley aleurone by acting as an antioxidant. *PLoS One* **2017**, *12* (11), e0188289.
22. Karakas, E.; Kisker, C., Structural analysis of missense mutations causing isolated sulfite oxidase deficiency. *Dalton Trans.* **2005**, (21), 3459-63.
23. Wang, X.-B.; Huang, X.-M.; Ochs, T.; Li, X.-Y.; Jin, H.-F.; Tang, C.-S.; Du, J.-B., Effect of sulfur dioxide preconditioning on rat myocardial ischemia/reperfusion injury by inducing endoplasmic reticulum stress. *Basic Res. Cardiol.* **2011**, *106* (5), 865.
24. Liang, Y.; Liu, D.; Ochs, T.; Tang, C.; Chen, S.; Zhang, S.; Geng, B.; Jin, H.; Du, J., Endogenous sulfur dioxide protects against isoproterenol-induced myocardial injury and increases myocardial antioxidant capacity in rats. *Lab. Invest.* **2011**, *91* (1), 12-23.
25. Jin, H.; Wang, Y.; Wang, X.; Sun, Y.; Tang, C.; Du, J., Sulfur dioxide preconditioning increases antioxidative capacity in rat with myocardial ischemia reperfusion (I/R) injury. *Nitric Oxide* **2013**, *32*, 56-61.
26. Chen, S.; Zheng, S.; Liu, Z.; Tang, C.; Zhao, B.; Du, J.; Jin, H., Endogenous sulfur dioxide protects against oleic acid-induced acute lung injury in association with inhibition of oxidative stress in rats. *Lab. Invest.* **2015**, *95* (2), 142-56.

27. Zheng, Y.; Yu, B.; De La Cruz, L. K.; Roy Choudhury, M.; Anifowose, A.; Wang, B., Toward Hydrogen Sulfide Based Therapeutics: Critical Drug Delivery and Developability Issues. *Med. Res. Rev.* **2018**, *38* (1), 57-100.
28. Ji, X.; Wang, B., Strategies toward Organic Carbon Monoxide Prodrugs. *Acc. Chem. Res.* **2018**, *51* (6), 1377-1385.
29. Schmidt, H. H. H. W.; Lohmann, S. M.; Walter, U., The nitric oxide and cGMP signal transduction system: regulation and mechanism of action. *Biochim. Biophys. Acta, Mol. Cell Res.* **1993**, *1178* (2), 153-175.
30. Yu, B.; Zheng, Y.; Yuan, Z.; Li, S.; Zhu, H.; De La Cruz, L. K.; Zhang, J.; Ji, K.; Wang, S.; Wang, B., Toward Direct Protein S-Persulfidation: A Prodrug Approach That Directly Delivers Hydrogen Persulfide. *J Am Chem Soc* **2018**, *140* (1), 30-33.
31. Knauert, M.; Vangala, S.; Haslip, M.; Lee, P. J., Therapeutic applications of carbon monoxide. *Oxid. Med. Cell. Longevity* **2013**, *2013*, 360815.
32. Brown, S. D.; Piantadosi, C. A., In vivo binding of carbon monoxide to cytochrome c oxidase in rat brain. *J. Appl. Physiol.* **1990**, *68* (2), 604-10.
33. Alonso, J. R.; Cardellach, F.; Lopez, S.; Casademont, J.; Miro, O., Carbon monoxide specifically inhibits cytochrome c oxidase of human mitochondrial respiratory chain. *Pharmacol. Toxicol.* **2003**, *93* (3), 142-6.
34. Zhang, J.; Piantadosi, C. A., Mitochondrial oxidative stress after carbon monoxide hypoxia in the rat brain. *J. Clin. Invest.* **1992**, *90* (4), 1193-9.
35. Du, S. X.; Jin, H. F.; Bu, D. F.; Zhao, X.; Geng, B.; Tang, C. S.; Du, J. B., Endogenously generated sulfur dioxide and its vasorelaxant effect in rats. *Acta Pharmacol. Sin.* **2008**, *29* (8), 923-30.

36. Cohen, H. J.; Fridovich, I.; Rajagopalan, K. V., Hepatic Sulfite Oxidase: A FUNCTIONAL ROLE FOR MOLYBDENUM. *J. Biol. Chem.* **1971**, *246* (2), 374-382.
37. Singer, T. P.; Kearney, E. B., Intermediary metabolism of l-cysteinesulfinic acid in animal tissues. *Arch. Biochem. Biophys.* **1956**, *61* (2), 397-409.
38. Mitsuhashi, H.; Yamashita, S.; Ikeuchi, H.; Kuroiwa, T.; Kaneko, Y.; Hiromura, K.; Ueki, K.; Nojima, Y., Oxidative Stress-Dependent Conversion of Hydrogen Sulfide to Sulfite by Activated Neutrophils. *Shock* **2005**, *24* (6), 529-534.
39. Kamoun, P., Endogenous production of hydrogen sulfide in mammals. *Amino Acids* **2004**, *26* (3), 243-54.
40. Qu, K.; Lee, S. W.; Bian, J. S.; Low, C. M.; Wong, P. T., Hydrogen sulfide: neurochemistry and neurobiology. *Neurochem Int.* **2008**, *52* (1-2), 155-65.
41. Zhang, D.; Wang, X.; Tian, X.; Zhang, L.; Yang, G.; Tao, Y.; Liang, C.; Li, K.; Yu, X.; Tang, X.; Tang, C.; Zhou, J.; Kong, W.; Du, J.; Huang, Y.; Jin, H., The Increased Endogenous Sulfur Dioxide Acts as a Compensatory Mechanism for the Downregulated Endogenous Hydrogen Sulfide Pathway in the Endothelial Cell Inflammation. *Front. Immunol.* **2018**, *9*, 882.
42. Stipanuk, M. H., Metabolism of sulfur-containing amino acids. *Annu. Rev. Nutr.* **1986**, *6*, 179-209.
43. Meng, Z.; Li, J.; Zhang, Q.; Bai, W.; Yang, Z.; Zhao, Y.; Wang, F., Vasodilator effect of gaseous sulfur dioxide and regulation of its level by Ach in rat vascular tissues. *Inhal. Toxicol.* **2009**, *21* (14), 1223-8.
44. Meng, Z.; Geng, H.; Bai, J.; Yan, G., Blood pressure of rats lowered by sulfur dioxide and its derivatives. *Inhal. Toxicol.* **2003**, *15* (9), 951-9.

45. Zhang, Q.; Meng, Z., The negative inotropic effects of gaseous sulfur dioxide and its derivatives in the isolated perfused rat heart. *Environ. Toxicol.* **2012**, *27* (3), 175-84.
46. Lovati, M. R.; Manzoni, C.; Daldossi, M.; Spolti, S.; Sirtori, C. R., Effects of sub-chronic exposure to SO₂ on lipid and carbohydrate metabolism in rats. *Arch. Toxicol.* **1996**, *70* (3-4), 164-173.
47. Haider, S. S., Effects of exhaust pollutant sulfur dioxide on lipid metabolism of guinea pig organs. *Ind. Health* **1985**, *23* (2), 81-87.
48. Mitsuhashi, H.; Nojima, Y.; Tanaka, T.; Ueki, K.; Maezawa, A.; Yano, S.; Naruse, T., Sulfite is released by human neutrophils in response to stimulation with lipopolysaccharide. *J. Leukocyte Biol.* **1998**, *64* (5), 595-599.
49. Bruske, I.; Hampel, R.; Baumgartner, Z.; Ruckerl, R.; Greven, S.; Koenig, W.; Peters, A.; Schneider, A., Ambient air pollution and lipoprotein-associated phospholipase A(2) in survivors of myocardial infarction. *Environ. Health Perspect* **2011**, *119* (7), 921-6.
50. Li, W.; Tang, C.; Jin, H.; Du, J., Regulatory effects of sulfur dioxide on the development of atherosclerotic lesions and vascular hydrogen sulfide in atherosclerotic rats. *Atherosclerosis* **2011**, *215* (2), 323-30.
51. Kajiyama, H.; Nojima, Y.; Mitsuhashi, H.; Ueki, K.; Tamura, S.; Sekihara, T.; Wakamatsu, R.; Yano, S.; Naruse, T., Elevated levels of serum sulfite in patients with chronic renal failure. *J. Am. Soc. Nephrol.* **2000**, *11* (5), 923-7.
52. Mitsuhashi, H.; Ikeuchi, H.; Yamashita, S.; Kuroiwa, T.; Kaneko, Y.; Hiromura, K.; Ueki, K.; Nojima, Y., Increased levels of serum sulfite in patients with acute pneumonia. *Shock* **2004**, *21* (2), 99-102.

53. Wu, W.; Jia, Y.; Du, S.; Tang, H.; Sun, Y.; Sun, L., Changes of sulfur dioxide, nuclear factor-kappaB, and interleukin-8 levels in pediatric acute lymphoblastic leukemia with bacterial inflammation. *Chin. Med. J. (Engl.)* **2014**, *127* (23), 4110-3.
54. Zhao, X.; Jin, H.-f.; Tang, C.-s.; Du, J.-b., Effects of sulfur dioxide, on the proliferation and apoptosis of aorta smooth muscle cells in hypertension: experiments with rats. *Zhonghua Yi Xue Za Zhi* **2008**, *88* (18), 1279-1283.
55. Yang, R. Y., Y; Dong, X; Wu, X; Wei, Y., Correlation between endogenous sulfur dioxide and homocysteine in children with pulmonary arterial hypertension associated with congenital heart disease. *Zhonghua Er Ke Za Zhi* **2014**, *8* (52).
56. Sun, Y.; Tian, Y.; Prabha, M.; Liu, D.; Chen, S.; Zhang, R.; Liu, X.; Tang, C.; Tang, X.; Jin, H.; Du, J., Effects of sulfur dioxide on hypoxic pulmonary vascular structural remodeling. *Lab. Invest.* **2010**, *90* (1), 68-82.
57. Yu, W.; Liu, D.; Liang, C.; Ochs, T.; Chen, S.; Chen, S.; Du, S.; Tang, C.; Huang, Y.; Du, J.; Jin, H., Sulfur Dioxide Protects Against Collagen Accumulation in Pulmonary Artery in Association With Downregulation of the Transforming Growth Factor beta1/Smad Pathway in Pulmonary Hypertensive Rats. *J. Am. Heart Assoc.* **2016**, *5* (10).
58. Jin, H. F.; Du, S. X.; Zhao, X.; Wei, H. L.; Wang, Y. F.; Liang, Y. F.; Tang, C. S.; Du, J. B., Effects of endogenous sulfur dioxide on monocrotaline-induced pulmonary hypertension in rats. *Acta Pharm. Sin.* **2008**, *29* (10), 1157-66.
59. Wang, X. B.; Huang, X. M.; Ochs, T.; Li, X. Y.; Jin, H. F.; Tang, C. S.; Du, J. B., Effect of sulfur dioxide preconditioning on rat myocardial ischemia/reperfusion injury by inducing endoplasmic reticulum stress. *Basic Res. Cardiol.* **2011**, *106* (5), 865-78.

60. Liu, D.; Huang, Y.; Bu, D.; Liu, A. D.; Holmberg, L.; Jia, Y.; Tang, C.; Du, J.; Jin, H., Sulfur dioxide inhibits vascular smooth muscle cell proliferation via suppressing the Erk/MAP kinase pathway mediated by cAMP/PKA signaling. *Cell Death Dis.* **2014**, *5*, e1251.
61. Naldini, L., Gene therapy returns to centre stage. *Nature* **2015**, *526* (7573), 351-60.
62. Malwal, S. R.; Sriram, D.; Yogeewari, P.; Konkimalla, V. B.; Chakrapani, H., Design, synthesis, and evaluation of thiol-activated sources of sulfur dioxide (SO₂) as antimycobacterial agents. *J. Med. Chem.* **2012**, *55* (1), 553-7.
63. Malwal, S. R.; Sriram, D.; Yogeewari, P.; Chakrapani, H., Synthesis and antimycobacterial activity of prodrugs of sulfur dioxide (SO₂). *Bioorg. Med. Chem. Lett.* **2012**, *22* (11), 3603-6.
64. Pardeshi, K. A.; Malwal, S. R.; Banerjee, A.; Lahiri, S.; Rangarajan, R.; Chakrapani, H., Thiol activated prodrugs of sulfur dioxide (SO₂) as MRSA inhibitors. *Bioorg. Med. Chem. Lett.* **2015**, *25* (13), 2694-7.
65. Li, M.; Feng, W.; Zhang, H.; Feng, G., An aza-coumarin-hemicyanine based near-infrared fluorescent probe for rapid, colorimetric and ratiometric detection of bisulfite in food and living cells. *Sens. Actuators, B* **2017**, *243*, 51-58.
66. Liu, Y.; Li, K.; Wu, M. Y.; Liu, Y. H.; Xie, Y. M.; Yu, X. Q., A mitochondria-targeted colorimetric and ratiometric fluorescent probe for biological SO₂ derivatives in living cells. *Chem. Commun. (Camb)* **2015**, *51* (50), 10236-9.
67. Xu, J.; Pan, J.; Jiang, X.; Qin, C.; Zeng, L.; Zhang, H.; Zhang, J. F., A mitochondria-targeted ratiometric fluorescent probe for rapid, sensitive and specific detection of biological SO₂ derivatives in living cells. *Biosens. Bioelectron.* **2016**, *77*, 725-32.

68. Wang, Q.; Wang, W.; Li, S.; Jiang, J.; Li, D.; Feng, Y.; Sheng, H.; Meng, X.; Zhu, M.; Wang, X., A mitochondria-targeted colorimetric and two-photon fluorescent probe for biological SO₂ derivatives in living cells. *Dyes Pigm.* **2016**, *134*, 297-305.
69. Liu, Y.; Li, K.; Xie, K. X.; Li, L. L.; Yu, K. K.; Wang, X.; Yu, X. Q., A water-soluble and fast-response mitochondria-targeted fluorescent probe for colorimetric and ratiometric sensing of endogenously generated SO₂ derivatives in living cells. *Chem. Commun. (Camb)* **2016**, *52* (16), 3430-3.
70. Malwal, S. R.; Gudem, M.; Hazra, A.; Chakrapani, H., Benzosultines as sulfur dioxide (SO₂) donors. *Org. Lett.* **2013**, *15* (5), 1116-9.
71. Malwal, S. R.; Chakrapani, H., Benzosulfones as photochemically activated sulfur dioxide (SO₂) donors. *Org. Biomol. Chem.* **2015**, *13* (8), 2399-406.
72. Kodama, R.; Sumaru, K.; Morishita, K.; Kanamori, T.; Hyodo, K.; Kamitanaka, T.; Morimoto, M.; Yokojima, S.; Nakamura, S.; Uchida, K., A diarylethene as the SO₂ gas generator upon UV irradiation. *Chem. Commun. (Camb)* **2015**, *51* (9), 1736-8.
73. Day, J. J.; Yang, Z.; Chen, W.; Pacheco, A.; Xian, M., Benzothiazole Sulfinate: a Water-Soluble and Slow-Releasing Sulfur Dioxide Donor. *ACS Chem. Biol.* **2016**, *11* (6), 1647-51.
74. Zhang, D.; Devarie-Baez, N. O.; Li, Q.; Lancaster, J. R., Jr.; Xian, M., Methylsulfonyl benzothiazole (MSBT): a selective protein thiol blocking reagent. *Org. Lett.* **2012**, *14* (13), 3396-9.
75. Xu, W.; Teoh, C. L.; Peng, J.; Su, D.; Yuan, L.; Chang, Y. T., A mitochondria-targeted ratiometric fluorescent probe to monitor endogenously generated sulfur dioxide derivatives in living cells. *Biomaterials* **2015**, *56*, 1-9.

76. Wang, K.; Peng, H.; Wang, B., Recent advances in thiol and sulfide reactive probes. *J. Cell. Biochem.* **2014**, *115* (6), 1007-22.
77. Wang, D.; Viennois, E.; Ji, K.; Damera, K.; Draganov, A.; Zheng, Y.; Dai, C.; Merlin, D.; Wang, B., A click-and-release approach to CO prodrugs. *Chem. Commun. (Camb)* **2014**, *50* (100), 15890-3.
78. Wang, K.; Peng, H. J.; Ni, N. T.; Dai, C. F.; Wang, B. H., 2,6-Dansyl Azide as a Fluorescent Probe for Hydrogen Sulfide. *J Fluoresc* **2014**, *24* (1), 1-5.
79. Zheng, Y.; Ji, X.; Ji, K.; Wang, B., Hydrogen sulfide prodrugs-a review. *Acta Pharm. Sin. B* **2015**, *5* (5), 367-77.
80. Ji, X.; Damera, K.; Zheng, Y.; Yu, B.; Otterbein, L. E.; Wang, B., Toward Carbon Monoxide-Based Therapeutics: Critical Drug Delivery and Developability Issues. *J. Pharm. Sci.* **2016**, *105* (2), 406-16.
81. Zheng, Y.; Yu, B.; Ji, K.; Pan, Z.; Chittavong, V.; Wang, B., Esterase-Sensitive Prodrugs with Tunable Release Rates and Direct Generation of Hydrogen Sulfide. *Angew. Chem., Int. Ed.* **2016**, *55* (14), 4514-8.
82. Nelb, R. G.; Stille, J. K., Three different consecutive orbital symmetry-controlled reactions in the novel stereospecific synthesis of 1-phenyl-4-(1-phenylethenyl)naphthalene. The reaction of 3,4-diphenylthiophene 1,1-dioxide with ethynylbenzene. *J Am Chem Soc* **1976**, *98* (10), 2834-2839.
83. Raasch, M. S., Annulations with tetrachlorothiophene 1,1-dioxide. *J. Org. Chem.* **1980**, *45* (5), 856-867.

84. Humphrey, R. E.; Ward, M. H.; Hinze, W., Spectrophotometric determination of sulfite with 4,4'-dithio-dipyridine and 5,5'-dithiobis(2-nitrobenzoic acid). *Anal. Chem.* **1970**, *42* (7), 698-702.
85. Guo, Z. X.; Li, Y. Z.; Zhang, X. X.; Chang, W. B.; Ci, Y. X., Flow injection determination of gaseous sulfur dioxide with gas permeation denuder-based online sampling and preconcentration. *Anal. Bioanal. Chem.* **2002**, *374* (6), 1141-6.
86. Li, Y.; Zhao, M., Simple methods for rapid determination of sulfite in food products. *Food Control* **2006**, *17* (12), 975-980.
87. Lin, V. S.; Chen, W.; Xian, M.; Chang, C. J., Chemical probes for molecular imaging and detection of hydrogen sulfide and reactive sulfur species in biological systems. *Chem. Soc. Rev.* **2015**, *44* (14), 4596-4618.
88. Lou, Y.; Chang, J.; Jorgensen, J.; Lemal, D. M., Octachloroazulene. *J. Am. Chem. Soc.* **2002**, *124* (51), 15302-15307.
89. Melhuish, W. H., Quantum Efficiencies of Fluorescence of Organic Substances: Effect of Solvent and Concentration of the Fluorescent Solute1. *J. Phys. Chem. A* **1961**, *65* (2), 229-235.
90. Baudin, J. B.; Hareau, G.; Julia, S. A.; Ruel, O., A direct synthesis of olefins by reaction of carbonyl compounds with lithio derivatives of 2-[alkyl- or (2' -alkenyl)- or benzyl-sulfonyl]-benzothiazoles. *Tetrahedron Lett.* **1991**, *32* (9), 1175-1178.
91. Blakemore, P. R., The modified Julia olefination: alkene synthesis via the condensation of metallated heteroarylalkylsulfones with carbonyl compounds. *Journal of the Chemical Society, Perkin Transactions 1* **2002**, (23), 2563-2585.

92. Yao, C. Z.; Li, Q. Q.; Wang, M. M.; Ning, X. S.; Kang, Y. B., (E)-Specific direct Julia-olefination of aryl alcohols without extra reducing agents promoted by bases. *Chem. Commun. (Camb)* **2015**, 51 (36), 7729-32.
93. Xu, S.; Gao, Y.; Chen, R.; Wang, K.; Zhang, Y.; Wang, J., Copper(I)-catalyzed olefination of N-sulfonylhydrazones with sulfones. *Chem. Commun. (Camb)* **2016**, 52 (24), 4478-80.
94. Uraguchi, D.; Nakamura, S.; Sasaki, H.; Konakade, Y.; Ooi, T., Enantioselective formal alpha-allylation of nitroalkanes through a chiral iminophosphorane-catalyzed Michael reaction-Julia-Kocienski olefination sequence. *Chem. Commun. (Camb)* **2014**, 50 (26), 3491-3.
95. Simlandy, A. K.; Mukherjee, S., Catalytic Enantioselective Synthesis of 3,4-Unsubstituted Thiochromenes through Sulfa-Michael/Julia-Kocienski Olefination Cascade Reaction. *J. Org. Chem.* **2017**, 82 (9), 4851-4858.
96. Robiette, R.; Pospíšil, J., On the Origin of E/Z Selectivity in the Modified Julia Olefination - Importance of the Elimination Step. *Eur. J. Org. Chem.* **2013**, 2013 (5), 836-840.
97. Borchardt, R. T.; Cohen, L. A., Stereopopulation control. II. Rate enhancement of intramolecular nucleophilic displacement. *J Am Chem Soc* **1972**, 94 (26), 9166-9174.
98. Valters, R., The Electronic and Steric Effects in Heterolytic Intramolecular Cyclisation Reactions. *Russ. Chem. Rev.* **1982**, 51 (8), 788-801.
99. Sun, Y.; Fan, S. W.; Zhang, S.; Zhao, D.; Duan, L.; Li, R. F., A fluorescent turn-on probe based on benzo[e]indolium for bisulfite through 1,4-addition reaction. *Sens. Actuators, B* **2014**, 193, 173-177.
100. Racker, E., Bioenergetics and the problem of tumor growth. *Am. Sci.* **1972**, 60 (1), 56-63.

101. Warburg, O., The Metabolism of Carcinoma Cells. *The Journal of Cancer Research* **1925**, 9 (1), 148-163.
102. Liberti, M. V.; Locasale, J. W., The Warburg Effect: How Does it Benefit Cancer Cells? *Trends Biochem. Sci.* **2016**, 41 (3), 211-218.
103. Shestov, A. A.; Liu, X.; Ser, Z.; Cluntun, A. A.; Hung, Y. P.; Huang, L.; Kim, D.; Le, A.; Yellen, G.; Albeck, J. G.; Locasale, J. W., Quantitative determinants of aerobic glycolysis identify flux through the enzyme GAPDH as a limiting step. *Elife* **2014**, 3.
104. Vander Heiden, M. G.; Cantley, L. C.; Thompson, C. B., Understanding the Warburg effect: the metabolic requirements of cell proliferation. *Science* **2009**, 324 (5930), 1029-33.
105. Ward, P. S.; Thompson, C. B., Metabolic reprogramming: a cancer hallmark even warburg did not anticipate. *Cancer cell* **2012**, 21 (3), 297-308.
106. Estrella, V.; Chen, T.; Lloyd, M.; Wojtkowiak, J.; Cornell, H. H.; Ibrahim-Hashim, A.; Bailey, K.; Balagurunathan, Y.; Rothberg, J. M.; Sloane, B. F.; Johnson, J.; Gatenby, R. A.; Gillies, R. J., Acidity generated by the tumor microenvironment drives local invasion. *Cancer Res.* **2013**, 73 (5), 1524-35.
107. Chang, C. H.; Qiu, J.; O'Sullivan, D.; Buck, M. D.; Noguchi, T.; Curtis, J. D.; Chen, Q.; Gindin, M.; Gubin, M. M.; van der Windt, G. J.; Tonc, E.; Schreiber, R. D.; Pearce, E. J.; Pearce, E. L., Metabolic Competition in the Tumor Microenvironment Is a Driver of Cancer Progression. *Cell* **2015**, 162 (6), 1229-41.
108. Gatenby, R. A.; Gillies, R. J., Glycolysis in cancer: a potential target for therapy. *Int. J. Biochem. Cell Biol.* **2007**, 39 (7-8), 1358-66.

109. Yu, X.; Hiromasa, Y.; Tsen, H.; Stoops, J. K.; Roche, T. E.; Zhou, Z. H., Structures of the human pyruvate dehydrogenase complex cores: a highly conserved catalytic center with flexible N-terminal domains. *Structure* **2008**, *16* (1), 104-14.
110. Roche, T. E.; Hiromasa, Y., Pyruvate dehydrogenase kinase regulatory mechanisms and inhibition in treating diabetes, heart ischemia, and cancer. *Cell Mol. Life Sci.* **2007**, *64* (7-8), 830-49.
111. Patel, M. S.; Nemeria, N. S.; Furey, W.; Jordan, F., The pyruvate dehydrogenase complexes: structure-based function and regulation. *J. Biol. Chem.* **2014**, *289* (24), 16615-23.
112. Patel, M. S.; Korotchkina, L. G., Regulation of the pyruvate dehydrogenase complex. *Biochem. Soc. Trans.* **2006**, *34* (2), 217-222.
113. Korotchkina, L. G.; Patel, M. S., Probing the mechanism of inactivation of human pyruvate dehydrogenase by phosphorylation of three sites. *J. Biol. Chem.* **2001**, *276* (8), 5731-8.
114. Saunier, E.; Benelli, C.; Bortoli, S., The pyruvate dehydrogenase complex in cancer: An old metabolic gatekeeper regulated by new pathways and pharmacological agents. *Int. J. Cancer* **2016**, *138* (4), 809-17.
115. Bowker-Kinley, M. M.; Davis, I. W.; Wu, P.; Harris, A. R.; Popov, M. K., Evidence for existence of tissue-specific regulation of the mammalian pyruvate dehydrogenase complex. *Biochem. J.* **1998**, *329* (1), 191-196.
116. Koukourakis MI, G. A., Sivridis E, Gatter KC, Harris AL, Pyruvate dehydrogenase and pyruvate dehydrogenase kinase expression in non small cell lung cancer and tumor-associated stroma. *Neoplasia (New York, NY)* **2005**, *7* (1), 1.
117. Lin, H. J.; Hsieh, F. C.; Song, H.; Lin, J., Elevated phosphorylation and activation of PDK-1/AKT pathway in human breast cancer. *Brit J Cancer* **2005**, *93* (12), 1372-81.

118. Kato, M.; Li, J.; Chuang, J. L.; Chuang, D. T., Distinct structural mechanisms for inhibition of pyruvate dehydrogenase kinase isoforms by AZD7545, dichloroacetate, and radicicol. *Structure* **2007**, *15* (8), 992-1004.
119. McFate, T.; Mohyeldin, A.; Lu, H.; Thakar, J.; Henriques, J.; Halim, N. D.; Wu, H.; Schell, M. J.; Tsang, T. M.; Teahan, O.; Zhou, S.; Califano, J. A.; Jeoung, N. H.; Harris, R. A.; Verma, A., Pyruvate dehydrogenase complex activity controls metabolic and malignant phenotype in cancer cells. *J. Biol. Chem.* **2008**, *283* (33), 22700-8.
120. Kolobova, E.; Tuganova, A.; Boulatnikov, I.; Popov, K. M., Regulation of pyruvate dehydrogenase activity through phosphorylation at multiple sites. *Biochem. J.* **2001**, *358*, 69-77.
121. Stacpoole, P. W., Therapeutic Targeting of the Pyruvate Dehydrogenase Complex/Pyruvate Dehydrogenase Kinase (PDC/PDK) Axis in Cancer. *J. Natl. Cancer Inst.* **2017**, *109* (11).
122. Lu, C. W.; Lin, S. C.; Chen, K. F.; Lai, Y. Y.; Tsai, S. J., Induction of pyruvate dehydrogenase kinase-3 by hypoxia-inducible factor-1 promotes metabolic switch and drug resistance. *J. Biol. Chem.* **2008**, *283* (42), 28106-14.
123. Wigfield, S. M.; Winter, S. C.; Giatromanolaki, A.; Taylor, J.; Koukourakis, M. L.; Harris, A. L., PDK-1 regulates lactate production in hypoxia and is associated with poor prognosis in head and neck squamous cancer. *Brit J Cancer* **2008**, *98* (12), 1975-1984.
124. Kim, J. W.; Dang, C. V., Cancer's molecular sweet tooth and the Warburg effect. *Cancer Res.* **2006**, *66* (18), 8927-30.
125. Contractor, T.; Harris, C. R., p53 negatively regulates transcription of the pyruvate dehydrogenase kinase Pdk2. *Cancer Res.* **2012**, *72* (2), 560-7.

126. Bonnet, S.; Archer, S. L.; Allalunis-Turner, J.; Haromy, A.; Beaulieu, C.; Thompson, R.; Lee, C. T.; Lopaschuk, G. D.; Puttagunta, L.; Bonnet, S.; Harry, G.; Hashimoto, K.; Porter, C. J.; Andrade, M. A.; Thebaud, B.; Michelakis, E. D., A mitochondria-K⁺ channel axis is suppressed in cancer and its normalization promotes apoptosis and inhibits cancer growth. *Cancer cell* **2007**, *11* (1), 37-51.
127. Sutendra, G.; Michelakis, E. D., Pyruvate dehydrogenase kinase as a novel therapeutic target in oncology. *Front. Oncol.* **2013**, *3*, 38.
128. Madhok, B. M.; Yeluri, S.; Perry, S. L.; Hughes, T. A.; Jayne, D. G., Dichloroacetate induces apoptosis and cell-cycle arrest in colorectal cancer cells. *Brit J Cancer* **2010**, *102* (12), 1746-52.
129. Garber, K., Energy deregulation: licensing tumors to grow. *Science* **2006**, *312* (5777), 1158-9.
130. Papandreou, I.; Goliassova, T.; Denko, N. C., Anticancer drugs that target metabolism: Is dichloroacetate the new paradigm? *Int. J. Cancer* **2011**, *128* (5), 1001-8.
131. Kankotia, S.; Stacpoole, P. W., Dichloroacetate and cancer: new home for an orphan drug? *Biochim. Biophys. Acta.* **2014**, *1846* (2), 617-29.
132. Sun, R. C.; Fadia, M.; Dahlstrom, J. E.; Parish, C. R.; Board, P. G.; Blackburn, A. C., Reversal of the glycolytic phenotype by dichloroacetate inhibits metastatic breast cancer cell growth in vitro and in vivo. *Breast Cancer Res. Treat.* **2010**, *120* (1), 253-60.
133. Chu, Q. S.; Sangha, R.; Spratlin, J.; Vos, L. J.; Mackey, J. R.; McEwan, A. J.; Venner, P.; Michelakis, E. D., A phase I open-labeled, single-arm, dose-escalation, study of dichloroacetate (DCA) in patients with advanced solid tumors. *Invest. New Drugs* **2015**, *33* (3), 603-10.

134. Li, J.; Kato, M.; Chuang, D. T., Pivotal role of the C-terminal DW-motif in mediating inhibition of pyruvate dehydrogenase kinase 2 by dichloroacetate. *J. Biol. Chem.* **2009**, *284* (49), 34458-67.
135. Knoechel, T. R.; Tucker, A. D.; Robinson, C. M.; Phillips, C.; Taylor, W.; Bungay, P. J.; Kasten, S. A.; Roche, T. E.; Brown, D. G., Regulatory roles of the N-terminal domain based on crystal structures of human pyruvate dehydrogenase kinase 2 containing physiological and synthetic ligands. *Biochemistry* **2006**, *45* (2), 402-15.
136. Kato, M.; Wynn, R. M.; Chuang, J. L.; Tso, S. C.; Machius, M.; Li, J.; Chuang, D. T., Structural basis for inactivation of the human pyruvate dehydrogenase complex by phosphorylation: role of disordered phosphorylation loops. *Structure* **2008**, *16* (12), 1849-59.
137. Stacpoole, P. W., The dichloroacetate dilemma: environmental hazard versus therapeutic goldmine--both or neither? *Environ. Health Perspect* **2011**, *119* (2), 155-8.
138. Schoors, S.; Bruning, U.; Missiaen, R.; Queiroz, K. C.; Borgers, G.; Elia, I.; Zecchin, A.; Cantelmo, A. R.; Christen, S.; Goveia, J.; Heggermont, W.; Godde, L.; Vinckier, S.; Van Veldhoven, P. P.; Eelen, G.; Schoonjans, L.; Gerhardt, H.; Dewerchin, M.; Baes, M.; De Bock, K.; Ghesquiere, B.; Lunt, S. Y.; Fendt, S. M.; Carmeliet, P., Fatty acid carbon is essential for dNTP synthesis in endothelial cells. *Nature* **2015**, *520* (7546), 192-197.
139. de Jong, L.; Meng, Y.; Dent, J.; Hekimi, S., Thiamine pyrophosphate biosynthesis and transport in the nematode *Caenorhabditis elegans*. *Genetics* **2004**, *168* (2), 845-54.
140. Comin-Anduix, B.; Boren, J.; Martinez, S.; Moro, C.; Centelles, J. J.; Trebukhina, R.; Petushok, N.; Lee, W. N.; Boros, L. G.; Cascante, M., The effect of thiamine supplementation on tumour proliferation. A metabolic control analysis study. *Eur. J. Biochem.* **2001**, *268* (15), 4177-82.

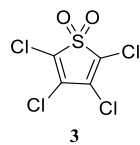
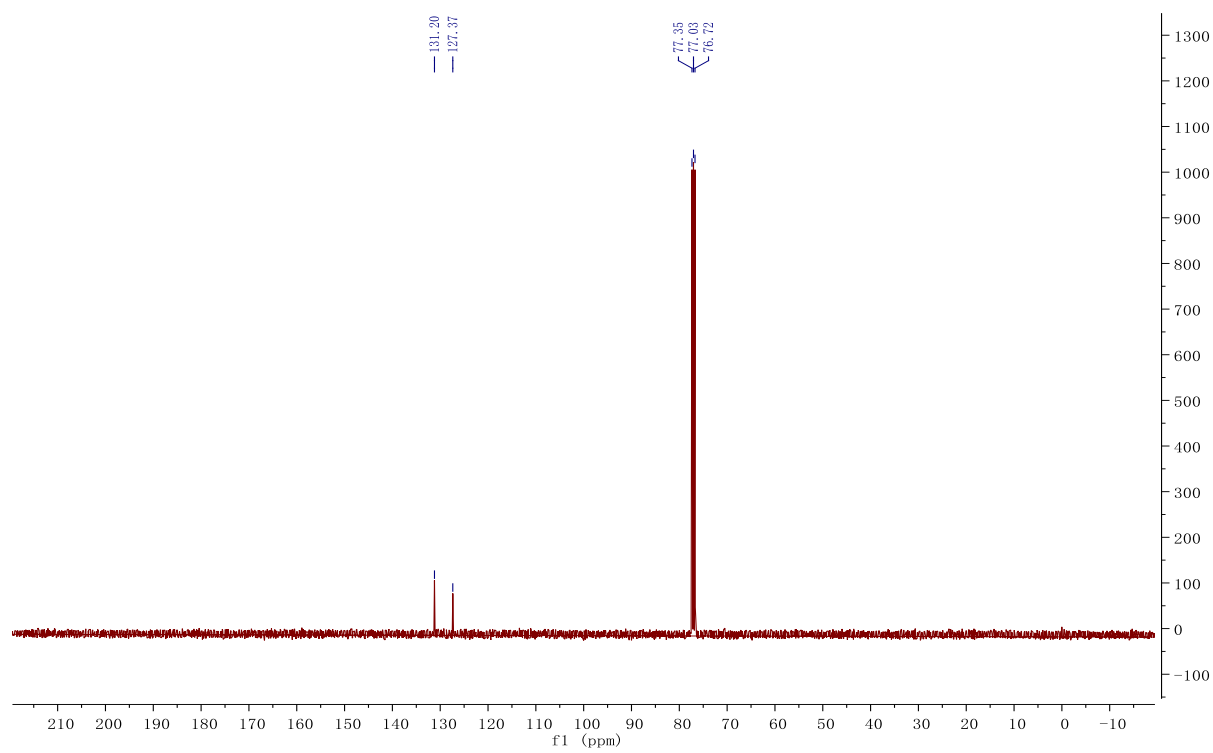
141. Hanberry, B. S.; Berger, R.; Zastre, J. A., High-dose vitamin B1 reduces proliferation in cancer cell lines analogous to dichloroacetate. *Cancer Chemother. Pharmacol.* **2014**, *73* (3), 585-94.
142. Smithline, H. A.; Donnino, M.; Greenblatt, D. J., Pharmacokinetics of high-dose oral thiamine hydrochloride in healthy subjects. *BMC Clin. Pharmacol.* **2012**, *12*, 4.
143. Pradere, U.; Garnier-Amblard, E. C.; Coats, S. J.; Amblard, F.; Schinazi, R. F., Synthesis of nucleoside phosphate and phosphonate prodrugs. *Chem. Rev.* **2014**, *114* (18), 9154-218.
144. Hwang, Y.; Cole, P. A., Efficient synthesis of phosphorylated prodrugs with bis(POM)-phosphoryl chloride. *Org Lett* **2004**, *6* (10), 1555-6.
145. Ruda, G. F.; Alibu, V. P.; Mitsos, C.; Bidet, O.; Kaiser, M.; Brun, R.; Barrett, M. P.; Gilbert, I. H., Synthesis and biological evaluation of phosphate prodrugs of 4-phospho-D-erythronohydroxamic acid, an inhibitor of 6-phosphogluconate dehydrogenase. *ChemMedChem* **2007**, *2* (8), 1169-80.
146. Dinh, H. T., Design and Synthesis of Thiamine Analogs as Anti-Cancer Therapeutics. *Thesis, Georgia State University* **2012**.
147. Temperini, A.; Annesi, D.; Testaferri, L.; Tiecco, M., A simple acylation of thiols with anhydrides. *Tetrahedron Letters* **2010**, *51* (41), 5368-5371.
148. Bondada, L.; Detorio, M.; Bassit, L.; Tao, S.; Montero, C. M.; Singletary, T. M.; Zhang, H.; Zhou, L.; Cho, J. H.; Coats, S. J.; Schinazi, R. F., Adenosine Dioxolane Nucleoside Phosphoramidates as Antiviral Agents for Human Immunodeficiency and Hepatitis B Viruses. *ACS Med. Chem. Lett.* **2013**, *4* (8), 747-751.

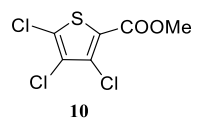
149. McGuigan, C.; Cahard, D.; Sheeka, H. M.; De Clercq, E.; Balzarini, J., Aryl phosphoramidate derivatives of d4T have improved anti-HIV efficacy in tissue culture and may act by the generation of a novel intracellular metabolite. *J. Med. Chem.* **1996**, *39* (8), 1748-53.
150. Bobek, M.; Kawai, I.; De Clercq, E., Synthesis and biological activity of 5-(2,2-difluorovinyl)-2'-deoxyuridine. *J. Med. Chem.* **1987**, *30* (8), 1494-1497.
151. Ple, N.; Turck, A.; Fiquet, E.; Queguiner, G., Metallation of diazines.III. New synthesis of analogues of trimethoprim and of bacimethrin. *J. Heterocycl. Chem.* **1991**, *28* (2), 283-287.

APPENDICES

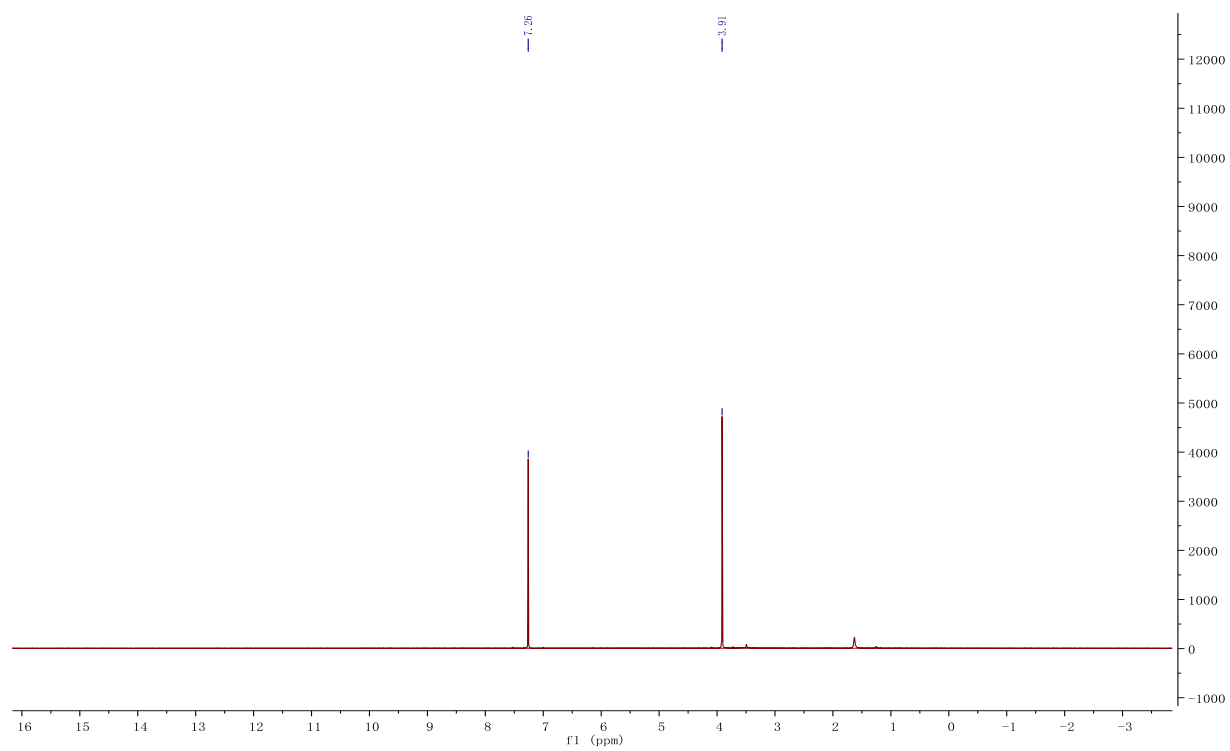
Appendix A NMR spectra of compounds in Chapter 1

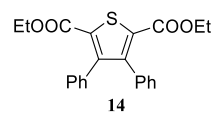
Appendix A.1 NMR spectra of compound in Chapter 1.2

 ^{13}C NMR

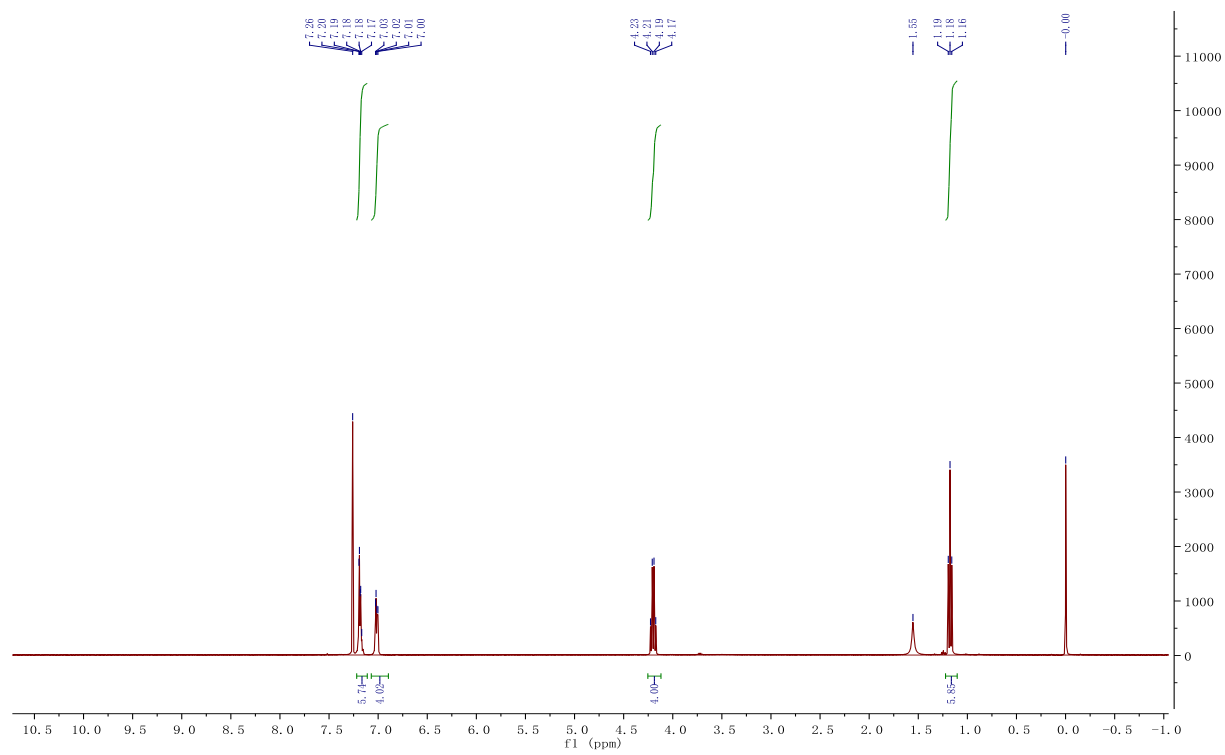


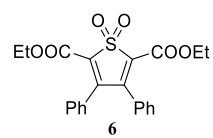
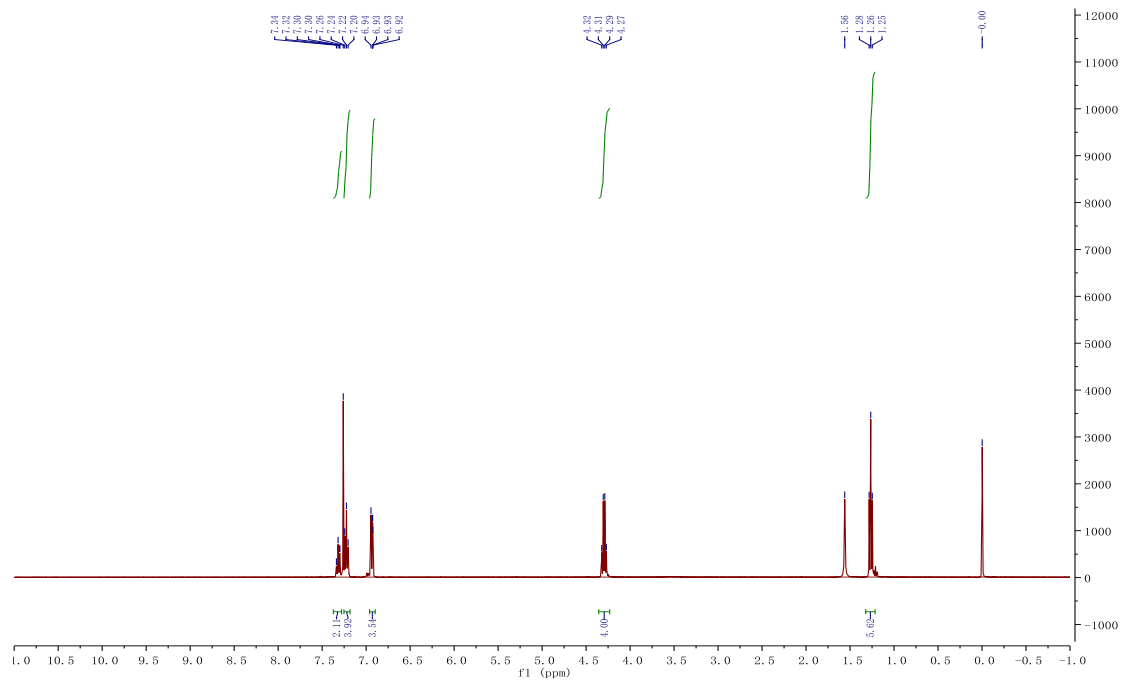
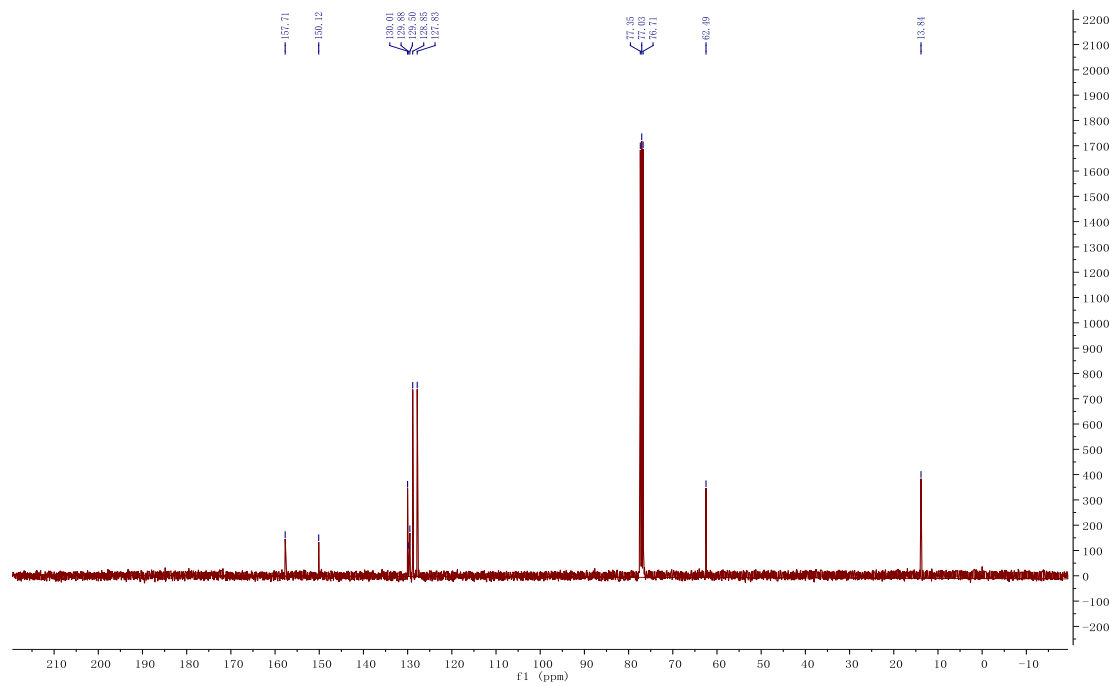
^1H NMR

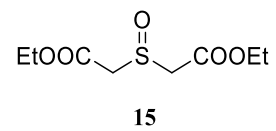




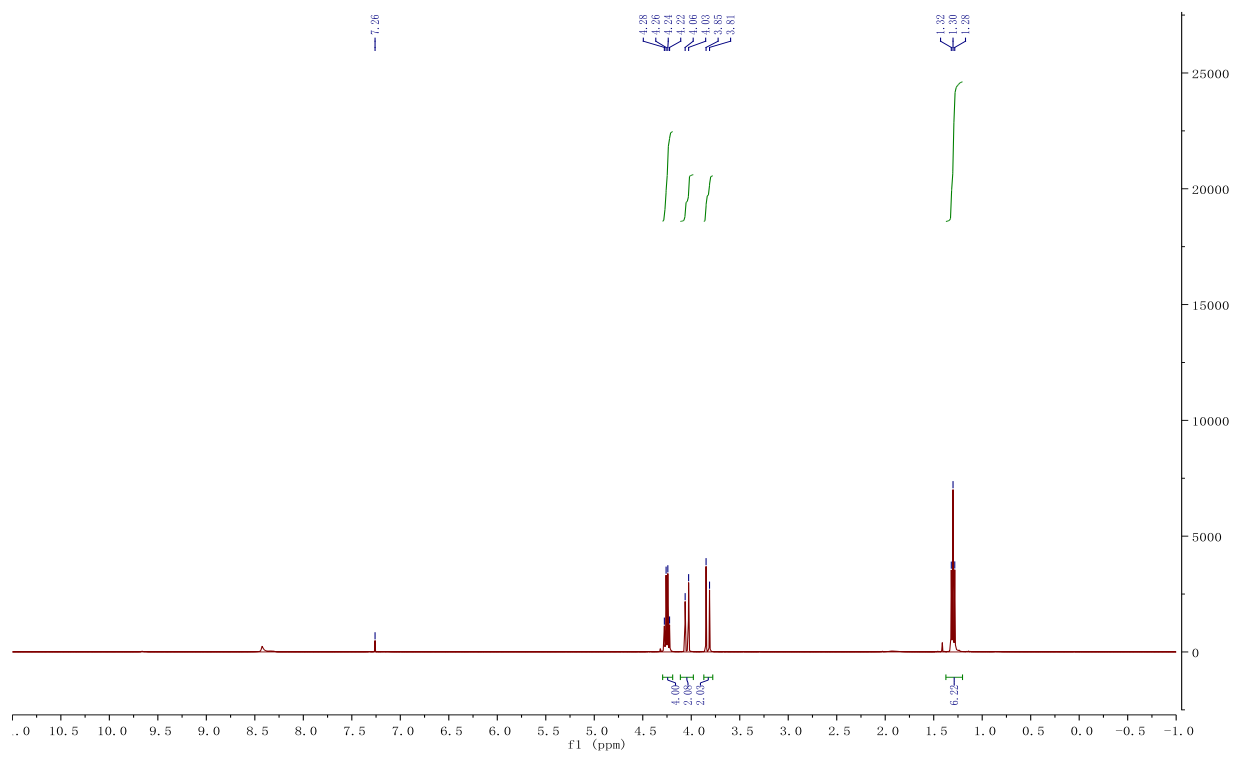
$^1\text{H NMR}$

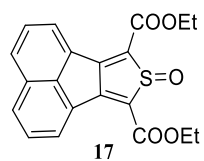
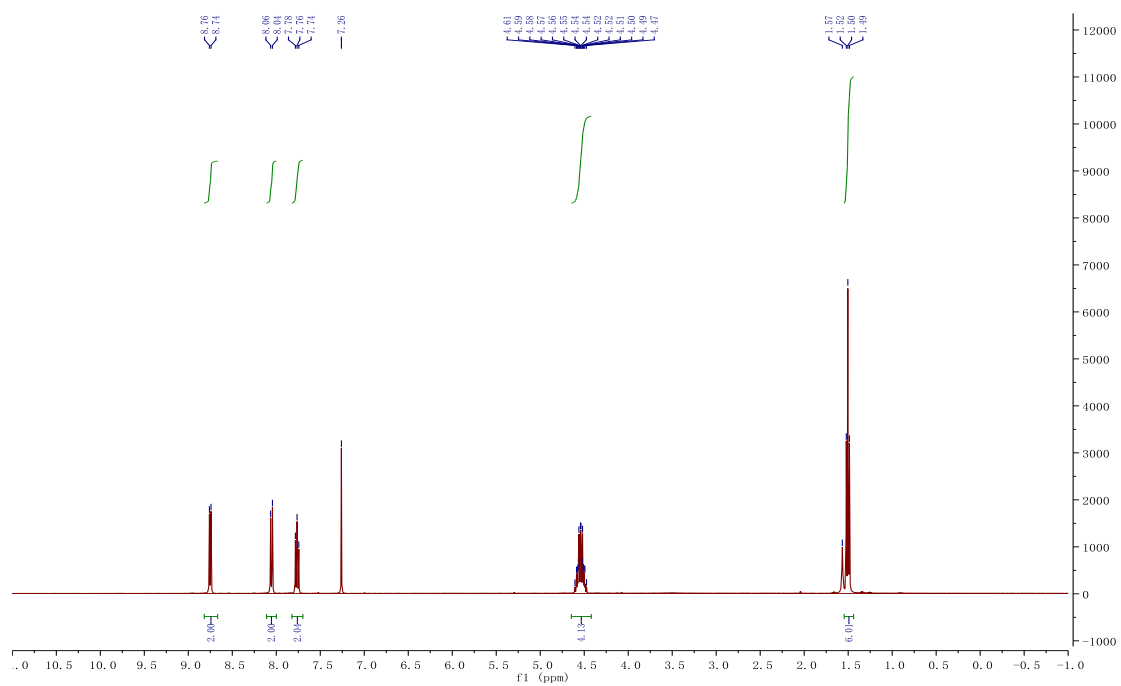
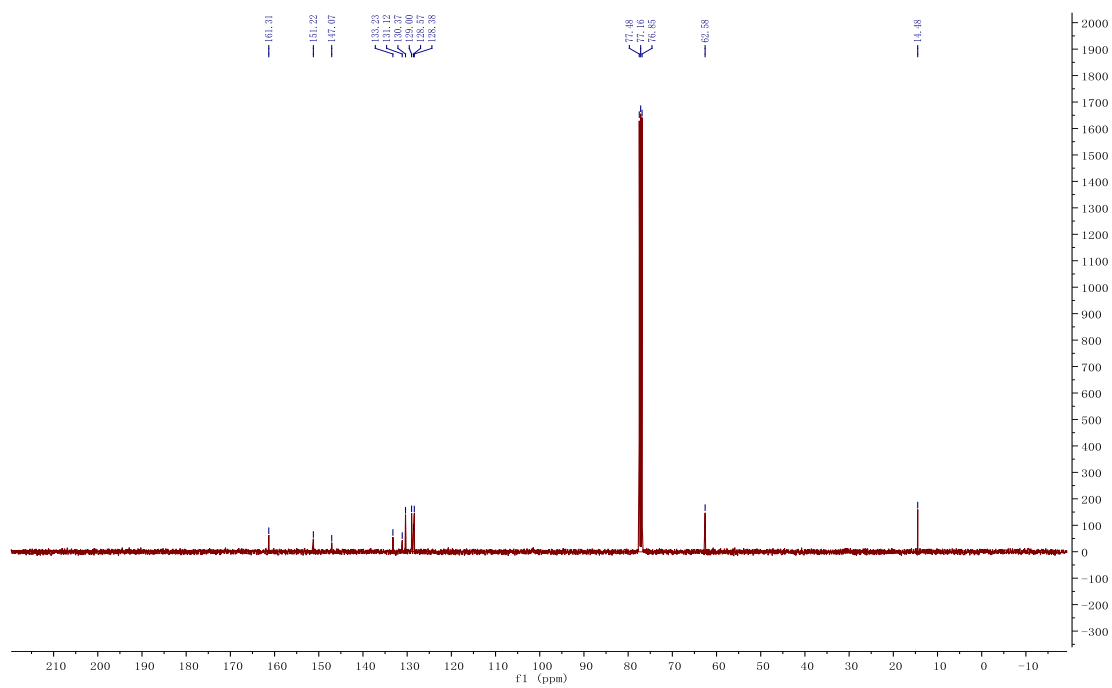


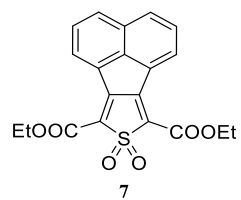
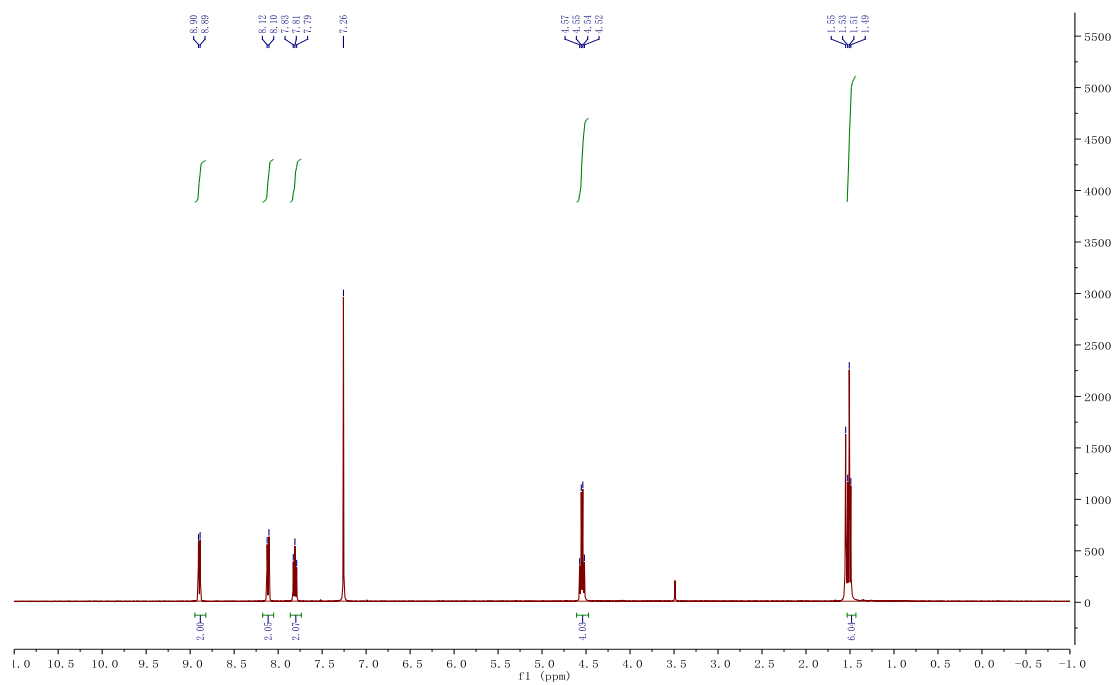
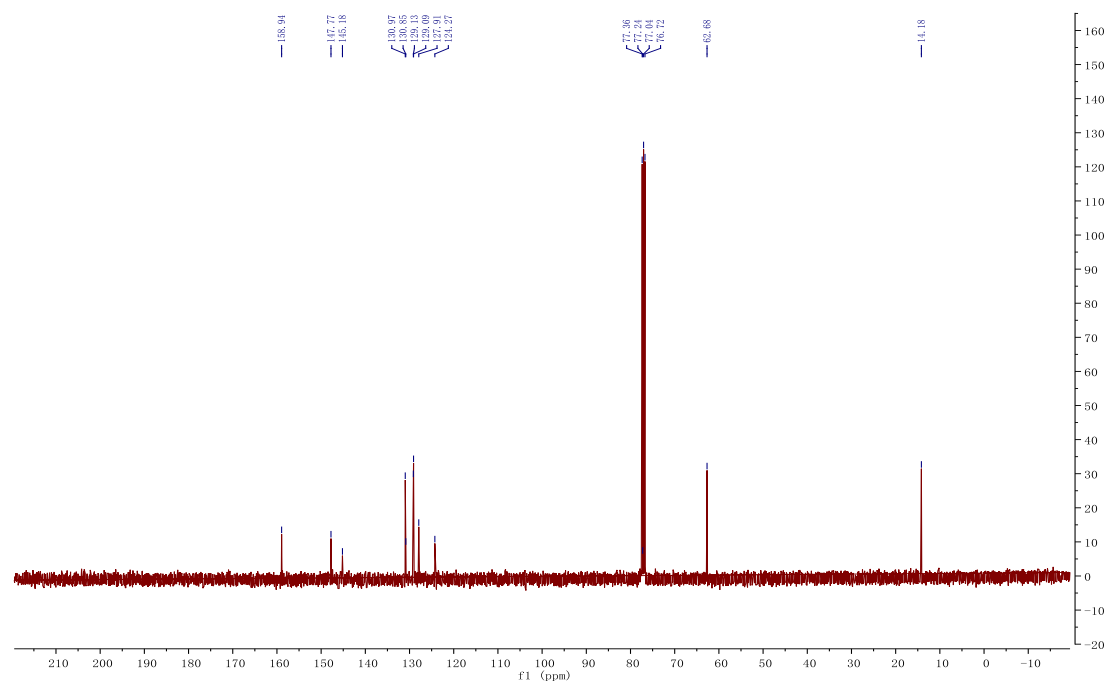
 ^1H NMR ^{13}C NMR

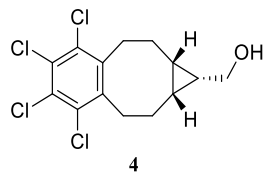


^1H NMR

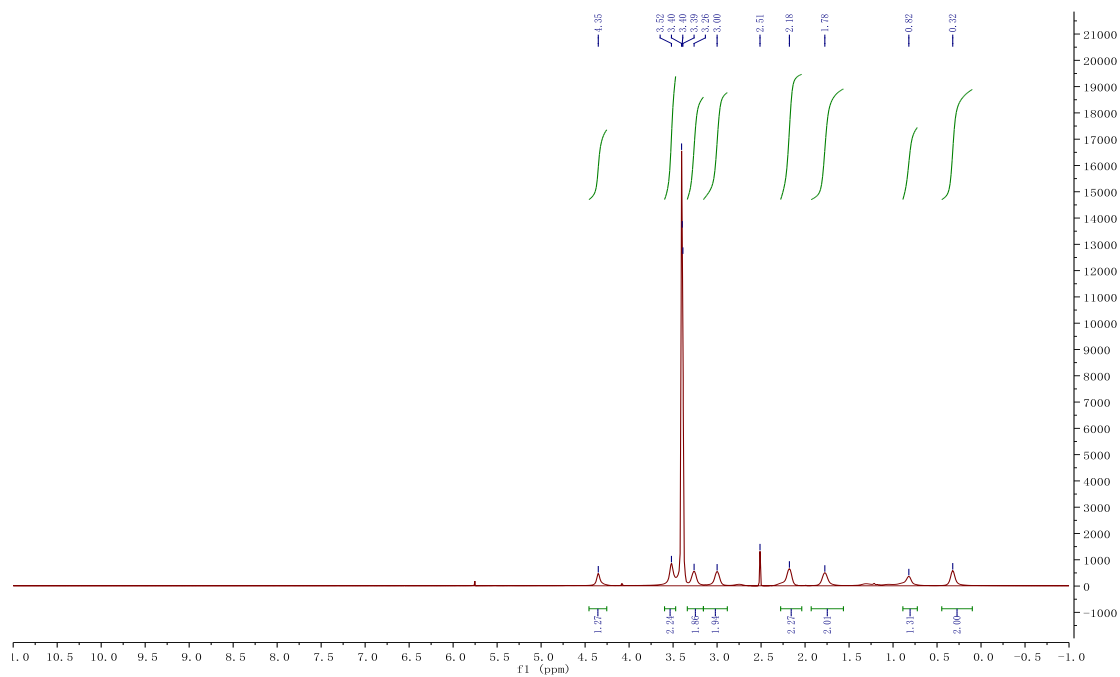


¹H NMR¹³C NMR

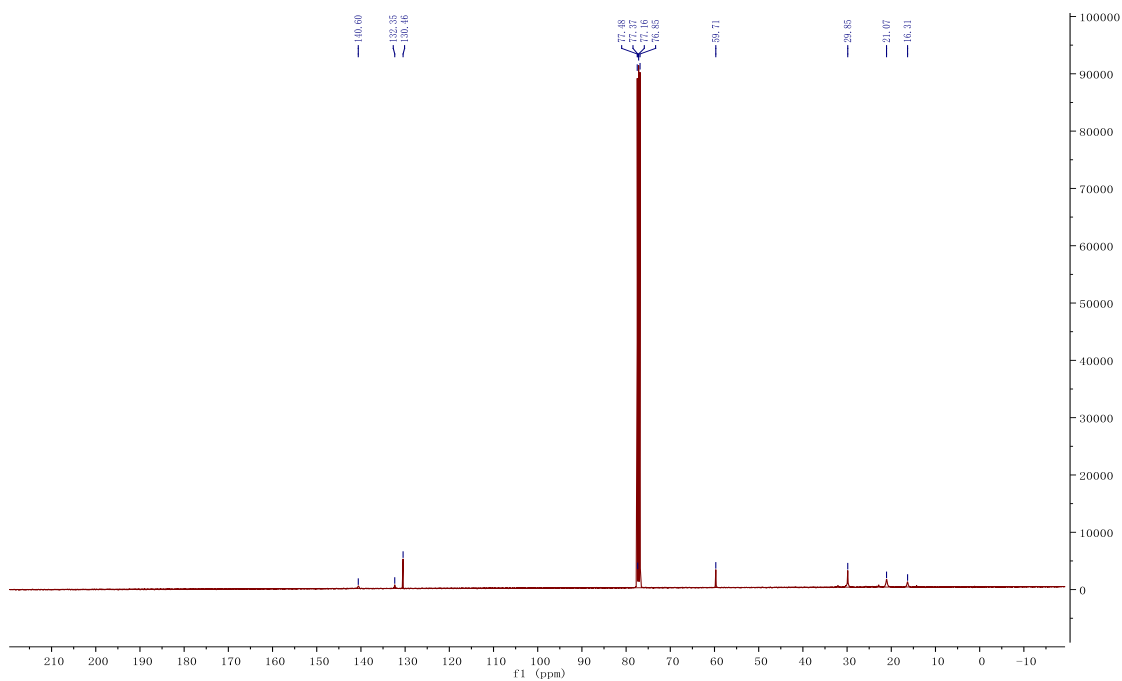
 $^1\text{H NMR}$  $^{13}\text{C NMR}$ 

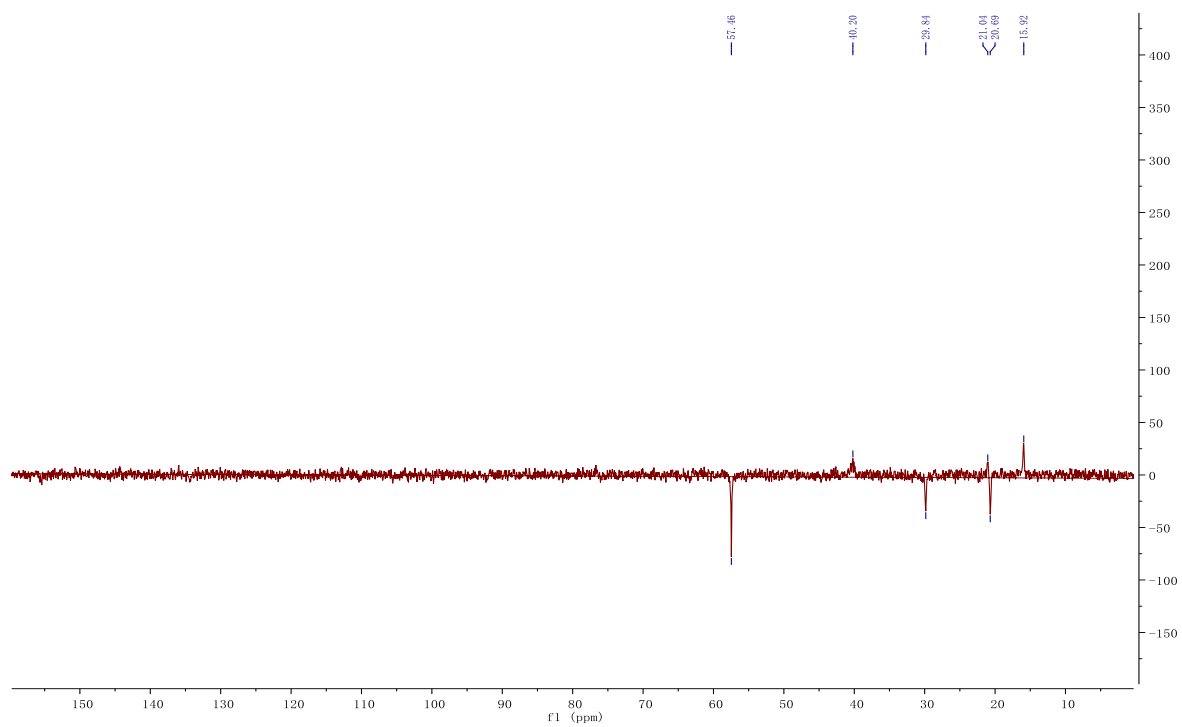
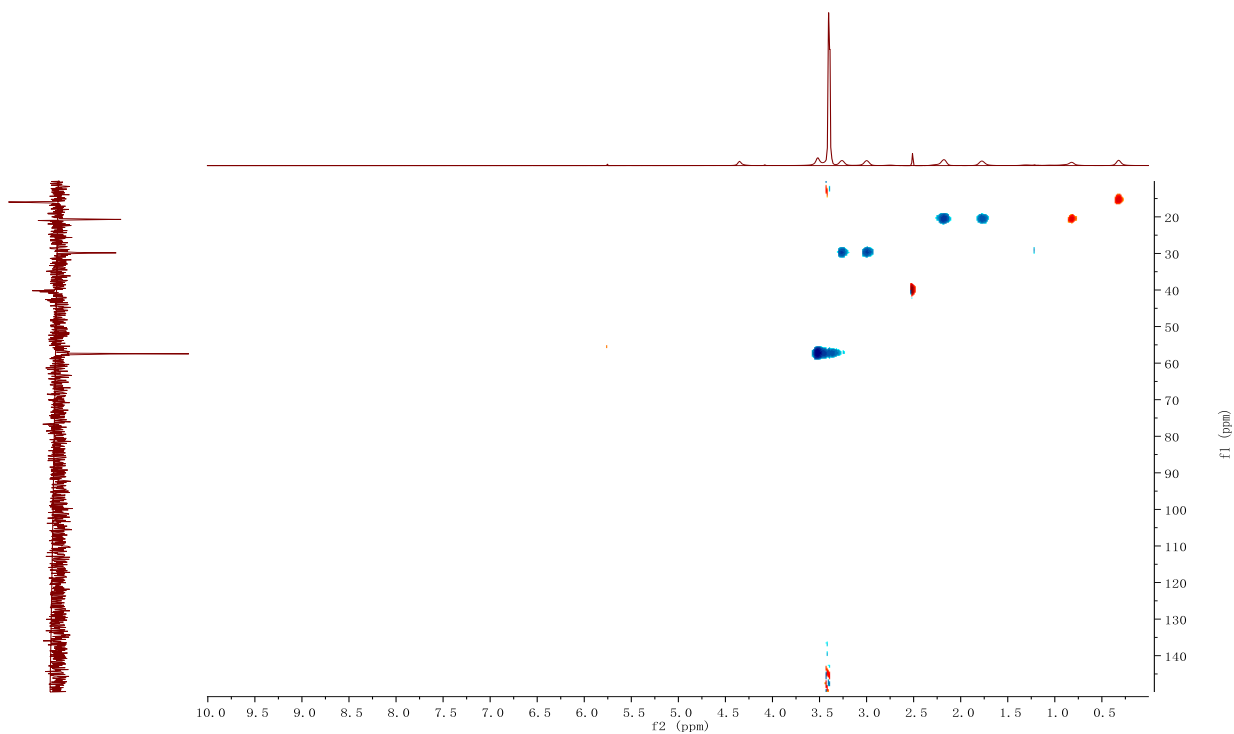


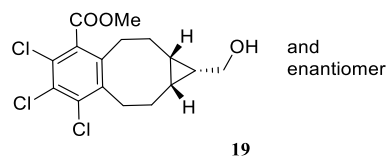
^1H NMR (600 MHz, DMSO- d_6)



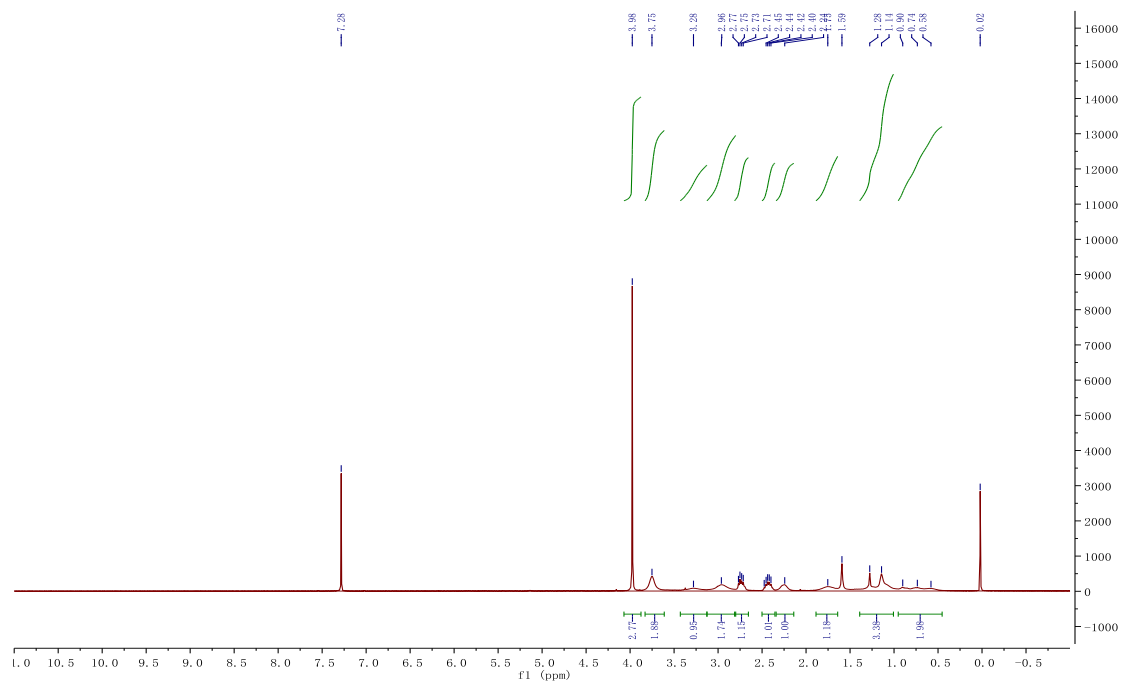
^{13}C NMR



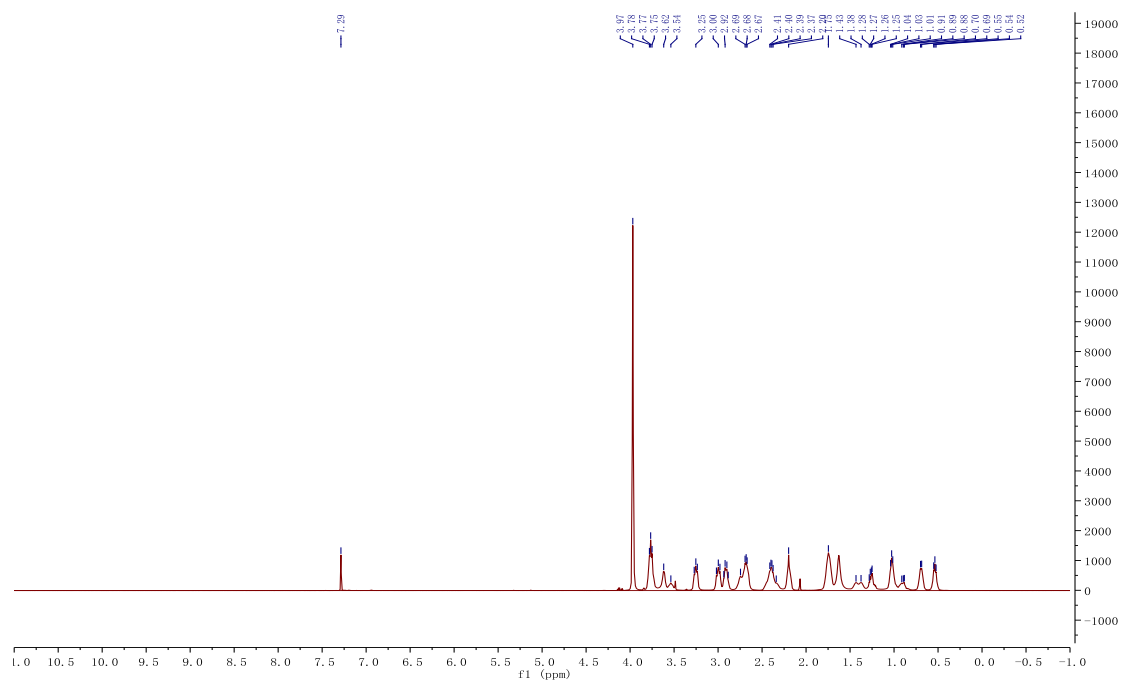
DEPT-135 (151 MHz, DMSO-d₆)Edited HSQC (DMSO-d₆)

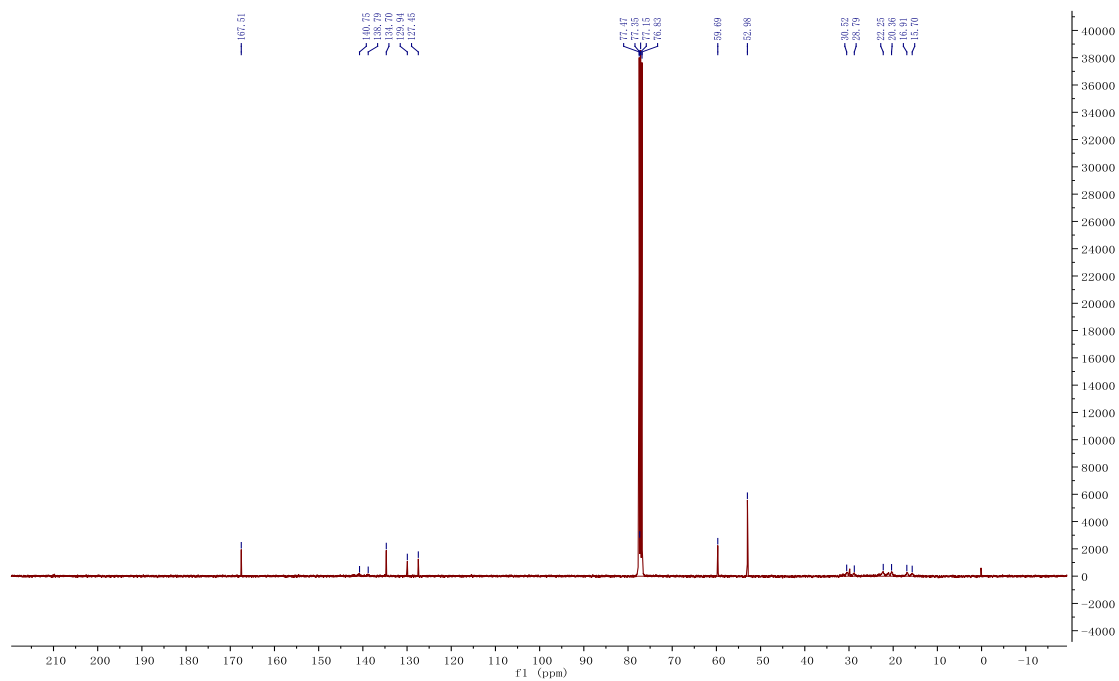
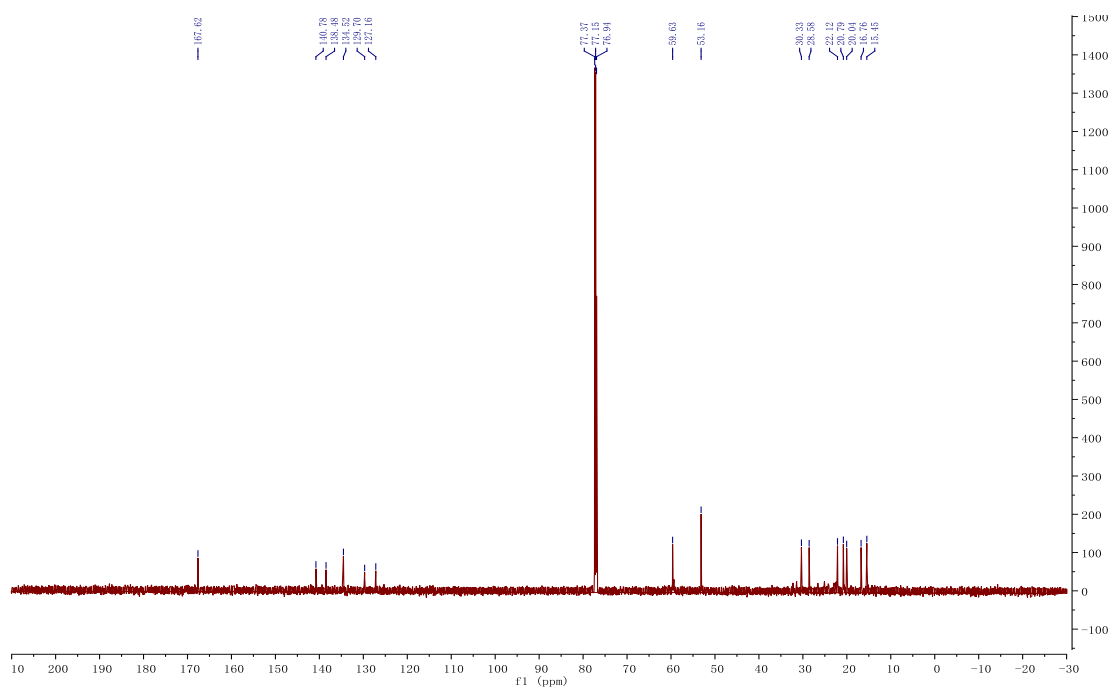


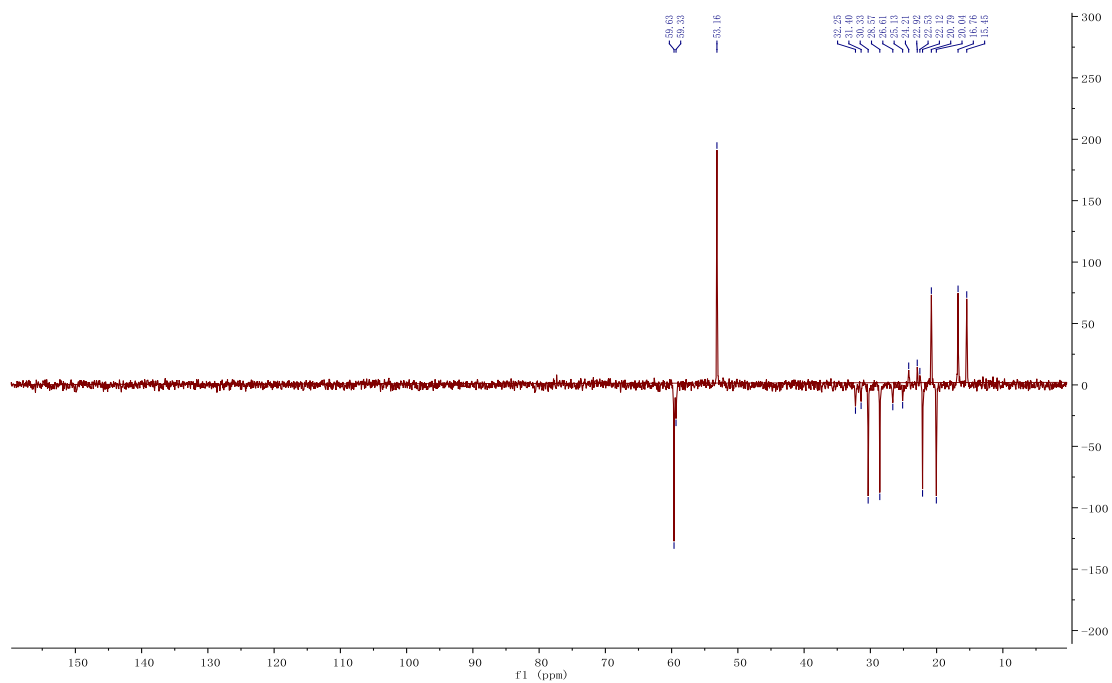
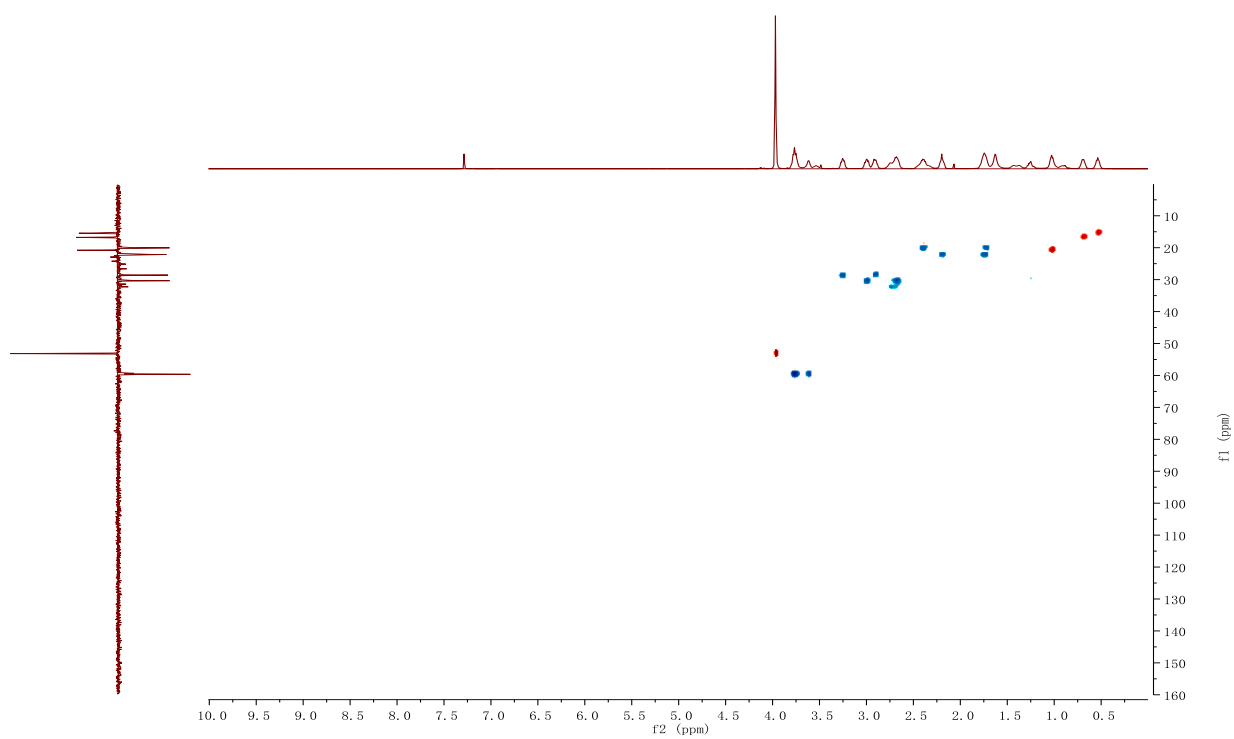
^1H NMR

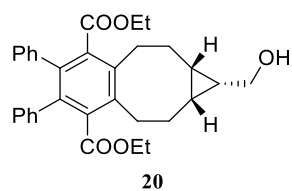


^1H NMR (600 MHz, CDCl_3 , 270 K)

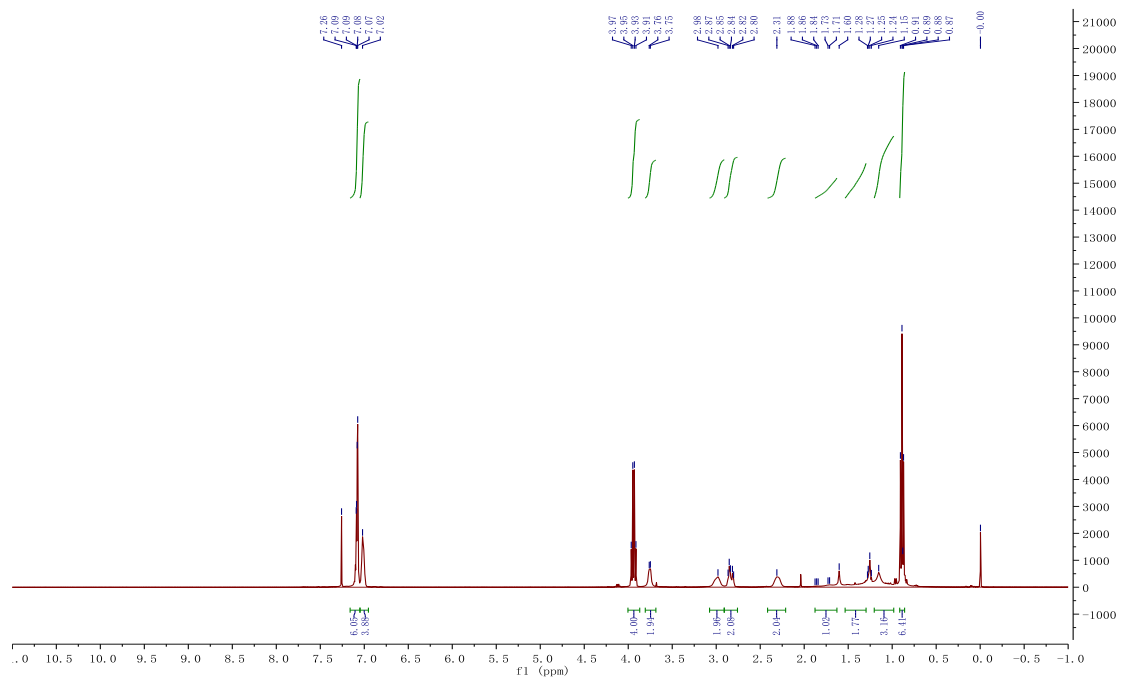


^{13}C NMR ^{13}C NMR (151 MHz, CDCl_3 , 270 K)

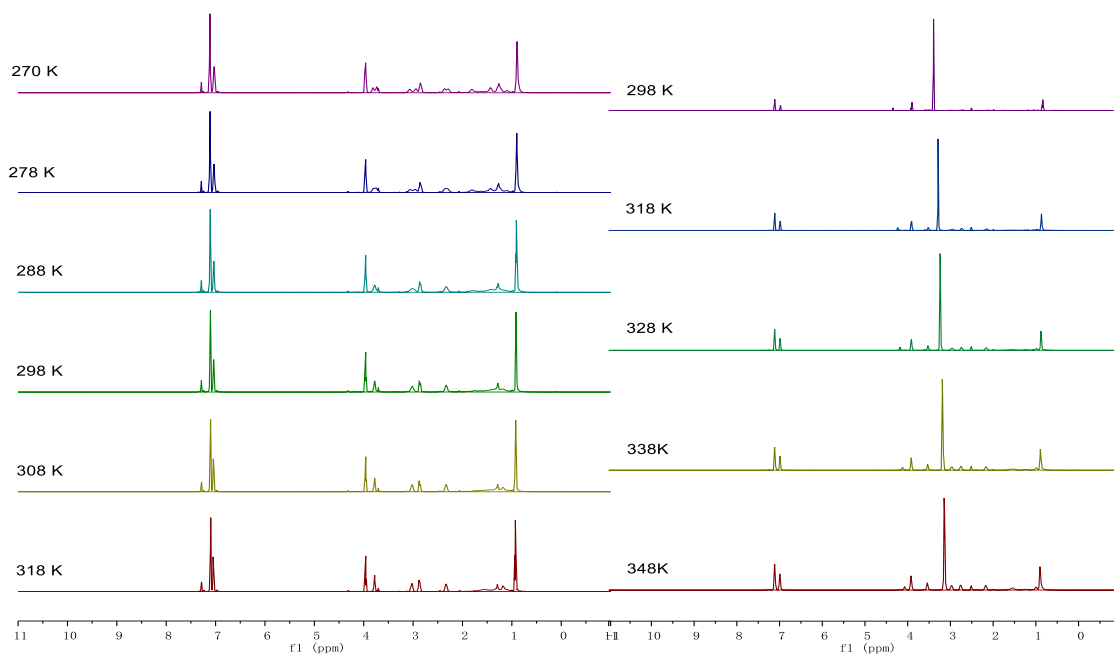
DEPT-135 (151 MHz, CDCl₃, 270 K)Edited HSQC (CDCl₃, 270 K)

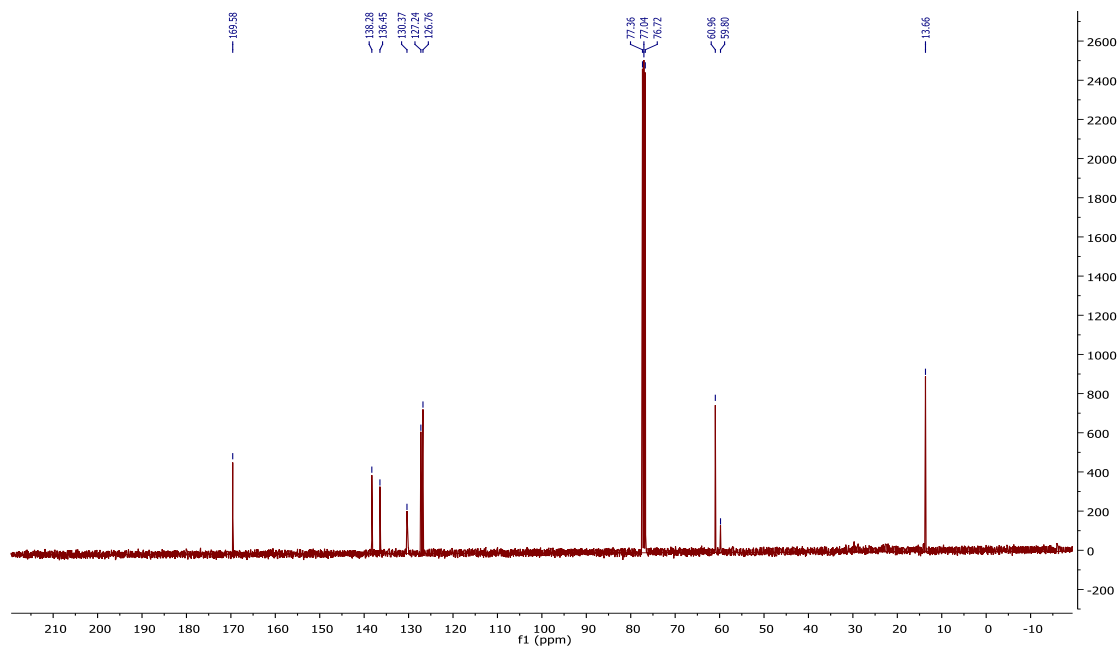


^1H NMR (400 MHz, CDCl_3)

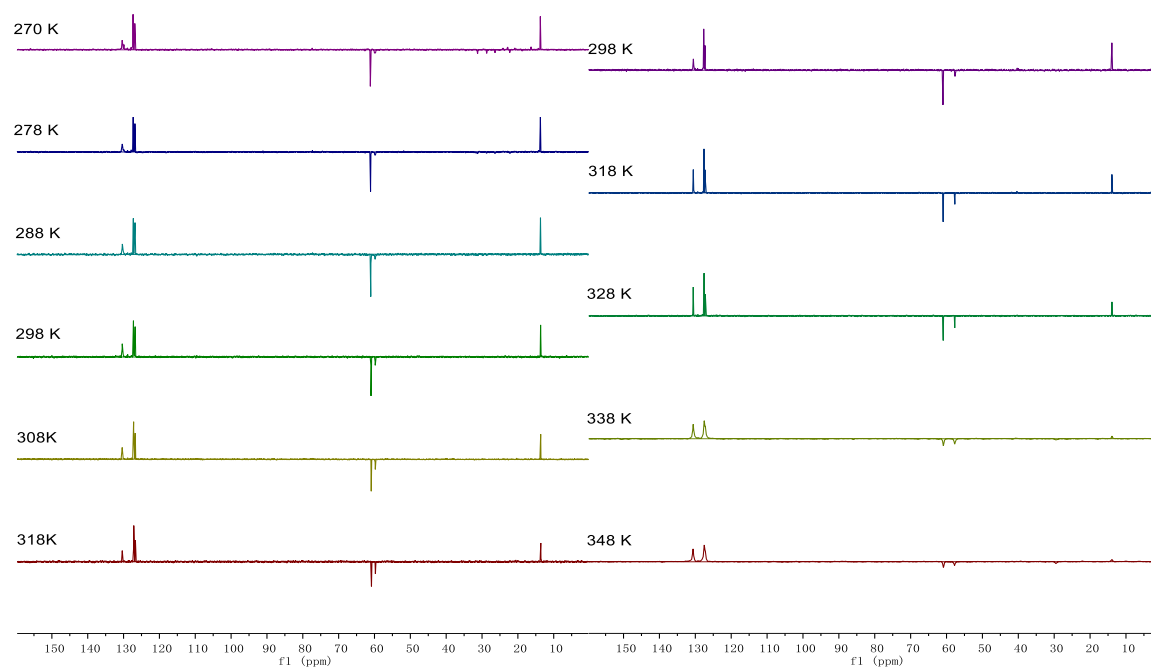


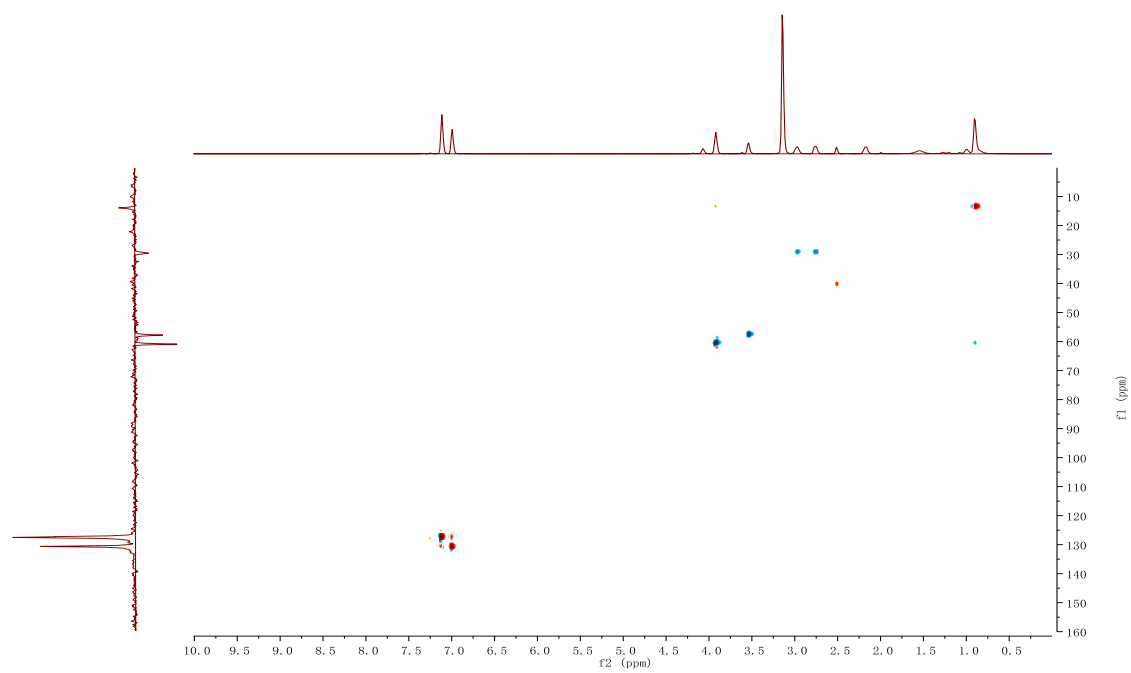
^1H NMR (600 MHz) at different temperature (left column: CDCl_3 , right column: DMSO-d_6)

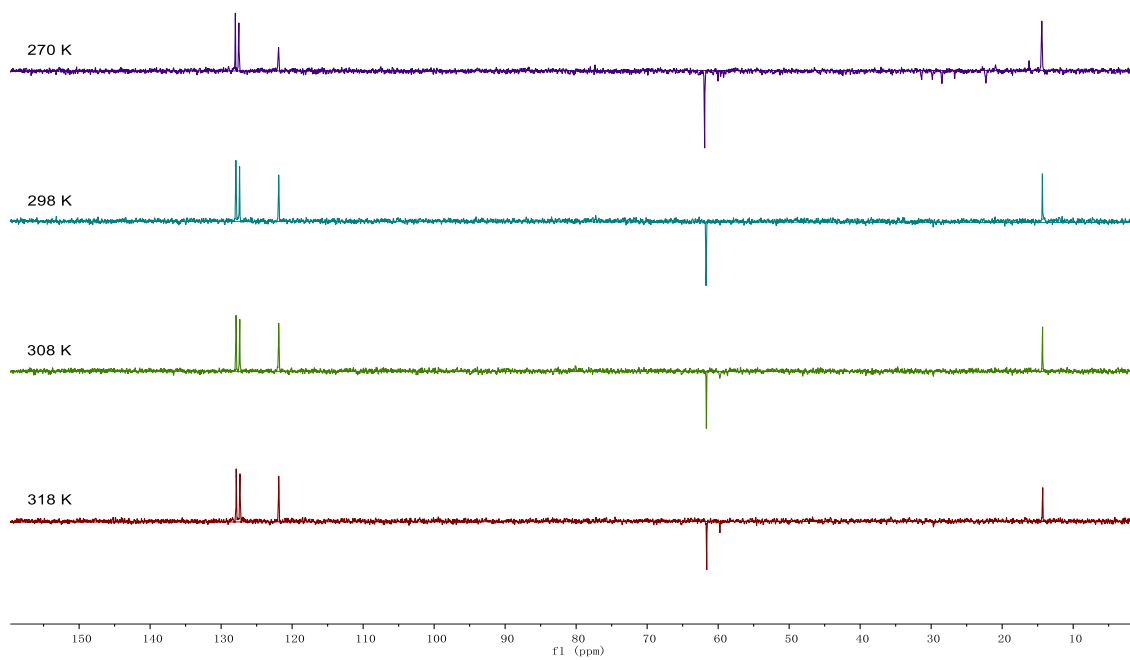
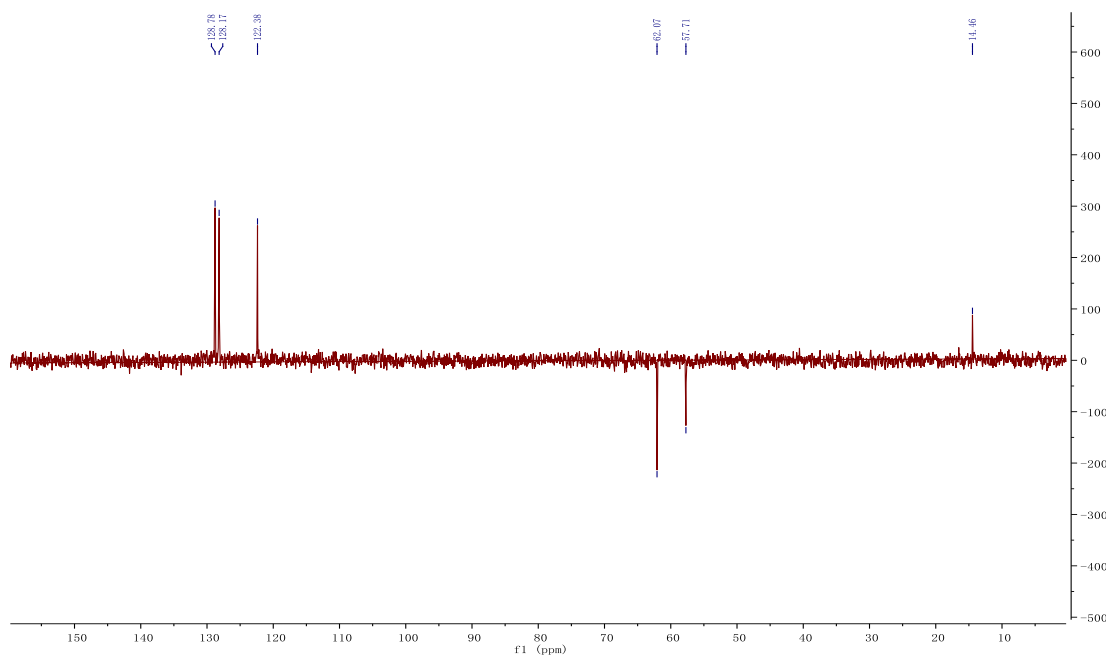


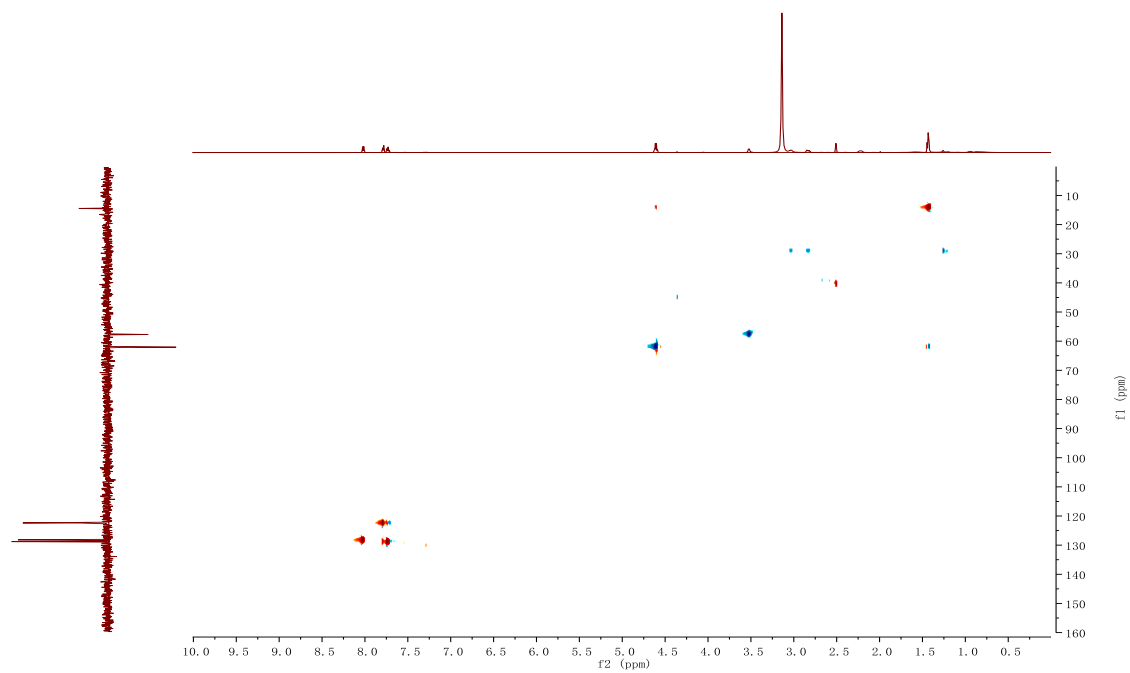
^{13}C NMR

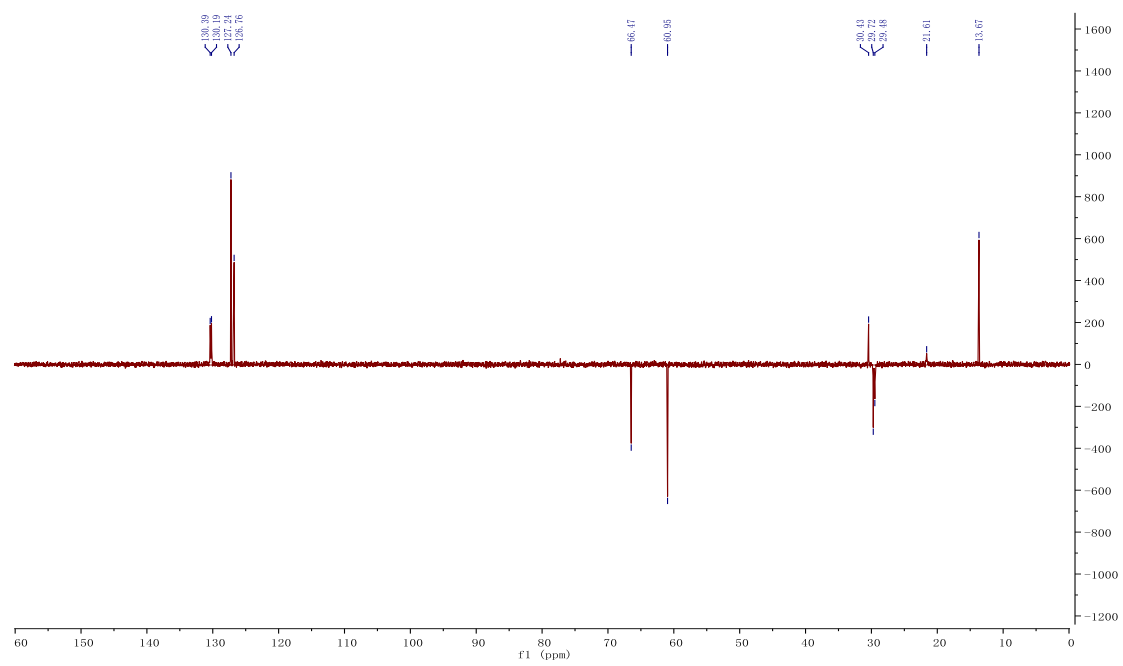
DEPT-135 (151 MHz) at different temperature (left column: CDCl_3 , right column: DMSO-d_6)



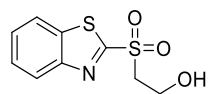
Edited HSQC (DMSO-d₆, 348 K)

DEPT-135 (151 MHz, CDCl₃) at different temperatureDEPT-135 (151 MHz, DMSO-d₆)

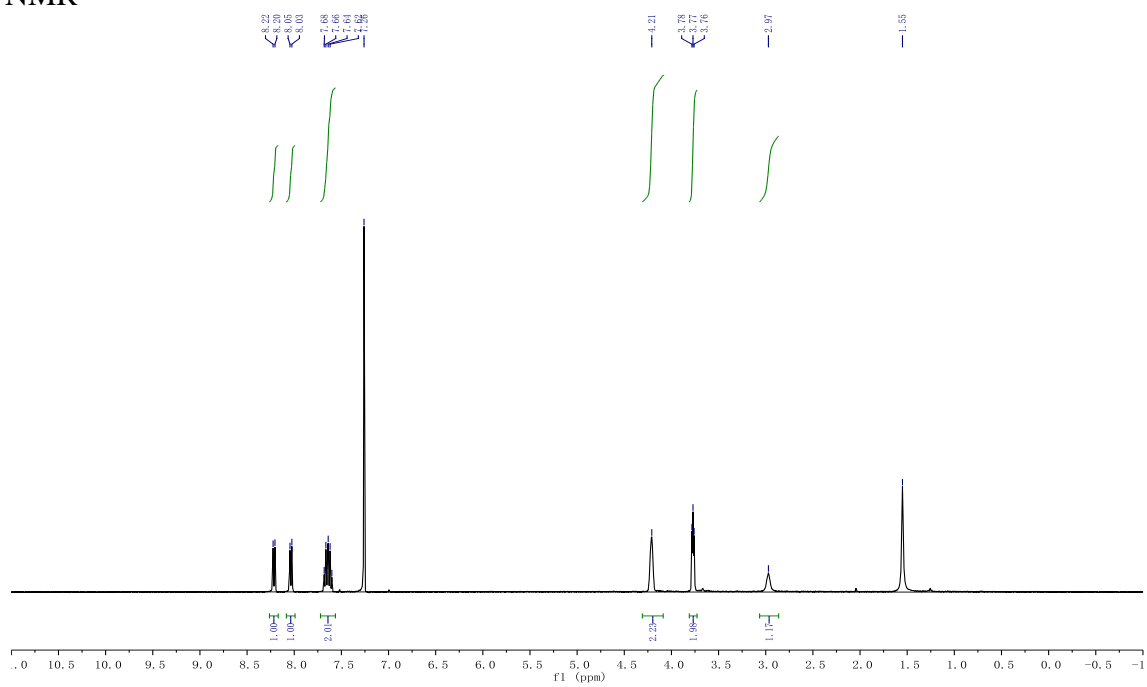
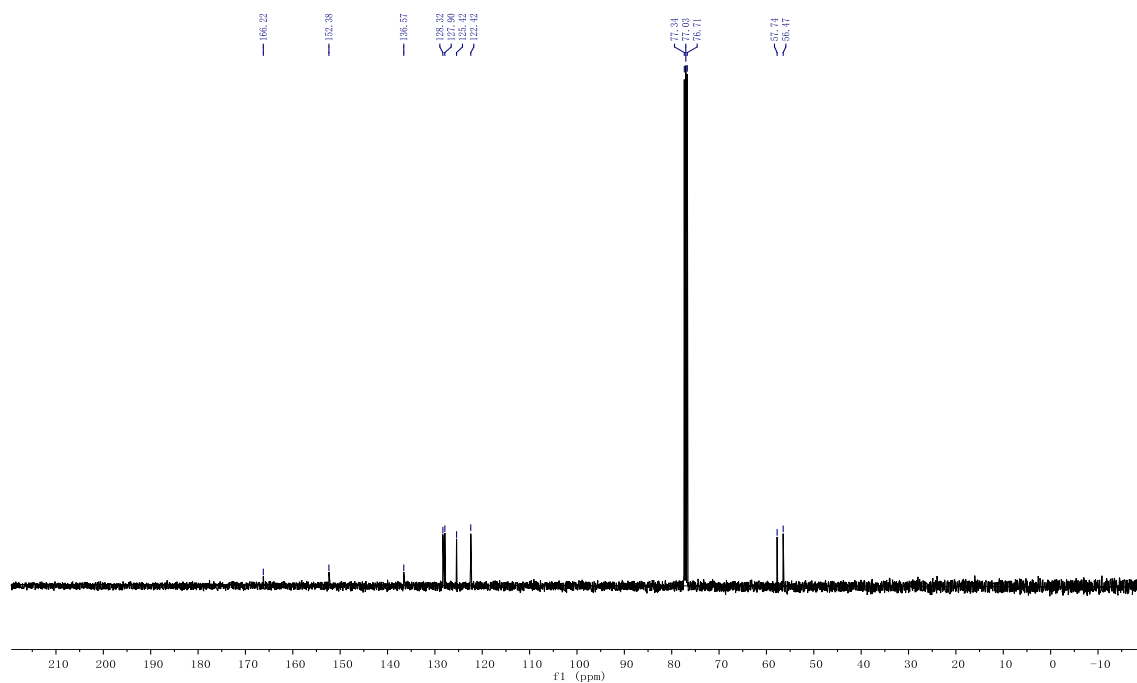
Edited HSQC (DMSO-d₆, 348 K)

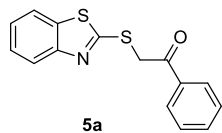
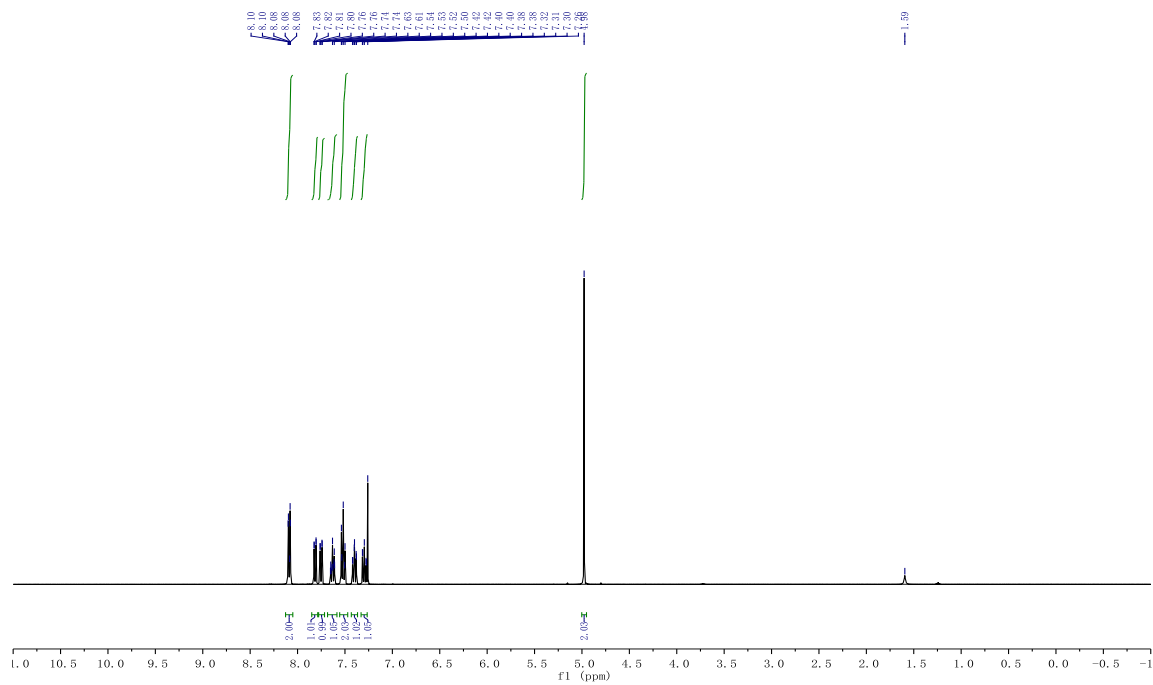
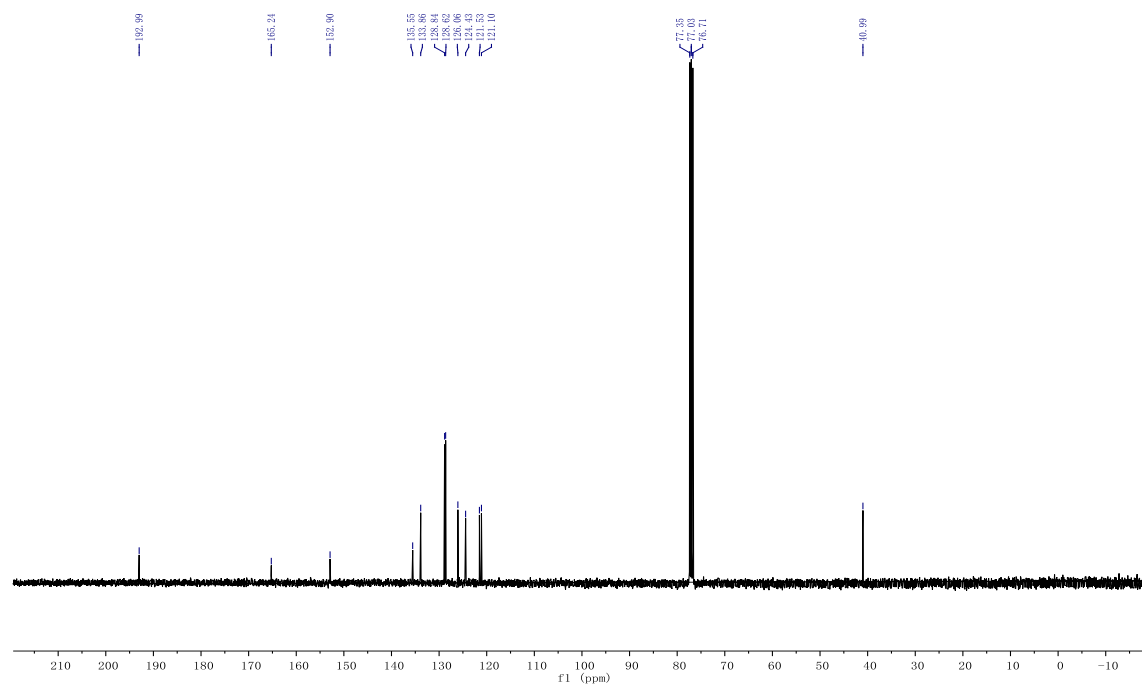
DEPT-135 (101 MHz, CDCl₃)

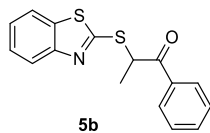
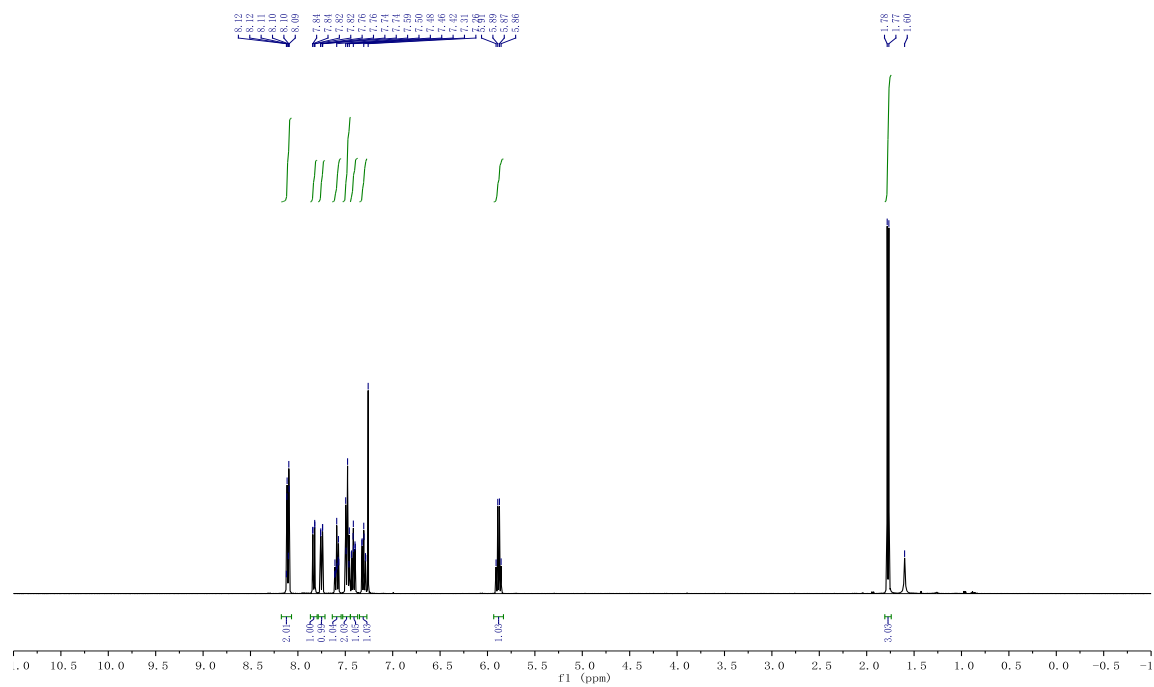
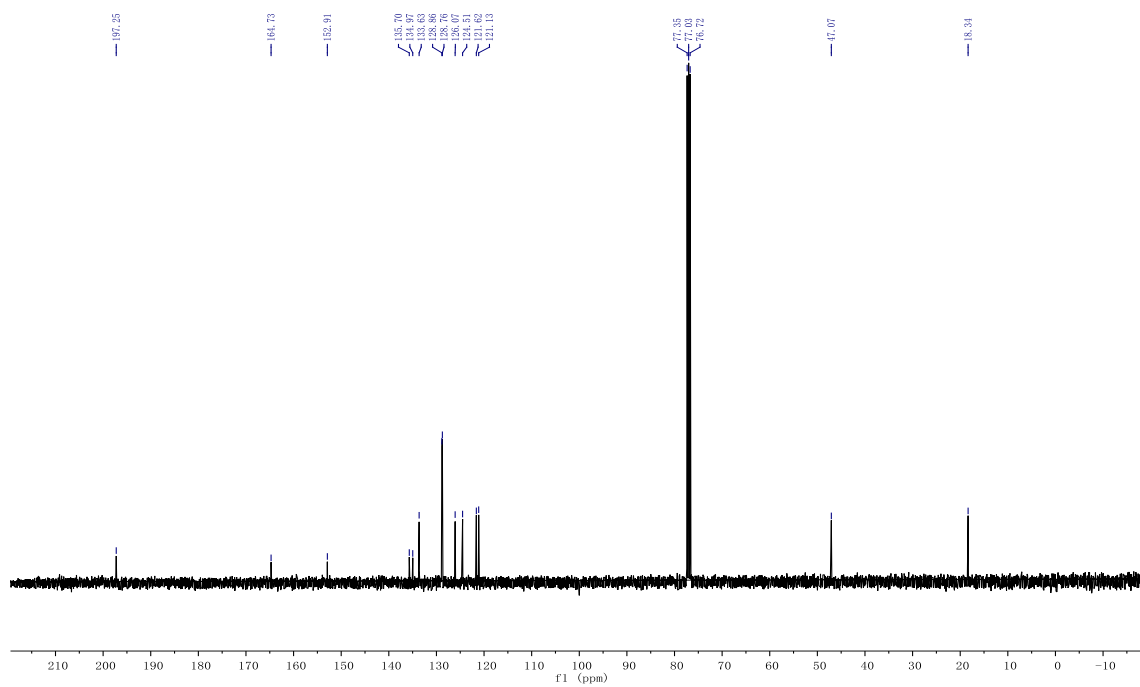
Appendix A.2 NMR spectra of compound in Chapter 1.3

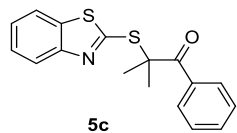
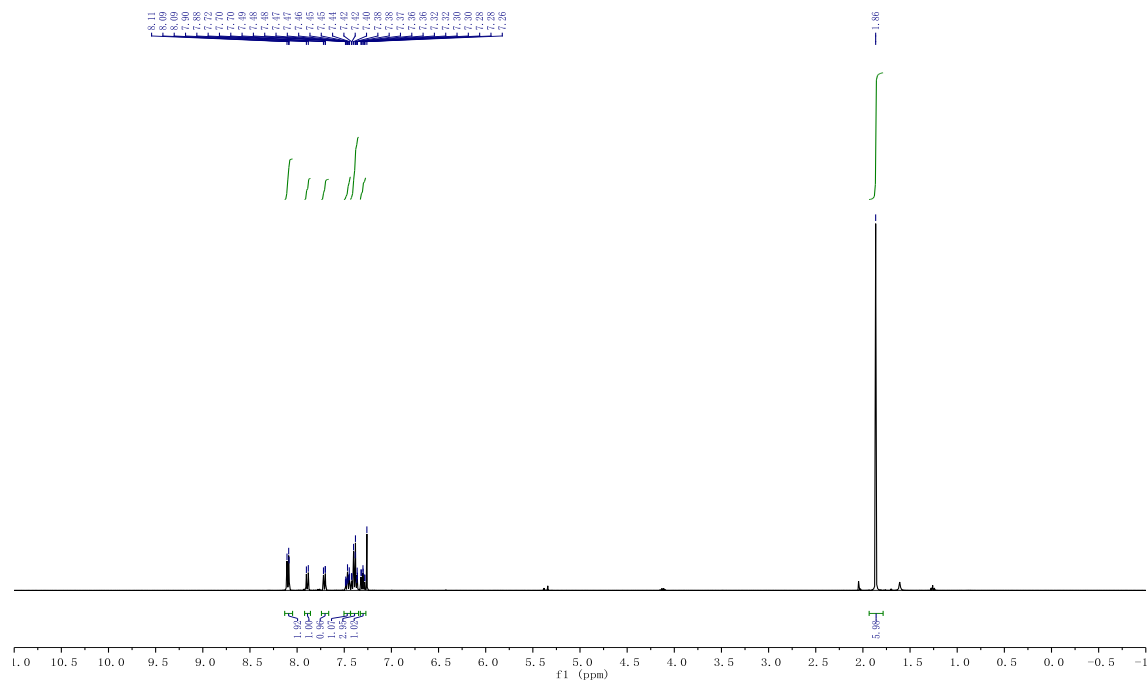
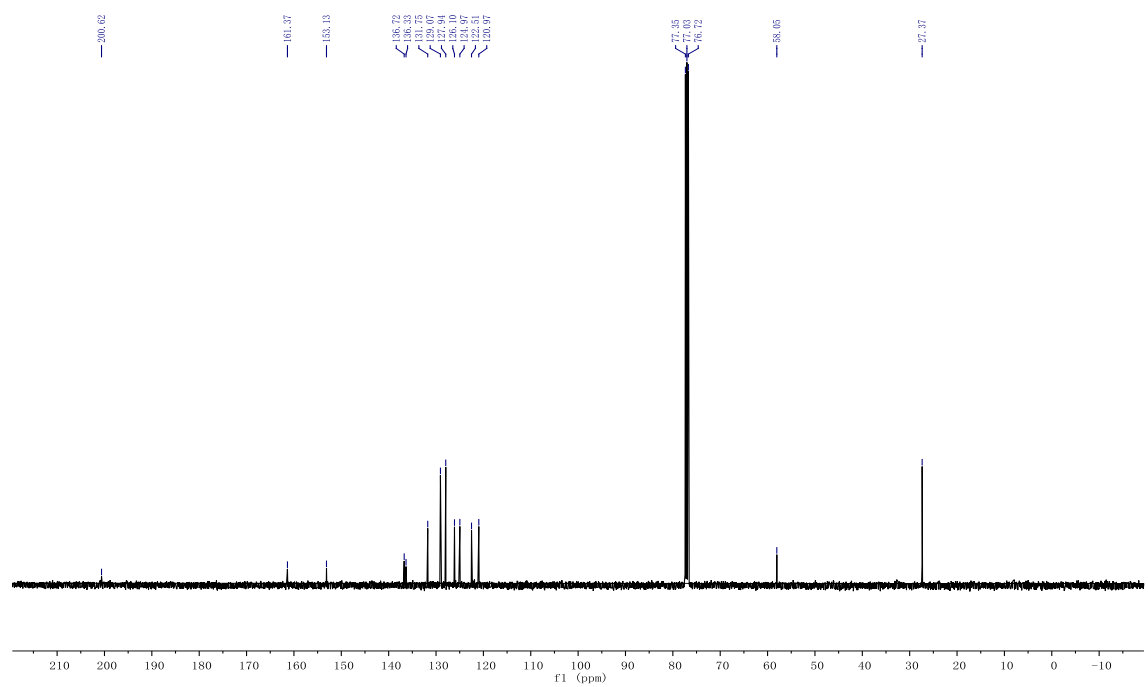


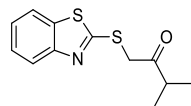
1

 ^1H NMR ^{13}C NMR

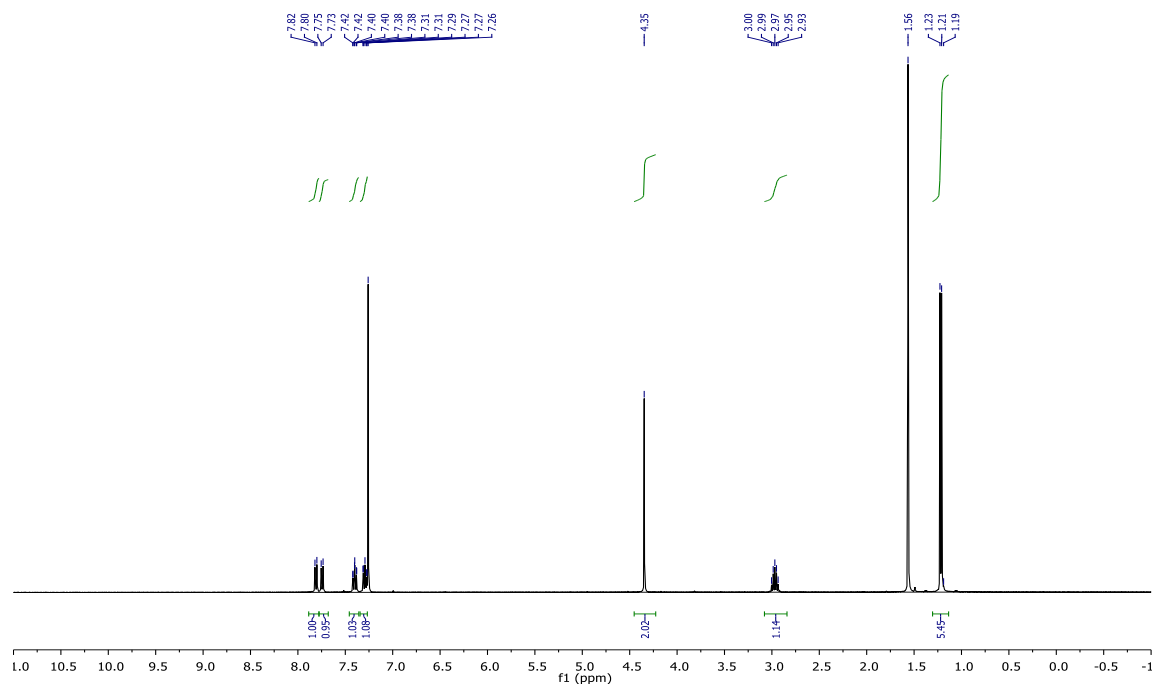
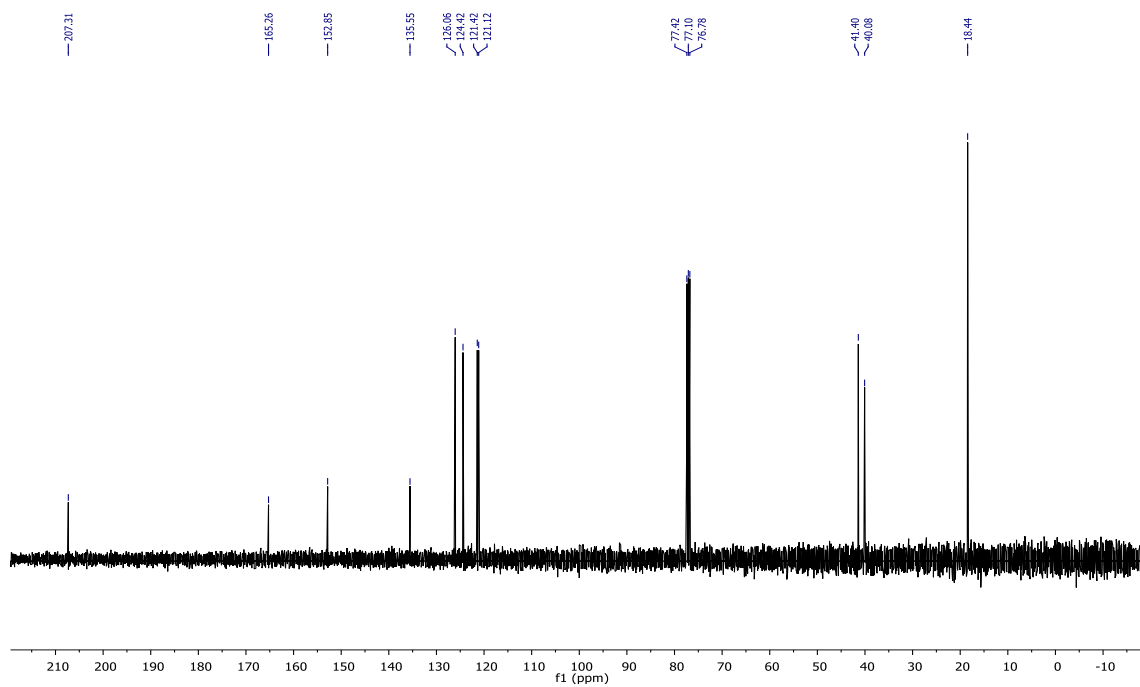
 $^1\text{H NMR}$  $^{13}\text{C NMR}$ 

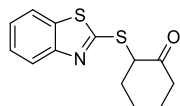
 ^1H NMR ^{13}C NMR

 $^1\text{H NMR}$  $^{13}\text{C NMR}$ 

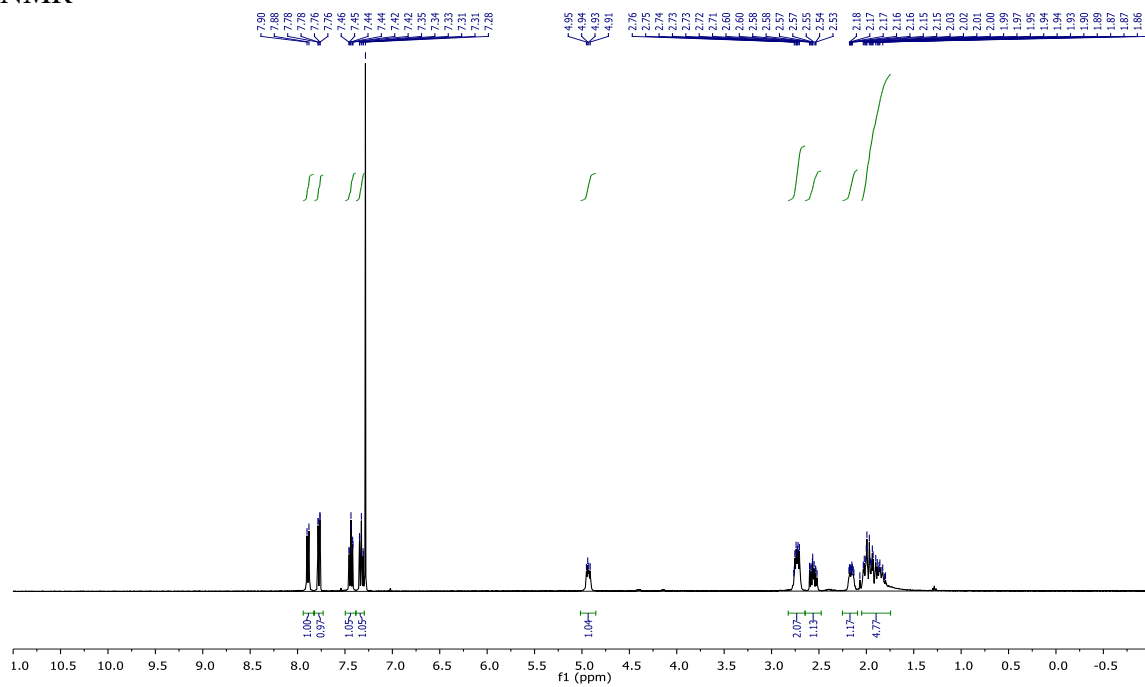
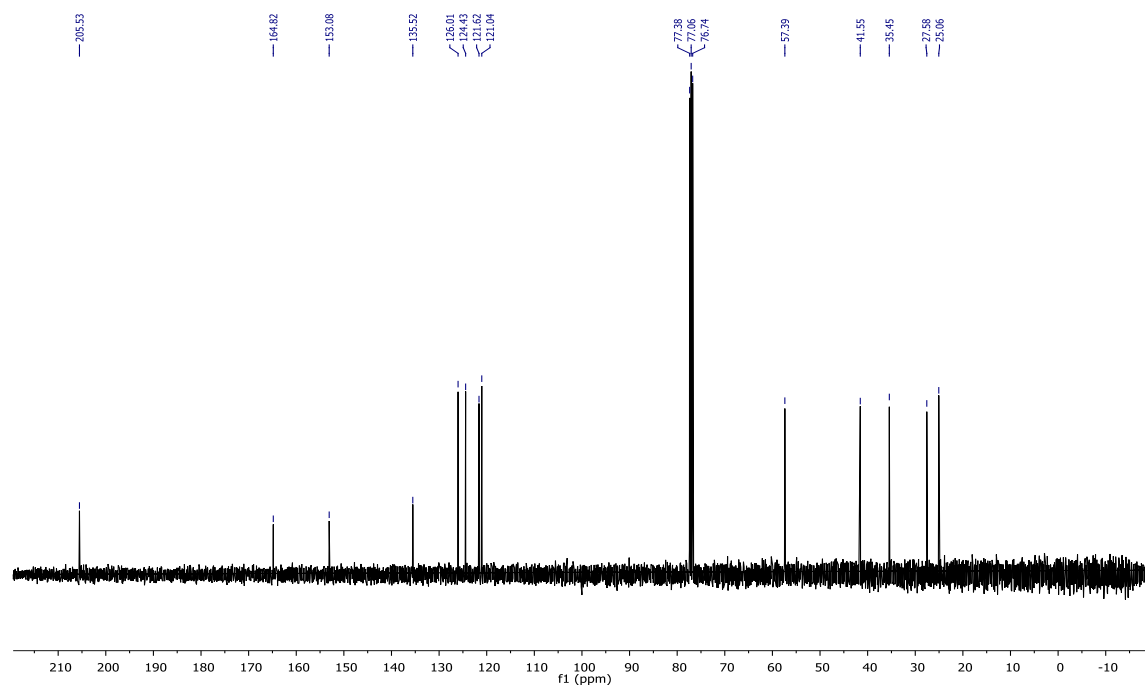


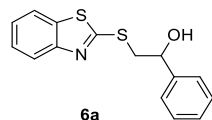
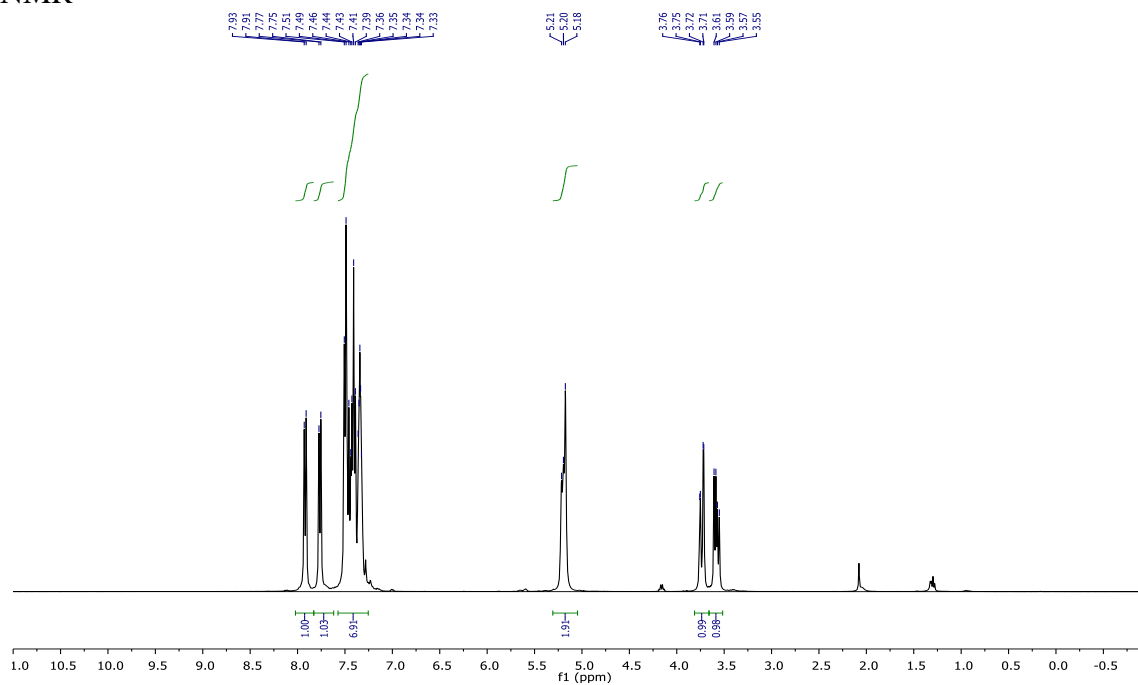
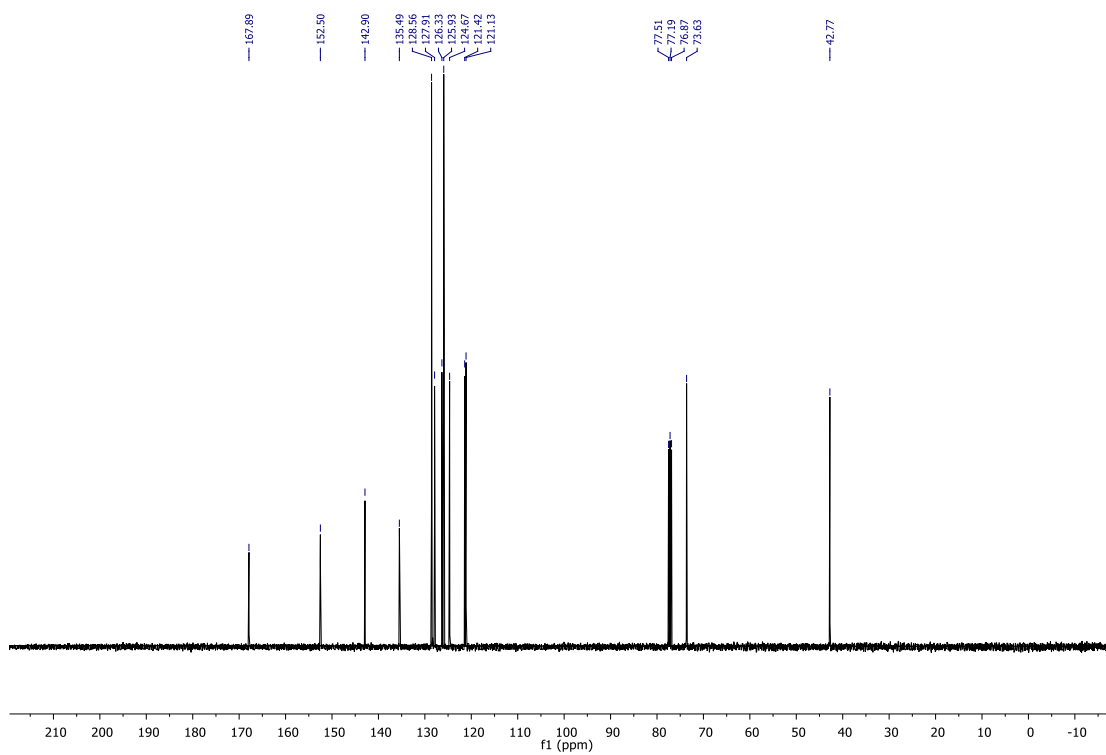
5d

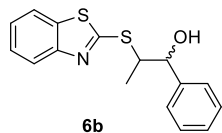
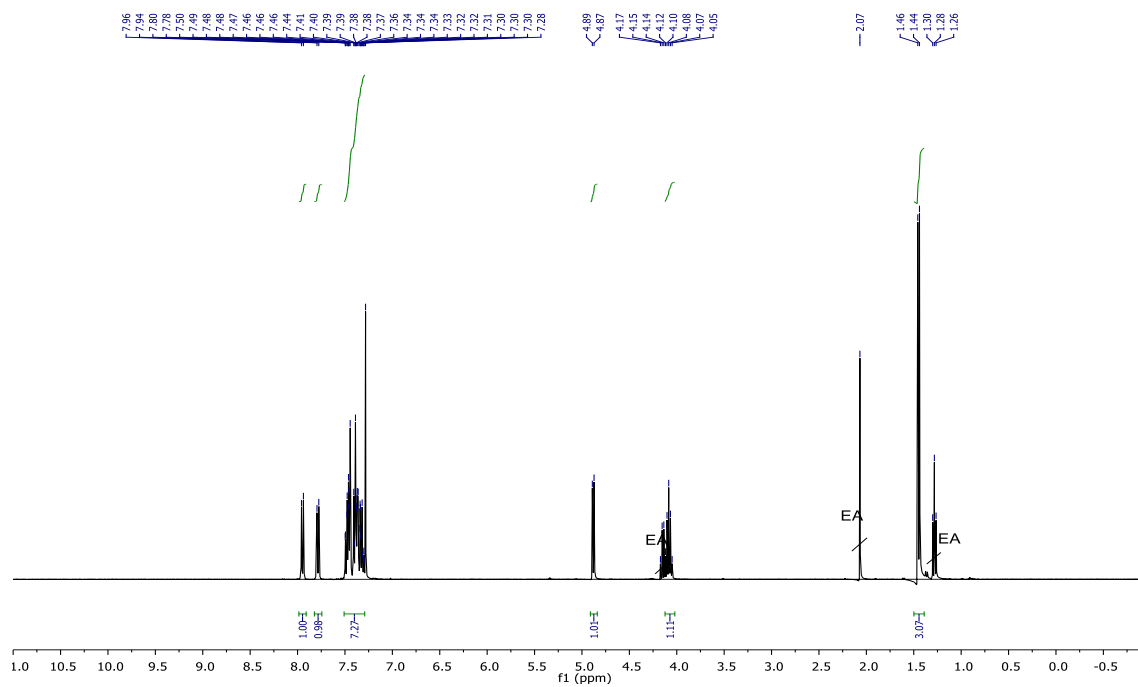
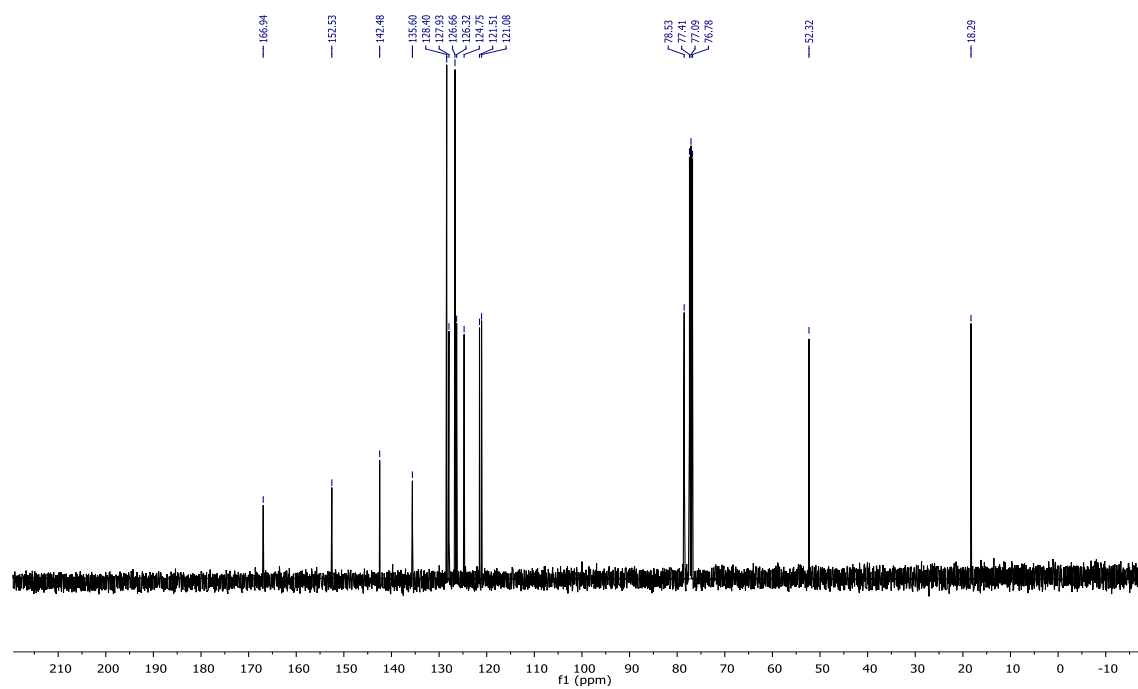
 ^1H NMR ^{13}C NMR

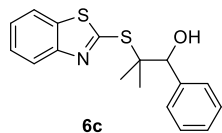


5e

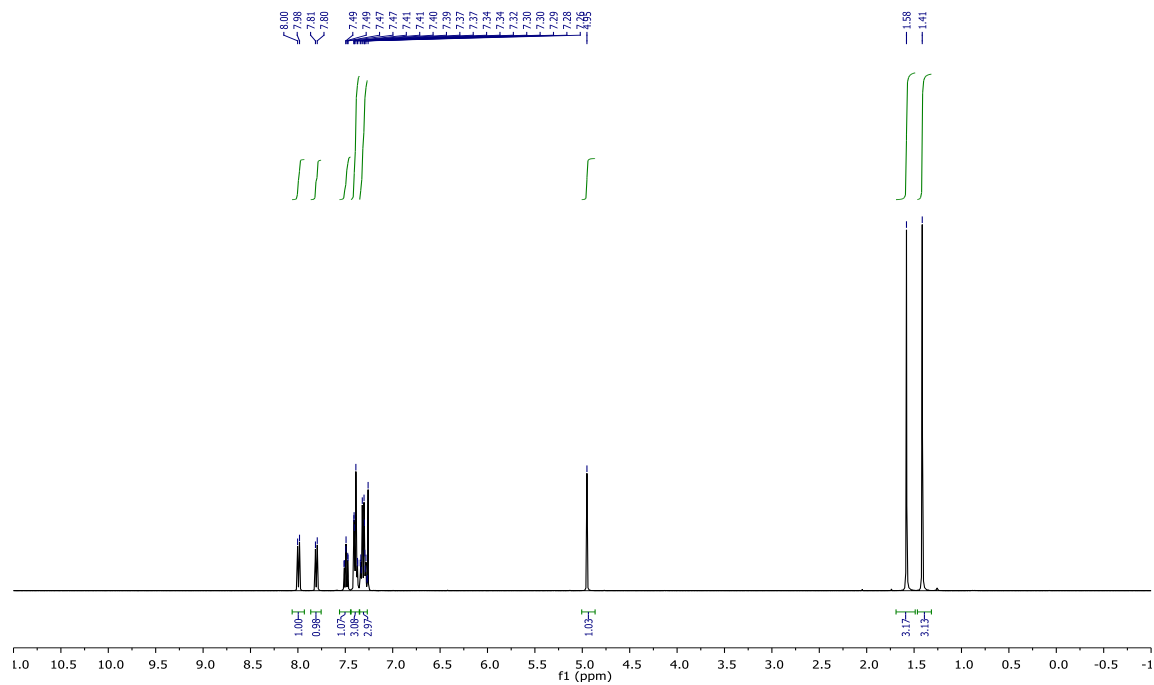
 ^1H NMR ^{13}C NMR

 $^1\text{H NMR}$  $^{13}\text{C NMR}$ 

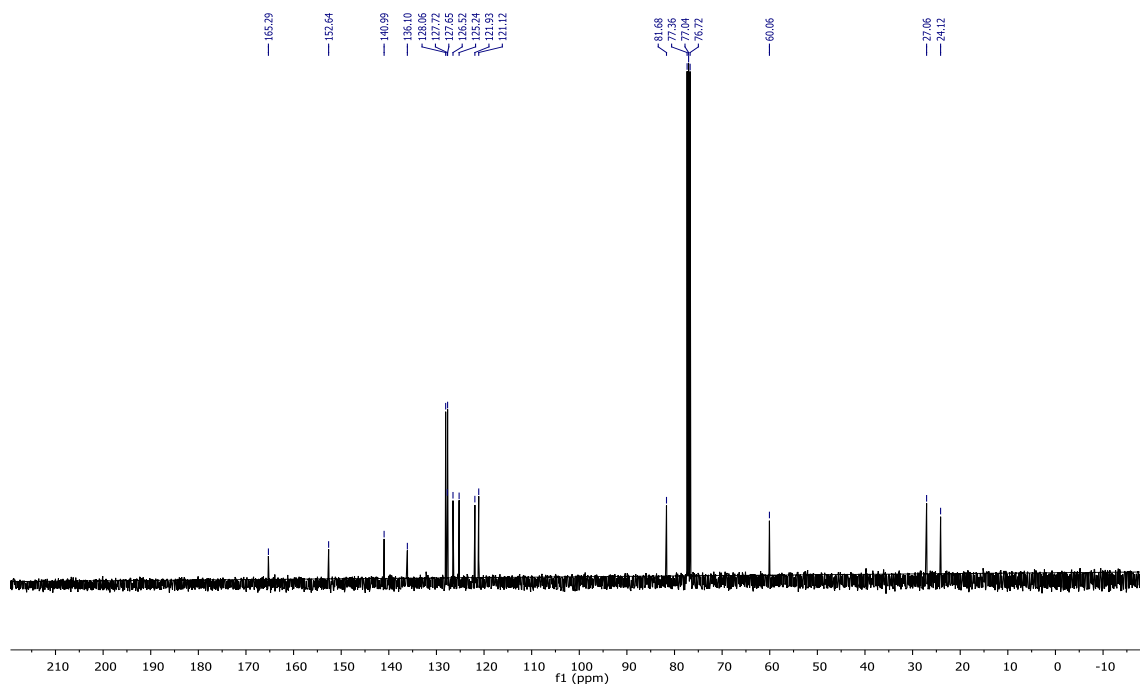
¹H NMR¹³C NMR

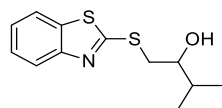


¹H NMR

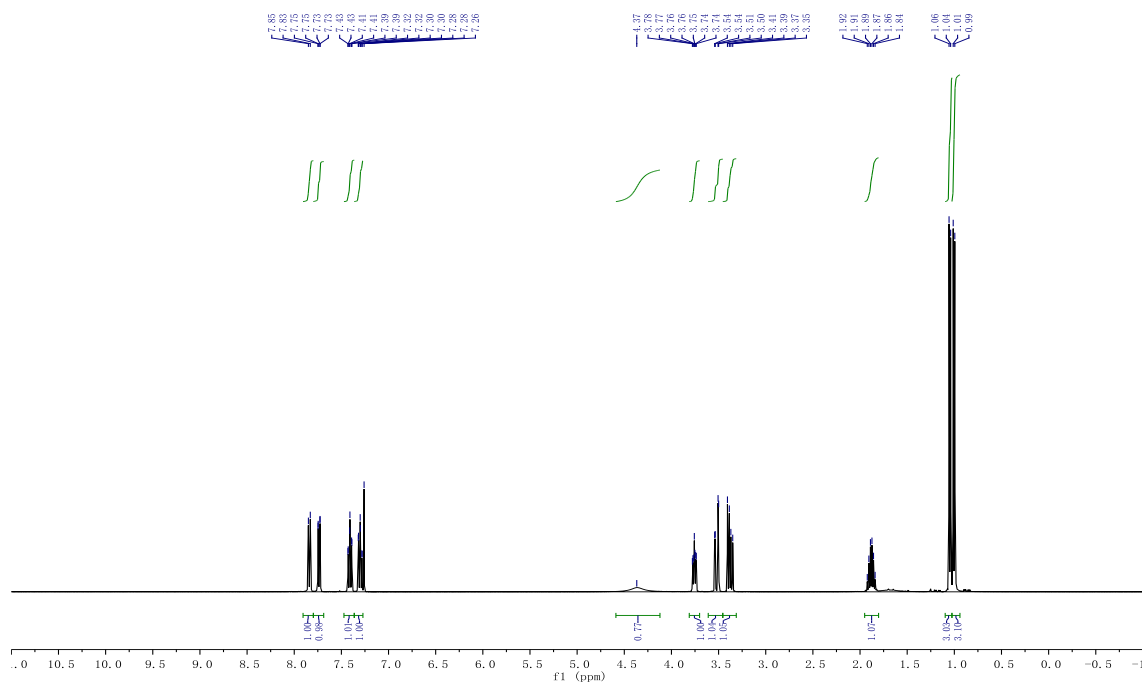
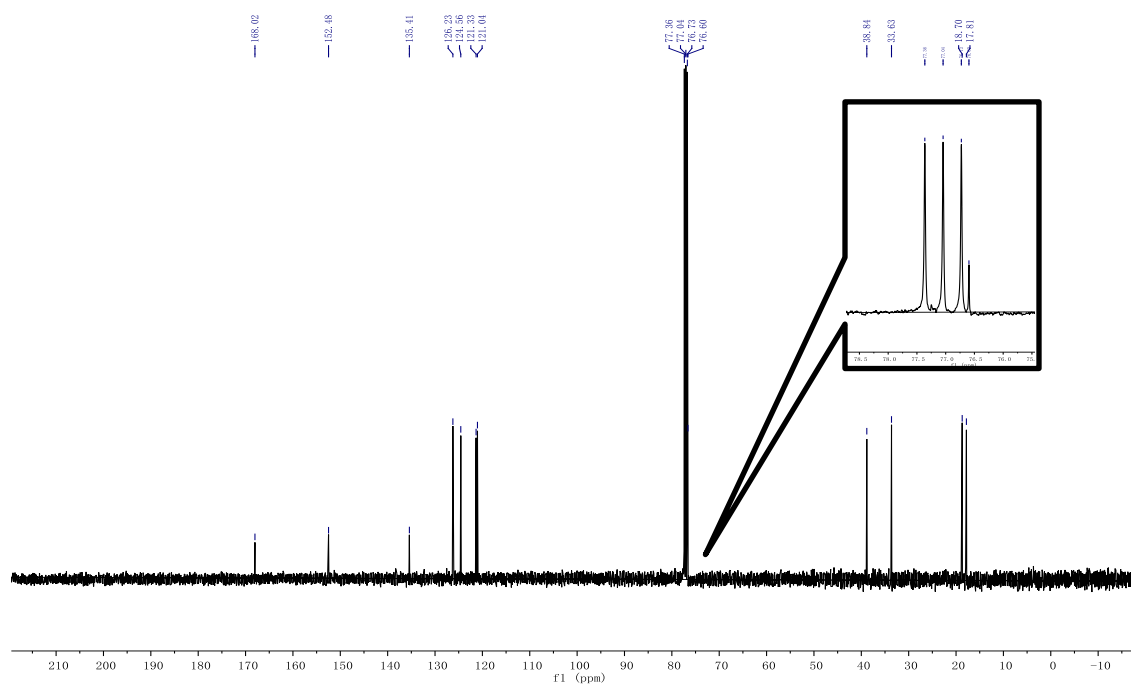


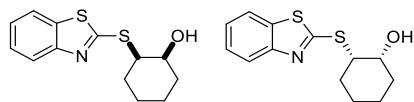
¹³C NMR



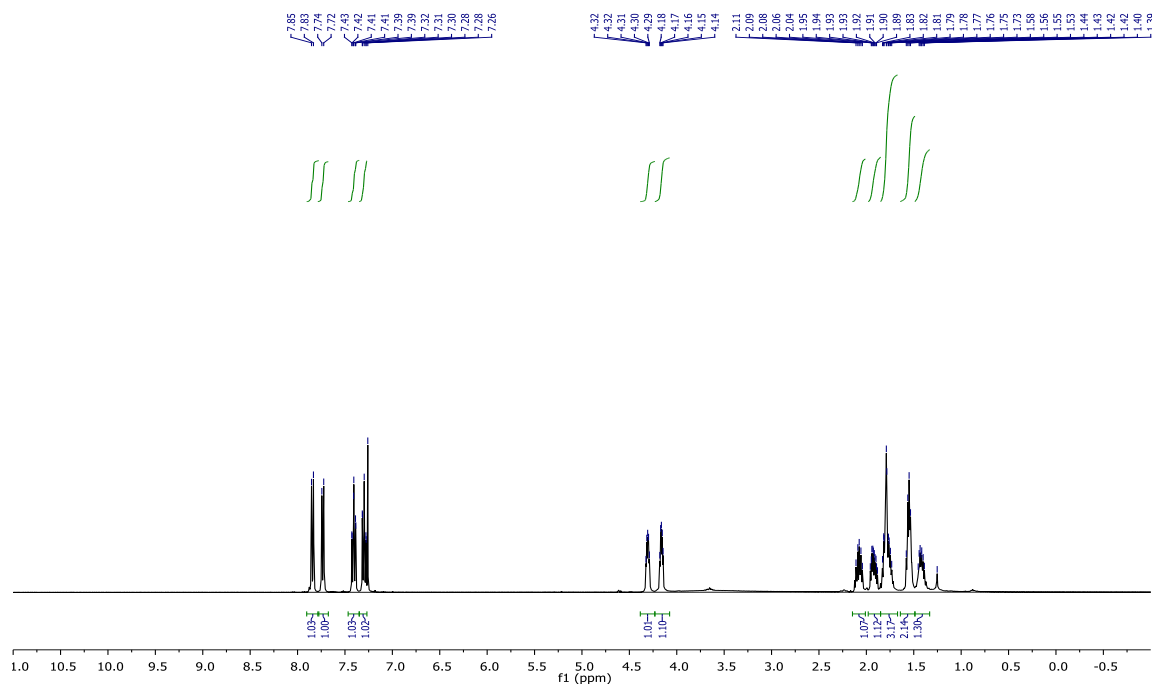
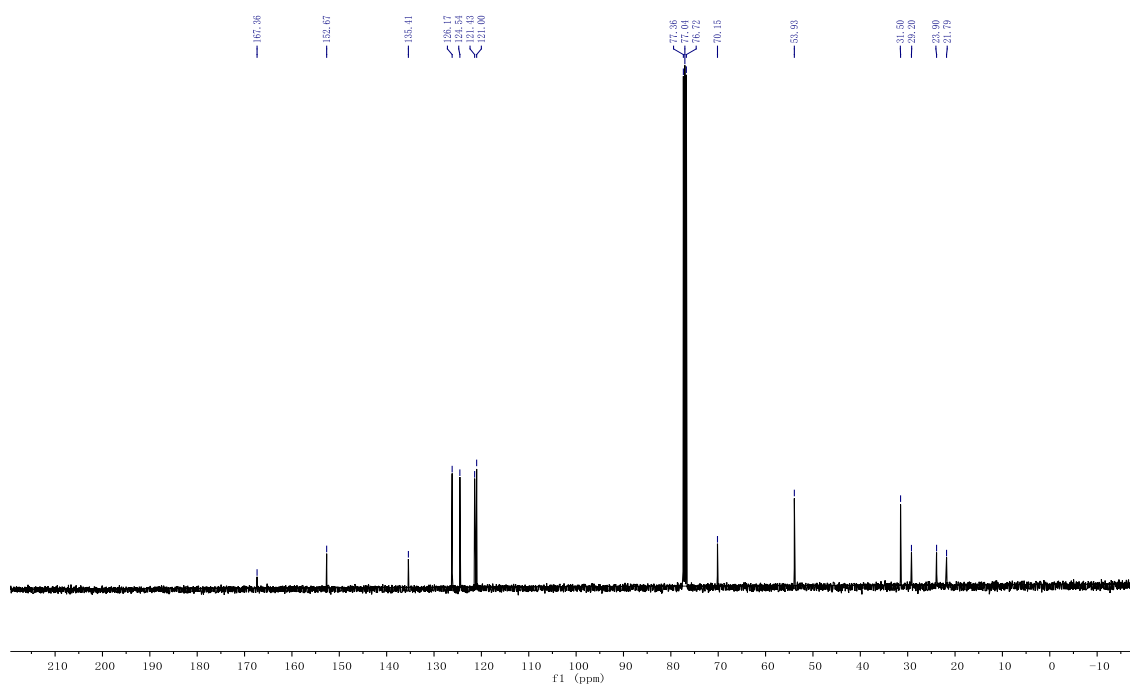


6d

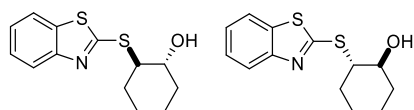
 ^1H NMR ^{13}C NMR



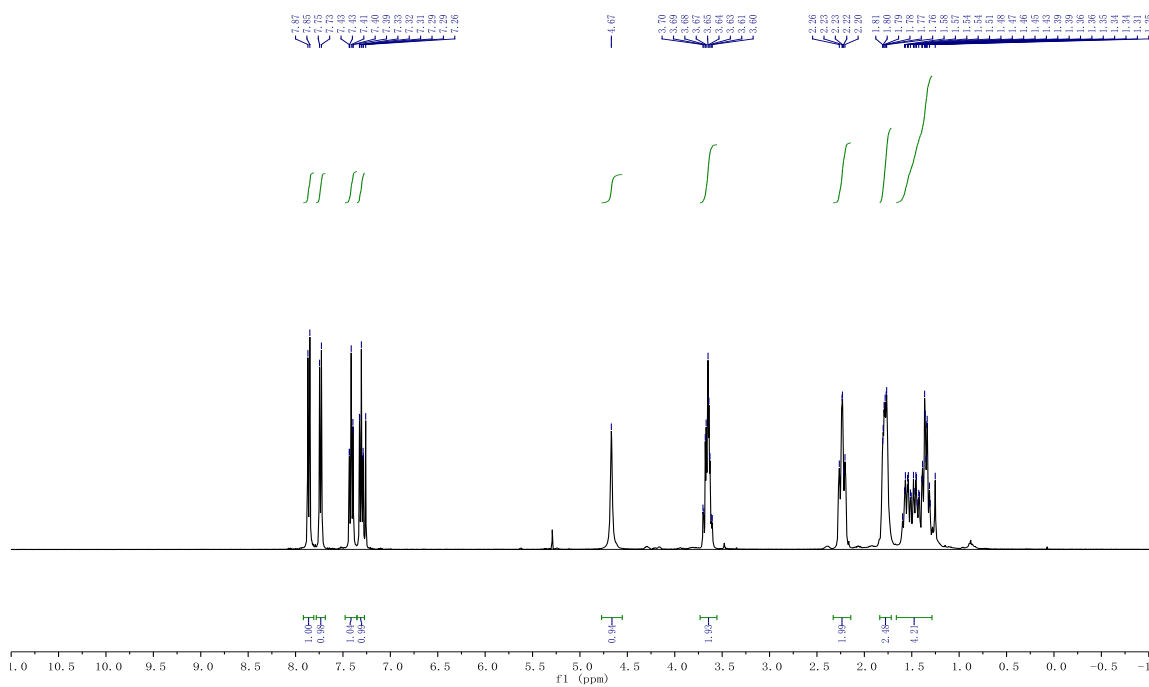
6d

 ^1H NMR ^{13}C NMR

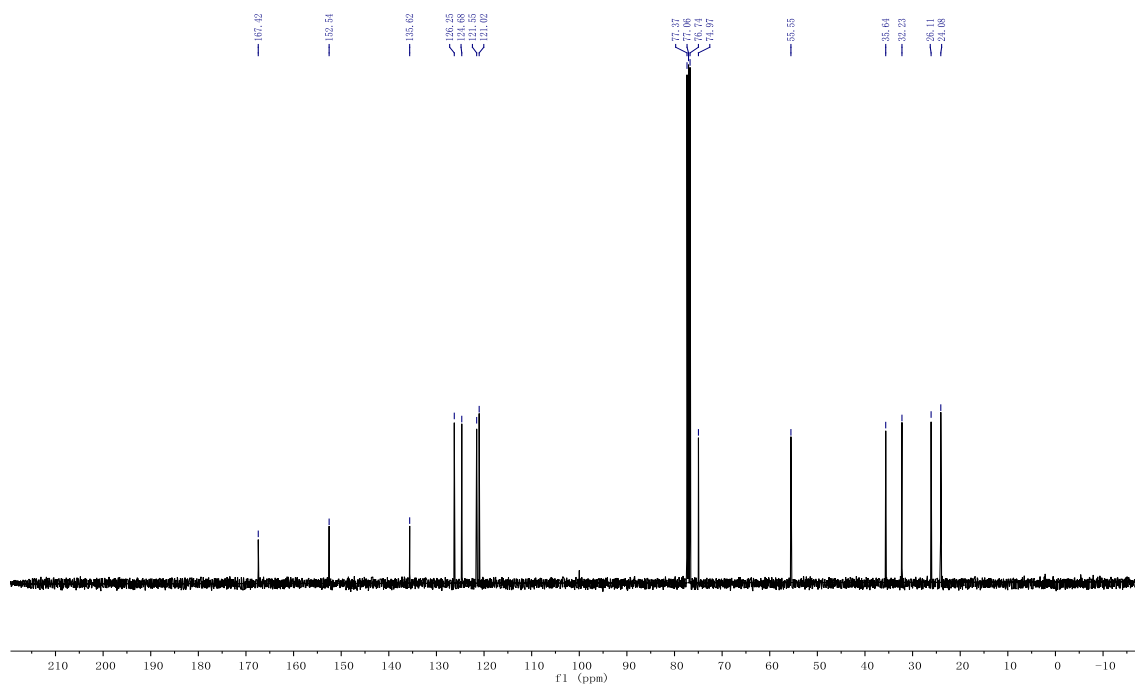
Trans-product:

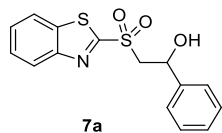
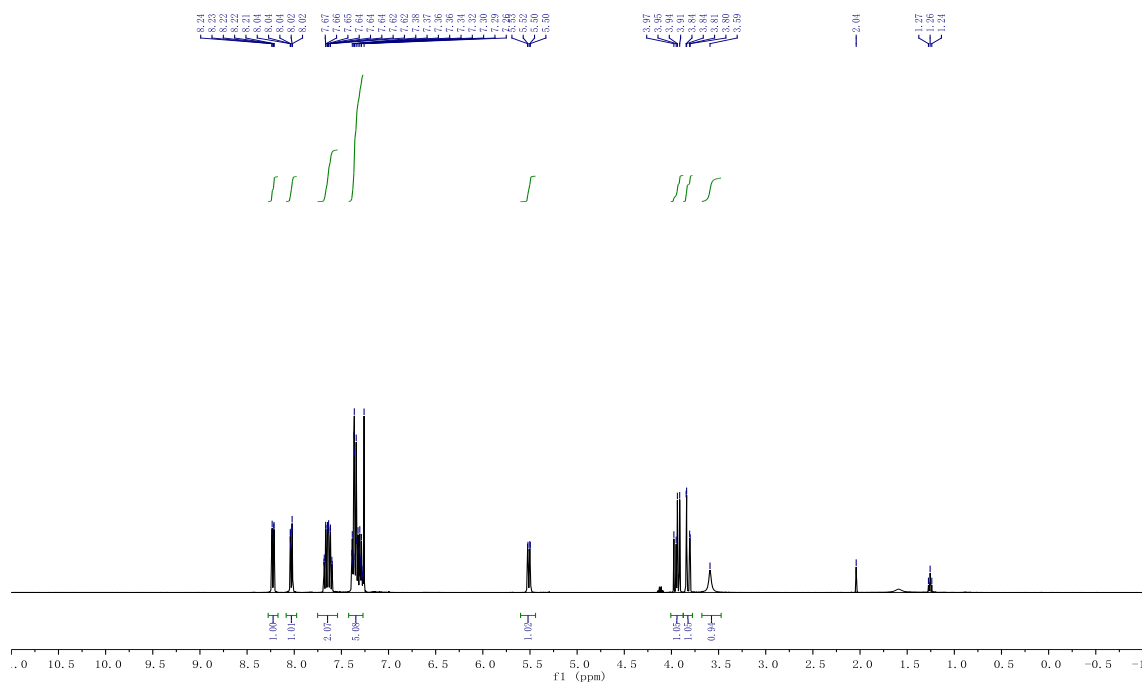
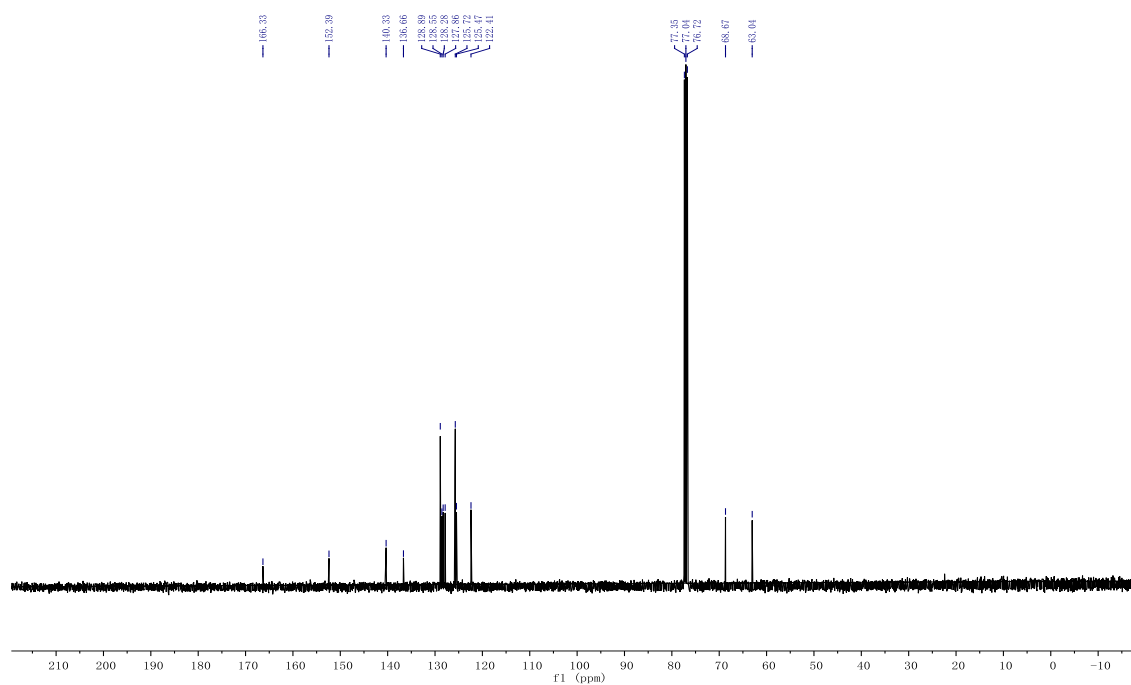


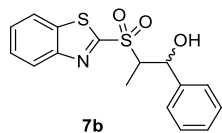
^1H NMR



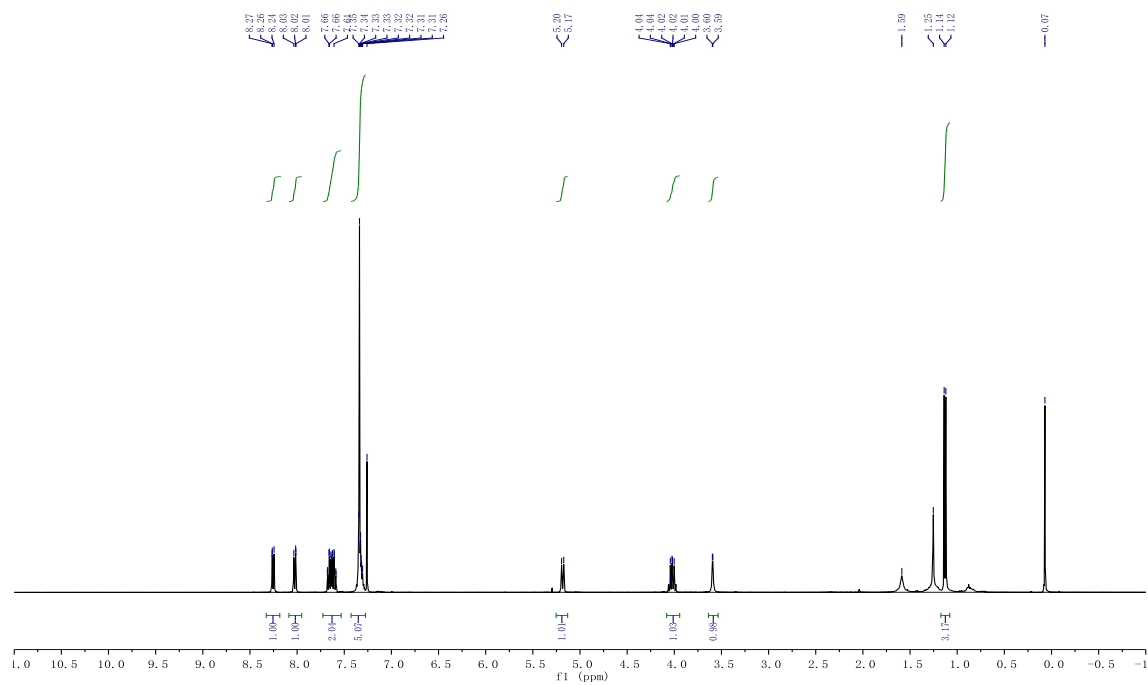
^{13}C NMR



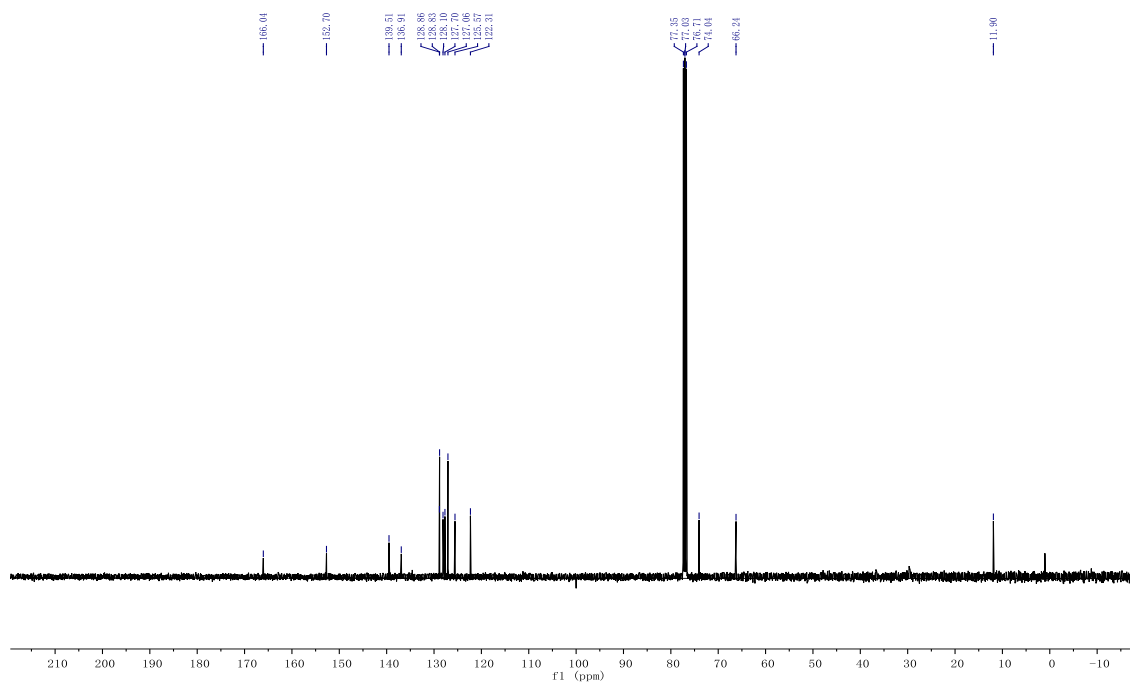
¹H NMR¹³C NMR

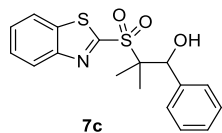
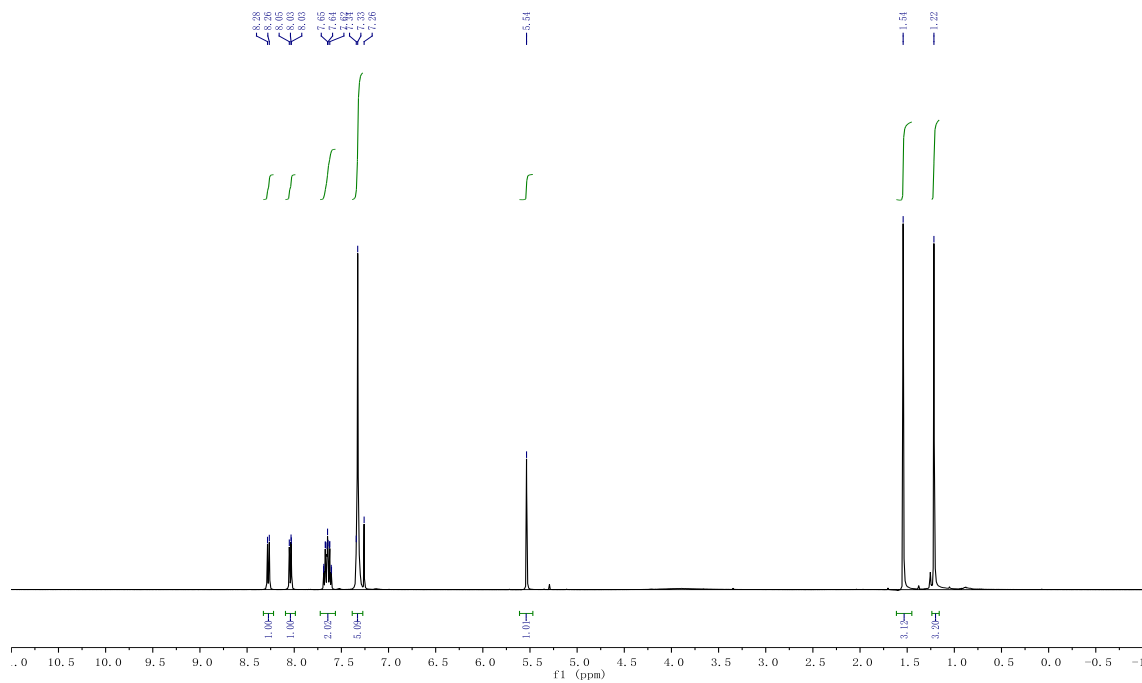
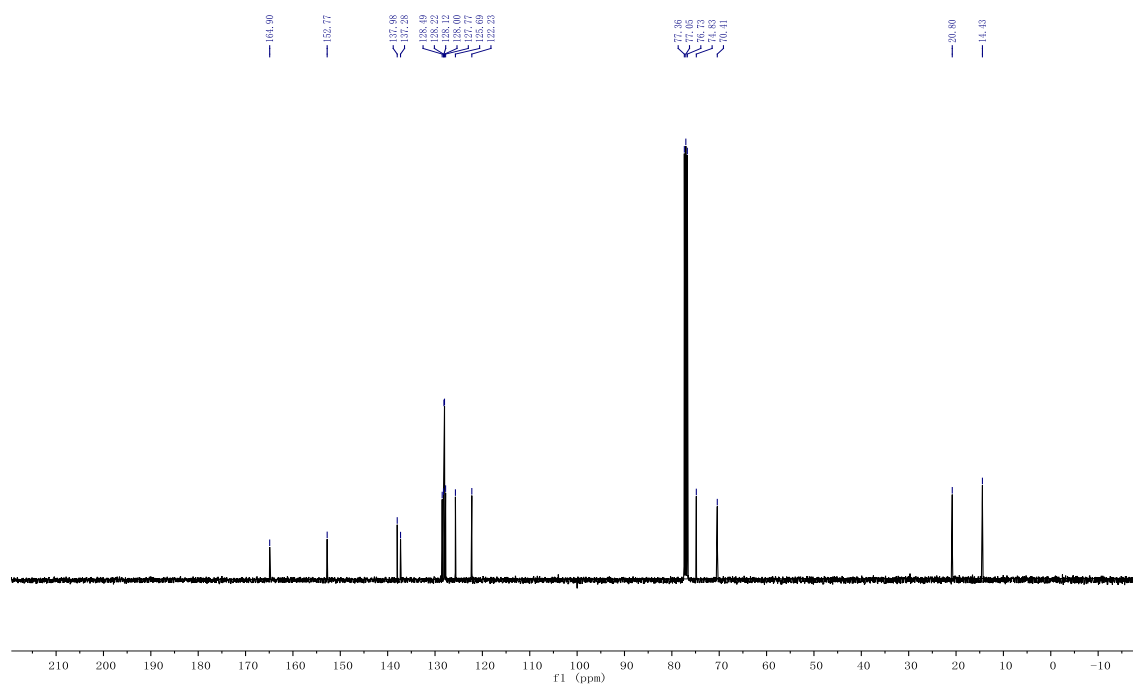


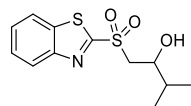
¹H NMR



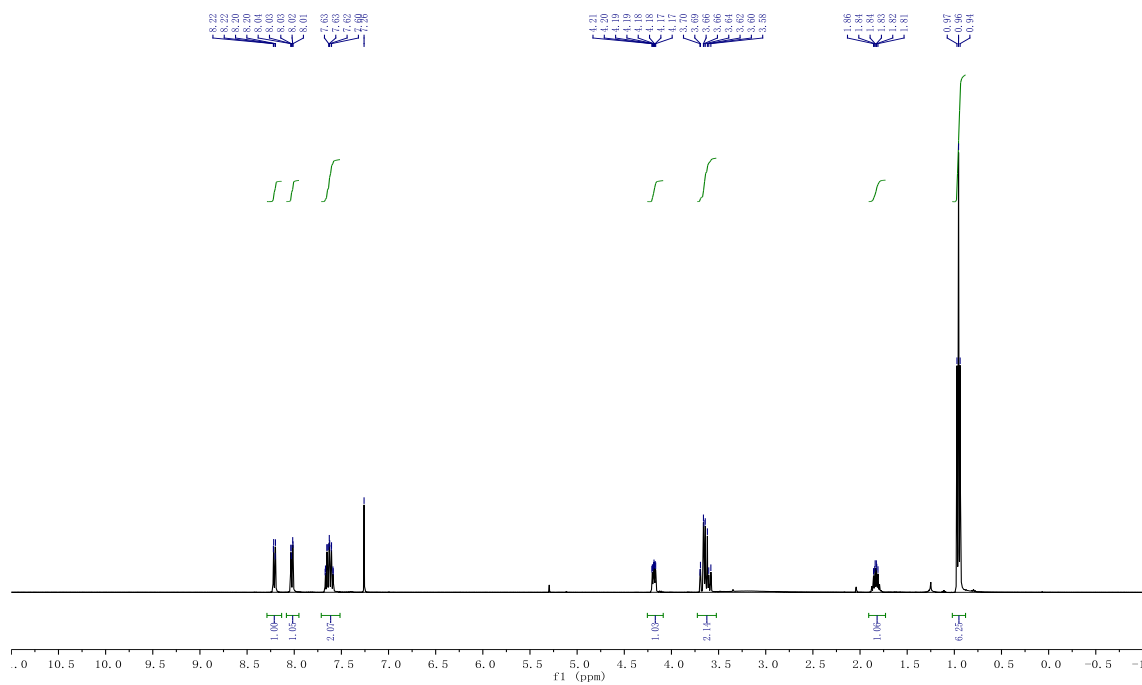
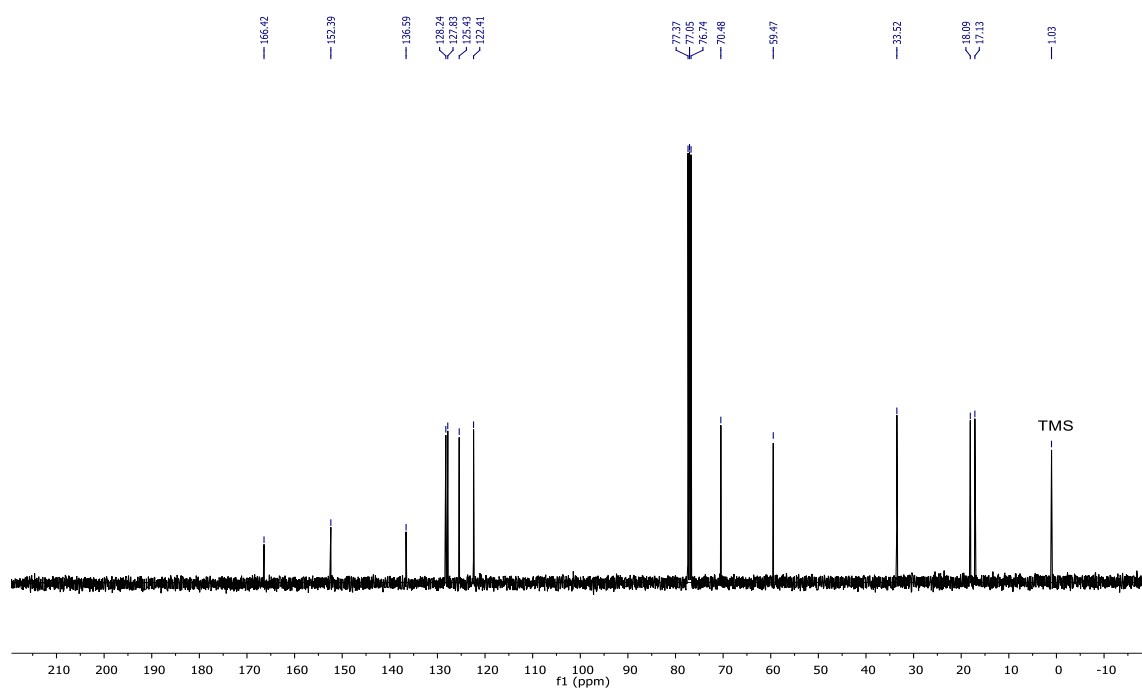
¹³C NMR

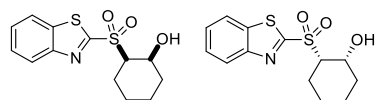


 ^1H NMR ^{13}C NMR

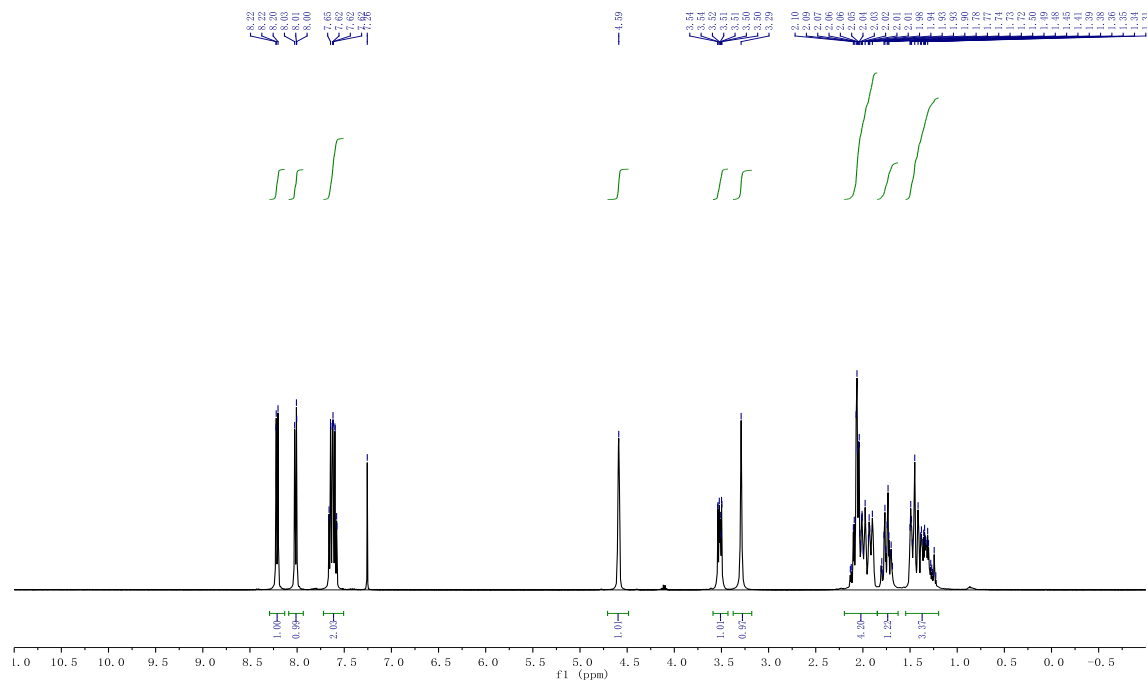
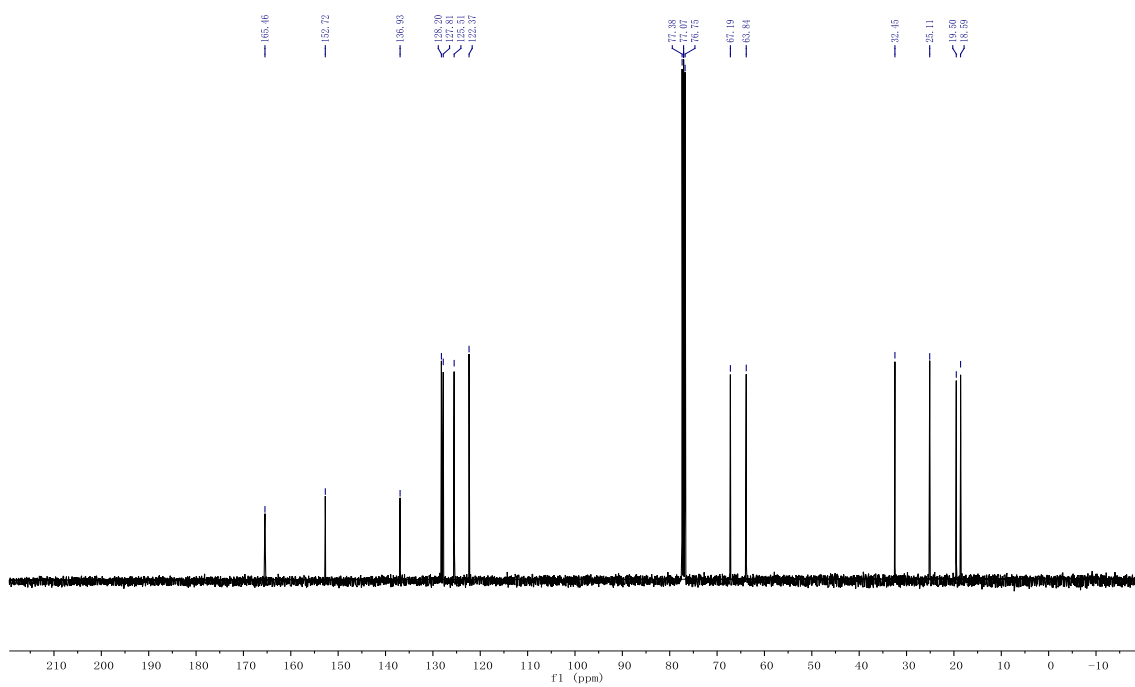


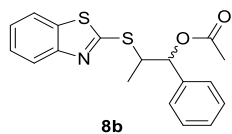
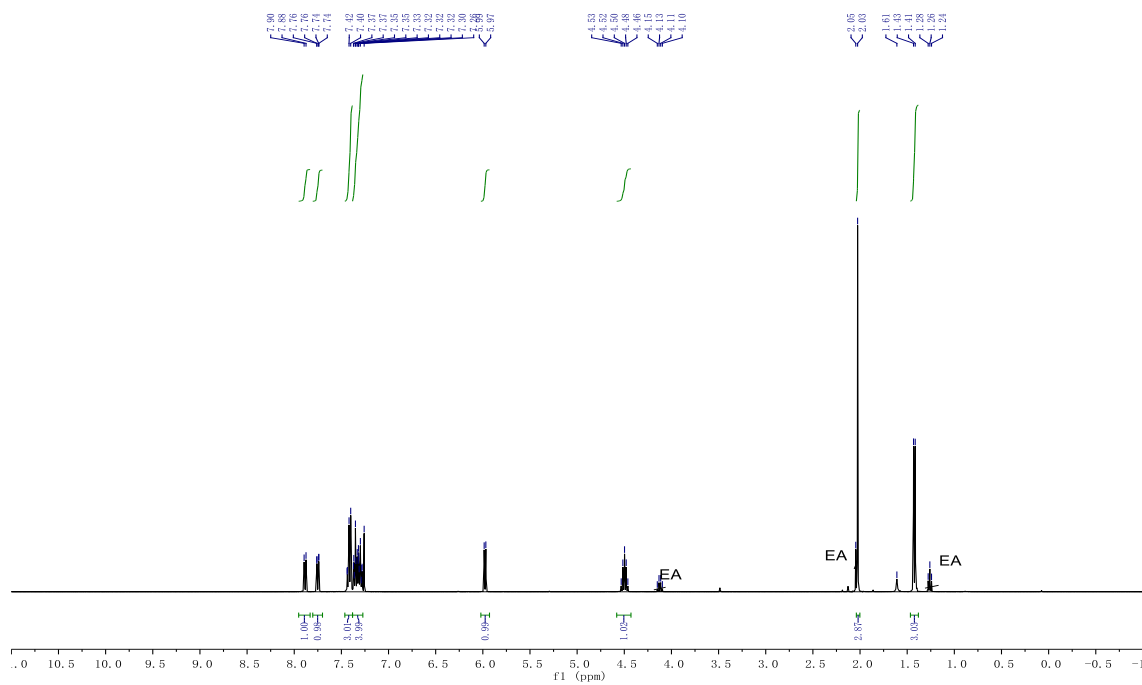
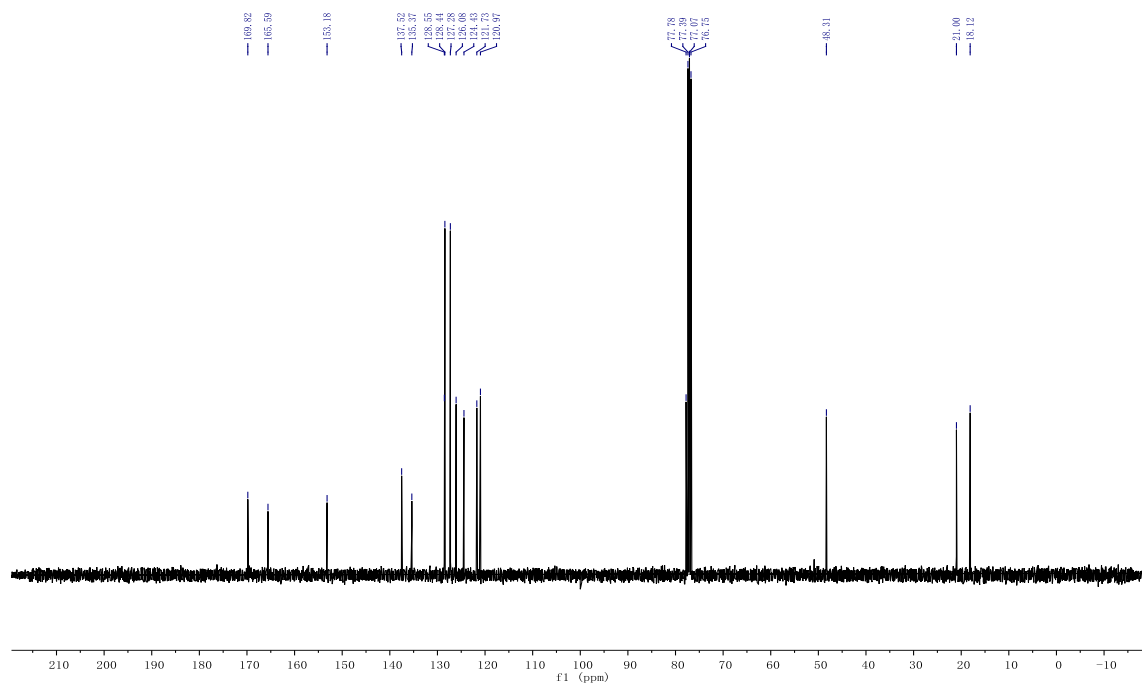
7d

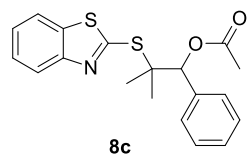
 ^1H NMR ^{13}C NMR



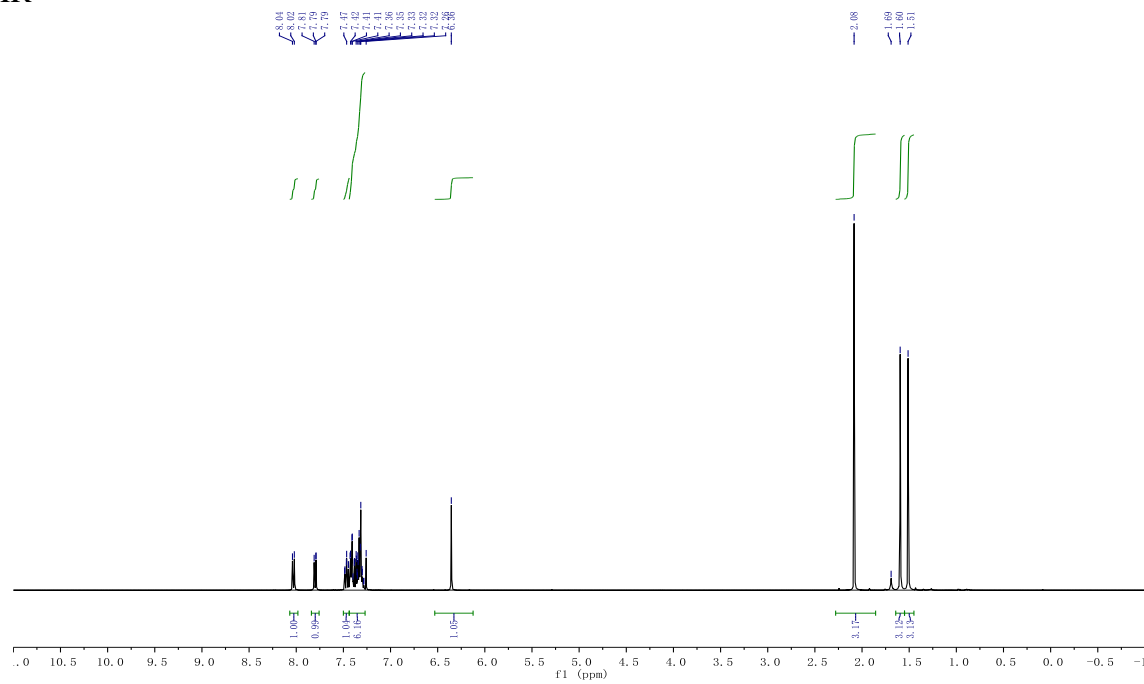
7e

 ^1H NMR ^{13}C NMR

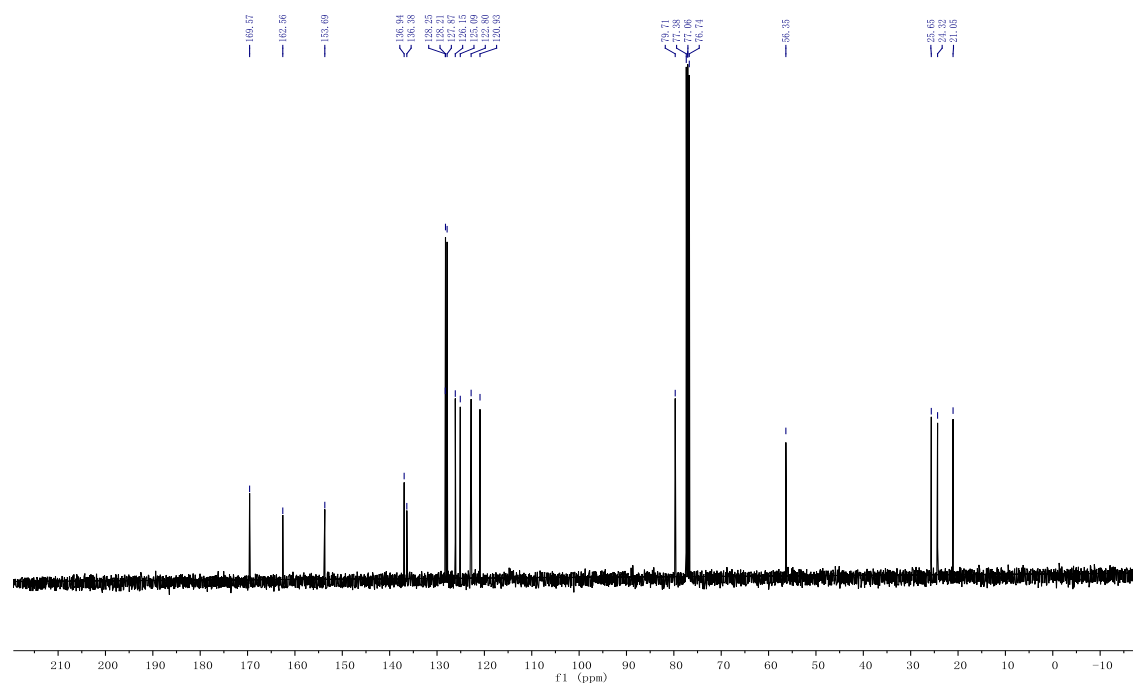
 ^1H NMR ^{13}C NMR

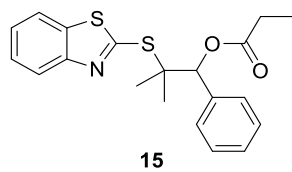
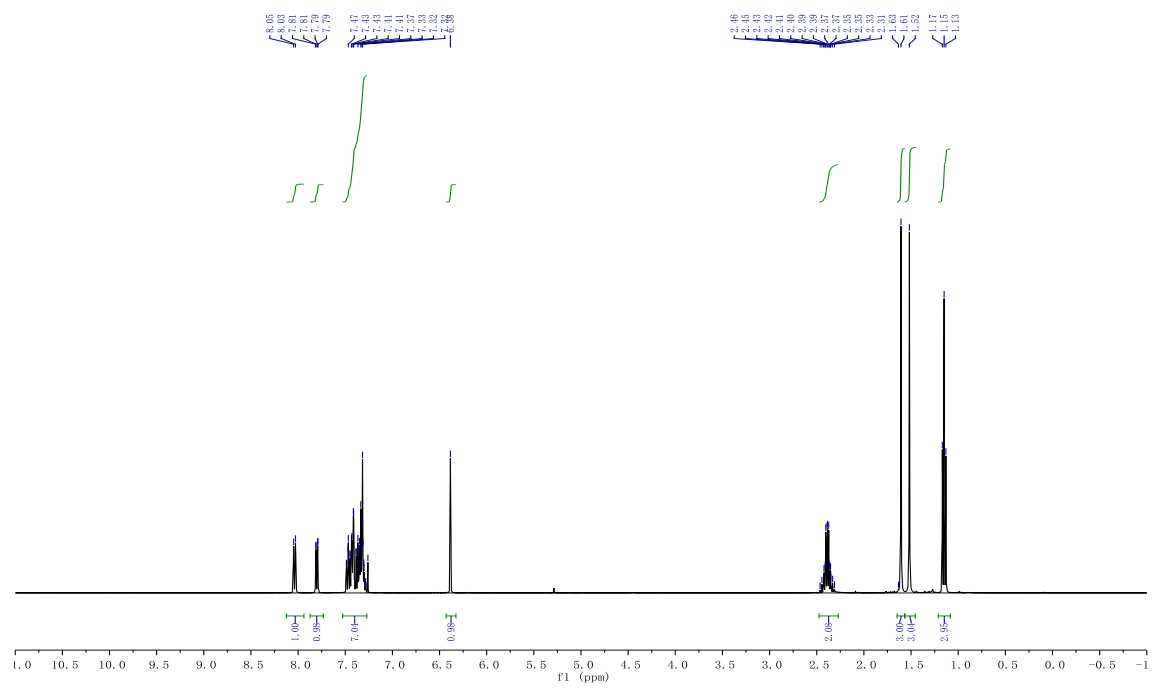
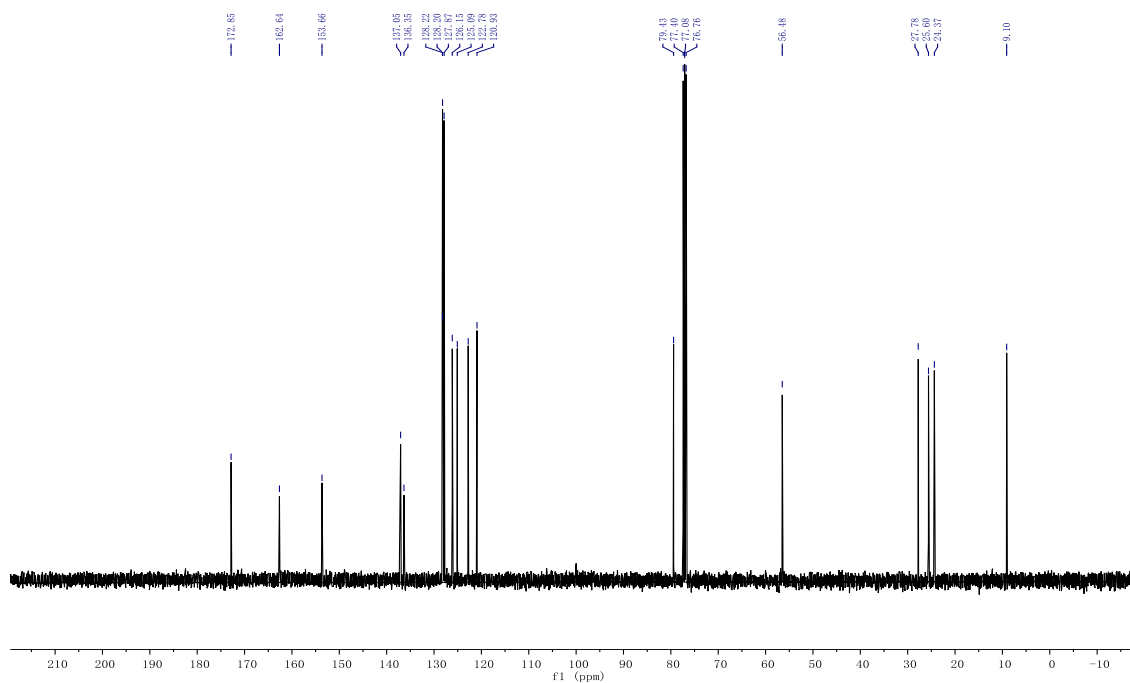


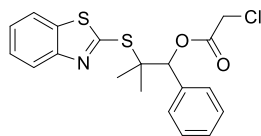
¹H NMR



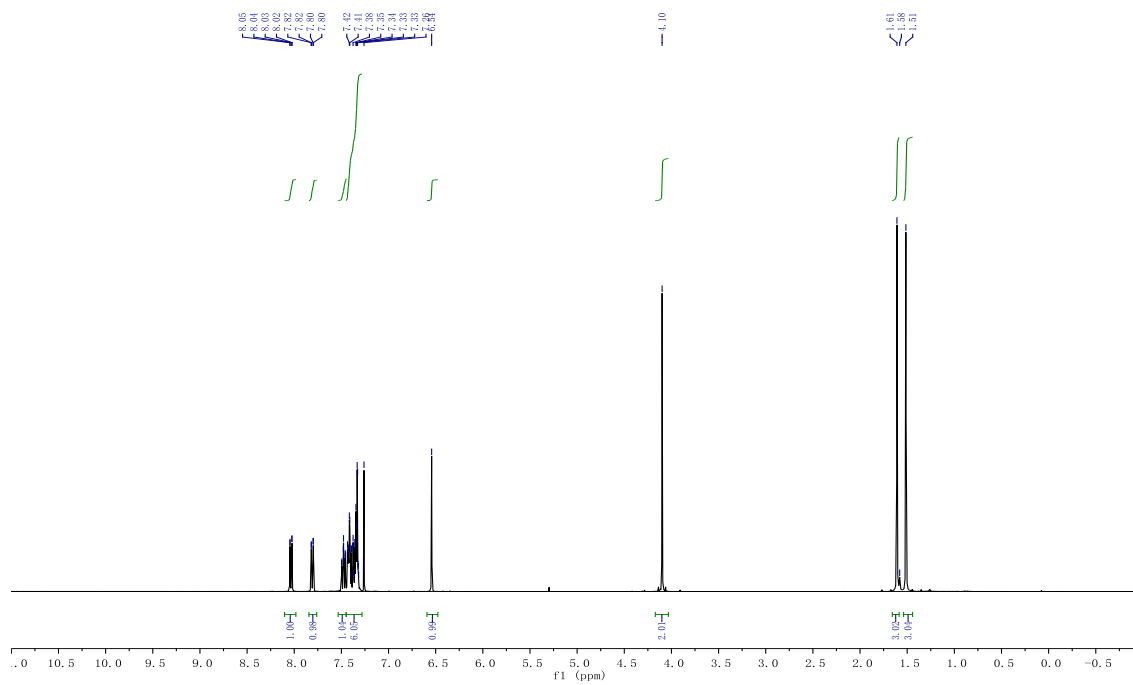
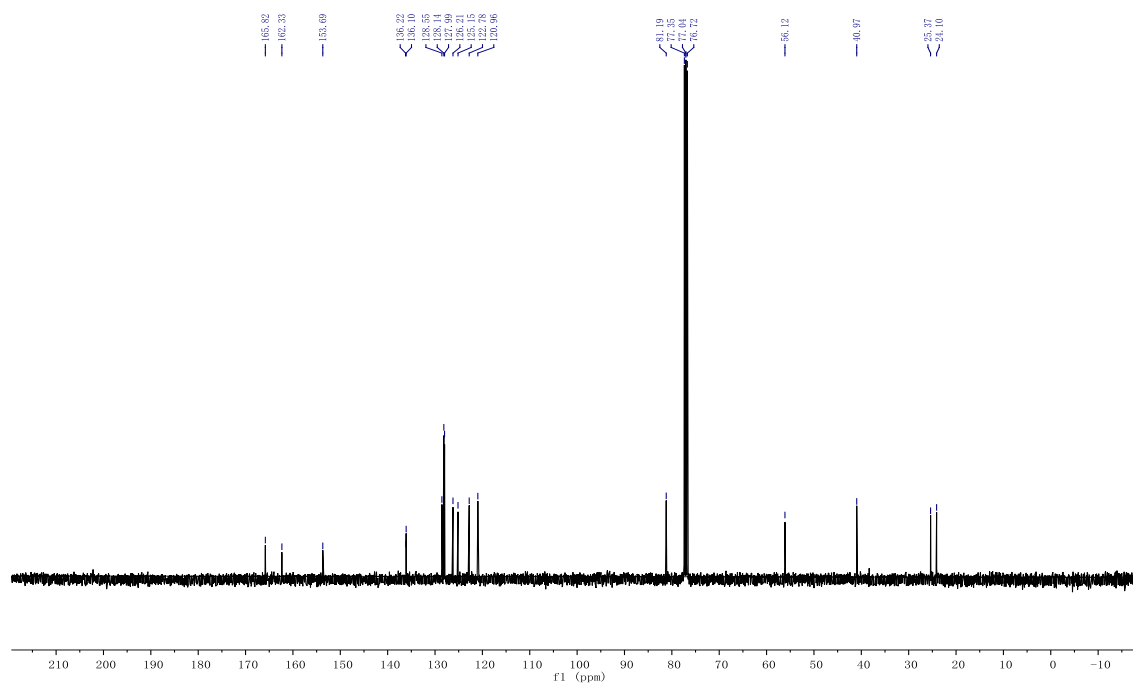
¹³C NMR

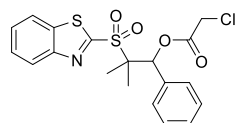


 $^1\text{H NMR}$  $^{13}\text{C NMR}$ 

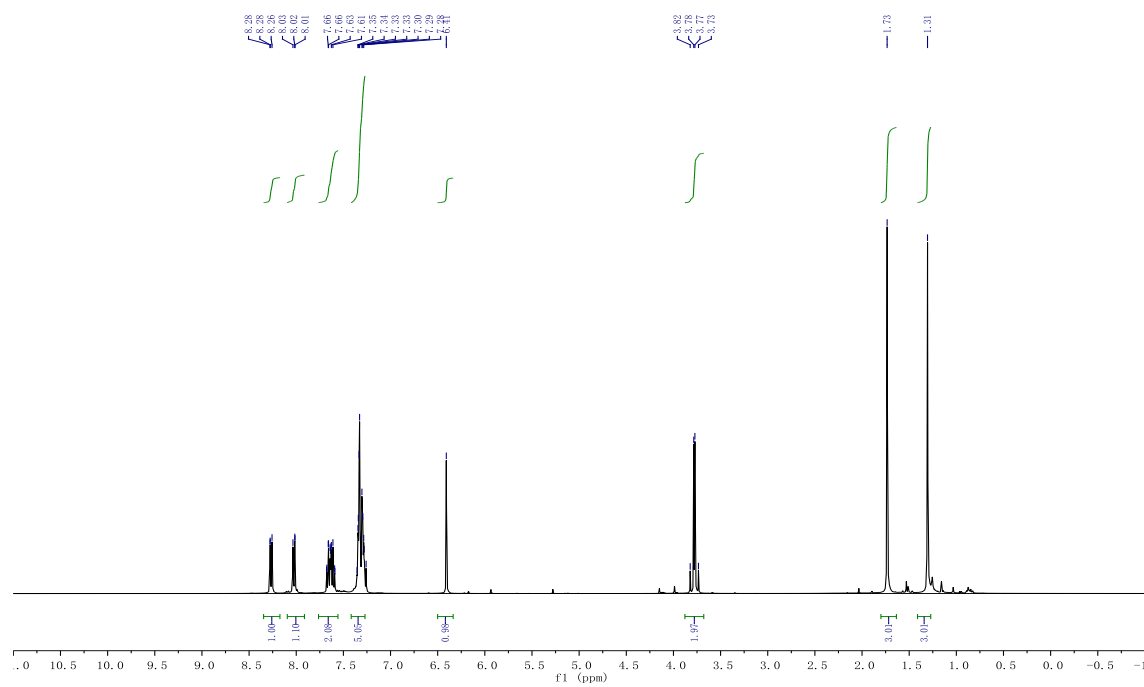
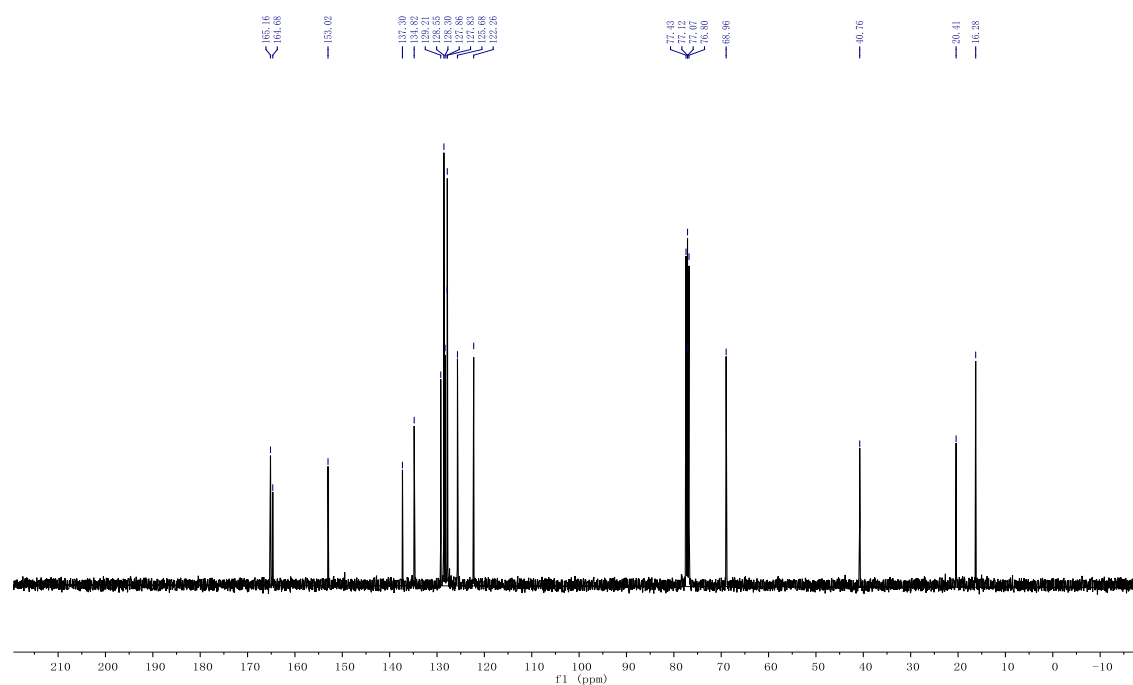


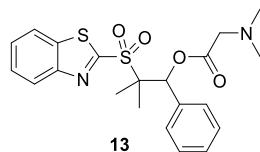
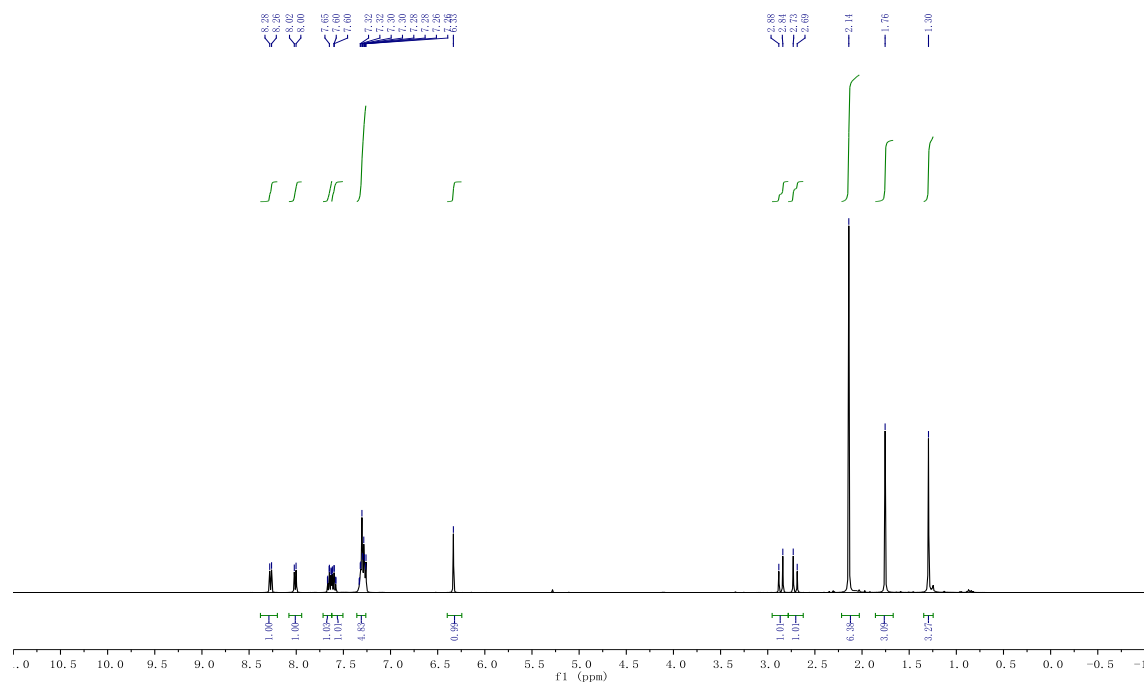
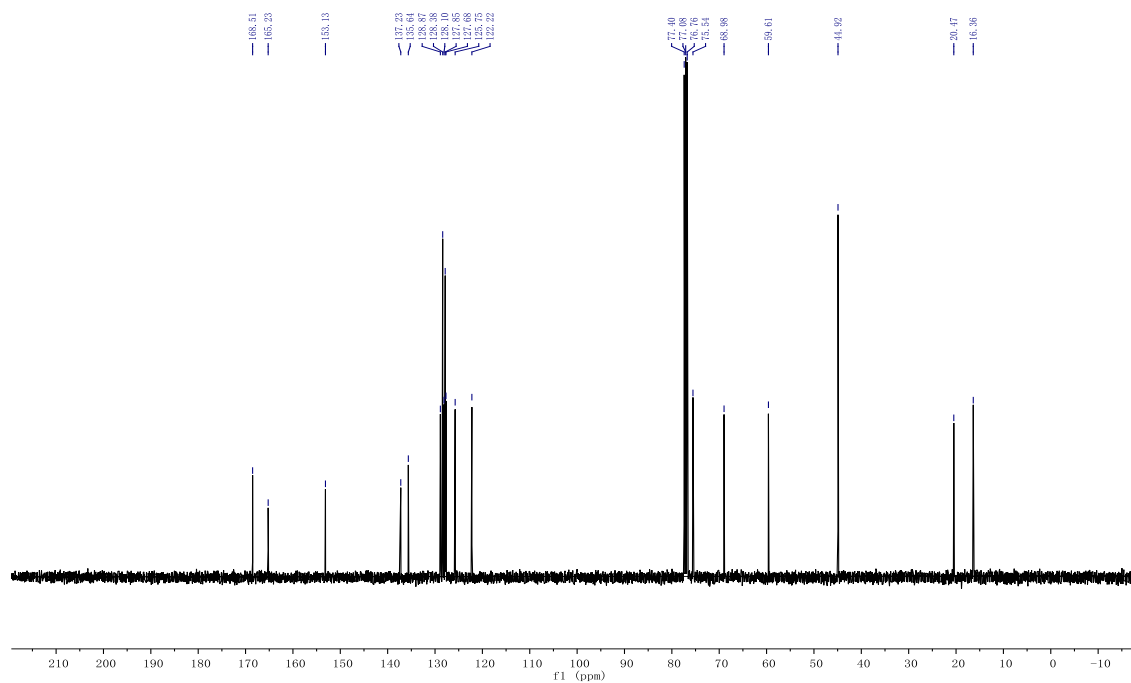
17

 ^1H NMR ^{13}C NMR

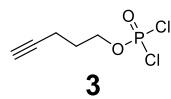
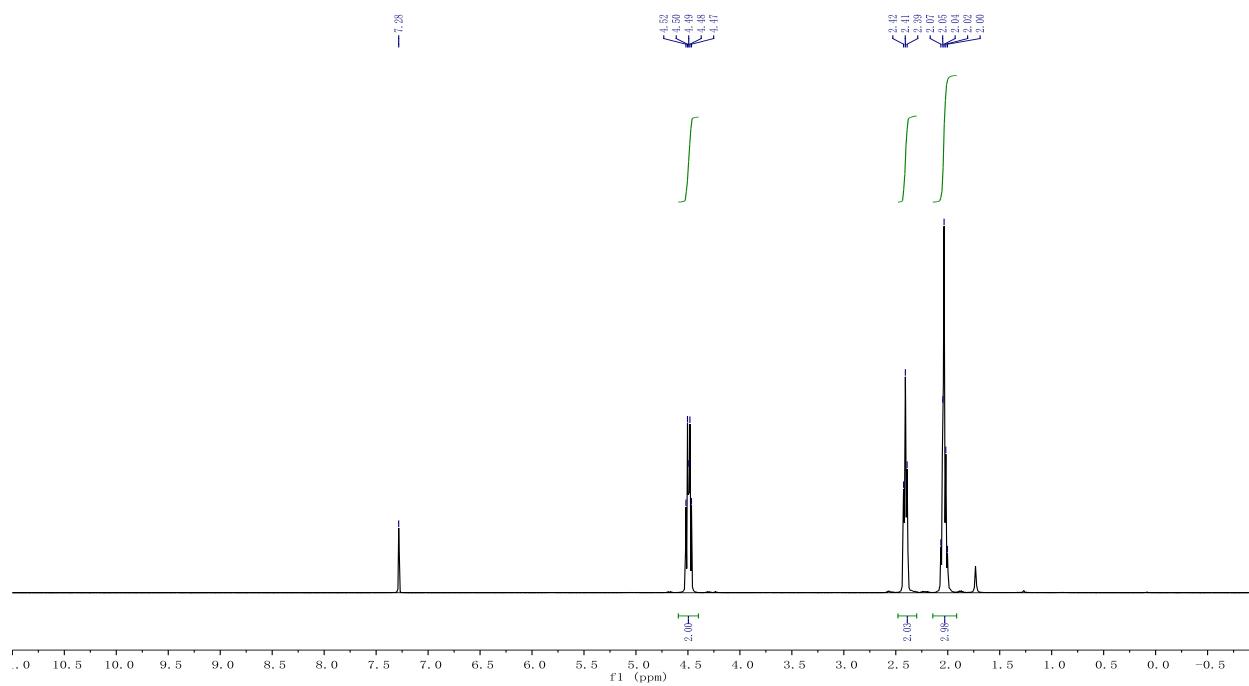
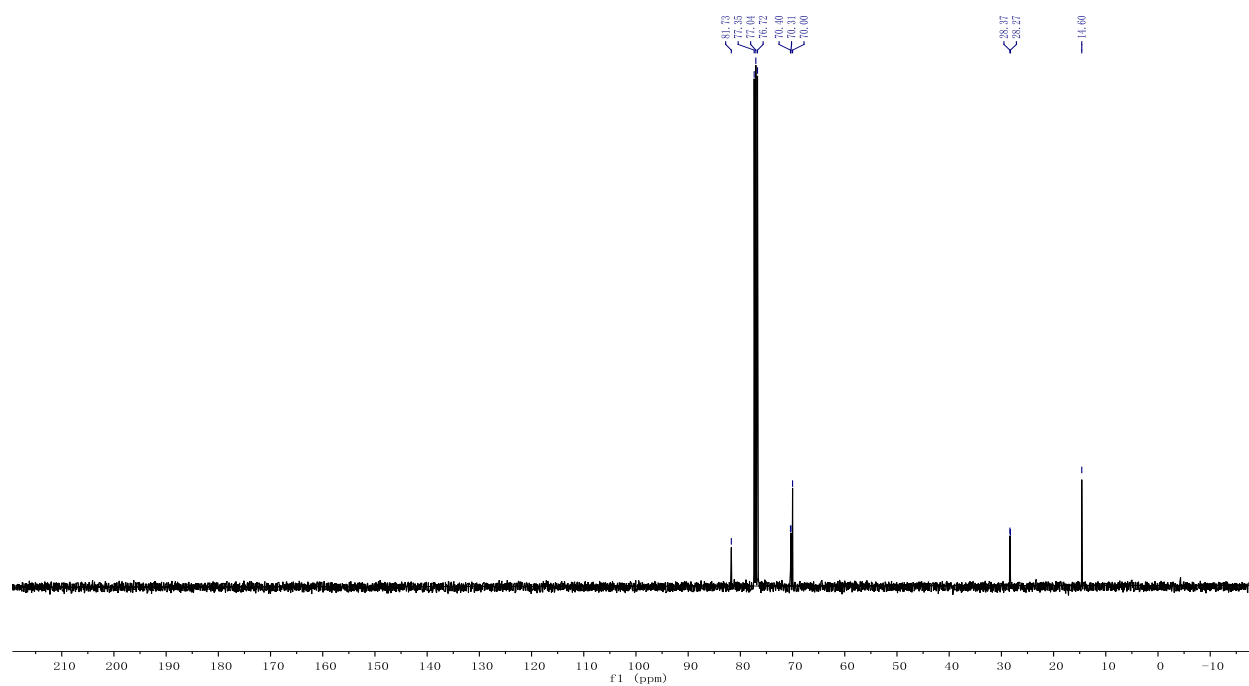


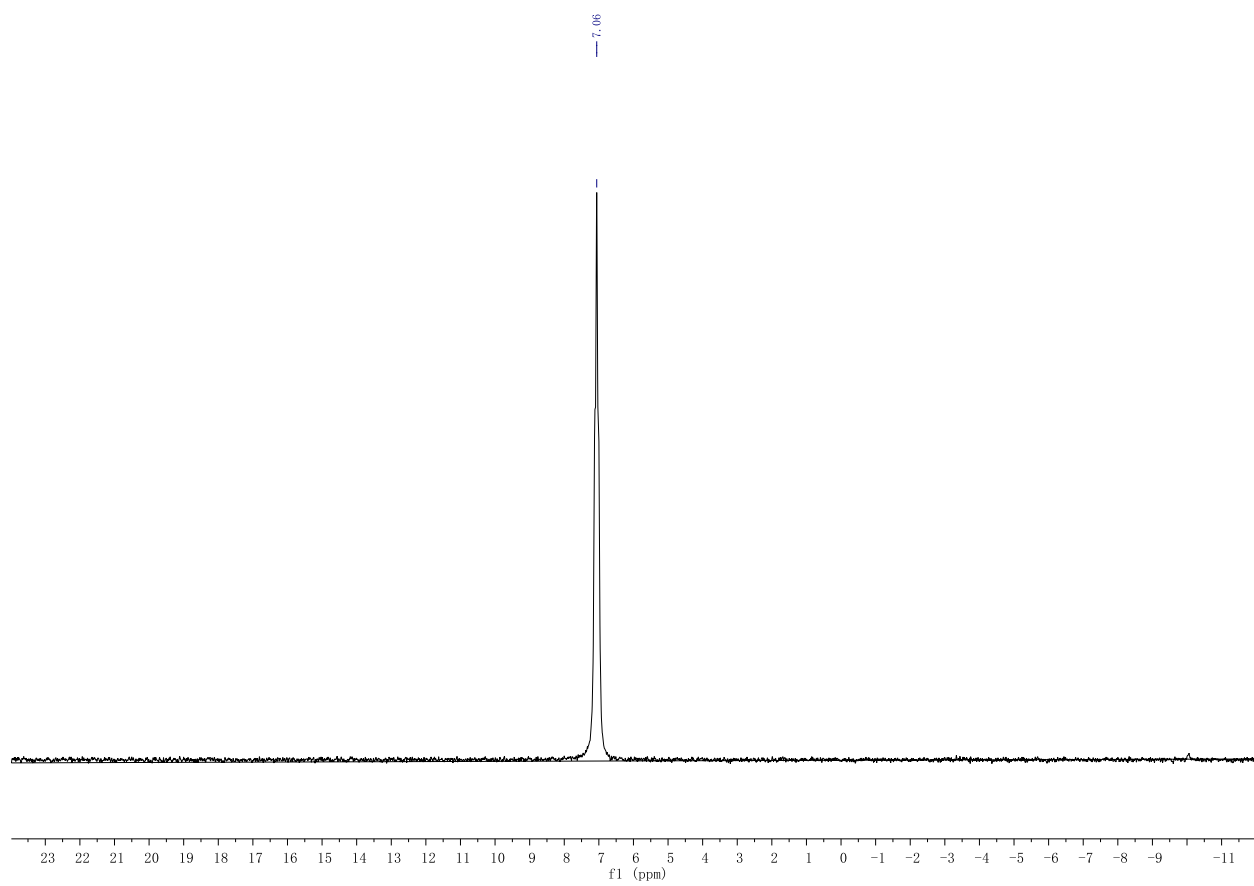
18

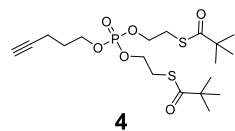
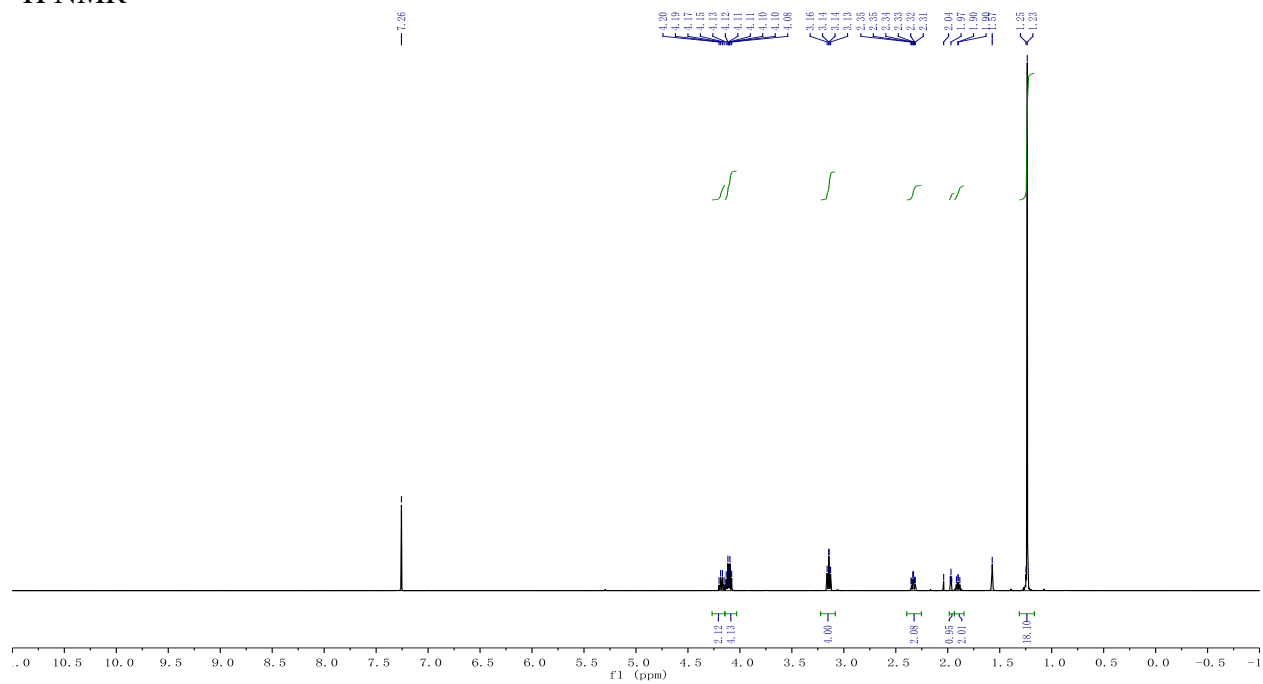
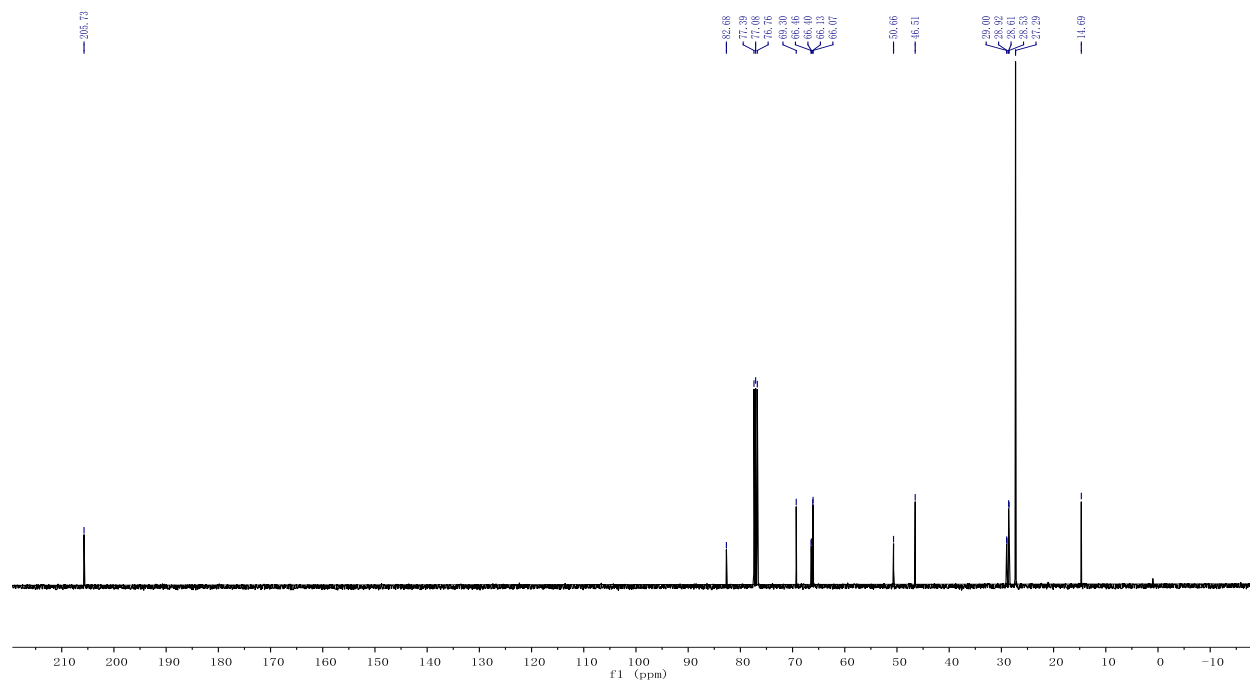
 $^1\text{H NMR}$  $^{13}\text{C NMR}$ 

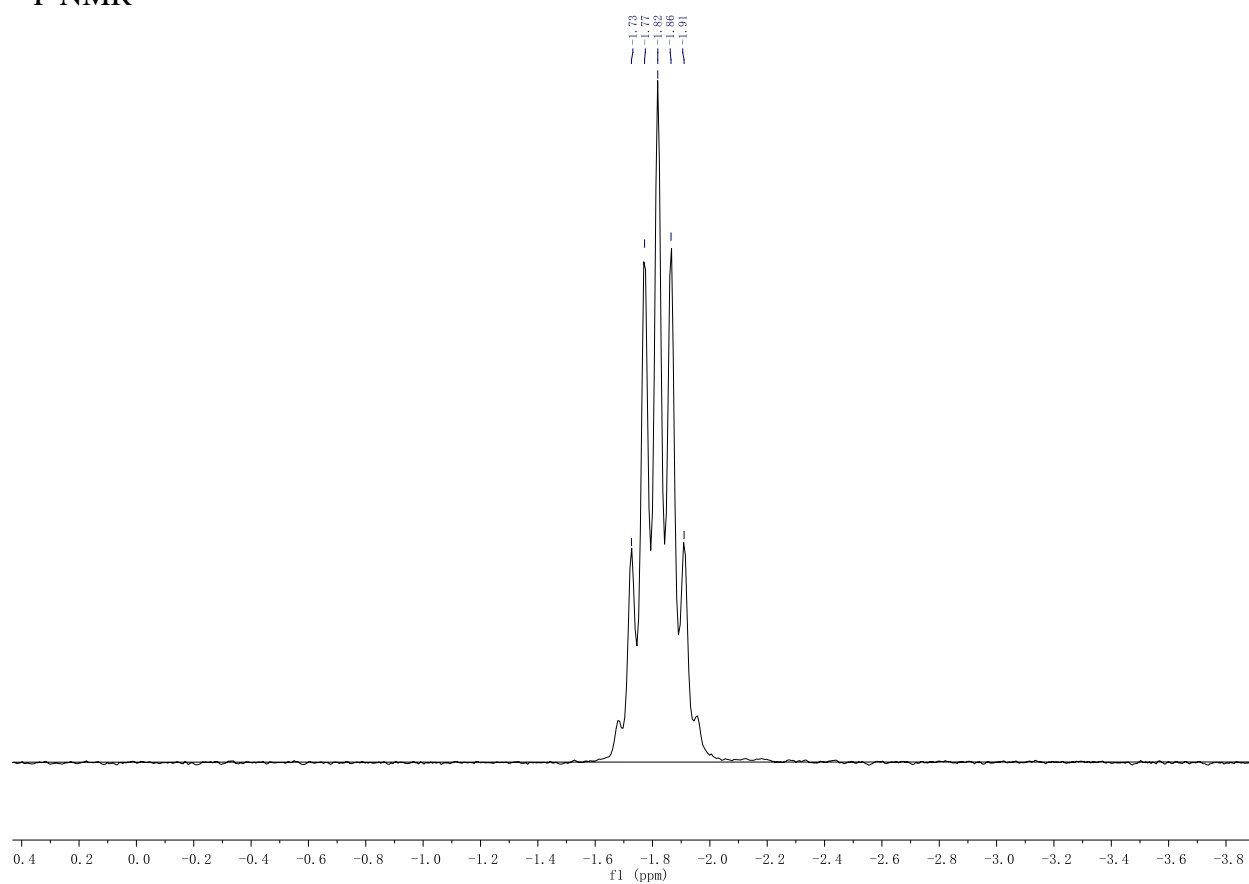
 ^1H NMR ^{13}C NMR

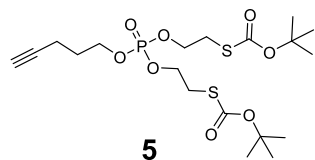
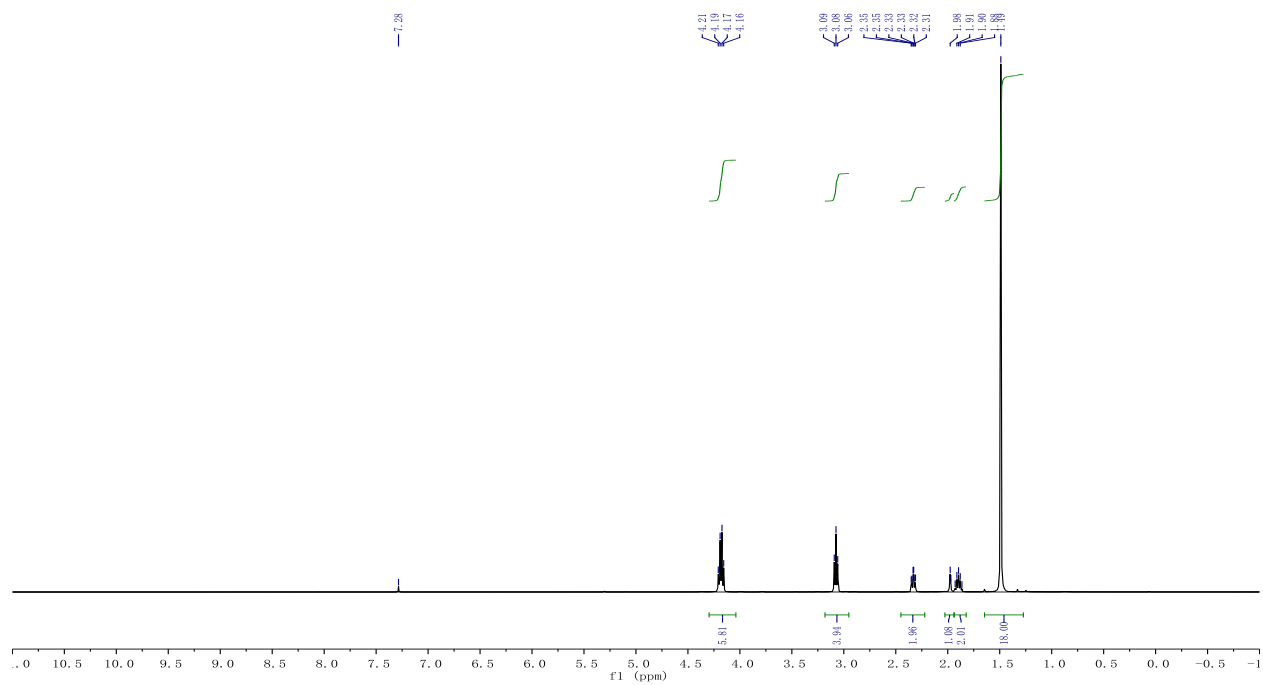
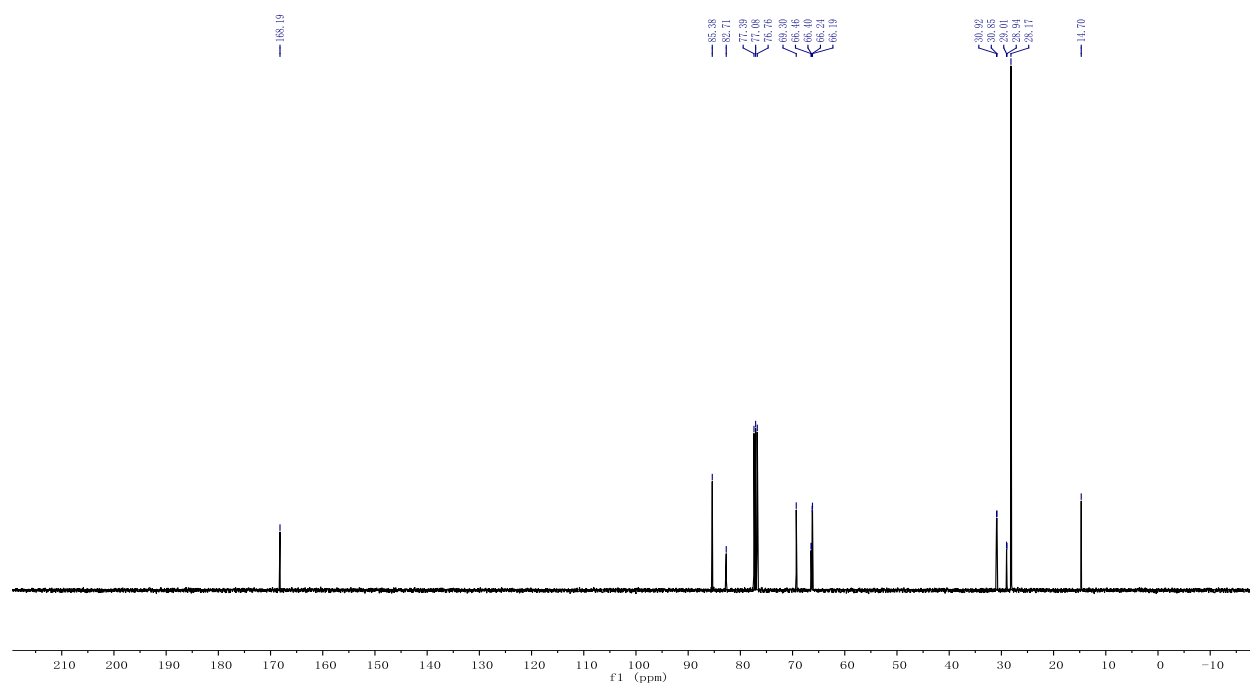
Appendix B NMR spectra of compound in Chapter 2

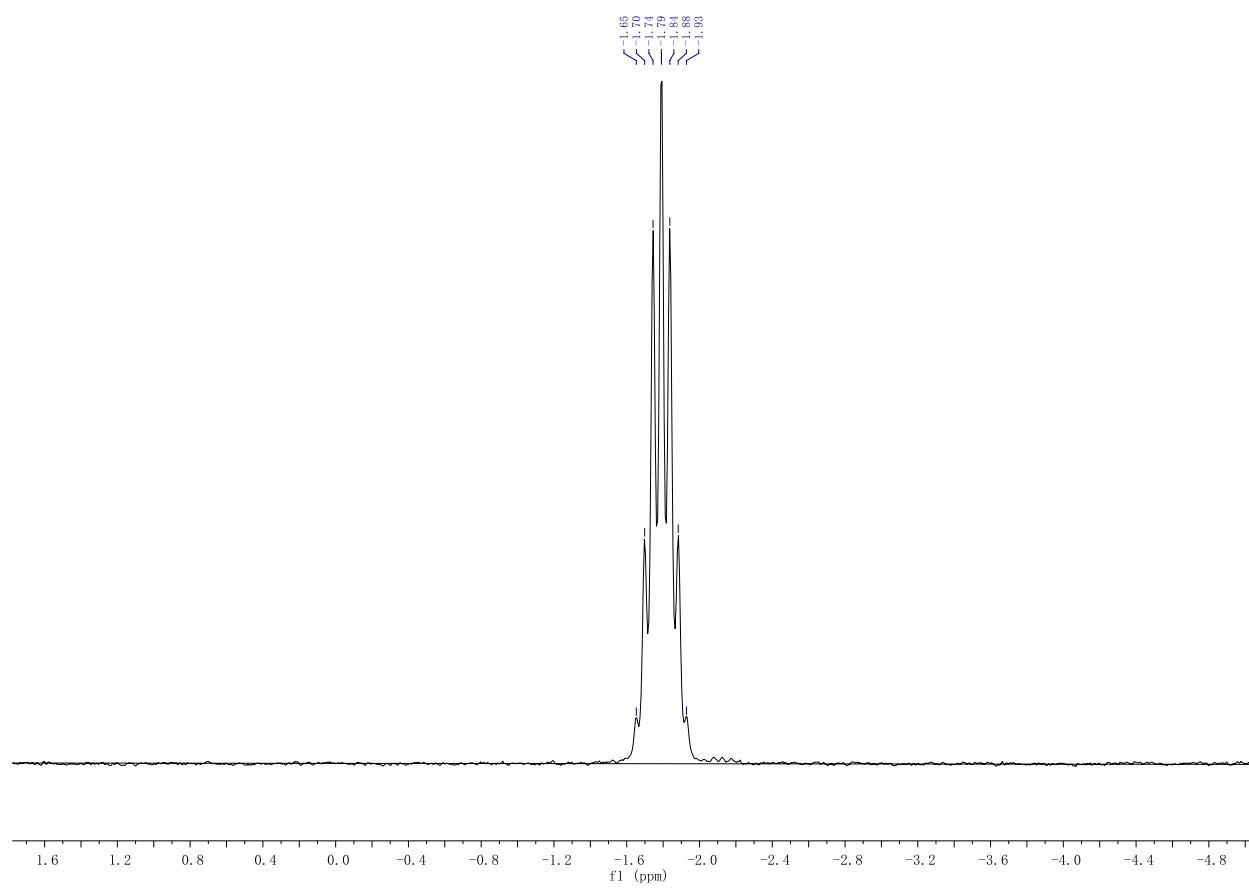
 ^1H NMR ^{13}C NMR

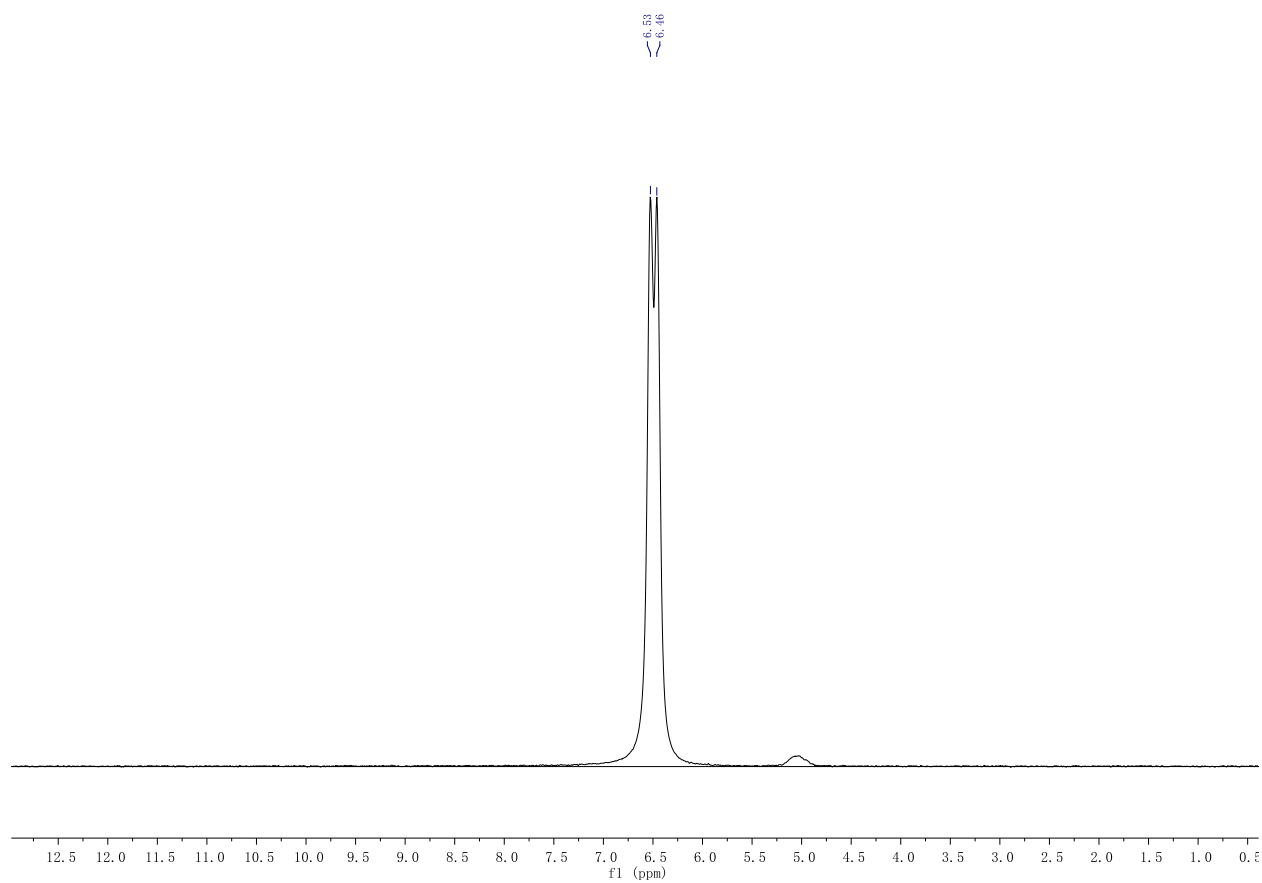
^{31}P NMR

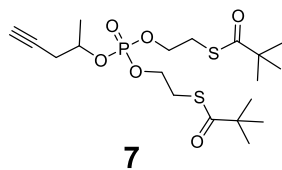
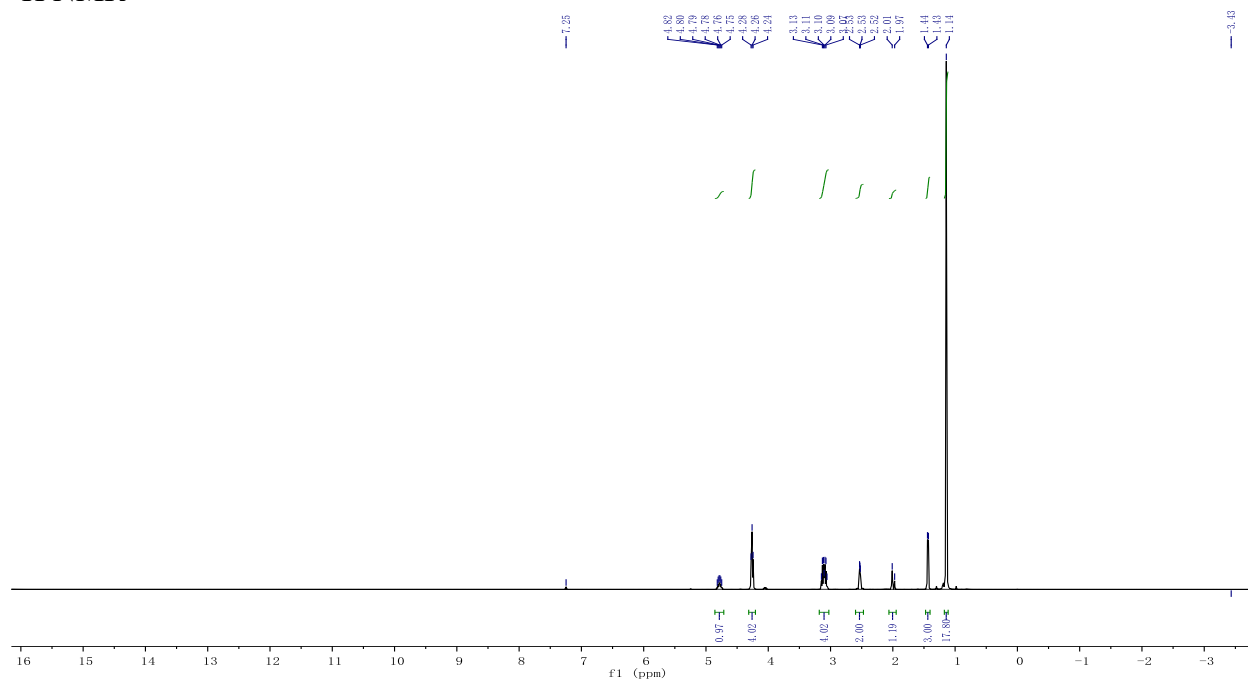
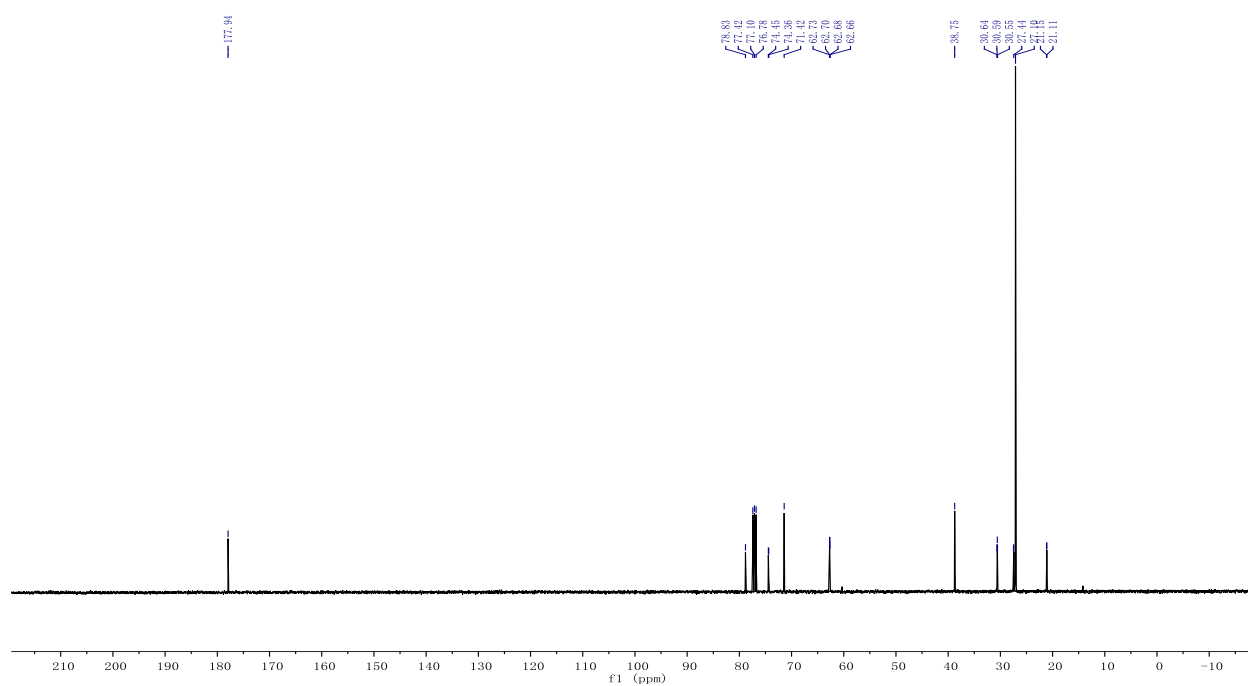
 $^1\text{H NMR}$  $^{13}\text{C NMR}$ 

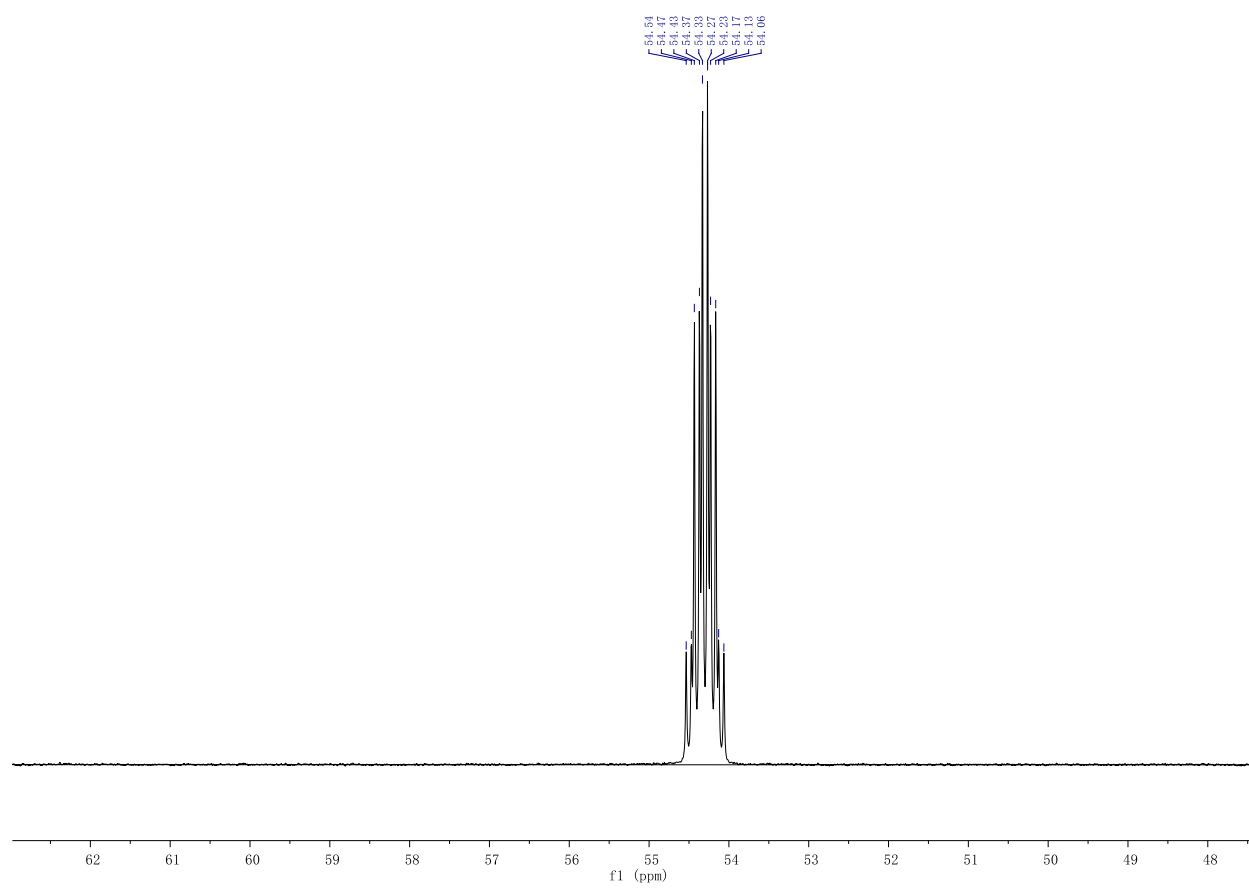
^{31}P NMR

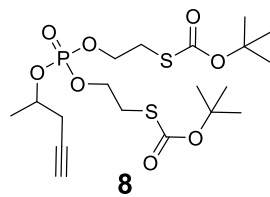
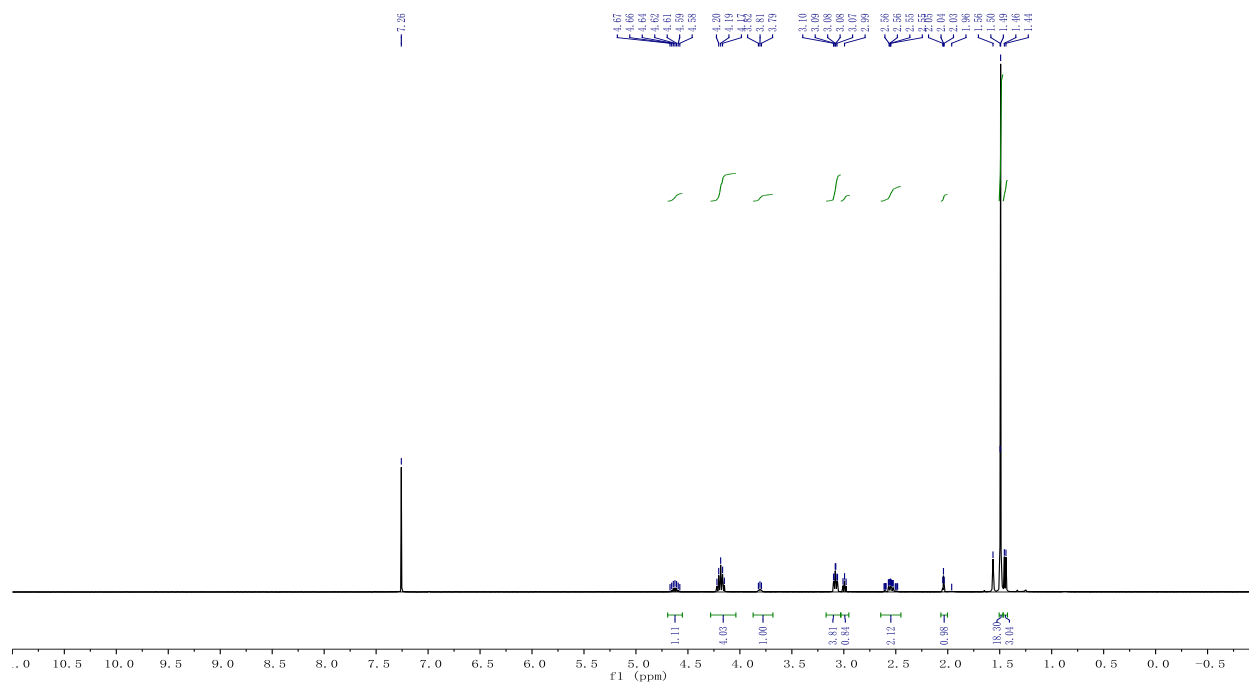
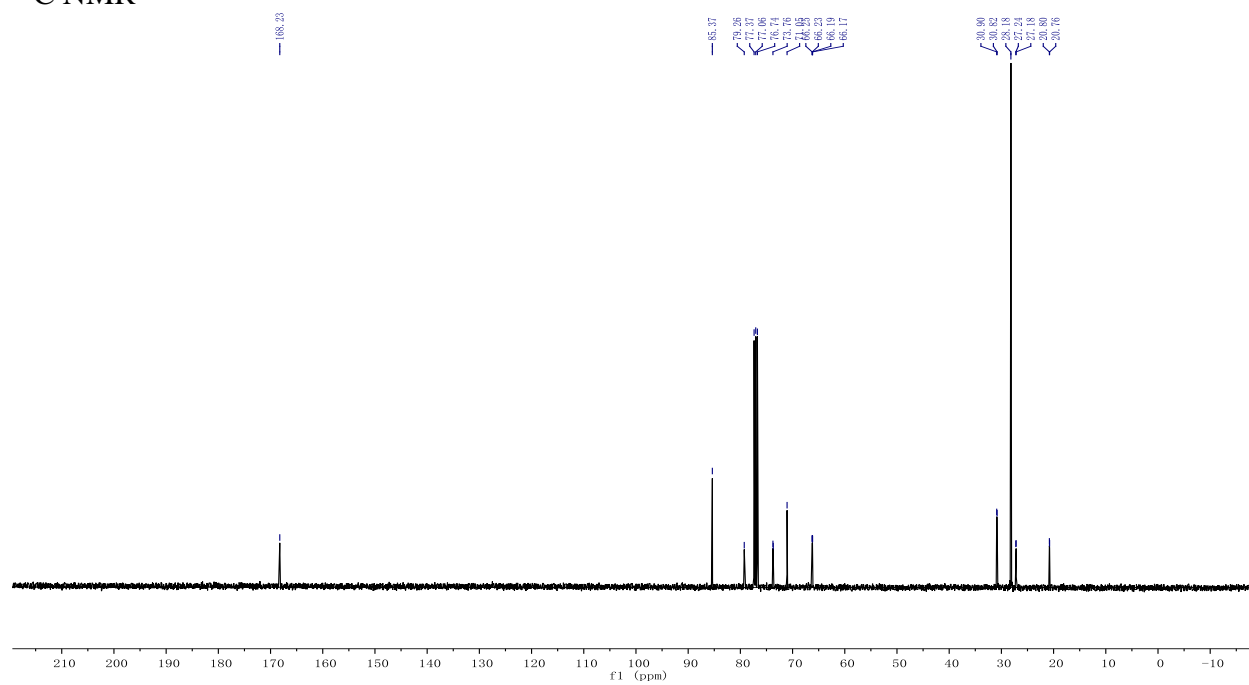
 $^1\text{H NMR}$  $^{13}\text{C NMR}$ 

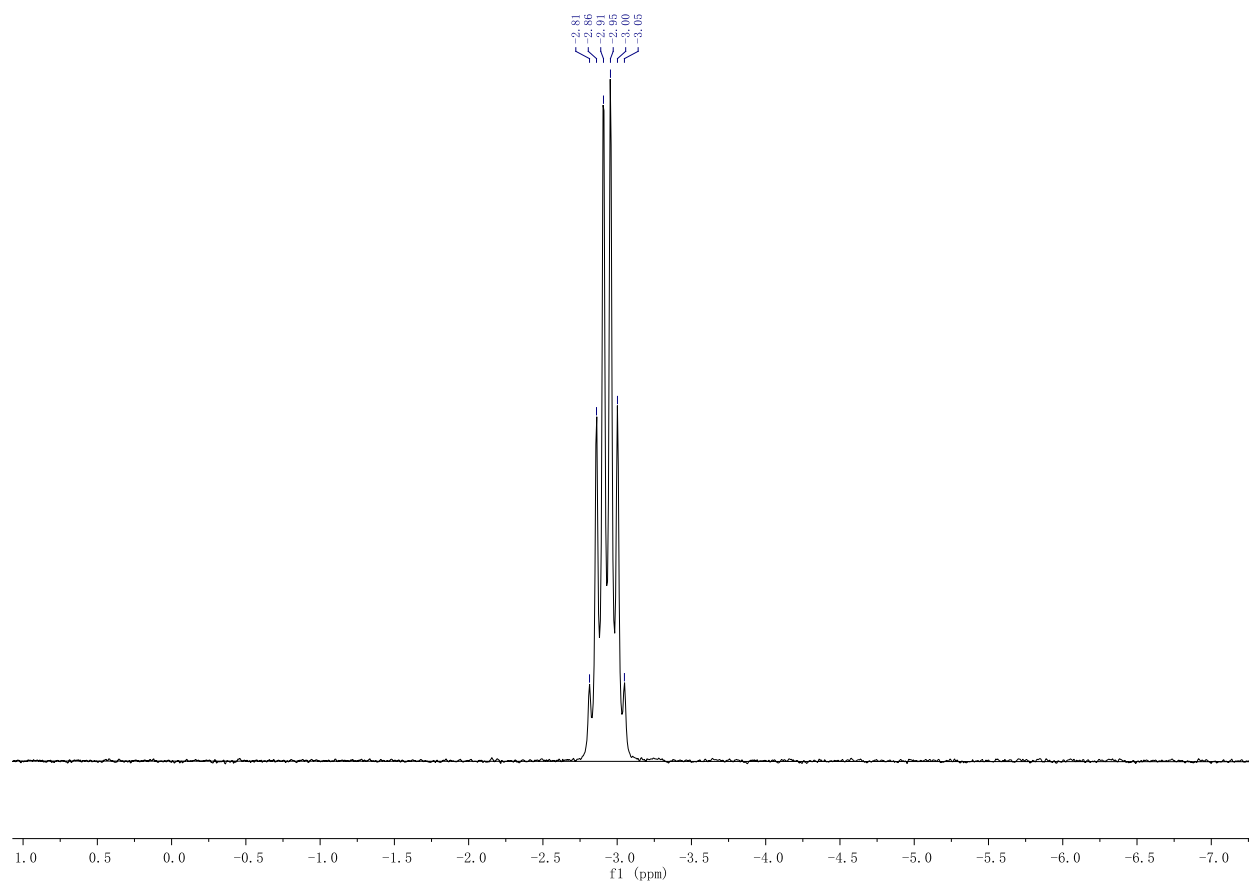
^{31}P NMR

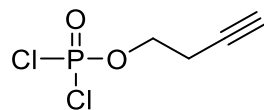
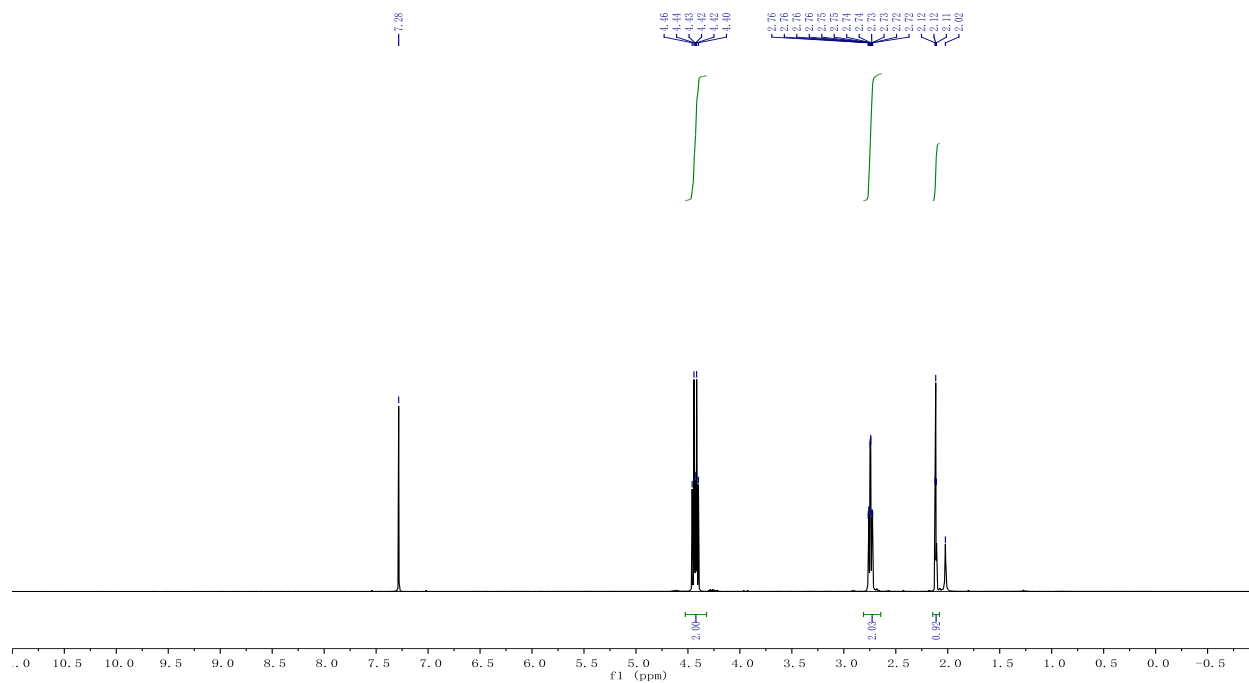
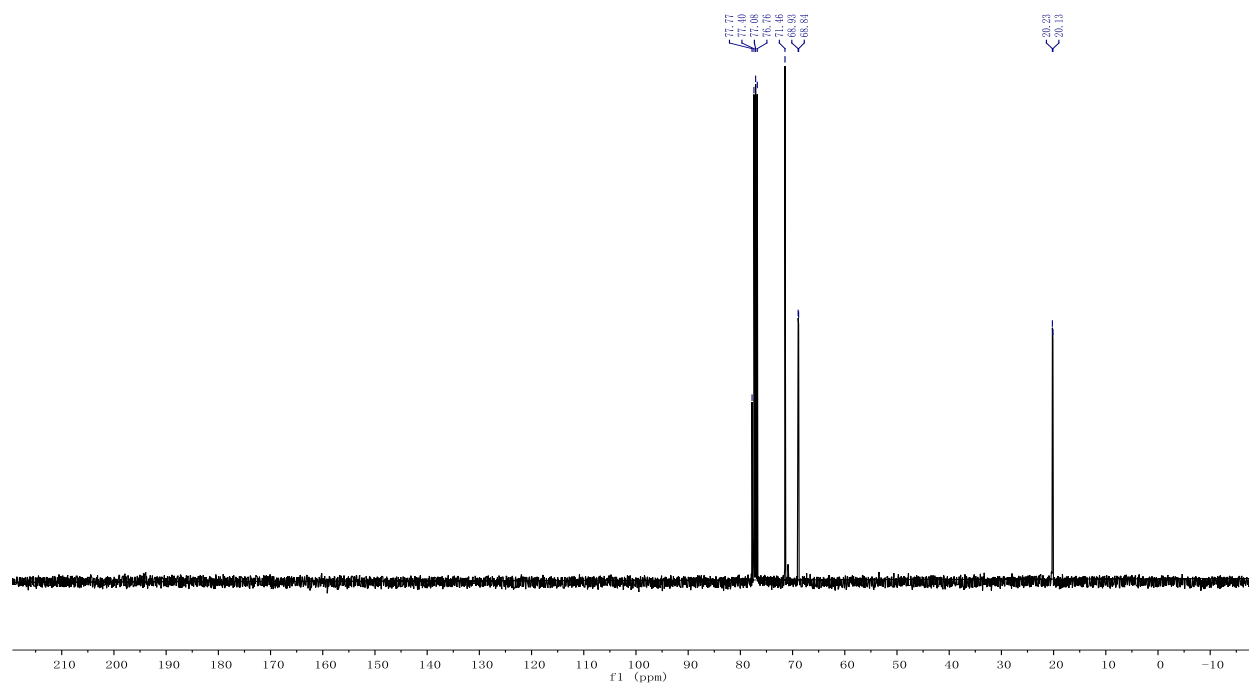
^{31}P NMR

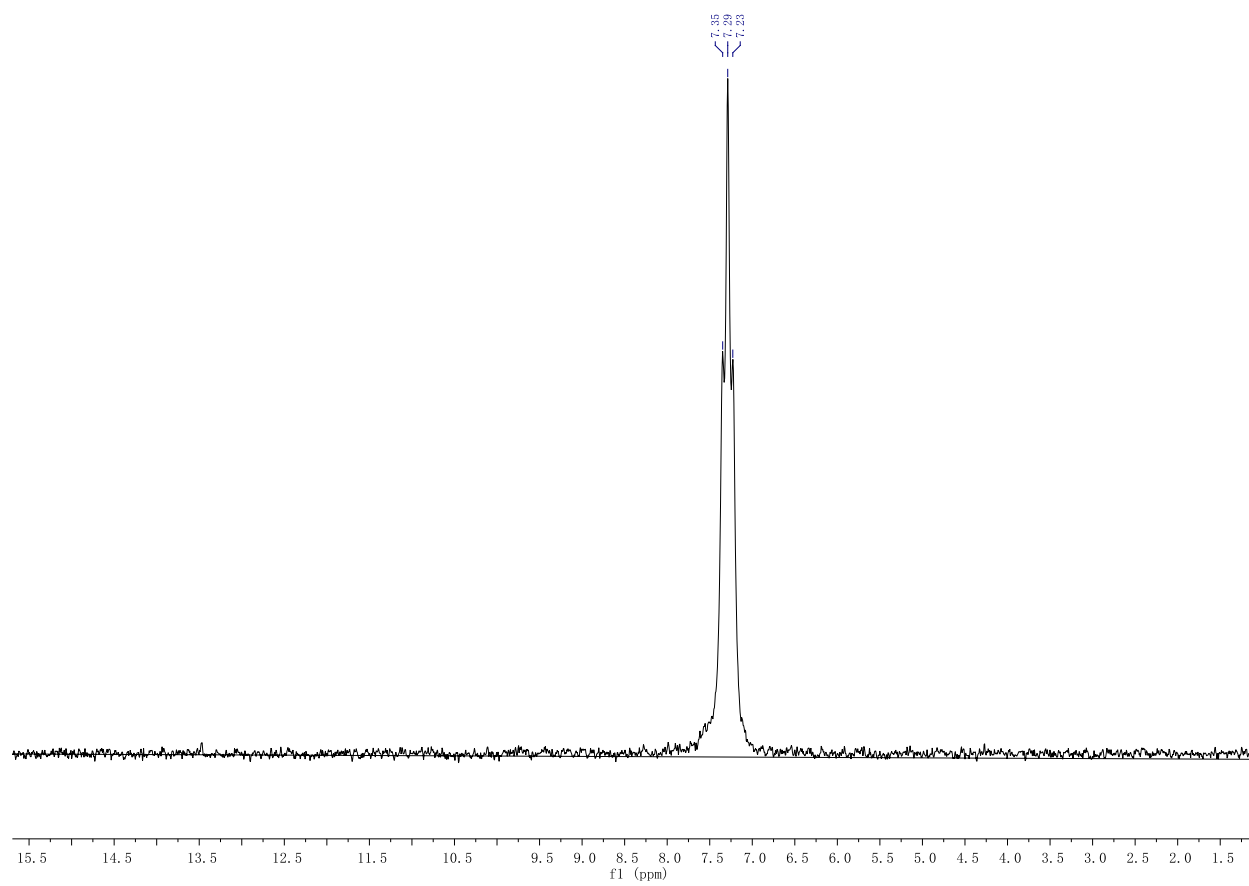
 ^1H NMR ^{13}C NMR

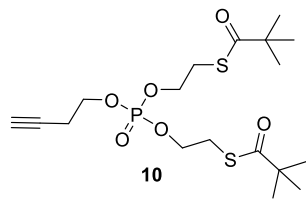
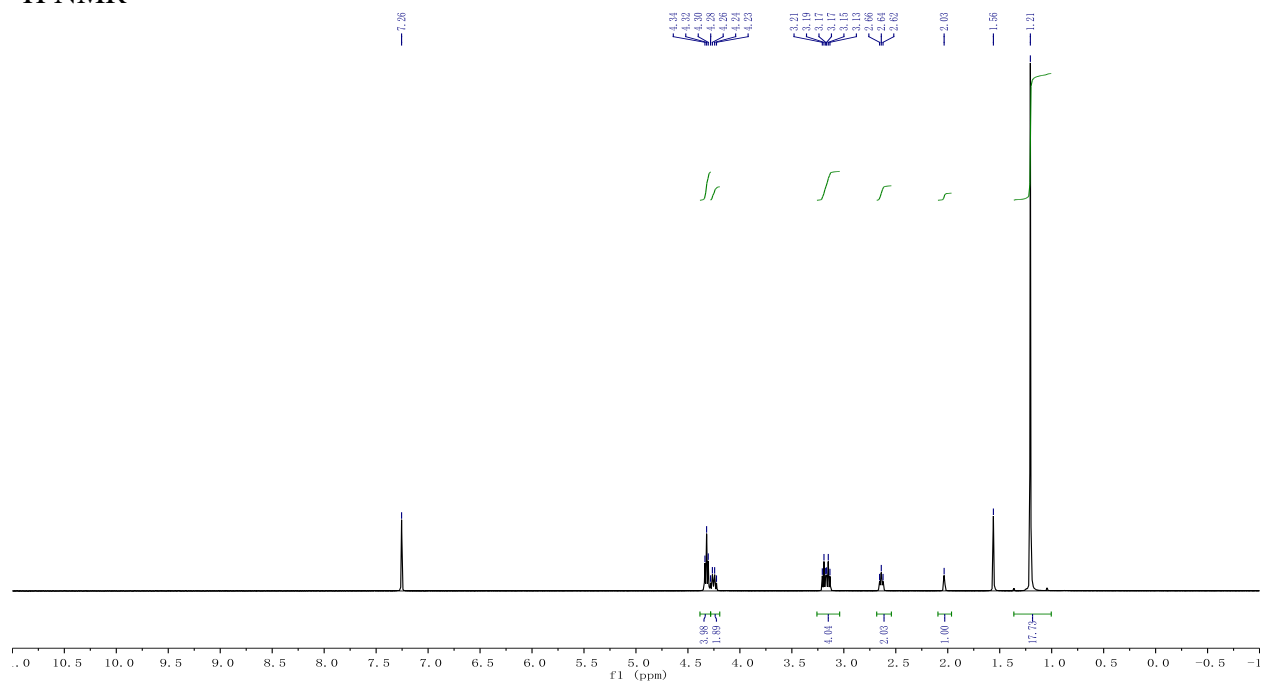
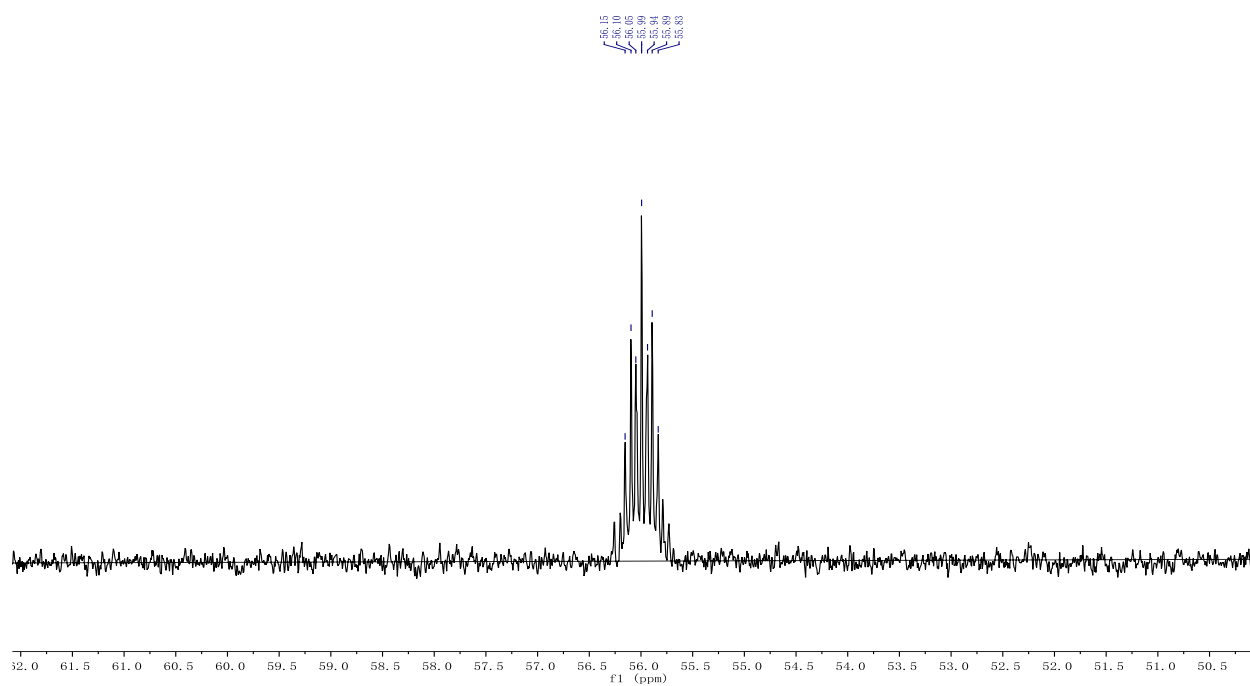
^{31}P NMR

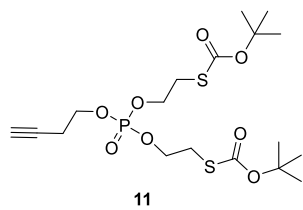
¹H NMR¹³C NMR

^{31}P NMR

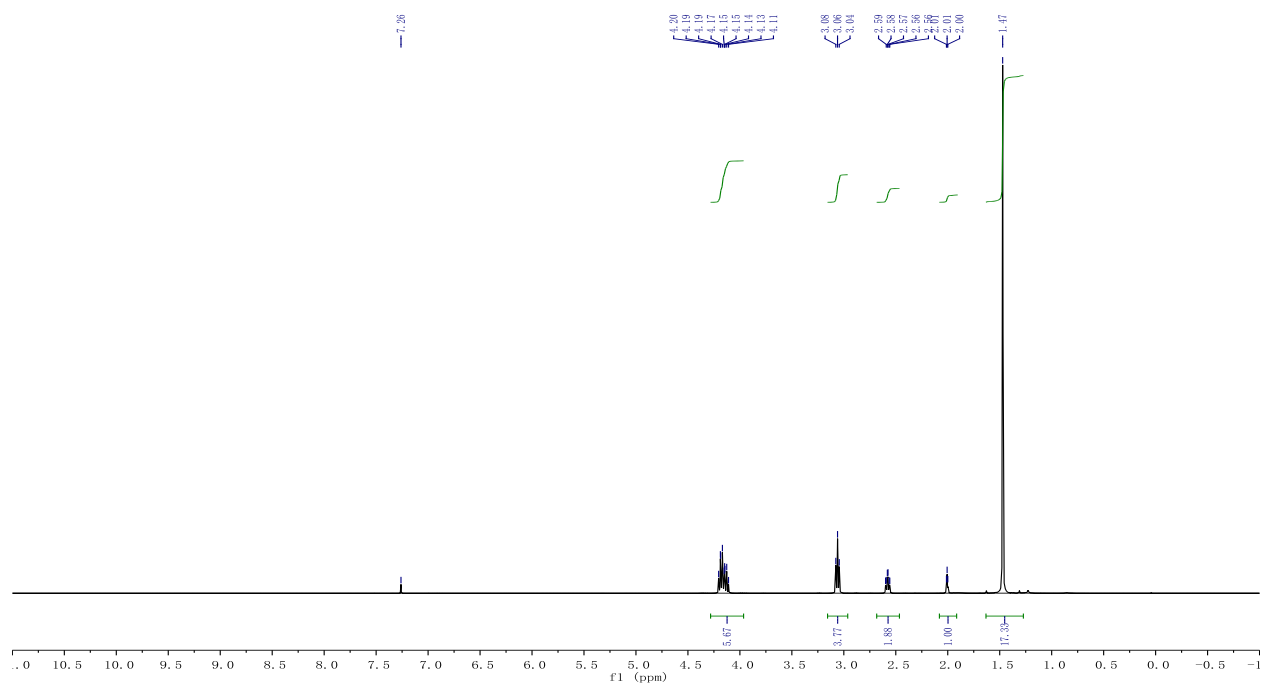
**9** ^1H NMR ^{13}C NMR

^{31}P NMR

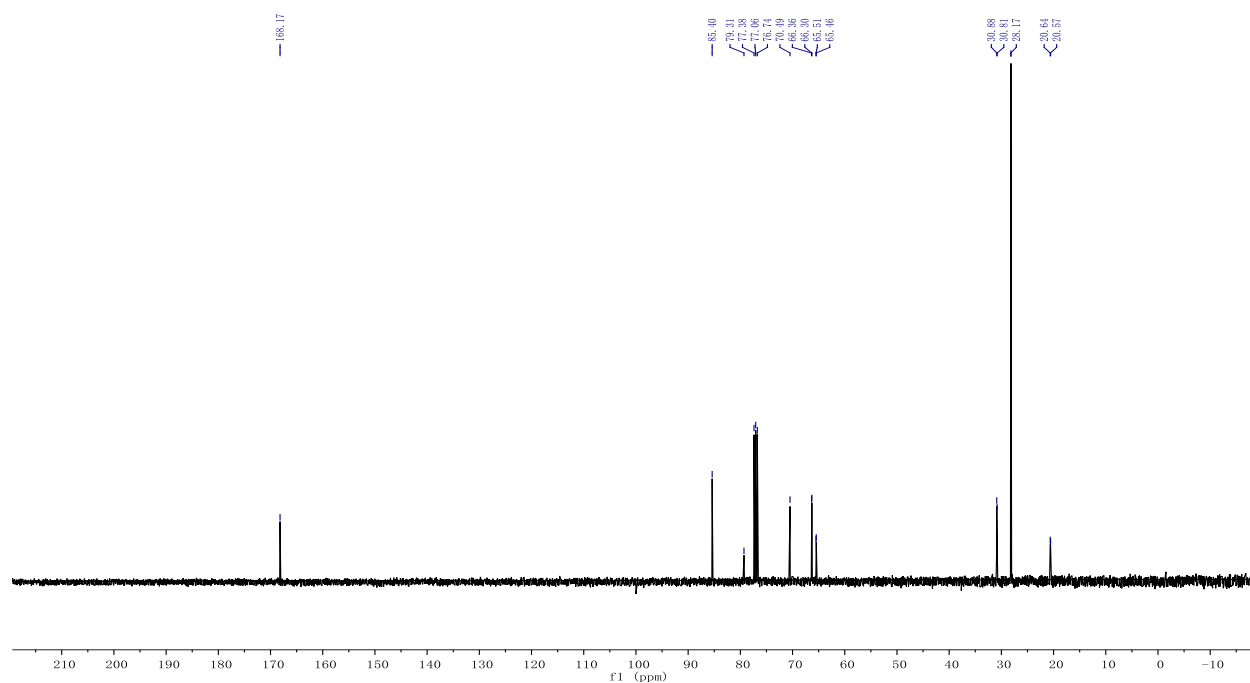
 ^1H NMR ^{31}P NMR

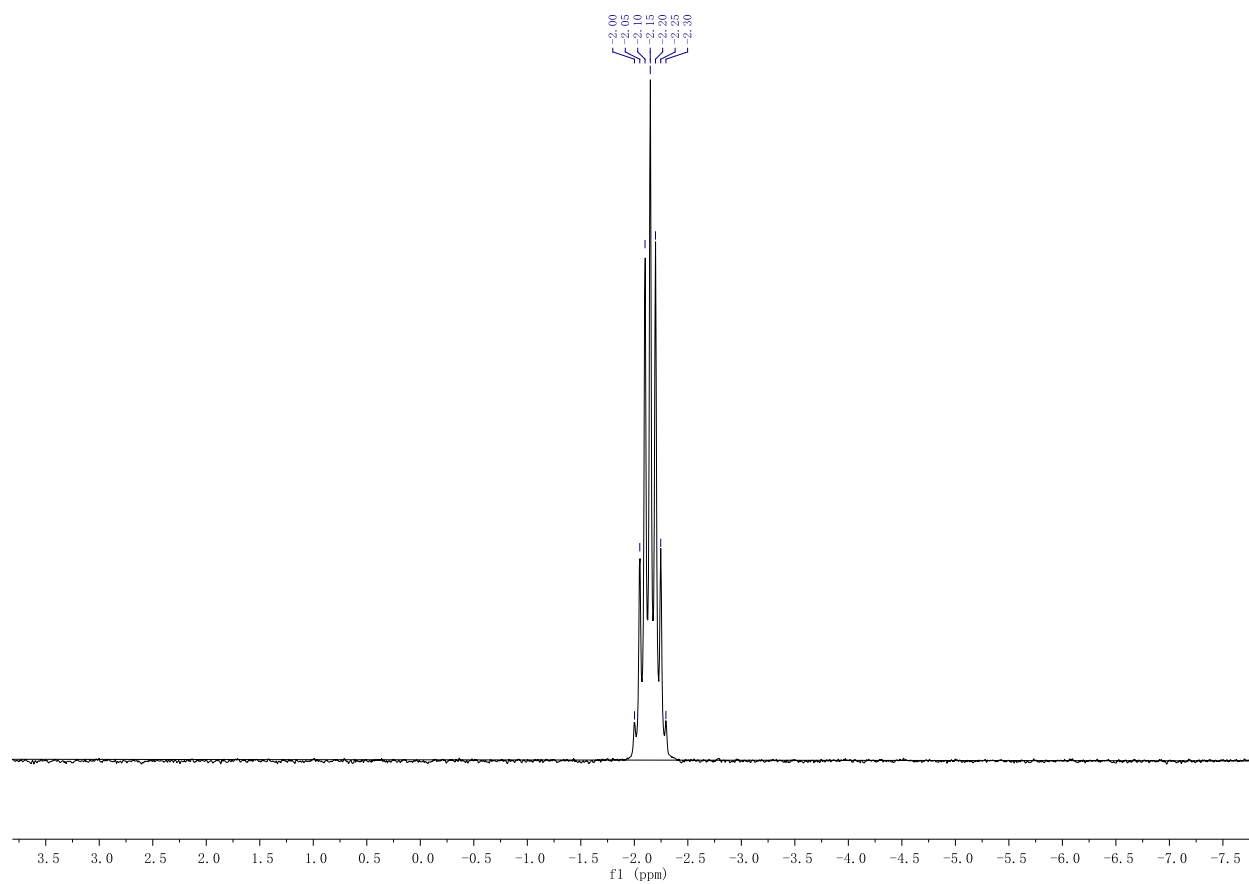


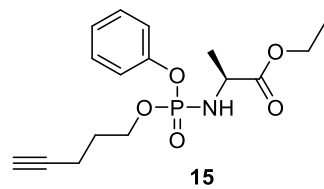
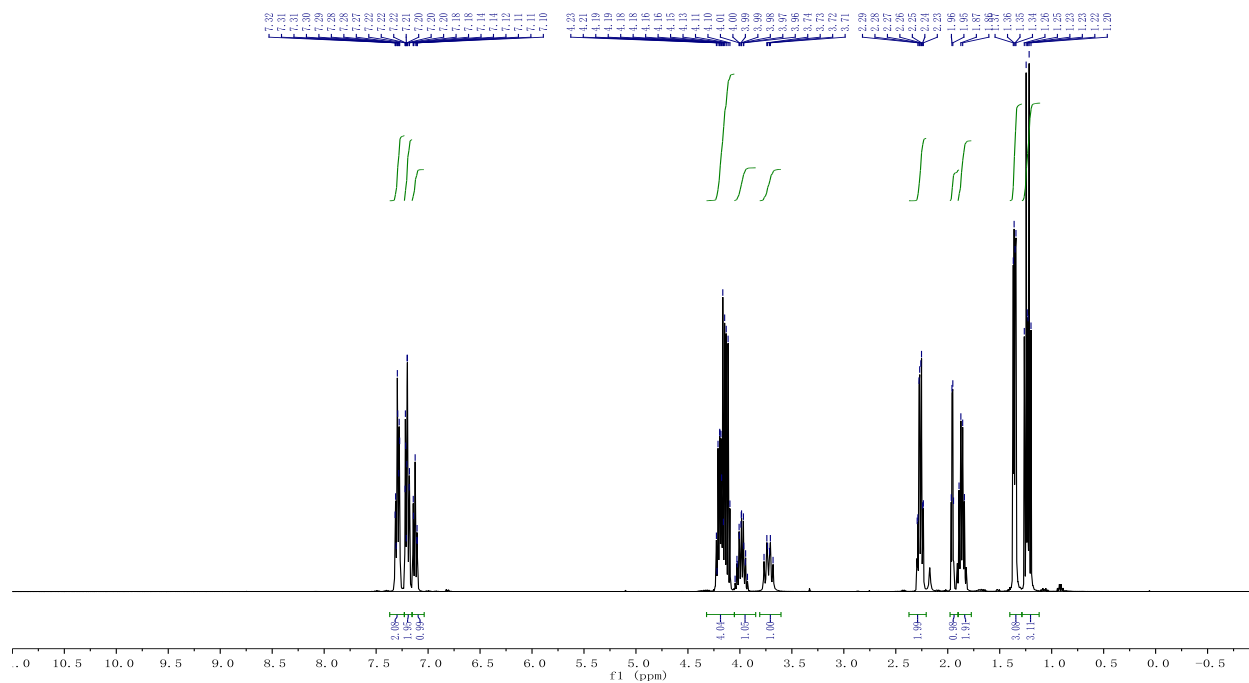
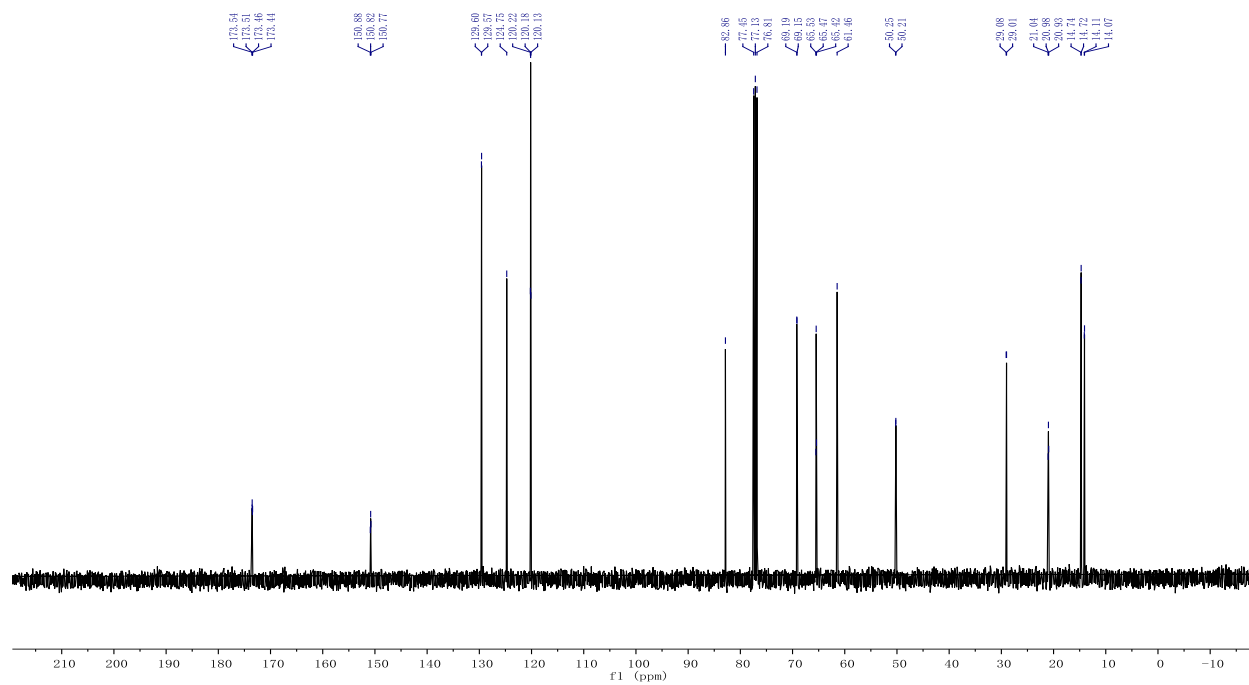
11
 $^1\text{H NMR}$

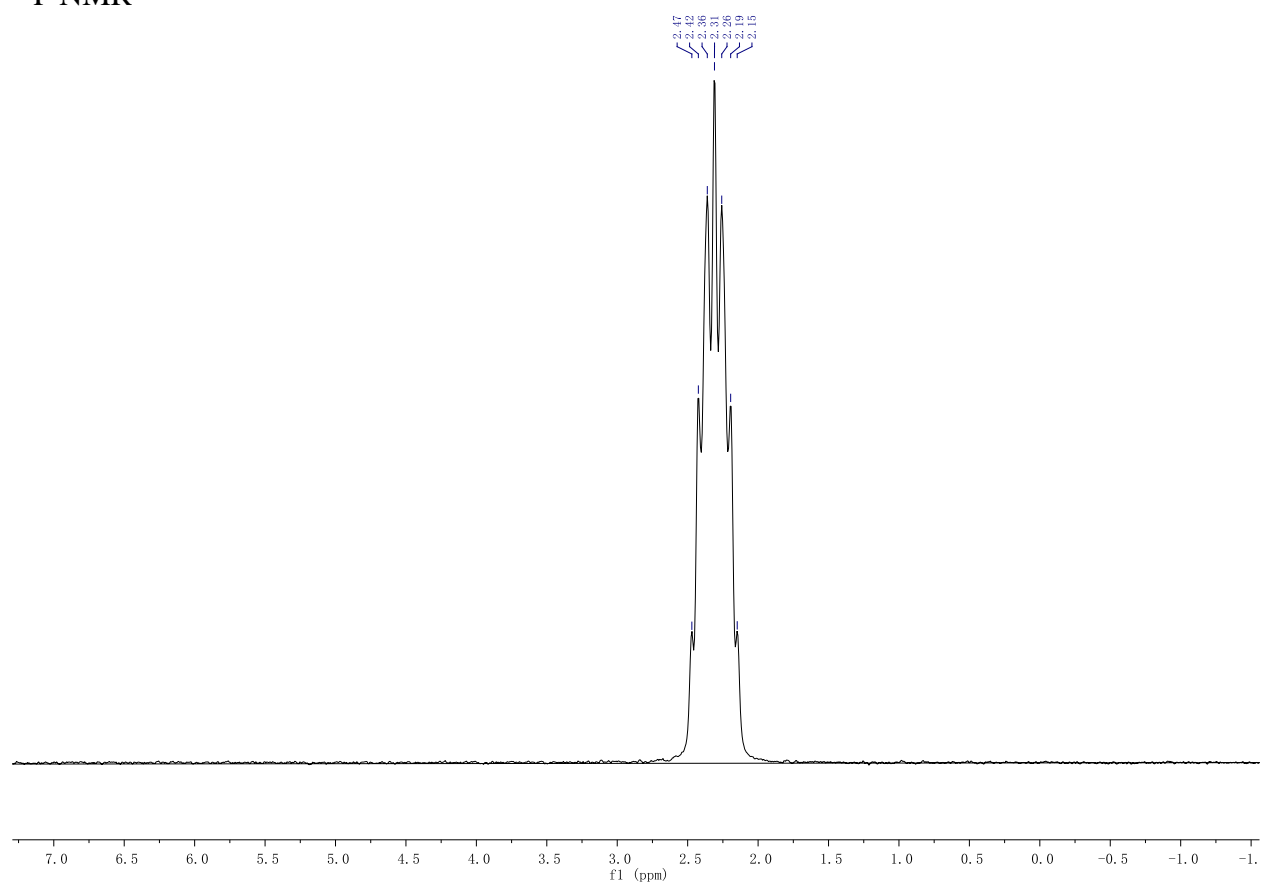


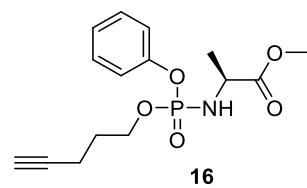
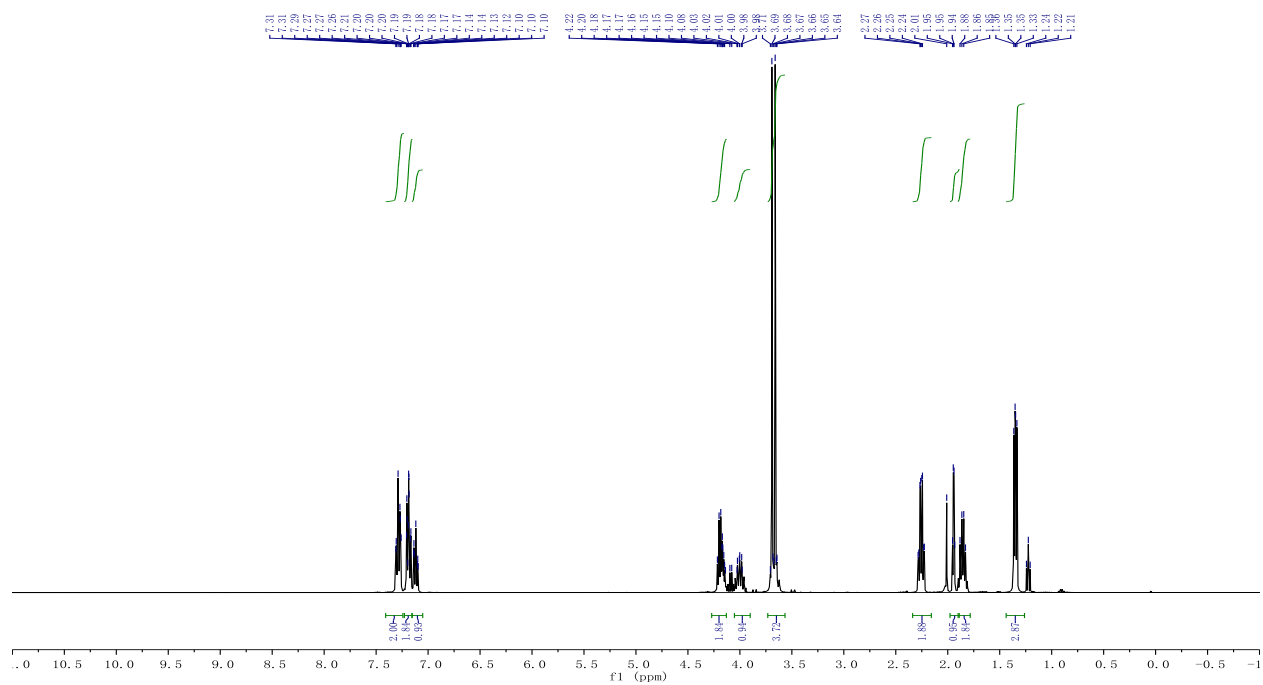
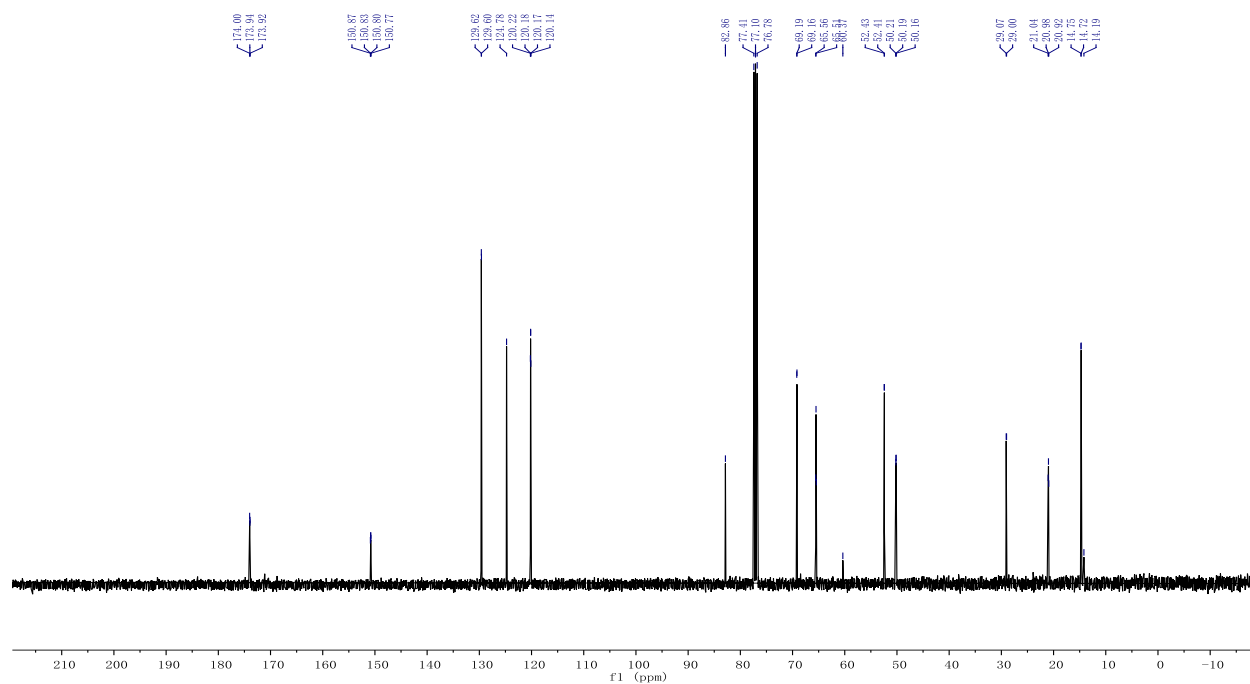
$^{13}\text{C NMR}$

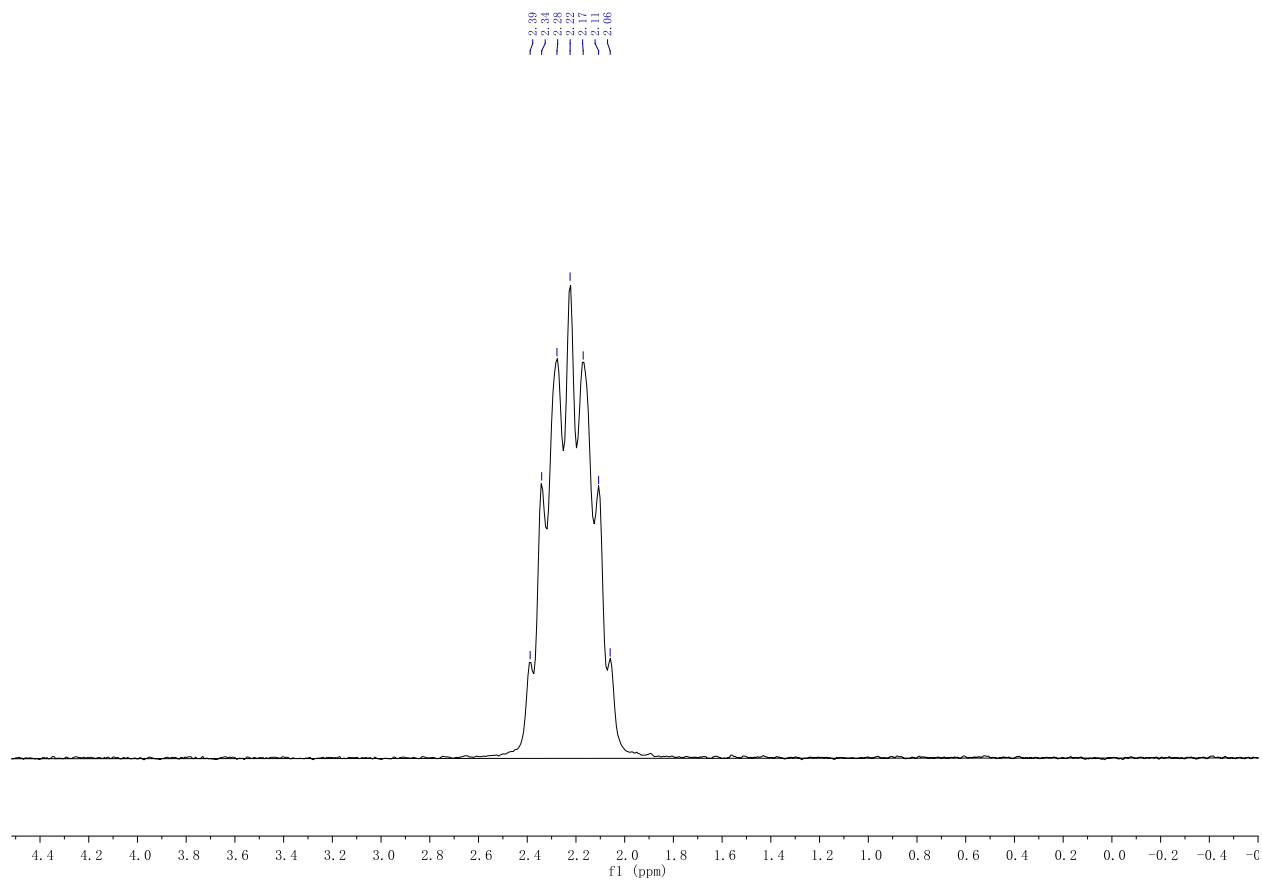


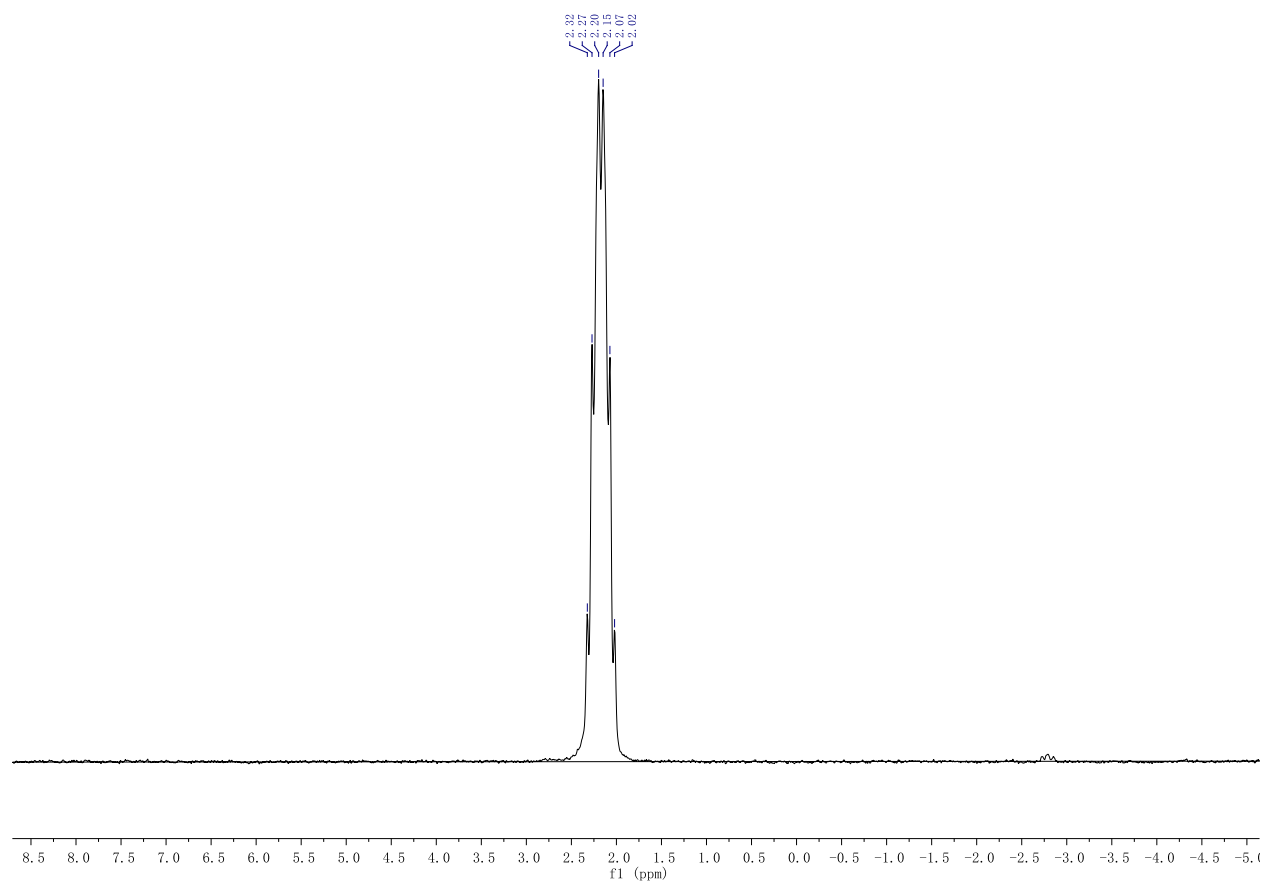
^{31}P NMR

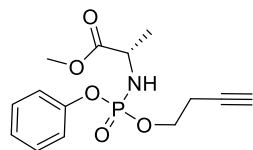
 ^1H NMR ^{13}C NMR

^{31}P NMR

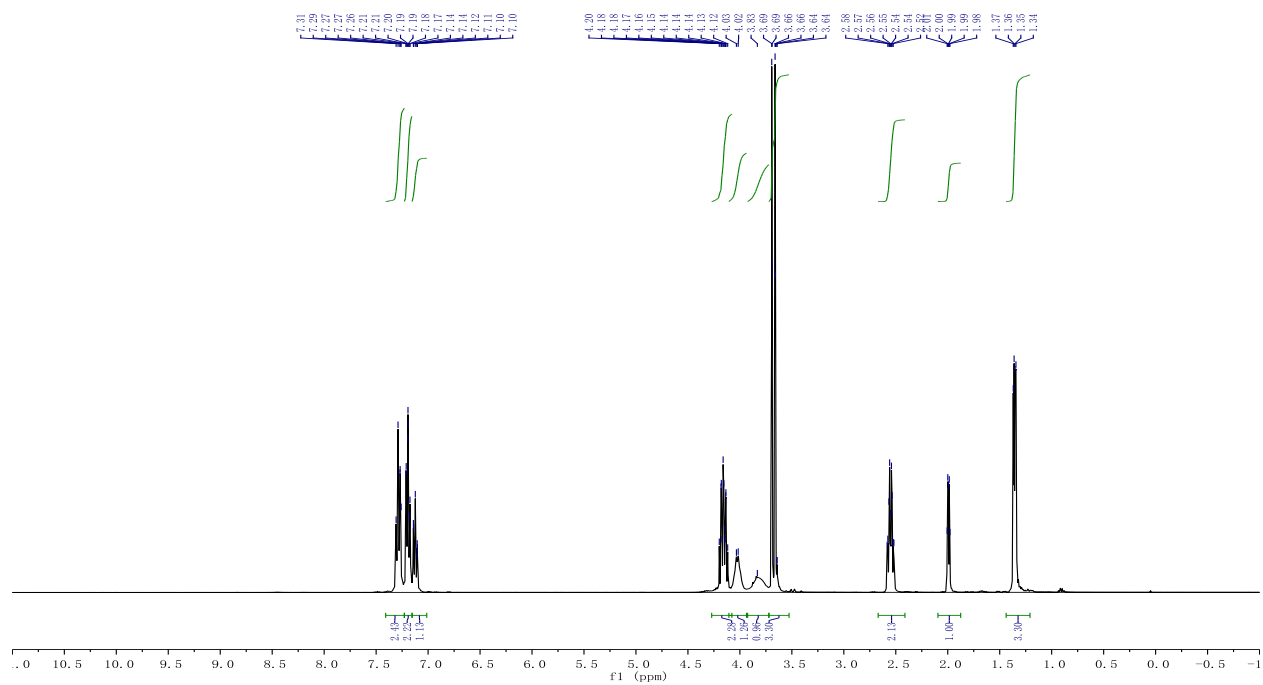
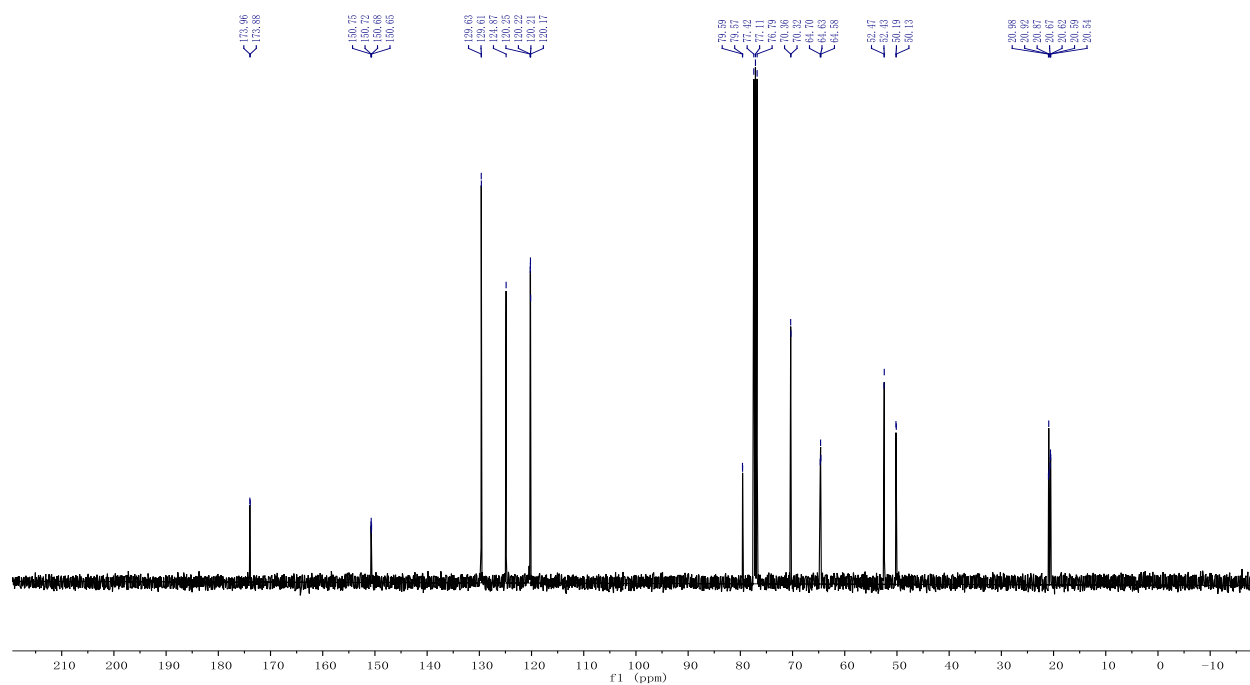
 $^1\text{H NMR}$  $^{13}\text{C NMR}$ 

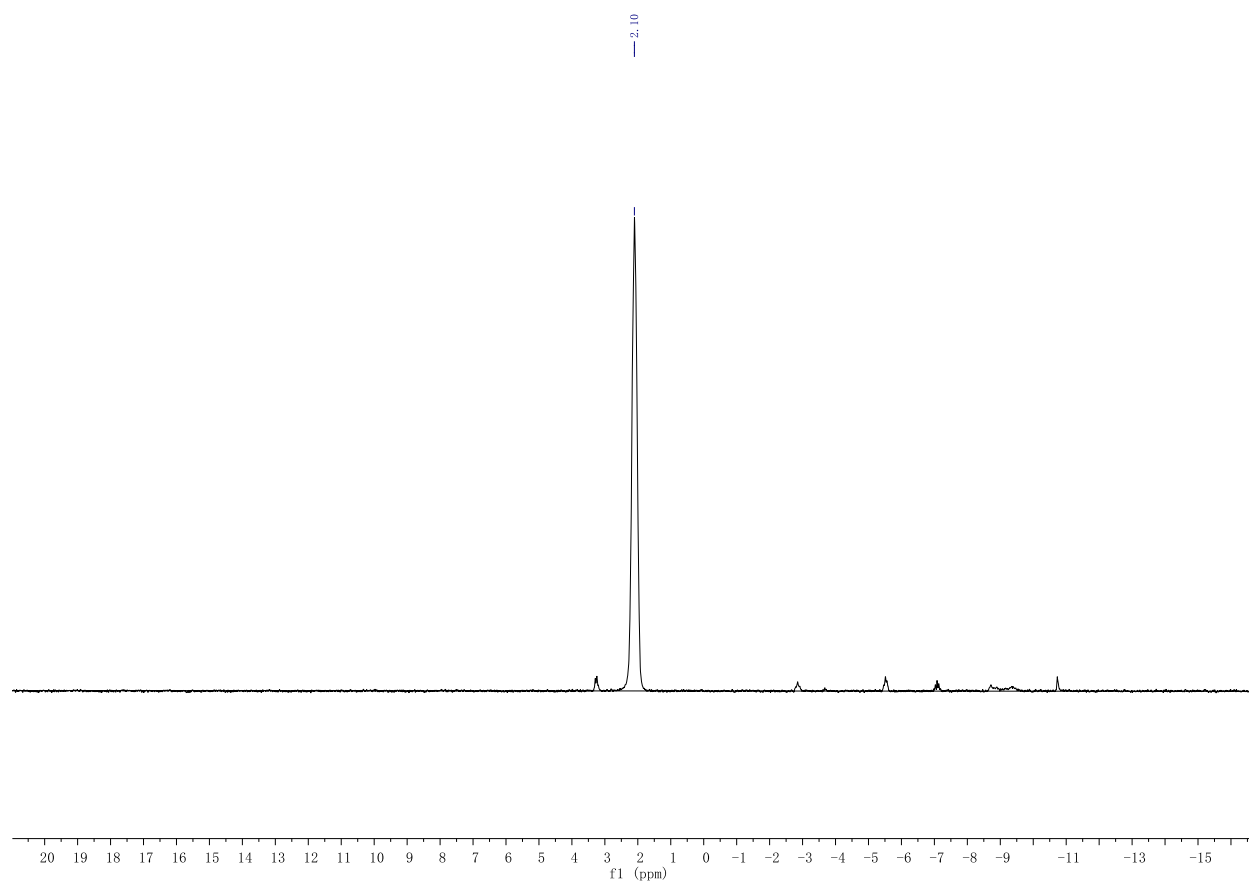
^{31}P NMR

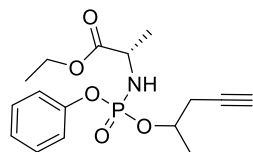
^{31}P NMR



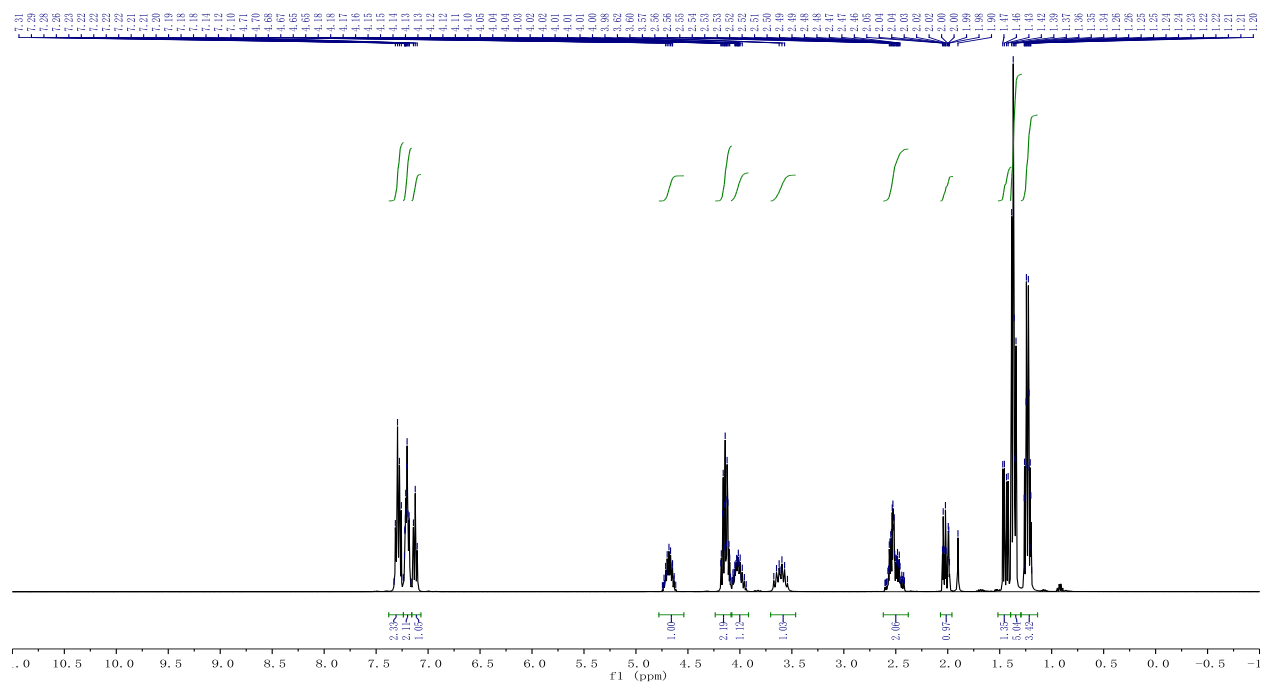
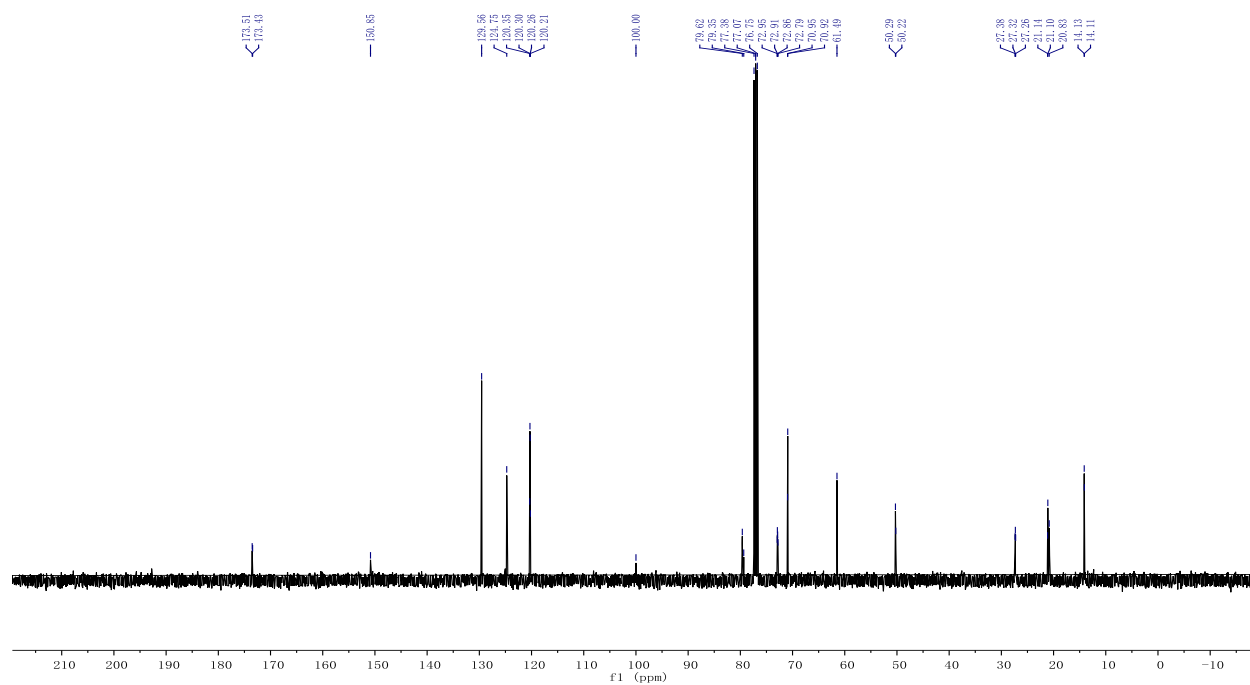
18

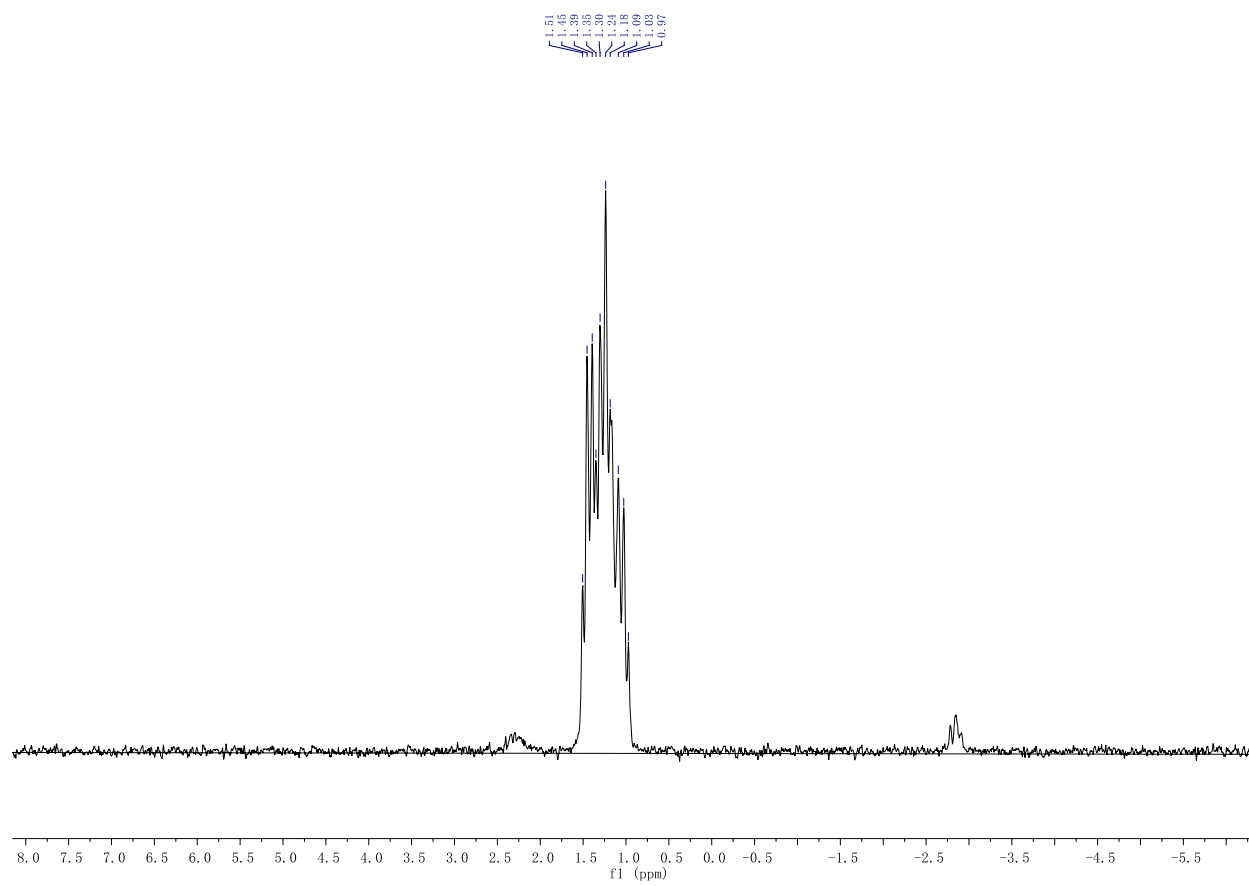
 ^1H NMR ^{13}C NMR

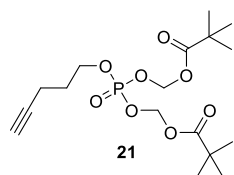
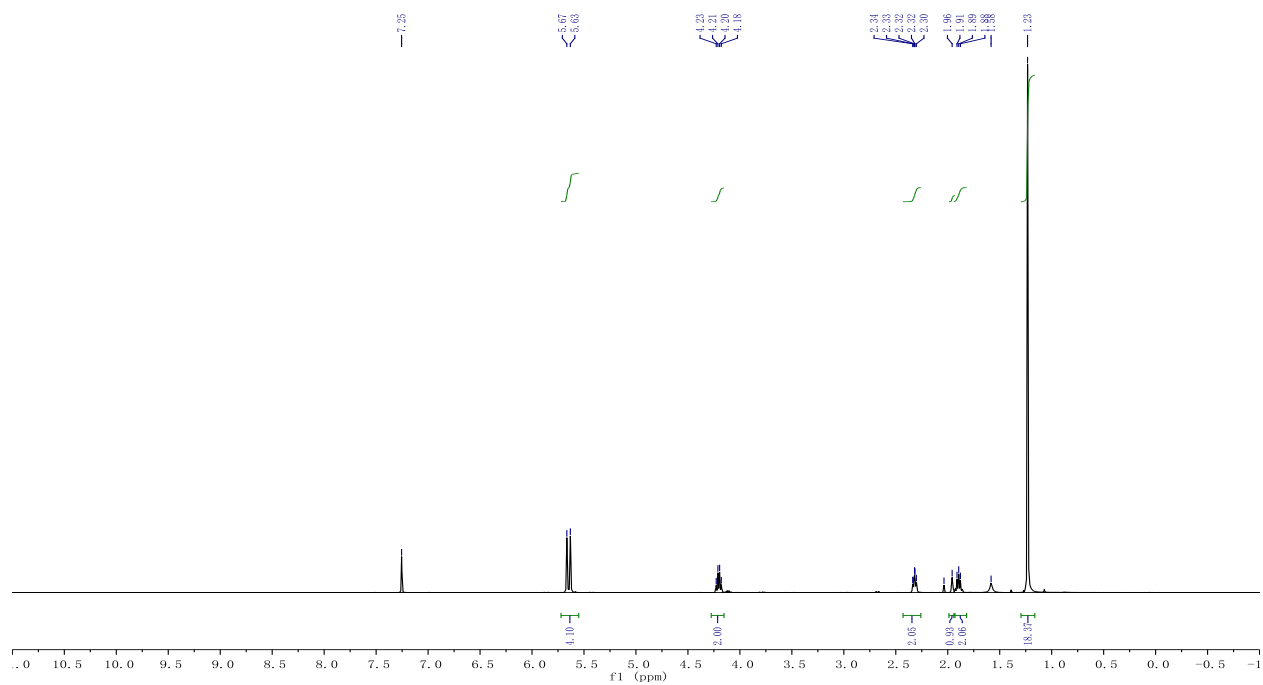
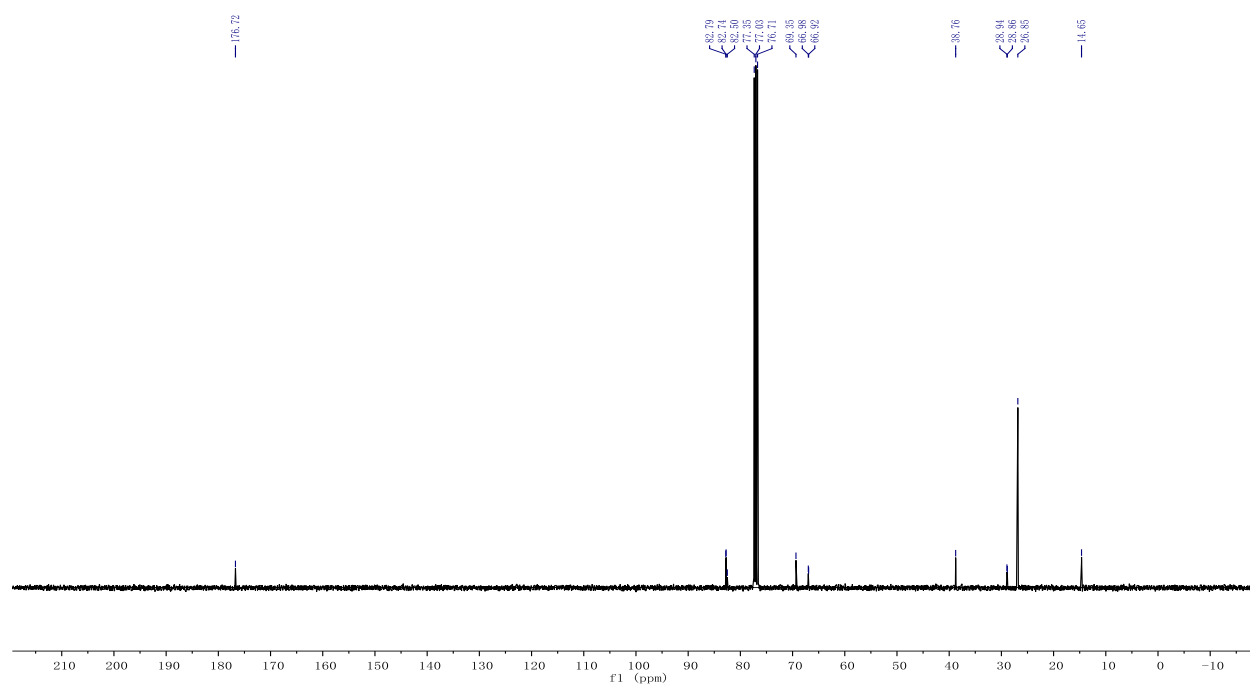
^{31}P NMR

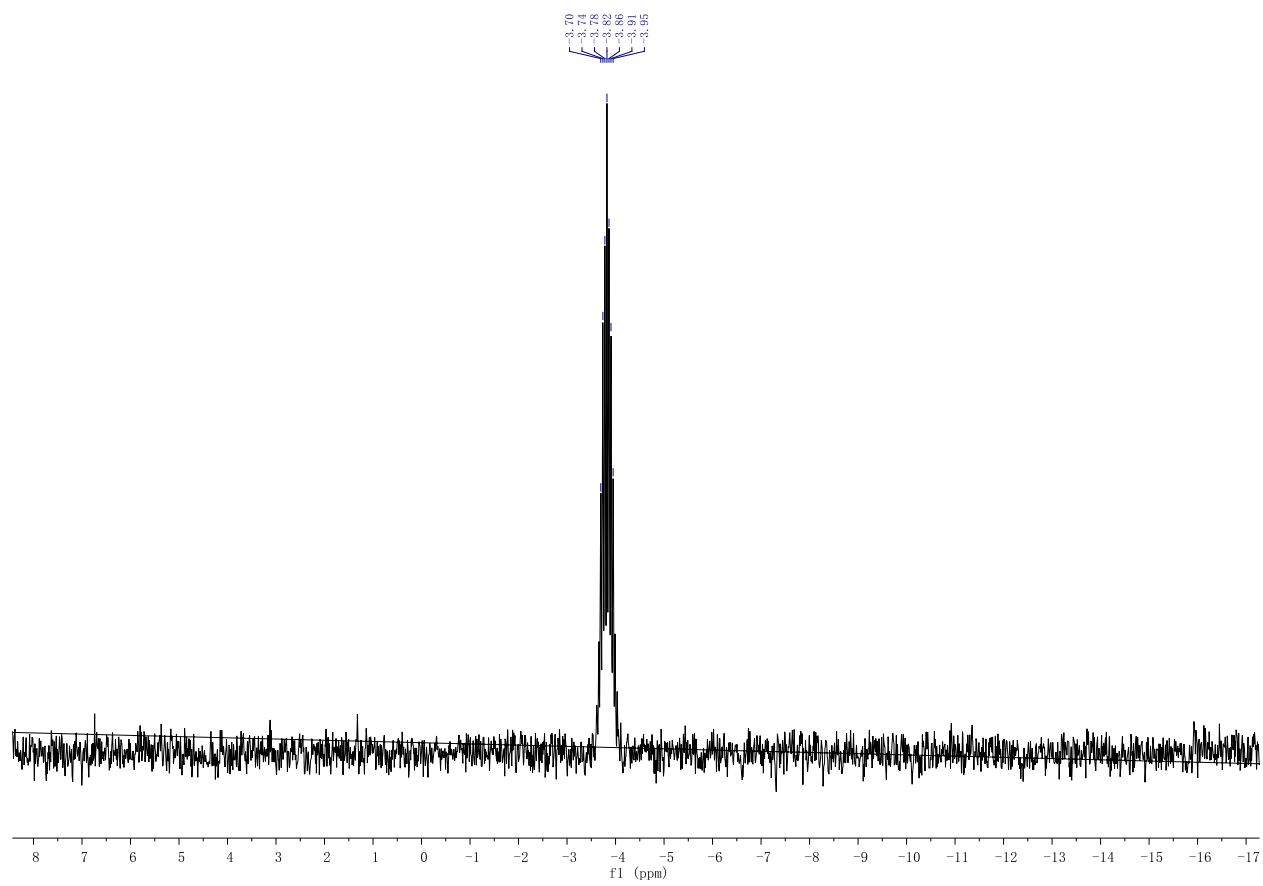


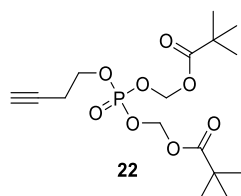
19

 ^1H NMR ^{13}C NMR

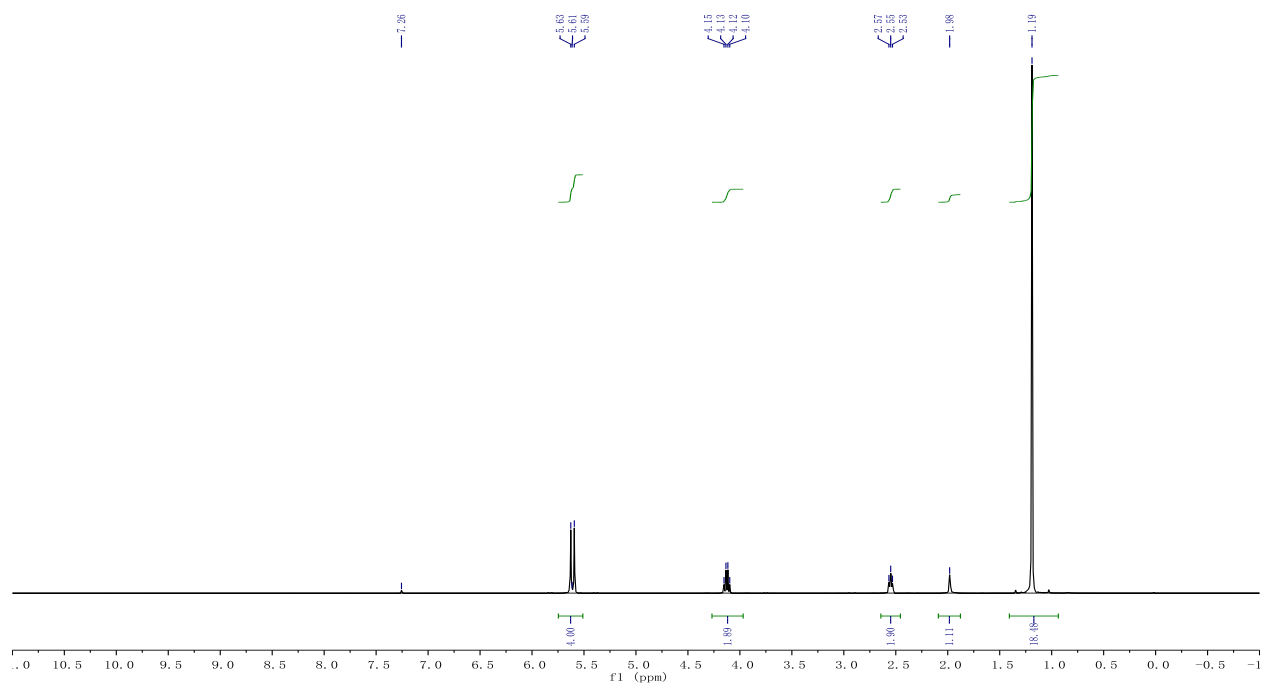
^{31}P NMR

¹H NMR¹³C NMR

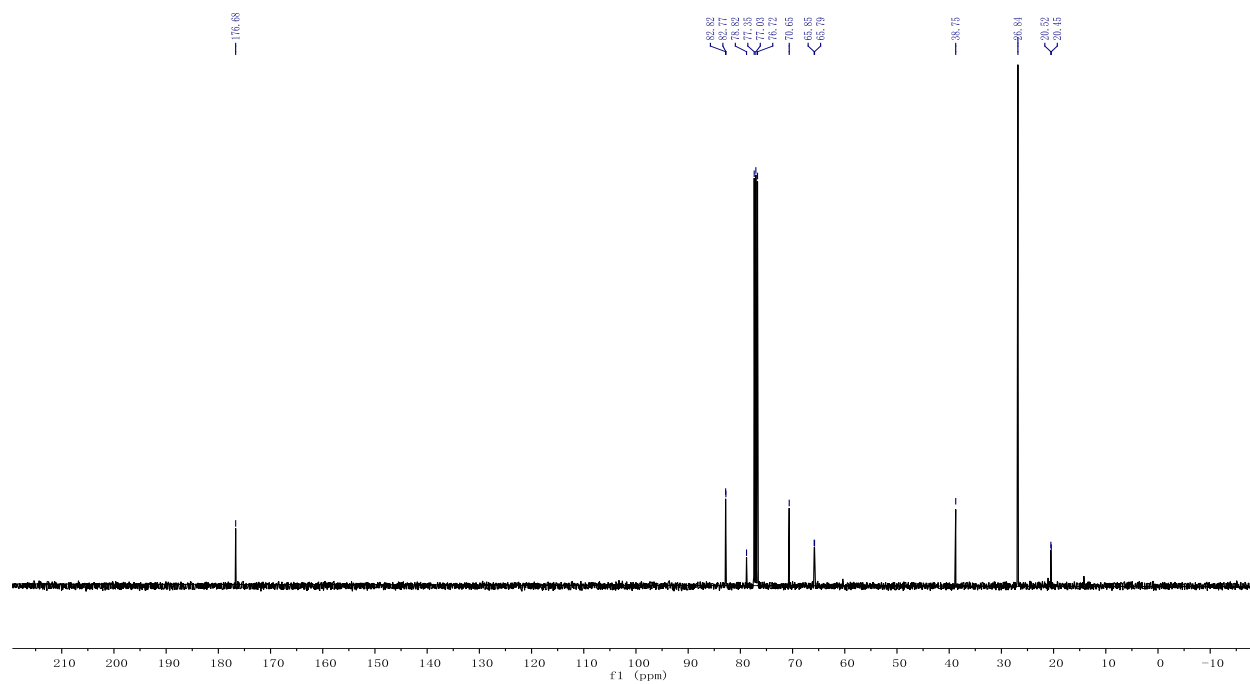
^{31}P NMR

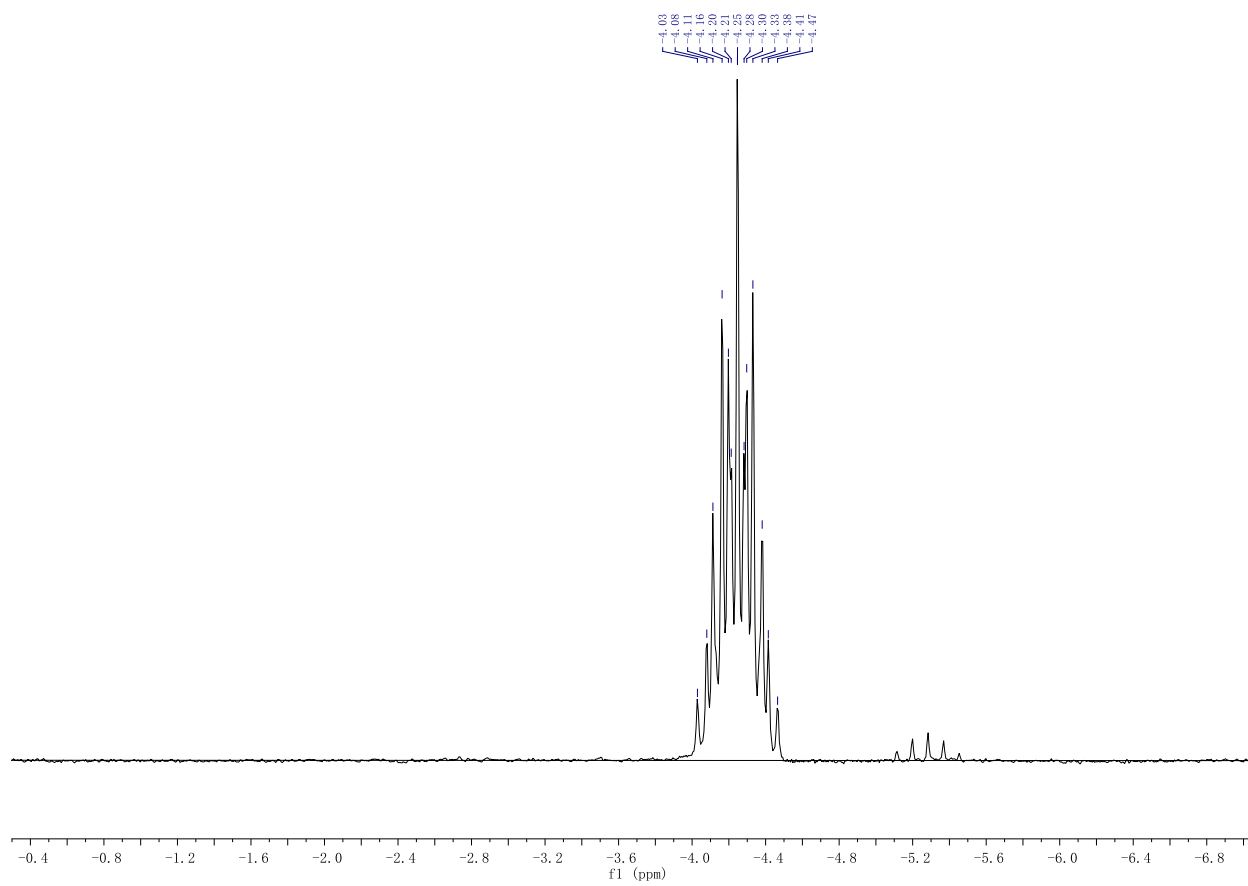


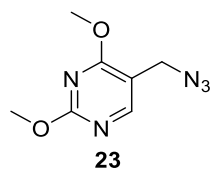
^1H NMR



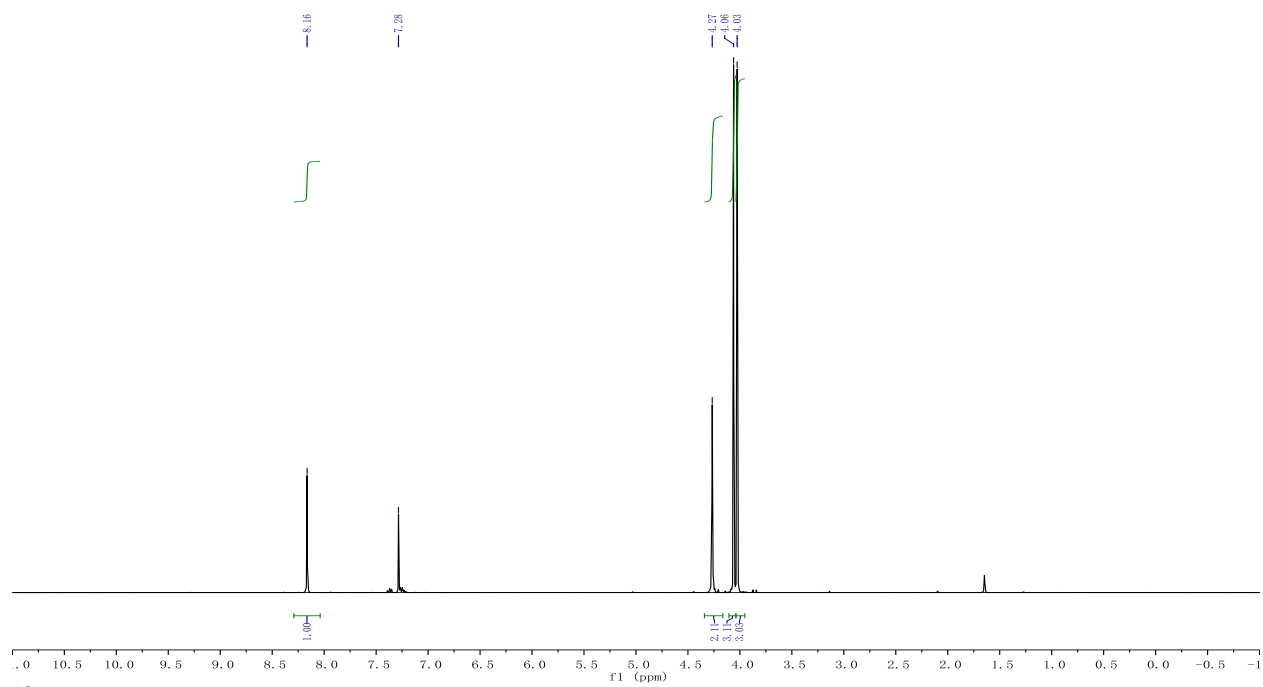
^{13}C NMR



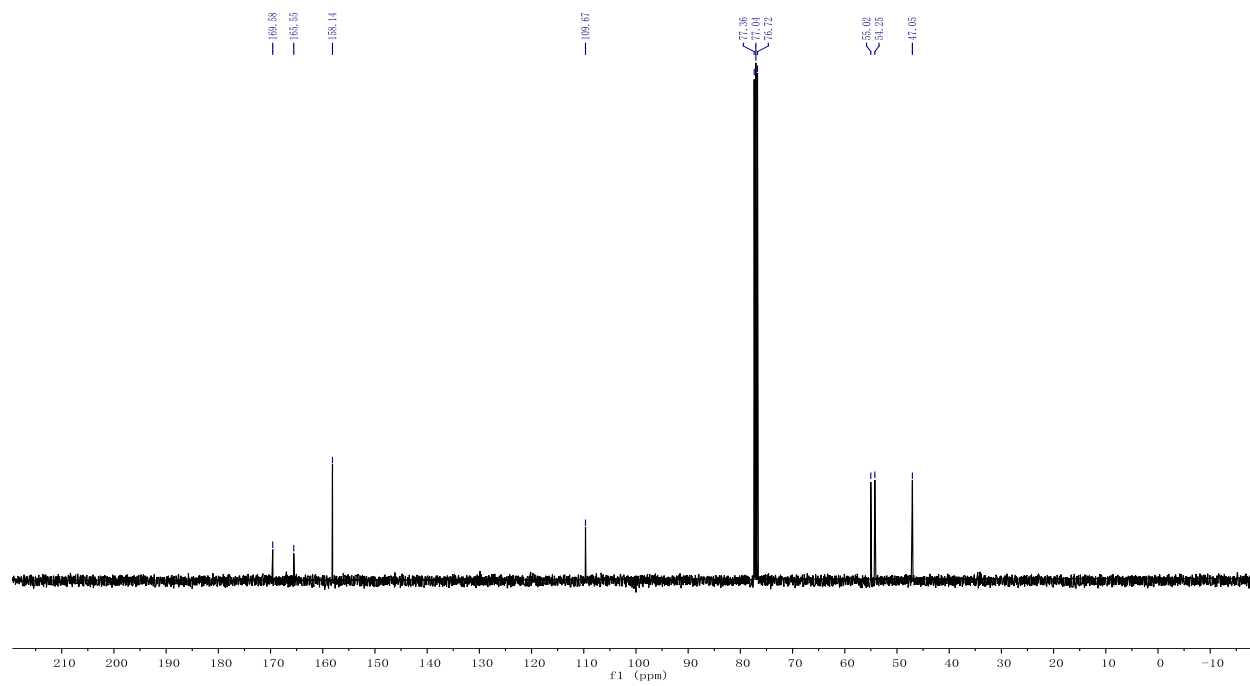
^{31}P NMR

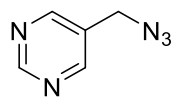
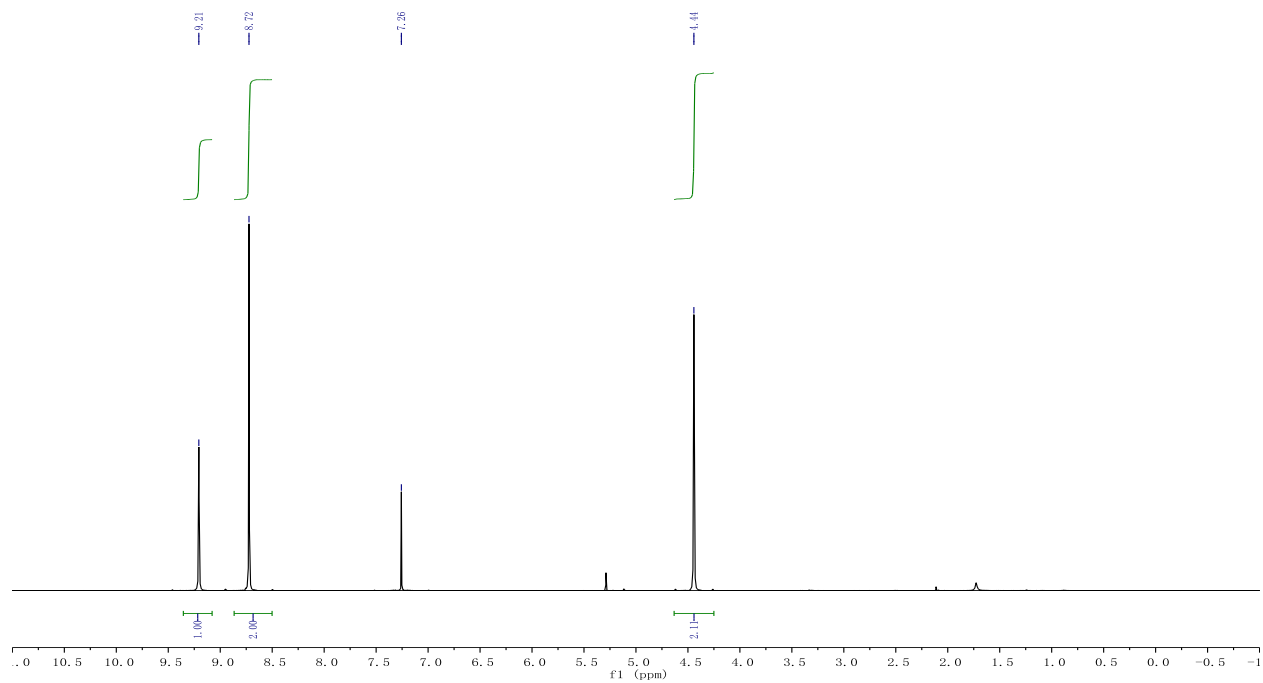
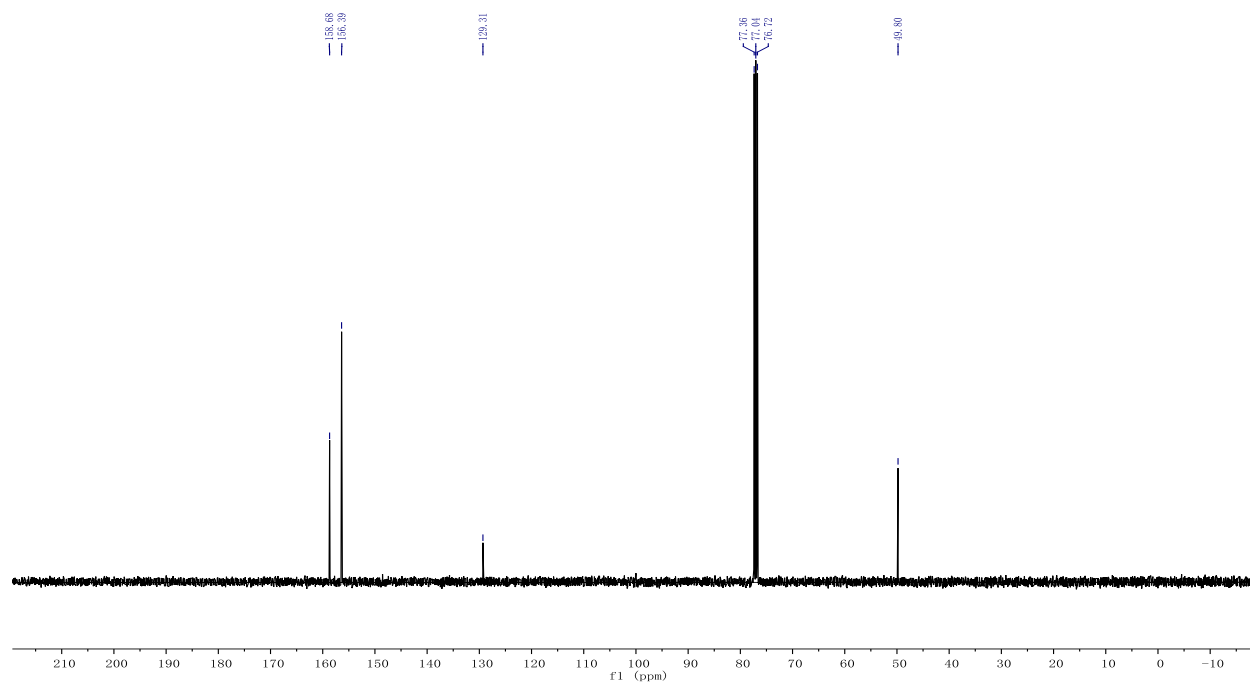


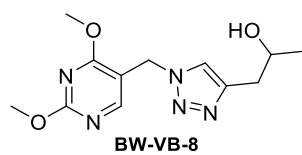
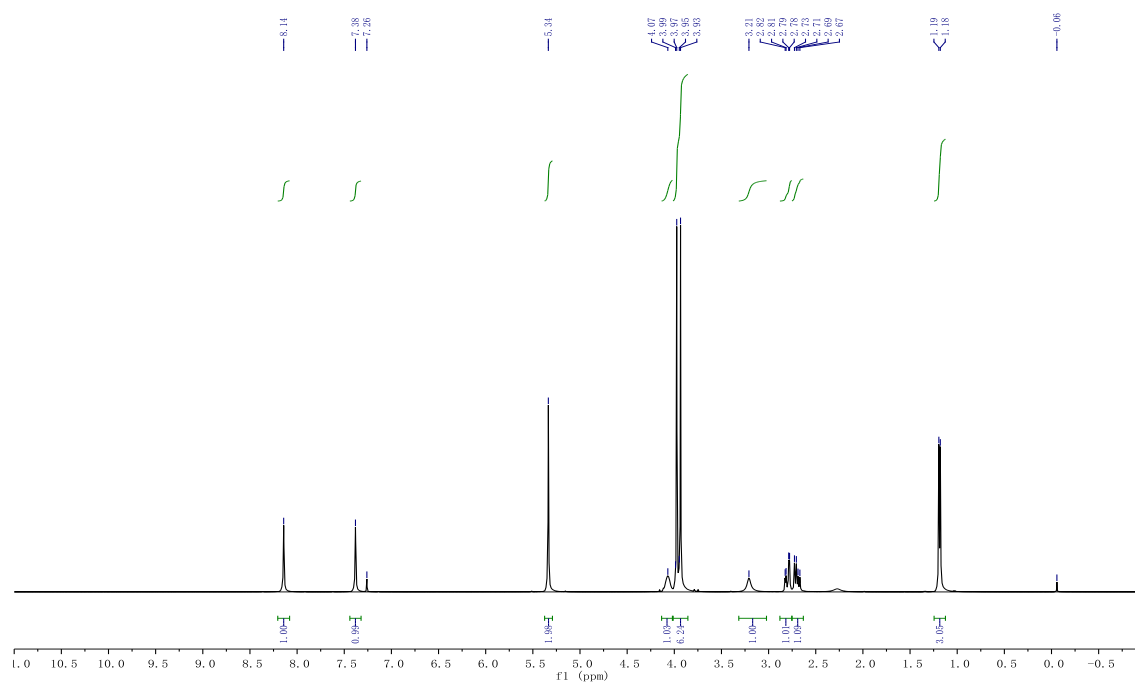
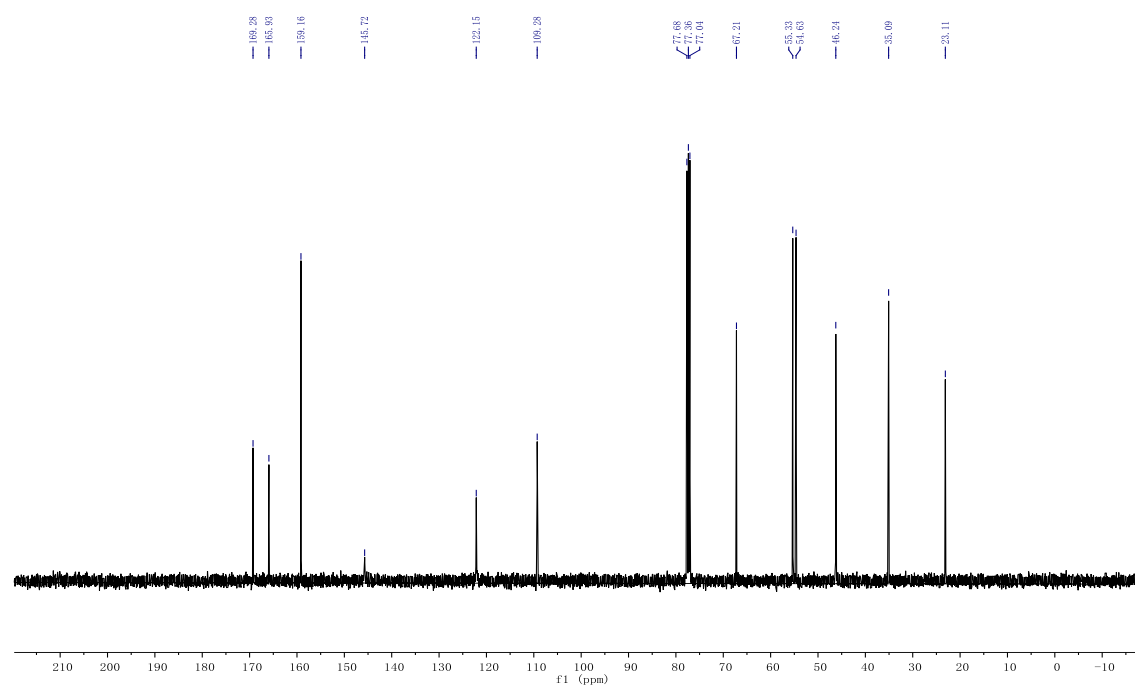
^1H NMR

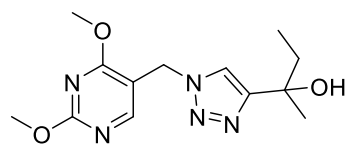


^{13}C NMR

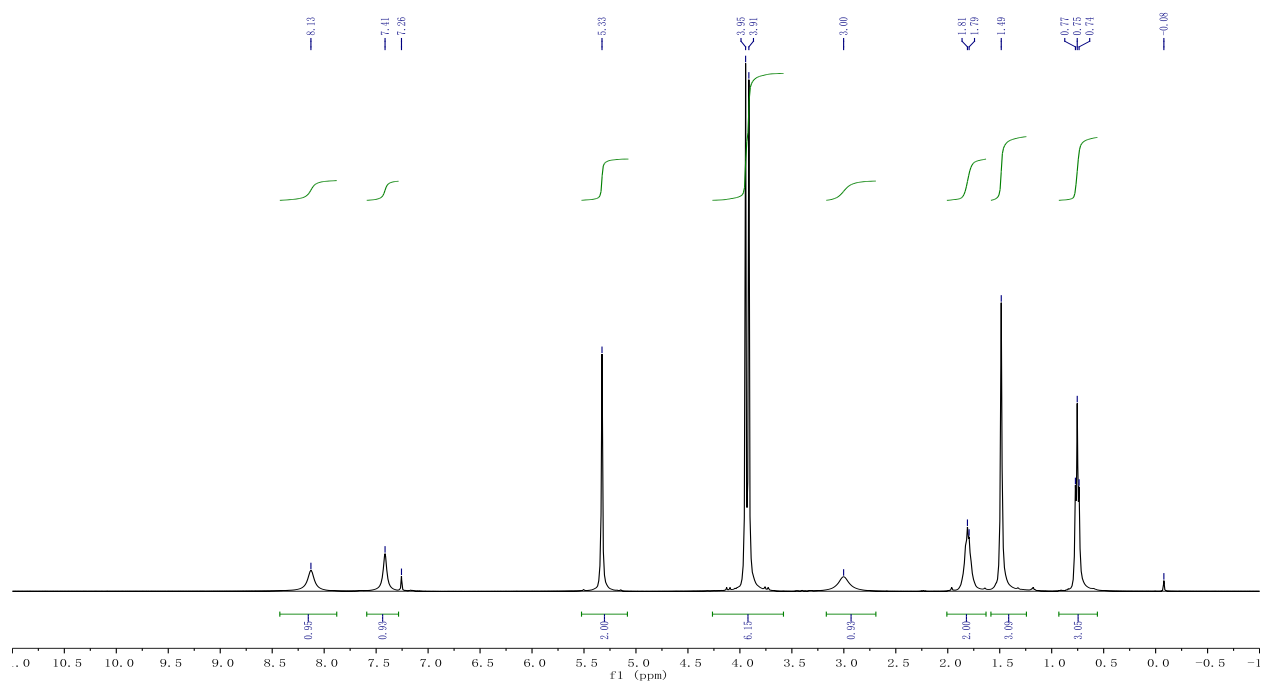
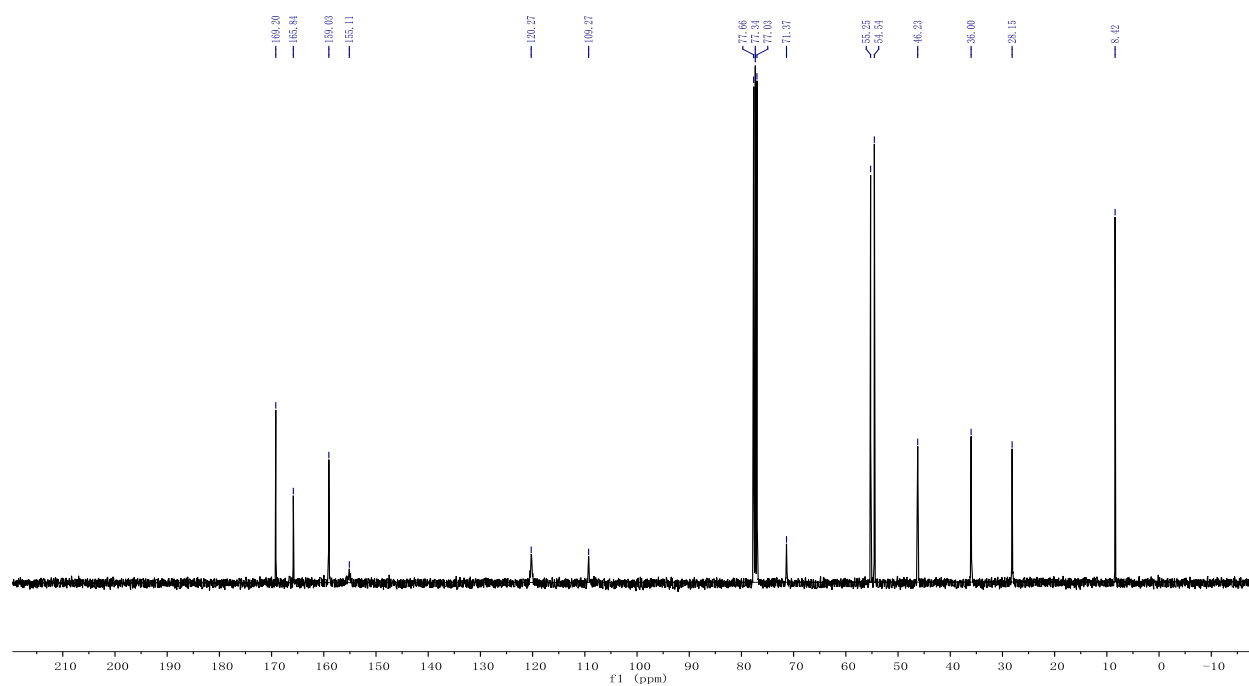


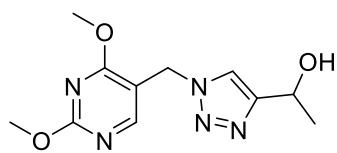
**25**¹H NMR¹³C NMR

¹H NMR¹³C NMR

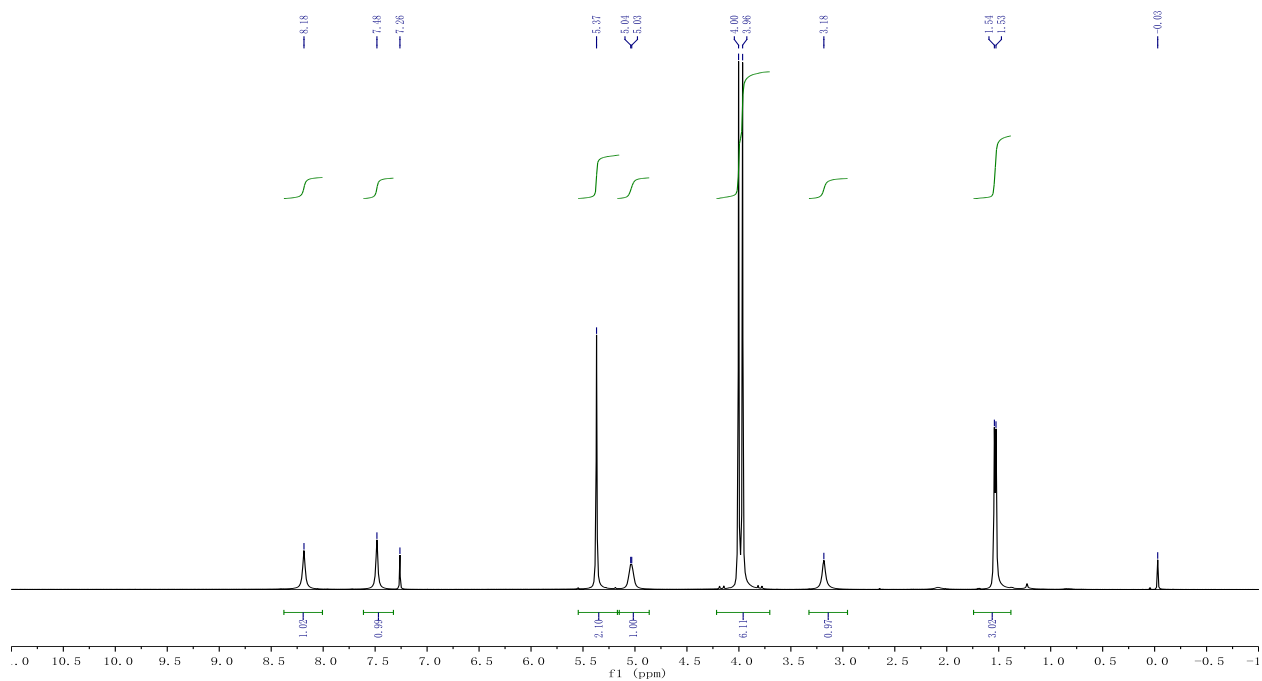
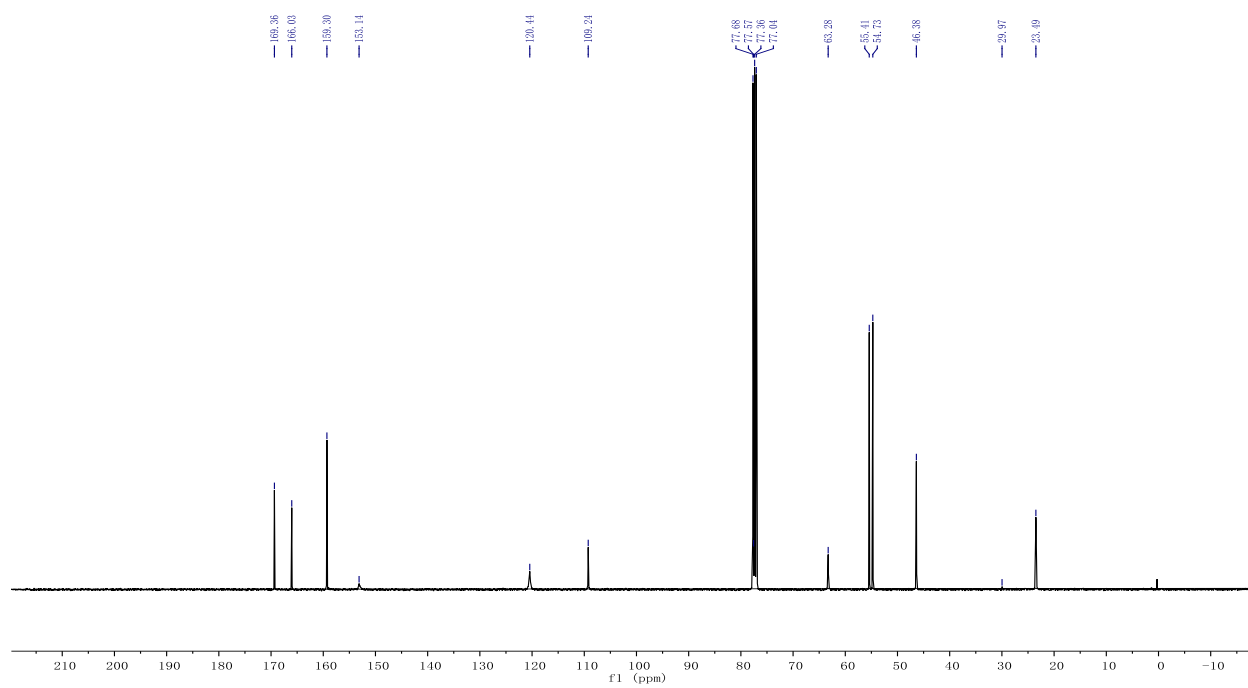


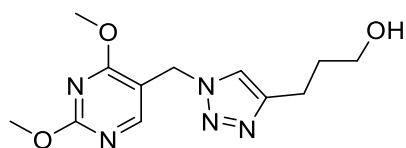
BW-VB-9

 ^1H NMR ^{13}C NMR

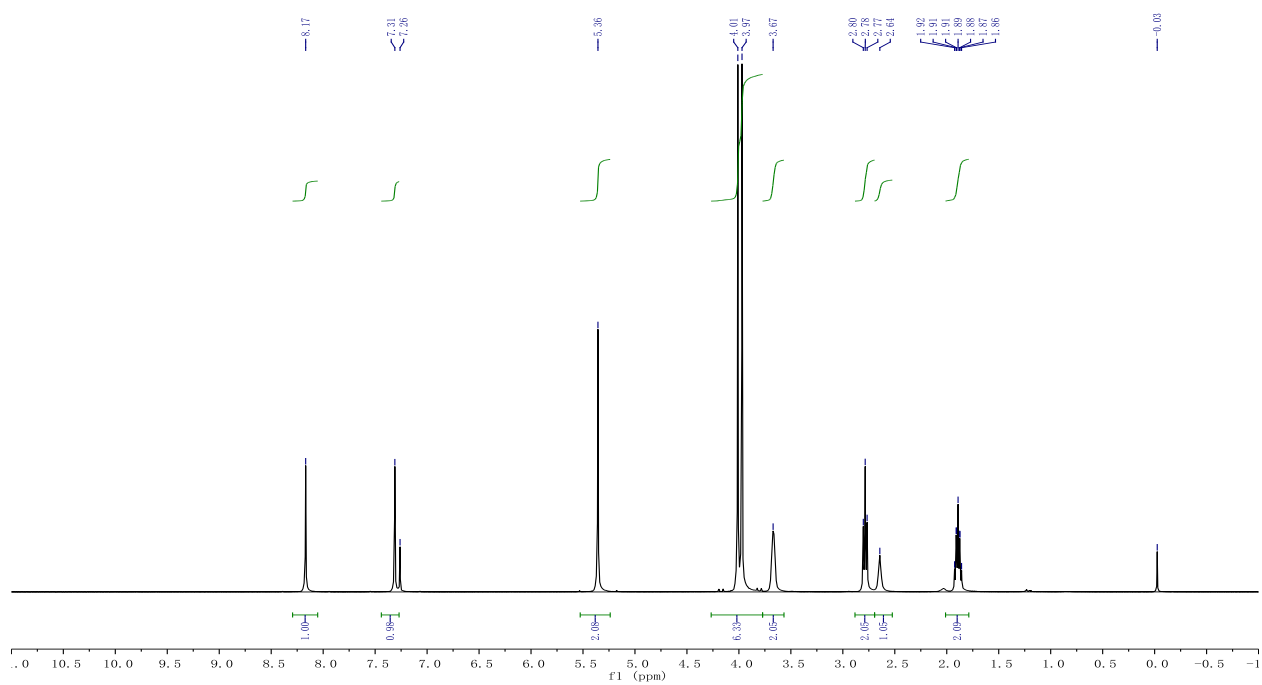
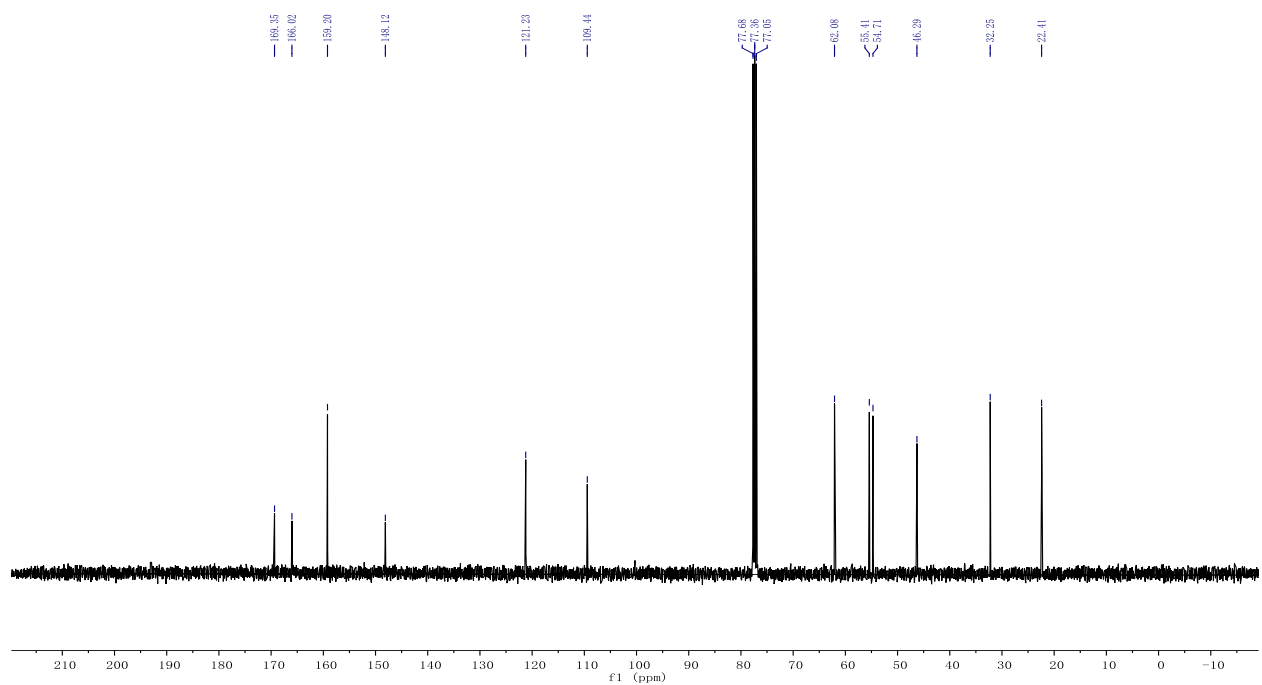


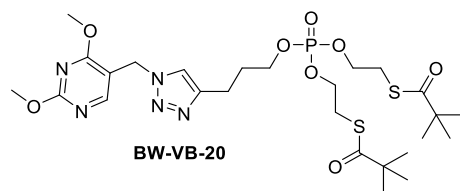
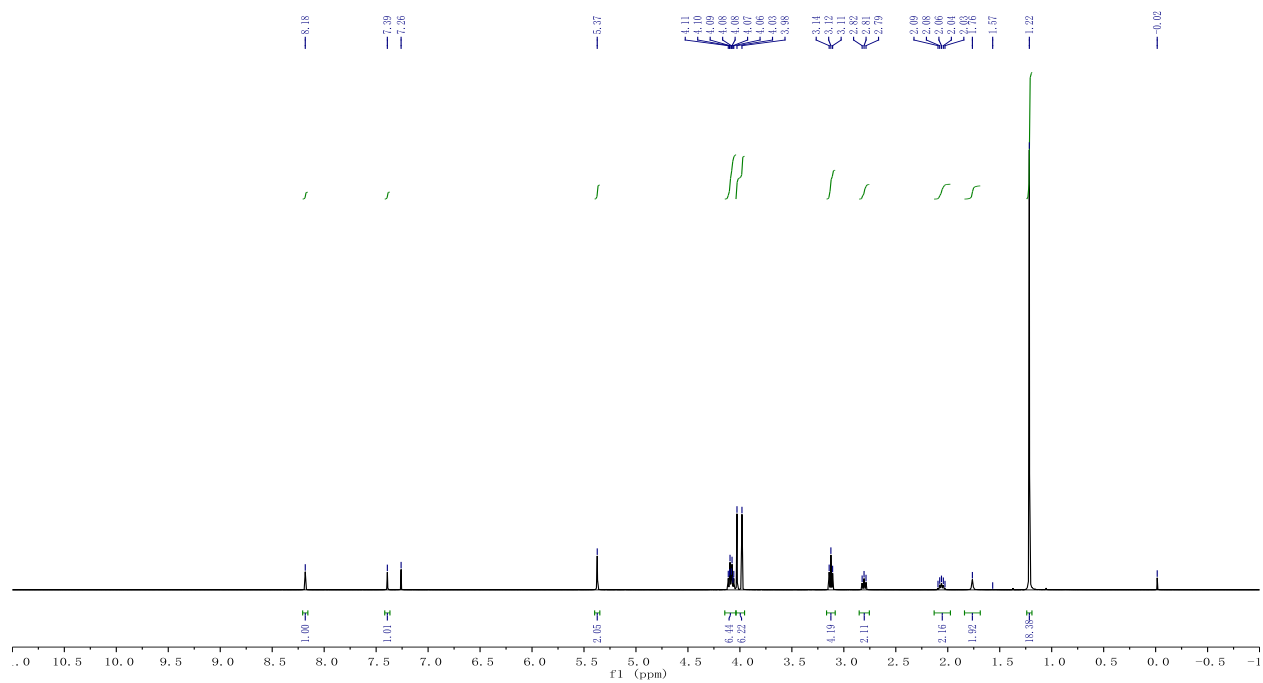
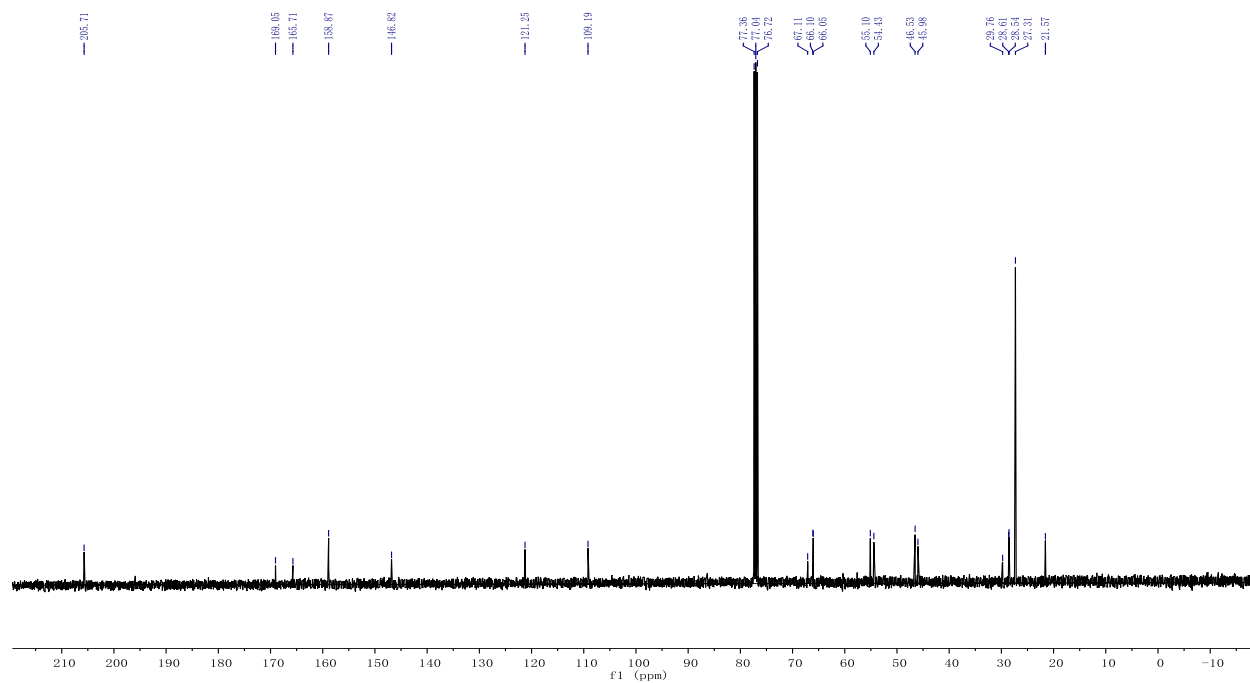
BW-VB-10

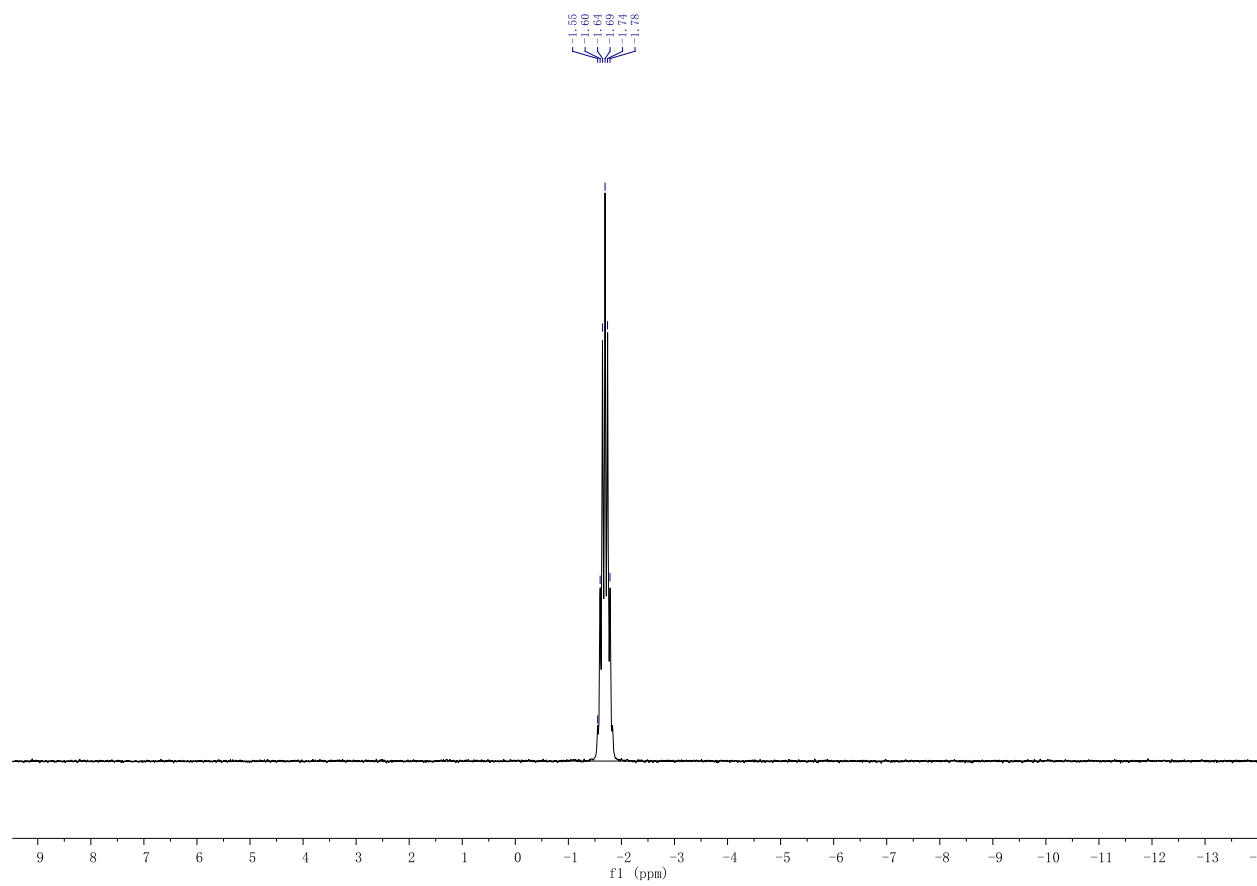
¹H NMR¹³C NMR

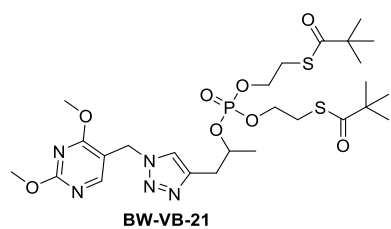
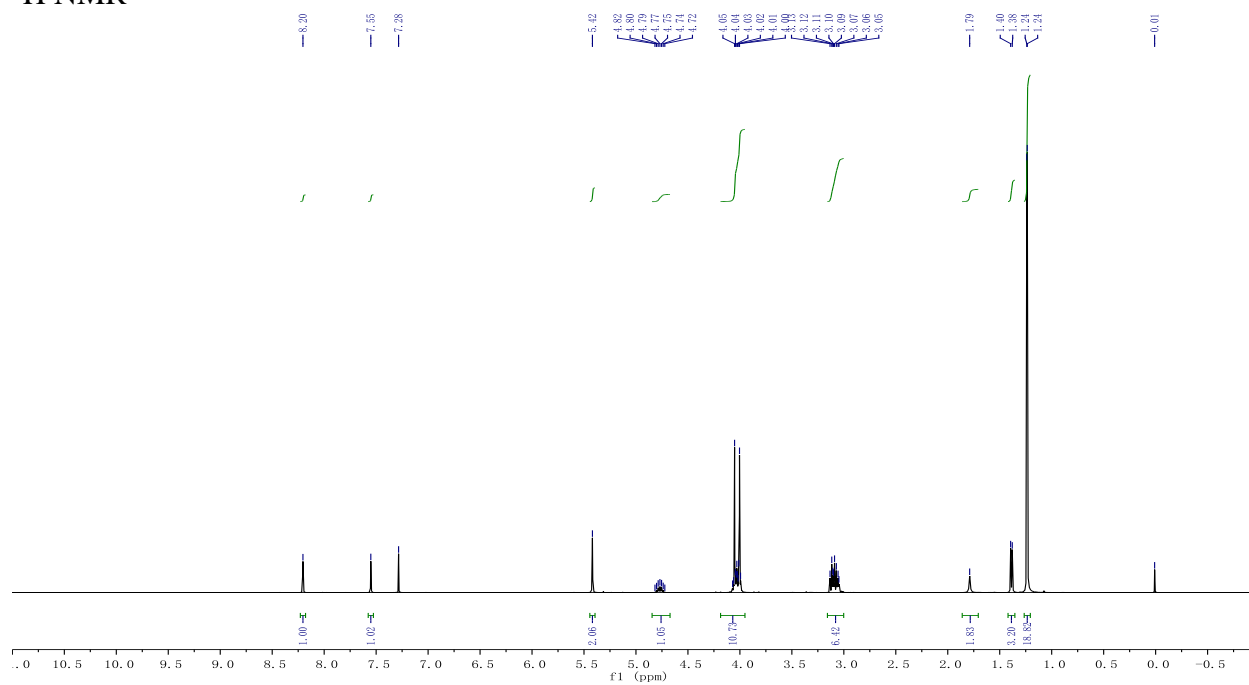
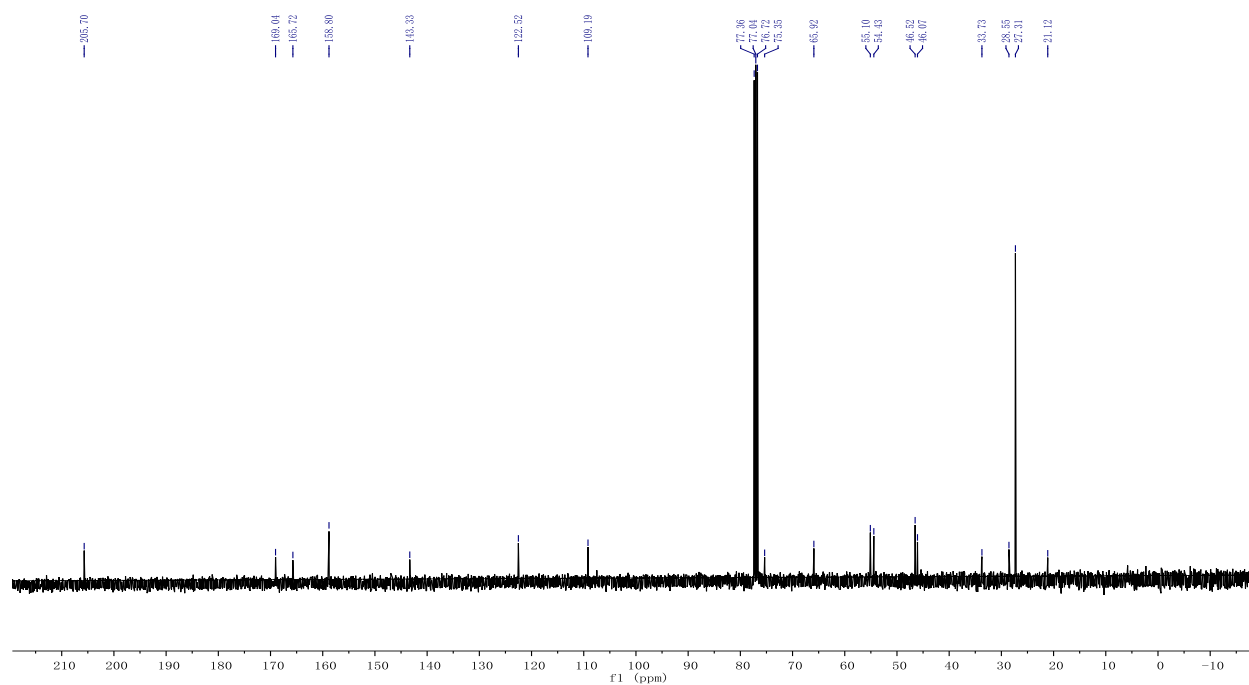


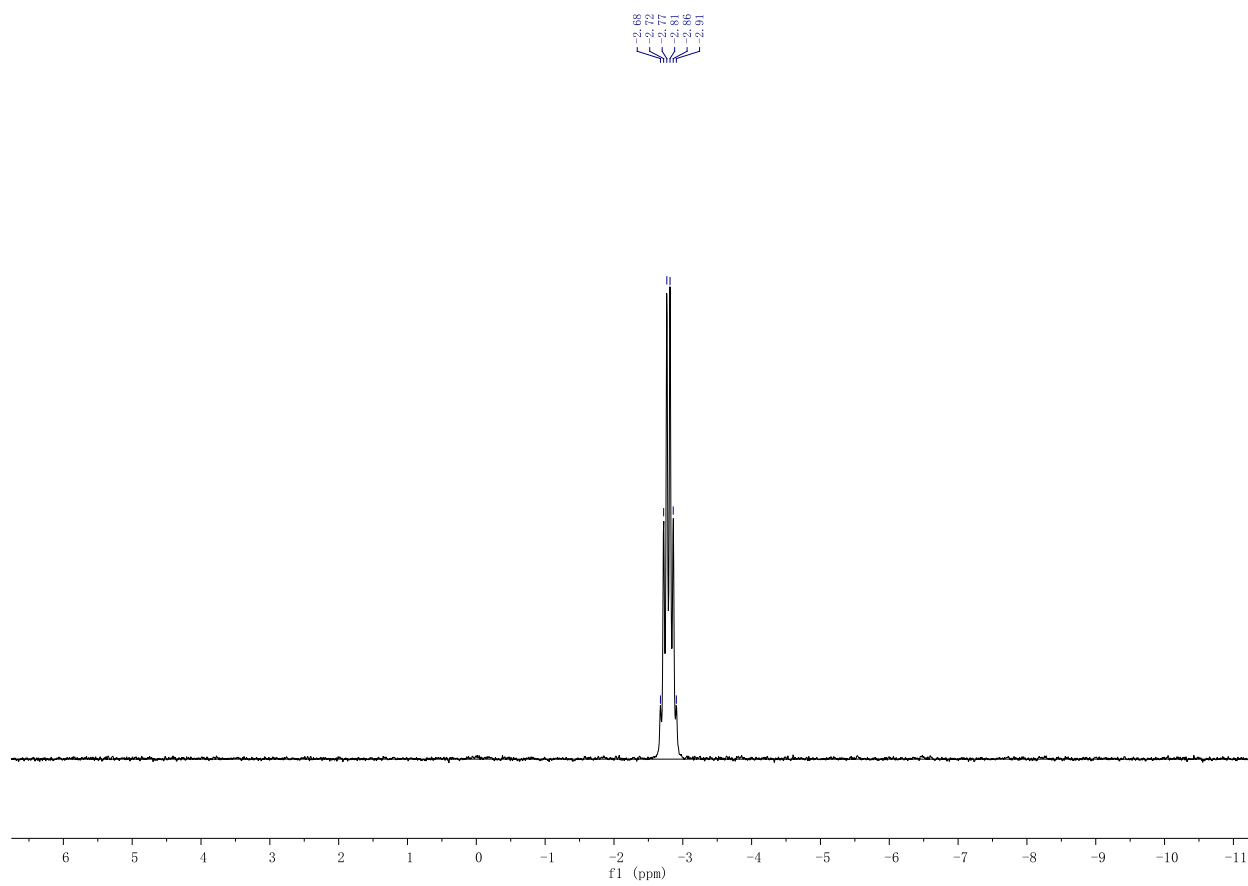
BW-VB-11

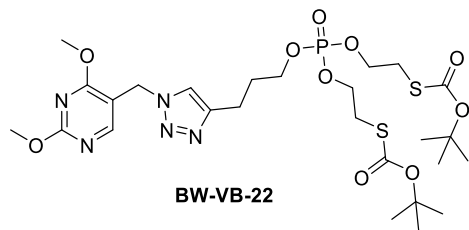
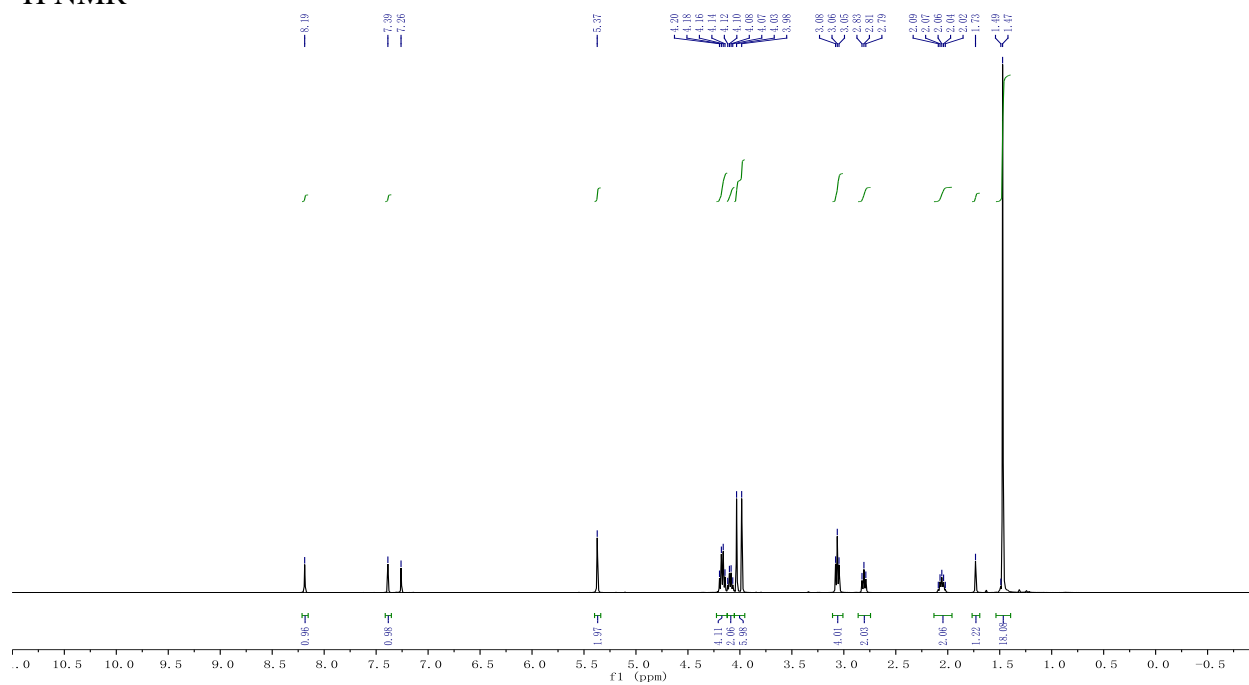
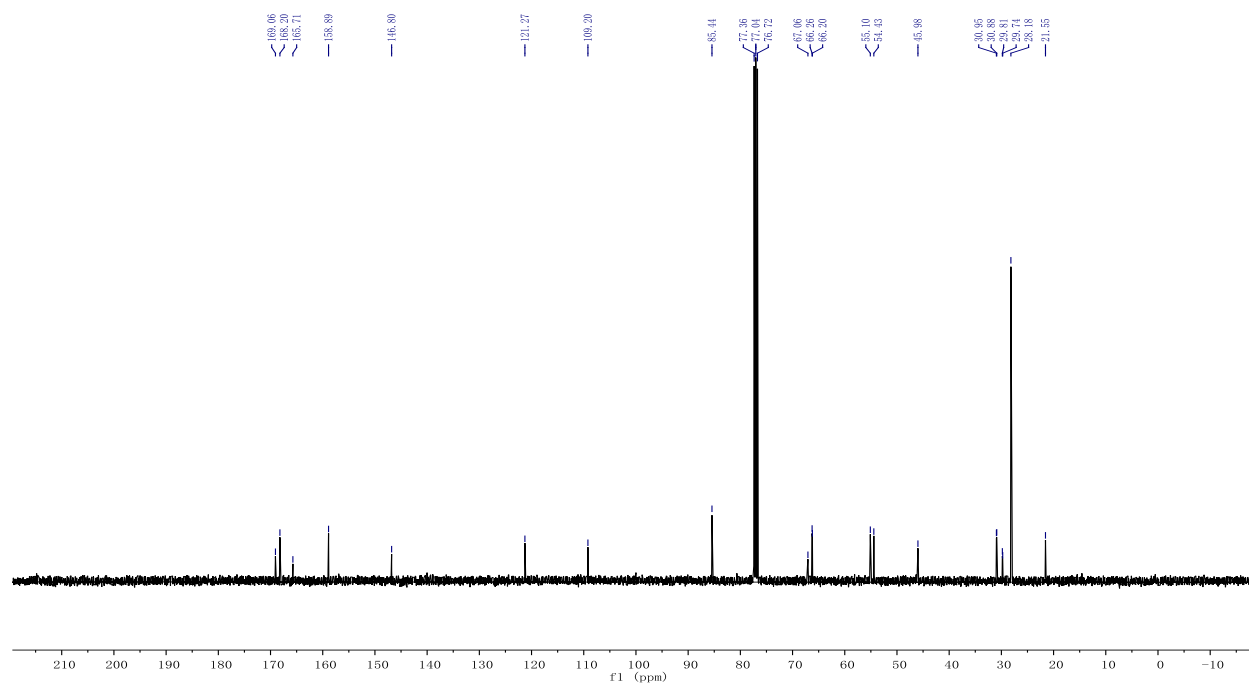
 ^1H NMR ^{13}C NMR

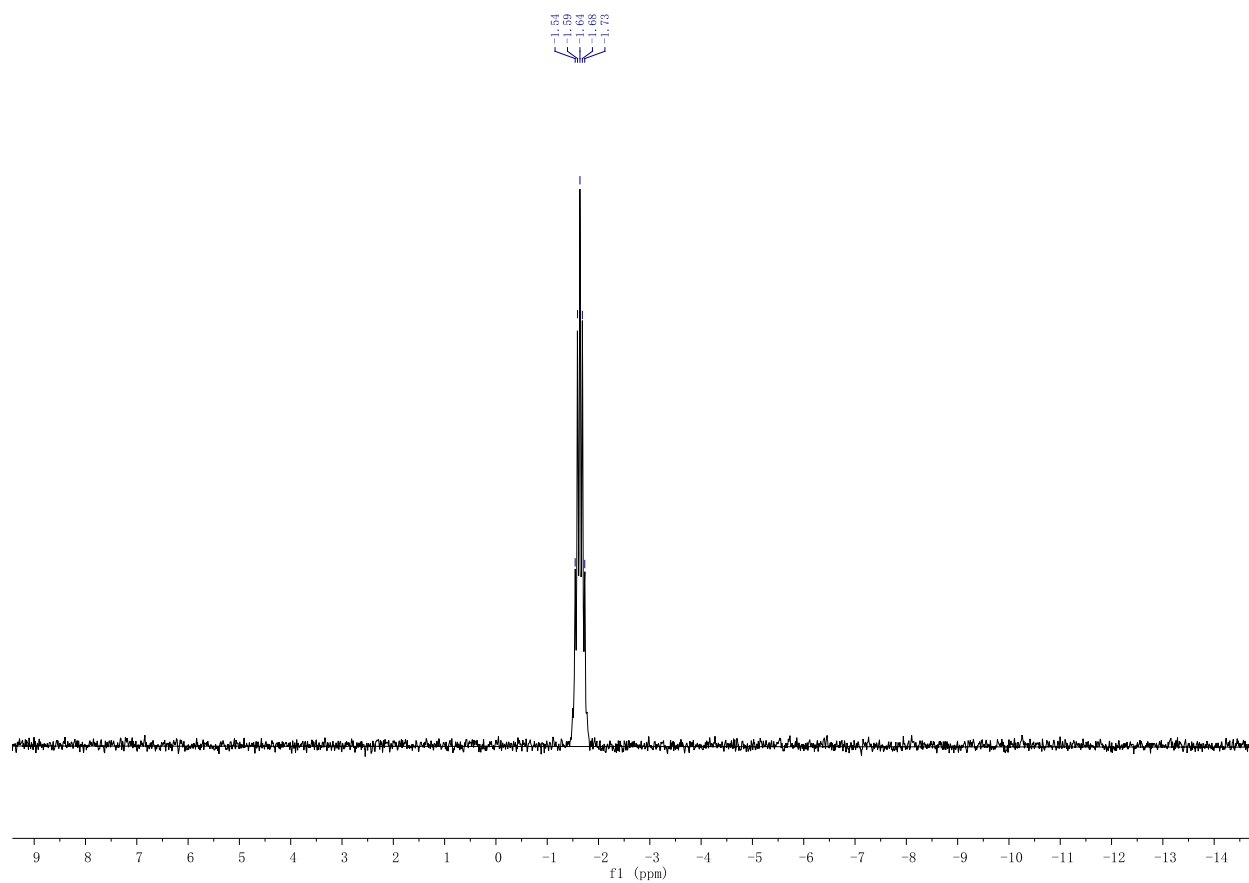
 ^1H NMR ^{13}C NMR

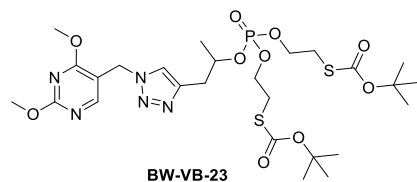
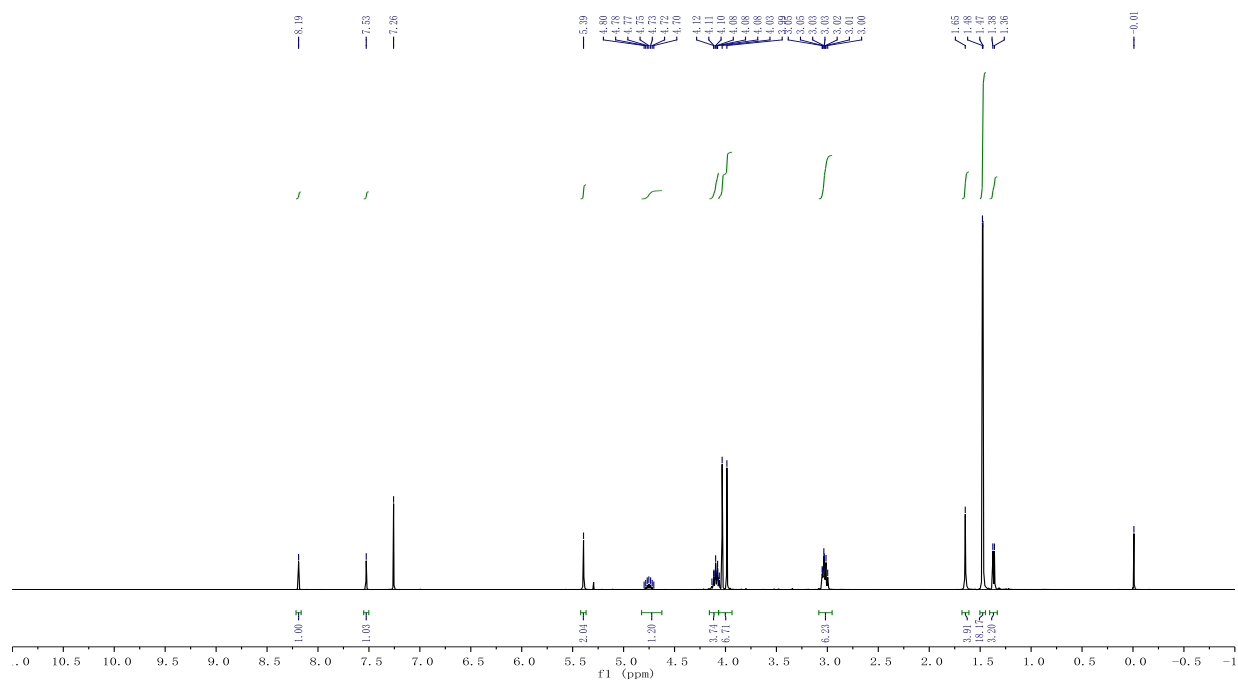
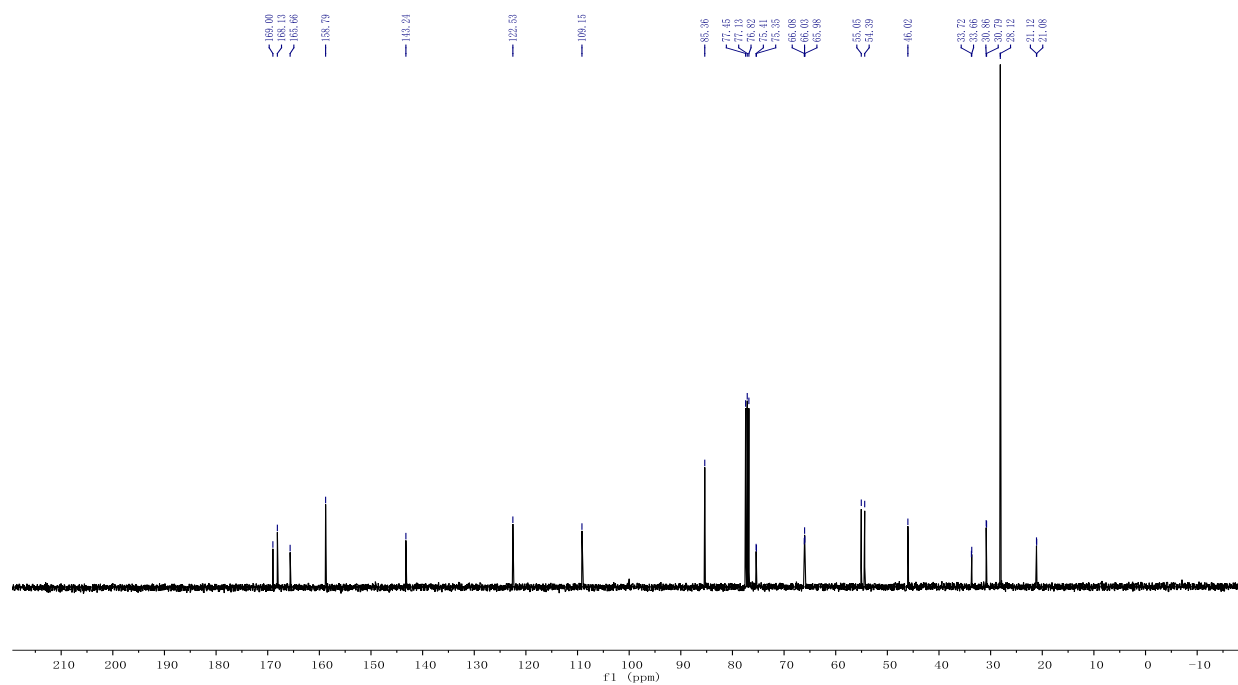
^{31}P NMR

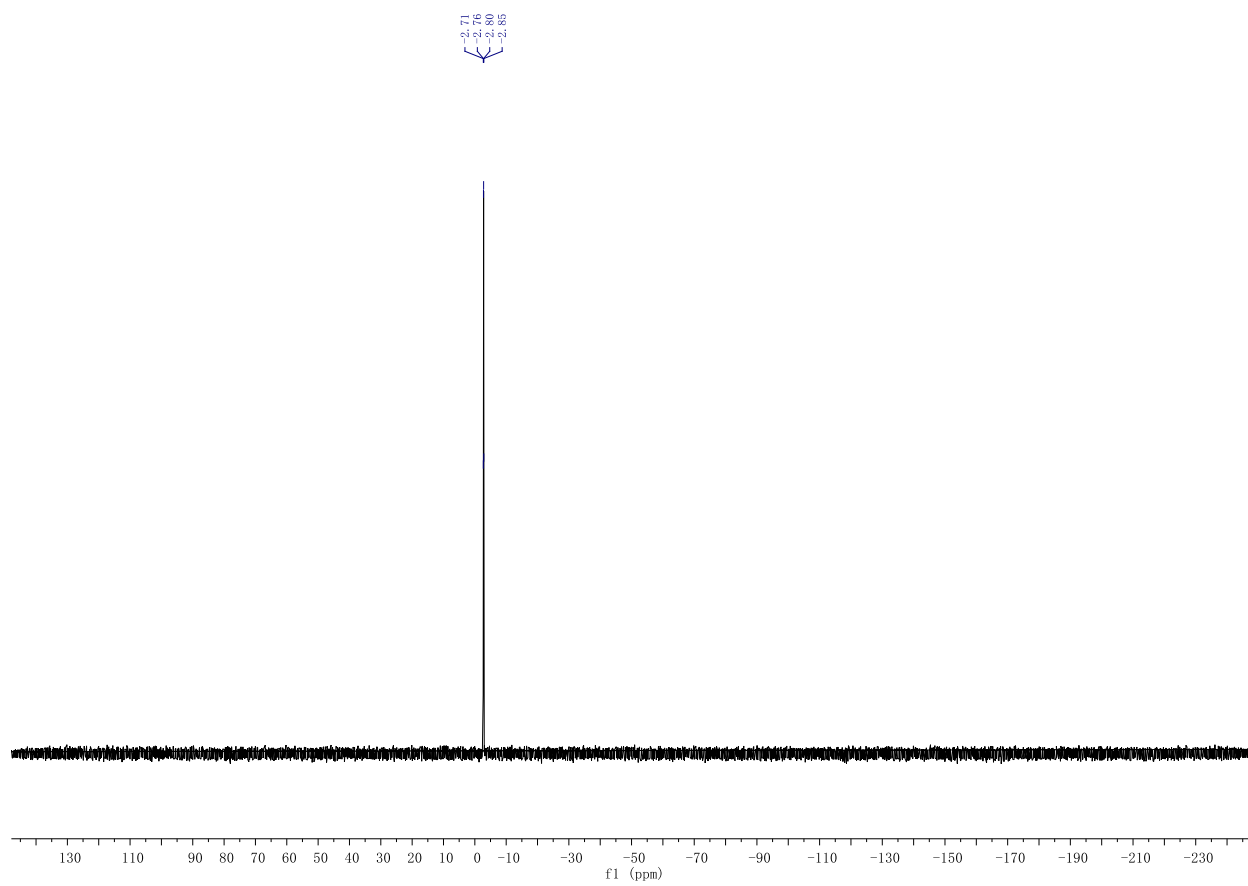
 ^1H NMR ^{13}C NMR

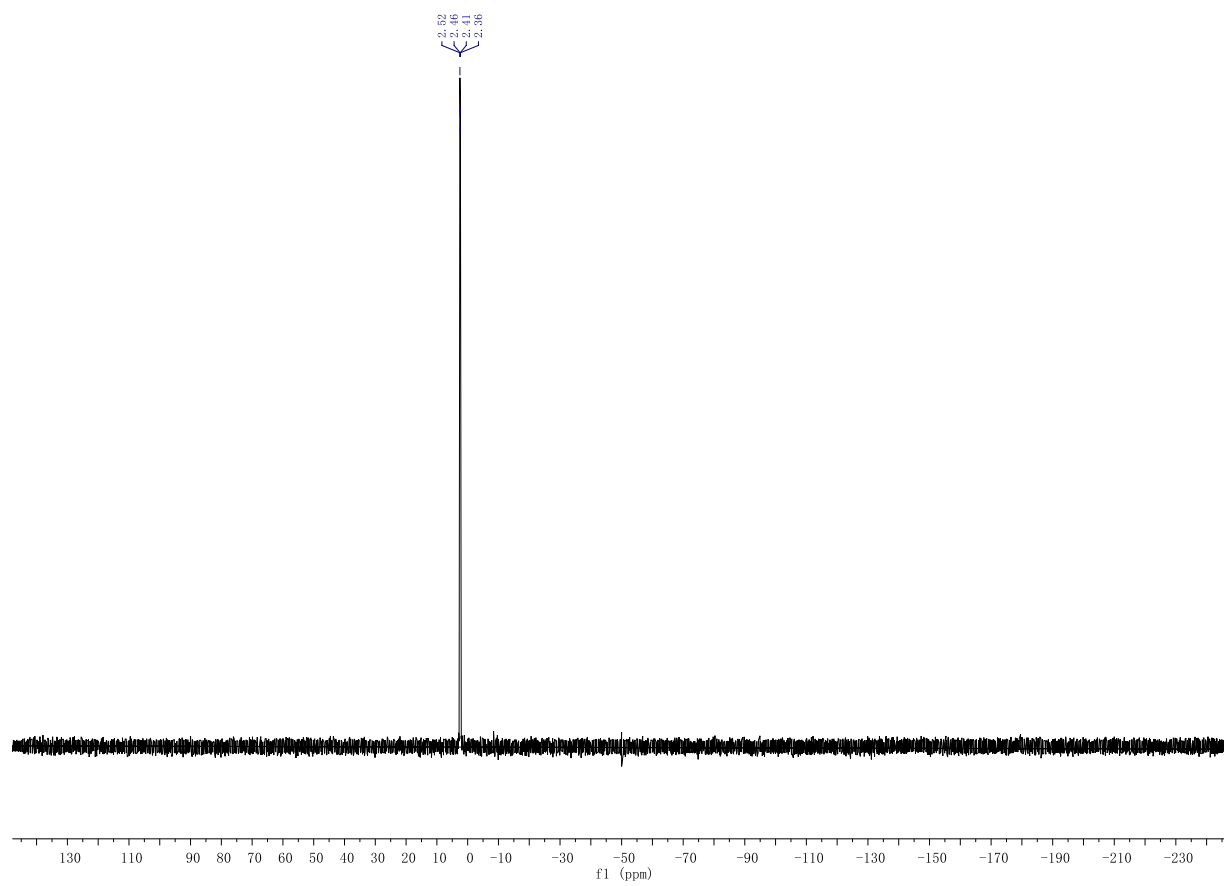
^{31}P NMR

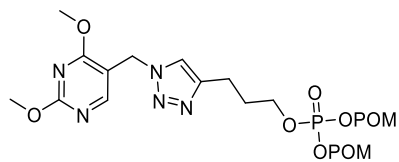
 $^1\text{H NMR}$  $^{13}\text{C NMR}$ 

^{31}P NMR

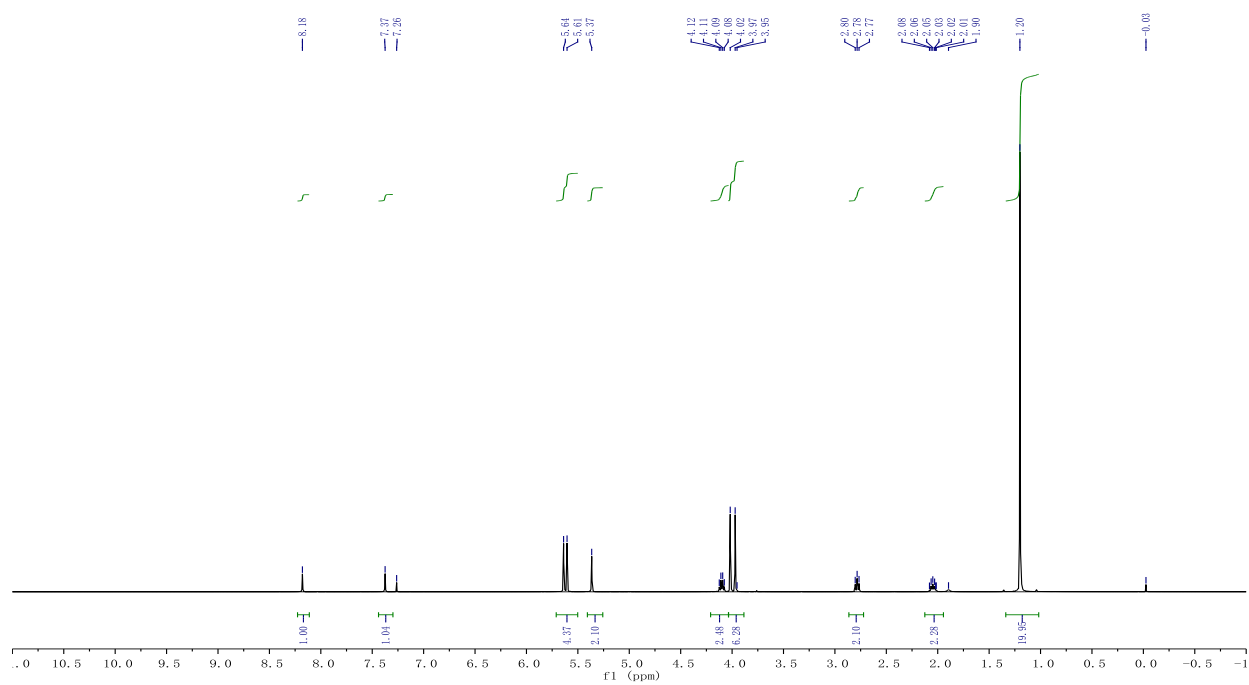
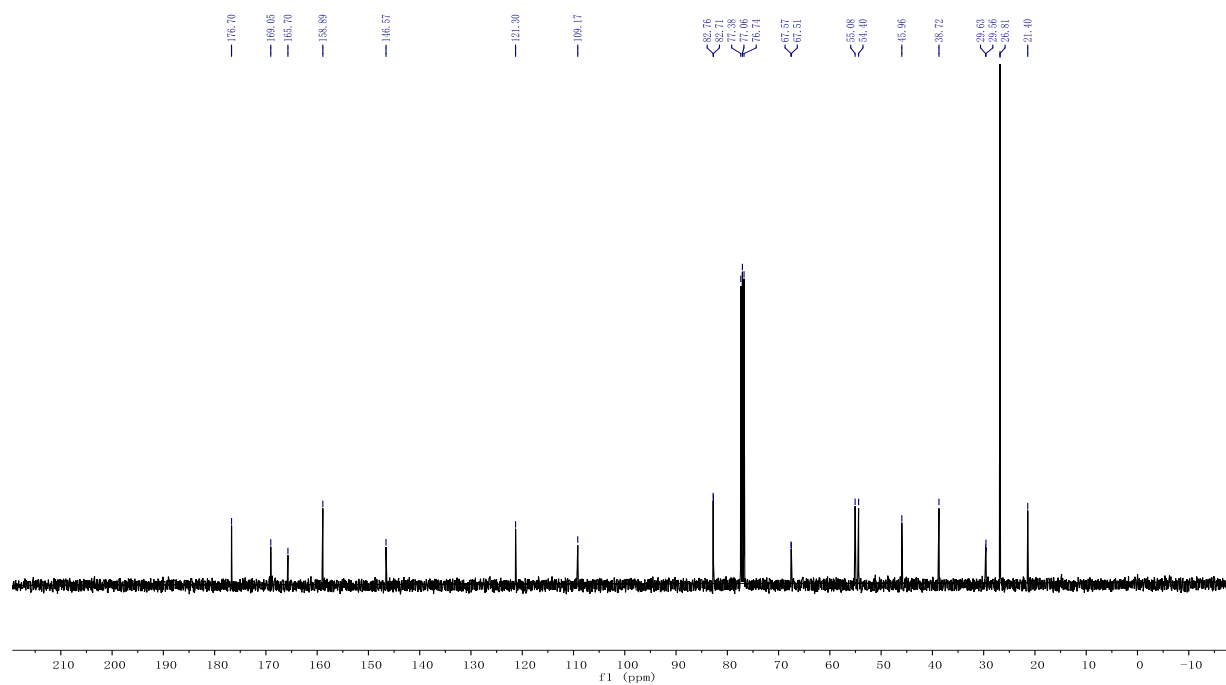
 ^1H NMR ^{13}C NMR

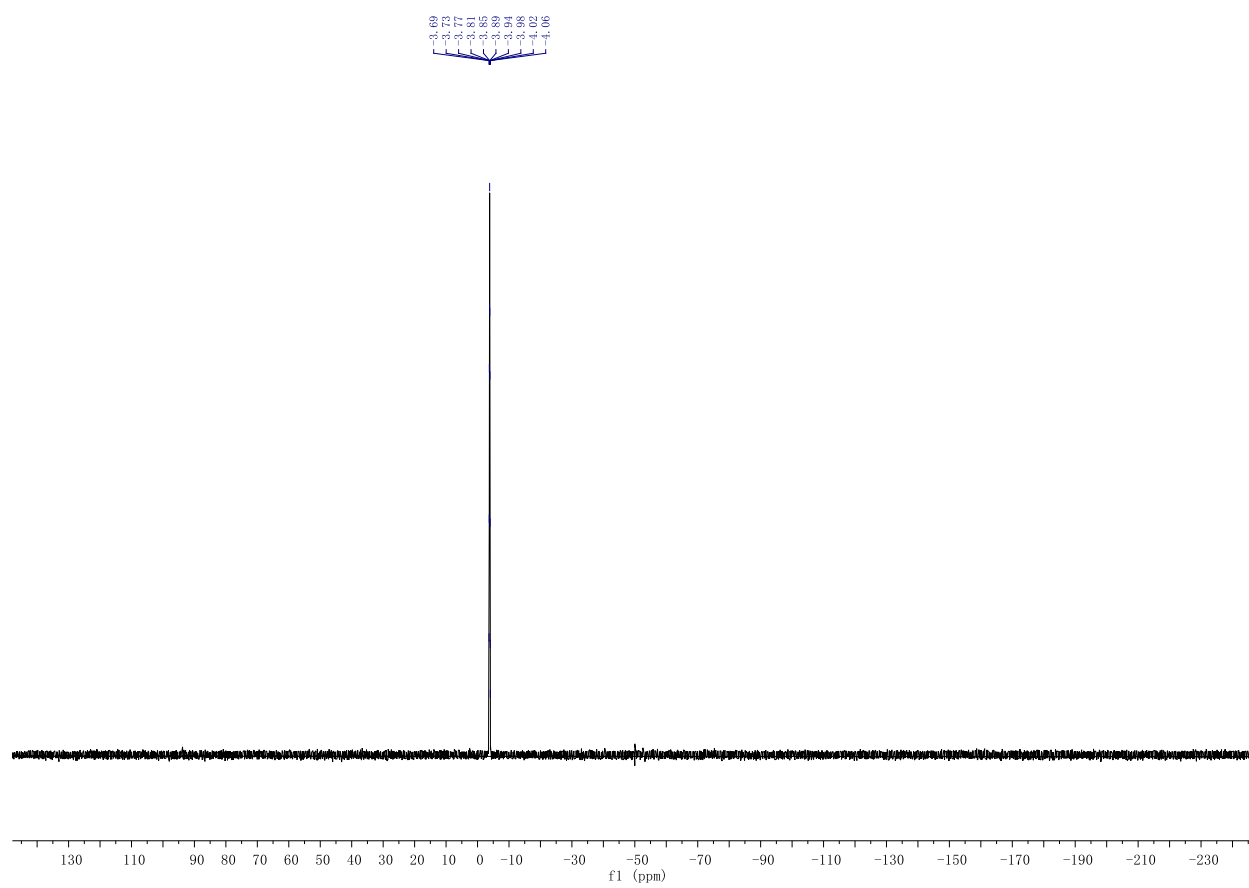
^{31}P NMR

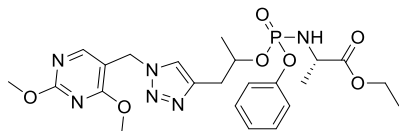
^{31}P NMR



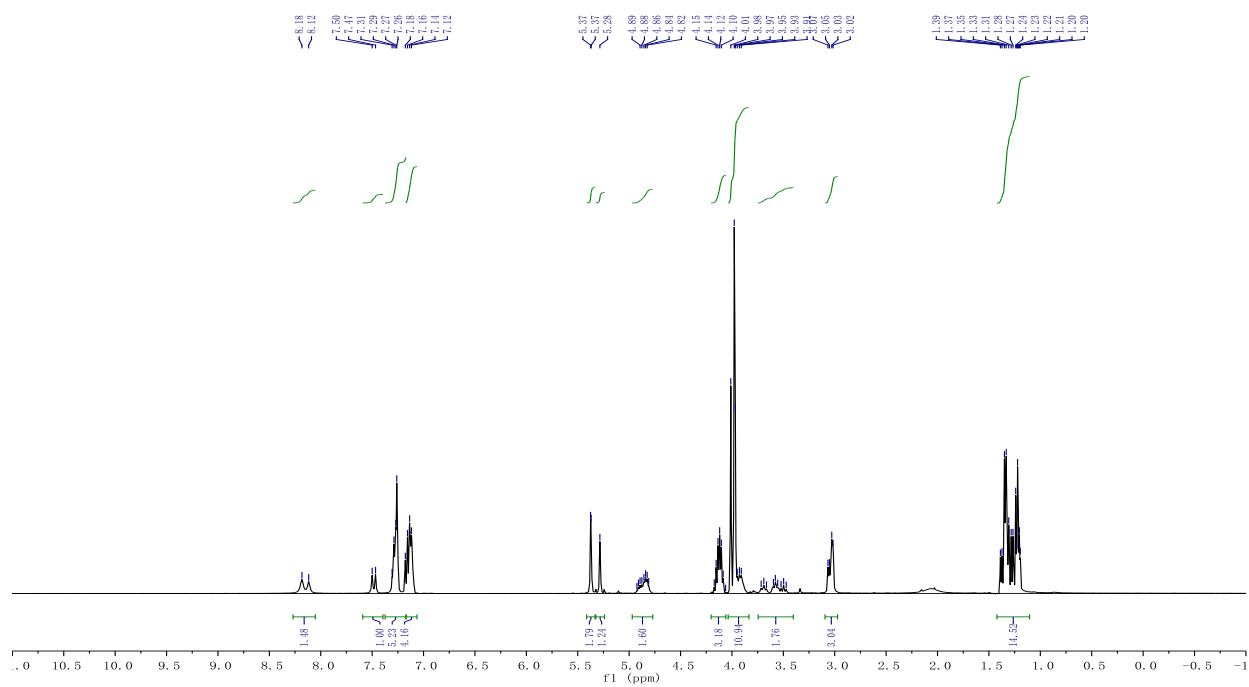
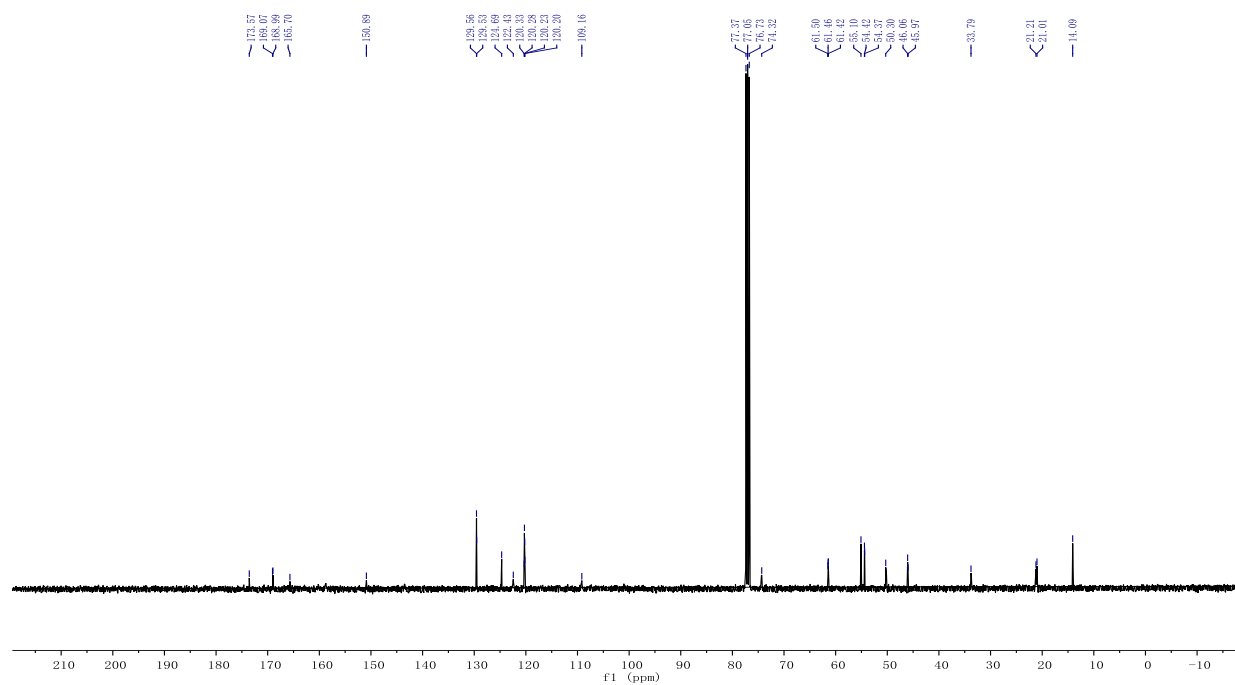
BW-VB-25

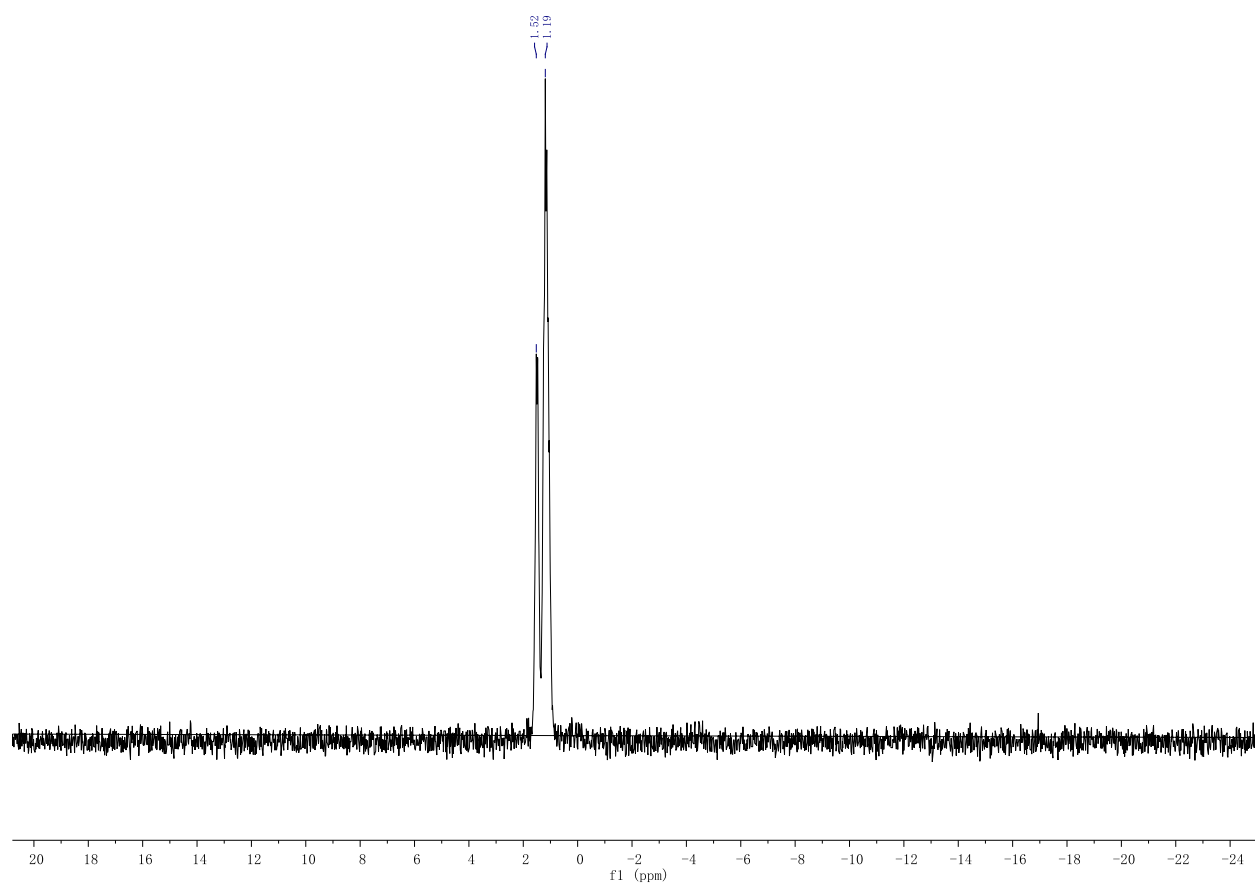
 ^1H NMR ^{13}C NMR

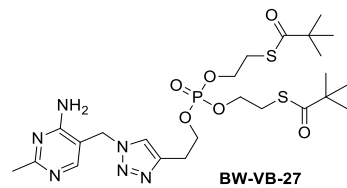
^{31}P NMR



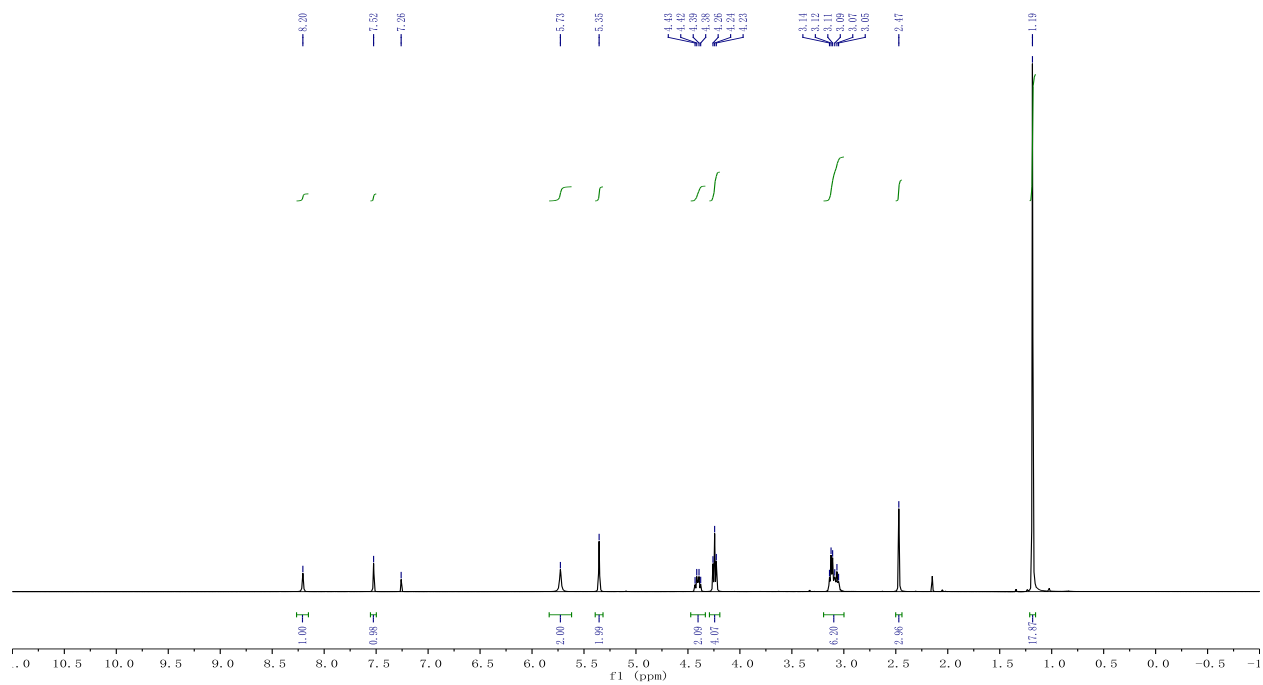
BW-VB-26

 ^1H NMR ^{13}C NMR

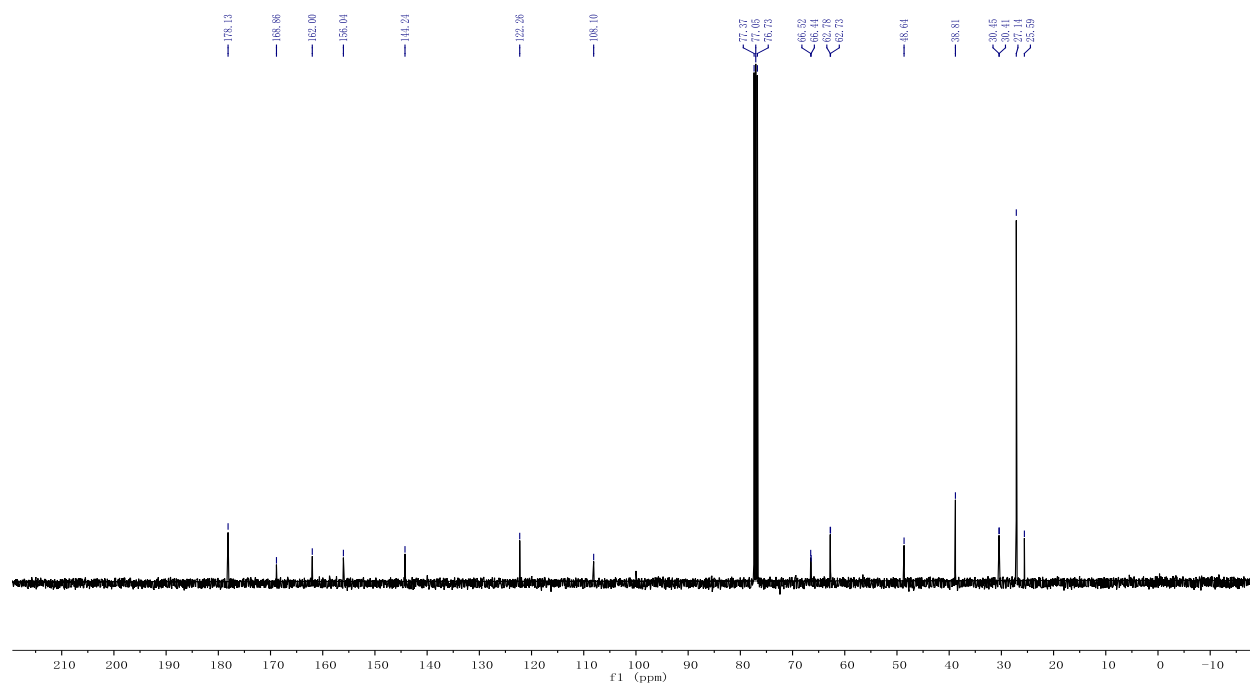
^{31}P NMR

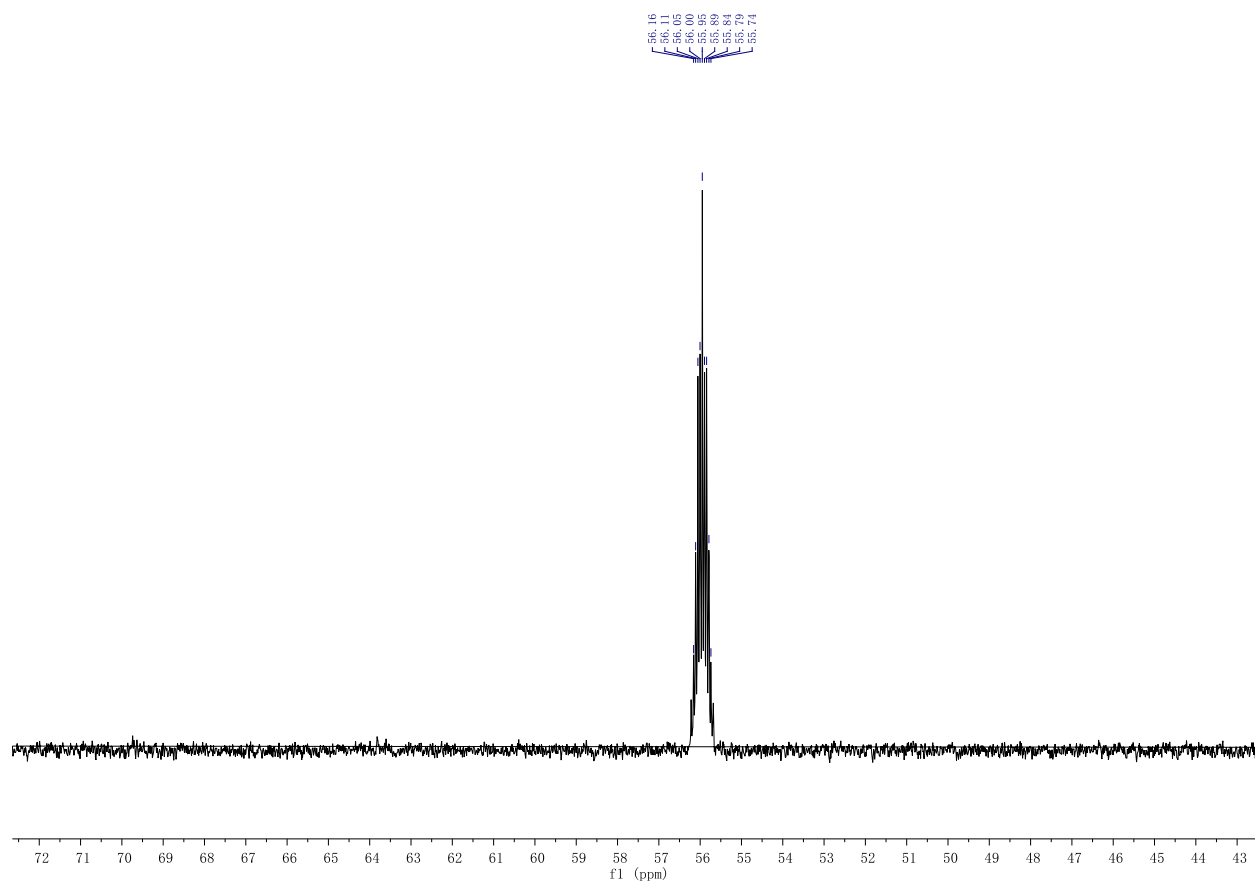


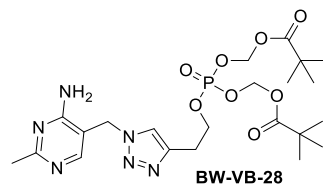
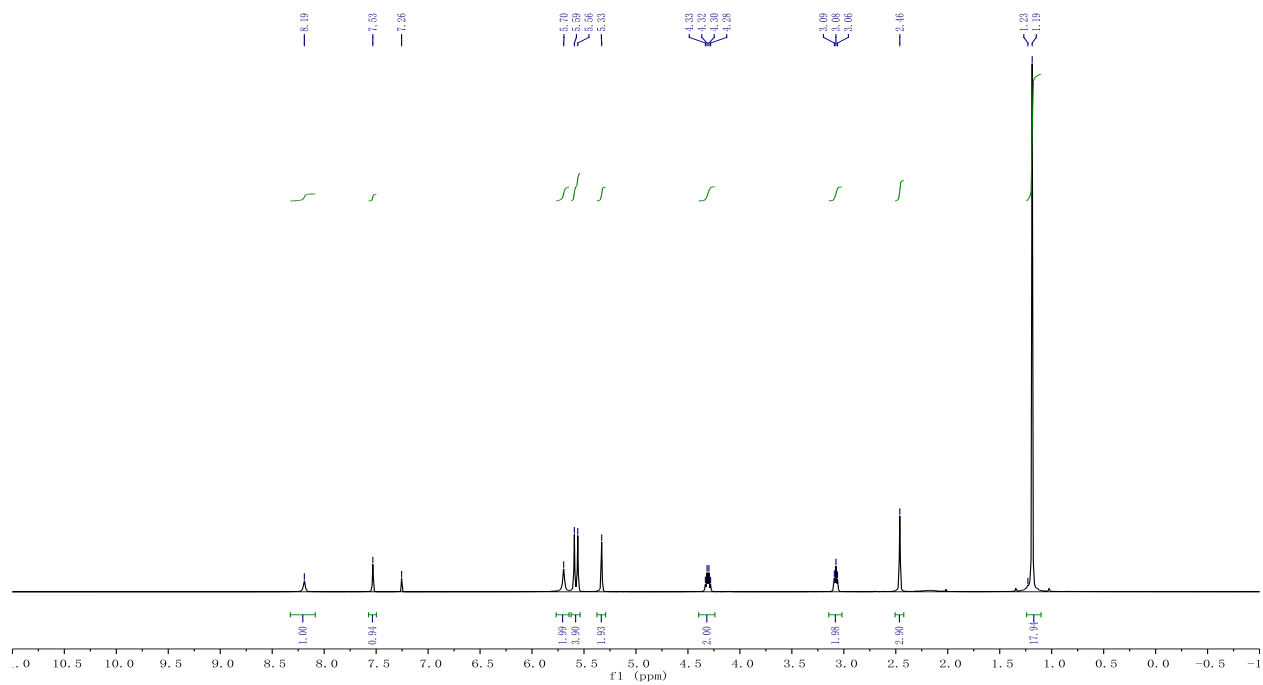
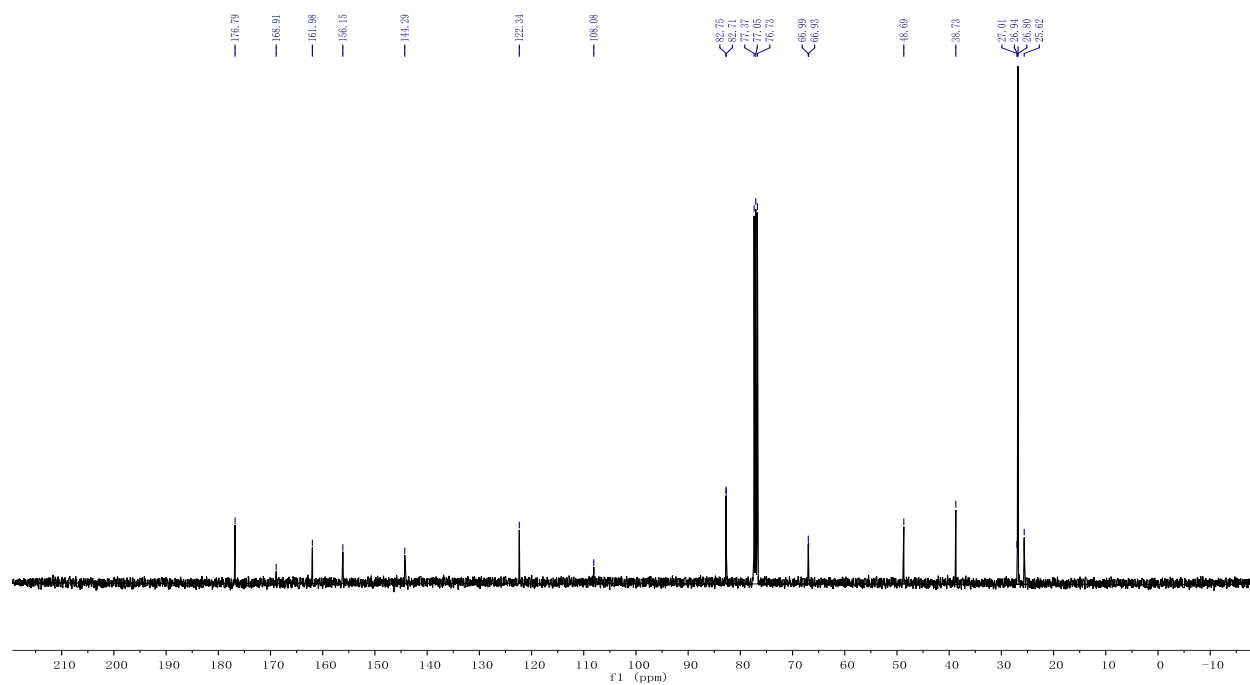
¹H NMR

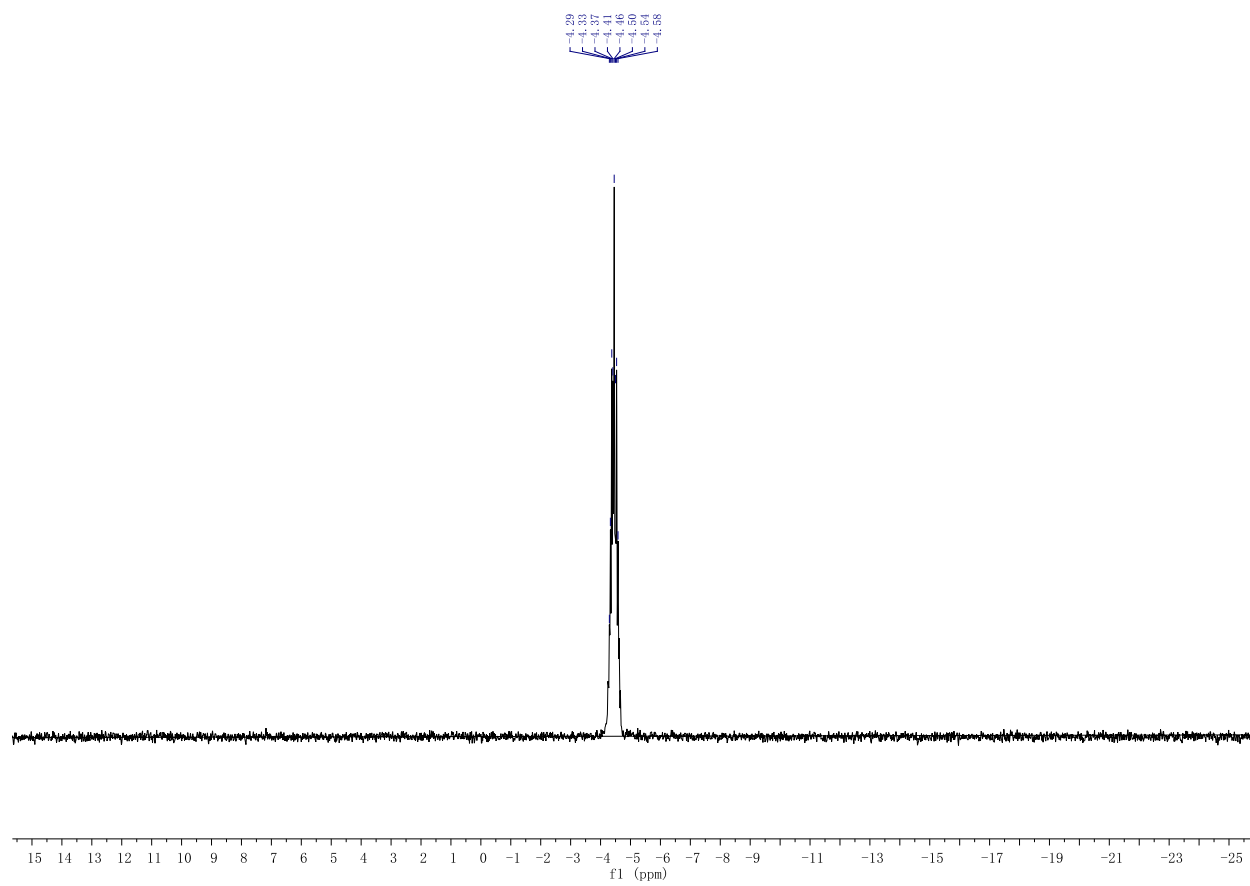


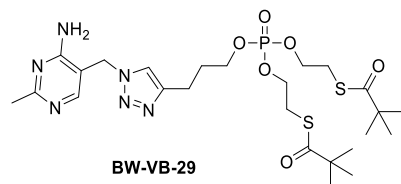
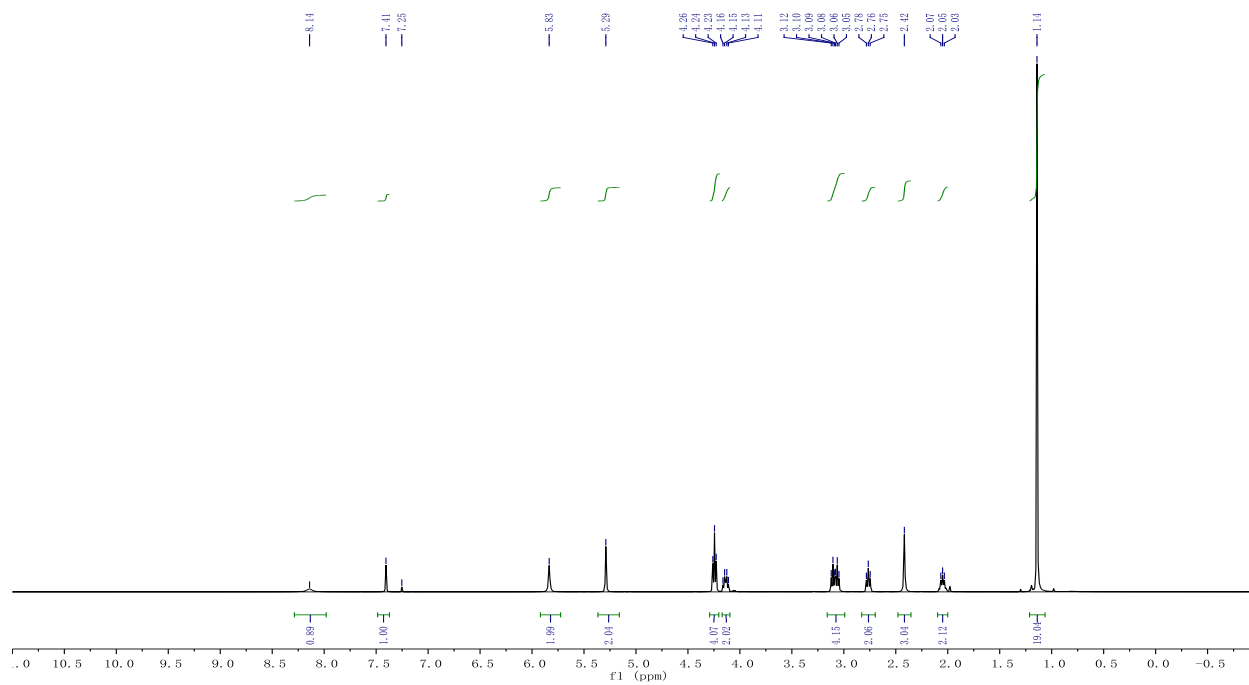
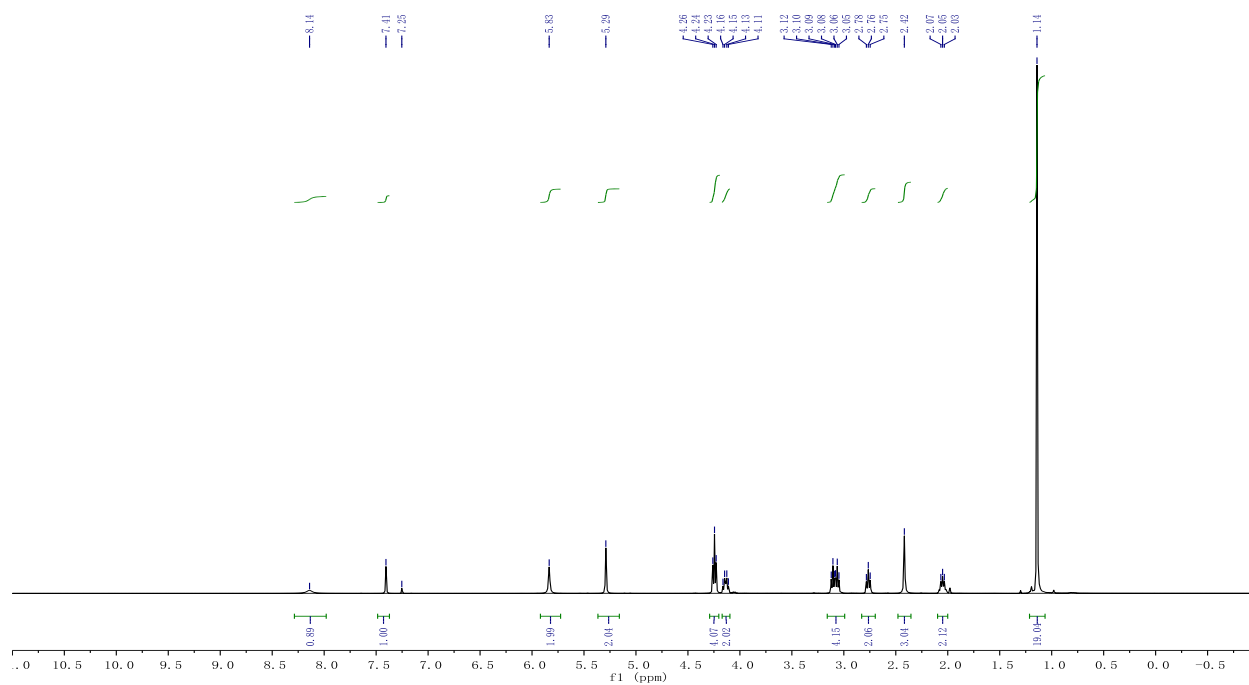
¹³C NMR

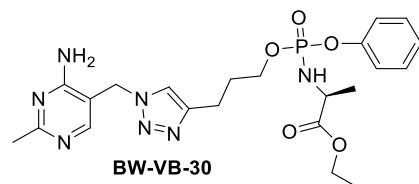
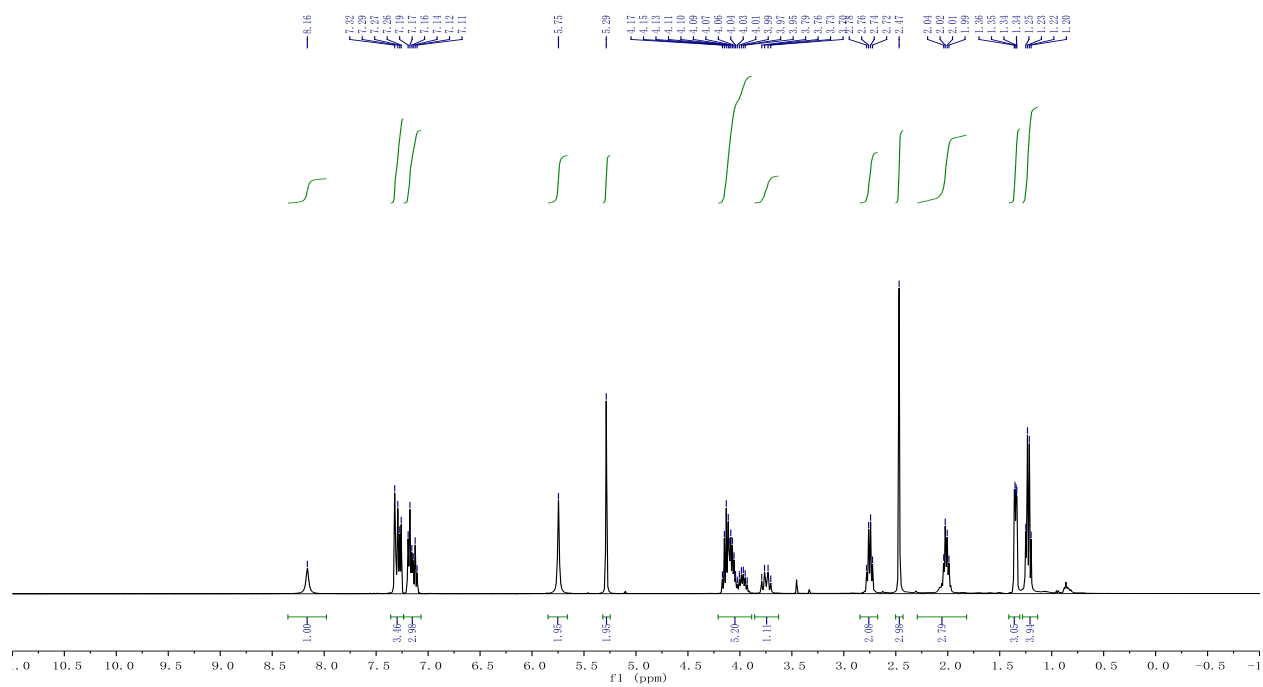
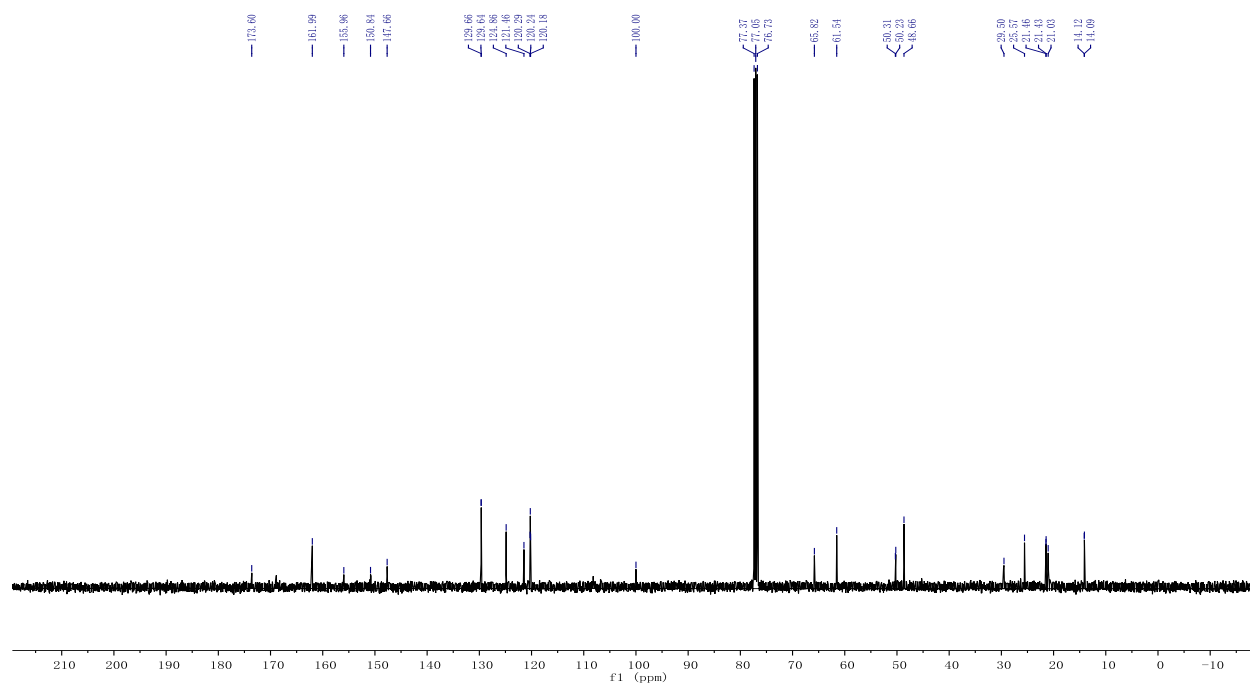


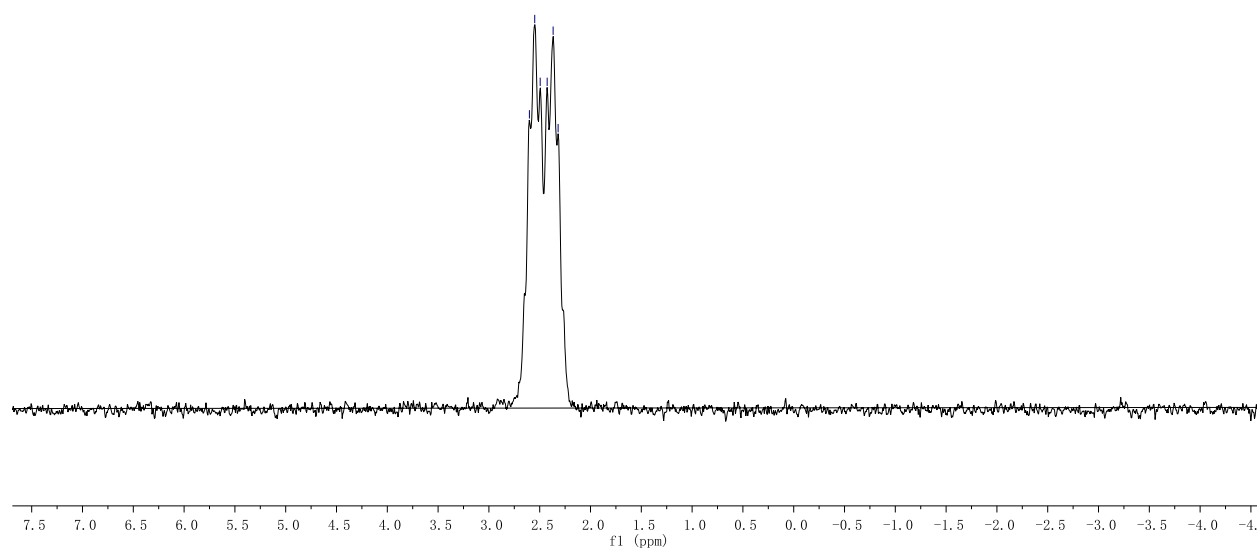
^{31}P NMR

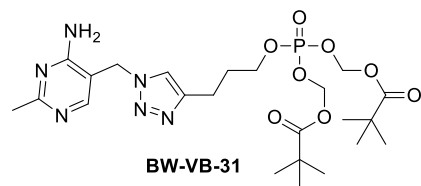
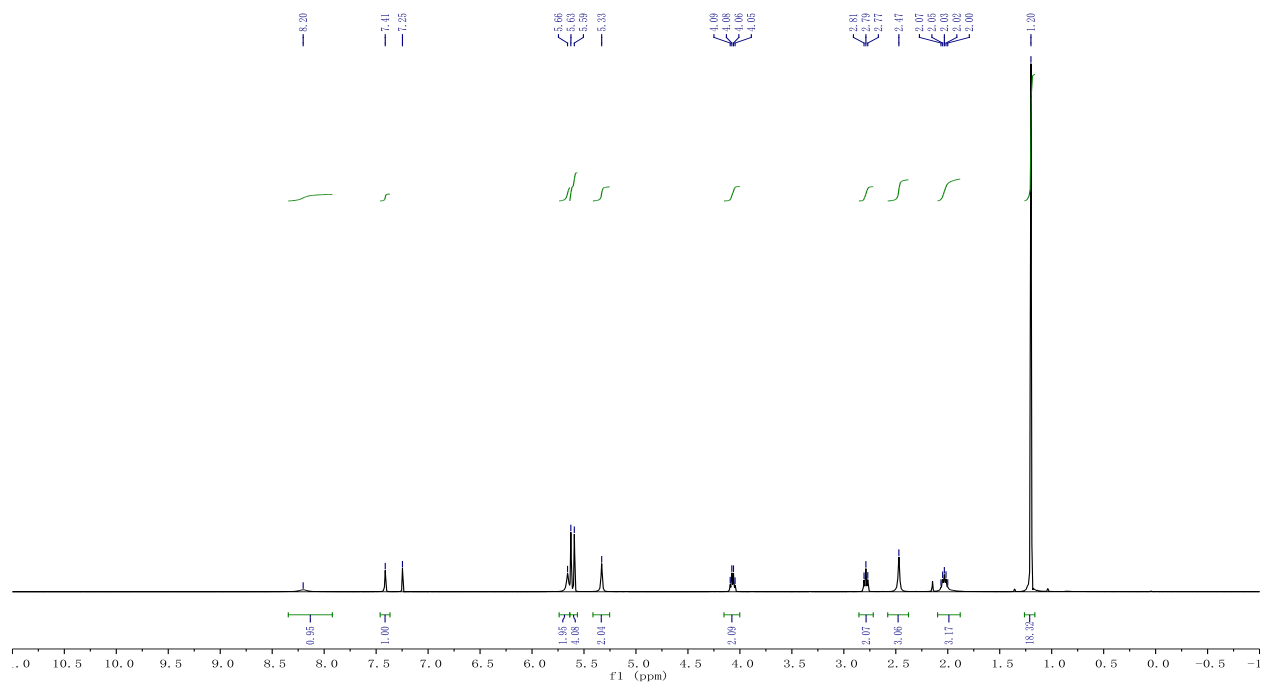
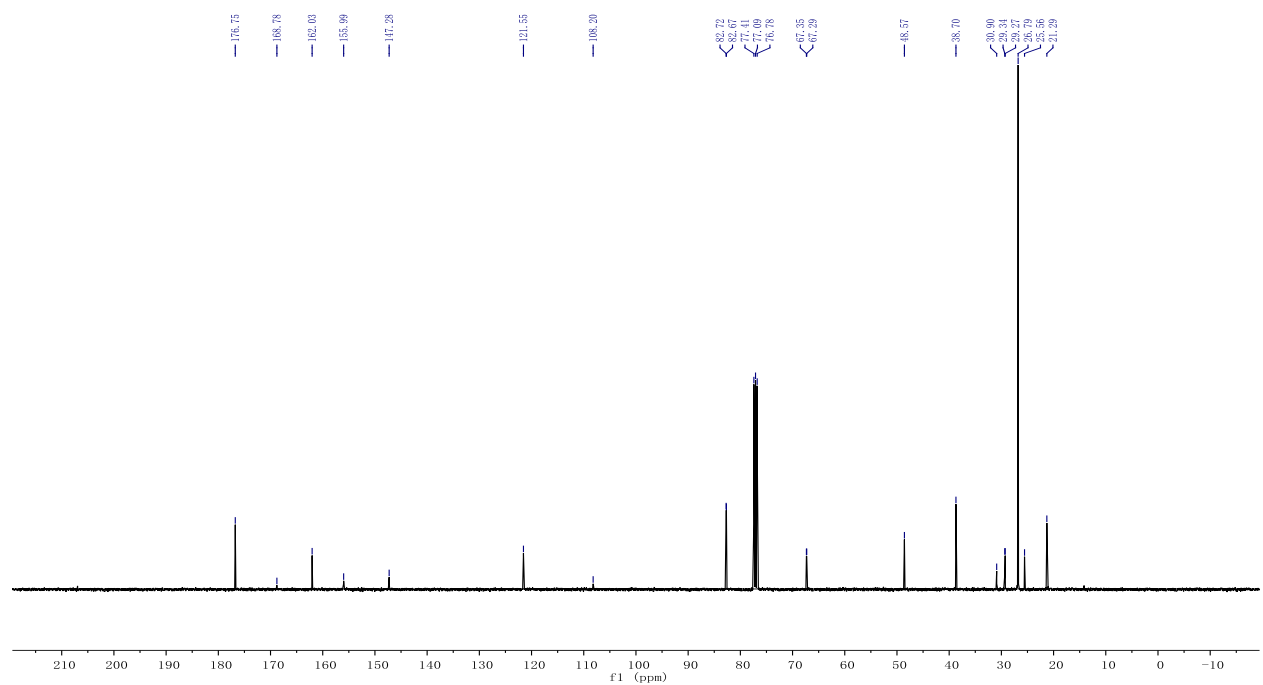
 ^1H NMR ^{13}C NMR

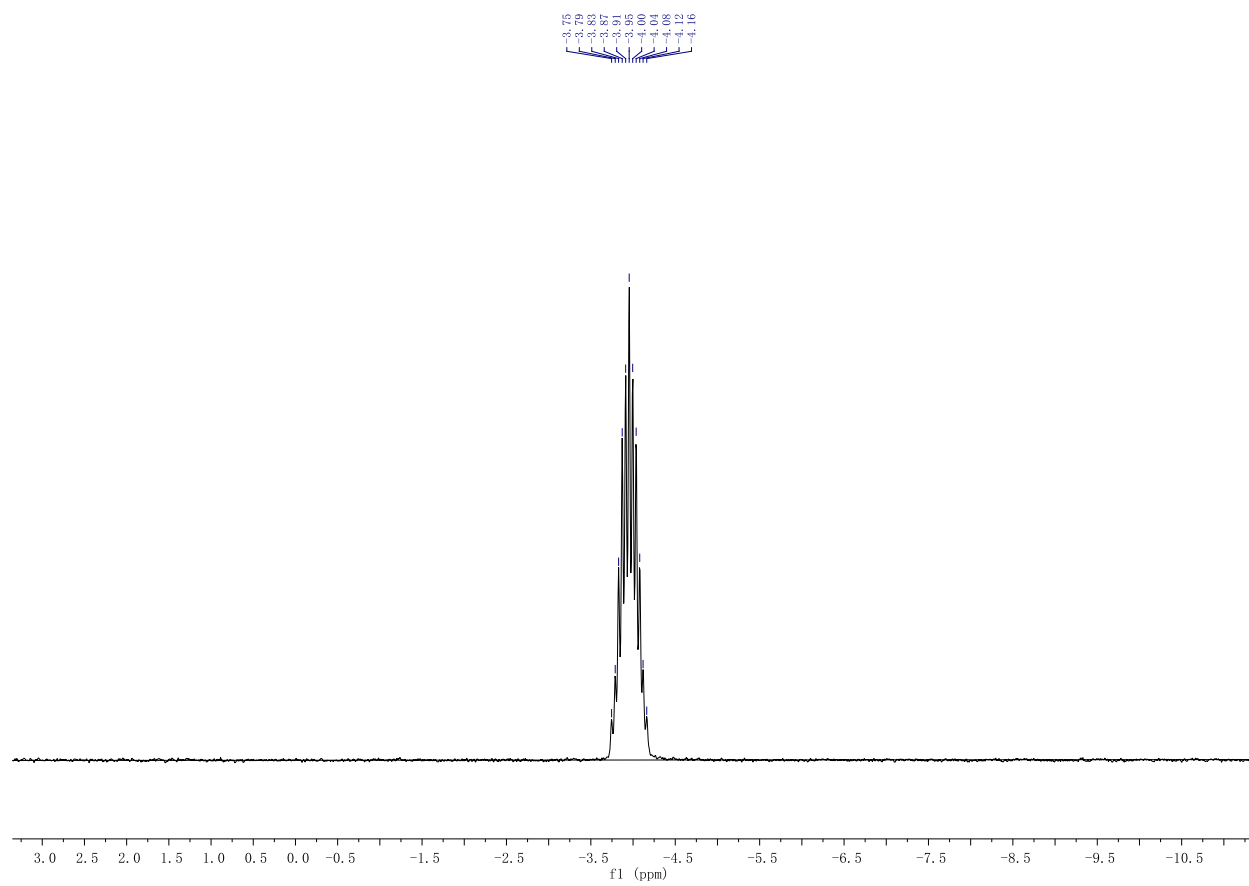
^{31}P NMR

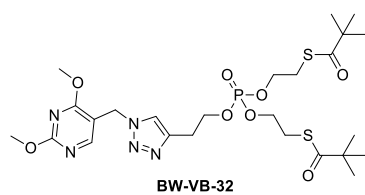
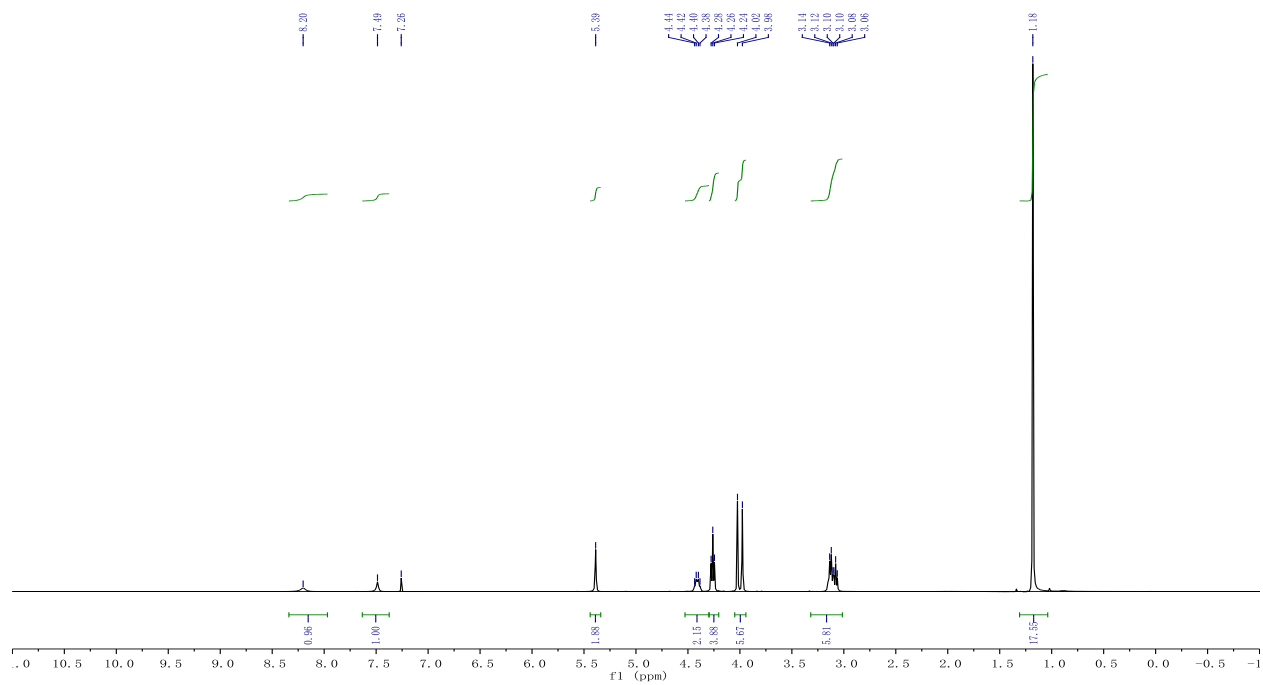
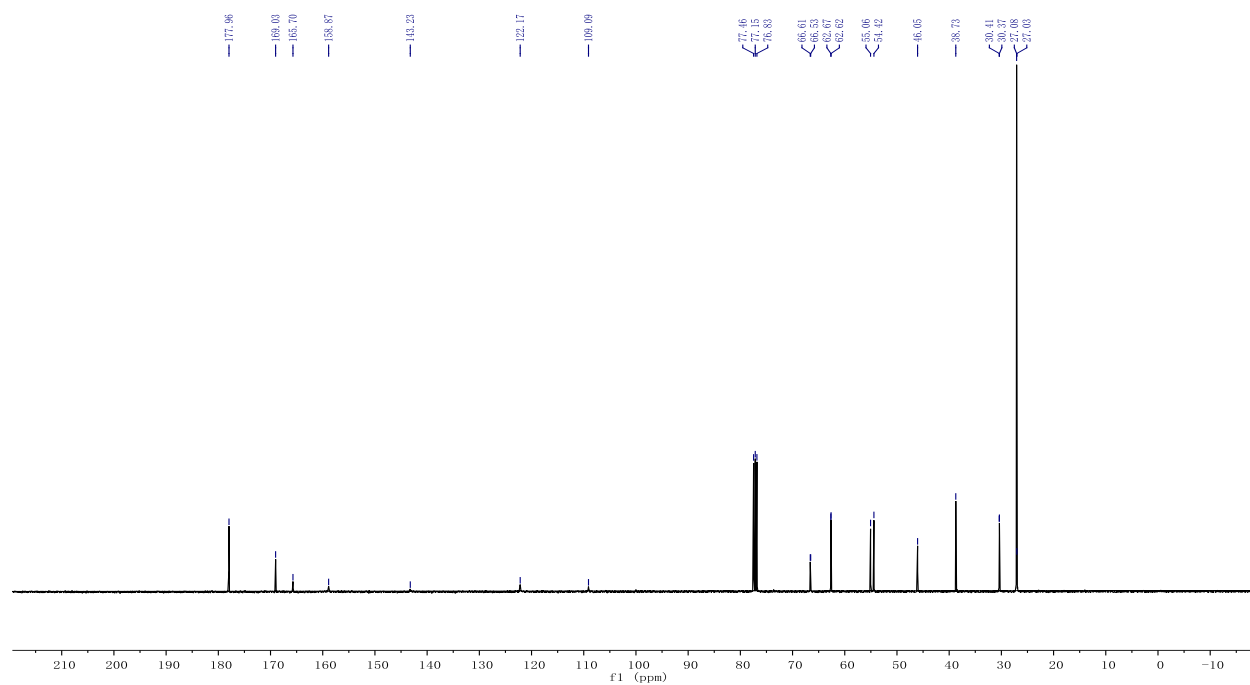
 ^1H NMR ^{13}C NMR

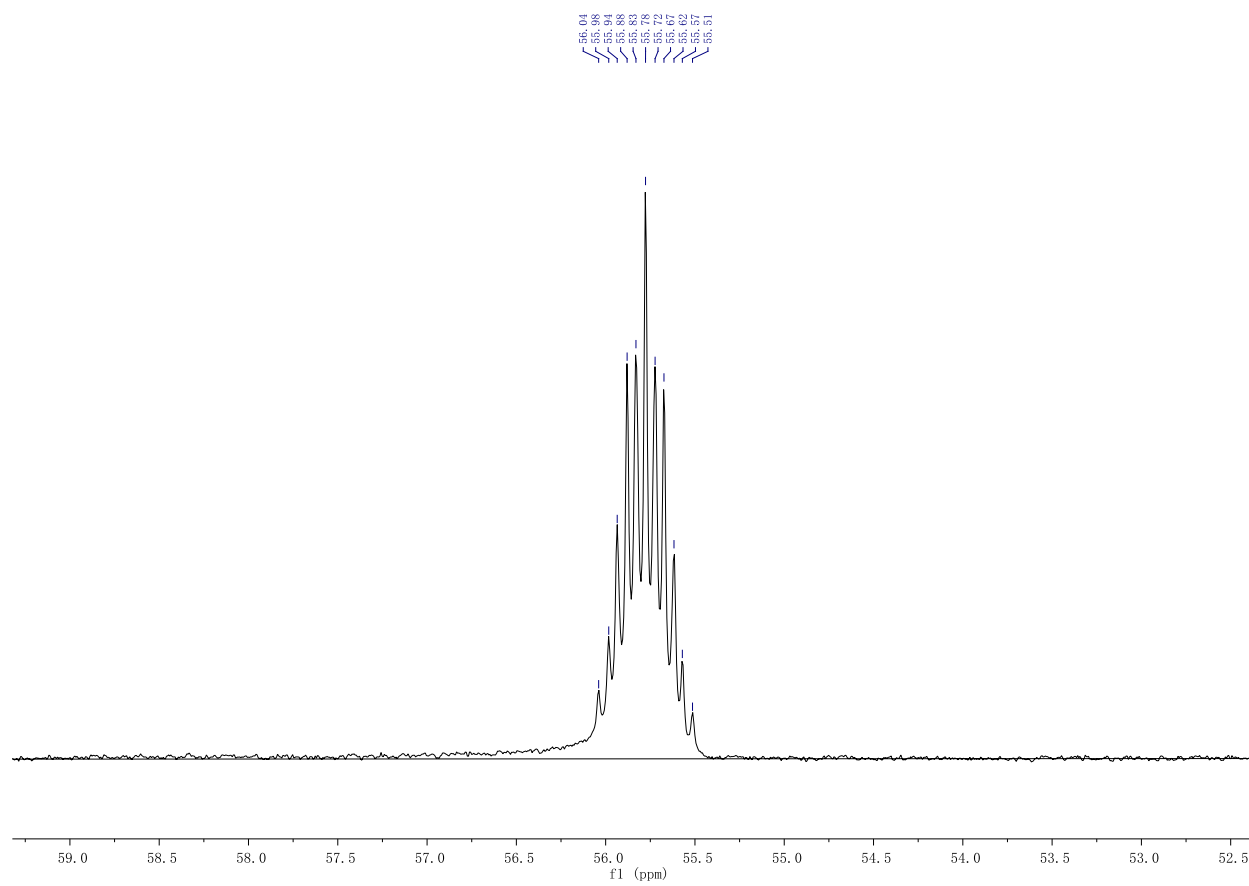
 ^1H NMR ^{13}C NMR

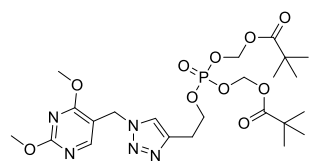
^{31}P NMR

 ^1H NMR ^{13}C NMR

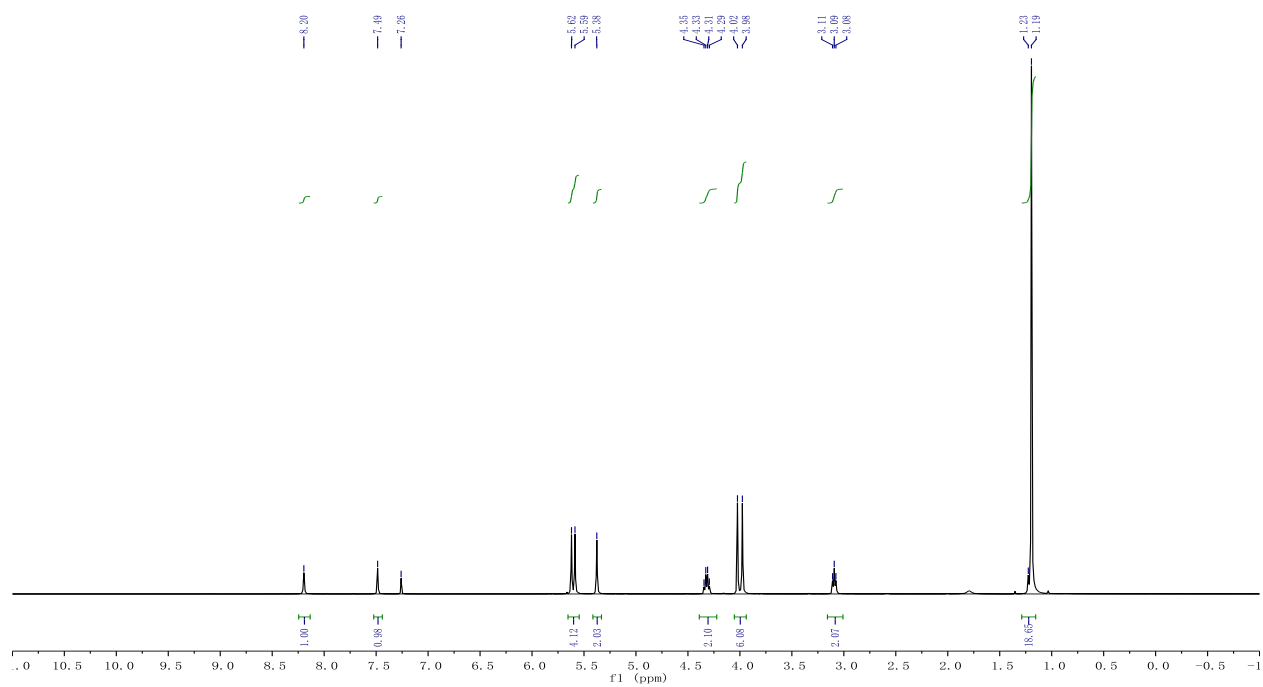
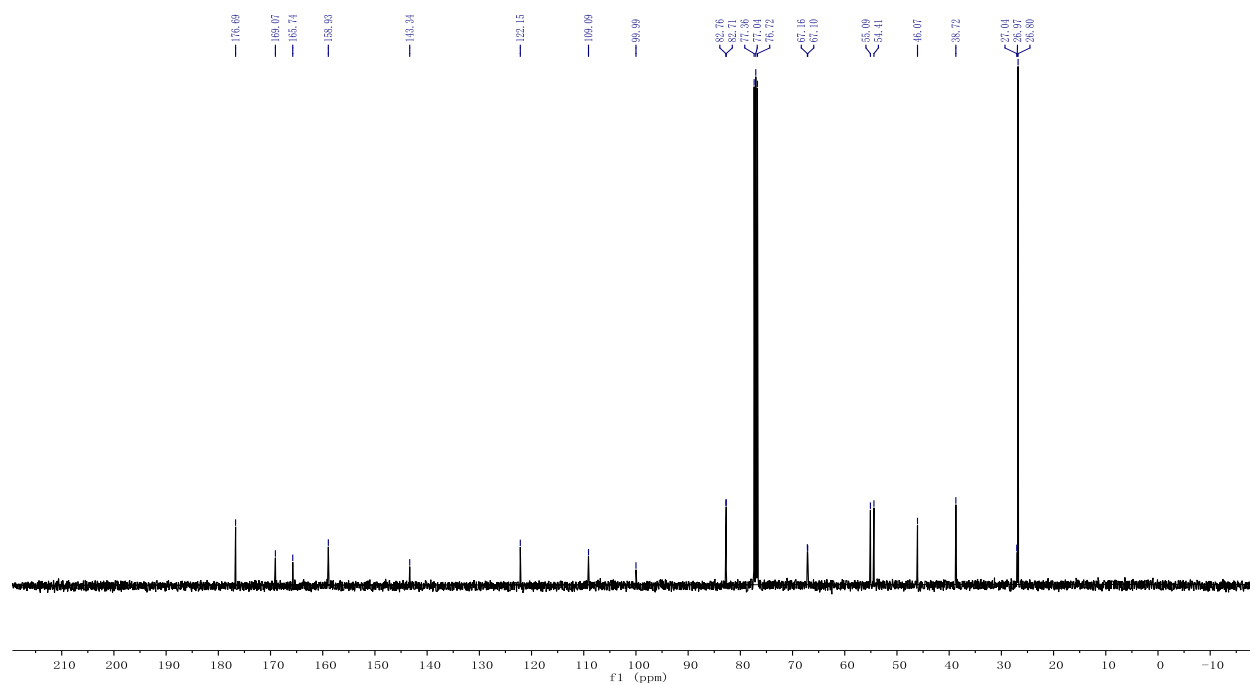
^{31}P NMR

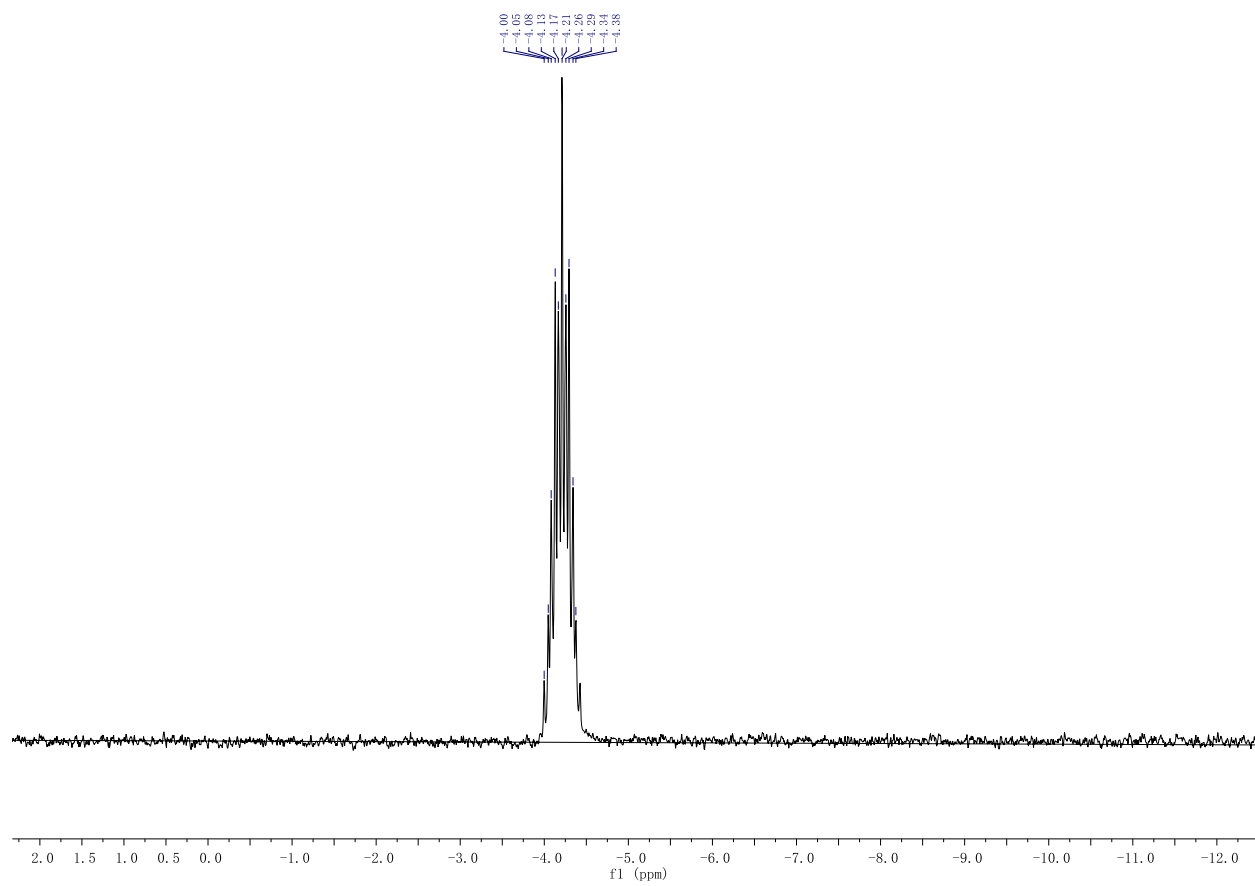
 ^1H NMR ^{13}C NMR

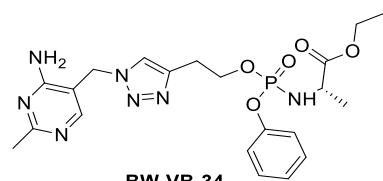
^{31}P NMR



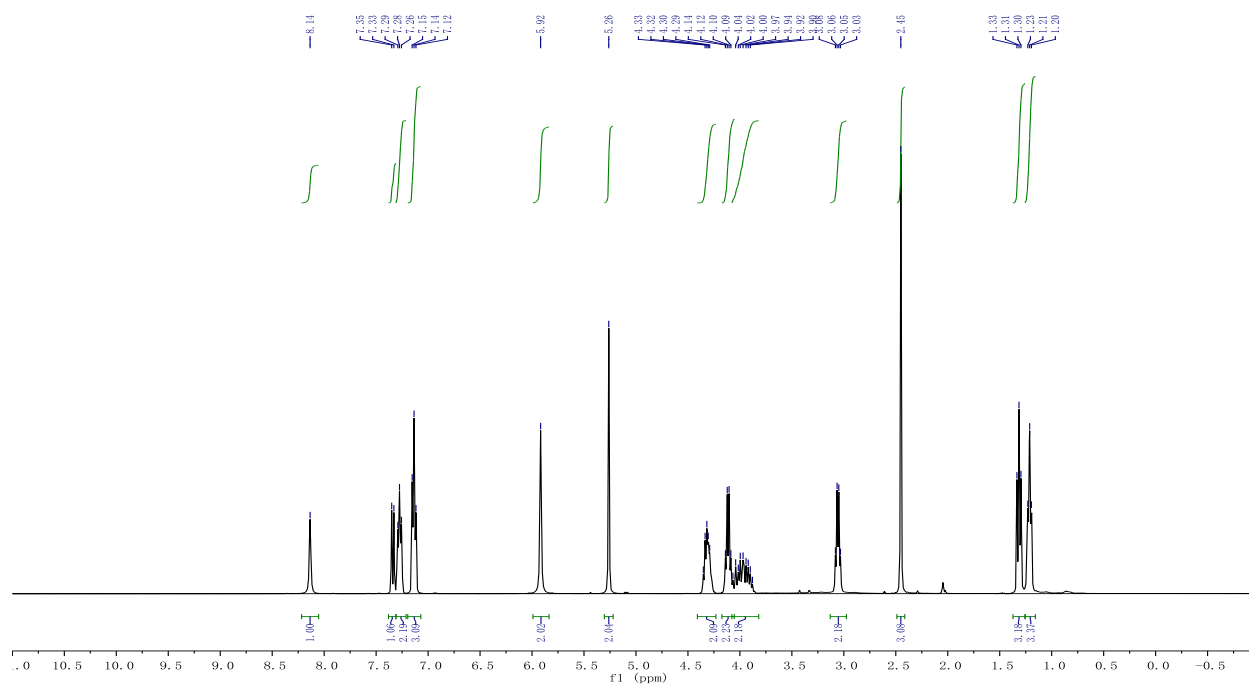
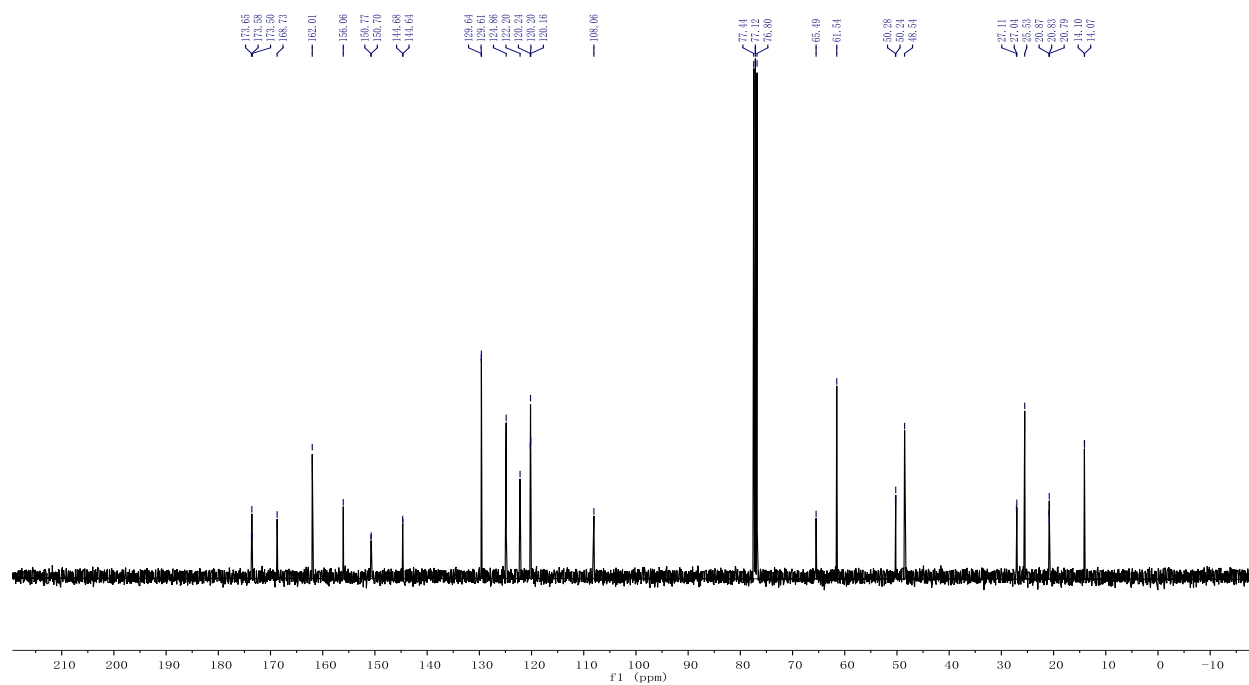
BW-VB-33

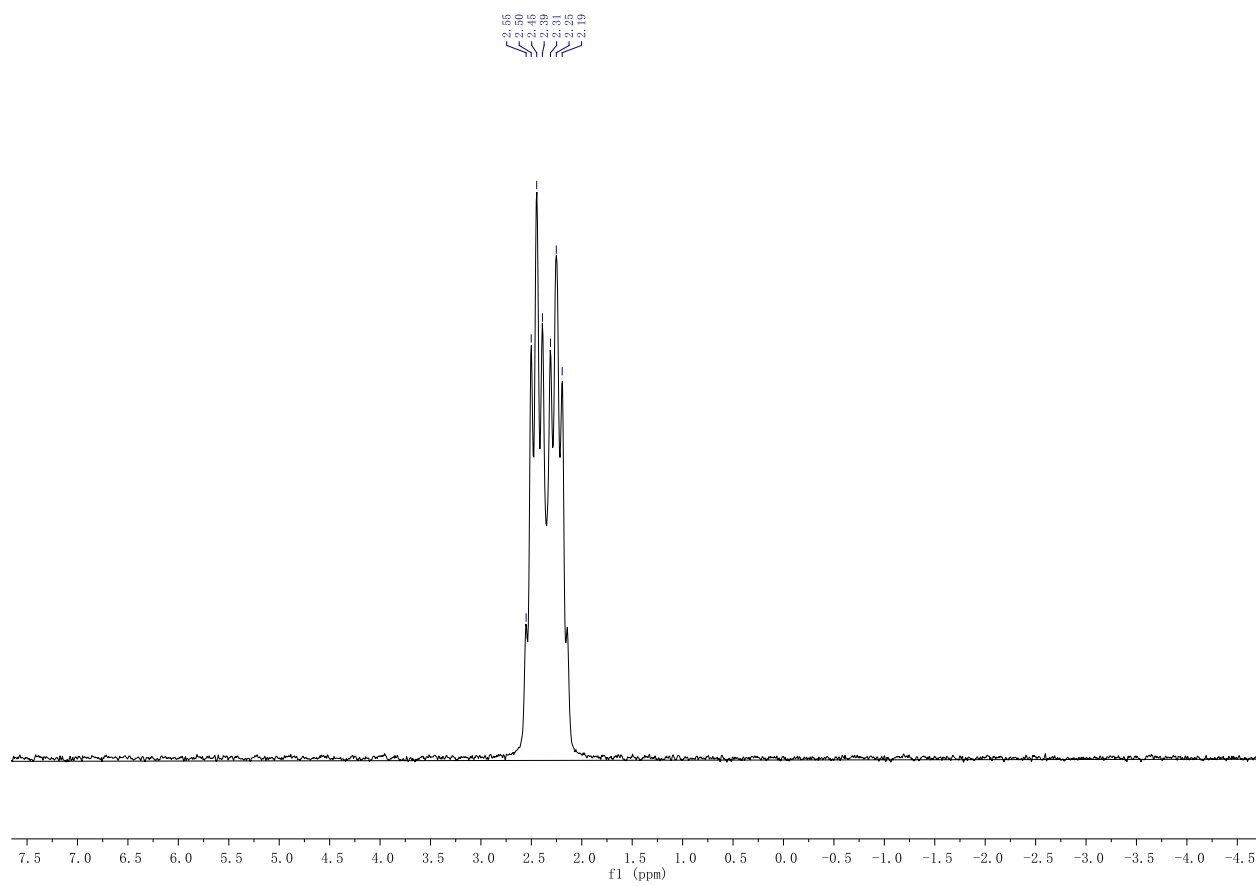
 ^1H NMR ^{13}C NMR

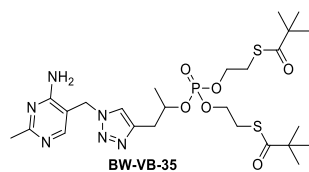
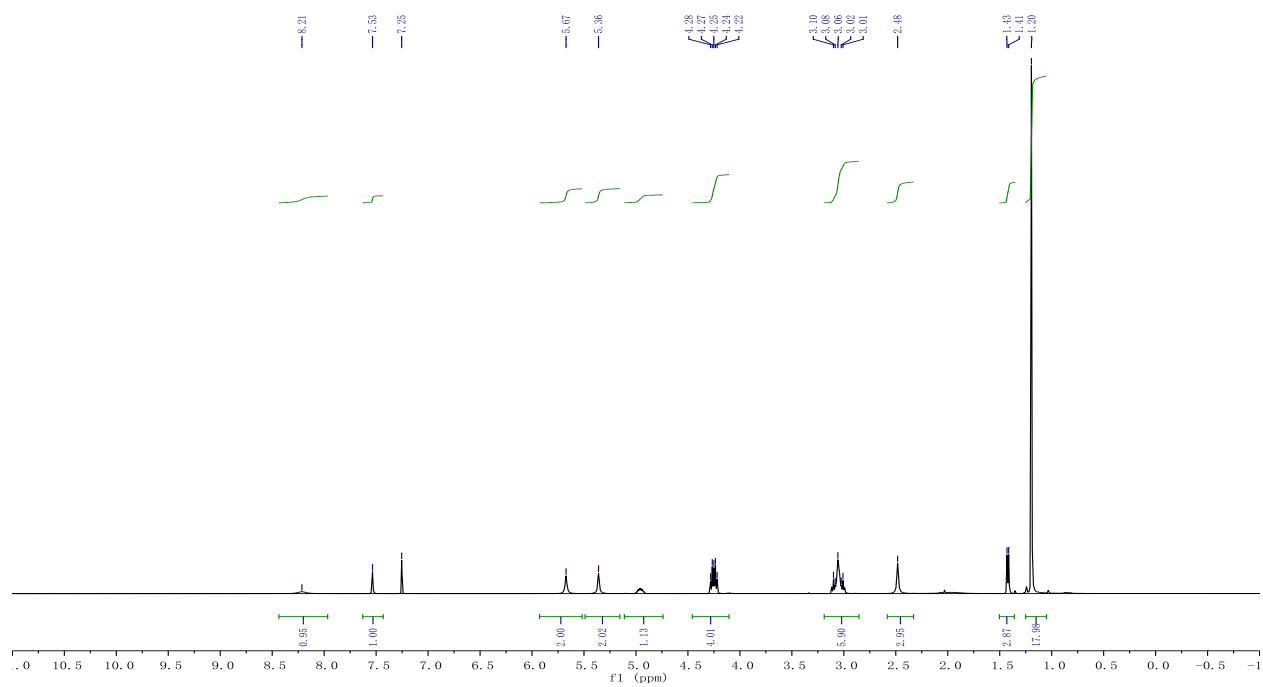
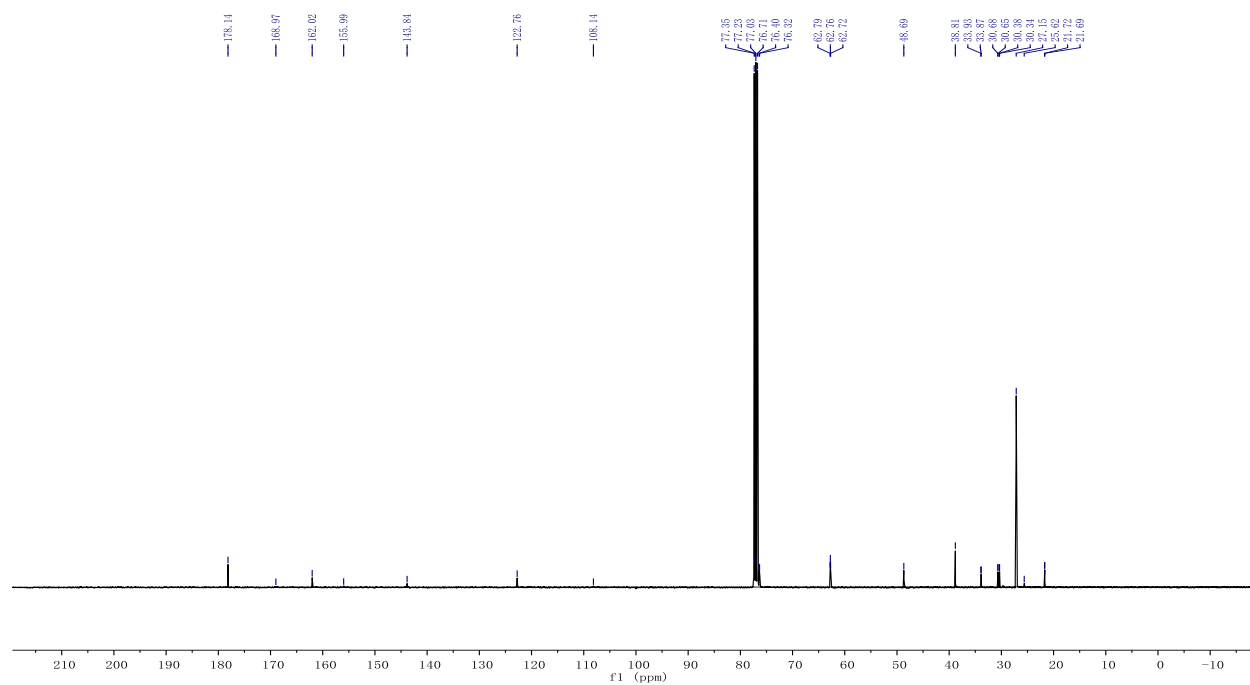
^{31}P NMR

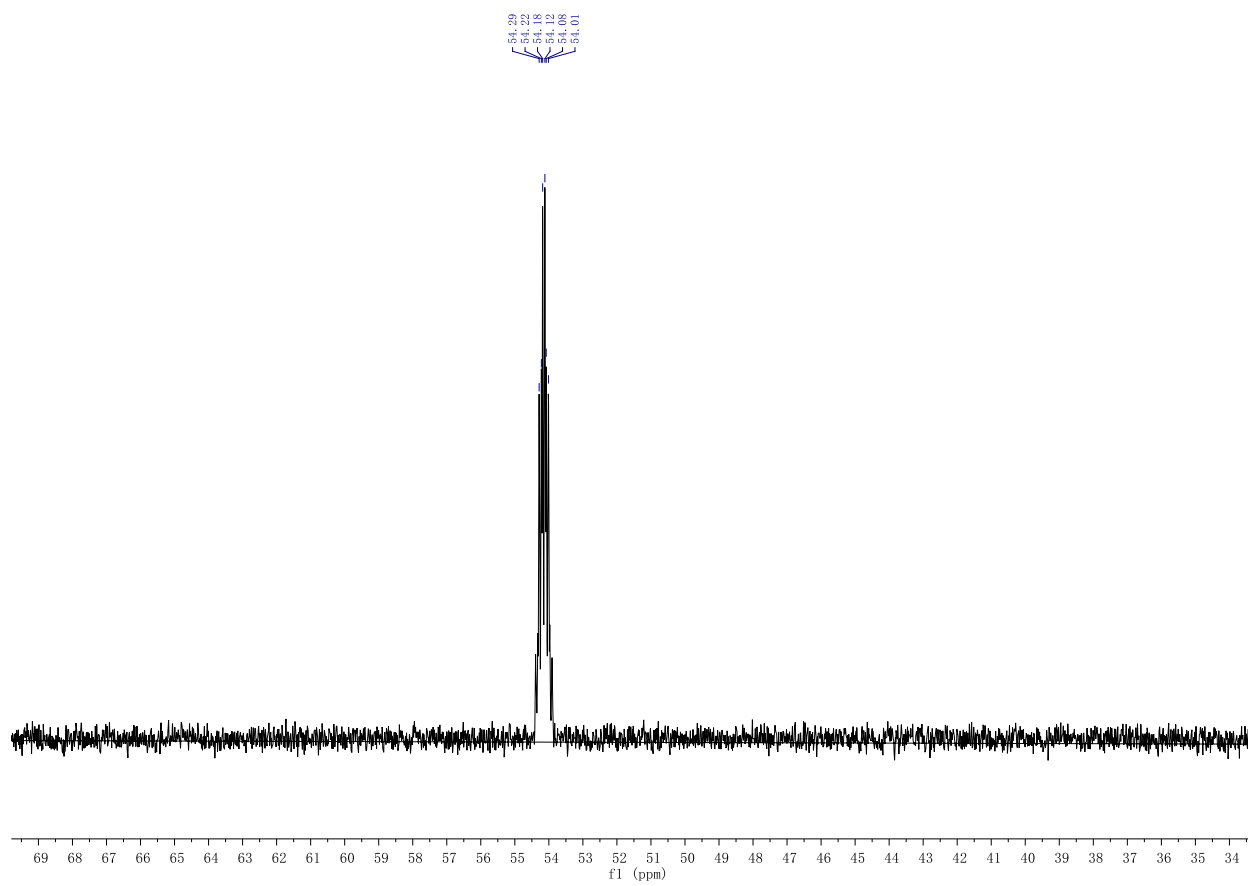


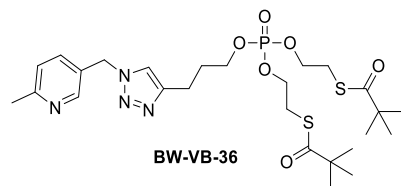
BW-VB-34

 ^1H NMR ^{13}C NMR

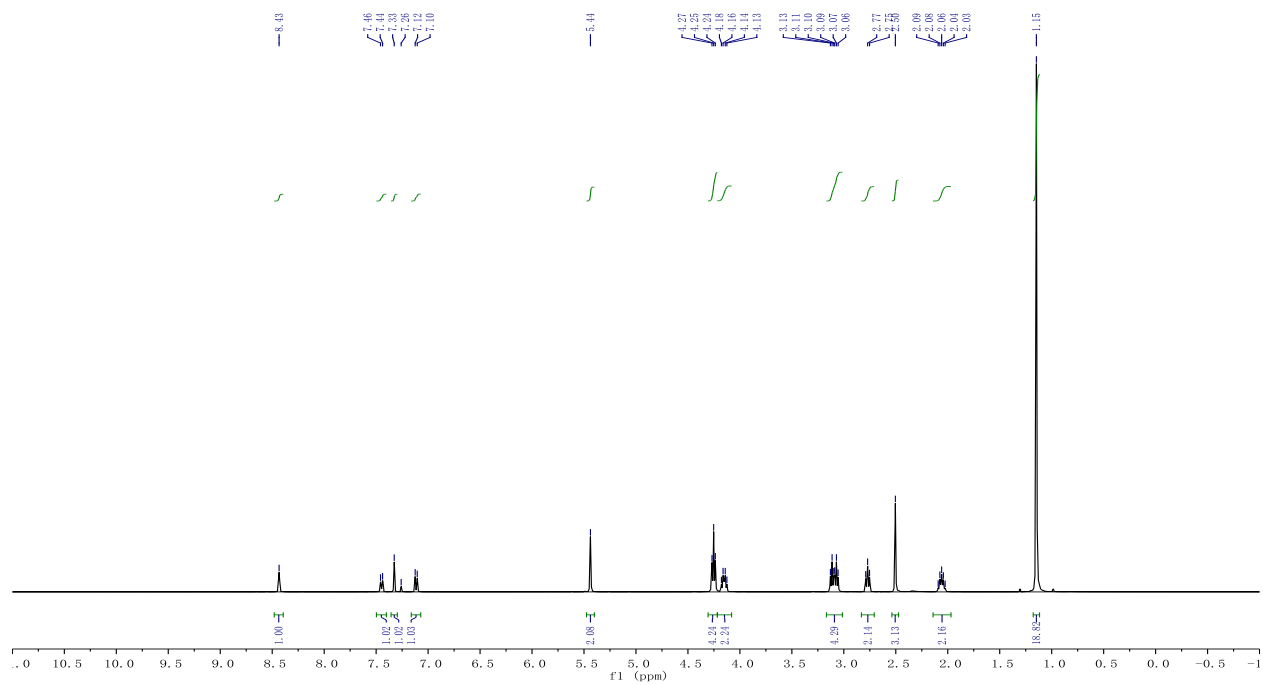
^{31}P NMR

 ^1H NMR ^{13}C NMR

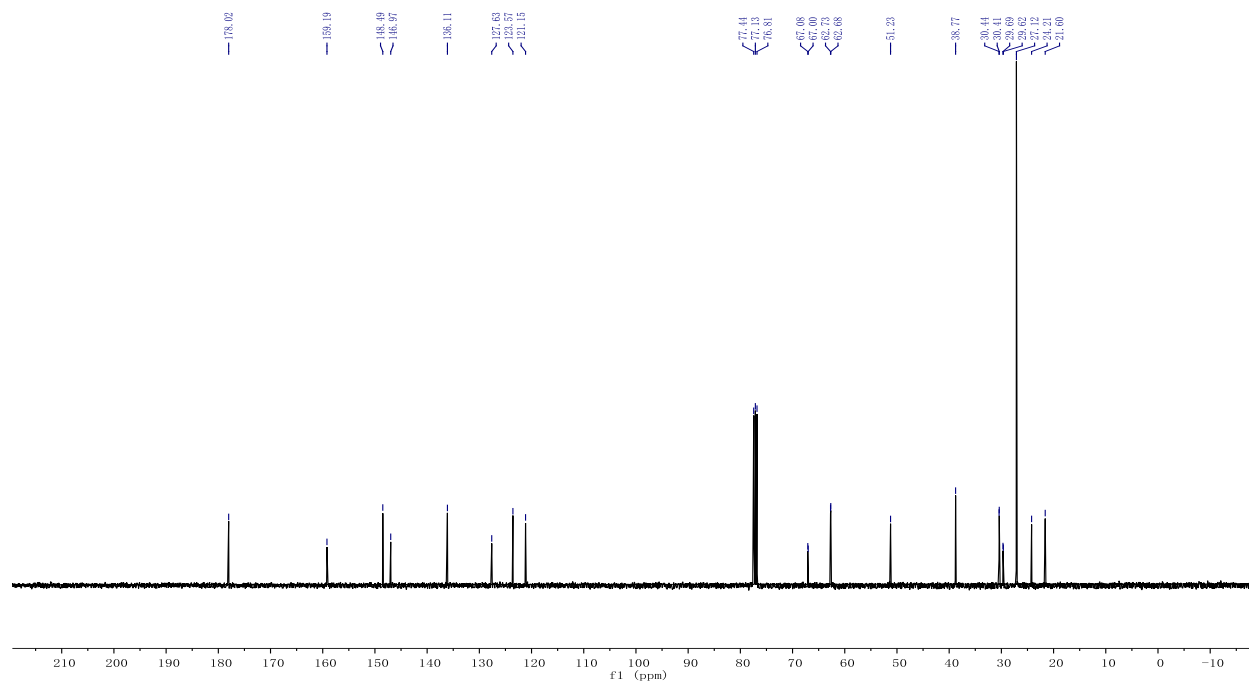
^{31}P NMR

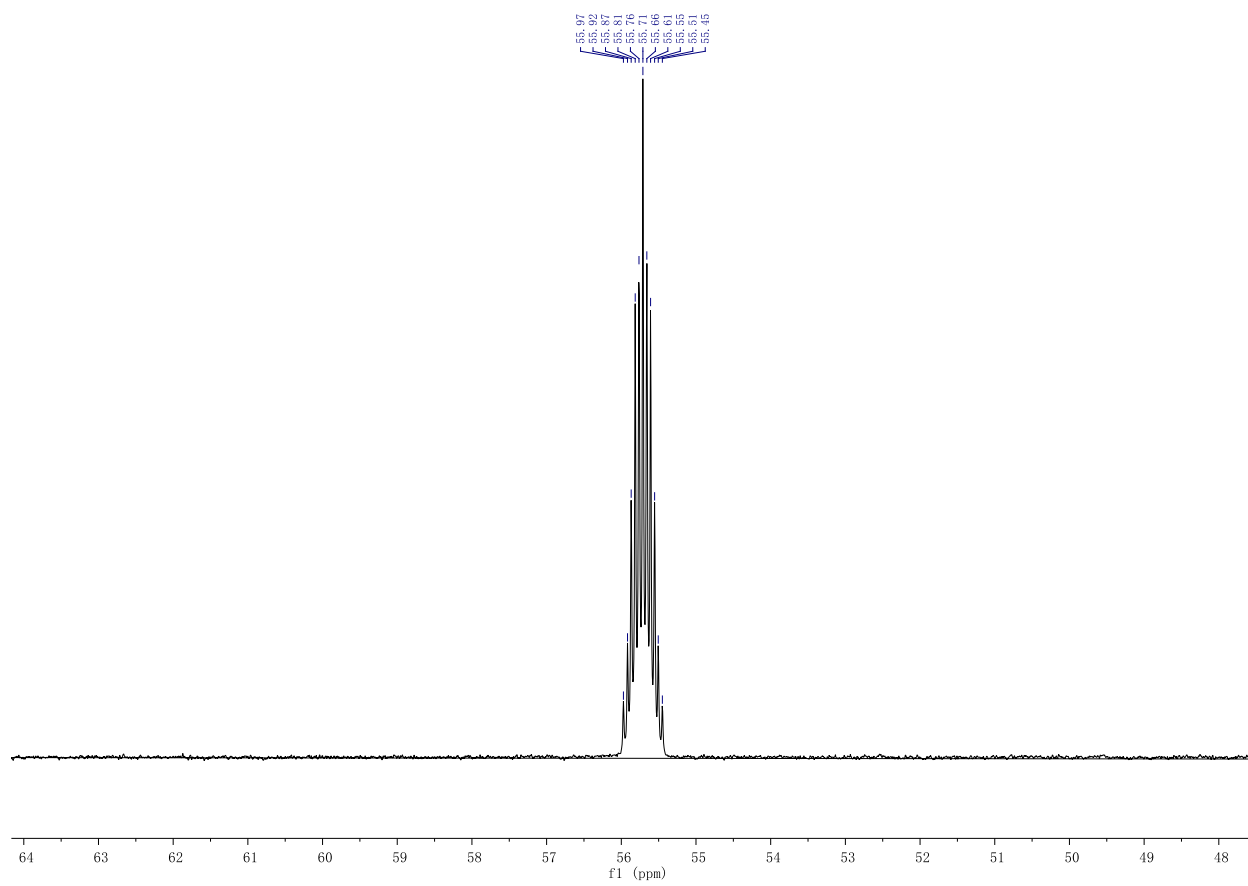


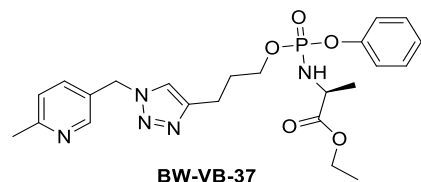
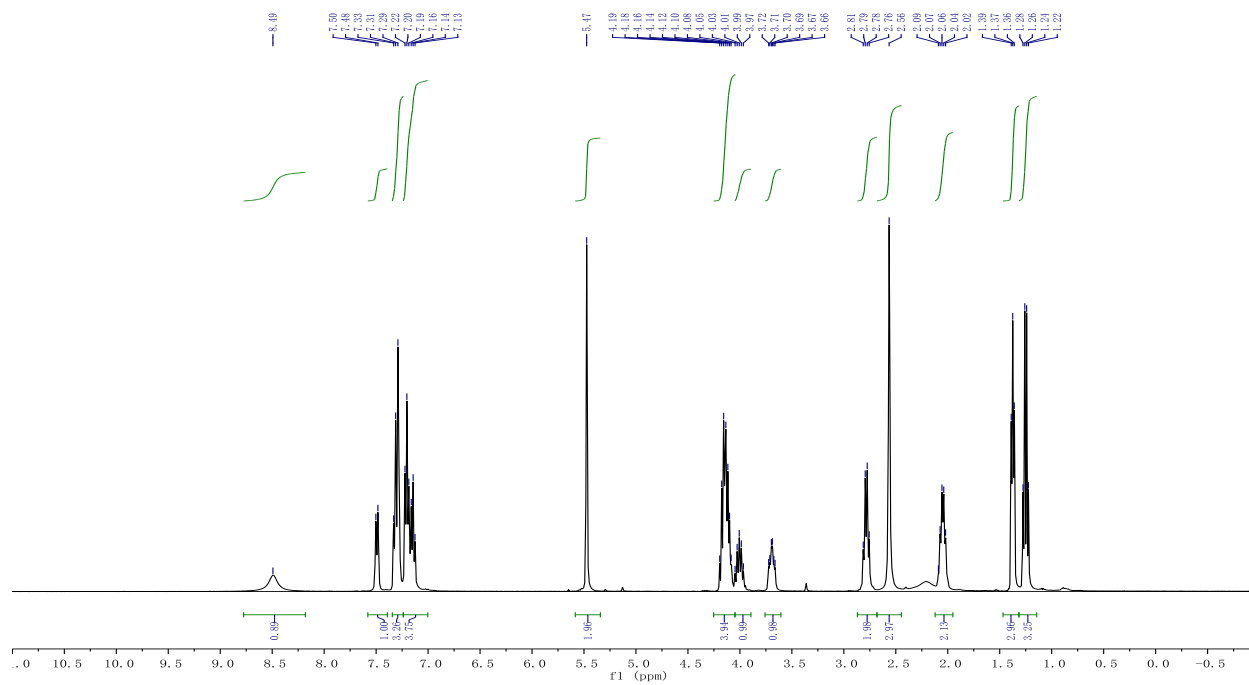
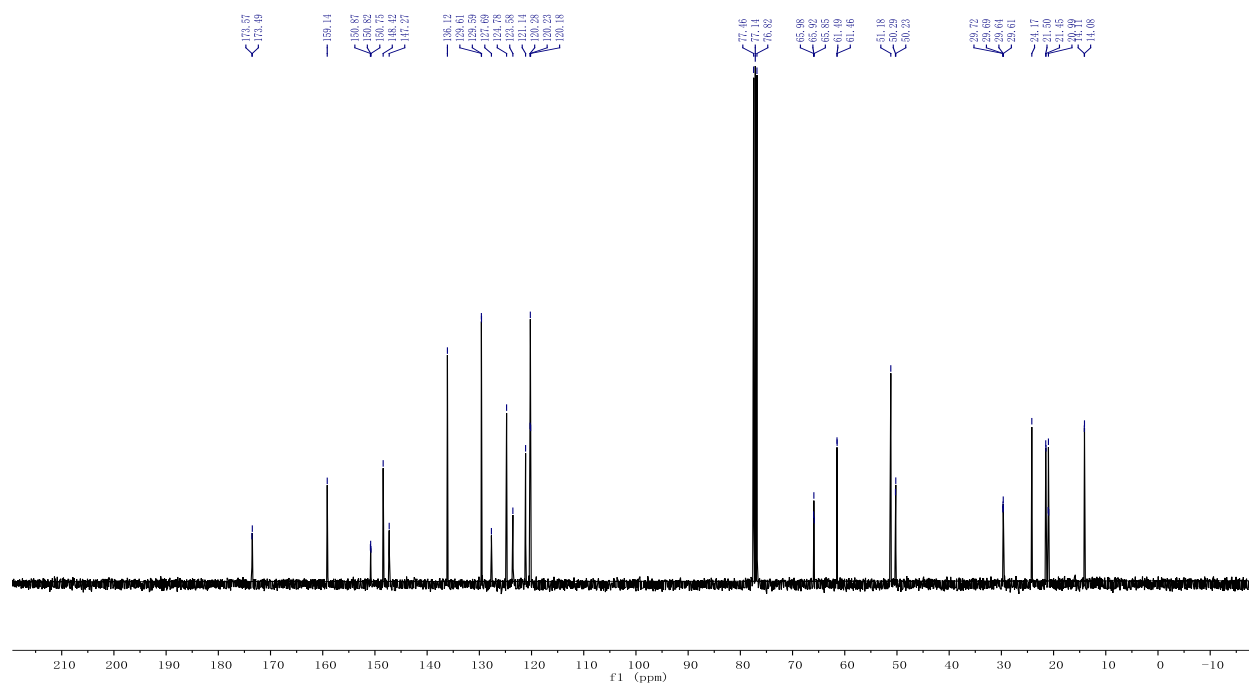
^1H NMR

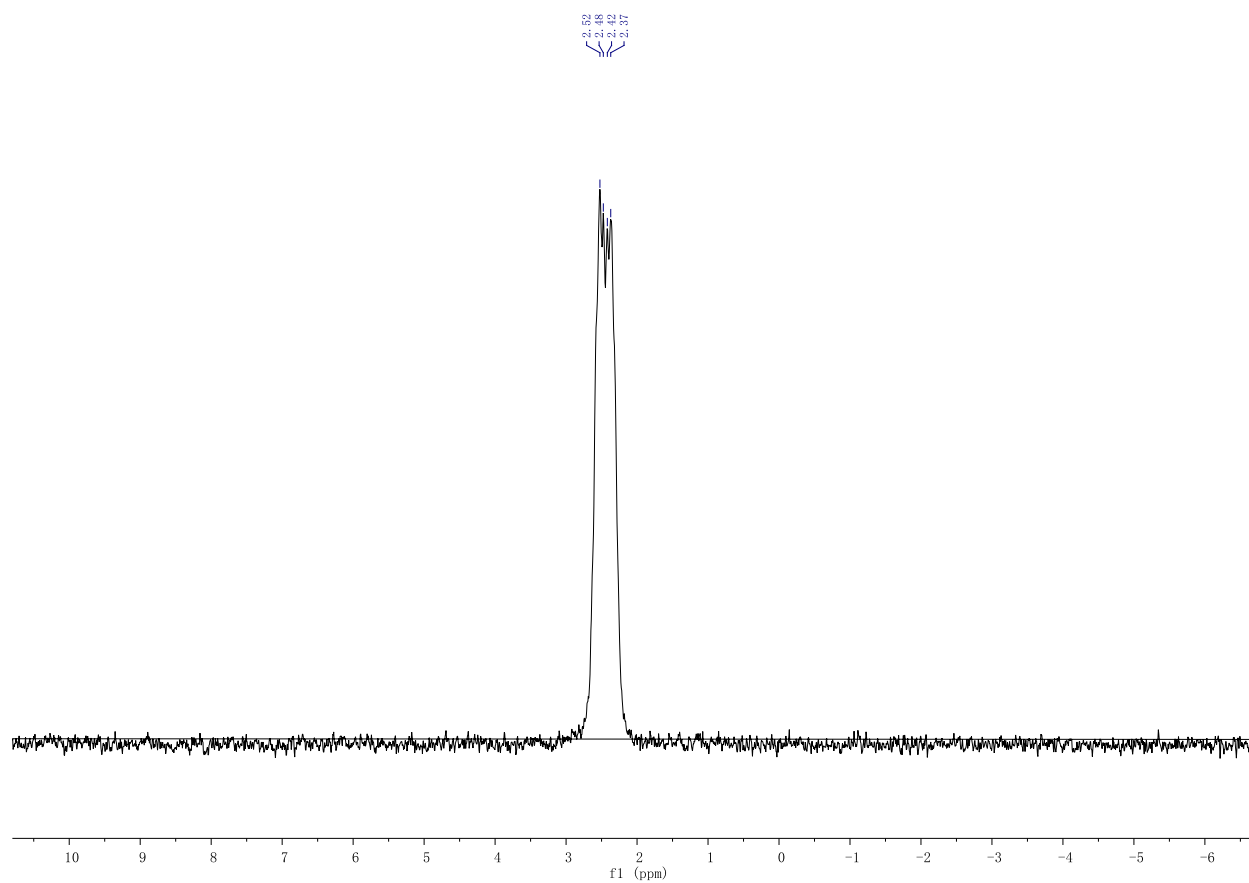


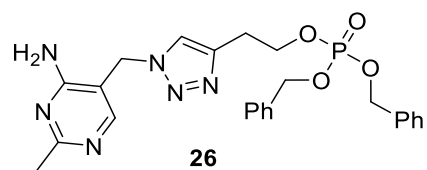
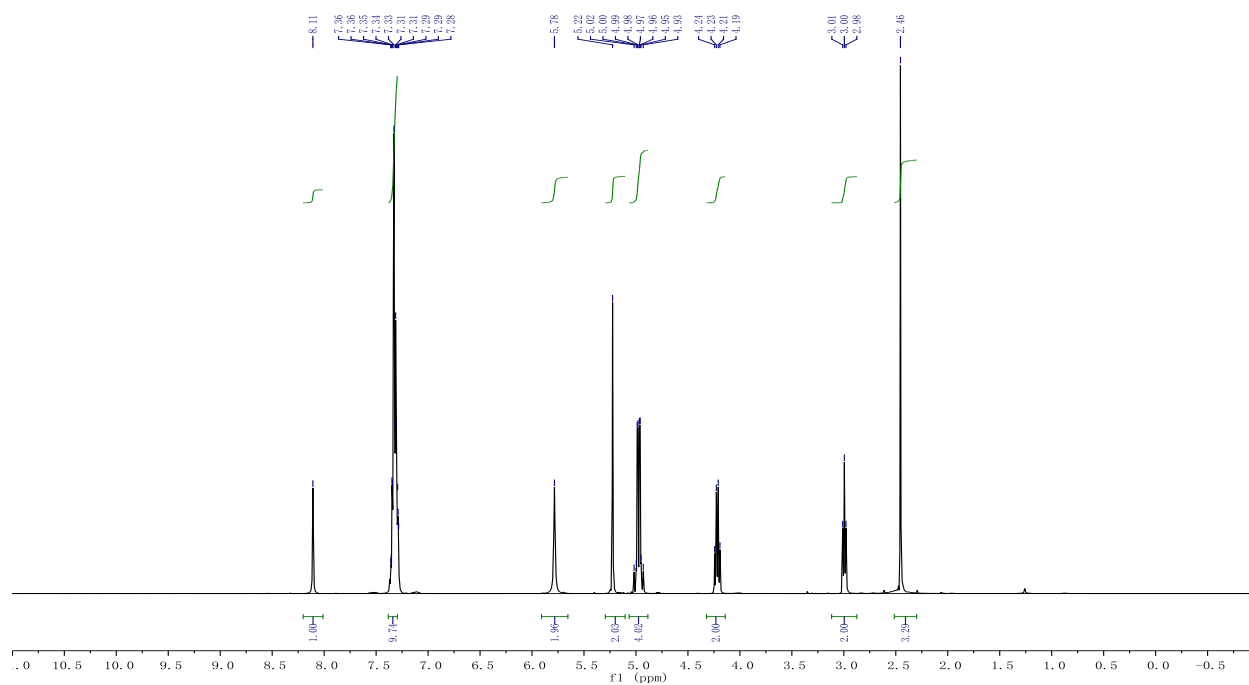
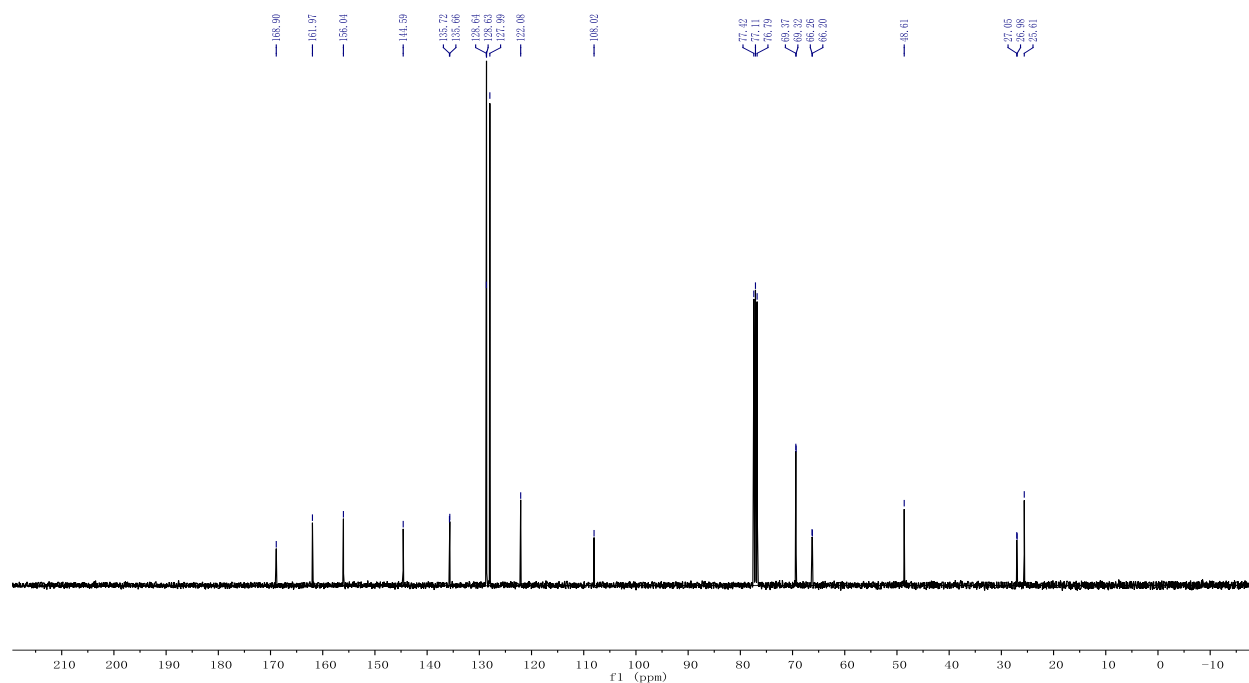
^{13}C NMR

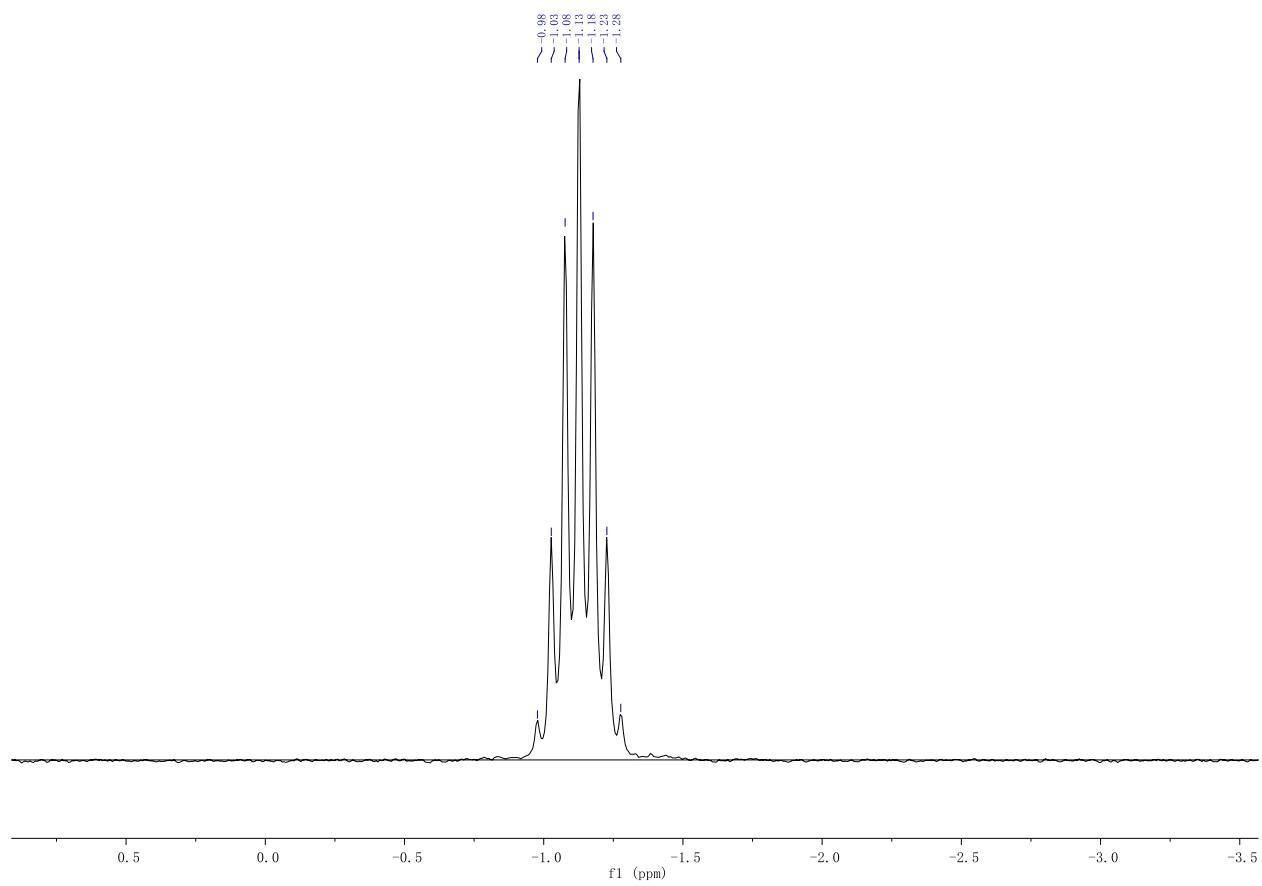


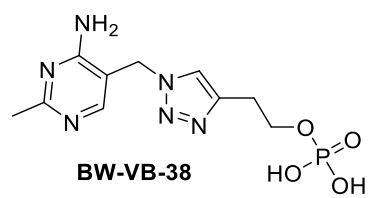
^{31}P NMR

 ^1H NMR ^{13}C NMR

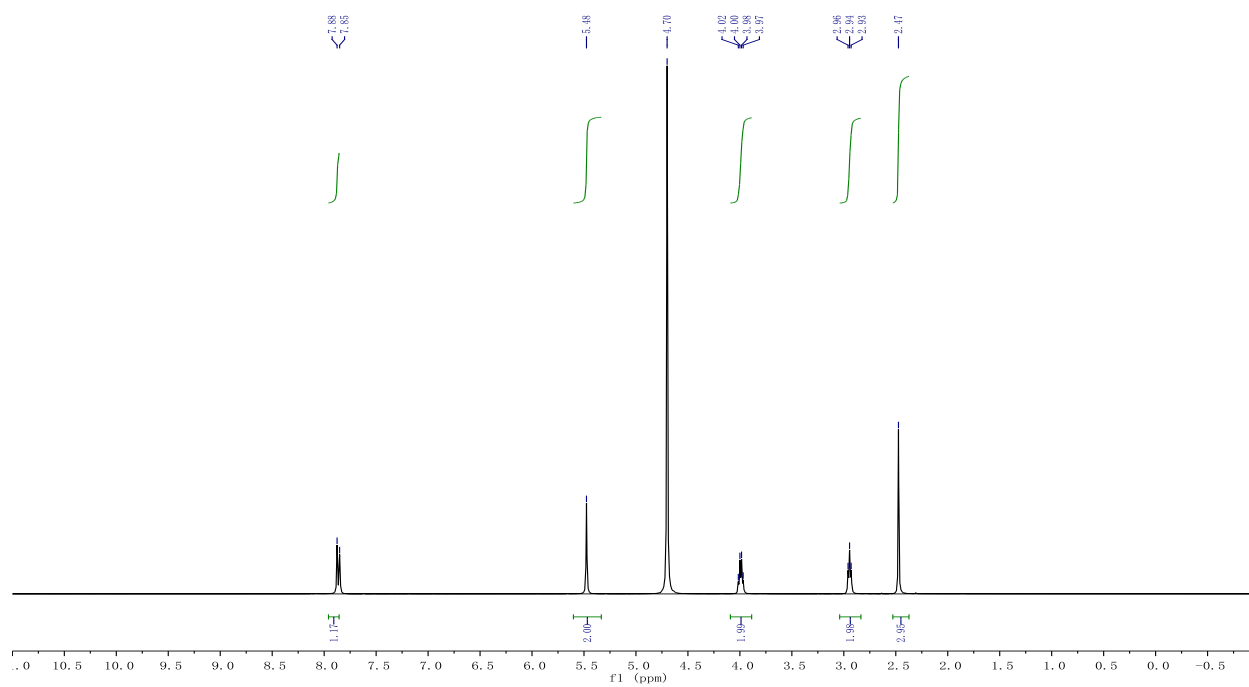
^{31}P NMR

¹H NMR¹³C NMR

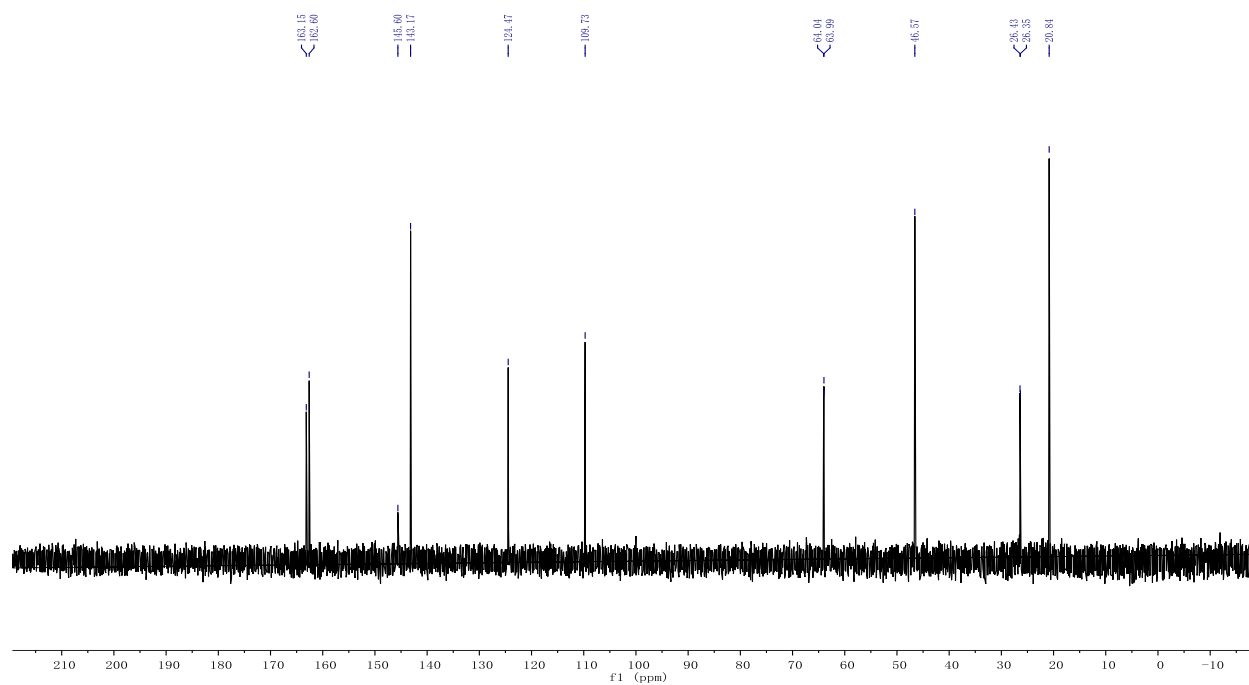
^{31}P NMR

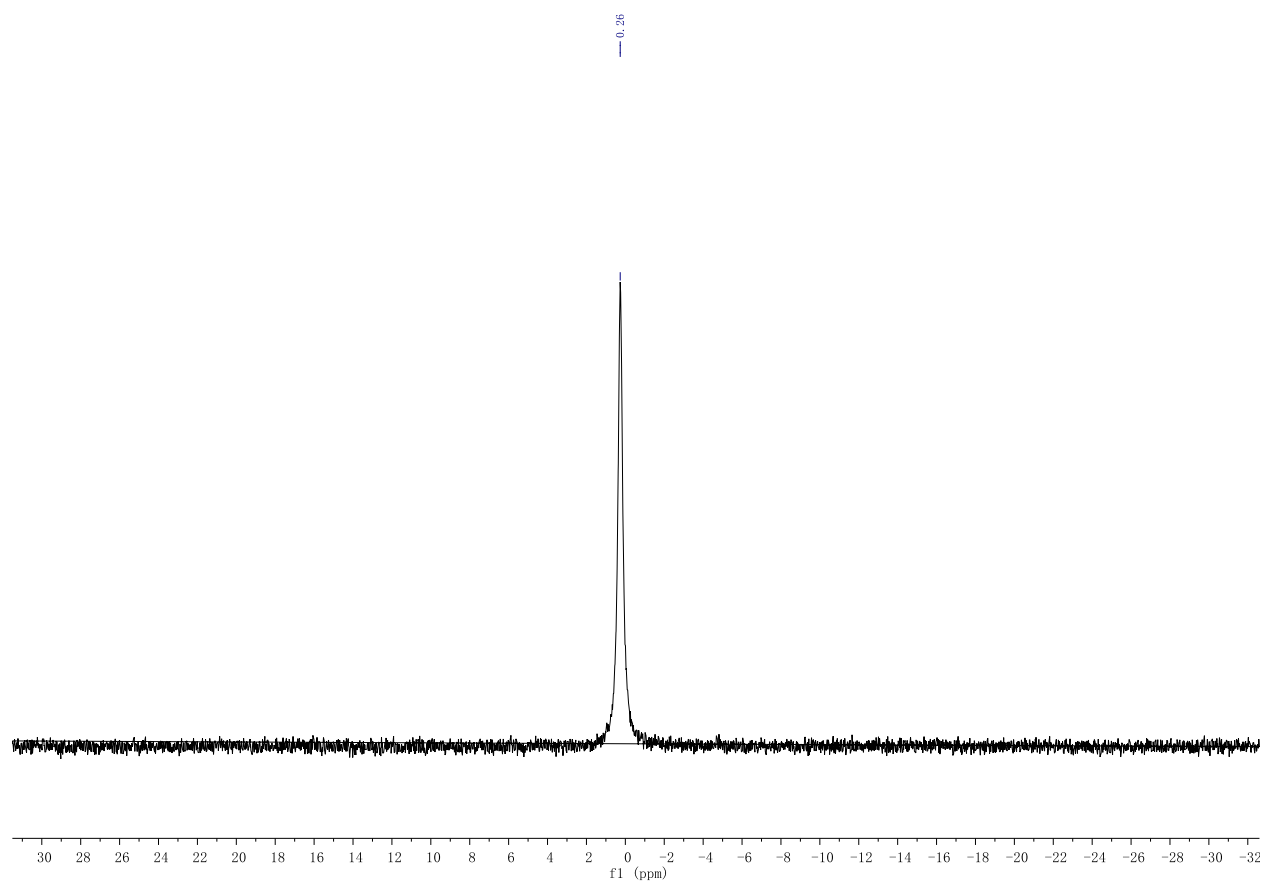


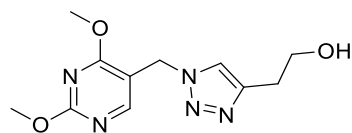
^1H NMR



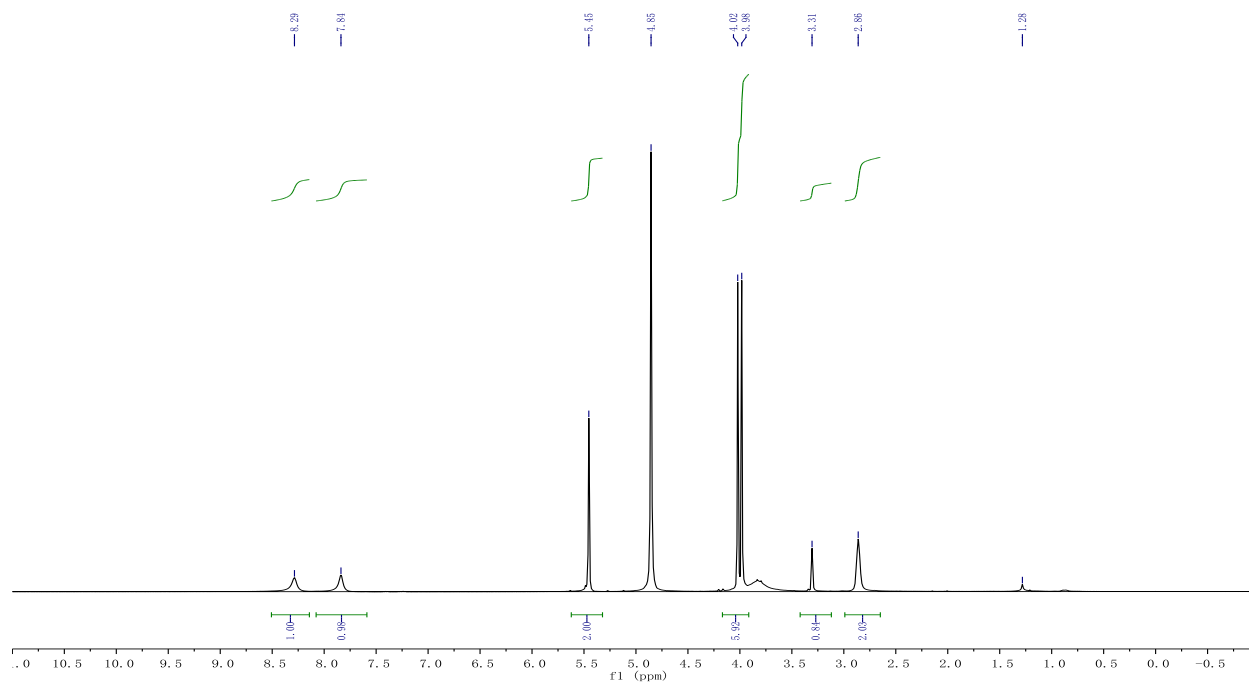
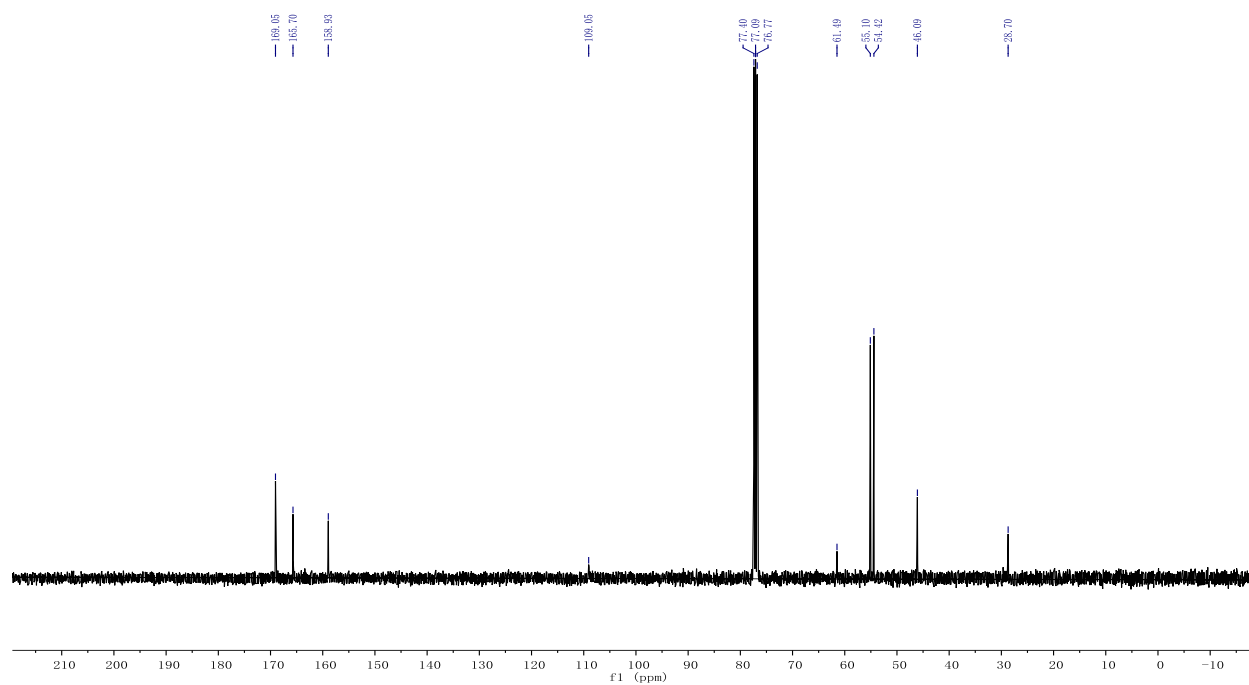
^{13}C NMR

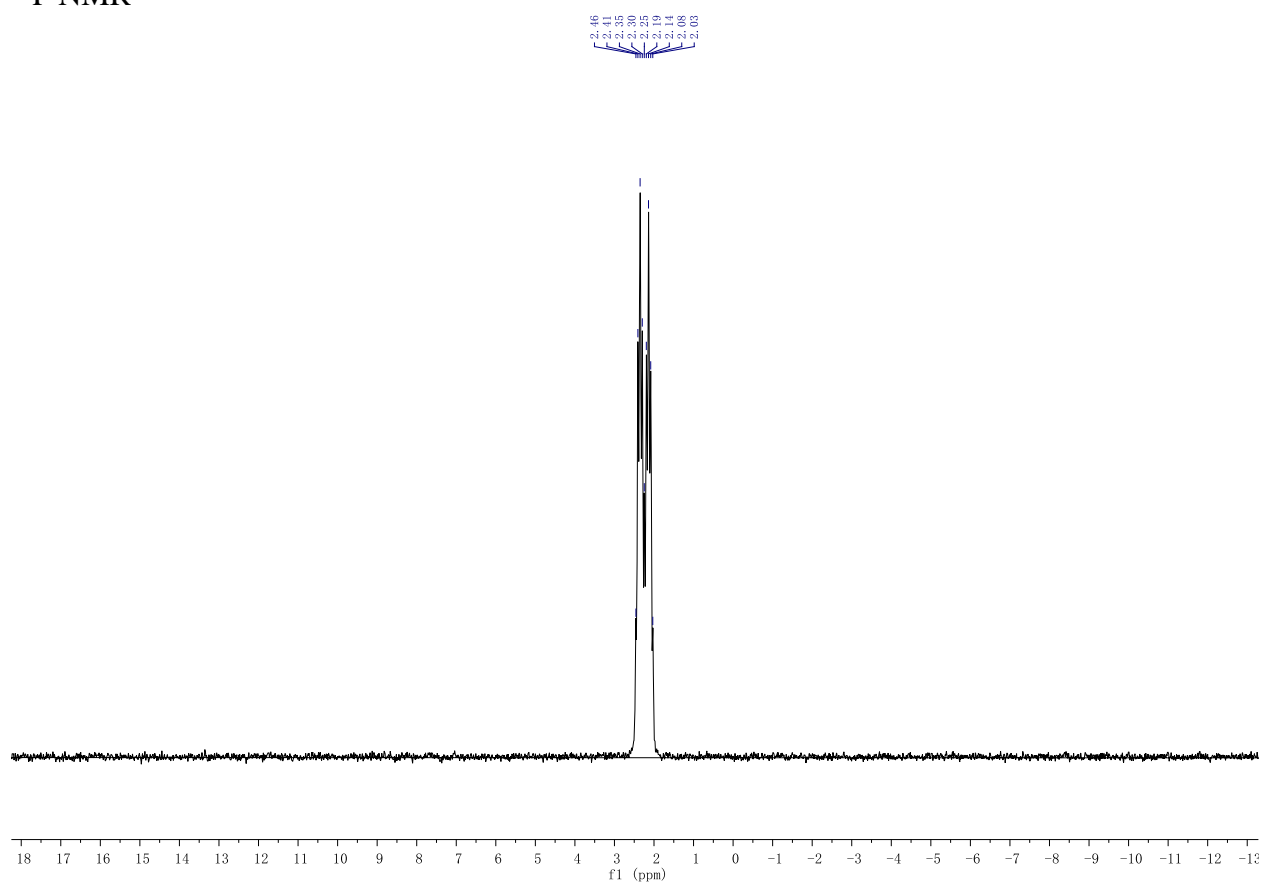


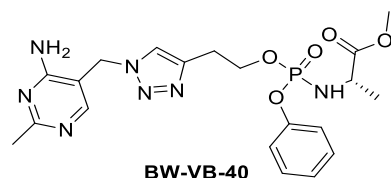
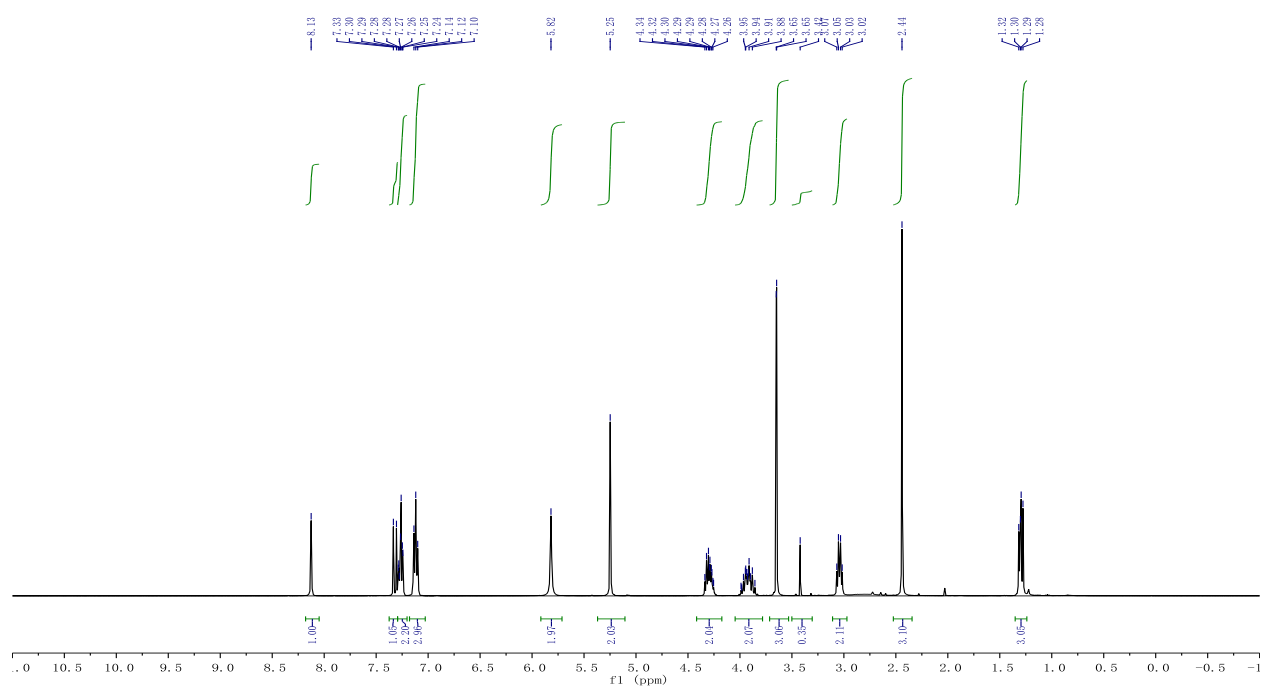
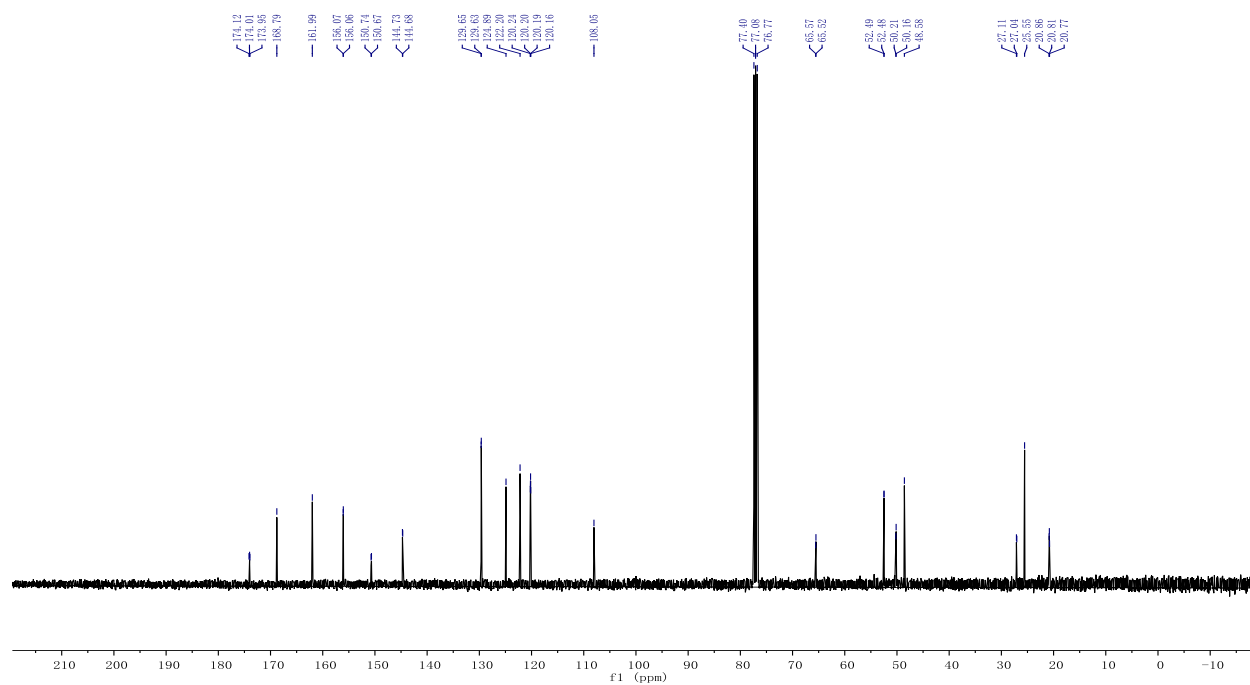
^{31}P NMR

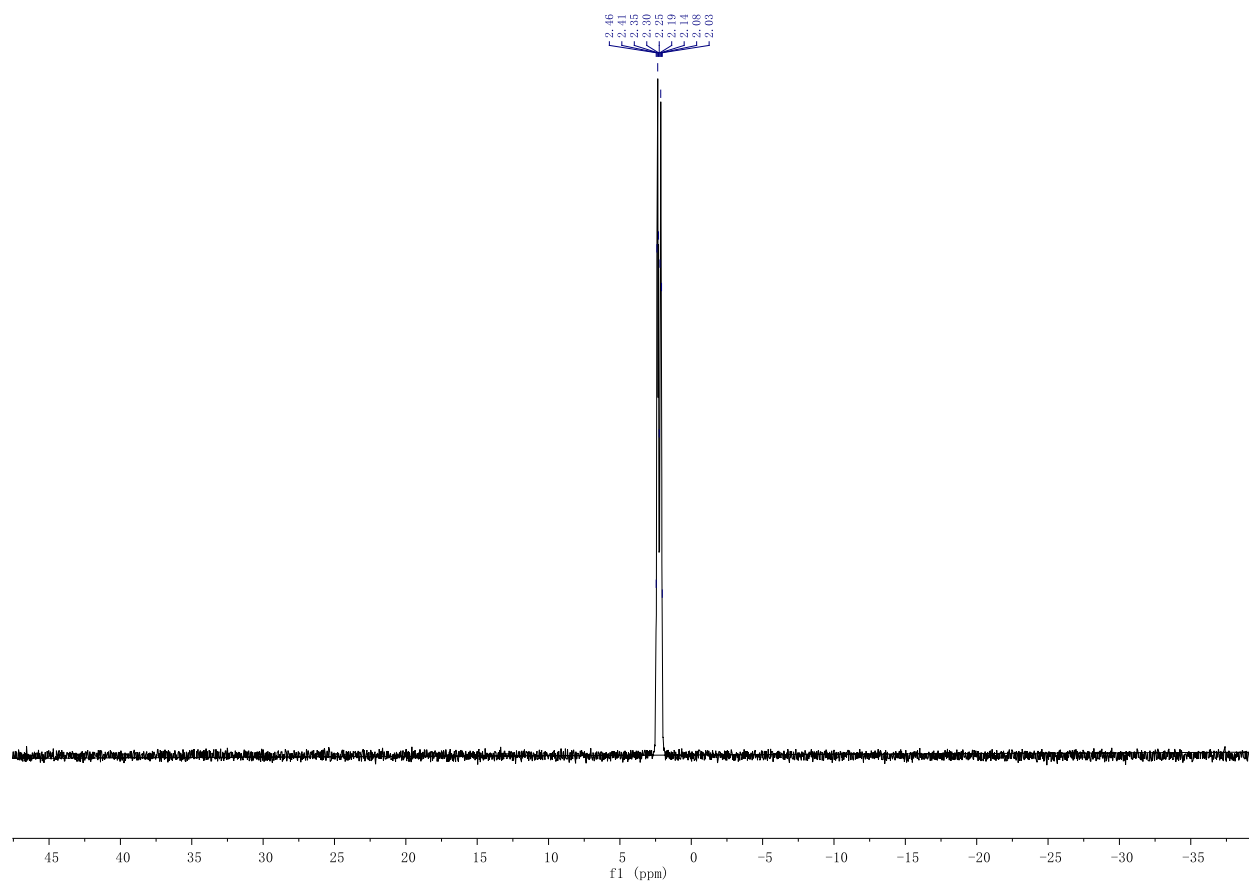


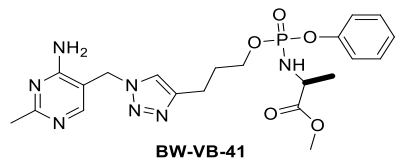
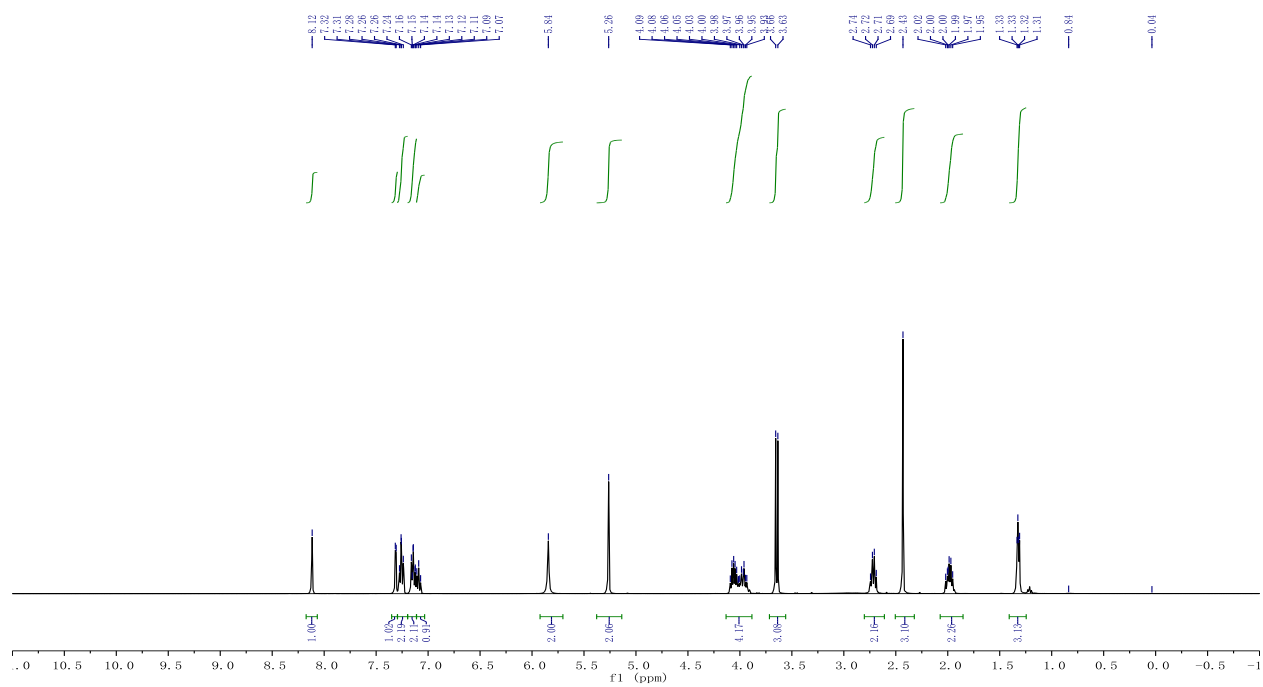
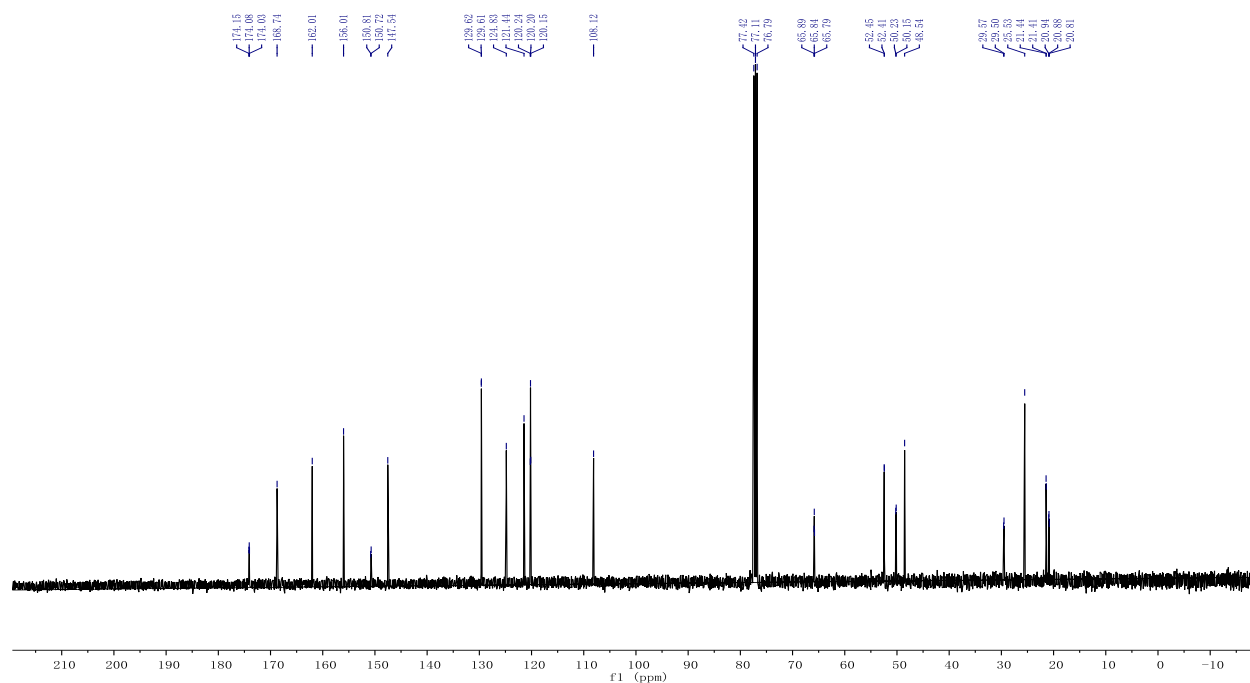
BW-VB-39

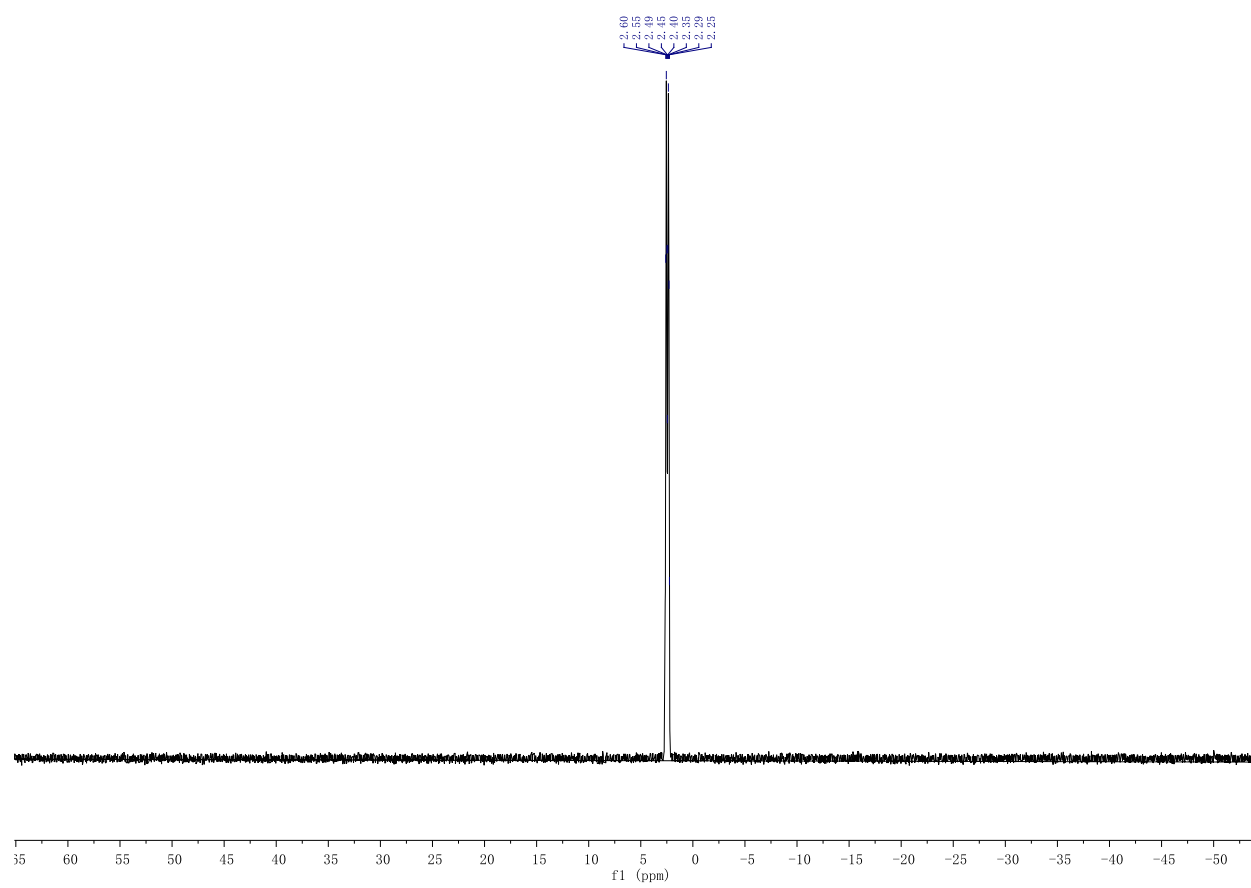
 ^1H NMR ^{13}C NMR

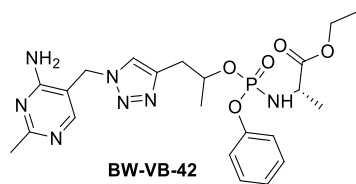
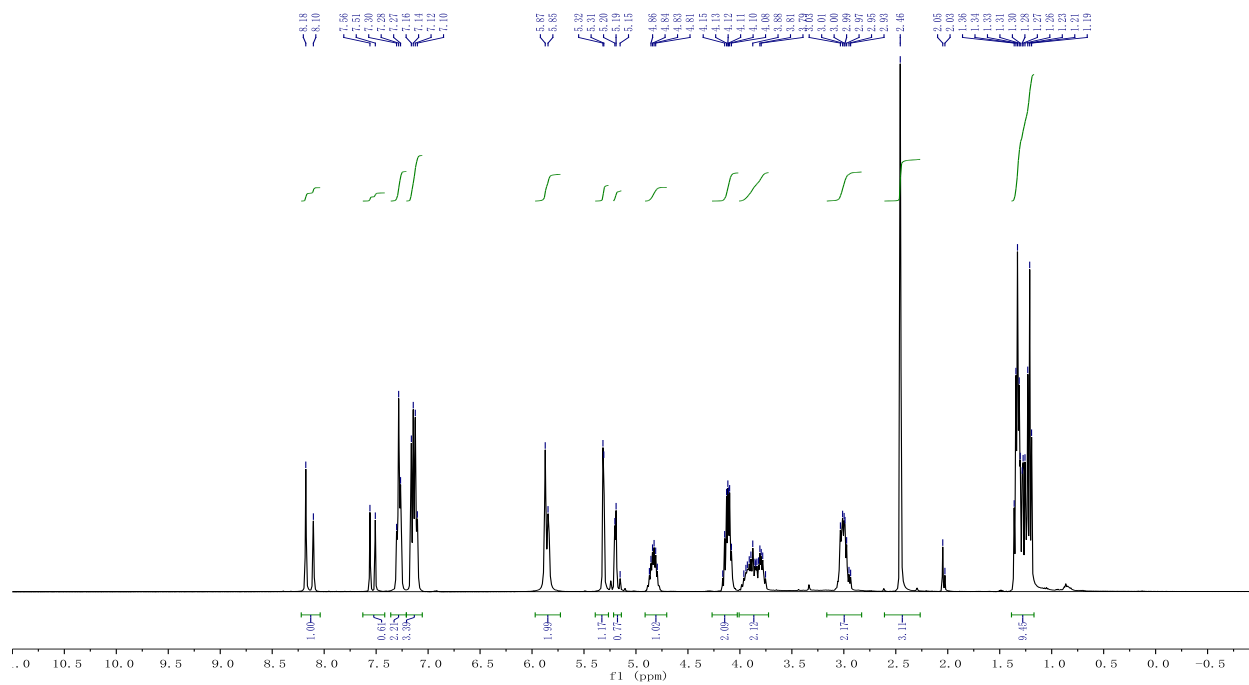
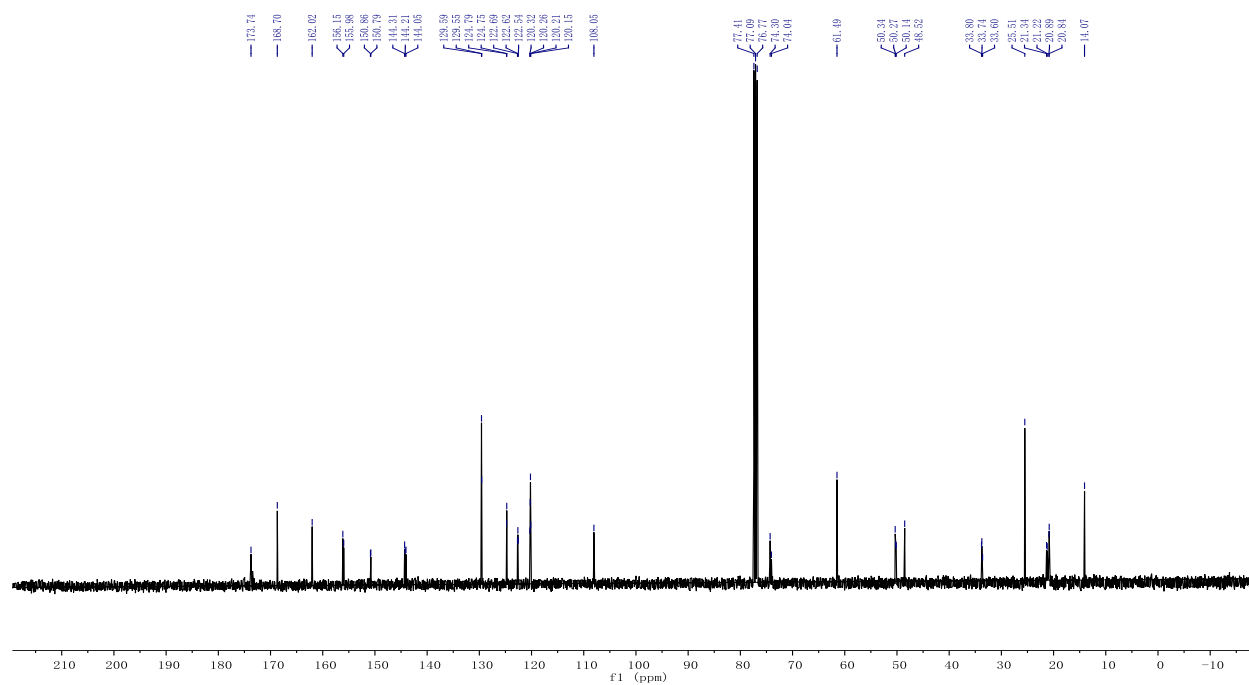
^{31}P NMR

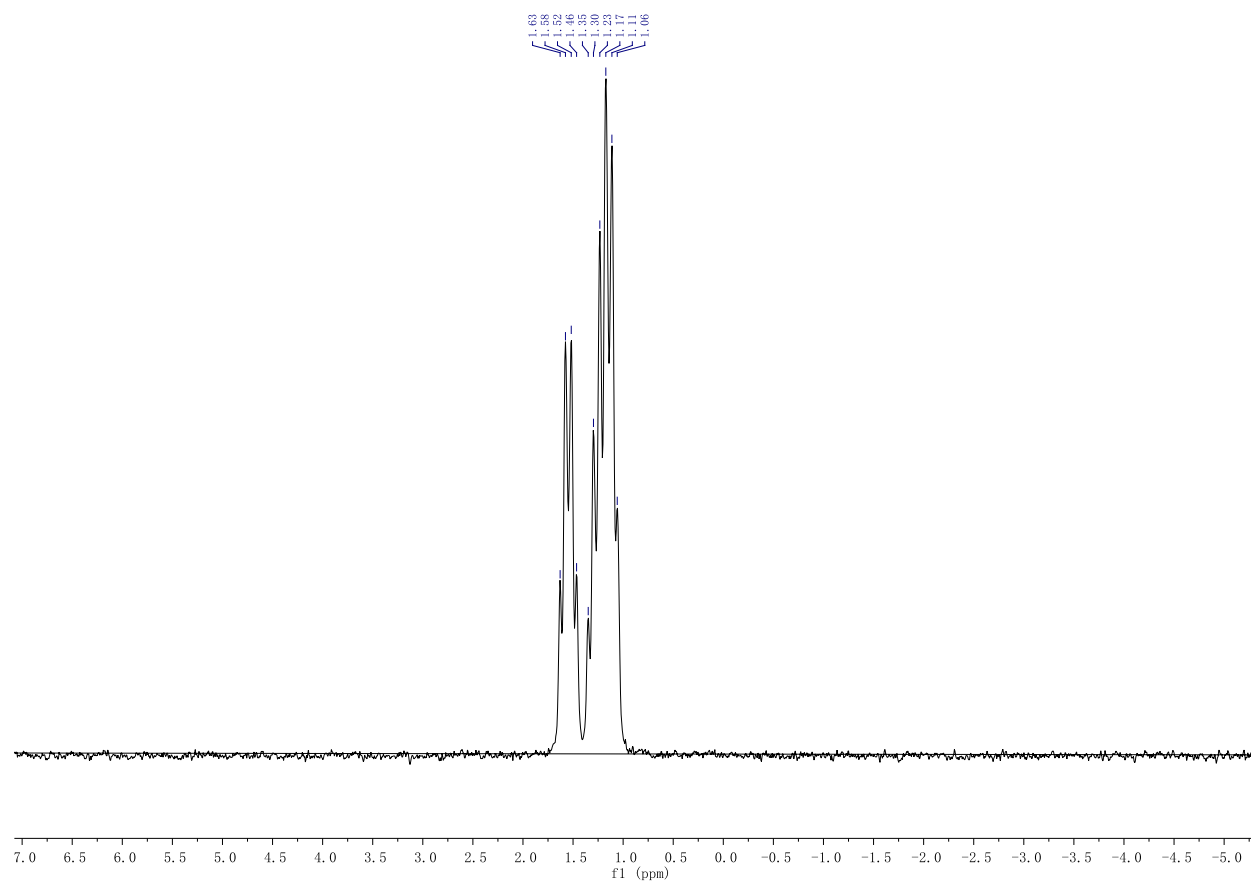
¹H NMR¹³C NMR

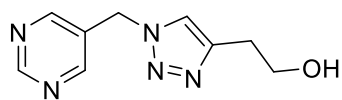
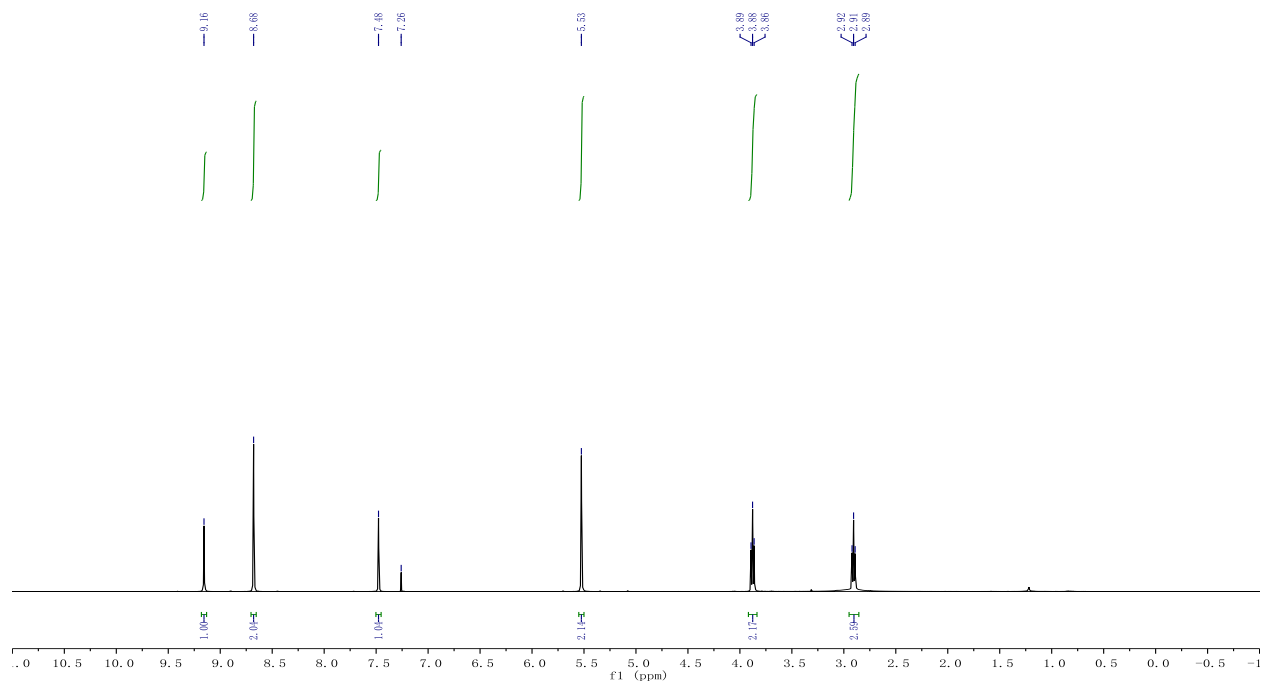
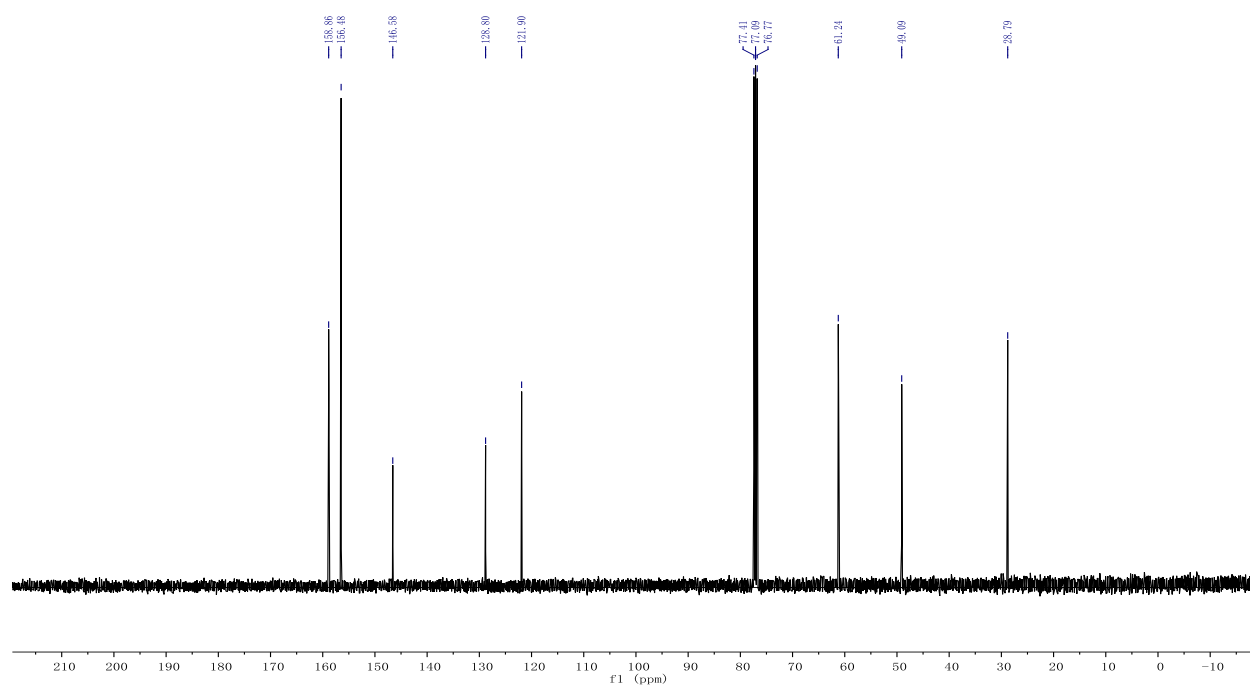
^{31}P NMR

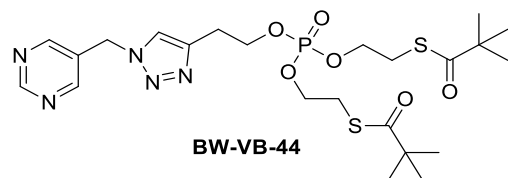
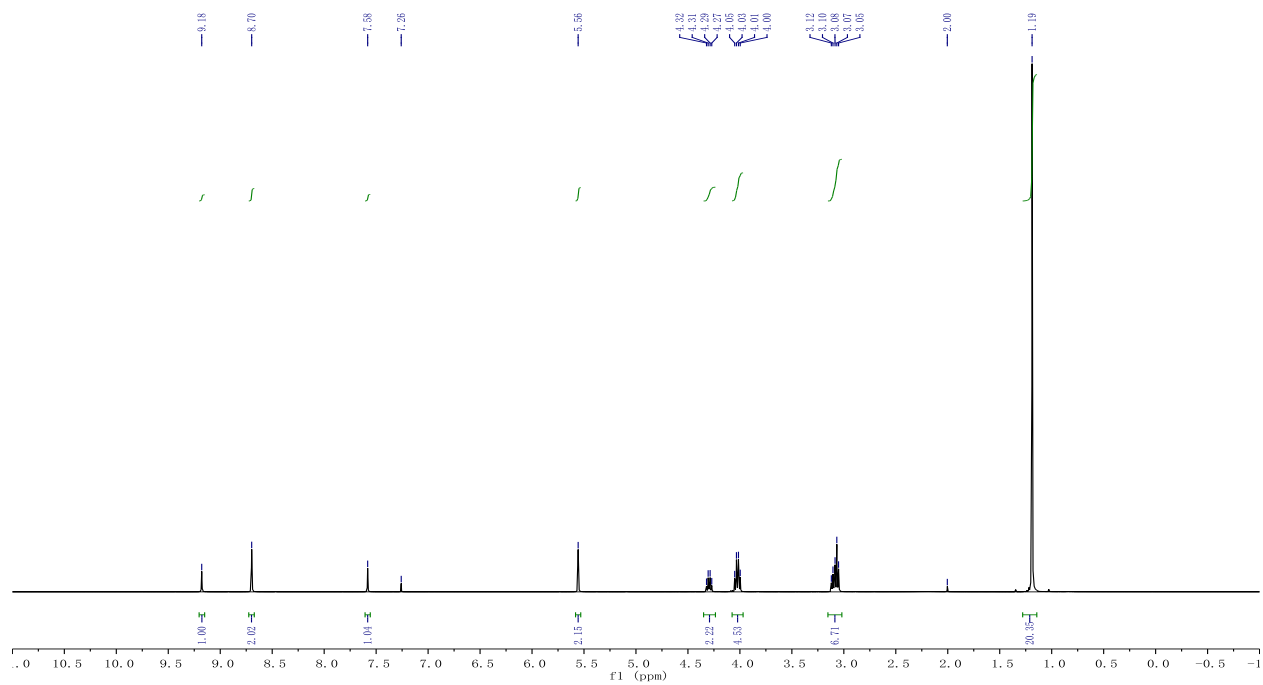
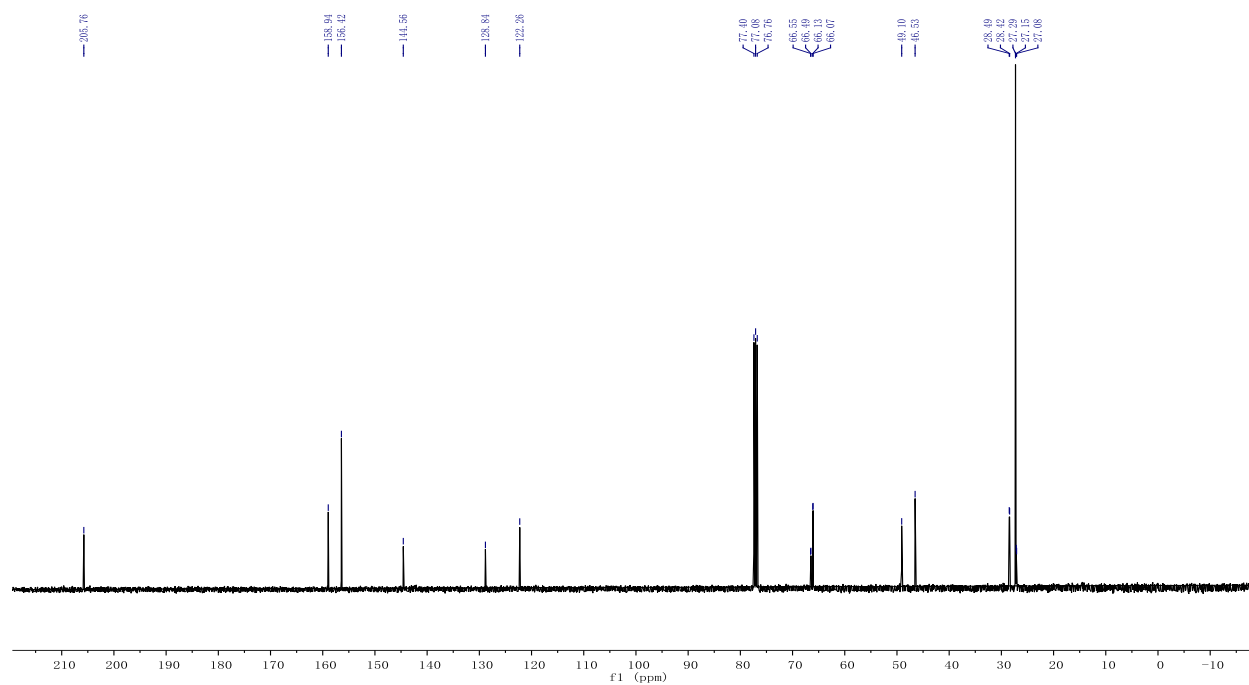
 ^1H NMR ^{13}C NMR

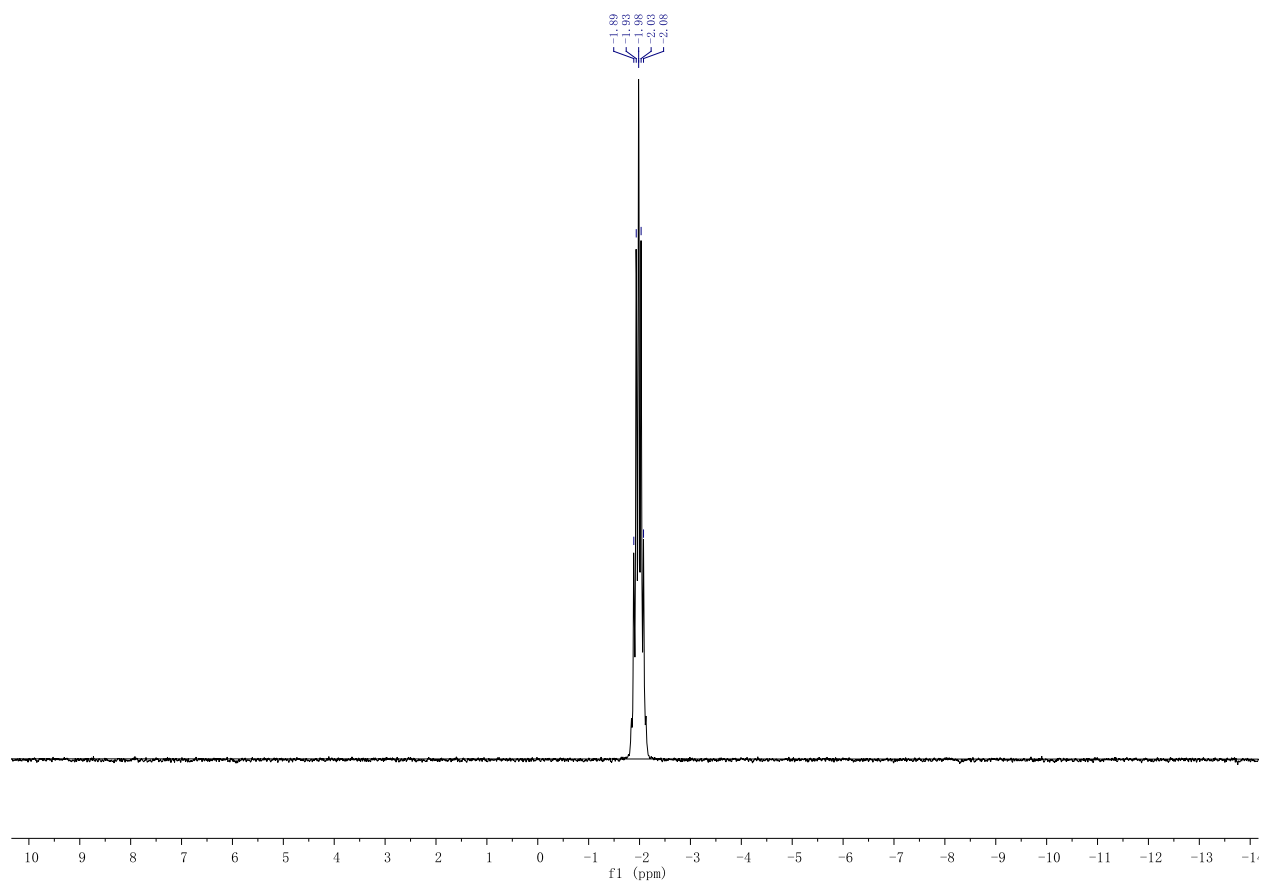
^{31}P NMR

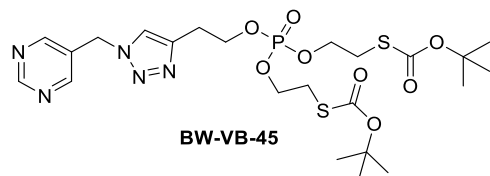
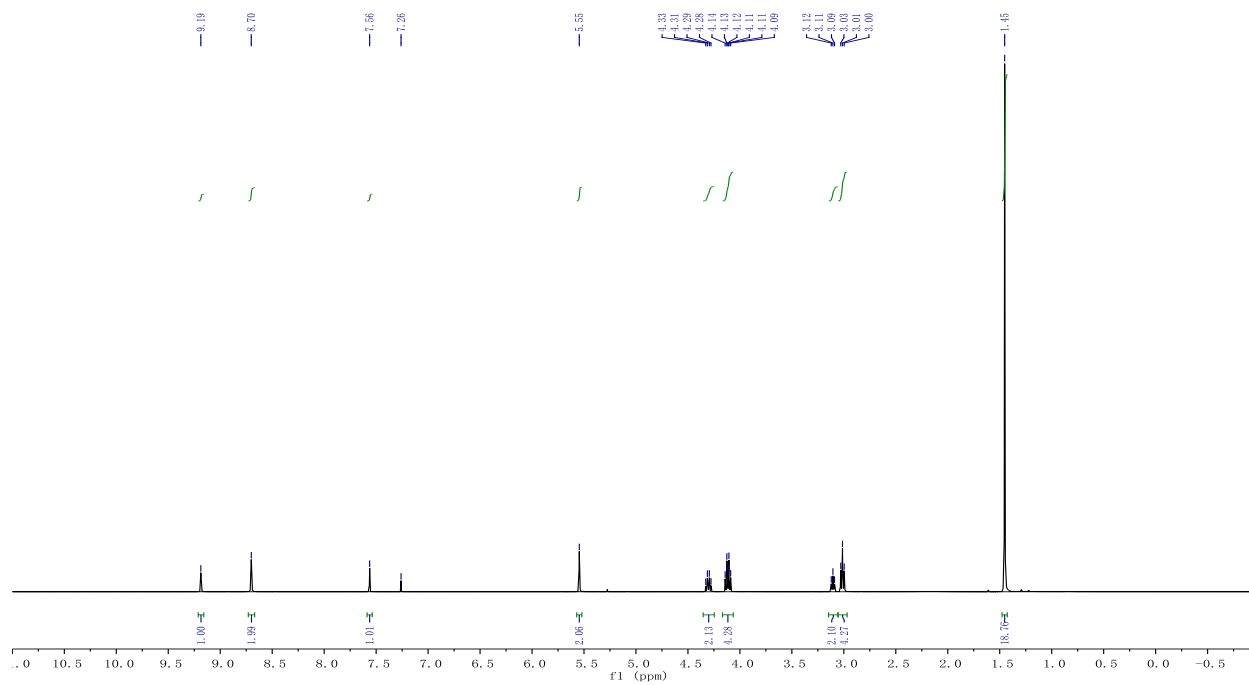
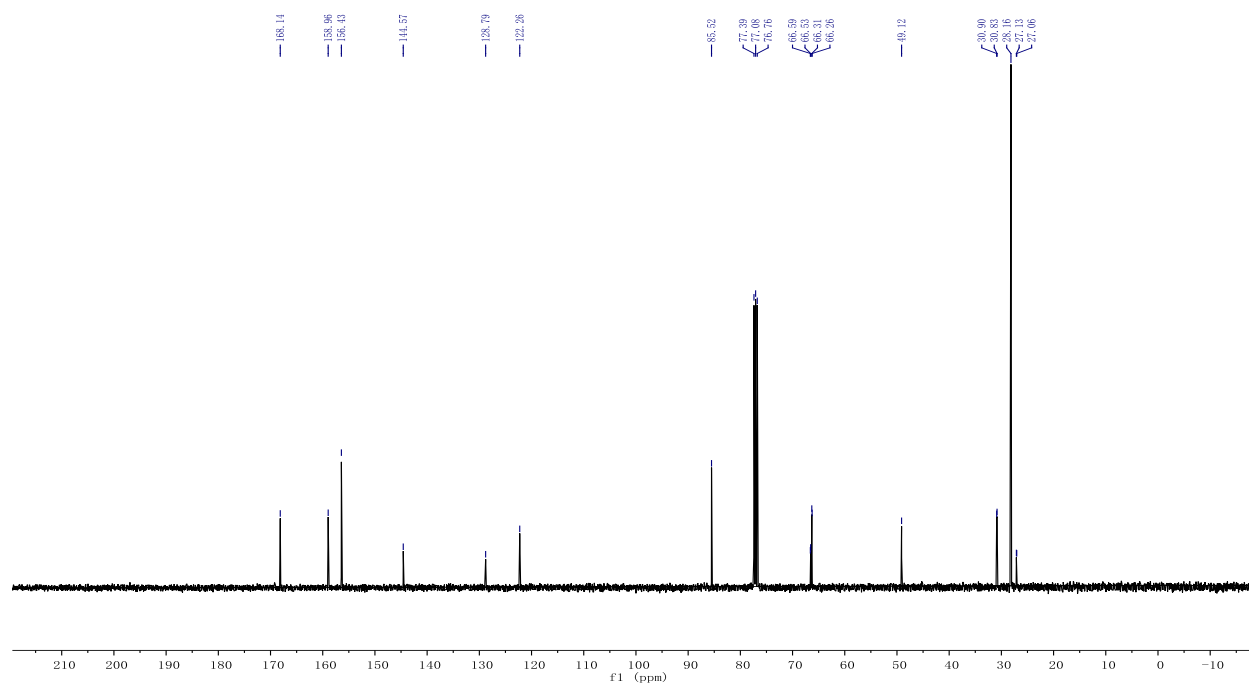
 ^1H NMR ^{13}C NMR

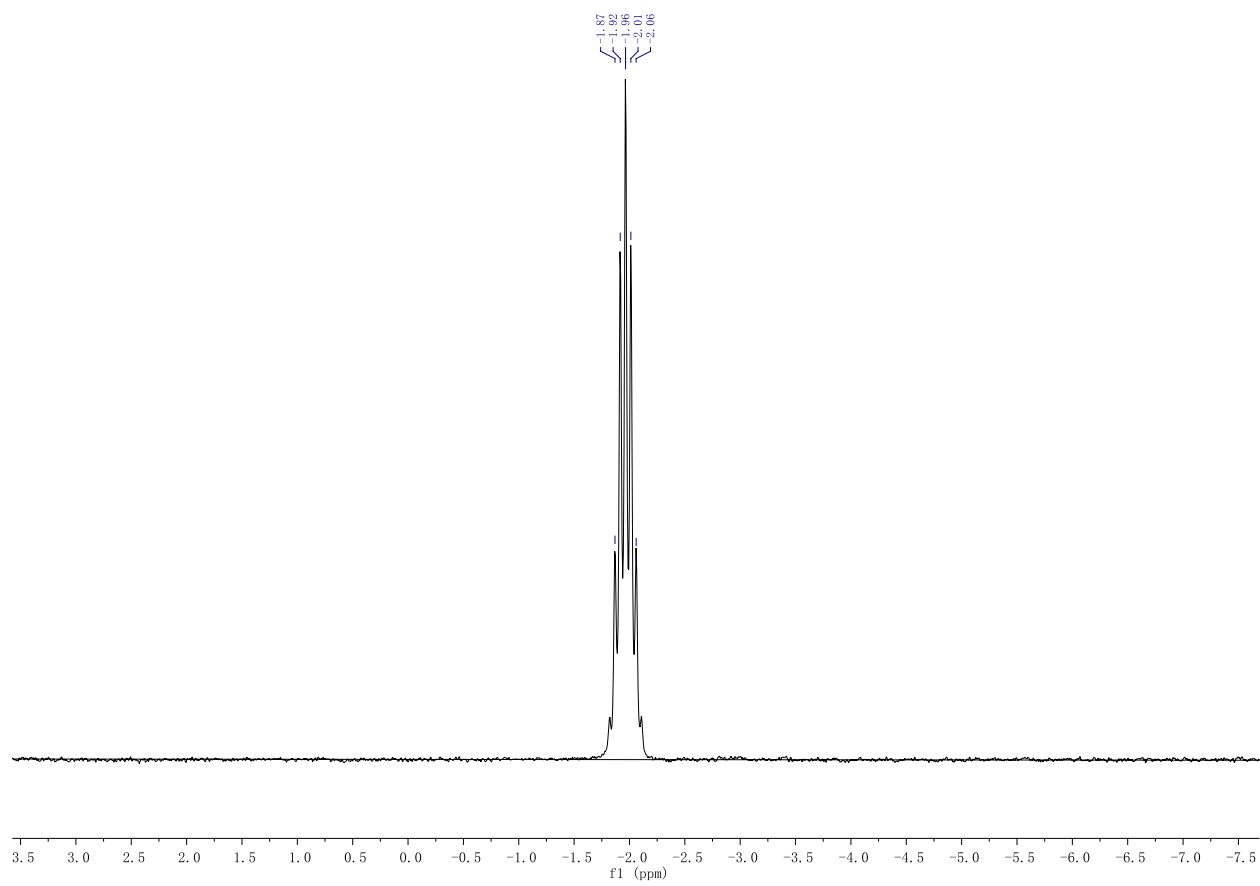
^{31}P NMR

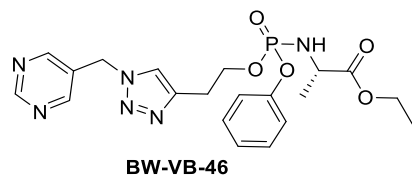
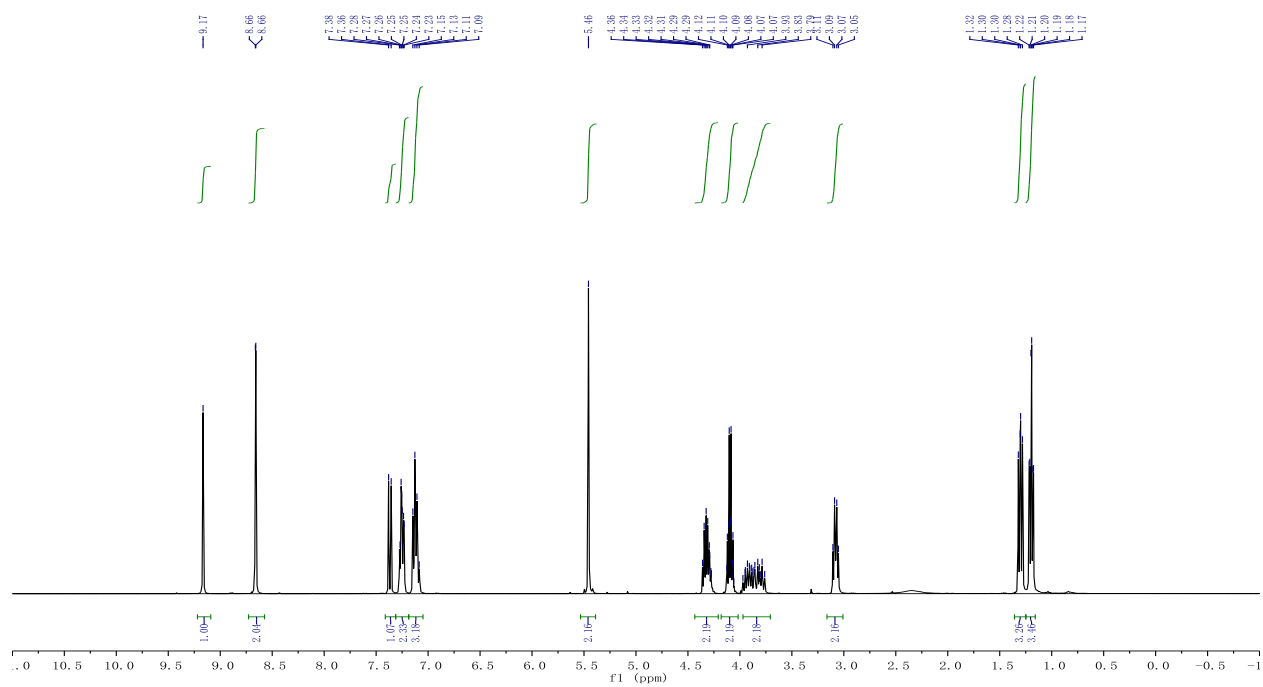
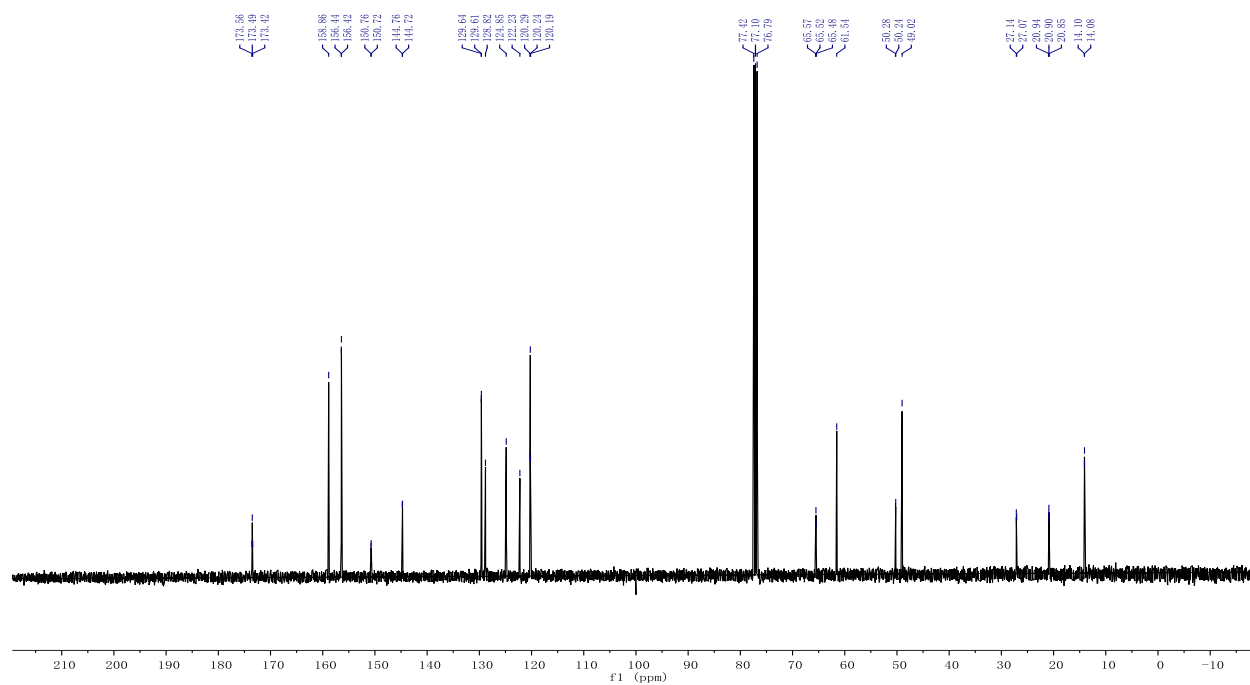
**BW-VB-43**¹H NMR¹³C NMR

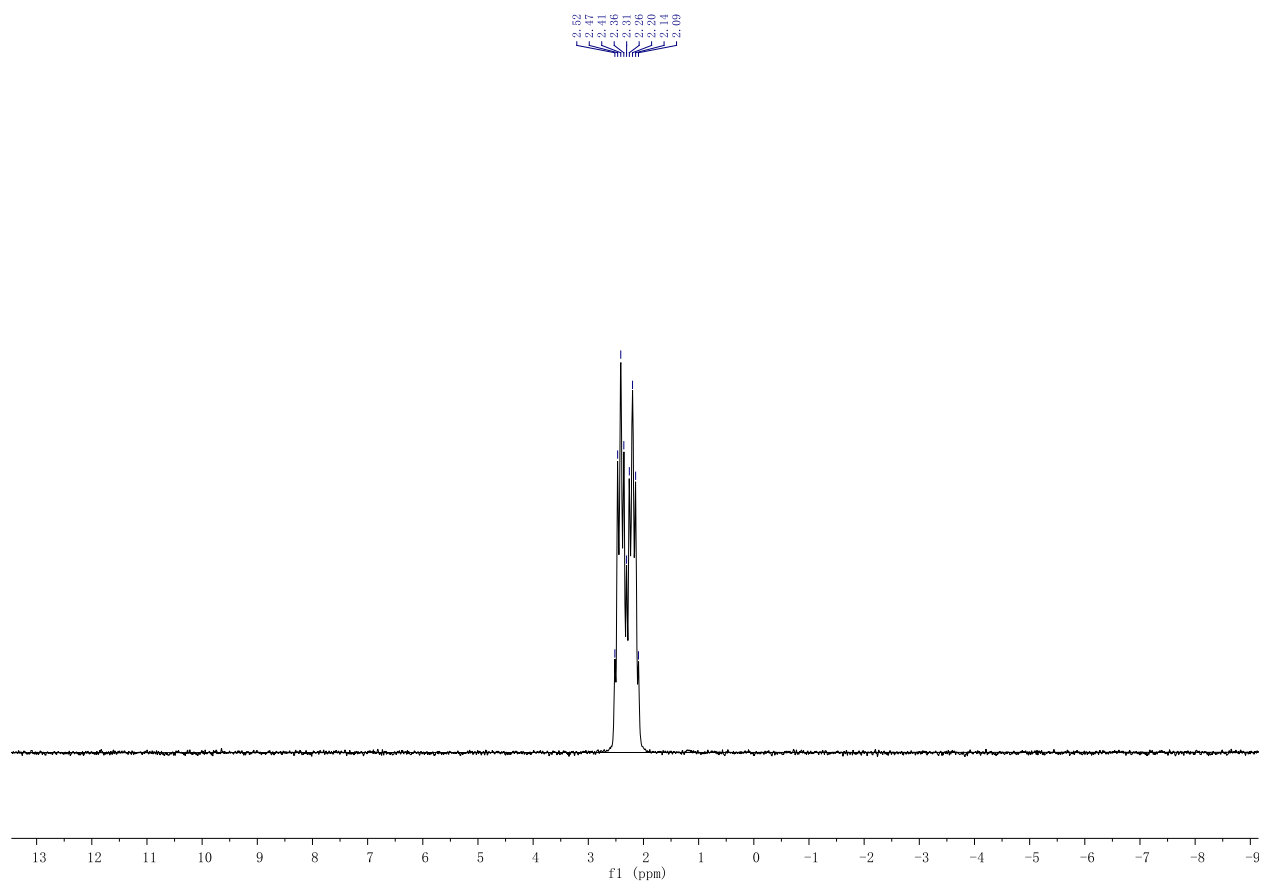
 ^1H NMR ^{13}C NMR

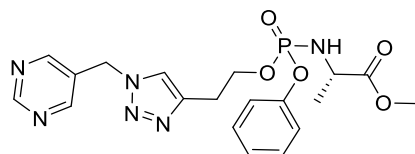
^{31}P NMR

 ^1H NMR ^{13}C NMR

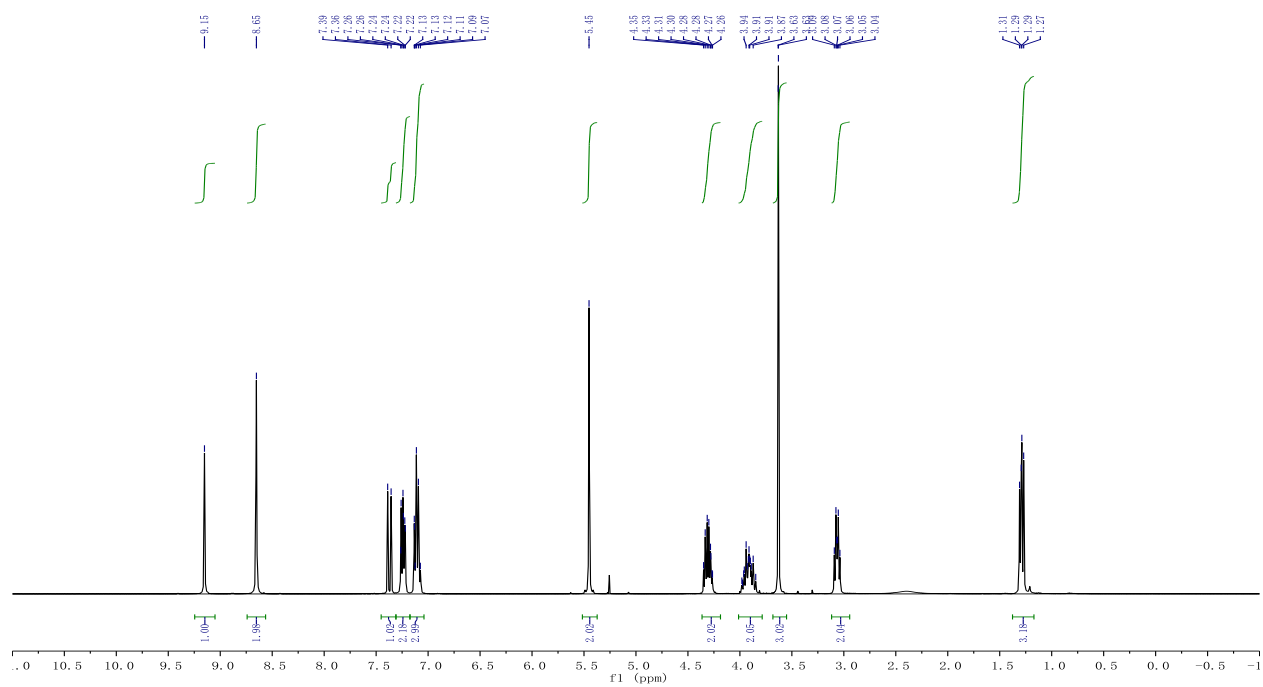
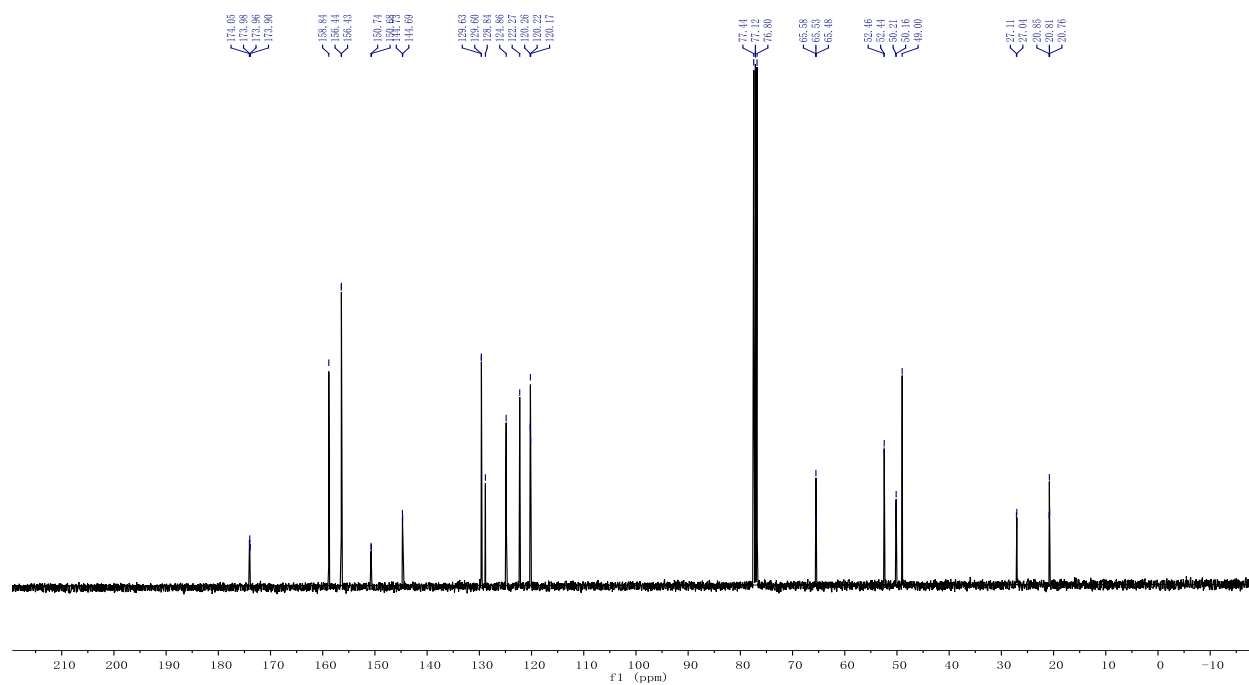
^{31}P NMR

 ^1H NMR ^{13}C NMR

^{31}P NMR



BW-VB-47

 ^1H NMR ^{13}C NMR

^{31}P NMR